ZooKeys 1215: 1–26 (2024)
DOI: 10.3897/zookeys.1215.128183

Review Article

Two new species of genus *Labronema* Thorne, 1939 (Nematoda, Dorylaimidae) from natural parks of Vietnam with an identification key to the species with a medium-sized odontostyle

Tam T. T. Vu[1,2], Milka Elshishka[3], Anh D. Nguyen[1,2], Thi Mai Linh Le[1,2], Aleksandar Mladenov[3], Vlada Peneva[3]

1 *Institute of Ecology and Biological Resources, Vietnam Academy of Science and Technology, 18 Hoang Quoc Viet, Cau Giay, Hanoi, Vietnam*
2 *Graduate University of Science and Technology, Vietnam Academy of Science and Technology, 18 Hoang Quoc Viet, Cau Giay, Hanoi, Vietnam*
3 *Institute of Biodiversity and Ecosystem Research, Bulgarian Academy of Sciences, 2 Gagarin Street, 1113 Sofia, Bulgaria*
Corresponding author: Vlada Peneva (esn.2006@gmail.com)

Abstract

Labronema Thorne, 1939 is a large and diverse dorylaimid genus with complicated taxonomy. Two new species, *Labronema porosum* **sp. nov.** and *Labronema bidoupense* **sp. nov.** from natural habitats in Vietnam were characterised both morphologically and molecularly (18S rDNA and 28 rDNA), and line drawings and microphotographs are provided. Phylogenetic analyses showed that the new species clustered together with *Labronema ferox* Thorne, 1939, the type species of the genus. The two new taxa belong to a group of *Labronema* species with medium body (L = 1.5–2.5 mm) and odontostyle (31–39 µm) length, and a lip region offset by a constriction. Based on morphological and molecular evidence, this study shows that the populations from Vietnam previously identified as *L. glandosum* Rahman, Jairajpuri, Ahmad & Ahmad, 1986 in fact represent *L. porosum* **sp. nov.** Evolutionary relationships of *Labronema* species are discussed. A key to the species of *Labronema* with a medium-sized odontostyle (31–39 µm) is provided as well as a list of the species of the genus considered valid.

Key words: Distribution, Dorylaimida, morphology, phylogeny, 18S rDNA, 28S rDNA

Academic editor: Sergei Subbotin
Received: 24 May 2024
Accepted: 20 August 2024
Published: 11 October 2024

ZooBank: https://zoobank.org/3D77FC3D-117D-444B-A5F6-9A2E056F739E

Citation: Vu TTT, Elshishka M, Nguyen AD, Le TML, Mladenov A, Peneva V (2024) Two new species of genus *Labronema* Thorne, 1939 (Nematoda, Dorylaimidae) from natural parks of Vietnam with an identification key to the species with a medium-sized odontostyle. ZooKeys 1215: 1–26. https://doi.org/10.3897/zookeys.1215.128183

Introduction

The genus *Labronema* was erected by Thorne (1939) when he described three new species and transferred six other species of the genus *Dorylaimus* Dujardin, 1845, with *Labronema ferox* Thorne, 1939 designated as a type species. Siddiqi (1969) raised the subfamily Qudsianematinae Jairajpuri, 1965 containing three genera including *Labronema* Thorne, 1939 to a full family rank. Based on an integrative approach including morphology, postembryonic development, and analysis of D2-D3 expansion segments of 28S rDNA sequences, Peña-Santiago and Álvarez-Ortega (2014) transferred the genus *Labronema* and seven other genera of the family Qudsianematidae to Dorylaimidae and proposed for it a new subfamily Labronematinae. Several studies showed that genus *Labronema* is a heterogeneous group of species with a very complicated taxonomy and

systematics (Andrássy 2009; Álvarez-Ortega et al. 2010; Peña-Santiago 2019; Peña-Santiago and Vinciguerra 2019; Peña-Santiago 2022). One of the main problems, similarly to other nematode taxa, is that the descriptions of many species do not entirely fit the genus diagnosis, often they do not conform to the modern taxonomic requirements and are insufficiently detailed (Peña-Santiago and Vinciguerra 2019; Altash et al. 2024; Elshishka et al. 2024). All that does not allow a good species differentiation. Furthermore, approximately 40% of the species (Andrássy 2011a) are described based on one sex, and this does not facilitate elucidating the systematics of the genus. Not less important is the limited molecular data (several 18S and 28S rRNA gene sequences), which are often not supported by morphological characteristics (Peña-Santiago 2019).

For several decades, a number of species, which were identified under *Crassolabium* Yeates, 1967, *Thonus* Thorne, 1974, *Eudorylaimus* Andrássy, 1959, *Aporcelaimellus* Heyns, 1965, *Talanema* Andrássy, 1991 have been transferred to or moved out *Labronema* (Andrássy 1991, 2009, 2011a; Peña-Santiago and Ciobanu 2011; Álvarez-Ortega and Peña-Santiago 2013, Imran et al. 2021). Two species of *Labronema* were transferred to *Nevadanema* Álvarez-Ortega & Peña-Santiago, 2012.

During the last ten years only three new species of the genus have been described: *L. mannai* Dattaray, Roy & Gantait, 2015 and *L. minimus* Dattaray, Roy & Gantait, 2015 from India, and *L. montanum* Peña-Santiago & Abolafia, 2019 from Spain. Furthermore, several studies presented new information on some known species contributing to the improvement of the taxonomy of the genus. Peña-Santiago (2019) provided a redescription of *L. ferox*, the type species of the genus, based on the population studied by Thorne (1974). This detailed study showed that *L. ferox* is a widespread species only in North America. Peña-Santiago and Vinciguerra (2019) redescribed three other species originally described from Italy: *L. angeloi* Vinciguerra & Clausi, 1994, *L. carusoi* Vinciguerra & Orselli, 1998, and *L. pulchrum* Vinciguerra & Zullini, 1980. In their paper, *L. pulchrum* was regarded as a junior synonym of *L. duhouxi* (Altherr, 1963).

Based on the morphological characters (species with a transverse vulva; a conoid, rounded or digitate tail, and non-contiguous ventromedian supplements) and molecular characterisation (D2-D3 expansion segments of 28S rRNA and 18S rRNA gene sequences), Imran et al. (2021) transferred *Labronema baqrii* Khan, Jairajpuri & Ahmad, 1989 to the genus *Talanema*. The authors regarded *L. neodiversum* Mondal, Manna & Gantait, 2012 as a junior synonym of *T. baqrii*, and transferred three other *Labronema* species (*L. malagasi* Furstenberg, Heyns & Swart, 1993, *L. digiturum* Vinciguerra, 1984, and *L. sphinctum* Mohilal & Dahanachand, 2001) to the genus *Talanema*. Peña-Santiago (2022) synonymized *L. loeffleri* Andrássy, 1978 and *L. macrosoma* Alekseyev, 1992 with *L. magnum* Altherr, 1972 on the base of the following morphological characters: large general size, very strong odontostyle, large spicules, and similar number of ventromedian supplements as well as similar habitats. Recently, Zahedi Asl et al. (2023) presented new integrative data (morphological and molecular) of *Labronema vulvapapillatum* (Meyl, 1954) Loof & Grootaert, 1981 from Iran.

Imran et al. (2021) considered that in terms of the lip region shape, *Labronema* spp. present a continuum of variation comprising (i) *L. ferox* type having offset lip region with arched lips, (ii) *L. vulvapapillatum* type having offset lip region

but lips not arched, and (iii) *L. hyalinum* (Thorne & Swanger, 1936) Thorne, 1939 type having lip region almost continuous with adjacent body. The species having atypical lip region were referred to as "atypical" ones (Álvarez-Ortega et al. 2010). However, in order to elucidate the status of these groups more integrative taxonomic studies are needed.

Currently, the genus *Labronema* includes 47 species (see Suppl. material 1), spread in all continents, except for Antarctica. In Vietnam, two species of the genus *Labronema*, *L. neopacificum* Rahman, Jairajpuri, Ahmad & Ahmad, 1986 and *L. glandosum* Rahman, Jairajpuri, Ahmad & Ahmad, 1986 have been reported (Álvarez-Ortega et al. 2010; Vu and Nguyen 2013). During an extensive study of the free-living nematodes of protected territories in Vietnam, two unknown species of *Labronema* were recovered. The objective of the present study is (i) to characterize these populations on the basis of an integrative approach and describe the new species, (ii) to discuss their phylogenetic relationships and (iii) to provide an identification key to the species with a medium-sized odontostyle.

Materials and methods

Nematode extraction, preservation, and morphological studies

Soil samples were collected from a pristine forest in the Natural Reserve Du Gia (Bac Me District, Ha Giang Province) and the National Park Bidoup-Nui Ba (Lac Duong District, Lam Dong Province), Vietnam. Nematodes were extracted from soil samples using modified Baermann funnel technique (Southey 1986). They were heat-killed, fixed in TAF solution (for morphological observations) or in a DESS mixture (Yoder et al. 2006) (for molecular analyses), transferred to anhydrous glycerol (Seinhorst 1962), and mounted on glass slides for microscopic observation. Drawings were prepared using an Olympus BX 51 compound microscope with a drawing tube. Photomicrographs were taken using an Axio Imager.M2-Carl Zeiss compound microscope equipped with a digital camera (ProgRes C7) and specialised software (CapturePro Software 2.8). Measurements were made using an Olympus BX 41 light microscope with a drawing tube and digitising tablet (CalComp Drawing Board III, GTCO CalCom Peripherals, Scottsdale, AZ, USA) and Digitrak 1.0f computer program (Philip Smith, John Hutton Institute, Dundee, UK). Terminology follows Peña-Santiago (2021). The locations of pharyngeal gland nuclei are given following Loof and Coomans (1970).

DNA isolation, amplification, and sequencing

Genomic DNA was isolated from single individuals as described by Holterman et al. (2006) and stored at –20° until used as a PCR template. The D2-D3 expansion segment of 28S and was amplified using the forward D2A (5'–ACAAGTACCGTGGGGAAAGTTG–3') and reverse D3B (5'–TCGG AAGGAACCAGCTACTA–3') primers (Subotin et al. 2006) and the 18S rDNA fragment was amplified using the primers 18S (18F: 5'-TCTAGAGCTAATACATGCAC-3'/18R: 5'-TACGGAAACCTTGTTACGAC-3') (Floyd et al. 2005). All PCR reactions contained 12.5 µl Hot start green PCR Master Mix (2×) (Promega, USA), 1 µl of the forward

and reverse primer (10 µM each), the 3 µl DNA template and sterile Milli-Q water to 25 µl of the total volume. All PCR reactions were performed in SimpliAmp Thermal cycler (Thermo Fisher Scientific) as follows: an initial denaturation step at 95 °C for 4 min, followed by 40 cycles at 95 °C for 30 s, 54 °C for 30 s and 72 °C for 60s with a final incubation for 5 min at 72 °C. Amplicons were visualised under UV illumination after Simplisafe gel staining and gel electrophoresis.

Phylogenetic analyses

For reconstructing the phylogenetic relationships, analyses were based on 18S and 28S rDNA sequences. The newly obtained rDNA sequences were analysed using the BioEdit and aligned with sequences available in GenBank using the ClustalW alignment tool implemented in the MEGA 7 version 11.0 (Kumar et al. 2016). The final 18S and 28S rDNA datasets for phylogenetic study included sequences from the present study and available sequences of members of the Dorylaimidae retrieved from GenBank. The prepared multiple alignments of 28S rDNA generated by the ClustalW algorithm were routinely manually edited in order to eliminate improper phylogenetic signals. Representative *Mononchus* sequences were used as the outgroup. The phylogenies were constructed with the MEGA 7 version 11.0. Maximum likelihood with K2+G+I substitution model for 28S; T92+G+I substitution model for 18S data set was used. Genetic distances (number of nucleotide positions and uncorrected p-distance) were calculated in MEGA7.

Taxon treatment

***Labronema porosum* sp. nov.**
https://zoobank.org/8C545ECD-4517-47DB-BD84-43D2A9F1DD28

Labronema glandosum sensu Vu and Nguyen (2013).

Material examined. Five females from the Natural Reserve Du Gia (Bac Me District, Ha Giang Province) in good condition.

Description. Females (for measurements see Table 1, Figs 1–3) Nematodes of a medium size. Body cylindrical, slightly ventrally curved after fixation. Cuticle three layered, especially obvious at caudal region, outer layer thin, intermediate – much thicker than the outer one, particularly at the caudal region; inner layer much thinner than the intermediate layer, especially distinct at the caudal region; cuticle 4–7 µm thick at anterior region, 5–7 µm at mid-body, and 7–9 µm posterior to anus. The intermediate layer with longitudinal striations seen at a certain optical section. Ventral and lateral pores conspicuous, present along the whole body, between fifth and sixth ventral pore a rudimentary duct was observed (at 95–112 µm from anterior end); dorsal pores 5–7 at anterior end. Lip region truncated, laterally weakly angular, offset by an appreciable constriction, 2.8–3.1 times wider than high, less than one-third (23–28%) of body diameter at pharynx base. Lips separated, outer labial and cephalic papillae very low, inner labial papillae slightly protruding. Amphid with stirrup-shaped fovea; its aperture 9–10.5 µm wide, occupying two-fifths to almost one-half (39–47%) of lip region diameter. Cheilostom nearly cylindrical, with thick walls. A peculiar

Table 1. Measurements of females of *Labronema porosum* sp. nov. and females and males of *Labronema bidoupense* sp. nov. from Vietnam. All measurements are in µm (except L in mm), and in the form mean ± standard deviation with range.

Character	*L. porosum* sp. nov.		*L. bidoupense* sp. nov.		
Type	**holotype**	**paratypes**	**holotype**	**paratypes**	
Number of specimens	♀	4 ♀♀	♀	5 ♀♀	6 ♂♂
L	1.94	1.95 ± 0.1 (1.92–2.02)	1.59	1.90 ± 0.1 (1.77–2.04)	1.72 ± 0.2 (1.41–1.96)
a	22.5	19.7 ± 2.1 (18.2–21.1)	23.4	22.4 ± 1.0 (20.9–23.3)	22.6 ± 2.2 (19.7–25)
b	3.8	4.0 ± 0.1 (3.9–4.0)	3.6	4.0 ± 0.1 (3.8–4.1)	4.1 ± 0.3 (3.6–4.5)
c	75.4	73.5 ± 5.9 (69.3–77.6)	58.9	69.2 ± 8.2 (57.8–77.2)	62.9 ± 3.1 (58.8–67.8)
c’	0.6	0.5 ± 0.1 (0.5–0.6)	0.6	0.6 ± 0.1 (0.5–0.6)	0.5 ± 0.03 (0.5–0.6)
V%	53	50.9 ± 1.6 (48.5–52)	57	55. 6 ± 1.2 (54–57)	–
Lip region diameter	24	23.4 ± 0.8 (22–24)	26	26.3 ± 0.9 (25–28)	23.9 ± 1.0 (23–26)
Odontostyle length	37	35.9 ± 0.9 (35–37)	39	38.3 ± 0.7 (37.5–39)	34.5 ± 1.0 (33–36)
Odontophore length	42	42.2 ± 2.0 (40–44)	42	43; 43; 43	50.7 ± 1.8 (48–53.5)
Guiding ring	21	20.7 ± 0.4 (20–21)	22	22.5 ± 0.4 (22–23)	20.1 ± 1.3 (18–21)
Neck length	510.5	491.1 ± 8.4 (484–500)	443	470.9 ± 11.9 (458–487)	422.9 ± 22.8 (388.5–450)
Body diameter at:					
- Pharynx base	85	93.7 ± 10.2 (82.5–103)	68	78.3 ± 2.4 (76–81)	71.7 ± 7.5 (57–77)
- Mid - body	86	101.5 ± 8.3 (91–111)	68	84.9 ± 3.5 (80.5–90)	76.7 ± 10.9 (59–89.5)
- Anus/cloacal aperture	45	51.4 ± 4.9 (48–55)	43	50.3 ± 2.4 (47–53)	50.9 ± 3.6 (45–55)
Distance vulva to anterior end	1030	992.8 ± 14.6 (979–1011)	912	1056.8 ± 63.7 (956–1124)	–
Prerectum length	92	87.3 ± 6.7 (82.5–92)	93	98.3 ± 14.4 (89–123)	–
Rectum length	52	51.8 ± 6.6 (47–56)	43	52.7 ± 3.1 (49.5–58)	–
Tail length	26	26.9 ± 1.2 (26–28)	27	28.3 ± 2.5 (26–31)	27.4 ± 3.0 (22–31)
Spicule length	–	–	–		77.4 ± 5.3 (68–83)
Ventromedian supplements	–	–	–		13–15

cuticular fold present on the dorsal site of stoma, its posterior end reaching the guide ring. Odontostyle strong, 5–6 times as long as broad, 1.4–1.6 times longer than lip region diameter, and 1.7–1.9% of total body length. Odontophore rod-like; 1.1–1.2 times odontostyle length. Pharynx conspicuously muscular, with its slender portion enlarging very gradually, the basal expansion 220–237 µm

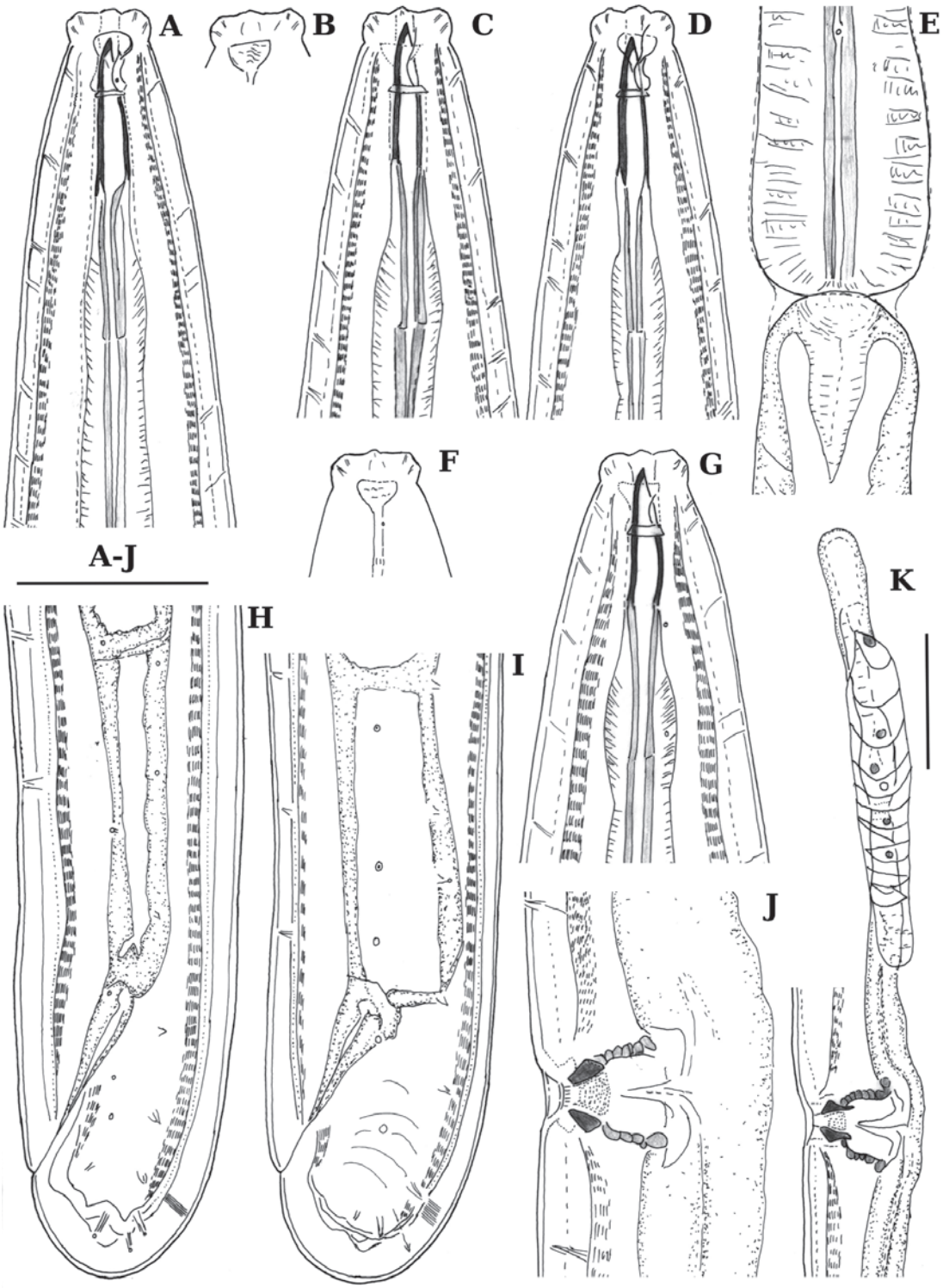

Figure 1. Line drawings of *Labronema porosum* sp. nov. female **A, C, D, G** lip region (C holotype) **B, F** amphids (B holotype) **E** pharyngo-intestinal junction (holotype) **H, I** tail ends (H holotype) **J** vulval region **K** anterior genital branch (holotype). Scale bars: 25 µm (**A–J**); 50 µm (**K**).

long, 45–47% of pharynx length; dorsal nucleus (DN) at 56–60% of pharyngeal length (*n* = 3). Pharyngo-intestinal junction well developed; cardia with conical projection into the intestinal lumen, measuring 46–59 × 20–25 µm. Prerectum 1.9–2.0 and rectum 1–1.2 times longer than anal body diameter. Genital system di-ovarian, with both branches well and equally developed. Ovaries large,

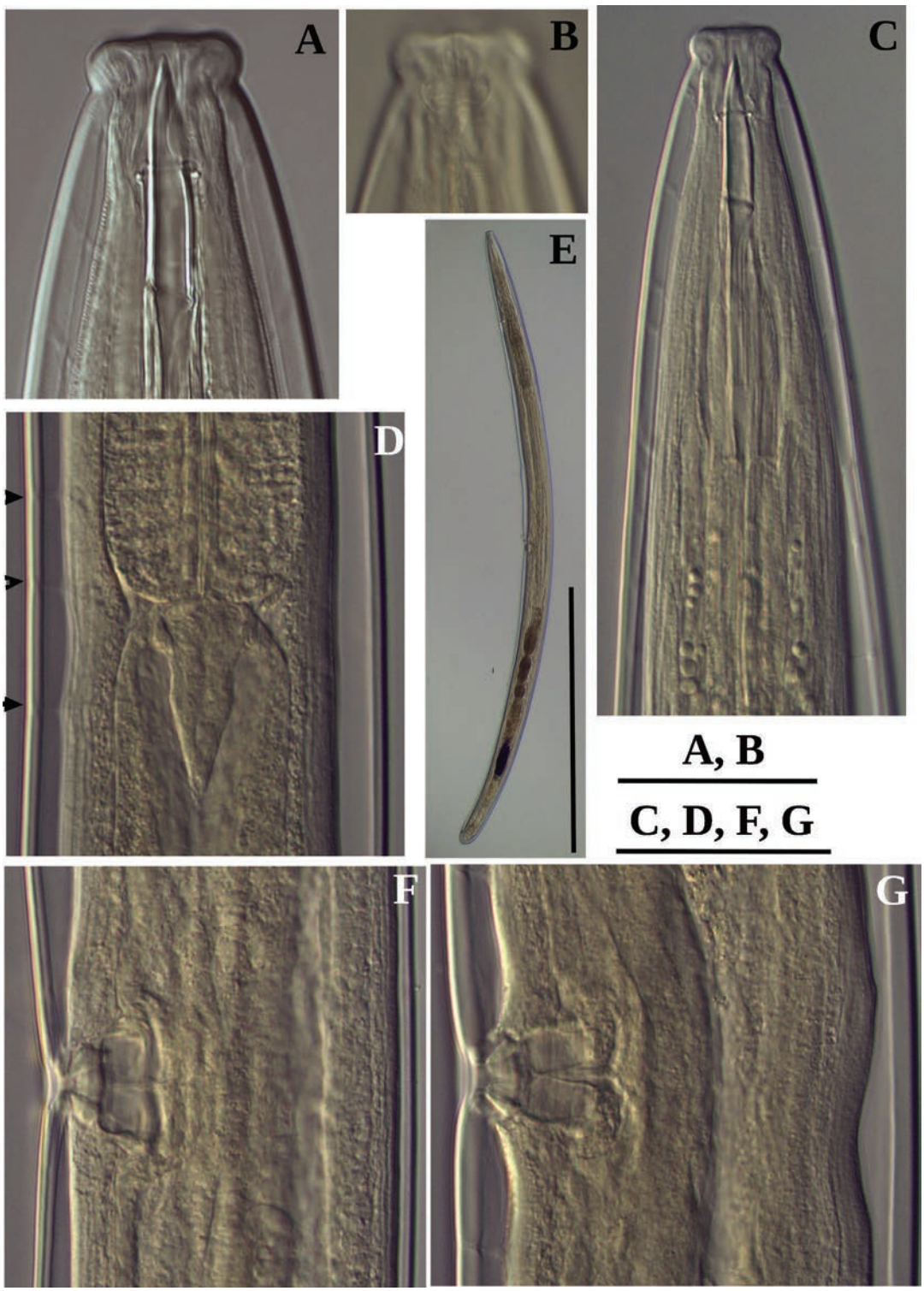

Figure 2. Photomicrographs of *Labronema porosum* sp. nov. females **A** lip region **B** amphidial fovea **C** anterior end **D** pharyngo-intestinal junction, arrows indicate dorsal pores **E** entire body **F, G** vulval region. Scale bars: 30 µm (**A, B**); 50 µm (**C, D, F, G**); 500 µm (**E**).

reaching oviduct/uterus junction, with oocytes first in two or more rows and then in a single row, anterior 161–229 µm and posterior ovary 170–249 µm long, respectively. Anterior oviduct 97–180 µm long and posterior 70–120 µm long (*n* = 3), respectively or 1.0–2.1 and 0.7–1.4 times longer than body diameter, *pars dilatata oviductus* weakly developed, sphincter at oviduct/uterus

junction 7–8 µm long, not cuticularised. Uteri not differentiated, tubular, sperm not present in them, anterior uterus 114–125 µm long, posterior uterus 95–100 µm long or slightly longer than the body diameter. Uterine egg observed in one female (107 × 53 µm). Vagina extending inwards to 37–45% of the body diameter: *pars proximalis vaginae* measuring 20–24 × 17–20 µm, surrounded by weakly developed musculature, *pars refringens* consisting of two small triangular sclerotized pieces (lateral view), with a combined width of 17–20 µm; *pars distalis* 7.5–9.0 µm long. Vulva a longitudinal slit, 8–10 µm long. Tail short, rounded. Hyaline part of tail 11–17 µm thick or 40–65% of total tail length.

Male. Unknown.

Remarks. This species is very close to the Vietnamese populations identified as *L. glandosum* and described by Vu and Nguyen (2013). It differs only in a slightly wider lip region (22–24 vs 21–22 µm) and somewhat longer odontostyle (35–37 vs 29–35 µm). The odontostyle of the specimens of Cuc Phuong population were measured again and an error was detected in the length of the shortest odontostyle, thus the range of odontostyle length becoming 32–35 µm. The Vietnamese specimens differ from these of the type population of *L. glandosum* by having a longer body (L = 1.6–2.25 vs 1.41–1.58 mm), odontophore (40–50 vs 38–39 µm), pharynx length (437–513 vs 407–420 µm) and tail (25–30 vs 21–24 µm). Besides, the lateral chord is without vs with gland-like structures in *L. glandosum*. Since there are no significant differences based on morphology between the new species and the previously reported Vietnamese populations of *L. glandosum* (Vu and Nguyen 2013), these two populations are considered conspecific.

Type locality and habitat. A pristine mountain area in the Natural Reserve Du Gia, Bac Me District, Ha Giang Province, Vietnam (22°43'5"N, 105°12'4"E, elevation 750 m a.s.l.)

Type material. The holotype female and four paratype females are deposited in the Nematode Collection of the Institute of Biodiversity and Ecosystem Research, Bulgarian Academy of Sciences, Bulgaria, under an accession number IBER-BAS NTC 110.

Representative DNA sequences. After sequencing the obtained *L. porosum* sp. nov. rDNA sequence fragments were deposited in GenBank under the following accession numbers: PP084891 (18s rDNA) originating from NR Bac Me, Ha Giang, Vietnam, and PP060468 (NR Bac Me, Ha Giang, Vietnam), PP060470 (NP Cuc Phuong, Ninh Binh, Vietnam) (28S rDNA).

Etymology. The species name reflects conspicuous ventral and lateral body pores characteristic of the species.

Differential diagnosis and relationships. The new species is characterised by its medium-sized body (1.6–2.25 mm), and odontostyle (32–37 µm), weakly angular and offset by a constriction lip region, 21–24 µm wide, presence of a peculiar cuticular fold on the dorsal side of stoma, not differentiated uterus, a longitudinal vulva (V = 48.5–59%), and short and rounded tail (25–30 µm, c = 53–90, c' = 0.5–0.6). In having medium body size (L = 1.5–2. 5 mm) and odontostyle (32–39 µm), and lip region offset by a constriction, the new species resembles *L. andrassyi* Gagarin, 1992, *L. brevicauda* Furstenberg, Heyns & Swart, 1993, *L. gerlachi* Andrássy, 2011, *L. glandosum*, and *L. obesum* Thorne, 1974. The new species can be differentiated from all of them by having a peculiar cuticular fold on the dorsal part of the stoma. Further, it differs from:

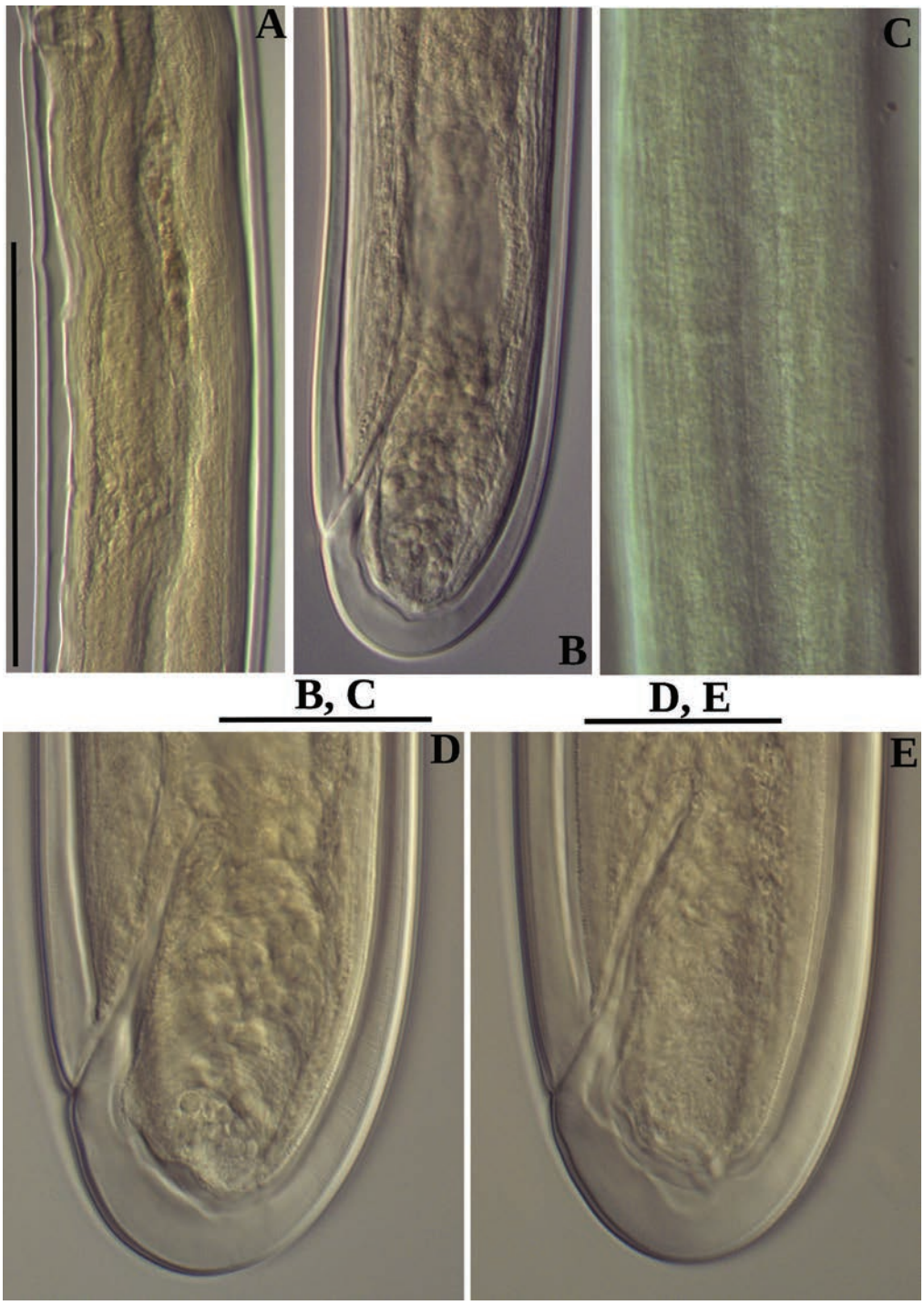

Figure 3. Photomicrographs of *Labronema porosum* sp. nov. females **A** posterior uterus **B, D, E** tail ends **C** lateral field. Scale bars: 200 µm (**A**); 50 µm (**B, C**); 30 µm (**D, E**).

L. andrassyi by having: a somewhat shorter body length (1.6–2.25 vs 2.1–2.7 mm), narrower lip region (21–24 vs 36–38 µm), shorter prerectum and tail (1.6–2.1 vs 3.5–5.4 times longer than anal body diameter, 25–30 vs 35–45 µm respectively) (Gagarin 1992);

L. brevicauda by having different shape of amphidial fovea (stirrup vs funnel shape), less robust odontostyle (5–6 vs 4 times as long as broad), absence of disc-shaped structure between pharynx and cardia vs present, smaller vulva (8–10 vs 13 or 14 µm long) stippled area large vs small (Furstenberg et al. 1993);

L. gerlachi by having: a somewhat wider lip region (21–24 vs 21–22 µm), more posterior vulva position (48.5–59 vs 45–48%), rectum straight vs angular, a longer prerectum (1.6–2.1 vs 1.3–1.4 anal body widths) and shorter tail (25–30 vs 30–35 µm, c = 53–90 vs 51–53) (Andrássy 2011b);

L. glandosum by having: a longer body (1.6–2.25 vs 1.41–1.58 mm), absence of a disc-shaped structure between pharynx and cardia vs present, lateral chord ornamentation (without vs with gland-like structures), wider lip region (21–24 vs 20–21 µm), somewhat longer odontostyle (32–37 vs 32–35 µm) and tail (25–30 vs 21–24 µm) (Rahman et al. 1986);

L. obesum by having: weakly vs strongly angular lip region, absence of a disc-shaped structure between pharynx and cardia vs present, tail longer (25–30 vs 37 µm, calculated from the drawing), and without vs with distinctive central core (Thorne 1974).

***Labronema bidoupense* sp. nov.**

https://zoobank.org/60E81CEC-448C-4A08-85BC-A217685F030B

Material examined. Six females, 6 males collected from National Park Bidoup-Nui Ba (Lac Duong District, Lam Dong Province) in good condition.

Description. Females (for measurements see Table 1, Figs 4–10) Nematodes of a medium size. Body cylindrical, slightly curved ventrally or adopted an open C shape after fixation. Cuticle three layered, especially obvious at caudal region, outer layer thin, intermediate layer much thicker than the outer one, particularly at the caudal region; inner layer much thinner than the intermediate layer; cuticle 7–8 µm thick at anterior region, 6–7 µm in mid-body, and 12–14 µm posterior to anus. The intermediate layer with longitudinal striations seen at a certain optical section. A narrow cervical lacuna between cuticle and epidermis observed. Ventral and lateral pores conspicuous, located all over the body, dorsal pores four or five at anterior end. After fifth or sixth ventral pore a structure resembling an excretory pore (duct with cuticularised walls) present (at 98–107 µm from anterior end). Lip region truncated, laterally somewhat angular, offset by a deep constriction, 3.2–3.6 times broader than high, less than one-third (33–38%) of body diameter at pharynx base. Lips weakly separated, labial and cephalic papillae very low, liplets around labial opening present (Fig. 9B). Amphid with stirrup-shaped fovea; its aperture 11 µm wide, occupying two-fifths to one-half of lip region diameter. Cheilostom nearly cylindrical, with thick walls. Odontostyle strong and slightly sigmoid, 6–7 times as long as broad, 1.4–1.5 times longer than lip region diameter, and 1.9–2.4% of total body length. Odontophore rod-like; 1.1 times odontostyle length. Pharynx strongly muscular, with its slender portion enlarging gradually, basal expansion 203–222 µm long, 43–46% of pharynx length; gland nuclei and their orifices located as follows: DO = 52%, DN = 57%, S_2N = 93% (*n* = 1). Pharyngo-intestinal junction well developed; cardia with long conical projection into the intestinal lumen measuring 50–65 × 17–24 µm; presence of a thin and irregular disc- or belt-like structure separating the pharyngeal base from the cardia. Genital system di-ovarian, with both branches well and equally developed. Ovaries are reflexed, anterior 204–261 µm long, posterior 208–262 µm long, reaching oviduct/uterus junction, with oocytes first in two or more rows and then in a single row. Anterior oviduct 92.5–149 µm

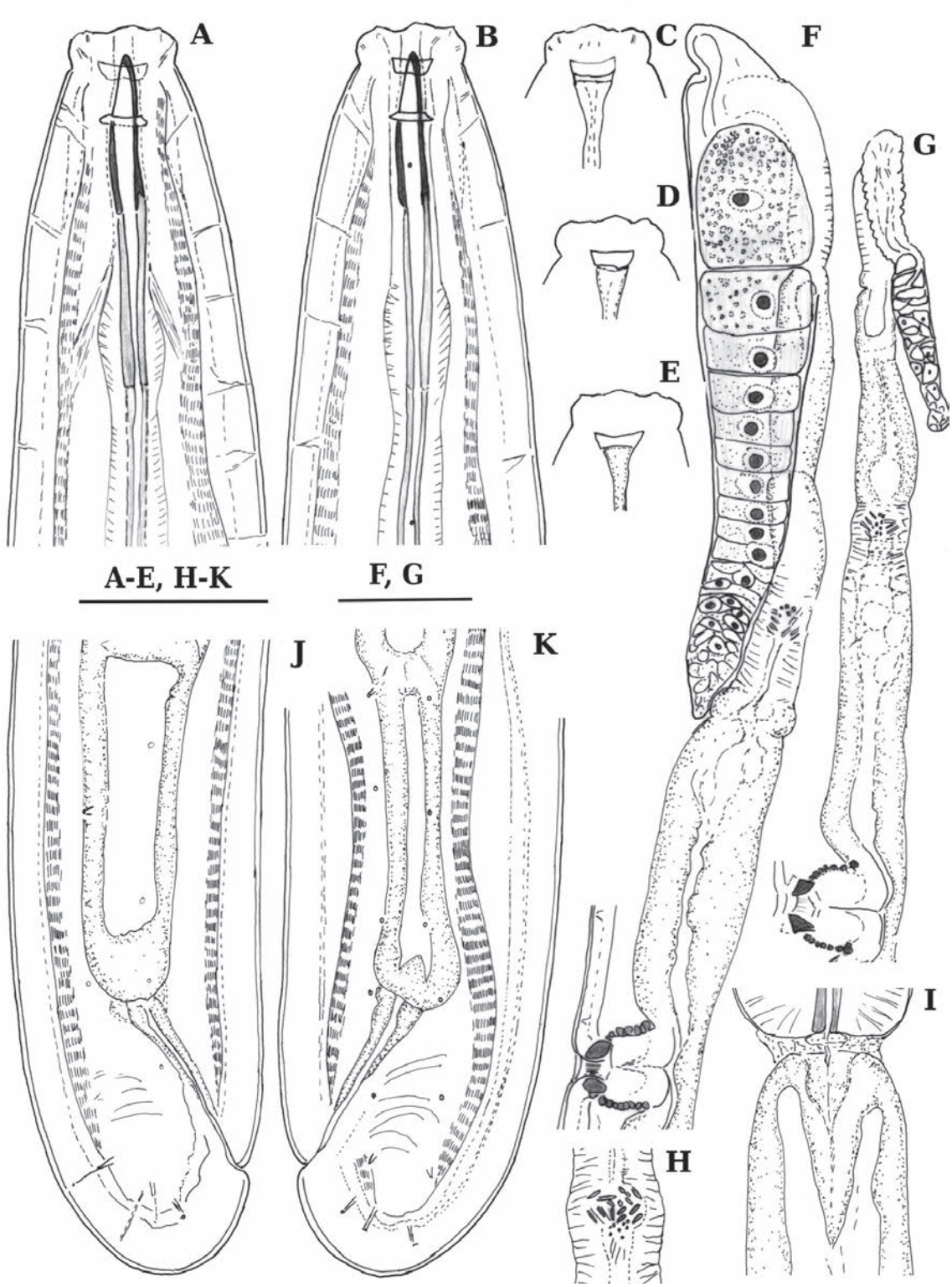

Figure 4. Line drawings of *Labronema bidoupense* sp. nov. female **A, B** lip region (**B** holotype) **C–E** amphids (D holotype) **F, G** anterior genital branch **H** uterine Z-differentiation (holotype) **I** pharyngo-intestinal junction (holotype) **J, K** tail ends (**J** holotype). Scale bars: 25 µm (**A–E, H–K**); 50 µm (**F, G**).

long and posterior oviduct 126–154 µm long, respectively, or 1.35–1.84× longer than body diameter, consisting of a moderately developed proximal *pars dilatata*. *Pars dilatata* elongated and measuring 56–80 × 17–21 µm (27–33 × 16 µm in one young female), often containing round spermatozoa. Uterus com-

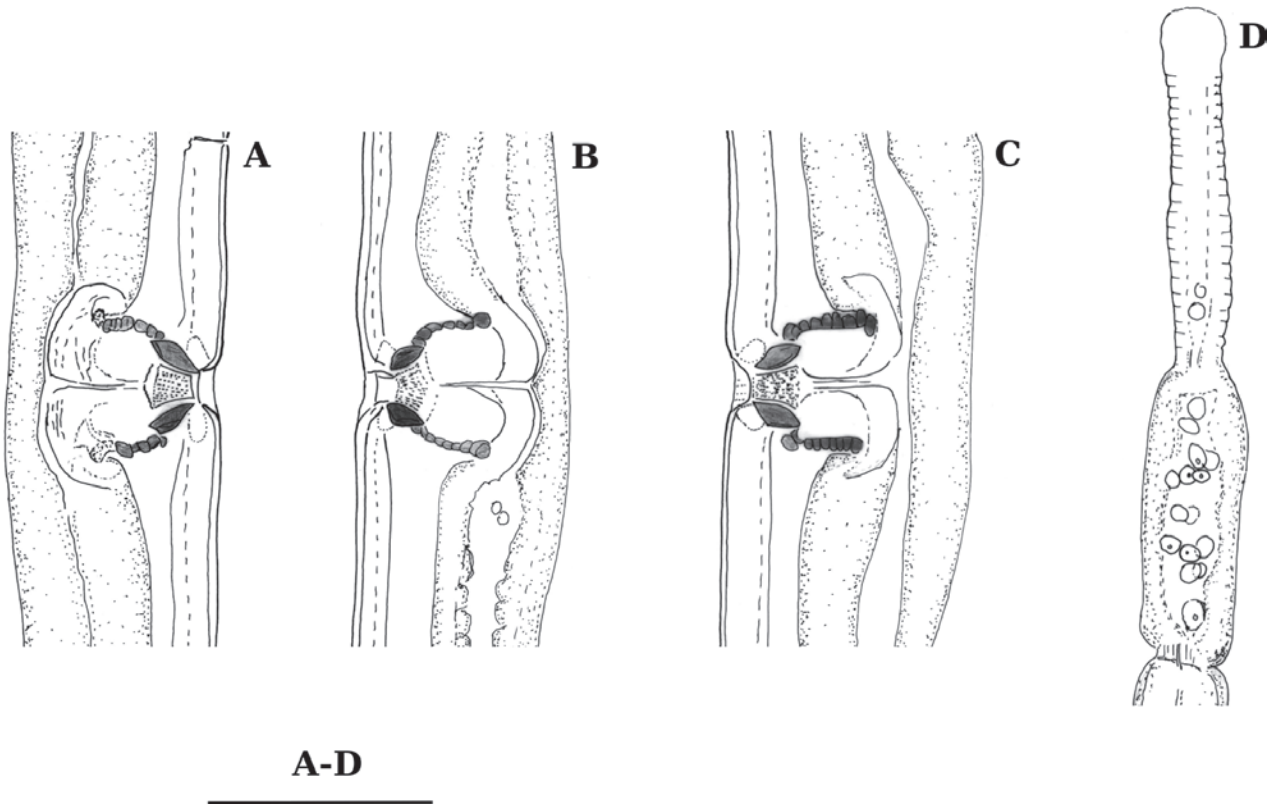

Figure 5. Line drawings of *Labronema bidoupense* sp. nov. female **A–C** vulval regions **D** anterior pars dilatata oviductus Scale bar: 25 µm.

plex, tripartite, anterior uterus 195–244 µm long, posterior uterus 193–241 µm long or 2.4–2.8 times longer than the body diameter; consisting of a thicker proximal region with lumen, a muscularised region (*pars musculosa uteri*) with Z-differentiation (Fig. 4F–H), ending with a tubular part. In the young female, the measurements are as follows: anterior ovary, oviduct, and uterus 106, 65, and 190 µm long, respectively, and posterior ovary, oviduct, and uterus 102, 65, and 217 µm long, respectively. Vagina extending inwards to 44% of the body diameter: *pars proximalis* 22–29 × 19–26 µm in size, *pars refringens* consisting of (lateral view) two small triangular sclerotized pieces, with a combined width of 18–22 µm; *pars distalis* 9 µm long. Vulva a longitudinal slit 7–9 µm long. Prerectum 1.7–2.4 and rectum 1–1.2 times longer than anal body diameter. Tail short and rounded, three pairs of caudal pores at the posterior half of the tail. Hyaline part of tail 12–14 µm thick or 42–53% of total tail length.

Males. General morphology similar to that of the female, except for the genital system. After the fourth or fifth ventral pore a structure resembling an excretory pore (duct with cuticularised walls) present (at 96–105 µm from anterior end). Genital system di-orchic, composed of two opposed testes, anterior 207–234 µm and posterior 191–225 µm long. Sperm oval, measuring 5 µm. Ventromedian supplements contiguous 13–15 in number, ad-cloacal pair located at 9–13 µm from cloacal aperture. Spicules 1.4–1.8 times body diameter at cloacal aperture long, 5–6 times as long as wide, spicule head 0.8–1.4 times longer than wide, occupying 9–11% of total spicule length, and with slender walls, median piece narrow, occupying 29–36% of spicule maximum width, and reaching the posterior end, which is 5–6 µm broad, curvature 140–150°, ventral

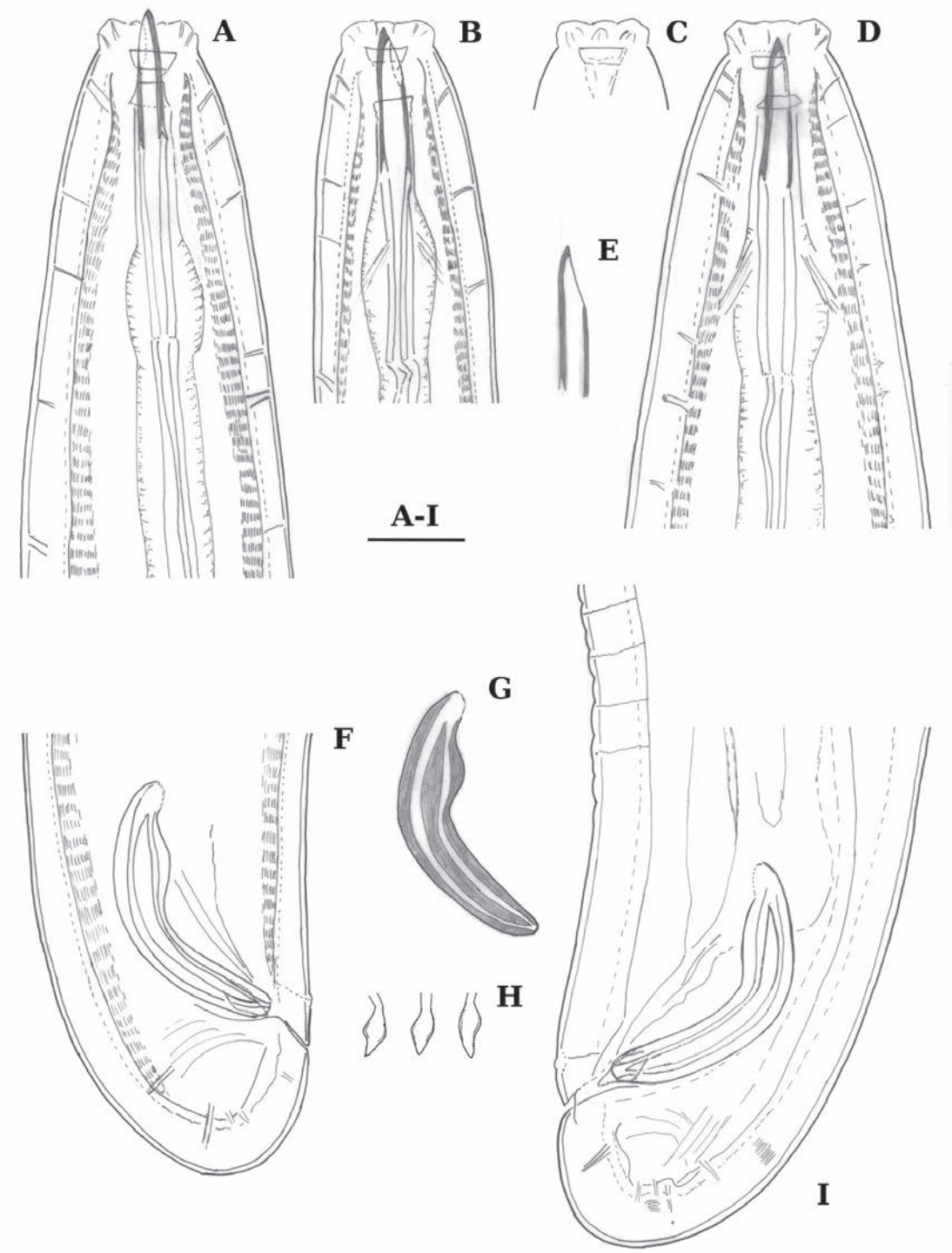

Figure 6. Line drawings of *Labronema bidoupense* sp. nov. male **A, B, D** lip region **C** amphidial fovea **E** odontostyle **F, I** tail ends **G** spicules **H** lateral guiding pieces. Scale bar**:** 25 µm.

hump located at 20–23 µm or 23.5–30% of spicule length from its anterior end, posterior tip 4.5–6 µm wide. Lateral guiding piece slightly curved, leaf-shaped (Fig. 6H), 17–19 µm long and 6 µm wide, ca 3 times longer than broad. Tail similar to that of female.

Type locality and habitat. A pristine forest in the Bidoup mountain, Lac Duong District, Lam Dong Province, Vietnam (12°04'47"N, 108°39'29"E, elevation 2130 m a.s.l.).

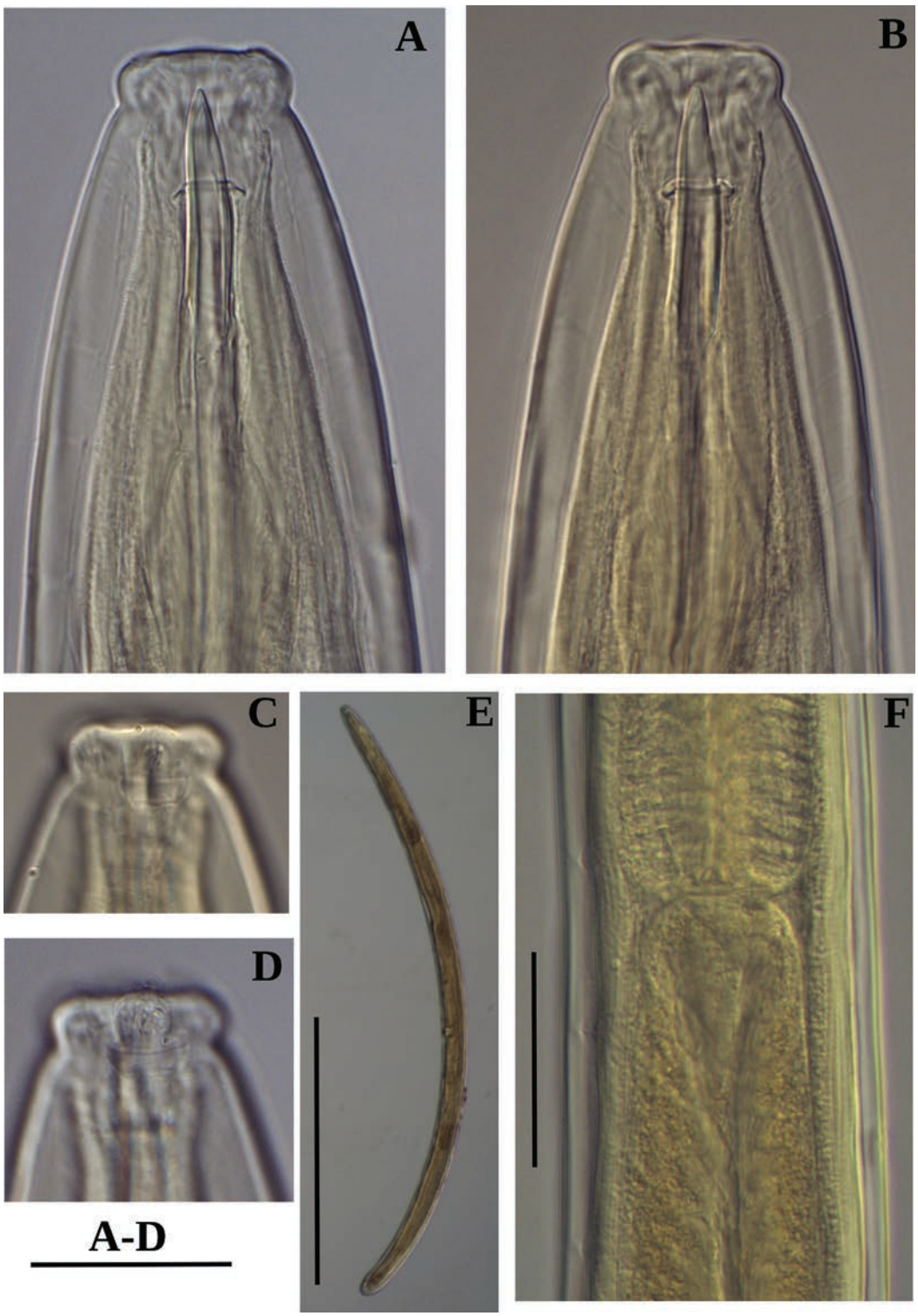

Figure 7. Photomicrographs of *Labronema bidoupense* sp. nov. female **A, B** lip region **C, D** amphidial fovea **E** entire body **F** pharyngo-intestinal junction Scale bars: 30 µm (**A–D**); 50 µm (**F**); 500 µm (**E**).

Type material. The holotype female, three paratype females, and two paratype males are deposited in the Nematode Collection of the Institute of Biodiversity and Ecosystem Research, Bulgarian Academy of Sciences, Bulgaria, under the accession numbers IBER-BAS NTC 111, 112, respectively. One paratype female and four paratype males are deposited in the Nematode collection of the Institute of Ecology and Biological Resources, Hanoi, Vietnam (accession

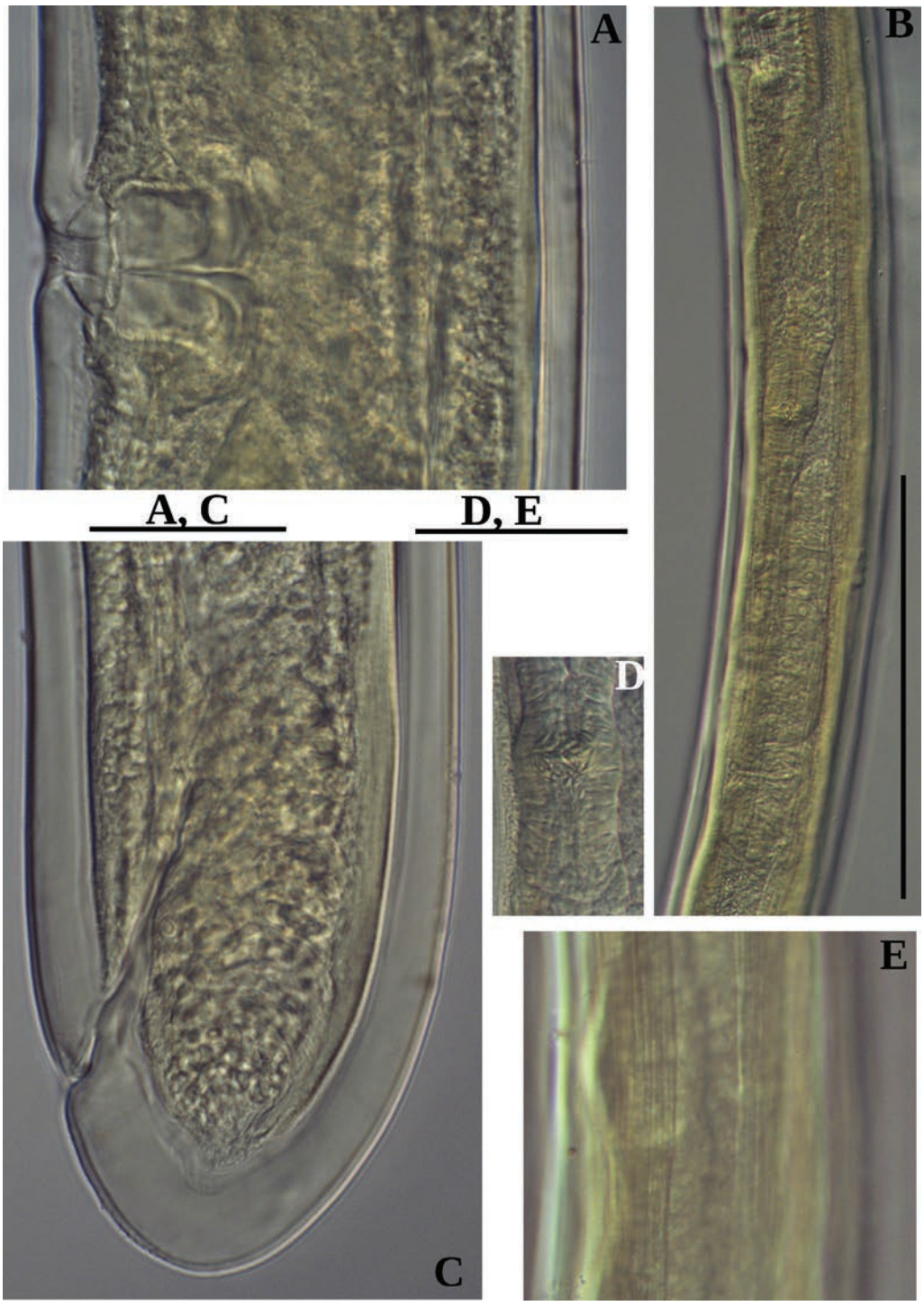

Figure 8. Photomicrographs of *Labronema bidoupense* sp. nov. female **A** vulval region **B** posterior genital branch **C** tail end **D** uterine Z-differentiation **E** lateral field. Scale bars: 30 µm (**A, C**); 200 µm (**B**); 50 µm (**D, E**).

number IEBR-FLN-DOR_04 and 05–08, respectively), one paratype female is deposited in the Wageningen Nematode Collection (**WANECO**), Wageningen, the Netherlands (WANECO accession number WT 4040), and one paratype female is deposited in the Nematode Collection of the U.S. Department of Agriculture (**USDA**), Beltsville, Maryland, USA (USDANC accession number T-8110p).

Representative DNA sequences. After sequencing the obtained *L. bidoupense* sp. nov. rDNA sequence fragments were deposited in GenBank

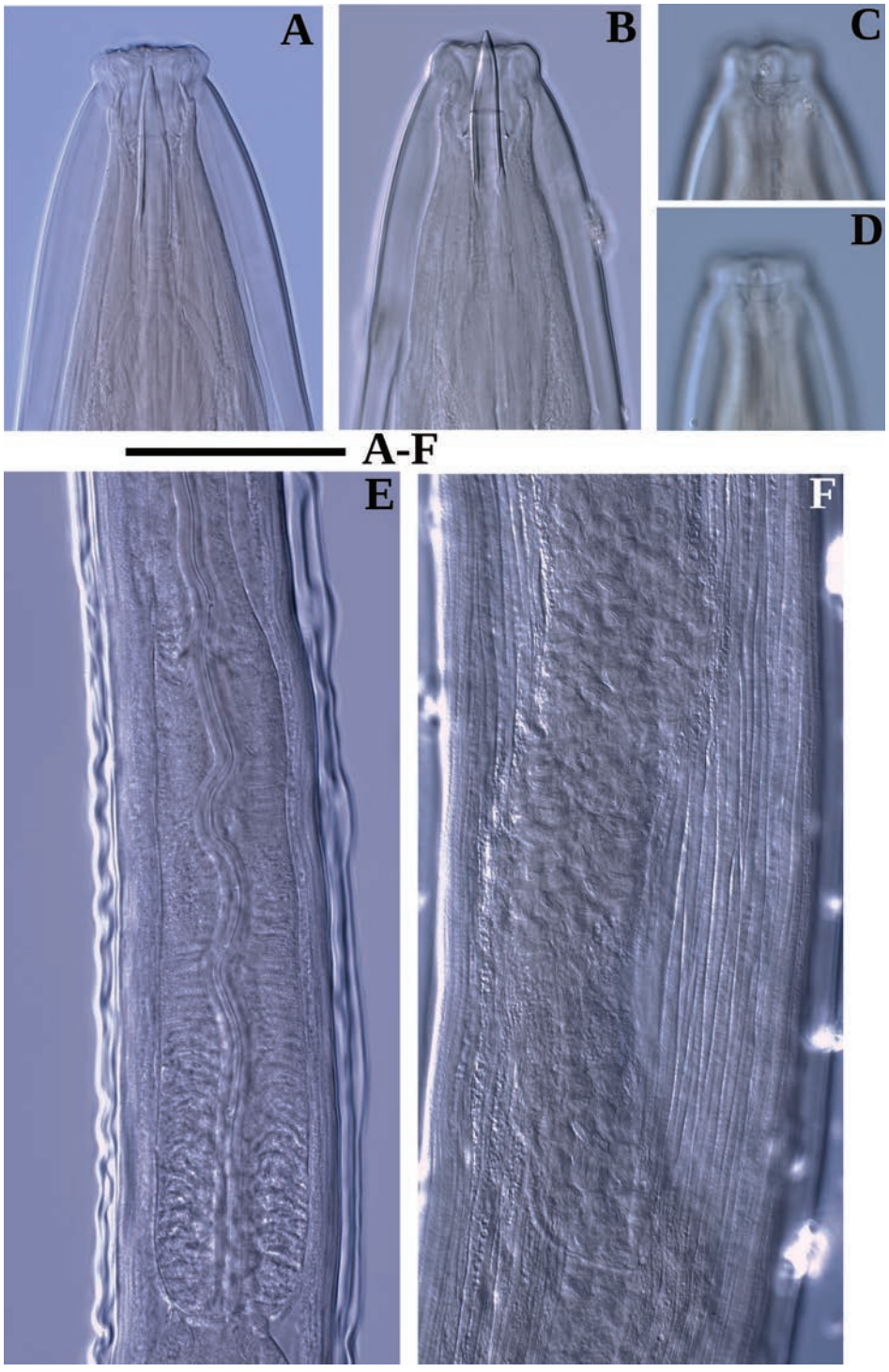

Figure 9. Photomicrographs of *Labronema bidoupense* sp. nov. male **A, B** lip region **C, D** amphidial fovea **E** pharyngeal expansion **F** sperm cells in testis. Scale bar: 50 µm.

under the following accession numbers PP084892 (18S rDNA) and PP060469 (28S rDNA), both originating from a specimen collected in NP Bidoup-NuiBa, Dak Lak, Vietnam.

Etymology. The species is named after the Bidoup Mountain, the place from where it was recovered.

Differential diagnosis and relationships. The new species is characterised by its medium-sizes body (1.59–2.04 mm long), lip region offset by a deep

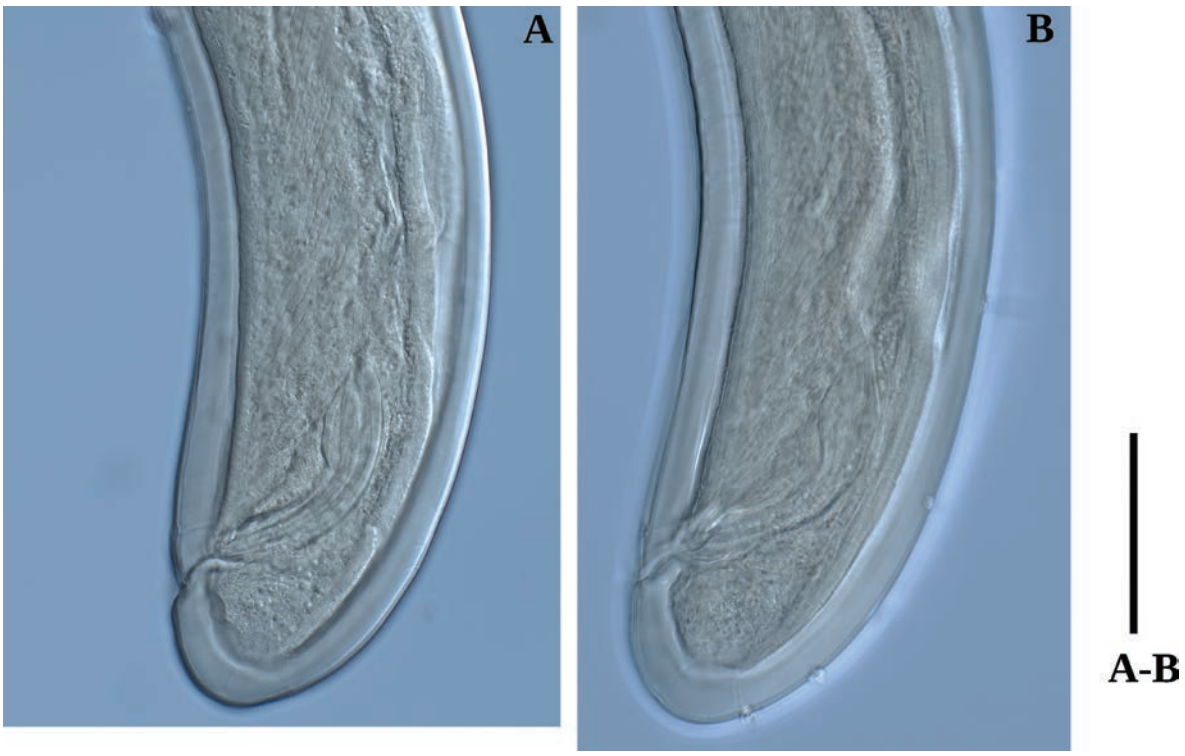

Figure 10. Photomicrographs of *Labronema bidoupense* sp. nov. male **A, B** tail ends. Scale bar: 50 µm.

constriction and 25–28 µm wide, odontostyle 37.5–39 µm long, uterus complex (tripartite), longitudinal vulva (V = 54–57%), short and rounded tail (26–31 µm, c = 57.8–77.2, c' = 0.5–0.6). Males with 68–83 µm long spicules, 5–6 times as long as wide and contiguous ventromedian supplements 13–15 in number, lateral piece leaf-shaped.

In having medium body size (L = 1.5–2.5 mm) and odontostyle (31–39 µm), and lip region offset by a constriction, the new species resembles *L. andrassyi*, *L. brevicauda*, *L. gerlachi*, *L. glandosum*, *L. obesum* and *L. porosum* sp. nov. The new species differs from:

L. porosum sp. nov. by having: a thicker body cuticle, wider lip region (25–28 vs 21–24 µm), slightly sigmoid vs straight odontostyle, longer odontostyle (37.5–39 vs 32–37 µm), a peculiar cuticular fold on the dorsal site of stoma absent vs present, shorter pharyngeal expansion (203–222 vs 220–237 µm), presence of disc-shaped structure between pharynx and cardia vs absence, complex vs simple uterus, males present vs absent;

L. andrassyi by having: a shorter body length (1.59–2.04 vs 2.1–2.7 mm), thicker body cuticle, narrower lip region (25–28 vs 36–38 µm), longer prerectum (1.7–2.4 vs 3.5–5.4 times longer than anal body diameter) and tail (26–31 vs 35–45 µm), males present vs absent (Gagarin 1992);

L. brevicauda by having: a different number of dorsal pores at anterior end (4 or 5 vs 6 or 8), wider lip region (25–28 vs 21–25 µm), longer and less robust odontostyle (37.5–39 vs 32–35.6 µm and 6–7 vs 4 times as long as broad), complex vs simple uterus, males present vs absent (Furstenberg et al. 1993);

L. gerlachi by having: a wider lip region (25–28 vs 21–22 µm), longer odontostyle (37.5–39 vs 33–35 µm), more posterior vulva position (54–57 vs 45–48%), rectum straight vs angular, shorter tail (26–28 vs 30–35 µm), males present vs absent (Andrássy 2011b);

L. glandosum by having: a differently shaped lateral chord (without vs with gland-like structures), a wider lip region (25–28 vs 20–21 µm), longer odontostyle (37.5–39 vs 32–35 µm) and tail (26–31 vs 21–24 µm), complex vs simple uterus, males present vs absent (Rahman et al. 1986);

L. obesum by having: a shorter body length (1.59–2.04 vs 2.2 mm), longer odontostyle (37.5–39 vs 33 µm), tail without vs with distinctive central core, males present vs absent (Thorne 1974).

Sequences and phylogenetic analyses

Molecular sequences of two specimens of *L. porosum* sp. nov. and one specimen of *L. bidoupense* sp. nov. were analysed in this study. After sequencing and editing, five sequences were obtained: a nearly full-length of 18S rRNA gene for *L. porosum* sp. nov., (1641 bp; PP084891) and *L. bidoupense* sp. nov., (1636 bp; GenBank: PP084892); two nearly full-length D2-D3 segment of 28S rRNA gene for *L. porosum* sp. nov., (828 bp; GenBank: PP060468, PP060470) and for *L. bidoupense* sp. nov. (856 bp; GenBank: PP060469). A BLAST search for matches to the partial 18S rDNA sequences revealed that *L. porosum* sp. nov. has a difference of 34 nt with *L. ferox* (AY552972), 24–40 nt with *L. vulvapapillatum* (AY284807 from The Netherlands, KC574385 from Iran), 32 nt with *L. montanum* (MK894247–MK894248) and 23 nt with the new species *L. bidoupense* sp. nov. The new species *L. bidoupense* sp. nov. has a difference of 34 nt with *L. ferox* (AY552972), 22–69 nt with *L. vulvapapillatum* (AY284807 from The Netherlands, KC574385 from Iran) and 36 nt with *L. montanum* (MK894247–MK894248). A BLAST search for matches the partial 28S rDNA sequences revealed that *L. porosum* sp. nov. has a difference of 76–78 nt with *L. vulvapapillatum* (AY592996–AY592997 from The Netherlands, ON685882 from Iran), 106 nt with *L. montanum* (MK894244–MK894246) and 31 nt with *L. bidoupense* sp. nov. *Labronema bidoupense* sp. nov. has 78 nt of difference with *L. vulvapapillatum* (AY592996–AY592997 from The Netherlands, ON685882 from Iran), 115 nt with *L. montanum* (MK894244–MK894246) from Spain. *Labronema porosum* sp. nov. population from Du Gia Nature Reserve, Bac Me district, Ha Giang Province (PP060468) was 100% identical with *Labronema* population from Cuc Phuong National Park, Ninh Binh Province (PP060470). The evolutionary relationships of the two new species as derived from the molecular analyses, are presented in the phylogenetic trees (Figs 11, 12). The 18S rDNA sequences of the two studied *Labronema* species from Vietnam clustered together in a group with *L. ferox* and were nested within the first clade (following Shokoohi et al. 2013), encompassing representatives of other species of *Labronema* (*L. vulvapapillatum*) and genera *Paractinolaimus* and *Pararhyssocolpus* (Fig. 11). Generally, this tree topology positioning was confirmed by the phylogenetic analyses based on the 28S rDNA data (Fig. 12). The 28S rDNA sequences of the two new species from Vietnam clustered together with *L. vulvapapillatum* from Iran (ON685882) and were positioned within a clade containing the genera belonging to the family Dorylaimidae (following the Peña-Santiago and Abolafia 2019 and Vazifeh et al. 2023) and encompassing representatives of the genera *Crassolabium*, *Nevadanema*, and *Dorylaimus*, as well as genera from other families *Talanema* (Qudsianematidae), *Pararhyssocolpus* (Pararhyssocolpidae), *Sylphodorylaimus* (Thornenematidae), and *Paractinolaimus* (Actinolaimidae). The close relationships of both Vietnamese species are

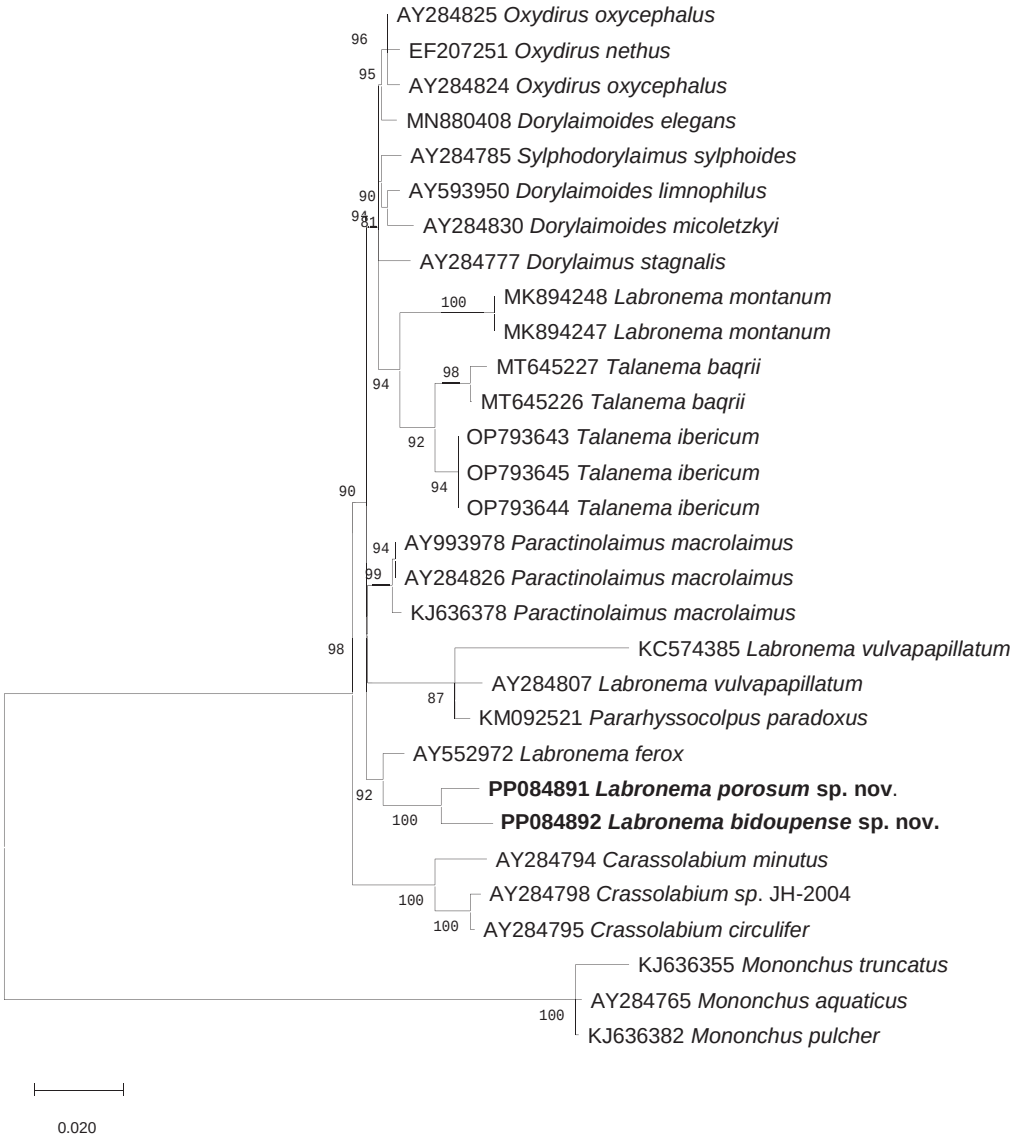

Figure 11. Phylogenetic relationships of *Labronema* from the analysis of the 18S rDNA sequences under ML (K2+G+I model). Numbers to the left of the branches are bootstrap values for 1000 replications.

also in agreement with their morphology. The main differences were described in detail in the diagnosis part, in the description of *L. bidoupense* sp. nov.

The most recent identification keys of all *Labronema* species known by that time is the key by Andrássy (1991). The same author also provided a key to the European species of the genus (Andrássy 2009). However, these keys are outdated due to the numerous taxonomic changes and several new species described during the last decades. Here we elaborated a partial key for determination of a group of species with a medium-sized odontostyle (31–39 µm) to which also belong the two new Vietnamese species. Some species are excluded from the key:

- *Labronema virgo* Monteiro 1970: this species fits the features of the genus *Labronema* (the presence of offset by constriction lip region, robust odontostyle 1.5 times lip region diameter, double guiding ring), but because of the transverse vulva non-typical for the genus, this species is not included in the key.

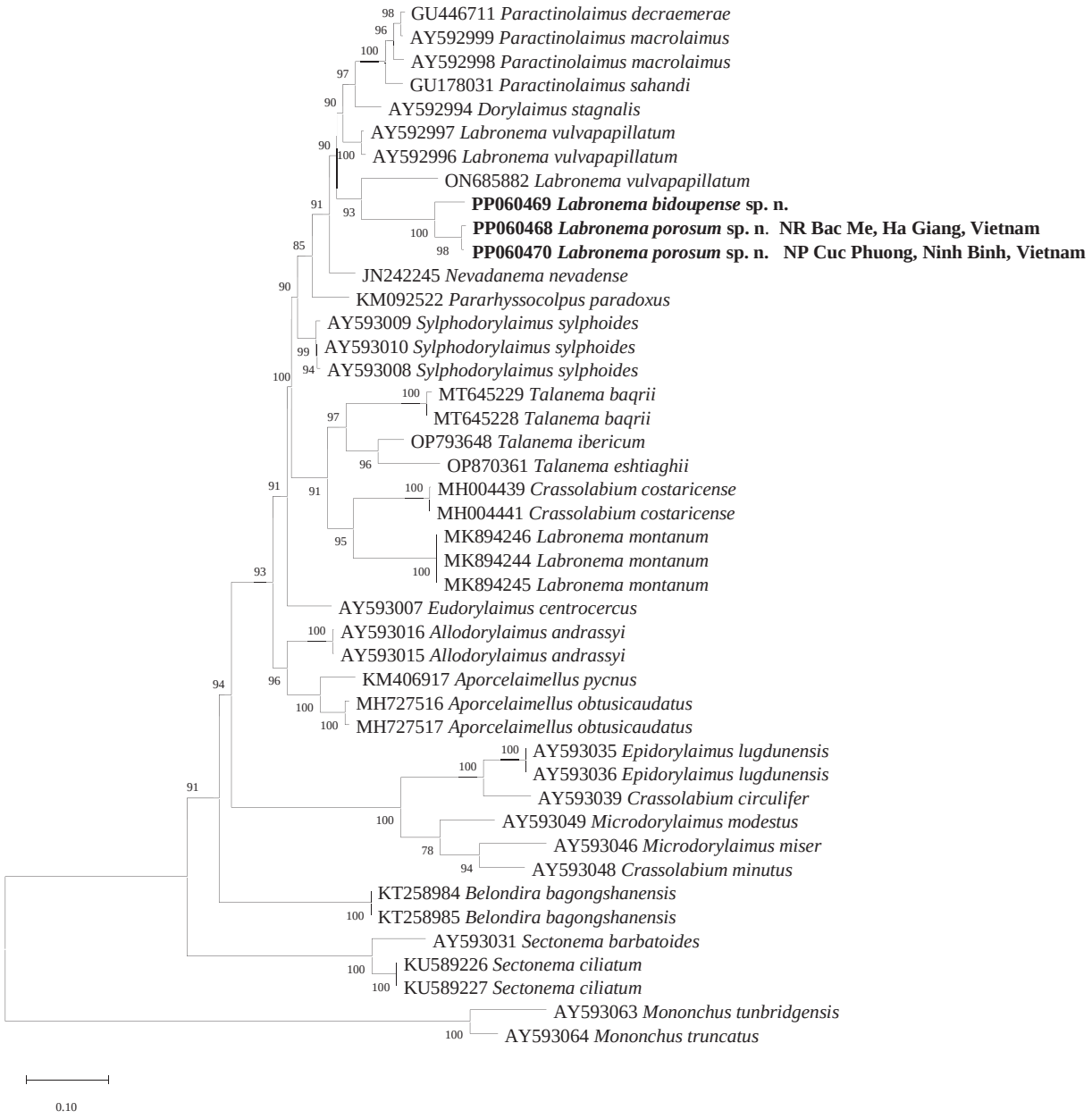

Figure 12. Phylogenetic relationships of *Labronema* from the analysis of the 28S rDNA sequences under ML (K2+G+I model). Numbers to the left of the branches are bootstrap values for 1000 replications.

- *Labronema enigmatum* Baniyamuddin & Ahmad, 2007: in the presence of a transverse vulva, spaced ventromedian supplements, and bluntly rounded tail, this species does not fit well with typical *Labronema* pattern. Andrássy (2009) transferred this species to the genus *Labronemella* Andrássy, 1985. According to Peña-Santiago et al. (2012), the identity of this species is questionable; therefore, it should be either considered a species *inquirenda* or retained under *Labronema*. Because of the problematic position of this species, it is not included in the key.
- *Labronema diversum* Andrássy, 2002: this species is characterised by sexual dimorphism in the tail region, females have a tail with a dorsally curved peg, while males have a rounded conoid tail. The sexual dimorphism is atypical for the genus *Labronema*. According to Andrássy (2011a) this pe-

culiar structure of the female tail is an atavistic character. The presence of robust odontostyle, double guiding ring, longitudinal vulva and contiguous ventromedian supplements fit with genus *Labronema* but its position is doubtful (Imran et al. 2021).

- *Labronema nemella* Mushtaq & Ahmad, 2007: according to Peña-Santiago et al. (2012) the true identity of this species is intriguing, because of the morphology of lip region and odontostyle (our remark). The authors consider that this species might be a member of *Labronemella*, but further data is needed to confirm this.
- Two of the atypical species of genus *Labronema* (characterised with lip region nearly continuous with the adjacent body) – *L. neopacificum* Rahman, Jairajpuri, Ahmad & Ahmad, 1986 and *L. pacificum* (Cobb, 1906) Thorne, 1939, which are distinguished by a medium-sized odontostyle are not included in this key because the lip region does not correspond to the typical offset lip region of members of the genus *Labronema*.

Key to the species of genus *Labronema* with medium sized odontostyle (31–39 µm)

1 Body large, 3 mm or more **2**
– Body < 3 mm **5**
2 Vulva pre-equatorial – ♀ L = 3.4–3.6 mm, a = 45.3–46.03, b = 4.7–4.8, c = 109.8–113.2, V = 47–49% **(India)** .... ***L. mannai* Dattaray, Roy, Gantait, 2015**
– Vulva equatorial **3**
3 Odontostyle nearly equal to lip region diameter, males present – ♀ L = 3.0–3.6 mm, a = 35, b = 4.1, c = 100, V = 50%, ♂ L = 3.0–3.5 mm, a = 43, b = 4.0–5.2, c = 100, ventromedian supplements 20–27 ..... ***L. ferox* Thorne, 1939 (USA)**
– Odontostyle longer than lip region diameter, males absent **4**
4 Prerectum longer, 3–4 times anal body diameter, paravulvae present anterior and posterior to vulva – ♀ L = 3.2–4.0 mm, a = 45–50, b = 4.3–5.4, c = 119–154, V = 49–56% **(India)** ..... ***L. deoriaensis* Khan, Jairajpuri & Ahmad, 1989**
– Prerectum shorter, twice as long as anal body diameter, paravulvae absent – ♀ L = 3.0–3.7 mm, a = 37–44, b = 3.8–4.9, c = 90–127, V = 51–54% **(USA)*** ..... ***L. thornei* Ferris, 1968**
5 Lip region off set by weak depression – ♀ L = 2.4–3.0 mm, a = 28–33, b = 4.3–5.0, c = 90–103, V = 44–49%, ♂ L = 2.20–2.76 mm, a = 33–38, b = 3.9–4.5, c = 74–93, ventromedian supplements 21–23 **(Ecuador).....** ***L. aequatoriale* Andrássy, 2011**
– Lip region off set by constriction **6**
6 Body length 2.3–3 mm; lip region diameter as long as odontostyle length – ♀ L = 2.1–2.8 mm, a = 19.5–28, b = 4.0–4.3, c = 54.7–73.7, V = 51–57% (**Russia)** ..... ***L. andrassyi* Gagarin, 1992***
– Body length < 2.2 mm, lip region diameter shorter than odontostyle length **7**

* In the original description, no data on vulva characterisation were presented.

7 Vulva pre-equatorial – ♀ L = 1.7–2.0 mm, a = 17–19, b = 3.7–4.0, c = 51–53, V = 45–48% **(Seychelles)** ..... ***L. gerlachi* Andrássy, 2011**
– Vulva equatorial **8**
8 Lateral chords with gland-like structures – ♀ L = 1.4–1.6 mm, a = 19–22, b = 3.4–3.7, c = 59–71, V = 53–54% **(India)**..... ..... ***L. glandosum* Rahman, Jairajpuri, Ahmad & Ahmad, 1986**
– Lateral chords without gland-like structures **9**
9 Tail with distinctive central core – ♀ L = 2.2 mm, a = 25, b = 4.1, c = 60, V = 53% **(USA)** ..... ***L. obesum* Thorne, 1974**
– Tail without central core **10**
10 Female genital system tripartite, males present – ♀ L = 1.6–2.0 mm, a = 20.9–23.4, b = 3.6–4.1, c = 57.8–77.2, V = 54–57%, ♂ L = 1.4–2.0 mm, a = 19.7–25, b = 3.6–4.5, c = 58.8–67.8, ventromedian supplements 13–15 in number **(Vietnam)** ..... ***L. bidoupense* sp. nov.**
– Female genital system simple, males absent **11**
11 The disc-like structure between the pharynx base and cardia present – ♀ L = 1.6–2.1 mm, a = 21.9–23, b = 3.7–4.0, c = 64–79, V = 50–52% **(Madagascar)** ..... ***L. brevicauda* Furstenberg, Heyns & Swart, 1993**
– The disc-like structure between the pharynx base and cardia absent – ♀ L = 1.6–2.25 mm, a = 18–25, b = 3.5–4.6, c = 53–90, V = 49–59% **(Vietnam)** ..... ***L. porosum* sp. nov.**

Discussion

The integrative taxonomy approach used in the study of *L. porosum* sp. nov. and *L. bidoupense* sp. nov. from Vietnam contributes to the knowledge of the large and complex genus *Labronema*. The two species are very close morphologically and genetically and form a well-supported clade with the type species (18S rDNA tree Fig. 11) and *L. vulvapapillatum*, Vakil Kandi population from Iran (28S rDNA tree Fig. 12). Other populations identified as *L. vulvapapillatum* from The Netherlands (AY284807) and Kerman Province, Iran (KC574385) clustered together in the 18S r DNA tree (Fig. 11) and are closely related to that clade (Fig. 11). Obviously, the populations of *L. vulvapapillatum* from The Netherlands and Kerman Province, Iran are not conspecific with that from Vakil Kandi population. This species has been reported from several countries in Europe and Asia (Shokoohi et al. 2013; Zahedi Asl. et al. 2023) and since the ranges for many characters (e.g., body, odontostyle, and tail length) are very wide (Shokoohi et al. 2013: table 5), most probably it represents a species complex (Shokoohi et al. 2013). However, it is difficult to delineate different species based on literature sources because in some descriptions data about reproductive system or illustrations of important characters are missing or it is difficult to be assessed from the photomicrographs.

In both phylogeny trees of 18S and 28S rDNA (Figs 11, 12), *L. montanum* stands independently with other species of *Labronema* (*L. ferox*, *L. vulvapapillatum* and the two new species from Vietnam) and it is closer to the species of *Talanema* and *Crassolabium costaricense* Varela-Benavides & Peña-Santiago, 2018. *Labronema montanum* is very similar to other three *Labronema* species: *L. angeloi*, *L. carussoi* (Vinciguerra an Orselli 1998) and

L. duxousi (= *L. pulchrum*) (Peña-Santiago and Vinciguerra 2019). As it was mentioned by Peña-Santiago and Abolafia (2019) that these four species represent a rather homogeneous group. They possess unique combination of several characters such as lip region shape, presence of structures resembling cardial glands, short conical cardia, and peculiar reproductive system in female – tripartite uterus with narrow often coiled intermediate part, *pars refringens vaginae* of similar appearance; and in males – the lateral piece is narrow and bifid. These four species have distinct range inhabiting the southern Europe and have been reported from France, Albania, Spain, Italy, Switzerland, and Romania (Peña-Santiago and Abolafia 2019).

The 28S rDNA sequences from the two populations of *Labronema* from Du Gia Nature Reserve (Bac Me District, Ha Giang Province) and Cuc Phuong National Park (Ninh Binh Province) confirmed that the population previously recorded as *L. glandosum* from Cuc Phuong National Park (Vu and Nguyen 2013) is identical with the new species *L. porosum* sp. nov.

It is very difficult to assess the phylogenetic relationships of the genus *Labronema* with other genera using the integrative approach due to the very low number of species studied, also affecting the reconstruction of the evolutionary history of dorylaimid groups of higher taxonomic ranks.

Additional information

Conflict of interest

The authors have declared that no competing interests exist.

Ethical statement

No ethical statement was reported.

Funding

The work is a part result of a research project NCXS01.04/23-25 funded by the Vietnam Academy of Science and Technology (VAST) and a research project "Studies on selected nematode taxa of the orders Mononchida and Dorylaimida from Vietnam and Bulgaria" funded by the Bulgarian Academy of Science (BAS), code number IC-VT/01/2023-2025. This study used facilities of the Institute of Biodiversity and Ecosystem Research – Bulgarian Academy of Sciences upgraded in the frames of the project DiSSCo-BG (Upgrade of the Research Infrastructure "Distributed System of Scientific Collections—Bulgaria") funded by the National Roadmap for Research Infrastructures, Ministry of Education and Science of the Republic of Bulgaria.

Author contributions

Conceptualization: VP. Data curation: TTTV, ME. Formal analysis: TTTV, ME, TMLL. Funding acquisition: VP. Investigation: ME, VP, TTTV. Methodology: ADN. Project administration: VP, TTTV. Resources: TTTV, ADN, TMLL. Visualization: AM, VP. Writing - original draft: ME. Writing - review and editing: AM, TTTV, ADN, VP, TMLL.

Author ORCIDs

Tam T. T. Vu https://orcid.org/0000-0003-1145-975X
Milka Elshishka https://orcid.org/0009-0002-3588-4566
Anh D. Nguyen https://orcid.org/0000-0001-9273-0040

Data availability

All of the data that support the findings of this study are available in the main text or Supplementary Information.

References

Altash S, Kostadinova A, Peneva V (2024) Integrative taxonomic study of mononchid nematodes from riparian habitats in Bulgaria. I. Genera *Mononchus* Bastian, 1865 and *Coomansus* Jairajpuri & Khan, 1977 with the description of *Mononchus pseudoaquaticus* sp. nov. and a key to the species of *Mononchus*. ZooKeys 1206: 137–180. https://doi.org/10.3897/zookeys.1206.124237

Altherr E (1963) Contribution à la connaissance de la faune des sables submergés en Lorraine. Nématodes. Annales de Spéléologie 18: 53–98.

Álvarez-Ortega S, Peña-Santiago R (2012) Nematodes of the order Dorylaimida from Andalucía Oriental, Spain. *Nevadanema nevadense* gen. n., sp. n. (Qudsianematidae) from Sierra Nevada National Park. Nematology 14(2): 249–264 https://doi.org/10.1163/138855411X589309

Álvarez-Ortega S, Peña-Santiago R (2013) Taxonomy of the genus *Aporcelaimellus* Heyns, 1965 (Nematoda, Dorylaimida, Aporcelaimidae). Zootaxa 3669(3): 243–260. https://doi.org/10.11646/zootaxa.3669.3.3

Álvarez-Ortega S, Vu TTT, Peña-Santiago R (2010, publ. 2012) Studies on four atypical species of the genus *Labronema* Thorne, 1939 (Dorylaimida, Qudsianematidae). Journal of Nematode Morphology and Systematics 13(2): 107–122. https://revistaselectronicas.ujaen.es/index.php/jnms/article/view/791

Andrássy I (1991) The superfamily Dorylaimoidea (Nematoda) – a review. Family Qudsianematidae, II. Opuscula Zoologica Budapest 24: 3–55.

Andrássy I (2009) Free-living nematodes of Hungary. III. Pedozoologica Hungarica n° 5. Hungarian Natural History Museum. Budapest, Hungary, 608 pp.

Andrássy I (2011a) Three new bisexual species of *Labronema* Thorne, 1939 (Nematoda: Qudsianematidae). Opuscula Zoologica Budapest 43: 107–120.

Andrássy I (2011b) Free living nematodes of Seychelles. In: Gerlach J (Ed.) Crustacea, Platyhelminthes, Nematoda, Annelida and Tardigrada of the Seychelles Islands. Siri Scientific Press, Manchester (160 pp), spec p. 15–57.

Elshishka M, Mladenov A, Altash S, Álvarez-Ortega S, Peña-Santiago R, Peneva V (2024) Cyber catalog and revision of the nematode genus *Enchodelus* (Nordiidae, Dorylaimida). Biodiversity Data Journal 12: e126315. https://doi.org/10.3897/BDJ.12.e126315

Floyd RM, Rogers AD, Lambshead PJD, Smith CR (2005) Nematode-specific PCR primers for the 18S small subunit rRNA gene. Molecular Ecology Notes 5(3): 611–612. https://doi.org/10.1111/j.1471-8286.2005.01009.x

Furstenberg JP, Heyns J, Swart A (1993) Four new species of *Labronema* Thorne, 1939 from islands in the Western Indian Ocean (Nematoda: Dorylaimoidea). Nematologica 39: 450–465. https://doi.org/10.1163/187529293X00394

Gagarin VG (1992) The free-living freshwater nematodes of the Soviet Union. Hidrometeoizdat, St. Petersburg, 152 pp. [In Russian]

Holterman M, van der Wurff A, van den Elsen S, van Megen H, Bongers T, Holovachov O, Bakker J, Helder J (2006) Phylum-wide analysis of SSU rDNA reveals deep phylogenetic relationships among nematodes and accelerated evolution toward crown clades. Molecular Biology and Evolution 23: 1792–1800. https://doi.org/10.1093/molbev/msl044

Imran Z, Abolafia J, Ahmad W (2021) On the identity of *Labronema baqrii* Khan, Jairajpuri & Ahmad, 1989 (Nematoda, Dorylaimida) and analysis of the relationships between the genera *Labronema* Thorne, 1939 and *Talanema* Andrássy, 1991. Zoologischer Anzeiger 291: 102–112. https://doi.org/10.1016/j.jcz.2021.02.003

Kumar S, Stecher G, Tamura K (2016) MEGA 7: Molecular Evolutionary Genetics Analysis version 7.0 for bigger datasets. Molecular Biology and Evolution 33: 1870–1874. https://doi.org/10.1093/molbev/msw054

Loof PAA, Coomans A (1970) On the development and location of the oesophageal gland nuclei in the Dorylaimina. Proceedings IX International Nematology Symposium (Warsaw 1967) Zeszyty Problemowe Postępów Nauk Rolniczych 92: 79–161.

Peña-Santiago R (2019) Taxonomy of the genus *Labronema* Thorne, 1939 (Nematoda: Dorylaimida: Dorylaimidae) with redescription of its type species, *L. ferox* Thorne, 1939. Nematology 21: 23–34. https://doi.org/10.1163/15685411-00003192

Peña-Santiago R (2021) Morphology and bionomics of dorylaims (Nematoda: Dorylaimida). Nematology Monographs & Perspectives 13: 1–6. https://doi.org/10.1163/9789004447851

Peña-Santiago R (2022) New synonyms in the genus *Labronema* Thorne, 1939 (Nematoda, Dorylaimida, Dorylaimidae). Nematology 24: 953–957. https://doi.org/10.1163/15685411-bja10175

Peña-Santiago R, Abolafia S (2019) Morphological and molecular characterization of *Labronema montanum* sp. n. (Dorylaimida, Dorylaimidae) from Spain. Journal of Nematology 51: 1–11. [e2019-29] https://doi.org/10.21307/jofnem-2019-029

Peña-Santiago R, Álvarez-Ortega S (2014) An integrative approach to assess the phylogeny and the systematics of rounded-tailed genera of the subfamily Qudsianematinae (Nematoda, Dorylaimida). Zoologica Scripta 43: 418–428. https://doi.org/10.1111/zsc.12058

Peña-Santiago R, Ciobanu M (2011) The genus *Crassolabium* Yeates, 1967 (Nematoda, Dorylaimida): A monographic study. University of Jaén, 195 pp.

Peña-Santiago R, Vinciguerra MT (2019) Re-description of three Italian species of the genus *Labronema* Thorne, 1939 (Dorylaimida, Dorylaimidae). Nematology 21: 753–766. https://doi.org/10.1163/15685411-00003250

Peña-Santiago R, Abolafia J, Pedram M (2012) New data on *Labronemella labiata* Andrássy, 1985 (Dorylaimida: Qudsianematidae) from Iran, with SEM study and a compendium of the genus. Zootaxa 3271: 43–54. https://doi.org/10.11646/zootaxa.3271.1.4

Rahman MF, Jairajpuri MS, Ahmad I, Ahmad W (1986) Two new species of *Labronema* Thorne, 1939 (Nematoda: Dorylaimida) from India. Nematologica 32(4): 367–373. https://doi.org/10.1163/187529286X00264

Seinhorst JW (1962) On the killing, fixation and transferring to glycerine of nematodes. Nematologica 8(1): 29–32. https://doi.org/10.1163/187529262X00981

Shokoohi E, Abolafia J, Mehrabi-Nasab A, Peña-Santiago R (2013) On the identity of *Labronema vulvapapillatum* (Meyl, 1954) Loof & Grootaert, 1981 (Dorylaimida, Qudsianematidae). Russian Journal of Nematology 21(1): 31–40.

Siddiqi MR (1969) *Crateronema* n. gen. (Crateronematidae n. fam.), *Poronemella* n. gen. (Lordellonematinae n. sub-fam.) and *Chrysonemoides* n. gen. (Chrysonematidae n. fam.) with a revised classification of Dorylaimoidea (Nematoda). Nematologica 15: 81–100. https://doi.org/10.1163/187529269X00128

Southey J F (Ed.) (1986) Laboratory methods for work with plant and soil nematodes. London: Her Majesty' Stationery Office, 202 pp.

Subotin SA, Sturhan D, Chizhov VN, Vovlas N, Baldwin, JG (2006) Phylogenetic analysis of Tylenchida Thorne, 1949 as inferred from D2 and D3 expansion frag-

ments of the 28S rDNA gene sequences. Nematology 8: 455–474. https://doi.org/10.1163/156854106778493420

Thorne G (1939) A monograph of the nematodes of the superfamily Dorylaimoidea. Capita Zoologica 8: 1–261.

Thorne G (1974) Nematodes of the Northern Great Plains. Part II. Dorylaimoidea in part (Nemata: Adenophorea). South Dakota State University Agricultural Experiment Station Technical Bulletin 41: 1–120.

Vazifeh N, Niknam G, Jabbariz H, Peña-Santiago R (2023) Morphological and Molecular Characterization of *Talanema eshtiaghii* sp. n. (Dorylaimida, Qudsianematidae) from Iran. Journal of Nematology e2023 55: 1–8. https://doi.org/10.2478/jofnem-2023-0022.

Vinciguerra MT, Orselli L (1998) Nematodes of Italian sand dunes. 3. Four new species of Qudsianematidae (Dorylaimida, Nematoda). Nematologia mediterranea 26: 255–266.

Vu TT, Nguyen TD (2013) New observation on *Labronema glandosum* (Dorylaimida: Qudsianematidae) from Vietnam and a key for differentiation to other species in Vietnam. Hội Nghị Khoa Học Toàn Quốc Về Sinh Thái Và Tài Nguyên Sinh Vật Lần Thứ 5: 223–226.

Yoder M, De Ley I T, King I, Mundo-Ocampo M, Mann J, Blaxter M, Poiras L, De Ley P (2006) DESS: a versatile solution for preserving morphology and extractable DNA of nematodes. Nematology 8: 367–376. https://doi.org/10.1163/156854106778493448.

Zahedi Asl E, Niknam G, Vazifeh N (2023) *Laimydorus zehsaziani* n. sp., a new member of the genus from northwest of Iran, with additional data on *Labronema vulvapapillatum* (Meyl, 1954) Loof & Grootaert, 1981 (Dorylaimida: Dorylaimidae). Journal of Helminthology 97: e65. https://doi.org/10.1017/S0022149X23000317

Supplementary material 1

An updated list of species of genus *Labronema* Thorne, 1939

Authors: Tam T. T. Vu, Milka Elshishka, Anh D. Nguyen, Thi Mai Linh Le, Aleksandar Mladenov, Vlada Peneva

Data type: docx

Link: https://doi.org/10.3897/zookeys.1215.128183.suppl1

ZooKeys 1215: 27–52 (2024)
DOI: 10.3897/zookeys.1215.132189

Research Article

A new genus of Assamiidae (Opiliones, Grassatores) from Xizang, China

Xiaoru Qi[1,2], Adriano B. Kury[3], Chao Zhang[1,2]

1 *Key Laboratory of Zoological Systematics and Application, College of Life Sciences, Hebei University, Baoding, Hebei 071002, China*
2 *Hebei Basic Science Center for Biotic Interaction, Hebei University, Baoding, Hebei 071002, China*
3 *Departamento de Invertebrados, Museu Nacional/Universidade Federal do Rio de Janeiro (UFRJ), Quinta da Boa Vista, São Cristóvão, 20.940-040, Rio de Janeiro, RJ, Brazil*

Corresponding author: Chao Zhang (opiliones@163.com)

Abstract

Knowledge of the family Assamiidae in the Eastern Himalayas is primarily concentrated from Nepal, while Bhutan, Xizang, and northeastern India remain much less studied. Herein, a new genus, *Linzhiassamia* **gen. nov.**, is described from Xizang, China, along with two new species, *Linzhiassamia medogensis* **sp. nov.** and *Linzhiassamia zayuensis* **sp. nov.** These represents the first records of the family Assamiidae from Xizang. A comparative analysis with other continental Asian Assamiidae is undertaken, with a focus on genital morphology. Potential closest relatives are identified, including the genus *Dhaulagirius* Martens, 1977 from Nepal.

Key words: Arachnida, Eastern Himalayas, genitalia, harvestmen, taxonomy

OPEN ACCESS

Academic editor: Shahan Derkarabetian
Received: 16 July 2024
Accepted: 3 September 2024
Published: 11 October 2024

ZooBank: https://zoobank.org/94EAABFF-DCCA-4DD4-93F1-5274684317AD

Citation: Qi X, Kury AB, Zhang C (2024) A new genus of Assamiidae (Opiliones, Grassatores) from Xizang, China. ZooKeys 1215: 27–52. https://doi.org/10.3897/zookeys.1215.132189

Introduction

The Paleotropical family Assamiidae encompasses more than 450 valid species (Kury et al. 2023). In stark contrast to families that have "prospered from renewed interest and revitalized sampling efforts," assamiids are ensnared in a "labyrinthine taxonomy" (Palmieri et al. 2023), a legacy of the Roewerian system. Currently, Assamiidae is divided into 13 mostly Roewerian subfamilies, the monophyly of which is not clearly supported, and some of which exhibit suspiciously disjunct geographic distributions. Palmieri et al. (2023) utilized a 10-locus Sanger dataset for a limited number of terminals and found that, as is common in most harvestmen, the phylogeny of Assamiidae is heavily dependent on geography and clades do not correspond to traditional subfamilies. However, the generic and subfamilial boundaries within the family remain entirely unclear.

Modern descriptions of assamiid species are sparse and even combined, they fail to encompass their entire taxonomic and geographic range. Specifically, Kauri (1961, 1985), Bauer and Prieto (2009), Santos and Prieto (2010), Lotz (2011), and Martens (2022) have contributed to the understanding of the Afrotropical clade sensu Palmieri et al. Suzuki (1969a, 1969b), Zhang and Zhang (2015), Zhang et al. (2010) and Zhao et al. (2023) have contributed to

knowledge of assamiids from Indochina (including Yunnan) and Borneo. Finally, Martens (1977, 2021) has contributed detailed descriptions from Nepal. Notably, there are no modern descriptions from the Indian subcontinent, and there are no records of the family from Xizang.

In this article, two new species from Xizang are described. Unable to find an existing genus that matches their characters, we have erected the new genus *Linzhiassamia* gen. nov. Additionally, we describe the intraspecific variation of *L. zayuensis* sp. nov., providing detailed morphological descriptions, observations of genitalia, and discussions on the taxonomic position of the new species.

Taxonomic background of the Assamiidae

Assamiidae was initially a monogeneric family for *Assamia* Sørensen, 1884 from the Indian highlands. Thorell (1889) added *Maracandus* and three new genera, then later added two more South-East Asian genera (Thorell 1890, 1891). Sørensen (1896) described four new African genera and merged Dampetroidae into Assamioidæ. Loman (1902) confirmed the inclusion of Dampetridae, added Samoidae to the synonymy, and described eight new genera. Roewer (1912) misspelled the family name, restored Samoidae as a subfamily of Phalangodidae, included two former Ethiopian Epedanidae, removed *Conomma* and *Mitraceras*, and distinguished three subfamilies: Assamiinae, Dampetrinae, and Trionyxellinae. Roewer (1923, 1927) added more genera and species. In 1935, Roewer created 14 new subfamilies and numerous new genera and species. Roewer (1940) added more genera and species without changing the suprageneric classification. Mello-Leitão (1949) separated the pseudonychiate subfamilies into the new family Trionyxellidae.

Kauri (1985: 42) introduced the subfamily Irumuinae, comprising specialized subterranean species that inhabit forest soil and humus layers. In contrast, Staręga (1992: 273) opted to omit subfamilies from his catalog of genera, as he did for other families, effectively synonymizing two subfamilies by merging their type genera into other subfamilies: Tsadseinae Roewer, 1935 into Erecinae Roewer, 1935, and Harsadiinae Roewer, 1935 into Sidaminae Roewer, 1935. Kury (2007) succinctly summarized the taxonomy of the family, criticizing the current subdivisions as unsatisfactory and artificial. More recently, Martens (2022) described a new subfamily from the Ethiopian highlands, characterized by unusual pedipalp dimorphism, although the male genitalia conform to the family's basic morphology.

Recent trends in taxonomy have seen a dismissal of subfamilies that are not clades. For instance, Palmieri et al. (2023: 6) highlighted the non-monophyly of certain subfamilies, thereby questioning the utility of several subfamily definitions. Similarly, Klementz and Sharma (2023: 34) referred to the "now taxonomically defunct Polycoryphinae or Mysoreinae subfamilies." However, this approach seems to reflect our current challenges in developing robust morphological diagnoses, which stem from a lack of comprehensive taxonomic groundwork. Discarding these subfamilies should be seen as a transition towards a more accurate and phylogenetically informed taxonomy, particularly considering the nearly 500 species within the Assamiidae that require intermediate taxa. Our focus should be on reforming and refining these subfamilies by leveraging both existing and new morphological data to enhance their utility and accuracy.

Materials and methods

Specimen preparation and examination

The specimens were preserved in 75% ethanol, examined under a Leica M205A stereomicroscope, and the overall drawings were made using a drawing tube-equipped Leica M205A stereomicroscope, while the detailed drawings were created using Inscape v. 1.3. Photographs were taken using a Leica M205A stereomicroscope, equipped with a DFC 450 CCD. The male genitalia were initially placed in hot lactic acid (40–50 °C) for about 1–2 min, then transferred to distilled water; the movable parts of the glans will mostly expand within 1 min (Schwendinger and Martens 2002).

Terminology

The terminology of genital structures follows Martens (1986) and Macías-Ordóñez et al. (2010), and the macrosetae terminology of male genitalia follows Kury and Machado (2021). Terminology for the outline of the dorsal scutum follows Kury and Medrano (2016). Type specimens of the new species are deposited in the Museum of Hebei University, Baoding, China (**MHBU**). All measurements are given in millimeters. The following abbreviations are used in the text: Pb pars basalis; Pd pars distalis.

Comparisons

In the diagnosis given here, *Linzhiassamia* sp. nov. is assessed in relation to genera that possess some features in common, such as the Nepalese highlanders *Dhaulagirius* Martens, 1977; *Micrassamula* Martens, 1977; *Nepalsia* Martens, 1977; and *Nepalsioides* Martens, 1977, as well as *Nilgirius* Roewer, 1915, which occurs in Yunnan and India. It is also compared with *Paktongius* Suzuki, 1969, from the lowlands of Laos, Malaysia, and Thailand.

Taxonomy

***Linzhiassamia* gen. nov.**
https://zoobank.org/909654AF-C499-4D06-A842-555ECAFC699F

Included species. *Linzhiassamia medogensis* sp. nov. (type species) and *Linzhiassamia zayuensis* sp. nov.

Etymology. The genus name is based on 林芝 (Linzhi), an alternative name for Nyingchi. This is associated with the pre-existing genus name *Assamia*. The gender is feminine.

Diagnosis. *Linzhiassamia* is similar to *Paktongius* for the sexually dimorphic coxa IV, which in males may reach areas III, IV or even V of the dorsal scutum, while in females it is much shorter, reaching area II, and not projected laterally (*Nilgirius* and the Nepalese genera treated here, all possess coxa IV monomorphic).

Linzhiassamia is similar to *Dhaulagirius* due to the sexually dimorphic chelicerae; however, in *Dhaulagirius*, the cheliceral hand is much more exaggeratedly developed. In the other genera compared here, the chelicerae are monomorphic.

Linzhiassamia is similar to *Nilgirius* and *Paktongius* for having a "pseudonychium" (tarsal process) in the tarsi of legs III and IV.

Linzhiassamia is similar to *Dhaulagirius*, *Micrassamula*, and *Nepalsia* for lacking a sharp annular joint-like constriction in the distal third of the truncus penis, between the pars basalis and pars distalis (in contrast to *Nepalsioides* and *Nilgirius*).

Linzhiassamia is similar to *Dhaulagirius*, *Nepalsia*, and *Nepalsioides* for having MS A organized in a triangle (in contrast to *Micrassamula*, which has MS A extended into a line, and *Nilgirius*, which has a ring-girdle formed by macrosetae D1, A1–A3, and B1).

Linzhiassamia is similar to *Dhaulagirius*, *Nepalsia*, and *Nilgirius* for not having a wide dorsal concavity, giving the distal truncus the aspect of an ice-cream scoop (in contrast to *Micrassamula* and *Nepalsioides*).

Linzhiassamia is similar to *Nepalsia* and *Nilgirius* for having all macrosetae concentrated distally (in contrast to *Dhaulagirius*, *Micrassamula*, and *Nepalsioides*).

Linzhiassamia is similar to *Dhaulagirius* for having the distal part of the truncus with constrictions, flaring to form a pyriform structure (in contrast to *Micrassamula*, *Nepalsia*, *Nepalsioides*, and *Nilgirius*, which have more or less continuous widening of the truncus, getting rounded apically).

***Linzhiassamia medogensis* sp. nov.**

https://zoobank.org/F56C8DB5-9ADA-4DDD-9E87-04D420941FC1

Figs 1–25

Type material. ***Holotype*** • male (MHBU-Opi-24ZC011501): China: Xizang, Nyingchi, Medog County, 29°33'N, 95°33'E, alt. 1116 m, 22 May 2019, H. Wang, L.Y. Wang leg. ***Paratypes*:** • one male (MHBU-Opi-24ZC011502) and two females (MHBU-Opi-24ZC011503-04), same collecting data as holotype • one male (MHBU-Opi-24ZC011601): China: Xizang, Nyingchi, Medog County, 29°33'N, 95°33'E, alt. 1116 m, 23 May 2019, H. Wang leg.

Diagnosis. Distal section of penis (pars distalis) markedly enlarged: ventral plate nearly triangle and frontal rim with median crevice (Figs 13, 15), convex in dorsal view and concave in ventral view (Figs 14, 16); The pars basalis and pars distalis of the penis are connected by joints (Figs 13–17). Glans partially sunken into a dorsally depressed portion of pars distalis of penis, its tip slightly extending the distal margin (Fig. 14) of the ventral plate. Opisthosomal region of scutum with abundant setiferous tubercles. Ocularium without spines, but with small, scattered tubercles. Pedipalpal femur ventrally with a row of six or seven setiferous tubercles.

Etymology. The species name originates from the specimen collection site: Medog County, Nyingchi, Xizang.

Description. Male (holotype and paratype). Habitus as in Figs 1, 7, 20–22. Coloration (Figs 20–22): entire body dorsally rusty yellow with brown patches; median area of prosoma with dark brown reticulations before and behind the interocular mound; around the ocularium dark brown patches; both lateral ridges of the prosomal and opisthosomal scuta with dark brown stripes; opisthosomal areas I–IV with dark brown, and the central region being lighter than the surrounding areas; there are transverse paler interspaces between areas I–III; area V and free tergites each with a transverse dark band; venter concolorous with the dorsum; chelicerae, pedipalps and legs rusty yellow, reticulated with light to dark brown.

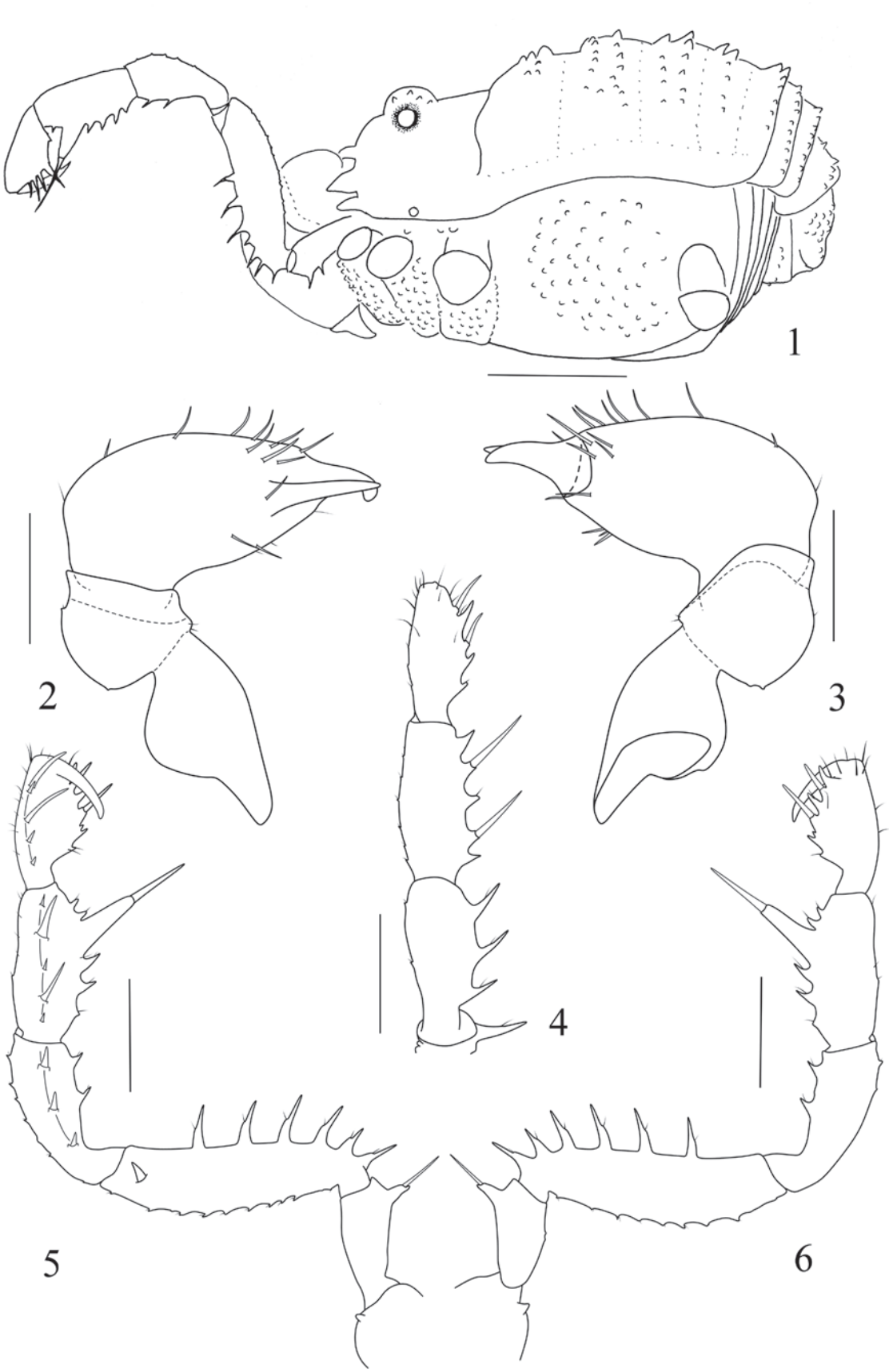

Figures 1–6. *Linzhiassamia medogensis* sp. nov., male (**2–6** holotype), male (**1** paratype) **1** male body, lateral view **2** left chelicera of male, ental view **3** left chelicera of male, ectal view **4** left pedipalp of male, dorsal view **5** left pedipalp of male, ental view **6** left pedipalp of male, ectal view. Scale bars: 1 mm (**1**); 0.5 mm (**2–6**).

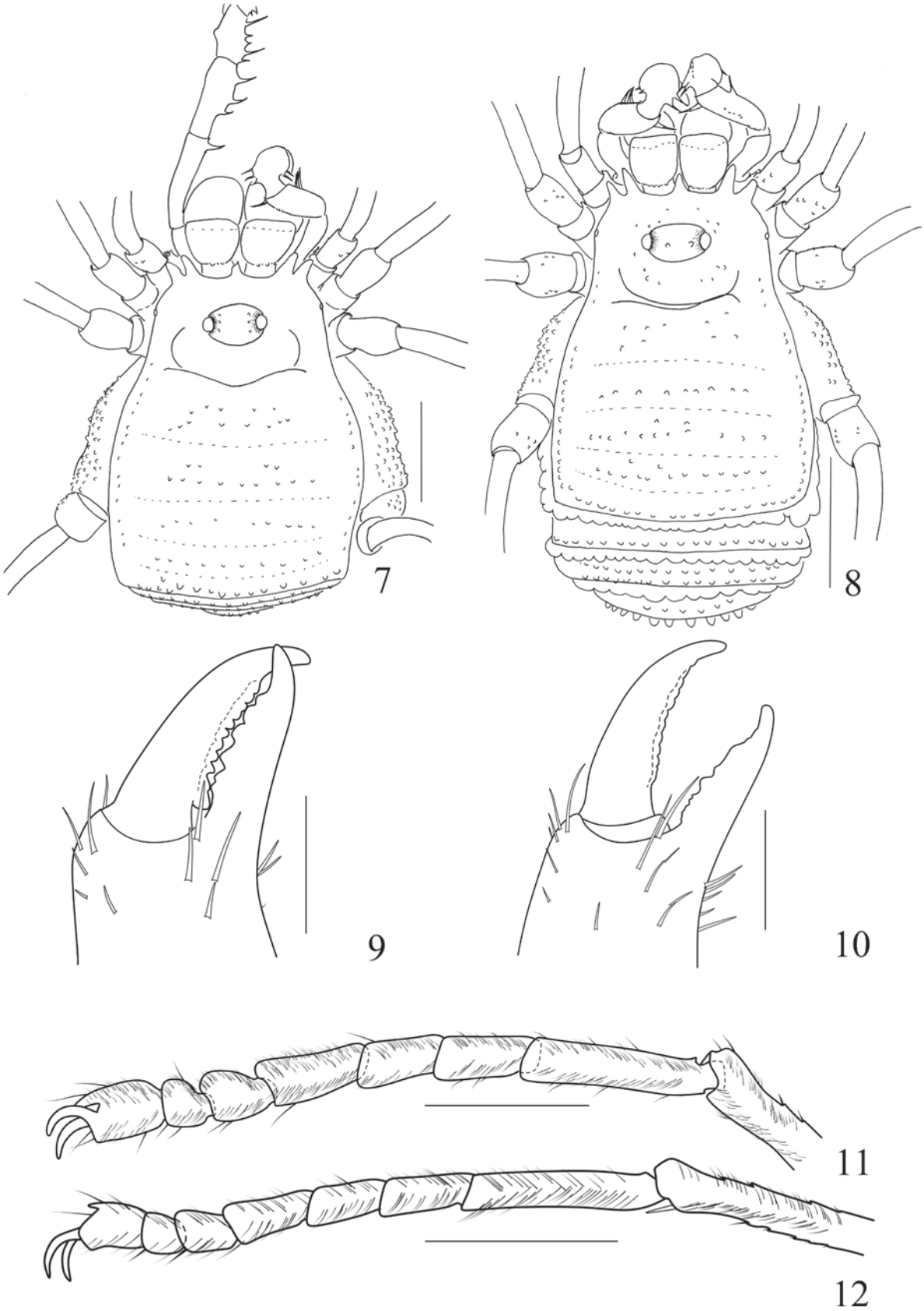

Figures 7–12. *Linzhiassamia medogensis* sp. nov., male (**9, 11** holotype), male (**7** paratype), female (**8, 10, 12** paratype) **7** male body, dorsal view **8** female body, dorsal view **9** left cheliceral fingers of male, frontal view **10** left cheliceral fingers of female, frontal view **11** right tarsal claw IV of male, lateral view **12** right tarsal claw IV of female, lateral view. Scale bars: 1 mm (**7, 8**); 0.5 mm (**11–12**); 0.25 mm (**9–10**).

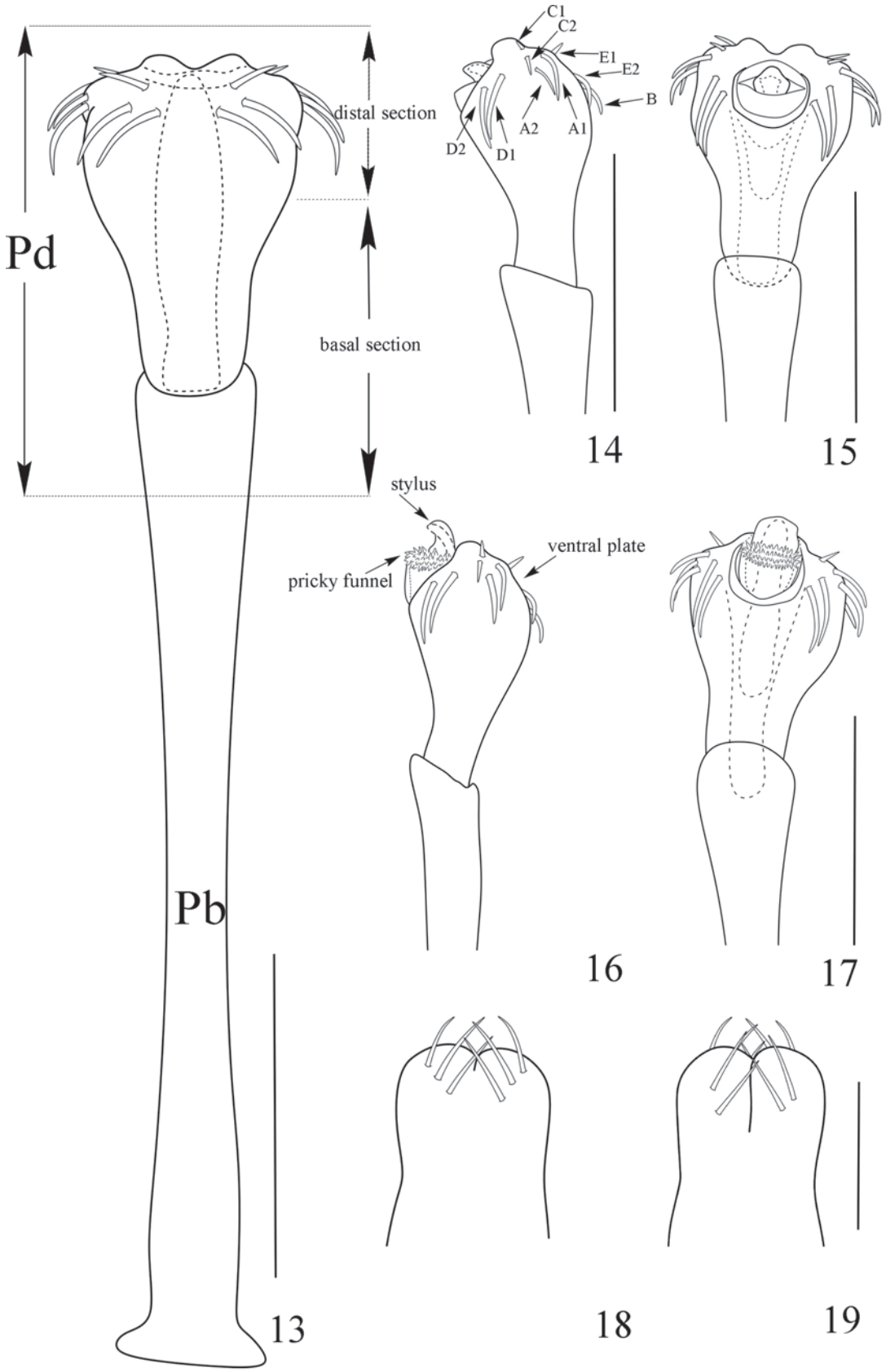

Figures 13–19. *Linzhiassamia medogensis* sp. nov., genitalia of male holotype (**13–17**) and female paratype (**18–19**) **13** penis, ventral view **14** distal part of penis, lateral view **15** same, dorsal view **16** distal part of penis (expanded), lateral view **17** same, dorsal view **18** ovipositor, dorsal view **19** same, ventral view. Pb, pars basalis, Pd pars distalis. Scale bars: 0.25 mm.

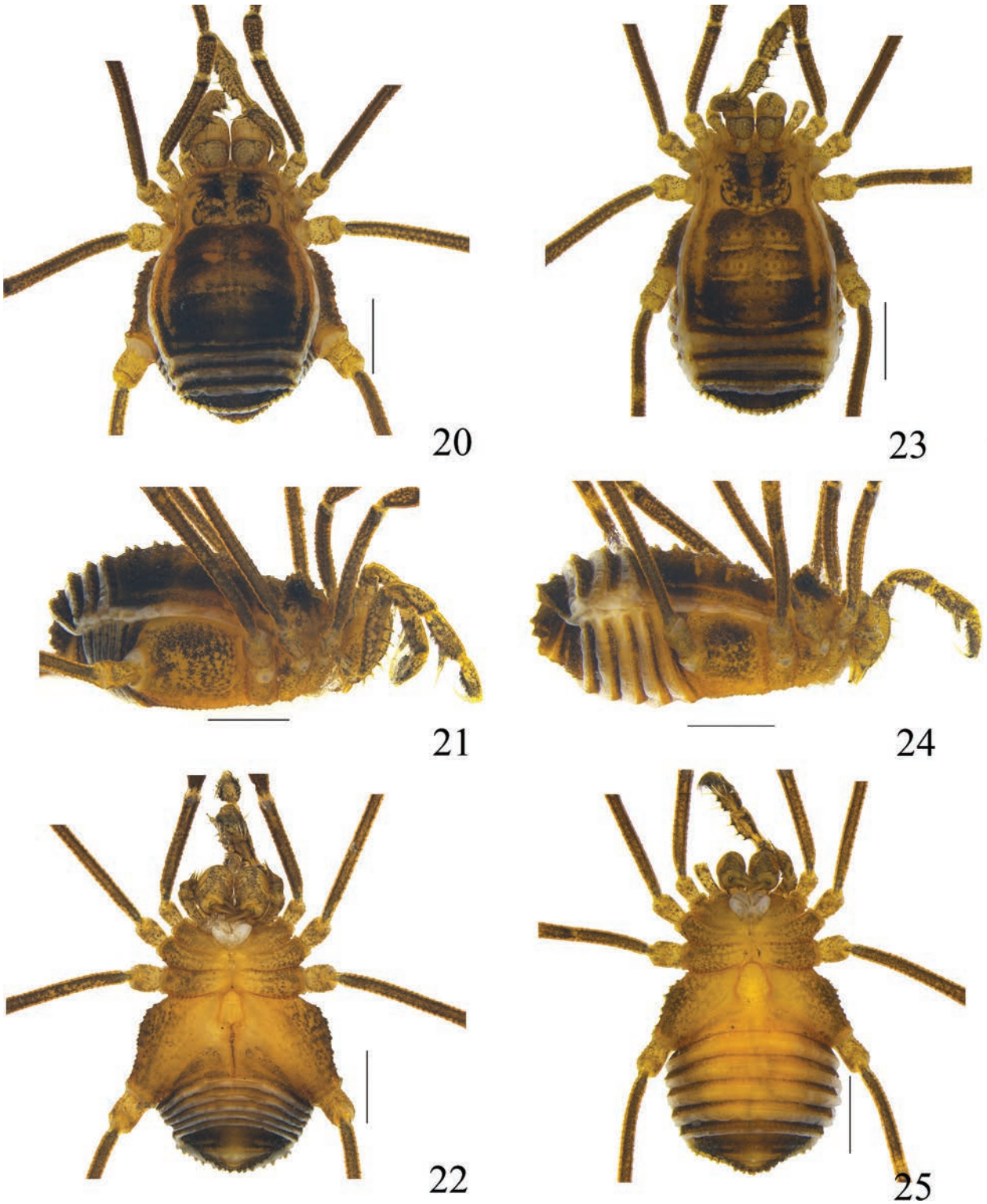

Figures 20–25. Photographs of male (**20–22** holotype) and female (**23–25** paratype) of *Linzhiassamia medogensis* sp. nov. **20, 23** body and parts of appendages, dorsal view **21, 24** body and parts of appendages, lateral view **22, 25** body and parts of appendages, ventral view. Scale bars: 1 mm.

Dorsum (Figs 7, 20). Dorsal scutum pyriform in shape, widest portion of body at scutal area II. Anterior margin of carapace with two spines at the lateral portion and a single median spine, the middle one is the smallest. Entire prosoma covered with small tubercles; anterior margin of prosoma with a row of small

tubercles at the lateral portion. Ocularium oval, removed from the anterior border of scutum by 0.13 mm, and scattered with small tubercles. Opisthosomal region of scutum with five areas. Opisthosomal areas I–IV are adorned with abundant seta-tipped tubercles and a longitudinal row of similar tubercles on the lateral margins. Area V and all free tergites with a transverse row of seta-tipped tubercles.

Venter (Fig. 22). Surface of all coxae tuberculated. Coxa I with a row of four tubercles prolaterally, and two rows of tubercles on the surface. Coxa II with a row of marginal tubercles on the prolateral surface, and disto-dorsally with an enlarged tubercle. Coxa III with prolateral and retrolateral rows of tubercles. Coxa IV larger than others, prolaterally with many scattered tubercles, Genital operculum with many hair-tipped granules. Free sternites with a row of minute tubercles, each with setae on top. Spiracles concealed.

Chelicera (Figs 2–3, 9). Basichelicerite elongate, dorsally with a slight bulla, without prominent armaments. Cheliceral hand unarmed, with sparse hairs only. Fingers relatively short, inner edges toothed as illustrated (Fig. 9): moveable finger with 11 teeth, the proximal one enlarged; fixed finger with six teeth, the proximal one diminished.

Pedipalpus (Figs 4–6). Coxa dorsally with one small tubercle. Trochanter ventrally with one long distal setiferous tubercle. Femur compressed laterally, widest at the middle of its length, ventrally with a row of 6 homogeneous setiferous tubercles; dorsally with a row of twelve low conical tubercles along the entire length; on the medial distal side with one setiferous tubercle. Patella with three ventromesal setiferous tubercles, and two ventroectal setiferous tubercles, dorsally with a row of six low conical tubercles along the entire length. Tibia ventromesally with two enlarged and three small setiferous tubercles; and ventroectally with one fairly enlarged and five setiferous tubercles. Tarsus with sparse hairs, ventromesally with two slightly enlarged and three small setiferous tubercle, and ventroectally with two slightly enlarged and five small setiferous tubercles. Tarsal claw slightly curved, shorter than tarsus.

***Legs*.** Slender and elongated. Trochanters I–IV with small, hair-tipped granules on the ventral surface. All femora with hair-tipped granules, femora III and IV curved. Tarsi III–IV with a pseudonychium and two bare claws (Fig. 11). Tarsal formula (I–IV): 5(2)/11–14(3)/6/7. Distitarsus I two-jointed and II three-jointed. The remaining leg segments with hair-tipped granules.

Penis (Figs 13–17). Truncus (pars basalis) slender, sides nearly parallel, then slightly enlarged (Fig. 13) and curved (Figs 14, 16) towards distal end. Distal portion of penis (pars distalis) markedly enlarged: ventral plate nearly triangle and frontal rim with median crevice (Figs 13–15), convex in dorsal view and concave in ventral view (Figs 14, 16); pars basalis and pars distalis of the penis connected by joints. Glans partially sunken into a dorsally depressed portion of pars distalis of penis, its tip slightly extending the distal margin (Fig. 14) of the ventral plate. Glans composed of two-thirds of prickly funnel and capsula externa near the base and one-third of stylus and capsula interna (Figs 14, 16). Capsula externa and capsula interna cylindrical, and the inner side of capsula interna with dense cover of fur-like microtrichia (Fig. 16). Stylus with irregular shape, constricted apically, the inverted stylus with capsula interna sunken into the spiny funnel, and all parts mentioned above surrounded totally by the

capsula externa (Fig. 16). Ventral plate with 18 large setae (Figs 13–15): four dorsal, eight lateral and six ventral.

Female (Figs 8, 10, 12, 18–19). In general appearance similar to the male; abdomen more rounded posteriorly (Figs 20, 23). Granulation and spination of body similar to the male (Figs 8, 23). Chelicerae not enlarged but of normal shape, with a slight difference in inner edges of the cheliceral finger (Fig. 10). Pseudonychium of legs IV in females reduced compared to that of male (Figs 11, 12). Femora of pedipalpi dorsally with a row of six setiferous tubercles. Tarsal formula (I–IV): 5(2)/11–12(3)/6/7.

Ovipositor (Figs 18, 19). Ventral side with four, dorsal side with six setae.

Measurements. Male holotype (female paratype): Body 3.53 (3.53) long, 2.29 (2.00) wide at the widest portion. Scutum 1.85 (1.64) long. Interocular mound 0.63 (0.57) long, 0.34 (0.34) wide, 0.24 (0.20) high, 0.13 (0.12) far from the anterior border of the scutum. Pedipalpal claw 0.39 (0.45) long. Penis 1.02 long. Measurements of left pedipalpus and legs as in Tables 1, 2.

Habitat. The specimens were collected under stones and on the leaves of the shrubbery.

Distribution. Known only from the type locality, the Medog County, Nyingchi City, Xizang Autonomous Region, China.

Variation. Specimens examined included three males and two females, the number of tarsal segments on the second legs was not constant, which varied from eleven to fourteen segments. On the fourth leg, the number of tarsal segments varies from seven to eight. The number of tarsal segments on the second leg and third leg is constant, with five segments on the second and six segments on the third. Another variation is the number of setiferous tubercles on the pedipalpus trochanter. For example, the male holotype (MHBU-Opi-24ZC011501) has only one setiferous tubercle on the pedipalpus trochanter (Figs 5, 6), while the male paratype (MHBU-Opi-24ZC011601) has two setiferous tubercles (Fig. 1).

Table 1. *Linzhiassamia medogensis* sp. nov. Measurements of the pedipalp and legs of the male holotype (MHBU-Opi-24ZC011501), as length/width.

	Trochanter	Femur	Patella	Tibia	Metatarsus	Tarsus	Total
Pedipalp	0.47/0.22	1.09/0.32	0.78/0.24	0.67/0.29		0.58/0.28	3.59
Leg I	0.36/0.25	1.73/0.21	0.63/0.28	1.26/0.18	1.98/0.09	1.18/0.05	7.14
Leg II	0.39/0.30	3.22/0.20	0.94/0.29	2.72/0.16	3.24/0.10	2.52/0.07	13.03
Leg III	0.46/0.37	2.30/0.24	0.81/0.35	1.51/0.21	2.68/0.16	1.40/0.11	9.16
Leg IV	0.60/0.36	3.75/0.26	1.02/0.42	2.23/0.21	4.32/0.18	1.89/0.12	13.81

Table 2. *Linzhiassamia medogensis* sp. nov. Measurements of the pedipalp and legs of the female paratype (MHBU-Opi-24ZC011503), as length/width.

	Trochanter	Femur	Patella	Tibia	Metatarsus	Tarsus	Total
Pedipalp	0.44/0.22	0.97/0.28	0.70/0.24	0.62/0.28		0.54/0.24	3.27
Leg I	0.45/0.28	2.45/0.16	0.72/0.25	2.35/0.15	2.83/0.08	2.08/0.08	10.88
Leg II	0.46/0.29	2.75/0.18	0.74/0.24	2.44/0.15	2.71/0.08	2.04/0.08	11.14
Leg III	0.42/0.35	2.03/0.23	0.58/0.31	1.32/0.22	2.21/0.13	1.21/0.11	7.77
Leg IV	0.54/0.33	3.09/0.23	0.78/0.32	1.92/0.23	3.45/0.14	1.52/0.08	11.30

***Linzhiassamia zayuensis* sp. nov.**
https://zoobank.org/65820C30-2533-44E6-A83F-94DABD451260
Figs 26–75

Type material. ***Holotype*** • male (MHBU-Opi-24ZC011801): China: Xizang, Nyingchi, Zayu County, 28°29'N, 97°30'E, alt. 1405 m, 13 July 2020, L.Y. Wang leg. ***Paratypes*:** • one female (MHBU-Opi-24ZC011802), China: Xizang, Nyingchi, Zayu County, 28°77'N, 96°72'E, alt. 1945 m, 27 May 2019, H. Wang leg • one male and one female (MHBU-Opi-24ZC011803-04), China: Xizang, Nyingchi, Zayu County, 28°53'N, 96°99'E, alt. 1509 m, 11 May 2023, Y. M. Hou, Z. Y. Yang leg • one male (MHBU-Opi-24ZC011901), China: Xizang, Nyingchi, Lulang Town, 29°96'N, 94°82'E, alt. 2472 m, 21 May 2019, H. Wang leg • one female (MHBU-Opi-24ZC011902), China: Xizang, Nyingchi, Bome County, 30°10'N, 95°07'E, alt. 2037 m, 02 June 2022, B. Liu leg • one male and one female (MHBU-Opi-24ZC011903-04), China: Xizang, Nyingchi, Bome County, 30°04'N, 95°02'E, alt. 2051 m, 17 July 2020, L. Y. Wang, Y. M. Hou, leg.

Diagnosis. The distal margin of the ventral plate is smooth and without any indentation (Figs 38, 63). Capsula externa cylindrical and capsula interna triangular, and the inner side of capsula interna with dense cover of fur-like microtrichia (Figs 41, 66). The ocularium has either a short spine or is unarmed, and there are two or three spines on the lateral anterior margin of the carapace (Figs 26, 32, 33, 45, 46, 48, 49, 51, 57, 58, 70, 71, 73–74).

Notes. The external morphological differences of this species are significant. The interocular have either a short spine or are smooth, and at the lateral portion there are two or three spines on the anterior margin of the carapace. However, the seta-tipped tubercles on the opisthosomal region of scutum are relatively small, which allows for a preliminary differentiation from the other three species. Additionally, by examining the expanded structure of the genitalia together with external morphological characteristics, this species can be accurately distinguished from others.

Etymology. The name of this species is derived from its collection locality in Zayu County, Nyingchi, Xizang.

Description. Male (holotype and paratype). Habitus as in Figs 26, 32, 45–47. Coloration (Figs 45–47): entire body dorsally rusty yellow with brown patches; median area of prosoma with dark brown reticulations before and behind the interocular mound; anterior margin of prosoma have dark brown patches at the lateral portion; both lateral ridges of the prosomal and opisthosomal scutum with dark brown stripes; opisthosomal areas I–IV with dark brown patches, and there is a longitudinal dark brown stripe along the entire length; area V and free tergites each with a transverse dark band; The venter is the same color as the dorsum; chelicerae, pedipalps and legs rusty yellow, reticulated with light to dark brown.

Dorsum (Figs 32, 45). Dorsal scutum pyriform in shape, widest portion of body at scutal area II. Anterior margin of carapace with three spines (two large spines and one small spine, with the middle one being the smallest) at the lateral portion and a single median spine; anterior margin of prosoma with two rows of small tubercles at the lateral portion. Ocularium oval, removed from the anterior border of scutum by 0.19 mm, and scattered with small tubercles. Opisthosomal region of scutum with five areas. Except for a few scattered small seta-tipped tubercles in areas II and III, opisthosomal areas I to IV are mostly smooth. Area V and all free tergites with a transverse row of seta-tipped tubercles.

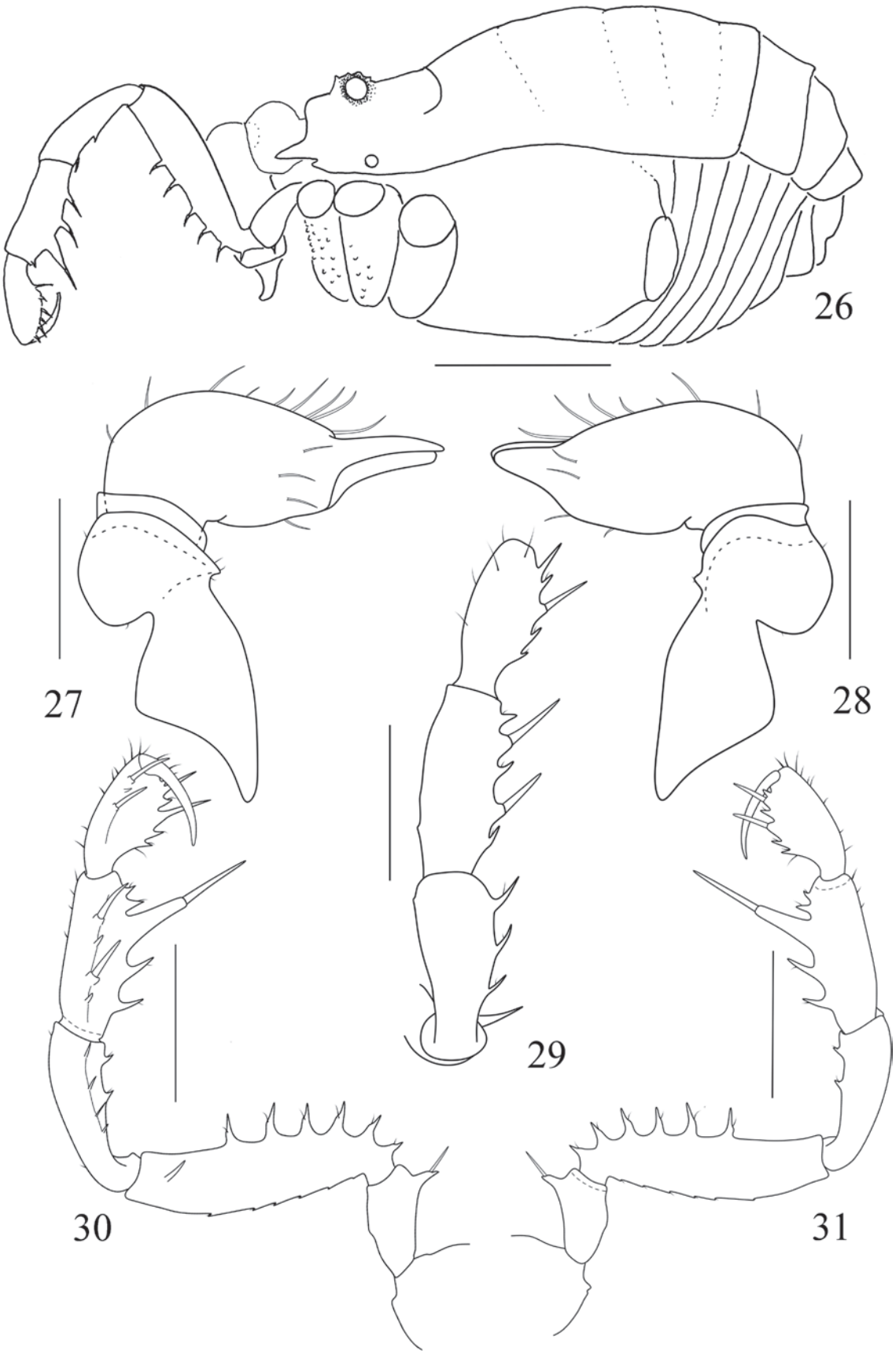

Figures 26–31. *Linzhiassamia zayuensis* sp. nov., male (**27–31** holotype), male (**26** paratype) **26** male body, lateral view **27** left chelicera of male, ental view **28** left chelicera of male, ectal view **29** left pedipalp of male, dorsal view **30** left pedipalp of male, ental view **31** left pedipalp of male, ectal view. Scale bars: 1 mm (**26**); 0.5 mm (**27–31**).

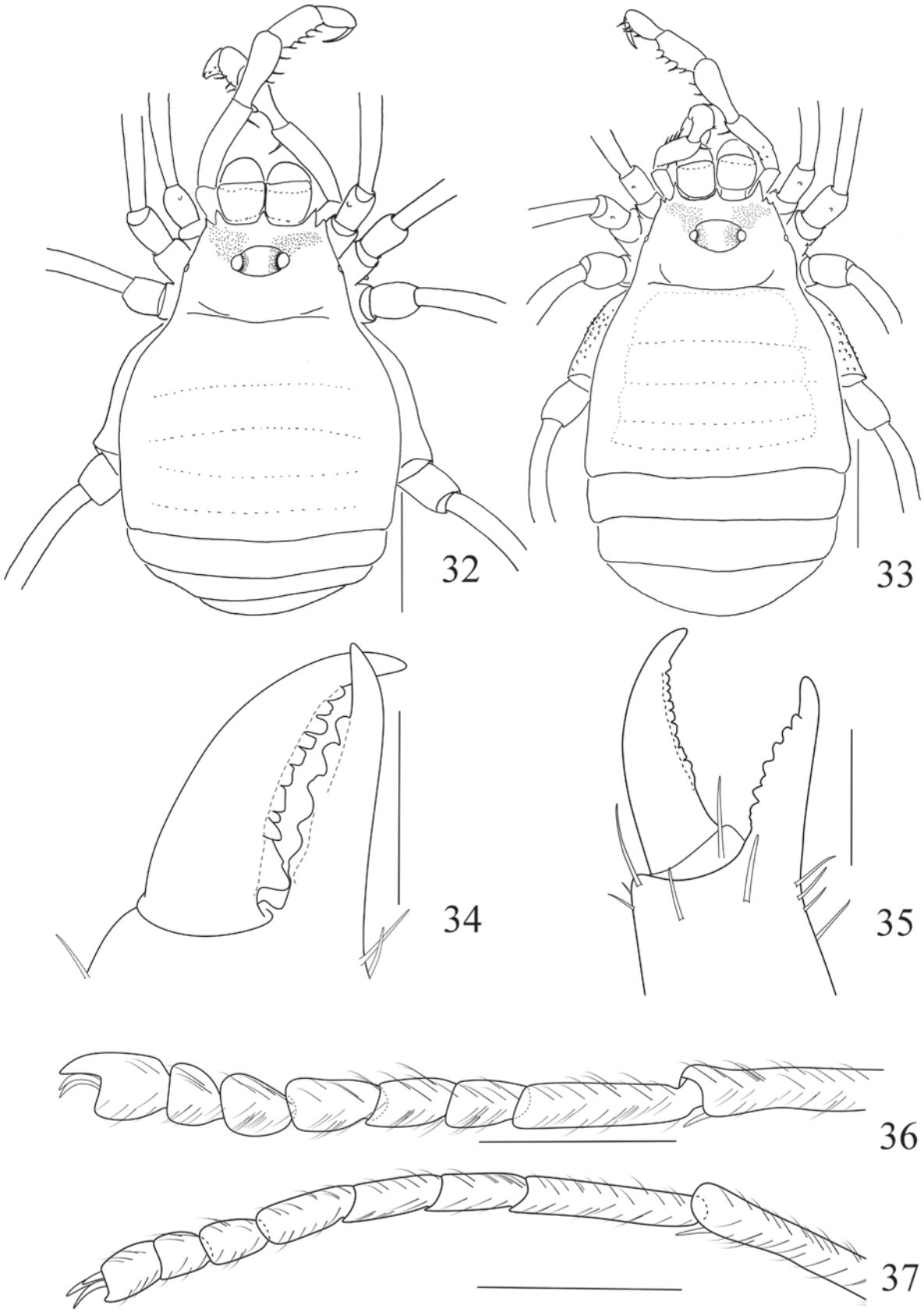

Figures 32–37. *Linzhiassamia zayuensis* sp. nov., male (**34, 36** holotype), male (**32** paratype), female (**33, 35, 37** paratype) **32** male body, dorsal view **33** female body, dorsal view **34** left cheliceral fingers of male, frontal view **35** left cheliceral fingers of female, frontal view **36** right tarsal claw IV of male, lateral view **37** right tarsal claw IV of female, lateral view. Scale bars: 1 mm (**32–33**); 0.5 mm (**36–37**); 0.25 mm (**34–35**).

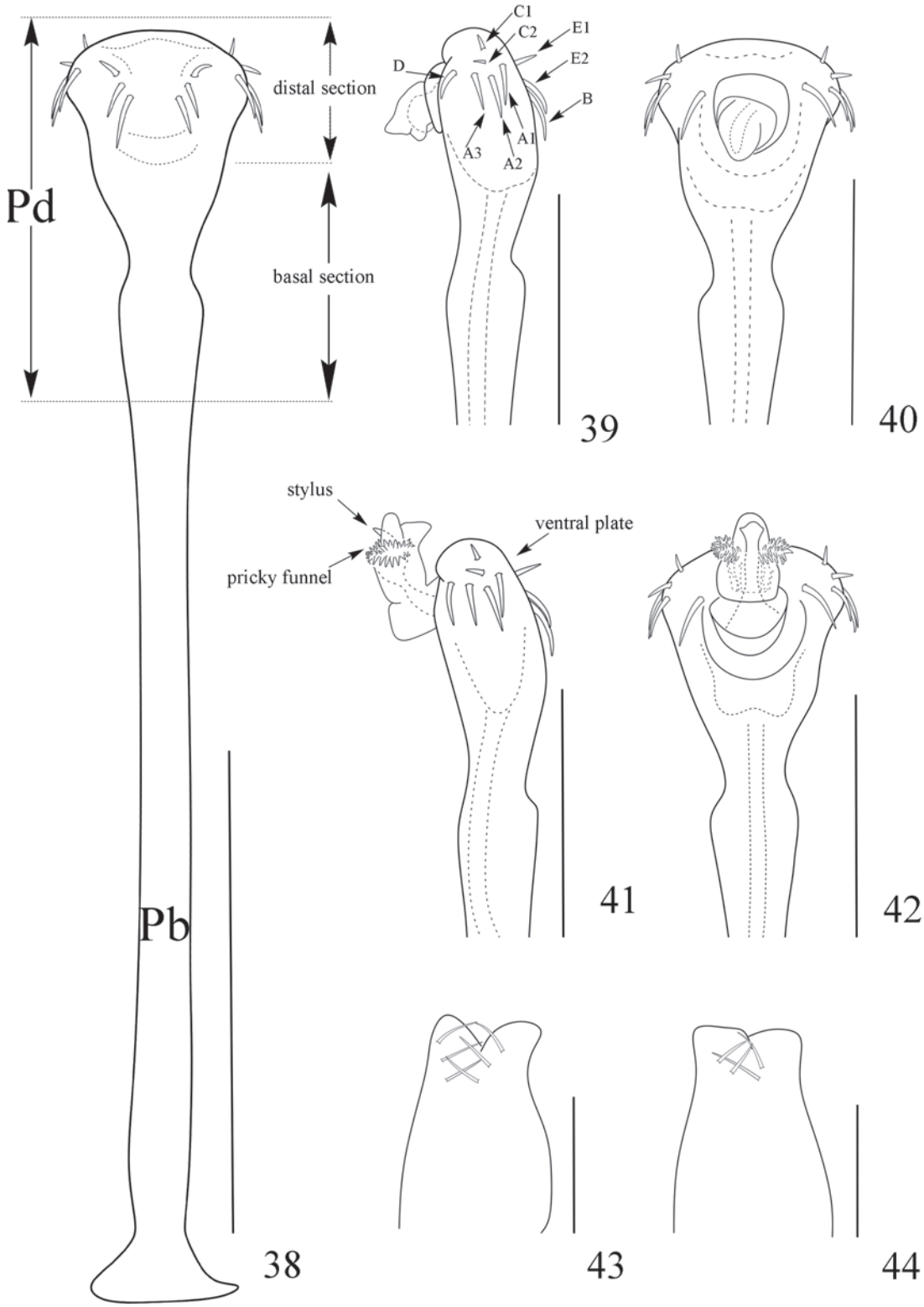

Figures 38–44. *Linzhiassamia zayuensis* sp. nov., genitalia of male holotype (**38–42**) and female paratype (**43, 44**) **38** penis, ventral view **39** distal part of penis, lateral view **40** same, dorsal view **41** distal part of penis (expanded), lateral view **42** same, dorsal view **43** ovipositor, dorsal view **44** same, ventral view. Pb, pars basalis, Pd pars distalis. Scale bars: 0.5 mm (**38**); 0.25 mm (**39–44**).

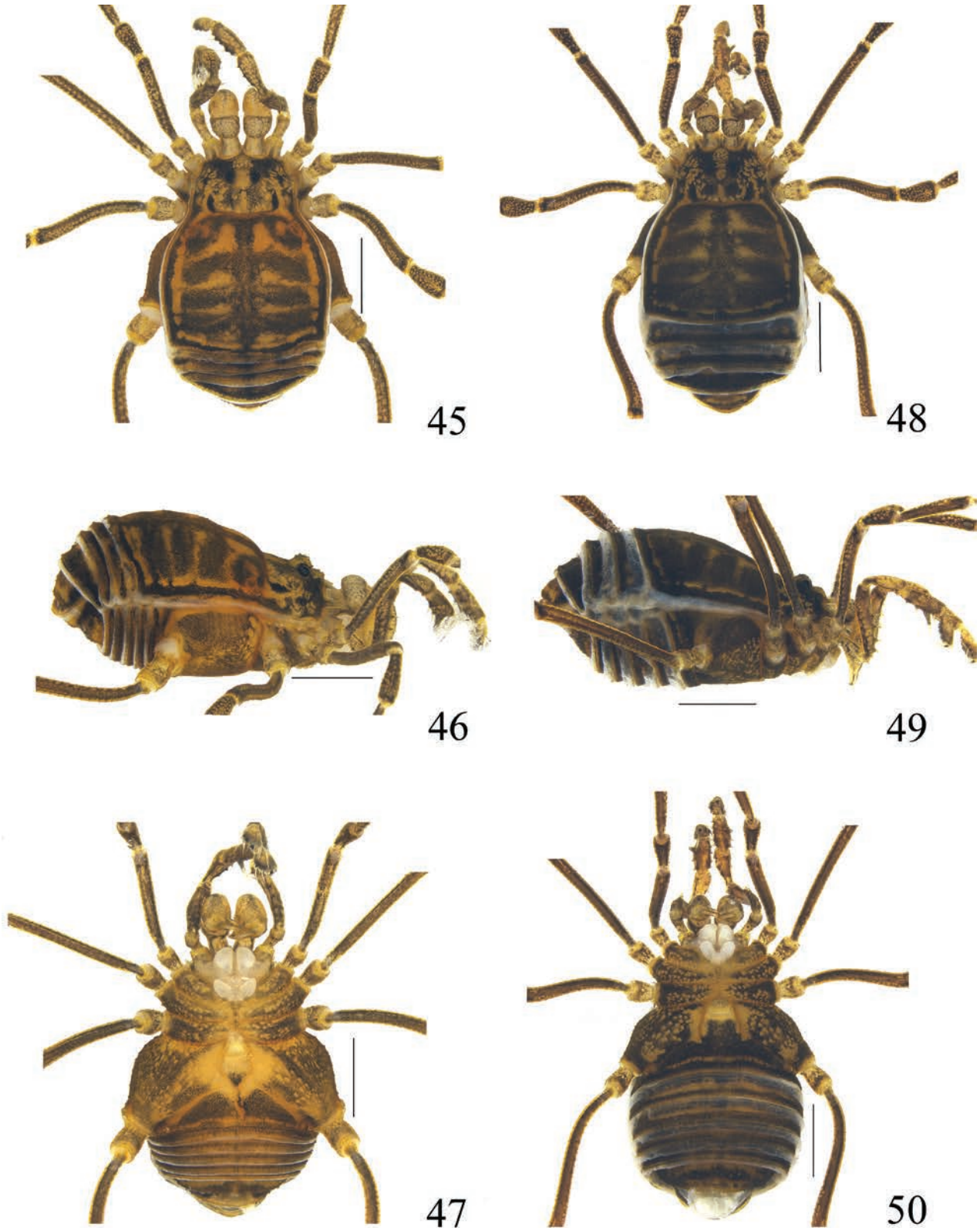

Figures 45–50. Photographs of male (**45–47** holotype) and female (**48–50** paratype) of *Linzhiassamia zayuensis* sp. nov. **45, 48** body and parts of appendages, dorsal view **46, 49** body and parts of appendages, lateral view **47, 50** body and parts of appendages, ventral view. Scale bars: 1 mm.

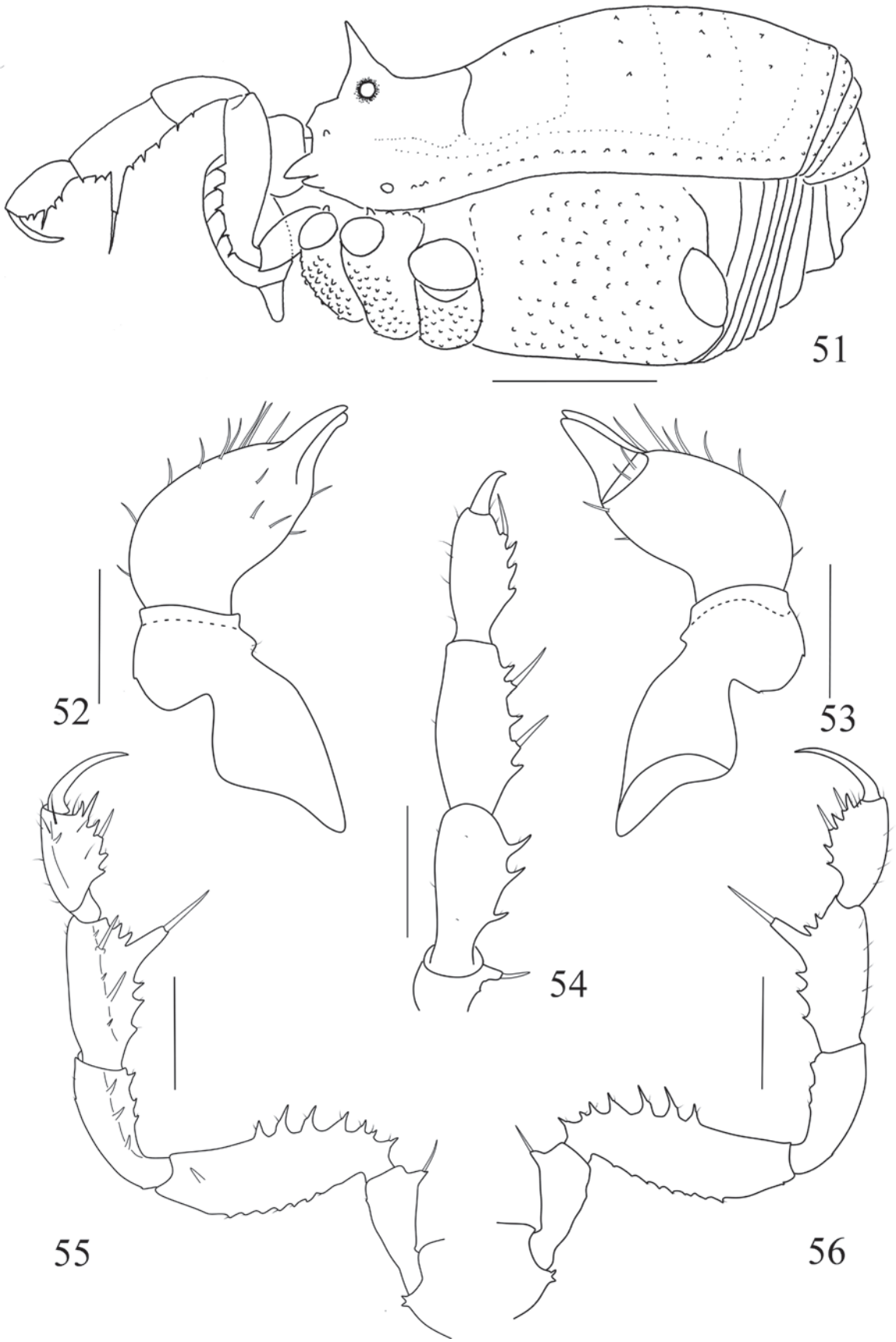

Figures 51–56. *Linzhiassamia zayuensis* sp. nov., male (**51–56** paratype) **51** male body, lateral view **52** left chelicera of male, ental view **53** left chelicera of male, ectal view **54** left pedipalp of male, dorsal view **55** left pedipalp of male, ental view **56** left pedipalp of male, ectal view. Scale bars: 1 mm (**51**); 0.5 mm (**52–56**).

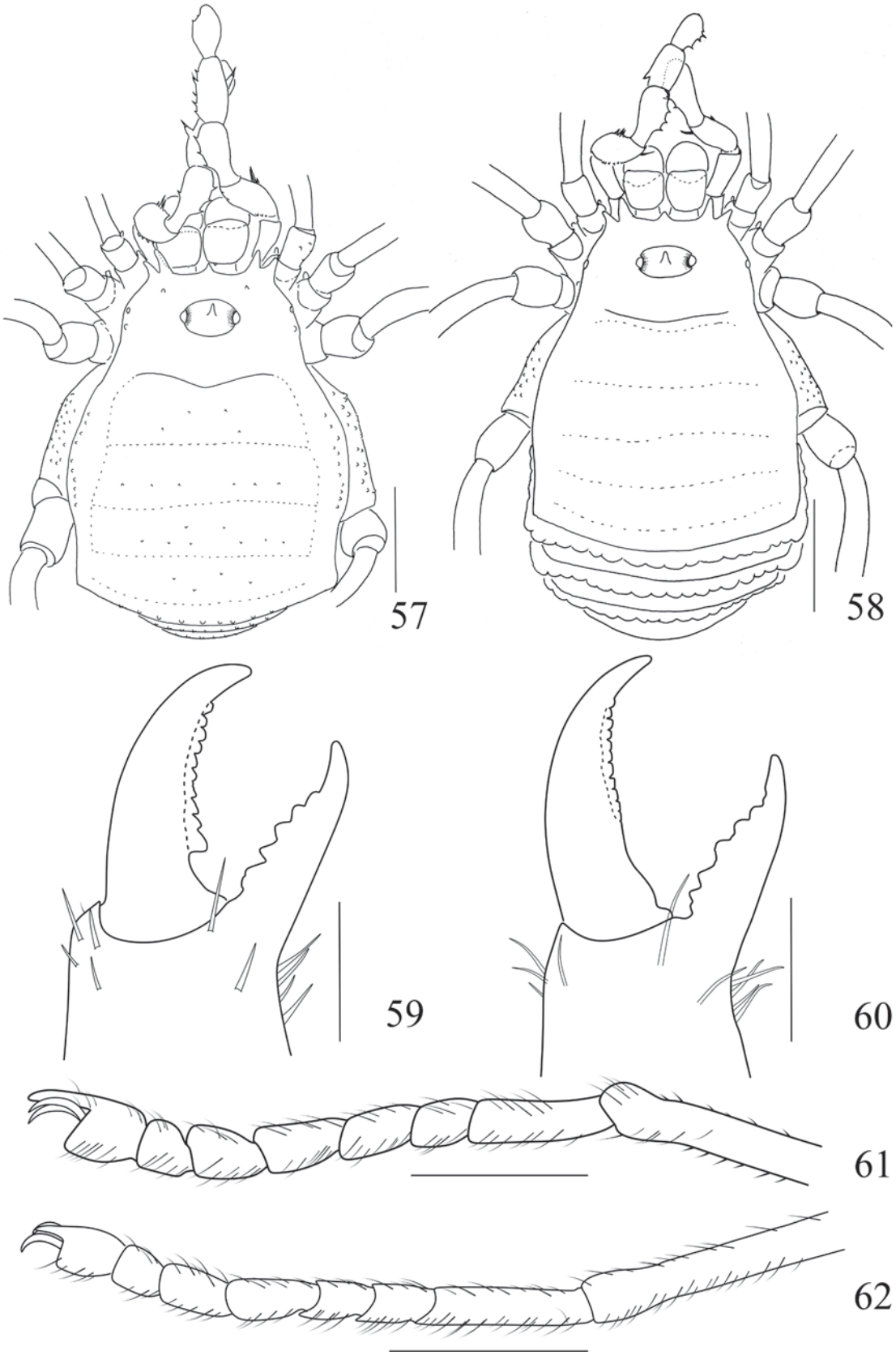

Figures 57–62. *Linzhiassamia zayuensis* sp. nov., male (**59, 61, 57** paratype), female (**58, 60, 62** paratype) **57** male body, dorsal view **58** female body, dorsal view **59** left cheliceral fingers of male, frontal view **60** left cheliceral fingers of female, frontal view **61** right tarsal claw IV of male, lateral view **62** right tarsal claw IV of female, lateral view. Scale bars: 1 mm (**57, 58**); 0.5 mm (**61–62**), 0.25 mm (**59–60**).

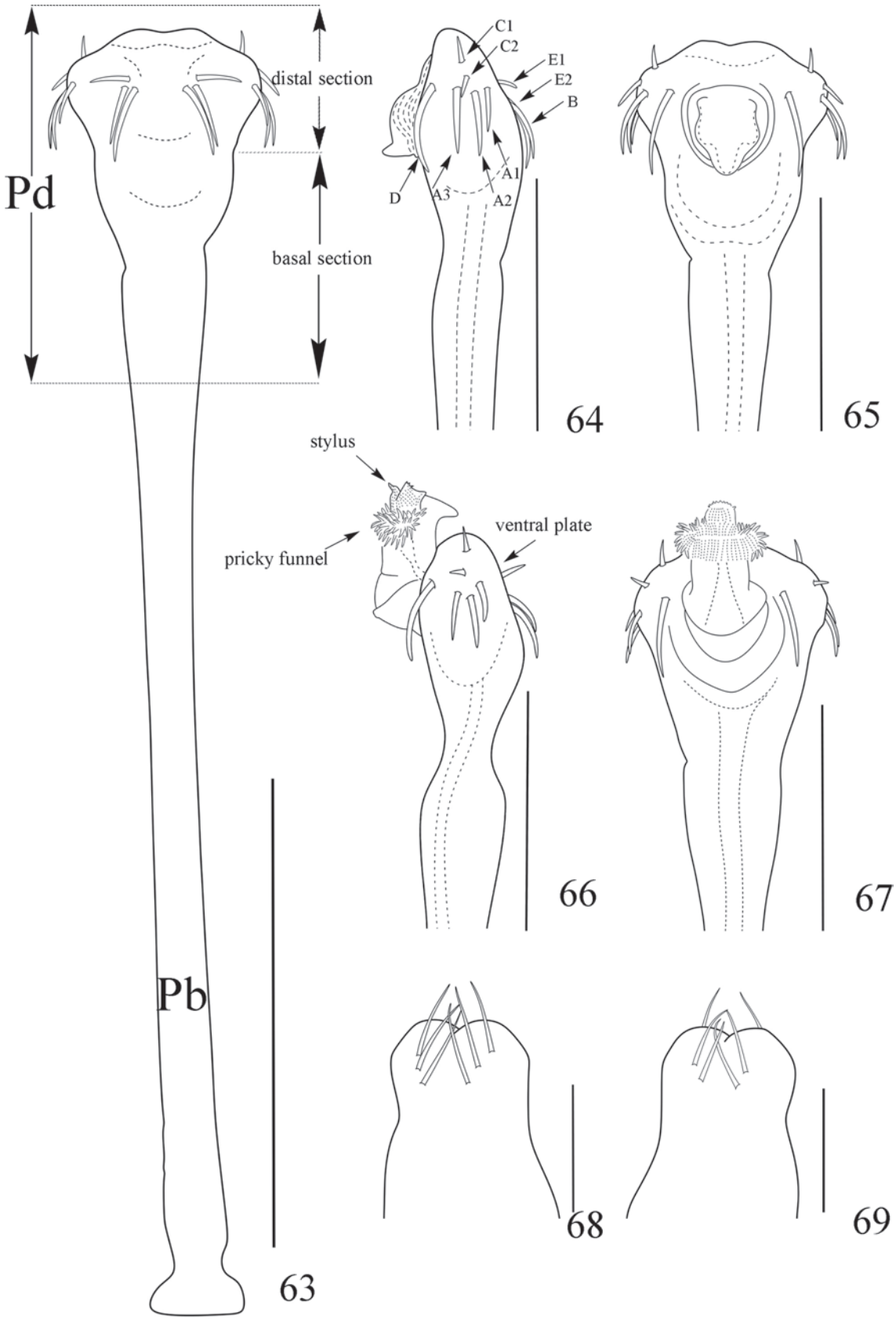

Figures 63–69. *Linzhiassamia zayuensis* sp. nov., genitalia of male paratype (**63–67**) and female paratype (**68–69**) **63** penis, ventral view **64** distal part of penis, lateral view **65** same, dorsal view **66** distal part of penis (expanded), lateral view **67** same, dorsal view **68** ovipositor, dorsal view **69** same, ventral view. Pb, pars basalis, Pd pars distalis. Scale bars: 0.5 mm (**63**); 0.25 mm (**64–69**).

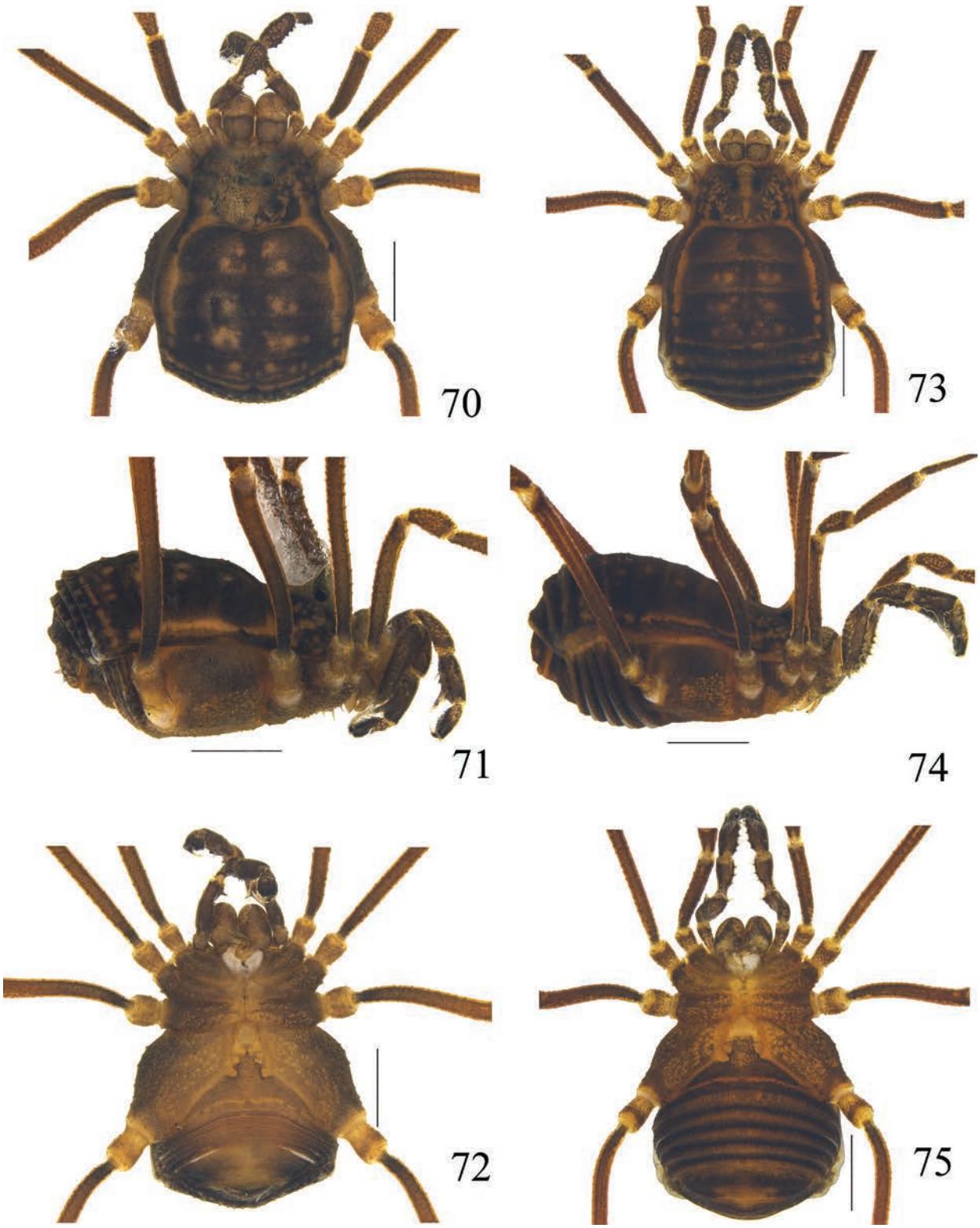

Figures 70–75. Photographs of male (**70–72** paratype) and female (**73–75** paratype) of *Linzhiassamia zayuensis* sp. nov. **70, 73** body and parts of appendages, dorsal view **71, 74** body and parts of appendages, lateral view **72, 75** body and parts of appendages, ventral view. Scale bars: 1 mm.

Venter (Fig. 47). Surface of all coxae tuberculated. Coxa I with a row of four tubercles prolaterally, and two rows of tubercles on the surface. Coxa II with a row of marginal tubercles on the prolateral surface, and disto-dorsally with an

enlarged tubercle. Coxa III with prolateral and retrolateral rows of tubercles. Coxa IV larger than others, prolaterally with a few scattered tubercles. Genital operculum with many hair-tipped granules. Free sternites with a row of minute tubercles. Spiracles concealed.

Chelicera (Figs 27–28, 34). Basichelicerite elongate, dorsally with a slight bulla, without prominent armaments. Cheliceral hand unarmed, with sparse hairs only. Fingers relatively short, inner edges toothed as illustrated (Fig. 34): moveable finger with 10 teeth, the proximal one enlarged; fixed finger with five teeth, the proximal one diminished.

Pedipalpus (Figs 29–31). Coxa dorsally with one small tubercle. Trochanter ventrally with one long distal setiferous tubercle. Femur compressed laterally, widest at the middle of its length, ventrally with a row of six homogeneous setiferous tubercles; dorsally with a row of six low conical tubercles along the entire length; on the medial distal side with one setiferous tubercle. Patella with two ventromesal setiferous tubercles and four ventroectal setiferous tubercles. Tibia ventromesally with two enlarged and two small setiferous tubercles; and ventroectally with one fairly enlarged and four setiferous tubercles. Tarsus with sparse hairs, ventromesally with two slightly enlarged and one small setiferous tubercle, and ventroectally with two slightly enlarged and five small setiferous tubercles. Tarsal claw slightly curved, shorter than tarsus.

***Legs*.** Slender and elongated. Trochanters I–IV with small hair-tipped granules on the ventral surface. All femora with hair-tipped granules, femora III and IV curved. Tarsi III–IV with a pseudonychium and two bare claws (Fig. 36). Tarsal formula (I–IV): 5(2)/9–10(3)/6/7. Distitarsus I two-jointed and II three-jointed. The remaining leg segments with hair-tipped granules.

Penis (Figs 38–42). Truncus (pars basalis) slender, sides nearly parallel, then slightly enlarged (Fig. 38). Distal portion of penis (pars distalis) markedly enlarged: ventral plate nearly triangle, convex in dorsal view and concave in ventral view (Figs 39, 41), distal margin smooth and without any indentation (Figs 38, 40). Glans partially sunken into dorsal depressed portion of pars distalis and not extending the distal margin of the ventral plate (Fig. 39). The glans is composed of three-quarters by the prickly funnel and capsula externa near the base, and one-quarter by the stylus and capsula interna (Fig. 41). Capsula externa cylindrical and capsula interna triangular, and the inner side of capsula interna with dense cover of fur-like microtrichia. Stylus with irregular shape, constricted apically, the inverted stylus with capsula interna sunken into the spiny funnel, and all parts mentioned above surrounded totally by the capsula externa (Fig. 41). Ventral plate with 18 setae (Figs 38–40): two dorsal, 10 lateral and six ventral.

Female (Figs 33, 35, 37, 48–50). In general appearance similar to the male (Figs 33, 48–50). The chelicerae are not enlarged and have a normal shape, with a slight difference in the inner edges of the cheliceral fingers compared to the males. The movable finger with 11 teeth and the fixed finger with seven teeth, both more than in males (Fig. 35). Pseudonychium of legs IV in female reduced compared to that of male (Fig. 37). Femora of pedipalpi dorsally with a row of six setiferous tubercles. Tarsal formula (I–IV): 5(2)/9–10(3)/6/7.

Ovipositor (Figs 43, 44). Ventral side with four, dorsal side with six setae.

Measurements. Male holotype (female paratype): body 3.42 (3.88) long, 2.33 (2.30) wide at the widest portion. Scutum 2.60 (1.74) long. Interocular mound 0.50 (0.54) long, 0.30 (0.23) wide, 0.19 (0.13) high, 0.19 (0.26) far from

the anterior border of the scutum. Pedipalpal claw 0.43 (0.33) long. Penis 1.34 long. Measurements of left pedipalpus and legs as in Tables 3, 4.

Habitat. These specimens were collected by sifting through the fallen leaves in the dark and humid undergrowth of the forest, as well as under stones and on the leaves of the shrubbery.

Distribution. Known only from the type locality, the Zayu County, Bome County, and Lulang Town, Nyingchi City, Xizang Autonomous Region, China.

Variation. Five male specimens were examined, displaying two distinct external morphologies, with a male paratype (MHBU-Opi-24ZC011901) chosen for discussion due to its differences from the male holotype (MHBU-Opi-24ZC011801). Compared to MHBU-Opi-24ZC011801, MHBU-Opi-24ZC011901 exhibits darker body coloration, there are no dark brown patches located on the sides of the anterior margin of the prosoma and larger dark brown patches on the opisthosomal areas I–IV (Figs 70–72). The carapace is shorter and rounder, with only two spines on each side of the anterior margin of the cephalothorax, ocularium armed with a conspicuous short median spine (Figs 51, 57, 70–71). Pedipalpus femur ventrally with a row of seven homogeneous setiferous tubercles, which has one more than MHBU-Opi-24ZC011801 (Figs 54–56). The chelicerae and inner edges of cheliceral finger show no significant differences (Figs 52, 53), the moveable finger with 10 teeth, fixed finger with six teeth (Fig. 59). There is no variation in pseudonychium of legs IV among male individuals. (Fig. 61).

Females also exhibit variation in morphological characteristics. Similar to the differences observed in males, females also display slight differences in body coloration (Figs 73–72). The number of spines on the anterior margin of carapace at the lateral portion from two to three, and the presence or absence of spines on the ocularium varies (Figs 73–75). Furthermore, the number of homogeneous setiferous tubercles on the pedipalpus femur ventrally ranges from six to seven. The chelicerae and inner edges of cheliceral finger show no

Table 3. *Linzhiassamia zayuensis* sp. nov. Measurements of the pedipalp and legs of the male holotype (MHBU-Opi-24ZC011801), as length/width.

	Trochanter	Femur	Patella	Tibia	Metatarsus	Tarsus	Total
Pedipalp	0.37/0.21	0.93/0.26	0.72/0.20	0.60/0.25		0.51/0.26	3.13
Leg I	0.31/0.23	1.32/0.18	0.59/0.24	1.06/0.17	1.49/0.07	0.71/0.07	5.48
Leg II	0.35/0.27	2.27/0.18	0.73/0.23	1.96/0.19	2.13/0.07	2.21/0.07	9.65
Leg III	0.43/0.34	1.69/0.19	0.62/0.31	1.22/0.24	1.91/0.12	1.14/0.08	7.01
Leg IV	0.52/0.36	2.41/0.19	0.79/0.36	1.74/0.26	2.78/0.16	1.54/0.10	9.78

Table 4. *Linzhiassamia zayuensis* sp. nov. Measurements of the pedipalp and legs of the female paratype (MHBU-Opi-24ZC011802), as length/width.1

	Trochanter	Femur	Patella	Tibia	Metatarsus	Tarsus	Total
Pedipalp	0.39/0.19	0.89/0.25	0.67/0.20	0.59/0.22		0.53/0.21	3.07
Leg I	0.29/0.21	1.30/0.19	0.58/0.20	0.98/0.17	1.40/0.07	1.02/0.06	5.57
Leg II	0.39/0.25	2.17/0.17	0.64/0.23	1.97/0.17	2.16/0.08	2.06/0.08	9.39
Leg III	0.37/0.27	1.71/0.20	0.57/0.26	1.11/0.21	1.86/0.08	1.19/0.07	6.81
Leg IV	0.43/0.26	2.27/0.22	0.66/0.27	1.55/0.21	2.82/0.09	1.52/0.07	9.25

significant differences, the moveable finger with 11 teeth, fixed finger with six teeth (Fig. 60). There is no variation in pseudonychium of legs IV and the ovipositor among females (Figs 62, 68, 69).

The observed external morphological differences initially led us to consider these as potentially separate species. However, upon dissecting the genitalia, we found remarkable similarities both before and after expansion, with only slight differences in the shapes of the stylus and prickly funnel (Figs 63–67). We speculate that these differences may be due to varying degrees of genitalia expansion. Despite the significant variations in external morphology, including coloration, interocular tubercles, pedipalp spines, and cheliceral teeth, our examination of the male genitalia did not reveal sufficient divergence to warrant the classification of distinct species at this time.

The Qinghai-Xizang Plateau is characterized by high altitude, thin atmospheric layers, and unique geographical and climatic conditions. These factors likely contribute to the observed morphological variations among specimens, particularly given the restricted gene flow between populations at different altitudes due to the limited dispersal capacity of harvestmen. While these variations may suggest the presence of more than one species, the current sample size and geographic coverage do not provide enough evidence to definitively separate these populations into distinct species. A more extensive collection of specimens from a broader range of localities is necessary before any formal taxonomic decisions can be made.

Discussion

The phylogenetic analysis by Palmieri et al. (2023) serves as an excellent foundation for comprehending the primary lineages of Assamiidae, particularly as they largely align with geographic distributions. However, the non-Afrotropical part of that study omits Himalayan species and only lightly addresses the Indian Trionyxellinae, primarily focusing on insular species (Dampetrinae).

We may endeavor to categorize the existing diversity of continental Asian Assamiidae into coherent groups of species, disregarding the Roewerian subfamilies which rely on superficial traits. This way, evaluating the affinities of any genus within Assamiidae becomes challenging due to the often concise nature of descriptions. To accurately categorize subfamilies, we should reduce each to their type genus, and ideally, to their type species if we wish to designate a subfamily by name.

a. The assamiids possessing tarsi III–IV with a tarsal process (often called "pseudonychium") were for a long time included together in the family Trionyxellidae Roewer, 1912, although there is no other evidence to assign these to a separate family. There are two subfamilies, the "true" Trionyxellinae and Mysoreinae, which should be restricted to southern India and Sri Lanka. This is the most poorly known group in Assamiidae, with no descriptions of genitalia.
b. Of the remnant pseudonychiate Asian assamiids, at least the species of *Paktongius* Suzuki, 1969 distributed in Laos and Thailand were said to possess a "gonyleptoid" condition: a lateral expansion of scutal areas III and IV and the hypertrophy of coxae IV (Klementz and Sharma 2023: 34). Some *Triaenopodium* Roewer, 1915 from Peninsular Malaysia, have similar genitalia and hints of this "gonyleptoid" condition (Suzuki 1976c:

figs 11, 12). Another possible representative of this group is *Bandona boninensis* Suzuki, 1974 from the Eastern Palearctic, with a male specimen from Yunnan depicted in Zhang et al. (2010: figs 1–16).

c. The Assamiinae sensu stricto having the distal part of the truncus shaped like an ice-cream scoop, with macrosetae elongated and prostrated. There are several examples from Nepal of this putative group, illustrated in Martens (1977), such as *Micrassamula* Martens, 1977 and *Nepalsioides* Martens, 1977 (Fig. 76). These "true" Assamiinae probably encompass species from Assam, West Bengal, Meghalaya, Arunachal Pradesh, Bangladesh, and Nepal.

d. There are also a few Assamiidae with strong sexual dimorphism on the chelicerae, and a peculiar genital configuration, which hail mostly from the highlands of Myanmar, Thailand, and Nepal. In *Euboeorix*, the distal truncus could be nicknamed "pancake bent": flattened dorso-ventrally, widening laterally towards the distal end until it curves and terminates as a semicircle. Possible representatives of this group are *Aboriscus* Roewer, 1940, *Euboeorix* Roewer, 1912, and *Dhaulagirius* Martens, 1977.

L. medogensis sp. nov. and *L. zayuensis* sp. nov. exhibit pseudonychiate tarsal claws, prompting comparisons with Indian Trionyxellidae such as *Nilgirius*. However, a preliminary examination of the genitalia of *Nilgirius scaber* Roewer, 1915 from southern India (Kury unpubl. data), reveals a markedly distinct genital structure. Our Tibetan species of *Linzhiassamia* also feature a pyriform distal truncus, which is not as depressed, with elongated macrosetae similar to

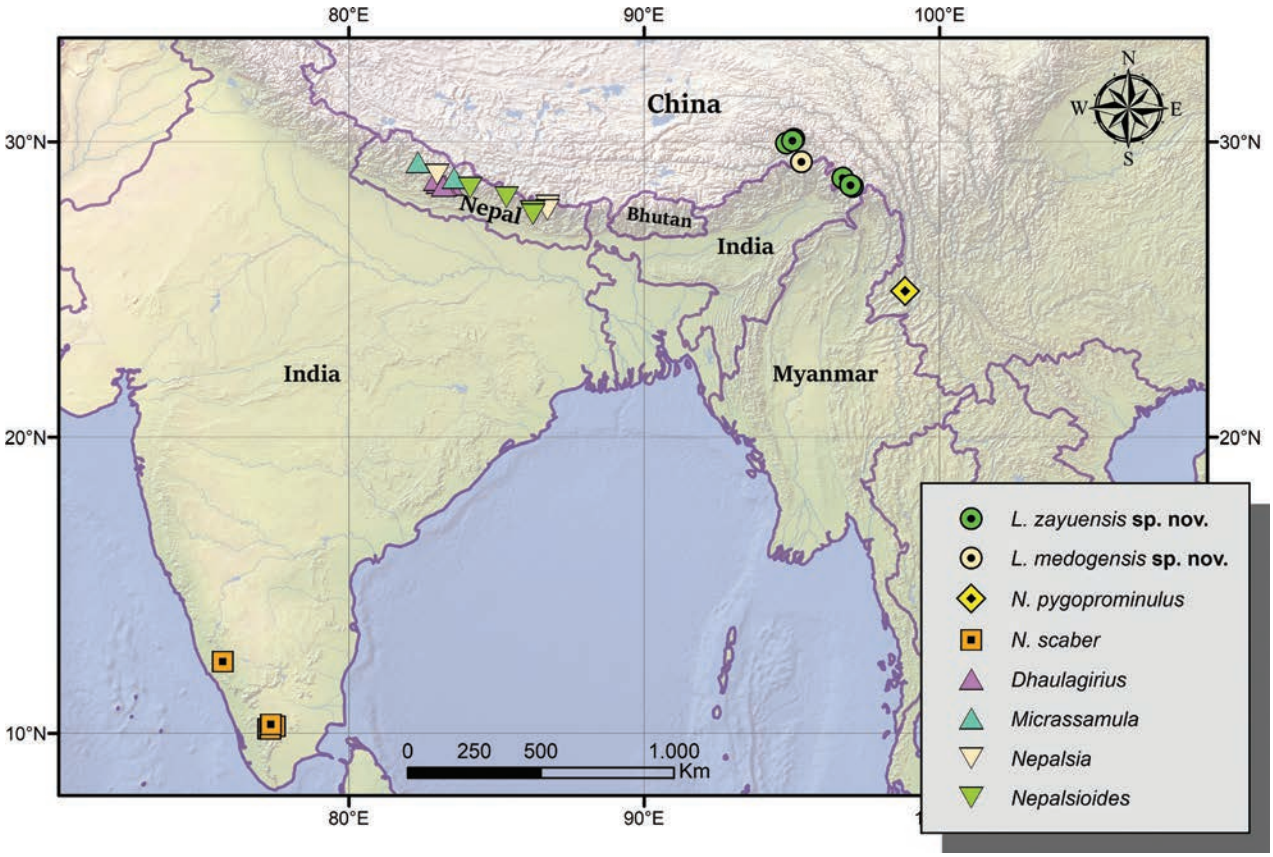

Figure 76. Eastern Himalaya and adjacent regions, showing the distribution of the species of *Linzhiassamia* and of probably related genera.

those observed in *Dhaulagirius altitudinalis* Martens, 1977. However, the sexual dimorphism in the chelicerae is much more subtle.

While a comparison with *Dhaulagirius* is not out of the question, defining suprageneric groups for these highlanders remains a distant prospect. Knowledge of the highlands of the Eastern Himalaya remains fragmentary. There are no assamiids known from Bhutan, and the few species known from Arunachal Pradesh come from modest altitudes (up to 600 m) with only limited descriptions by Roewer.

Acknowledgements

Many thanks are due to Peter Jäger for providing literature and to Luyu Wang, Hui Wang, Zhiyong Yang, and Yanmeng Hou for collecting the specimens. Special thanks are given to Willians Porto and Shahan Derkarabetian for insightful comments of the manuscript.

Additional information

Conflict of interest

The authors have declared that no competing interests exist.

Ethical statement

No ethical statement was reported.

Funding

This work was supported by (1) the Survey of Wildlife Resources in Key Areas of Tibet (ZL202203601) (2) # E-26/200.085/2019 (Apoio Emergencial ao Museu Nacional) from Fundação de Amparo à Pesquisa do Estado do Rio de Janeiro (FAPERJ) (3) # E-26/210.148/2019 (249116) (APQ1-Auxílio à Pesquisa básica- 2019) from Fundação de Amparo à Pesquisa do Estado do Rio de Janeiro (FAPERJ) (4) #311531/2019-9 (Produtividade em Pesquisa) from the Conselho Nacional de Desenvolvimento Científico e Tecnológico (CNPq) (5) #430748/2018-3 (Chamada MCTIC/CNPqN° 28/2018-Universal) from the Conselho Nacional de Desenvolvimento Científico e Tecnológico (CNPq) to ABK.

Author contributions

All authors have contributed equally.

Author ORCIDs

Xiaoru Qi https://orcid.org/0009-0006-9458-2532
Adriano B. Kury https://orcid.org/0000-0002-8334-6204
Chao Zhang https://orcid.org/0000-0003-1702-1206

Data availability

All of the data that support the findings of this study are available in the main text.

References

Bauer C, Prieto CE (2009) Three new Assamiidae (Arachnida: Opiliones) from Cameroon, with a redescription of *Chilon robustus* and comments on related species. Zootaxa 2059(1): 1–22. https://doi.org/10.11646/zootaxa.2059.1.1

Kauri H (1961) Opiliones. In: Hanström B, Brinck, P, Rudebeck G (Eds) South African Animal Life. Results of the Lund University Expedition in 1950–1951. Vol. 8. Almquist & Wiksell, Uppsala, 9–197.

Kauri H (1985) Opiliones from central Africa. Zoologische Wetenschappen (Annales du Musée Royal de l'Afrique Centrale). Sciences Zoologiques 245: 1–168.

Klementz BC, Sharma PP (2023) New species of *Paktongius* and convergent evolution of the gonyleptoid-like habitus in Southeast Asian Assamiidae (Opiliones: Laniatores). Zootaxa 5389(1): 034–054. https://doi.org/10.11646/zootaxa.5389.1.2

Kury AB (2007) Assamiidae Sørensen, 1884. In: Pinto-da-Rocha R, Machado G, Giribet G (Eds) Harvestmen: the Biology of the Opiliones. Harvard University Press, Cambridge and London, 173–176.

Kury AB, Machado G (2021) The genus *Eurytromma* from Sri Lanka: the homology of penial macrosetae in Podoctidae matches the gonyleptoid AE11 pattern (Opiliones: Laniatores: Epedanoidea). The Journal of Arachnology 49: 358–370. https://doi.org/10.1636/JoA-S-20-078

Kury AB, Medrano M (2016) Review of terminology for the outline of dorsal scutum in Laniatores (Arachnida, Opiliones). Zootaxa 4097(1): 130–134. https://doi.org/10.11646/zootaxa.4097.1.9

Kury AB, Mendes AC, Cardoso L, Kury MS, Granado A de A Giribet G, Cruz-López JA, Longhorn SJ, Medrano M, Oliveira ABR de, Kury IS, Souza-Kury, MA (2023) World Catalogue of Opiliones. WCO-Lite version 2.6. https://wcolite.com/ [Accessed on 2024-9-13]

Loman JCC (1902) Neue aussereuropäische Opilioniden. Zoologische Jahrbücher, Abteilung für Systematik, Ökologie und Geographie der Tiere 16(2): 163–216. https://doi.org/10.5962/bhl.part.17151

Lotz L (2011) Three new harvestmen species from southern Africa (Arachnida: Opiliones: Caddidae, Neopilionidae, Assamiidae). Journal of Afrotropical Zoology 7: 3–8.

Macías-Ordóñez R, Machado G, Pérez-González A, Shultz J (2010) Genitalic evolution in Opiliones. In: Leonard J, Córdoba-Aguilar A (Eds) The Evolution of Primary Sexual Characters in Animals. Oxford University Press, New York, 285–306.

Martens J (1977) Opiliones aus dem Nepal-Himalaya. III. Oncopodidae, Phalangodidae, Assamiidae (Arachnida). Senckenbergiana Biologica 57: 295–340.

Martens J (1986) Die Großgliederung der Opiliones und die Evolution der Ordnung (Arachnida). In: Barrientos JA (Ed.) Actas del X Congreso Internacional de Aracnología. Editorial Juvenil, Barcelona, 289–310.

Martens J (2021) Assamiidae from the Nepal Himalayas, including a new genus and a new species, with notes on *Dhaulagirius altitudinalis* Martens (Arachnida: Opiliones). In: Hartmann M, Barclay MVL, Weipert J (Eds) Biodiversität und Naturausstattung im Himalaya VII. Naturkundemuseum Erfurt, Erfurt, 175–184.

Martens J (2022) From the Ethiopian Bale Mountains hotspot—Filopalpinae subfam. nov., a new taxon of Laniatorean harvestmen based on external and genital morphology (Arachnida, Opiliones, Assamiidae). Zootaxa 5159(2): 221–244. https://doi.org/10.11646/zootaxa.5159.2.3

Mello-Leitão CF (1949) Famílias, subfamília, espécies e gêneros novos de opiliões e notas de sinonimia. Boletim do Museu Nacional 94: 1–33.

Palmieri L, Giribet G, Sharma PP (2023) Too early for the ferry: the biogeographic history of the Assamiidae of southeast Asia (Chelicerata: Opiliones, Laniatores). Molecular Phylogenetics and Evolution 178: 107647. https://doi.org/10.1016/j.ympev.2022.107647

Roewer CF (1912) Die Familien der Assamiiden und Phalangodiden der Opiliones-Laniatores. (= Assamiden, Dampetriden, Phalangodiden, Epedaniden, Biantiden, Zalmoxiden, Samoiden, Palpipediden anderer Autoren). Archiv für Naturgeschichte, Berlin, Abt. A, Original-Arbeiten 78(3): 1–242.

Roewer CF (1915) 106 neue Opilioniden. Archiv für Naturgeschichte, Berlin, Abt. A, Original-Arbeiten 81(3): 1–152.

Roewer CF (1923) Die Weberknechte der Erde. Systematische Bearbeitung der bisher bekannten Opiliones. Gustav Fischer, Jena, 1116 pp.

Roewer CF (1927) Weitere Weberknechte I. 1. Ergänzung der: "Weberknechte der Erde", 1923. Abhandlungen des Naturwissenschaftlichen Vereins zu Bremen 26(2): 261–402.

Roewer CF (1935) Alte und neue Assamiidae. Weitere Weberknechte VIII (8. Ergänzung der "Weberknechte der Erde" 1923). Veröffentlichungen aus dem Deutschen Kolonial-und Übersee-Museum in Bremen, Bremen 1(1): 1–168.

Roewer CF (1940) Neue Assamiidae und Trogulidae. Weitere Weberknechte X. Veröffentlichungen aus dem Deutschen Kolonial- und Übersee-Museum in Bremen 3(1): 1–31.

Santos R, Prieto C (2010) Los Assamiidae (Opiliones: Assamiidae) de Río Muni (Guinea Ecuatorial), con la descripción de ocho nuevas especies. Revista de Biologia Tropical 58(1): 203–243. https://doaj.org/article/4ed83522feb847e08547c2b4f76b36a8

Schwendinger PJ, Martens J (2002) A taxonomic revision of the family Oncopodidae III: Further new species of *Gnomulus* Thorell (Opiliones, Laniatores). Revue Suisse de Zoologie 109(1): 47–143. https://doi.org/10.5962/bhl.part.79580

Sørensen WE (1896) Opiliones Laniatores a cl. Dr. Yngwe Sjöstedt in Kamerun (Africa Centrali) collectos. Entomologisk Tidskrift 17(2–3): 177–202.

Staręga W (1992) An annotated check-list of Afrotropical harvestmen, excluding the Phalangiidae (Opiliones). Annals of the Natal Museum 33: 271–336. https://hdl.handle.net/10520/AJA03040798_283

Suzuki S (1969a) On a collection of opilionids from Southeast Asia. Journal of Science of the Hiroshima University 22: 11–77.

Suzuki S (1969b) Some phalangids from Thailand. Journal of Science of the Hiroshima University 22: 79–101.

Suzuki S (1976c) Report on a collection of opilionids from Pasoh Forest Reserve, West Malaysia. Nature and Life in Southeast Asia 7: 9–38.

Thorell TTT (1889) Aracnidi Artrogastri Birmani raccolti da L. Fea nel 1885–1887. In: Viaggio di Leonardo Fea in Birmania e regione vicine. XXI. Annali del Museo Civico di Storia Naturale di Genova 7(3): 521–729. https://doi.org/10.5962/bhl.title.10400

Thorell TTT (1890) Aracnidi di Nias e di Sumatra raccolti nel 1886 dal Sig. E. Modigliani. Annali del Museo Civico di Storia Naturale di Genova 10: 5–106. https://doi.org/10.5962/bhl.title.10511

Thorell TTT (1891) Opilioni nuovi o poco conosciuti dell'Arcipelago Malese. Annali del Museo Civico di Storia Naturale di Genova 10: 669–770.

Zhang C, Zhang F (2015) The assamiids harvestmen (Opiliones: Laniatores: Assamiidae) from Champasak Province, Laos. Zootaxa 3964(3): 335–351. https://doi.org/10.11646/zootaxa.3964.3.3

Zhang C, MacDermott J, Zhang F (2010) First Description of the male of *Bandona boninensis* Suzuki 1974 (Opiliones: Laniatores: Assamiidae). Acta Arachnologica 59(2): 87–91. https://doi.org/10.2476/asjaa.59.87

Zhao J, Cheng Z, Zhang C (2023) Description of *Nilgirius pygoprominulus* sp. n. (Opiliones, Assamiidae, Trionyxellinae) from China, with notes on its sexual dimorphism. Biodiversity Data Journal 11: e102954. https://doi.org/10.3897/BDJ.11.e102954

ZooKeys 1215: 53–64 (2024)
DOI: 10.3897/zookeys.1215.128976

Research Article

A new species of *Metaurus* Stål, 1866 (Hemiptera, Fulgoromorpha, Dictyopharidae), supplemented with mitogenome data from China

Yan-Li Zheng[1,2,3,4], Thierry Bourgoin[5], Lin Yang[2], Xiang-Sheng Chen[2]

1 *School of Geography and Resources, Guizhou Education University, Guiyang, Guizhou, China 550018, China*
2 *The Provincial Key Laboratory for Agricultural Pest Management of Mountainous Region; Institute of Entomology, Guizhou University, Guiyang, Guizhou 550025, China*
3 *Guizhou Provincial Key Laboratory of Geographic State Monitoring of Watershed, Guizhou Education University, Guiyang 550018, China*
4 *Mountain Research Institute, Guizhou Education University, Guiyang, Guizhou, China 550018, China*
5 *Institut Systématique, Evolution, Biodiversité (ISYEB), MNHN-CNRS-Sorbonne Université-EPHE-Univ. Antilles, Museum National d'Histoire Naturelle,75005, Paris, France*

Corresponding author: Xiang-Sheng Chen (chenxs3218@163.com)

Abstract

A new planthopper species, *Metaurus mohanensis* Zheng & Chen, **sp. nov.**, is described and illustrated from Yunnan, China. A key to differentiate species within the genus *Metaurus* is provided. The geographical distribution of *Metaurus* species and mitochondrial genome data of the newly described species are also included.

Key words: Auchenorrhyncha, distribution, Fulgoroidea, identification key, morphology, planthoppers, taxonomy

Academic editor: Mike Wilson
Received: 4 June 2024
Accepted: 4 September 2024
Published: 11 October 2024

ZooBank: https://zoobank.org/6C46F16B-B4D7-429C-A218-3967DE86DD81

Citation: Zheng Y-L, Bourgoin T, Yang L, Chen X-S (2024) A new species of *Metaurus* Stål, 1866 (Hemiptera, Fulgoromorpha, Dictyopharidae), supplemented with mitogenome data from China. ZooKeys 1215: 53–64. https://doi.org/10.3897/zookeys.1215.128976

Introduction

With a global distribution of 748 species across 160 genera (Bourgoin 2024), the family Dictyopharidae Spinola, 1839 represents a moderately sized taxon within the Hemiptera: Fulgoromorpha. Like all planthoppers, Dictyopharidae are strictly phytophagous insects, known to feed on over 25 families. Their diet predominantly includes dicots, particularly Asterales (13%), Caryophyllales (9%), Fabales (9%), and Fagales (7%), as well as monocots such as Poales (13%) and Liliales (7%) (Bourgoin 2024). Several dictyopharid species are recognized as economically significant agricultural pests (Wilson and O'Brien 1987; Wilson et al. 1994).

Dictyopharidae is currently classified into 19 tribes, plus two fossil ones, divided between two subfamilies: Dictyopharinae Spinola, 1839 and Orgeriinae Fieber, 1872 (Song et al. 2018; Bourgoin 2024). The genus *Metaurus* Stål, 1866 was initially placed in the tribe Dictyopharini Spinola, 1838, but was transferred to Orthopagini Emeljanov, 1983 by Emeljanov (2011) and later revised by Song and Liang (2012). In this latter study, the authors described a new species, *M. ramusitis* Song & Liang, 2012 from Laos and China (Yunnan), in addition to the type species *M. reticulatus* Stål, 1866 known from Cambodia. They also identified an unnamed species from Thailand, which is

definitively distinct but could not be formally described due to the absence of its abdomen.

We formally describe here a third species of *Metaurus* from Yunnan, China, *M. mohanensis* sp. nov. In addition to its morphological description, we also provide its complete mitogenome.

Materials and methods

Morphology

The specimens examined have been deposited in the Institute of Entomology, Guizhou University, Guiyang, China (GUGC). Dry specimens were used for the descriptions and illustrations. Genital segments of the specimens were macerated in a boiling solution of 10% NaOH, transferred to preparations of glycerin jelly, and examined under a Leica MZ12.5 stereomicroscope. Photographs of adult habitus were obtained using a Keyence VHX-1000 system. Illustrations were scanned with Canon Cano Scan LiDE 200 and imported into Adobe Photoshop CS6 for labeling and composition of figures.

The morphological terminology follows Yang and Yeh (1994) for the head and body, Bourgoin et al. (2015) for the forewing venation, and Bourgoin (1987, 1993) and Yang and Yeh (1994) for male and female genitalia, respectively. The usual standardized notation is used for the wing venation as follows: A1 first anal vein; bc, basal cell; CuA cubitus anterior; CuP cubitus posterior; MP: media posterior; R: radius; Sc: subcosta. The following abbreviations are used in the text for measurements: BL body length (from apex of cephalic process to tip of forewings); HL head length (from apex of cephalic process to base of eyes); HW head width (including eyes); FWL forewing length.

Biogeographical realms are named according to Holt et al. (2013).

Molecular methods

Total genomic DNA was extracted from the muscle tissue from the hind legs of the holotype specimen using the Takara Genome DNA Extraction Kit (Sangon Biotech, Shanghai, China) according to the manufacturer's instructions. The mitogenome was sequenced using a next-generation sequencing platform with Illumina Hiseq 2500 at OriGene (Beijing, China).

The quality of the raw sequences was evaluated using FastQC v.0.11.4 (www.bioinformatics.babraham.ac.uk/projects/fastqc). Putative mitogenome reads with an average quality value of < Q30 were removed before assembly. Then, the clean sequences were assembled using MitoZ v.2.4 software with default parameters and the mitogenome of *Orthopagus splendens* (Fulgoroidea: Dictyopharidae; GenBankNo. MW441850) as a reference (Zheng et al. 2021). The mitogenome was initially annotated using Galaxy Community 2022 with invertebrate genetic codes. PCGs were predicted by determining their open reading frames using the invertebrate mitochondrial genetic codon. rRNA genes and the AT-rich regions were determined by comparisons with the homologous sequences of other planthoppers from GenBank. Mitogenomic circular maps were depicted and annotated using Geneious R9. Strand asymmetry was calculated according to the following

formulas: AT skew = (A-T)/(A+T) and GC skew = (G-C)/(G+C). The mitogenome sequences of the new species have been deposited in GenBank under the accession number PP863288.

Taxonomy

Subfamily Dictyopharinae Spinola, 1839
Tribe Orthopagini Emeljanov, 1983

Genus *Metaurus* Ståhl, 1866

Metaurus Ståhl, 1866a: 151. Type species: *Metaurus reticulatus* Ståhl, 1866; by subsequent designation by Melichar (1912).
Metaurus Ståhl: Ståhl 1866b: 391; Atkinson 1886: 24; Melichar 1912: 46; Metcalf 1946: 38; Song and Liang 2012: 2564.

Diagnosis. See Song and Liang (2012).

Distribution. Oriental region (Cambodia; Laos; southwestern China; Thailand) (Song and Liang 2012).

Key to the species of *Metaurus* Ståhl (modified from Song and Liang 2012)

1 In lateral view, cephalic process in front of eyes distinctly longer than distance from curved point to posterior margin of eyes, with the ratio about 1.4: 1 ..... ***M.* indet. sp.**
– In lateral view, cephalic process in front of eyes slightly shorter or as long as distance from curved point to posterior margin of eyes **2**
2 In lateral view, cephalic process in front of eyes slightly shorter than distance from curved point to posterior margin of eyes, with the ratio about 0.7–0.8: 1. In dorsal view, segment X of males short and small, with ratio of the maximum length to width near base about 1.1: 1. In lateral view, apical ventral margins protruded ventrally into a small process. Aedeagus with ventral outer apical lobes curved anteriorly in ventral view..... ..... ***M. ramusitis* Song & Liang**
– In lateral view, cephalic process in front of eyes as long as distance from curved point to posterior margin of eyes. In dorsal view, segment X of males large and elongate, with ratio of the maximum length to width near base > 1.5. In lateral view, apical ventral margins protruded ventrally into a large rounded process. Aedeagus with ventral outer apical lobes directed posteriorly in ventral view **3**
3 In dorsal view, segment X of males with ratio of the maximum length to width near base about 1.6: 1; its ventral margins irregularly incised at midlength in lateral view. Aedeagus with ventral outer apical lobes directed posteriorly in ventral view ..... ***M. reticulatus* Ståhl**
– In dorsal view, segment X of males with ratio of the maximum length to width near base about 2.3: 1; its ventral margins only slightly concave, not incised at midlength in lateral view. Aedeagus with dorsal apical lobes (Figs 11, 16) produced in a pair of long lobes, directed posteriorly in lateral

view, and two lobes on it, base extends forward to form a leaf projection; ventral lobes (Figs 10, 17) with two pairs of lobes .... ***M. mohanensis* Zheng & Chen, sp. nov.**

***Metaurus mohanensis* Zheng & Chen, sp. nov.**
https://zoobank.org/9761682E-75C4-449E-BF12-10C12713C931

Type material. ***Holotype*** • ♂, China: Yunnan, Xishuangbanna Mengla County, Mohan, 16 June 2019, Feng-E Li (GUGC, no. GUGC-20220811-Y13). ***Paratypes*** • 2♂♂, same collection site as the holotype but 22 June 2019, Yalin Yao (GUGC).

Diagnosis. The new species is similar to *Metaurus ramusitis* Song & Liang, but can be distinguished from the latter by the shape of the phallobase and segment X: dorsal apical lobes of the phallobase (Figs 11, 16) produced in a pair of long lobes, directed posteriorly in lateral view, and two lobes on it, base extends forward to form a leaf projection in dorsal view (not in *M. ramusitis*). Segment X in dorsal view is relatively narrow, with ratio of the maximum length to width near base about 2.3: 1 (Fig. 13); ventral margin is protruded ventrally into a large rounded process at base in lateral view and slightly concave, not incised medially (Figs 8, 12); in *M. ramusitis*: segment X is relatively broader in dorsal view, and with an irregular incision medially in lateral view.

Description. Measurements (in mm). ♂, BL: 17.3–17.1 mm; HL: 3.6–3.7 mm; HW: 1.7–1.8 mm; FWL: 12–12.1 mm.

***Coloration*.** Body green. General colour greenish ochraceous; darker on apical part of cephalic process, on a longitudinal spot before eyes on genae, and on a small anterior spot on lower lateral carina behind eyes on pronotum. Rostrum blackish at extreme apex. Fore and hind wing membrane transparent, veins green, stigmal area green, anterior margin yellow. Legs green, apex of hind femora and base of hind tibiae black, tips of lateral spines on hind tibiae and tips of apical teeth on tarsomeres black.

***Morphology*.** Head and thorax (Figs 1–5). Cephalic process in front of eyes strongly upturned (about 45°), as long as distance from curved point to posterior margin of eyes in lateral view. Head shorter than pronotum and mesonotum combined, its ratio of length: width about 1:0.45 . Vertex relatively narrow, median longitudinal carina distinct only at the base, and lateral carina deeply concave and strongly tapered in front of the compound eyes. Frons elongate, with median carina complete and elevated, 2.5 times as long as wide, anterior portion distinctly narrowed and protruded anteriorly and upwardly in ventral and lateral views; lateral carinae ridged, frons distinctly expanded outwards below antennae. Postclypeus and anteclypeus strongly convex at middle, with distinct median carina. Rostrum long, extending up to abdominal sternite VI. Pronotum distinctly shorter than mesonotum medially, ratio length about 0.4:1, narrow anteriorly, broad posteriorly. Mesonotum tricarinate, lateral carinae incurved anteriorly towards median carina.

Forewings (Figs 1, 2, 6) hyaline, much longer than abdomen, nearly three times as long as broad; anterior margin distinctly expanded into a narrow, sclerotized costal area; costal cell without transverse veins, Sc+R forked apicad of junction of claval veins; MP first branching in MP_{1+2} and MP_{3+4} veins near basal one-third, anterior to first CuA branching, MP_{1+2} fork situated posterior to MP_{3+4}

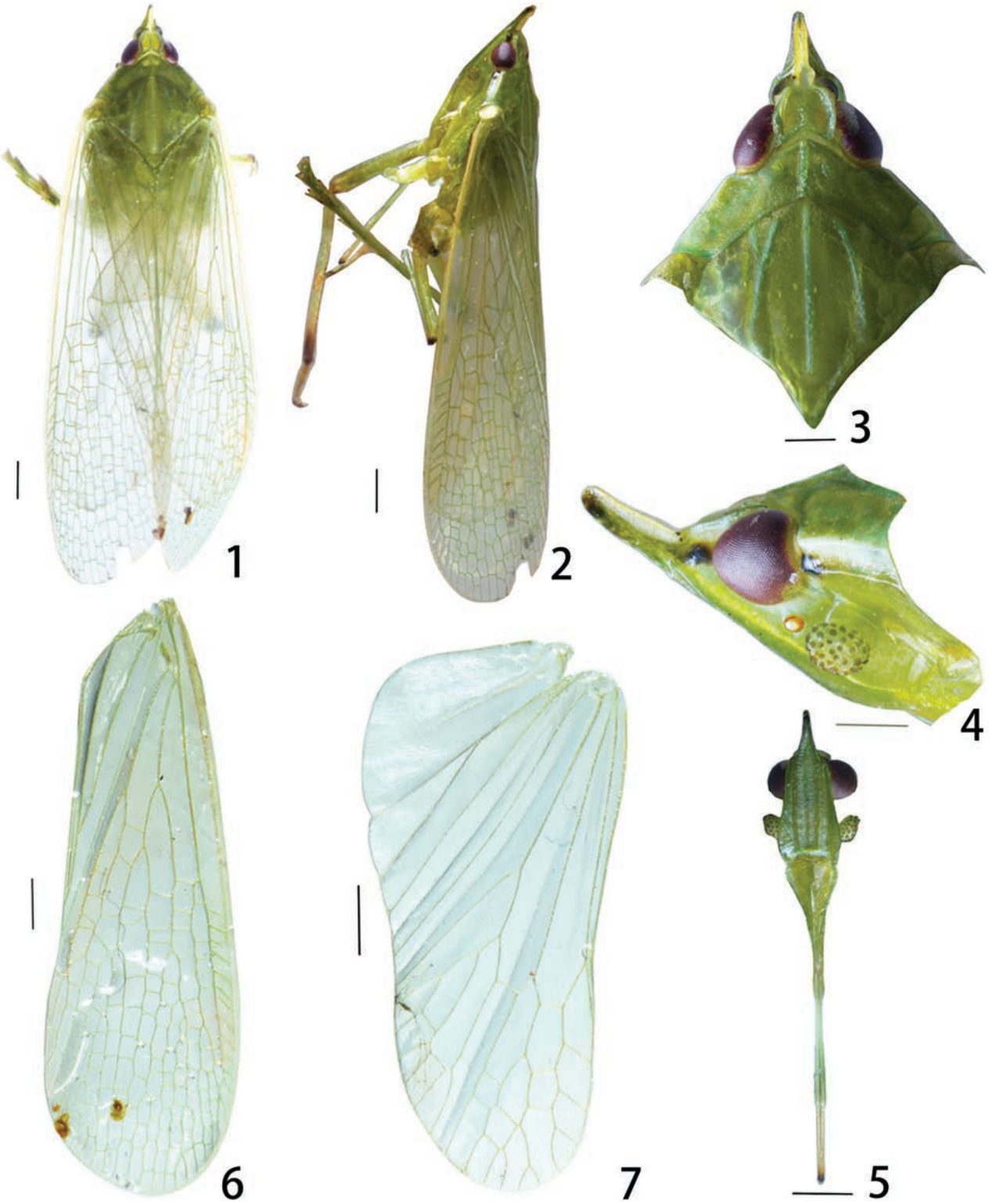

Figures 1–7. *Metaurus mohanensis* Zheng & Chen, sp. nov. **1** male, holotype, dorsal view **2** male, lateral view **3** male, head and thorax, dorsal view **4** male, frons and clypeus, ventral view **5** male, head and pronotum, lateral view **6** male, forewing **7** male, hind wing. Scale bars: 1 mm.

fork and then branching into a dozen of terminals; numerous transverse veins among Sc+R, MP and CuA on apical two-thirds; 22 apical cells; Pcu and A1 fused into a short Pcu+A1 vein at apical third of clavus; pterostigmal area not differentiated, elongate, with nine cells.

Hindwings (Fig. 7) hyaline. CuA first branching into CuA_1 and CuA_2 near middle; MP and CuA_1 branching to several accessory veins on apical two-thirds, with several transverse veins; 14 apical cells.

Legs narrow and long, fore femora flattened and dilated, with a distinct spine near apex, hind tibiae with 7 lateral spines and 7 apical teeth, hind tarsomeres I with 10 and tarsomeres II with 11 apical teeth. Metatibiotarsal formula: 7-7/10:11

***Male genitalia*.** Pygofer large and broad, ventrally distinctly longer than dorsally (about 5: 1); posterior margin with two obtuse processes near middle in lateral view (Figs 8, 12), upper process slightly smaller than lower one. Segment X (anal tube) large and broad in dorsal view, with ratio of the maximum length to width near base about 2.3: 1 (Figs 8, 12, 13); ventral margins in basal third protruded ventrally into a large triangular process in lateral view. Gonostyli relatively small in lateral view, posterior margin with directed tooth-like dorsal process medially and a directed tooth-like ventral process submedially on outer upper edge; apical part elongate and rounded (Figs 8, 12, 14); dorsal process short, acute apically. Aedeagus (Figs 9–13) large and robust, dorsal and lateral parts and most of ventral part of phallobase sclerotized and pigmented, the remainder membranous; with 3 pairs of apical membranous lobes; dorsal apical lobes (Figs 15, 16) long, directed posteriorly in lateral view, each bearing two smaller projections (Figs 15c, 16c) on it, base extending forward to form a leaf-like projection (Figs 15a, 16a); ventral lobes (Figs 10, 15, 17) large and slender, with two pairs of projections (Figs 10, 15, 17): the inner ones very slender (Figs 15f, 17f), directed posteriorly, with additional two smaller membranous projections on their median part (Fig. 17h), and one large basal lobe (Figs 15d, 17d); the outer ones slender and elongate, directed posteriorly (Fig. 17e), with two small projections medially in ventral view (Figs 15g, 17g).

Etymology. The species name *"mohanensis"* refers to the collecting site in the town of Mohan, in the Yunnan Province in southwestern China. Adjective.

Mitochondrial genome of the new species

The complete mitogenome of *Metaurus mohanensis* Zheng & Chen, sp. nov. is 15,469 bp in length and consists of 13 protein-coding genes (PCGs), 2 ribosomal RNA genes (rRNAs), 22 transfer RNA genes (tRNAs) and one large non-coding region (D-loop: [A+T]-rich region) (Fig. 18). The D-loop part is 1233 bp, taking place between 12S rRNA and trnI. The overall base composition is A: 48%, T: 28.8%, C: 15%, and G: 8.2%. AT skew ((A-T)/(A+T)) and GC skew ((G-C)/(G+C)) are 0.25 and - 0.293, respectively. All 13 PCGs started with ATN, GTG (nad1, nad5) and ended with TAN or a single T (nad1, nad4, atp6 and nad5) residue. The length of 22 tRNA ranged from 57 bp (trnV) to 70 bp (trnK). Genes of 16S rRNA and 12S rRNA are 1, 201 bp and 732 bp, respectively.

The genomic data from this study are openly available in the National Center for Biotechnology Information (NCBI) at https://www.ncbi.nlm.nih.gov, accession number: PP863288. Associated BioProject, SRA, and BioSample accession numbers are PRJNA1114399, SUB14549433 and SAMN41484364 respectively (https://www.ncbi.nlm.nih.gov/bioproject/PRJNA1114399).

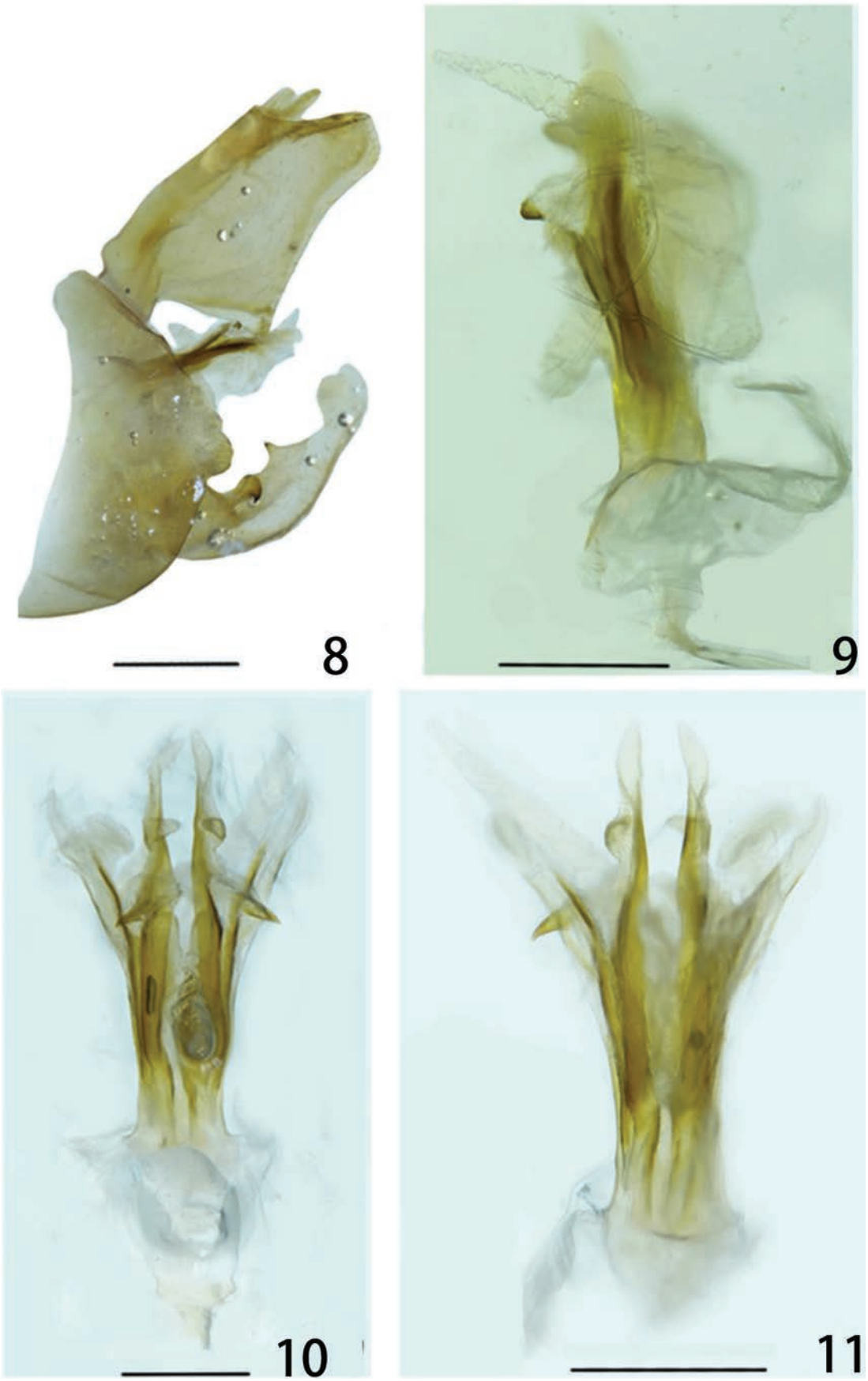

Figures 8–11. *Metaurus mohanensis* Zheng & Chen, sp. nov. **8** genitalia, lateral view **9** aedeagus, lateral view **10** aedeagus, ventral view **11** aedeagus, dorsal view. Scale bars: 1 mm (**8**); 0.5 mm (**9–11**).

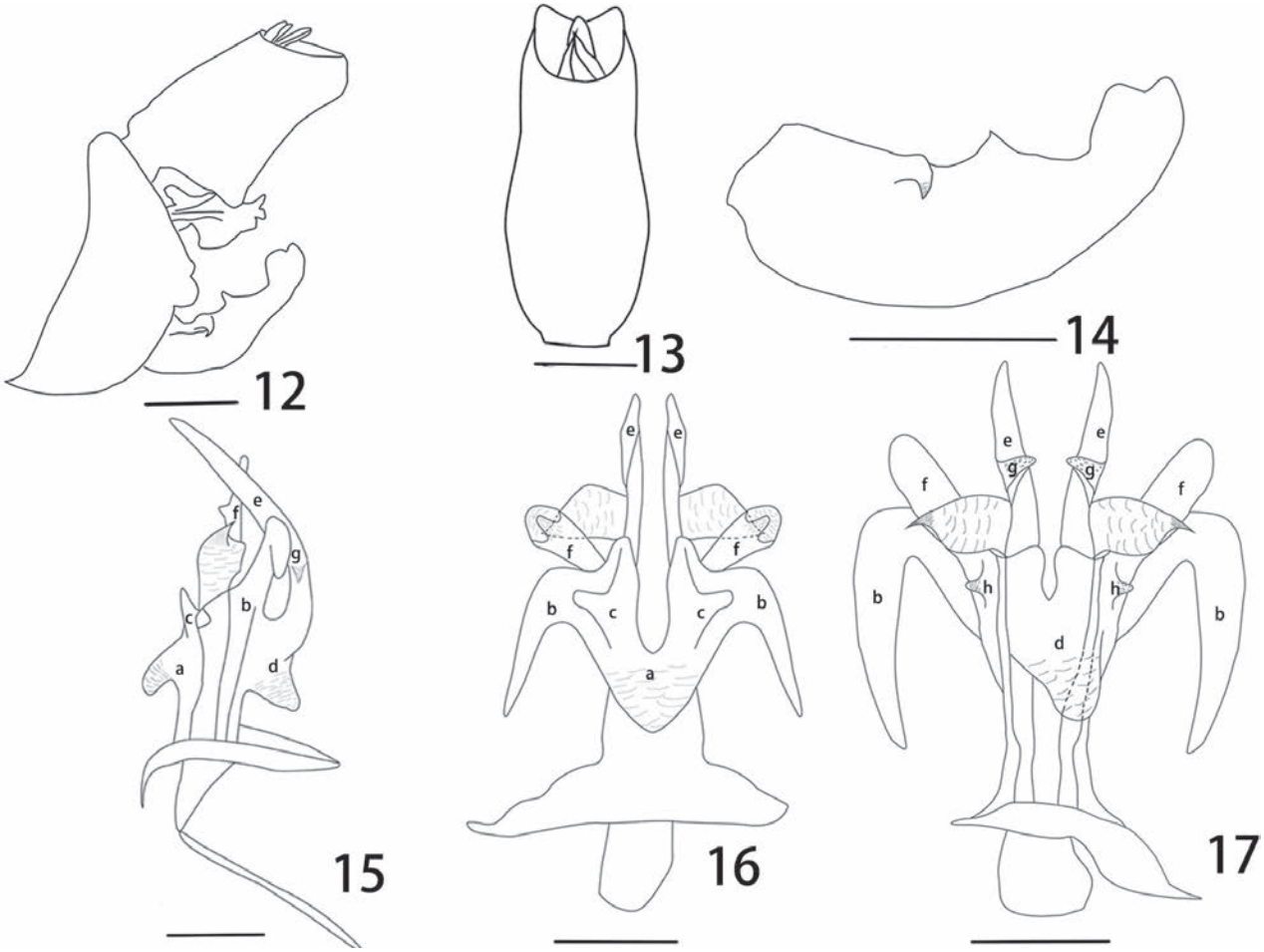

Figures 12–17. *Metaurus mohanensis* Zheng & Chen, sp. nov. **12** genitalia, lateral view **13** segment X, dorsal view **14** gonostyles, lateral view **15** aedeagus, lateral view **16** aedeagus, dorsal view **17** aedeagus, ventral view **a–h** 3 pairs of apical membranous lobes (same letters representing the same parts). Scale bars: 1 mm (**12**); 0.5 mm (**13–17**).

Discussion and conclusions

The Oriental genus *Metaurus* exhibits a continental distribution in southeastern Asia, being restricted to Thailand, Cambodia, Laos and southwestern China(-Fig. 19). *Metaurus ramusitis* Song & Liang, 2012 is known from Laos and only by one female from Yunnan, China. The new species in this study was also collected from Yunnan, China.

Species of *Metaurus* are externally quite similar to those of *Centromeria* Stål, 1870, a more diversified genus of Orthopagini with 14 species known to date (Song et al. 2016; Bourgoin 2024), but with a wider southeastern Asian distribution corresponding to the Oriental zoogeographic region as defined by Holt et al. (2013). *Metaurus* can be separated from *Centromeria* by the following characters: 1) Head in front of the eyes is strongly upturned, forming a slender, straight process, with the vertex's median carina only weakly ridged at the base (versus a frontal process that is moderately to strongly curved upwards in *Centromeria*); the vertex in *Centromeria* has lateral carinae that are moderately or abruptly constricted, strongly upturned in front of the eyes, and then gradually convergent anteriorly, culminating in an acuminate apex; 2) MP vein first forks into MP_{1+2} and MP_{3+4} veins before CuA, close to the basal one-third of corium,

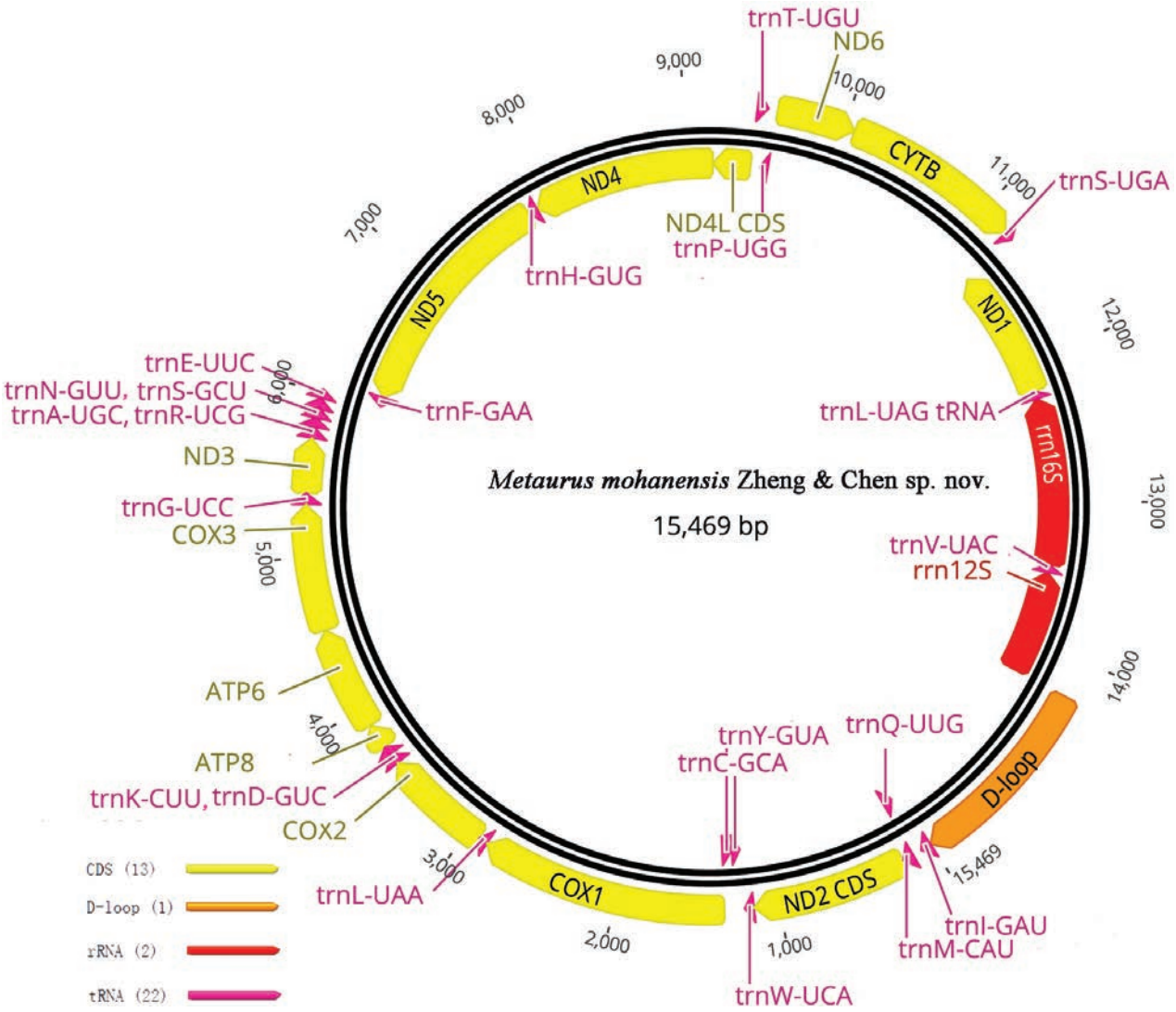

Figure 18. Circular map of the mitogenome of *Metaurus mohanensis* Zheng & Chen, sp. nov.

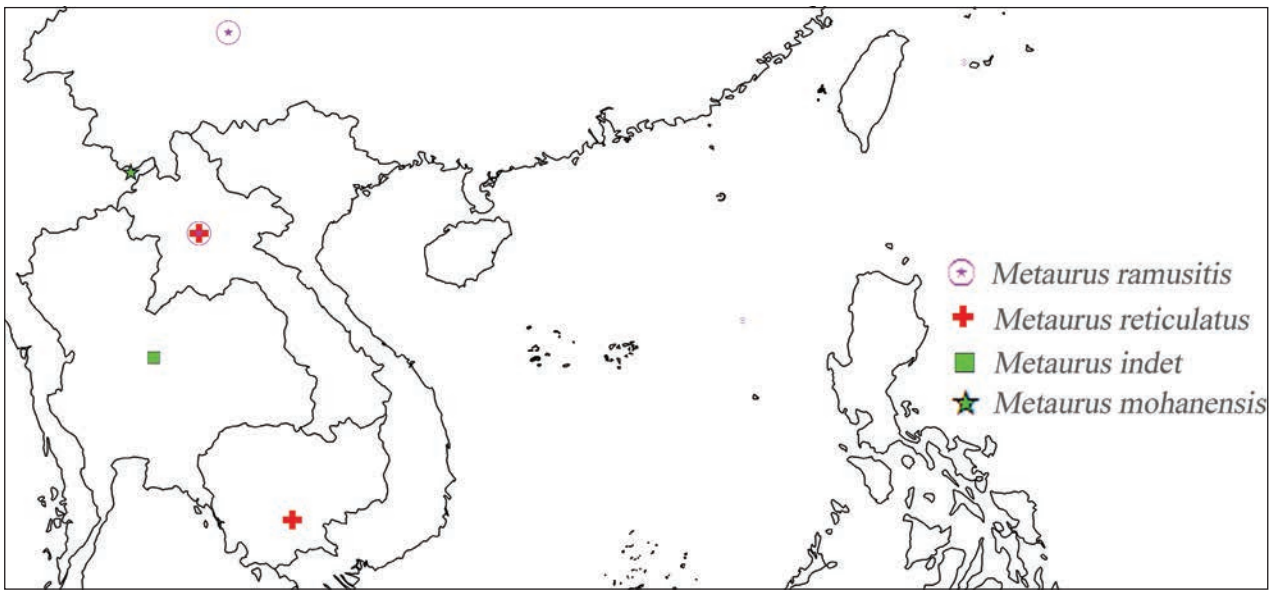

Figure 19. Geographical distribution of *Metaurus* species.

which is branched and with numerous accessory veins on the apical two-thirds of the corium (while MP bifurcating into MP_{1+2} and MP_{3+4} near middle, and posterior to CuA in *Centromeria*); and 3) Hind tibiae in *Metaurus* have 7 apical teeth, compared to only 6 apical teeth in *Centromeria*.

The mitogenome of *Metaurus mohanensis* Zheng & Chen, sp. nov. differs from *Orthopagus splendens* (Fulgoroidea: Dictyopharidae: Orthopagini; GenBankNo. MW441850) (Zheng, Bourgoin et al. 2021) by the following characteristics: 1) full length 15469 (15346 in *O. splendens*); 2) overall base composition: A: 48%, T: 28.8%, C: 15%, and G: 8.2%. AT skew ((A-T)/(A+T)) and GC skew ((G-C)/(G+C)) 0.25 and - 0.293, respectively (versus A: 47.2%, T: 30.2%, C: 14.6%, and G: 8%. AT skew ((A-T)/(A+T)): 0.22 and GC skew ((G-C)/(G+C)): - 0.294 in *Orthopagus splendens*); and 3) In *M. mohanensis*, all 13 PCGs start with ATN or GTG (nad1, nad5) and end with TAN or a single T (nad1, nad4, atp6 and nad5) residue. The length of 22 tRNA ranges from 57 bp (trnV) to 70 bp (trnK). Genes of 16S rRNA and 12S rRNA are 1,201 bp and 732 bp, respectively. In *O. splendens*, all 13 PCGs start with ATN and end with TAN or a single T (nad1, nad5 and atp6) residue. The length of 22 tRNA ranges from 59 bp (trnS) to 70 bp (trnK). Genes of 16S rRNA and 12S rRNA are 1,177 bp and 729 bp, respectively.

Additional information

Conflict of interest

The authors have declared that no competing interests exist.

Ethical statement

No ethical statement was reported.

Funding

The project was supported by the 2021 Guizhou Normal University award and subsidy fund project (No. 2023GZJB009); Guizhou Provincial Department of Education College Humanities Society, scientific research project No. 23RWJD191; Scientific research fund project of Guizhou Normal University (No. 2021ZD001).

Author contributions

All authors have contributed equally.

Author ORCIDs

Yan-Li Zheng https://orcid.org/0000-0002-6964-5988
Thierry Bourgoin https://orcid.org/0000-0001-9277-2478

Data availability

All of the data that support the findings of this study are available in the main text.

References

Atkinson ET (1886) Notes on Indian Rhynchota. No. 5. Journal of the Asiatic Society of Bengal 55: 12–83.

Bourgoin T (1987) A new interpretation of the homologies of the Hemiptera male genitalia, illustrated by the Tettigometridae (Hemiptera, Fulgoromorpha). In: Vidano C, Arzone A, Consiglio nazionale delle ricerche (Eds) Proceedings of the 6th Auchenorrhyncha meeting Turin, Italy, 7–11 September, 113–120.

Bourgoin T (1993) Female genitalia in Hemiptera Fulgoromorpha, morphological and phylogenetic data. Annales de la Société Entomologique de France (Nouvelle Série) 29: 225–244. https://doi.org/10.1080/21686351.1993.12277686

Bourgoin T (2024) FLOW (Fulgoromorpha Lists On the Web), a world knowledge base dedicated to Fulgoromorpha. Version 8. [accessed 2024-5-1]

Bourgoin T, Wang RR, Asche M, Hoch H, Soulier-Perkins A, Stroiński A, Yap S, Szwedo J (2015) From micropterism to hyperpterism: recognition strategy and standardized homology-driven terminology of the forewing venation patterns in planthoppers (Hemiptera: Fulgoromorpha). Zoomorphology 134 (1): 63–77. https://doi.org/10.1007/s00435-014-0243-6

Emeljanov AF (2011) Improved tribal delimitation of the subfamily Dictyopharinae and description of new genera and new species (Homoptera, Fulgoroidea, Dictyopharidae). Entomologicheskoe Obozrenie 90: 299–328. [English translation in Entomological Review 91: 1122–1145, 2011] https://doi.org/10.1134/S0013873811090053

Holt BG, Lessard JP, Borregaard MK, Fritz SA, Araujo MB, Dimitrov D, Fabre PH, Graham CH, Graves GR, Jonsson KA, Nogues-Bravo D, Wang ZH, Whittaker RJ, Fjeldsa J Rahbek C (2013) An update of Wallace's zoogeographic regions of the world. Science 339(6115): 74–78. https://doi.org/10.1126/science.1228282

Melichar L (1912) Monographie der Dictyophorinen (Homoptera). Abhandlungen der K. K. Zoologisch-Botanischen Gesellschaft in Wien 7(1): 1–221. [In German]

Metcalf ZP (1946) General catalogue of the Hemiptera, Fasc. IV. Fulgoroidea, Part 8 Dictyopharidae. Smith College, Northampton, MASS., 246 pp.

Song ZS, Liang AP (2012) Taxonomic revision of the Oriental genus *Metaurus* Stål (Hemiptera: Fulgoromorpha: Dictyopharidae), with description of a new species. Journal of Natural History 46: 41–42, 2563–2575. https://doi.org/10.1080/00222933.2012.708456

Song ZS, Webb MD, Liang AP (2016) Phylogenetic analysis of the Oriental genera of Orthopagini Emeljanov, 1983 (Hemiptera: Fulgoromorpha: Dictyopharidae: Dictyopharinae), with a systematic revision of the genus *Centromeria* Stål, 1870. Zoological Journal of the Linnean Society 178: 33–87. https://doi.org/10.1111/zoj.12401

Song ZS, Bartlett CR, O'Brien LB, Liang AP, Bourgoin T (2018) Morphological phylogeny of Dictyopharidae (hemiptera: fulgoromorpha). Systematic Entomology 43(4): 637–658. https://doi.org/10.1111/syen.12293

Stål C (1866a) Hemiptera Homoptera Latr. Hemiptera of Africa 4: 1–276.

Stål C (1866b) Analecta Hemipterologica. Berliner entomologische Zeitschrift 10: 381–394. https://doi.org/10.1002/mmnd.18660100410

Wilson SW, O'Brien LB (1987) A survey of planthoppers pests of economically important plants (Homoptera: Fulgoroidea). In: Proceedings of the 2nd Inter. Workshop on Leafhoppers and Planthoppers of Economic Importance. Commonwealth Institute of Entomology, London, 343–360.

Wilson SW, Mitter C, Denno RF, Wilson MR (1994) Evolutionary patterns of host plant use by delphacid planthoppers and their relatives. In: Denno RF, Perfect J (Eds) Planthoppers: Their Ecology and Management. Chapman and Hall, New York, 7–113. https://doi.org/10.1007/978-1-4615-2395-6_2

Yang CT, Yeh WB (1994) Nymphs of Fulgoroidea (Homoptera: Auchenorrhyncha) with descriptions of two new species and notes on adults of Dictyopharidae. Chinese Journal of Entomology, Special Publication 8: 1–187.

Zheng YL, Bourgoin T, Yang L, Chen XS, Luo XQ, Luo GJ (2021) Complete mitochondrial genome of the planthopper *Orthopagus splendens* (Germar, 1830) (Hemiptera: Fulgoromorpha: Dictyopharidae). Mitochondrial DNA, B 6: 2667–2668. https://doi.org/10.1080/23802359.2021.1964400

ZooKeys 1215: 65–90 (2024)
DOI: 10.3897/zookeys.1215.130416

Forum Paper

A survey of keys for the identification of newly described insect genera: recommendations for authors, reviewers, editors, and publishers

Laurence Packer[1]

1 *Department of Biology, York University, 4700 Keele St., Toronto, ON M3J 1P3, Canada*
Corresponding author: Laurence Packer (xeromelissa@gmail.com)

Abstract

Large numbers of new taxa are described annually and while there is a great need to make them identifiable, there seems little consistency in how this might be facilitated. 427 papers published in 2021 and 2022 were surveyed, which described 587 new insect genera. Only 136 of these papers included keys, and these allowed the identification of 233 of the new genera (31.9% of papers and 39.7% of the new genera). The proportion of papers that included a key varied significantly among insect orders but not among the handful of journals wherein the bulk of the new genera were described. Overall, for 17 key-related variables assessed in a binary fashion (optimal vs suboptimal), the average key had almost six criteria that were scored as being suboptimal. For example, less than one-fifth facilitated retracing and less than 12% had illustrated keys where the images were conveniently located close to the relevant key couplets. Progress towards confirming a putative identification was possible in all papers, through the inclusion of a diagnosis, habitus images, or both.

Based upon this analysis, and expanding on previous suggestions for key construction, 23 recommendations are made on how to make an identification key maximally useful for users and I indicate the relative ease with which each could be adhered to. Identification keys should accompany all new taxon descriptions, guidelines for effective key construction should be added to journals' instructions to authors, editors and reviewers should check keys carefully, and publishers should be attentive to the needs of users through, for example, permitting duplication of images to make keys easier to use. Recommendations are likely relevant to all levels in the taxonomic hierarchy for all organisms, despite the data being derived from generic-level keys for insects.

Key words: Best practices, biodiversity assessment, ease-of-use, entomology, identification keys, images, key construction guidelines, taxonomy

OPEN ACCESS

Academic editor: Fedor Konstantinov
Received: 24 June 2024
Accepted: 30 August 2024
Published: 11 October 2024

ZooBank: https://zoobank.org/A9D55886-E95E-4620-9B2E-27DA6B42E9E4

Citation: Packer L (2024) A survey of keys for the identification of newly described insect genera: recommendations for authors, reviewers, editors, and publishers. ZooKeys 1215: 65–90. https://doi.org/10.3897/zookeys.1215.130416

"… the most important impact of taxonomy is the usage of identification keys"
(Krell 2002)

Introduction

With increasing concern about declines in abundance and diversity of insects (e.g., Didham et al. 2020; Wagner 2020; Sánchez-Bayo and Wyckhuys 2021), there is a growing need for efficient tools to identify them. Yet resources to permit insect identifications are scattered and diverse, vary greatly in how easy they are to use and the extent to which they are taxonomically and/or geographically relevant. Furthermore, new taxa are being described at a high rate, but despite the recommendations of Walter and Winterton (2007), there seem to be no consistently applied criteria as to how they are to be made readily identifiable by others.

There are four means whereby new taxa can be made identifiable by those other than the original author(s): the diagnosis, the description, illustrations, and an identification key. In this paper I assess the current status of the identification keys (if provided) that accompany the description of new insect genera. I also assess the frequency with which the keys referred to appropriate illustrations and whether diagnoses were also provided (a formal assessment of the nature of insect genus level diagnoses is in preparation). Accurate assessment of the quality of descriptions for a wide range of insect taxa is likely beyond the ability of any one entomologist and I also do not assess the validity of the new genera as this would require a deep understanding of the systematics of most of the world's known biota. However, it is worth noting that a small minority of new genus descriptions were associated with the phylogenetic information that would provide a thorough justification (pers. obs.).

Generic level keys were chosen for assessment because their number was expected to be tractable for analyses for all insect orders for which new genera were described and thus the results of this analysis should be broadly applicable to entomological taxonomic research. Furthermore, at publication, the information in the paper describing a new genus would likely be the only way it could be identified. Consequently, I assessed papers for newly described insect genera published over two years starting from January 2021 to see whether they included an identification key and if so, how well the key fit a range of criteria (see below).

Methods

I searched for relevant papers using Scopus searches for "new gen*" or "gen* n*" for all insect orders (including names that are not generally in current use such as Heteroptera, Homoptera, and Isoptera), during the time period January 2021 to December 2022. The journal Entomological Review publishes translations of papers originally in Russian wherein taxonomic acts often formally date to the year previous. Those discovered in English translation in the above two years were included in the sample. Papers were downloaded using Google Scholar, ResearchGate, or the library resources available to me at York

University. I requested PDFs from corresponding authors of papers in Zootaxa (wherein the largest number of new insect genera were described) when these were not otherwise available. I separated out those papers that included one or more identification keys for analysis. Those that did not include a key were not investigated further except for calculation of the proportion of papers that included a key and the proportion of new genera that were associated with an identification key. This was calculated separately for each insect order and journal as well as in aggregate.

Five journals had far more new genus descriptions than others and in the text below they are denoted by the following abbreviations: **EJT** – European Journal of Taxonomy, **SE** – Systematic Entomology, **ZJLS** – Zoological Journal of the Linnean Society, **ZK** - ZooKeys, **ZT** – Zootaxa.

I did not include papers that dealt solely with fossil taxa because of the difference in approaches required with the study of such material. Similarly, I only included keys to adult insects unless adults were not treated in the paper as is commonly the case with some groups (Ephemeroptera, Aleyrodidae, male Strepsiptera).

Some keys treating new genera also included fossils and/or taxa above or below the level of genus (e.g., tribes, genus groups, subgenera, species) or included couplets that led to groups that were not further treated in the key. In such cases, only couplets that eventually led to a generic level identification were included in numerical analyses. However, if a couplet that led to a different taxonomic level in one lead, but to further couplets leading to genera in the other, these were included among the statistics with respect to both the number of couplets required to get to a generic level identification and the proportion of leads that were illustrated. As a result of these issues, the number of couplets assessed and included in tabulations sometimes differed from those in the published key.

Some papers provided more than one genus-level key either because males and females were treated separately (*n* = 3 papers, Cumming et al. 2021; Cumming and Le Tirant 2022; Benda et al. 2022) or because the new taxa belonged to different intermediate taxonomic levels (*n* = 2 papers, Brunke 2021, Sharkey et al. 2021). Thus, the number of keys assessed was slightly larger than the number of papers that included keys.

Terms associated with key structure are shown in Fig. 1. This is a hypothetical example couplet for a dichotomous key where features are treated in parallel. Most, but not all, keys followed this approach (see below). Each half of a dichotomous couplet is termed a lead and when more than one discriminating aspect of the organisms is included, they are henceforth called features (note that Walter and Winterton (2007), among others, use the terms character and character state for the same key components, but it seems desirable to avoid those words due to their usage in phylogenetics). It is common for authors to add ancillary information that might not be perfectly discriminatory of the groups defined by the two leads. Such information may be helpful and is usually shown in brackets before the next couplet number or the identification. Ancillary information commonly includes geographic features as in the example given below. I did not assess ancillary information as it is, by design, not decisive.

For each of the keys, I assessed the variables outlined below. Initially, I used the criteria noted by Walter and Winterton (2007: table 2) but it rapidly became

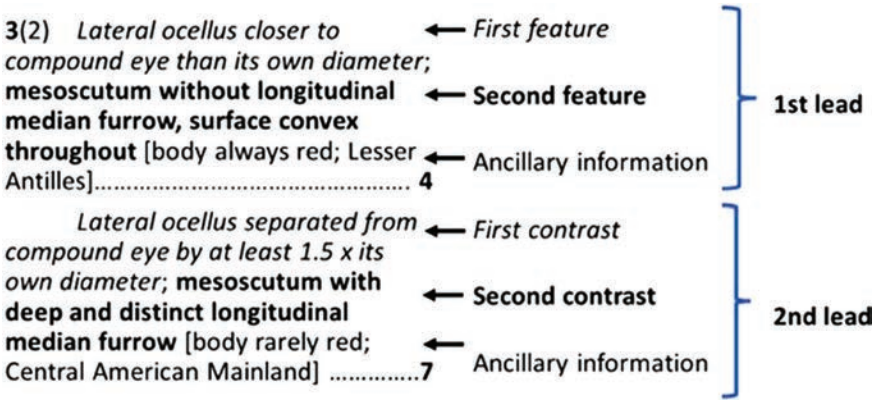

Figure 1. Schematic of a key couplet to outline some terms used in this paper.

evident that there were additional issues that required consideration. When the same, or a similar, topic was treated by them the fact is denoted by WW# where # relates to the number in their table 2.

i) Was the text freely available and was the key in the main body of the paper or as supplementary materials only? This was assessed at two levels of availability: a) generally freely available through Google Scholar searches for open access papers among those included in the sample and, if not, b) whether the paper was freely available through subscription content available through York University Libraries [this involves a system called Omni, which is the discovery service used by a large proportion of universities in Ontario]. I note that institutions using different discovery services would likely have access to a different suite of journals.
ii) Was it possible to determine that the paper included a key by using standard online search protocols? This was done by checking whether the term "key" was found in the title, abstract, or keywords in each paper.
iii) Was it possible for the user to ensure that the key was relevant to the specimen to be identified by stating the discriminating features of the taxonomic group and sex (and for social insects, caste) to which the key applied? These variables were assessed by searching the paper for descriptive or diagnostic information for the taxon at the level to which the key as a whole applied and whether it was overtly stated that the key applied only to one sex or, where relevant, to one caste.
iv) For the variables assessed in iii), was it easy to locate the necessary information? Where was it provided in relation to the key?
v) Is the key of the standard dichotomous structure and free of errors or surprises? A few keys were of the yoked style, wherein all taxa agreeing with the first lead of the first "couplet" are identified before the second lead of that "couplet" is reached. Errors arise through incorrect numbering and surprises may be encountered through the insertion of a non-dichotomous "couplet" among typical dichotomous ones. An additional non-standard key component is the leap-frog couplet, of which the following would be an example:

3(2) Head longer than wide; hind tibia with apicoventral spines.....9
– Head shorter than wide; hind tibia lacking apicoventral spines, surface flat.....4

In this instance, users may go to couplet 4 instead of couplet 9 from the first lead simply because it is expected that the first lead should take the user to the next couplet as this is standard practice.

vi) Does the key allow retracing? (WW7). The standard way of denoting this is shown in Fig. 1 and the above example; in each case, couplet three was reached from couplet 2. This is useful because users often reach a dead-end where the specimen seemingly agrees with neither lead and going backwards unassisted or restarting the key from the beginning is time-consuming and increasingly so the longer the key.

vii) How many steps does it take to get to an identification? (WW8). This variable requires some explanation and concerns the extent to which keys are fan- or comb-shaped and is an important characteristic for a user as the average number of steps to attain an identification increases with an increase in number of taxa far faster in comb-shaped keys than in fan-shaped ones (Walter and Winterton 2007; Packer et al. 2016). For example, the average number of steps from the beginning to identify the taxa in a 16-taxon comb-shaped key is 8.4 but varies from one to 15; whereas for a perfectly fan-shaped key for the same number of taxa it is only, and always, 4. For 128 taxa, these averages increase to 64.5 in a comb-shaped key but only to seven for a fan-shaped one (see the discussion for some added complexity concerning the number of steps to achieve an identification).

I calculated the average number of couplets leading to all the genera in a key averaging in cases where the same taxon came out more than once. I also assessed where those numbers fell between the calculated maximum and minimum numbers of steps that could have been required. For these calculations, I used the equations below.

The average maximum number of steps per taxon, i.e., for an entirely comb-shaped key, for n taxa is:

$$S_{MAX} = ((n+1)/2) - 1/n$$

whereas for a maximally fan-shaped key the average number of steps required for identification is:

$$S_{MIN} = (Q*(2^Q - x) + (Q+1)*2x)/n$$

where $Q = \lfloor \log2(n) \rfloor$ and $x = n - 2Q$.

(surrounding an expression by $\lfloor$ and $\rfloor$ indicates that its numerical value is to be rounded down to the next lowest integer, e.g., both 4.01 and 4.99 become 4). Note that this is the same as the equation given in Packer et al. (2016), i.e., log(n)/log(2), only in the special case where n belongs to the geometric series base 2, i.e., when x = 0.

viii) Are couplets monothetic? (WW2) A monothetic couplet is one in which only a single feature is used in the two leads. Such couplets will be impossible to use if that structure is missing and unnecessarily difficult to use if

the structure is obscured in the specimen at hand or requires dissection. I counted the number of couplets in each key that were monothetic.

ix) Are the features in a couplet dealt with in parallel in both leads (WW4) and is each contrasted? If the sequence of observations in the first lead is the same as in the second lead, it is easier to make the necessary comparisons than if they are not. If one feature is not contrasted, then that comparison is impossible and inclusion of that feature not only unhelpful but wastes users' time. I compared the leads for each couplet to detect non-parallel sequences or absent contrasts.

x) Are the features ambiguous? (WW3). Another way of stating this is to ask whether a couplet might be indecisive. There are multiple ways in which a couplet might be indecisive. Terms such as "usually", "often", "normal", etc., will not work if the specimen at hand is not of the "usual" phenotype.

Another way in which a couplet might be indecisive would be if a non-overlapping range of variables was given. For example, body length 9–12 mm versus body length 11–15 mm.

Similarly, features that are relative may be difficult for a user to interpret. For example, stating that a structure is strongly or weakly convex is a comparison that requires elaboration; the author of a key will know what is strongly convex for the taxonomic group under study but what is "strongly" convex in that group may be "weakly" convex in another. I noted all instances where a couplet was partially, or entirely, made up of relative statements and whether the difficulties were resolved through reference to illustrations. Optimally, the taxon with the least convex "strongly convex" condition and the taxon with the most convex "weakly convex" condition should be illustrated. It was not possible to evaluate the extent to which this approach was taken in the illustrated exemplars, but I considered a potentially indecisive feature to be resolved if both leads were illustrated for the relevant feature(s).

I noted all instances where a couplet contained indecisive features or whether entire couplets were ambiguous.

xi) Is at least one feature from each lead illustrated (WW5) and if so, are the images close to the relevant key couplet? (WW6). I assessed the proportion of leads that cited at least one figure and where the images were in relation to the relevant couplets.

xii) Are diagnoses provided for the genera? (WW9). Diagnoses are meant to be relatively short statements that note the characteristics of the named taxon either as a list or a combination in a manner that permits its differentiation from similar taxa (Austral Entomology 2024; see also Borkent 2021; Rheindt et al. 2023). A user may go to the diagnosis for a taxon as a confirmatory step, once a putative identification has been made using the key (Borkent 2021). I checked whether confirmation of an identification was possible through presentation of diagnoses for the new genera or all genera in the key.

xiii) Are habitus images provided? With the increasing availability and affordability of good quality imaging, provision of a picture of the organism could relatively easily allow the user to decide whether the putative identification might be correct. I assessed whether papers had habitus illustrations of new genera and whether they were photographs, drawings, or scanning electron micrographs.

Some keys could not be assessed for all variables considered. For example, keys that were emendations of previously published ones could not always be assessed for the number of couplets taken to get to an identification of the new genus (or any other) because that information was presented elsewhere, was not always accessible and I wanted to assess the articles as stand-alone papers. However, data for most of the other variables noted above could be assessed for just the emendations and one paper (Engel et al. 2022) emended the beginning of a key and so it could be included in all analyses relevant to just the new genus [Anderson and Bermudez-Higinio (2022) emended two previous keys using a single couplet that would fit at the beginning of the key for one, and much later in the key in the other; it was included as the latter]. Similarly, keys that included trichotomies were not assessed for minimum and maximum numbers of couplets required to get to an identification because equations 1 and 2 rely on all couplets being dichotomous. They could, however, be included for most of the other variables. As a result of these considerations, sample sizes vary among different analyses.

Taking the above criteria 'en masse', it is possible to assess the extent to which keys are suboptimal. To achieve this, the following variables were assessed as binary: whether 1) the key was available, 2) the term key would be located in standard key word searches, 3) the characteristics a specimen at hand must possess for the key to be relevant to it were overtly stated, 4) it was stated clearly that the key applied to just one caste, sex, and lacked sex specific features or couplets based on sexual dimorphism, 5) there were no formatting errors, 6) there were no leap-frog couplets, 7) all couplets were dichotomous, 8) retracing was possible, 9) the key was as fan-shaped as possible, 10) there were no monothetic couplets, 11) all features were contrasted, 12) no couplets were entirely indecisive, 13) images were available for each lead and 14) conveniently placed close to the couplet, 15) all taxa were diagnosed, 16) a habitus image was provided, 17) the key was an emendation but did not require the previous key to be usable. Thus, each key was assessed for an overall score out of 17. However, because some criteria were not applicable to some keys (e.g., whether retracing was made possible is not relevant to a key with a single couplet), overall key scores were also assessed through the percentage of relevant criteria for which they were suboptimal.

Results

Summary data

I found 427 papers that described a total of 587 new genera although 28 papers, describing 34 new genera, were not available for a range of reasons: unavailable through university library resources or Google Scholar combined with a lack of response to requests for a pdf or inactive or unlocatable corresponding author email addresses; an additional paper, describing one genus, was not written in English. Thus, the sample analysed included a total of 398 papers that described a total of 552 new genera. Only 136 papers (34.2%) included identification keys that treated 232 (42.0%) of the new genera (all papers are listed in Suppl. material 1 and the number of new genera in each is shown in Suppl. material 2, column H). These were among the total 1507 genera included among the keys that incorporated a total of 1448 couplets (note that the total number of couplets should equal the number of genera in all keys minus the number of

keys; however. this assumes all genera came out just once in each key and that all keys were fully dichotomous, neither assumption was upheld – see below).

Except in cases where only a few papers illustrate a point being made, consultation of Suppl. material 2 is required to find out which papers exhibited the state for a particular variable.

A total of 141 keys were found among the 136 papers (some papers included separate keys for males and females or to different taxonomic subgroups, see Suppl. material 2, column J). Ten keys were emendations to earlier ones (Suppl. material 2, column K) of which only one (Engel et al. 2022) did not require the original key to be available to permit identification of the new genus. Four were to incomplete and seemingly unidentifiable subgroups of genera ("to the species described in this paper" Namaki-Khameneh et al. 2021a; "selected genera" Sublett and Cook 2021; "to the genera discussed" Yasunaga et al. 2021; "most of the genera" He et al. 2021). Two other papers provided keys to a "phyletic group" (Polak and Mulaomerović 2021) or "phyletic series" (Ćurčić et al. 2021); the reference for both terms is Jeannel (1924), a 436-page article in French that seems difficult to access.

Among the six orders that were represented by more than 20 papers (see Suppl. material 2, column D), there was significant variation in the proportion of papers that included a key (χ^2 = 36.6, p = 7.19 × $10e^{-7}$), ranging from 5.3% for Lepidoptera to 47.1% for Coleoptera. The proportion of papers with a key among the remaining orders combined (maximum number of papers *n* = 8) was 44.4% not significantly different from the papers to the six more frequently studied orders combined (χ^2 = 2.04, p > 0.1).

Among the six journals with more than ten papers describing new genera (see Suppl. material 2, column C), the proportion of papers that included a key ranged from 33.6% for ZT to 50.0% for EJT and ZK. Variation among journals in the preponderance of papers with keys was not significant (χ^2 = 6.13, p = 0.29). The remaining journals had eight or fewer papers describing new genera but the proportion among their total that included a key was only 25.5%, significantly less than among the above six journals combined (χ^2 = 7.95, p < 0.005).

The number of genera in keys ranged from two to 130 with an average of 11.43 but with far from a normal distribution (Fig. 2; see also Suppl. material 2, column I).

The number of couplets in a key was not always what might be expected - the expectation being n-1, where n is the number of genera treated in the key (Suppl. material 2, column H). This was for a range of reasons, primarily when

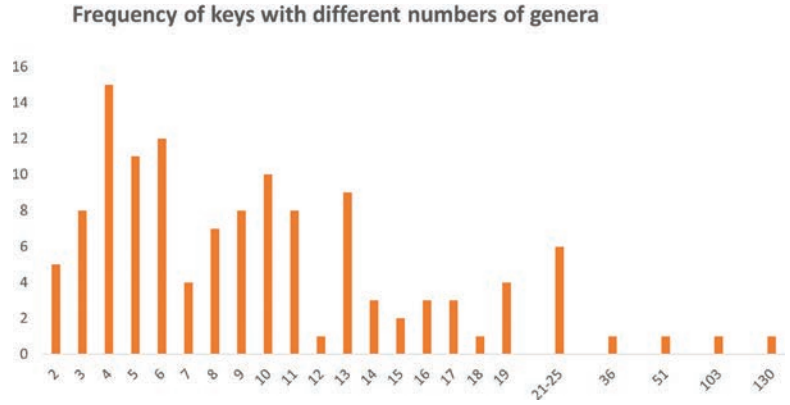

Figure 2. The frequency of keys that were to different numbers of genera. Note the disjunctions in the y-axis due to the small number of keys with more than 19 genera.

the same genus came out multiple times in the key (e.g., Viswayjothi and Clark 2022). The reasons are explained in the footnote to the relevant column.

Twenty-one keys (14.9%) were to the genera within a family, 35 (24.8%) were to those within a subfamily, 50 (35.5%) treated genera within a tribe, 11 (7.8%) were to those of a subtribe, 21 (14.9%) were to groups of genera and three (2.1%) were to ecologically defined subsets of higher-level taxa (Suppl. material 2, Column D).

Almost half of the keys (45.39%) were global in extent for the higher-level grouping to which the new genus belonged, although often the entire group was geographically restricted. Forty-nine keys (34.75%) were for a continental fauna or one that spanned two adjacent continents. Twenty-six (18.4%) were to single countries (data for Australian taxa were included in the continent statistics) or for a few nearby countries (e.g., India / Sri Lanka and Bosnia and environs) and two (1.4%) were to a part of a single country (see Suppl. material 2, column E).

Key assessment

i) Was the text freely available?

Of the 136 key-containing papers, 101 (74.3%) were freely available through Google Scholar, ResearchGate or open-source journal websites. Another seven (5.1%) were available through library resources (most of the previous 101 were also available through this route). Thirty (20.6%) were not available to me from either of the aforementioned approaches but were received after requesting a pdf from the senior author. This method of obtaining the papers permitted the identification of 50 new genera (21.5%) and 279 genera (18.9%) in total. When these are added to the 29 papers for 35 new genera for which citations were found but the papers seemingly unavailable (see above), a total of 59 papers (13.8%) for 85 new genera (14.5%) were either not accessible at all or required contacting the author.

Two of the keys were available only in the supplementary materials (Castro-Huertas et al. 2021; Xu et al. 2021), relevant to seven new genera (3%) and 154 genera (10.2%) in total.

ii) Was the term “key” discoverable using standard online search protocols?

The term “key” was first found in the title of twelve papers (8.8%), among the keywords in seven (5.2%), and in the abstract for 77 (56.6%). Thus, the fact that the paper included a key would be readily discovered using standard search terms for 96 (70.6%) of the papers, representing 169 new genera (72.5%) and 1009 (70.2%) of all genera (Suppl. material 2, column L).

iii) Was it possible for the user to ensure that the specimen to be identified belonged to the group for which the key was constructed through the text stating the characteristics that had to be present for the key to be useful and/or sex or caste of the specimen?

Twenty-one papers had keys to genera within a family for which instructions on how to identify the group might be considered unnecessary, nonetheless, two papers (Ardila-Camacho et al. 2021; López-Pérez, Zaragoza-Caballero 2021)

stated how to do so. Fifty-nine keys (41.8%) were in papers that explained how to identify the taxonomic group below the family level for which the key was relevant. Five of these stated the apomorphies that helped define the group. Seven papers stated a single feature, though in two of these (Huo et al. 2022; Yin and Kurbatov 2022) the feature required males to be available and so use of the key might not be embarked upon for female specimens. Nineteen papers provided a formal diagnosis of the group keyed (most, but not all, when a new taxon above the generic level was also being described). An additional 28 keys were associated with lists or combinations of features that users might check to determine whether the key was relevant to a specimen at hand but without a formal diagnosis. The number of features stated to make the key relevant ranged from one to 40 and averaged 8.2 (but with high variance: SD = 9.5; Suppl. material 2, column N). Thus, overall, 53.7% of all genera and 52% of the new genera were in keys where how to determine whether the key might be appropriate for a specimen was not explained (below family level).

For twelve keys (8.5%) for a total of 14 new genera (6.0%), both sexes were known but the key permitted identification of only one without overtly stating so (Suppl. material 2, column O). This issue arose for 181 (8.2%) of all genera.

Five keys were to specific castes of social insects, three to ant workers, one to bee workers, and one to termite soldiers. In one key to worker ants (Camacho et al. 2022) and one to bees (Engel et al. 2022) (1.4% of all keys), for one new genus each, it was not clearly stated in the heading to the key that it applied only to one caste (Suppl. material 2, column O). This issue was relevant to 13 genera in total (0.9%) and two new genera (0.9%).

iv) Where was this information placed within the paper?

The placement of the information enabling the user to decide whether the key was taxonomically appropriate was not consistent. Most usefully, it was immediately above the key, as in 23 cases (37.7%). It was in the introduction section of the paper also in 23 articles, elsewhere in the results in 12, and once each immediately beneath the key, in the methods or the diagnosis for the new genus.

v) Is the key of the standard dichotomous structure without errors or surprises?

Reasons for there being a different number of couplets in a key than expected based upon the number of genera are explained in Suppl. material 2, column H. In eleven keys, one or more genera came out more than once. In most cases only one or two genera keyed out twice but in Viswayjothi and Clark (2022) 37 of the 130 genera came out between two and five times although only two of the ten new genera were repeated, each twice. Two keys (Huo and Du 2021; Nieves-Aldrey 2022) had more than one genus coming out in one lead so those were not separable, though the newly described genera were not among them.

Some keys did not have the standard dichotomous structure: six had one or more trichotomies or a quadrichotomy, one had a “looped” key structure whereby the same couplet could be reached through two different paths (Tshernyshev 2021) and three were in the yoked style wherein all taxa agreeing with the first half of the first “couplet” were keyed before the second half of that

"couplet" was reached (Storozhenko 2021; Davidian 2022; Kluge et al. 2022) (Suppl. material 2, column Q). None of these issues inevitably add to the potential for the key failing, though they may increase the probability of user error.

Four keys had errors in numbering with duplicated and/or missing and/or incorrect couplet numbers (Castro-Huertas et al. 2021; Jałoszyński 2021; Lucañas 2021; Polak and Mulaomerović 2021) and a fifth (Namaki-Khameneh et al. 2021b) lacked numbers at the beginning of any couplet (Suppl. material 2, column R). I found no errata corrections associated with errors in these papers (search conducted in May 2024), although Jałoszyński (2021) has been superseded by Jałoszyński (2024) which contains a key to the world genera of the relevant group. Thus, five keys were unnecessarily difficult to follow due to errors in formatting and these difficulties applied directly to 37 (2.5%) genera in total, only three of which (1.3%) were newly described (these numbers are less than the total number of genera and new genera in these papers because only those taxa directly affected by the numerical errors were included in the calculations).

Leap-frogging was found in five keys 4.2% of those for which it would be possible (i.e., keys that had both three couplets or more and that were in a standard dichotomous format; Suppl. material 2, column S). In most cases a single couplet suffered from this, though in Gaimari and Havill (2021) all couplets where neither lead resulted directly in an identification had the leap-frog sequence. Overall, 58 genera (4.4%) were affected by leapfrogging, and six of them were new (2.6%).

vi) Does the key allow retracing?

Of the 120 keys for which retracing may have been sensible (i.e., those with more than two couplets and without the yoked format) only 19 stated which couplet led to the current one, while one more provided that information for the sole couplet that did not continue from the one immediately above it (Prathapan and Konstantinov 2021). Thus only 20 keys (16.7%) where retracing might have been sensible permitted it (Suppl. material 2, column T). This applied to 22.6% of both all genera and new genera. While retracing steps may be deemed unnecessary in keys with relatively few couplets, the number of couplets in keys with retracing versus those without it was not significantly different ($z = 1.3232$, $p = 0.19$) and the shortest keys with retracing had three couplets, the longest one without it had 186.

vii) How many steps does it take to get to an identification? (WW8).

The actual average number of couplets leading to all the genera in a key is provided in Suppl. material 2 column U. The same data, as well as the maximum (for a comb-shaped key) and minimum (for a maximally fan-shaped key) using equations 1 and 2 (see methods), are shown on logarithmic scales, in Fig. 3.

Thirteen keys (11.1% of those to more than three genera) were as fan shaped as possible given the number of taxa in the key (Suppl. material 2, column V). These keys involved a total of 56 genera, 19 of which were new (4.4% and 2.3% of the totals respectively). Unsurprisingly, these were all to relatively few taxa (with an average of 5.3 genera, the largest key that was as fan shaped as possible was to 9 genera), significantly fewer genera than in keys that were not perfectly fan-shaped ($z = 3.93$, $p < 0.0001$).

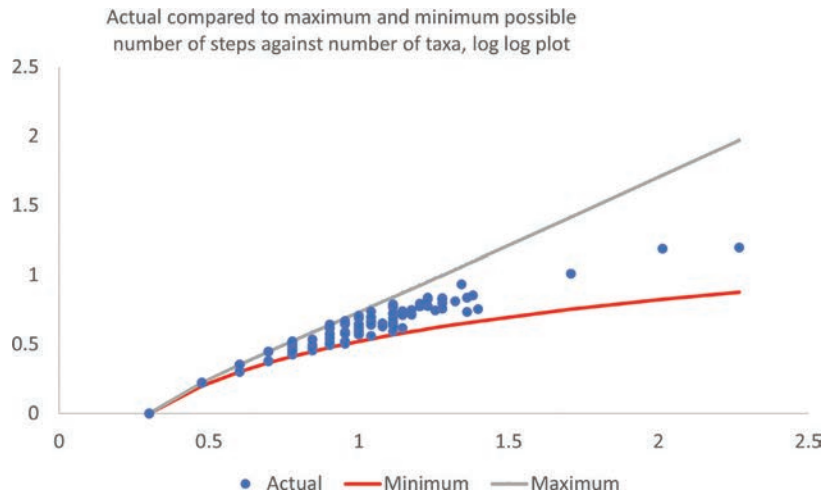

Figure 3. Log-log plot of mean number of steps required to obtain an identification against number of taxa in the key (blue dots) compared to the minimum for a fan-shaped (red line) and maximum number of steps (grey line) for a comb-shaped key.

vii) Are couplets monothetic?

Nine keys (6.4%) relevant to one new genus each (3.4%) were composed of only monothetic couplets, whereas 38 (27.0%) had no couplets based on a single structure (Suppl. material 2, column W). Overall, the identification of 1212 (77.1%) genera required negotiation of one or more monothetic couplets, 167 of these genera were new (71.7% of all new genera). The identification of all genera in a key was subject to monothetic couplets in 69 cases (48.9%), most often due to the first couplet being monothetic. The average proportion of couplets that were monothetic for one or both sexes was 33.9% on a per paper basis and 38.5% across all 1445 couplets. The proportion of couplets that were monothetic per key is shown in Suppl. material 2, column X.

viii) Are the features in a couplet dealt with in parallel in both leads and contrasted?

I found only two exceptions to sequences of features being the same in both leads in a couplet (Allsopp 2022; Kirejtshuk and Kovalev 2022), although identification of the new genus was not dependent upon such a couplet in the first of these. I found nineteen keys where a feature in one lead was not contrasted in the other (Suppl. material 2, column Y), but no single couplet in these keys was entirely composed of uncontrasted features except in one emendation key for a single new genus (Gilasian et al. 2021).

ix) Are features included in a couplet ambiguous or indecisive?

Such features were found in 89 keys (63.1%) and made up all parts of one or more leads in 30 (21.3%) although in three of these (Storozhenko 2021; Zettel and Laciny 2021; Pacheco et al. 2022) the ambiguities were resolved through illustration. Thus, 27 keys (19.1%) had couplets sufficiently indecisive as to make identification of some taxa in the key uncertain (Suppl. material 2, column Z). This uncertainty applied to 48 of the 233 new genera (20.6%).

x) Are features illustrated and if so, are the figures close to the key couplet to which they are relevant?

Sixty-three keys (44.7%) had no figures cited in any couplet encompassing 105 new genera (45.1%) and 653 genera overall (43.3%). At the opposite extreme 28 (19.9%) had at least one figure for each lead, relevant to 40 (17.2%) of the new genera and 239 of all genera (15.8%) (Suppl. material 2, column AA). Overall, the average proportion of leads that were illustrated was 33.8%.

With respect only to those couplets leading to newly described genera, 27.2% of keys had one or more features illustrated in each lead, an additional 9% had only the half of the couplet leading to the new genus illustrated, and 3.6% illustrated only the alternative lead (i.e., the one not leading to the new genus).

Seven keys had the images right next to the couplets and eight had them on an adjacent page (Suppl. material 2, column AB). Two keys had either one (David et al. 2021, the one most relevant for the new genus) or all (Colombo et al. 2022) images hyperlinked to the couplet. Other figures cited in keys were dispersed throughout the manuscript except in three papers (Ślipiński et al. 2021; Yeshwanth and Konstantinov 2021; Viswayjothi and Clark 2022) in which they were grouped, along with all other figures, at the end of the paper.

xi) Are diagnoses provided for the genera?

Eight keys (5.7%) had no diagnosis even for the new genus/genera being described (11 new genera, 4.7%) and another 13 (9.2%) (for 15 new genera, 6.4%) had no diagnosis section but had the kind of information that might be expected in one somewhere in the paper. Thirty-one papers (24.6%) had all taxa in the key diagnosed (Suppl. material 2, column AC) and this applied to 73 (37.4%) of the new genera and 364 of all genera (25.6%). An additional 18 (13.2%) papers had some of the previously described taxa diagnosed, primarily the genus considered most closely related to the new one such as when the new genus was being separated from the one to which it previously belonged. These were relevant to 37 (16.5%) of the new genera. While it might be expected that all genera were more likely to be diagnosed associated with keys to fewer genera, there was no significant difference in numbers of genera in keys with all, versus those with none, of the additional genera diagnosed ($U = 1295.5$, $p > 0.9$).

xii) Are habitus images provided?

Descriptions of nine new genera (6.1%) shared among four papers were not associated with habitus illustrations (Suppl. material 2, column AD) although images of at least parts of specimens of new genera were found in all but one. All the rest were associated with one or more high quality photographs except for four: one was indicated by SEM and three by line drawings.

Overall key assessment

For all seventeen variables that could be assessed as binary, the average number of criteria that were suboptimal among the keys was 5.7 (SD = 1.99) with a range from 1 to 11 (Suppl. material 2 column AE). Because some features were

not applicable to some keys, a more appropriate measure is the proportion of applicable criteria where a key was suboptimal, here the minimum was 7.7%, the maximum 68.8% and the average 36.1% (SD = 12.0%) (Suppl. material 2, column AF).

It is worth noting that these rather coarse evaluations are not likely to indicate the actual relative quality of the keys for a number of reasons including that all variables are treated as equally important, and the analysis does not incorporate the relative difficulty of identifying different taxa. However, the analysis does indicate the number of aspects that could have been made easier for the user.

Discussion

Much has been said in recent years about crises in taxonomy and the impediment that lack of taxonomic information produces for other branches of science (most recently by Löbl et al. 2023). While there are suggestions to the contrary (e.g., Wheeler 2005: "Taxonomy does not exist to answer the question "What species is this?"") most taxonomists understand the importance of their work in making the world's biota identifiable by others, at least at grant-writing time or in the introduction to manuscripts where they point out the importance of their research. Indeed, as Krell (2002) has stated "the most important impact of taxonomy is the usage of identification keys". Given the considerable interest in insect identification for biodiversity survey work, conservation, biosecurity, and other applications, one might expect an ever-increasing need for relatively easy to use identification tools. Walter and Winterton (2007) noted the increased interest in insect identification, conducting a Google Search for "insect key" and found that the number of "hits" obtained increased by almost 20-fold in a single year (from 1,120 in March 2005 to 20,100 in March 2006). In April 2024, I found that the same search yielded "about 203,000,000" hits [though it should be noted that these search terms are highly imprecise]. While there is increasing accuracy of identifications based upon photographs (MacPhail et al. 2020) sometimes even for bulk samples (Fujisawa et al. 2023) and/or using convolutional neural network approaches (e.g., An et al. 2023), growing application of DNA barcode-based identifications (e.g., Gostel and Kress 2022), which also work for bulk samples (e.g., Gleason et al. 2023) not all people wishing to identify an insect want, or are able, to use these methods. Furthermore, newly described taxa will rarely be amenable to either of these approaches.

The number of new insect genera being described indicates that traditional aspects of taxonomic research remain essential and, of course, all identification methods associated with naming an organism require those names to be available in the first place (but see Ratnasingham and Hebert 2013). But making a name available is not the same as making it accessible. The standard way of making a newly available name accessible is through an identification key. Consequently, it was disappointing to find that a minority of the new genus descriptions was accompanied by a key that permitted identification and that when a key was provided, it rarely followed standard recommendations concerning effective key construction.

Recommendations

Based upon the empirical assessment provided above, a set of best practices can be suggested for the description of new taxa dealing specifically with aspects of key construction. While my focus has been on keys associated with the description of new insect genera, these recommendations apply to any level in the taxonomic hierarchy for any taxonomic group. These recommendations are shown in Table 1, which also gives a partial rationale, cites an example for each best practice (when uncommon), and indicates whether adherence to the recommendation might be expected to take a large amount of research effort, journal space, or costs. How to adhere to these recommendations should be readily understood in most cases, although some additional explanation is given when this seems worth noting: such instances are denoted by an asterisk (*) in the first column of the table. The number at the beginning of a paragraph below the table refers to the recommendation number in the table.

Table 1. Recommendations concerning keys associated with new taxon descriptions, rationales for the recommendation, examples of best practices when these were uncommon and possible impediments to their implementation. Notes: * - see further discussion in recommendations section; Ψ - W much, w little- extra effort required; A much, a little - extra space required; $ much, ¢ little - extra cost likely involved; § - all keys in ZJLS.

Recommendation	Rationale	Example	Issues Ψ
1. Include a key	At description, a new taxon will be best identified through use of a key. If it is an emendation to an earlier key either:		WA**$**
	a) put the couplet to the new genus near the very beginning or	Engel et al. 2022;	wa¢;
	b) state overtly and immediately above the key the features that should be present in a specimen for the key to be relevant.	Brunke 2021	wa¢
2.* Avoid placing a key in supplementary materials– unless	Supplementary materials often do not get as much attention from editors and reviewers as the rest of the text. IF they are necessary, put them in a stand-alone file with all necessary ease-of-use features as outlined below.		-A¢
3.* Make the key freely accessible	Open access identification tools will be seen, used and, perhaps most importantly, cited more often.		--$
4. Announce the presence of a key	Why hide the most useful part of your work from potential users? State the word "key" in the title, abstract, and/or keywords so it can be located using standard search methods.		---
5. Title the key appropriately	State the criteria for which the key is relevant: taxonomic group, geographic region, sex, caste: i.e., make it clear to a user whether the key will work for the specimen they wish to identify.		---
6. Diagnose the higher taxonomic group to which the key applies	State the features that make an individual belong to the taxonomic group dealt with in the key so users can tell easily whether they should use the key for a specimen at hand.		-a¢
7. Place that diagnosis usefully	Stating the features a specimen must possess for the key to be relevant immediately after the subheading to the key is most useful.	Prathapan and Konstantinov 2021	---
8.* Avoid monothetic couplets	Likely impossible to implement exhaustively, but at least try to avoid couplets that rely on a structure that is easily broken off (e.g., antennae) or requires dissection (e.g., genitalia).		Wa¢
9.* Make couplets decisive	Avoid couplets made entirely of features with exceptions or that are based on relative statements.		Wa$
10.* Avoid jargon	If a simpler synonymous term is available, use it.	Esteves and Fisher 2021	--- ;
	Illustrate what is meant, provide a glossary,	Wood et al. 2022	WA¢
	or cite a standard reference a user might be expected to have.		---
11.* Illustrate all leads	"A picture is worth a thousand words". Many obscure features can be made perfectly clear through reference to an image.	Sharkey et al. 2021	WA$
12.* Place images within the key	Flipping backwards and forwards in a hardcopy or scrolling to and fro in a pdf can be extremely irritating. Hyperlinking is an excellent solution.	Sharkey et al. 2021; Colombo et al. 2022	WA$; w--
13. Allow retracing	Getting lost in a long key and having to go backwards or start from the beginning again wastes users' time.	Xu et al. 2021	---

Recommendation	Rationale	Example	Issues ψ
14*. Make keys as fan shaped as possible	Users are likely no less busy than are taxonomists and a fan-shaped key for 120 taxa will average an order of magnitude less effort to use than a comb-shaped one for the same taxa [but see points 17 and 18 below].	Bocakova et al. 2022	W--
15. Avoid leapfrogging	Leapfrog couplets are too easy to use incorrectly and are entirely unnecessary.		---
16. Avoid polychotomies… Unless	A user might not notice the third lead as almost all couplets are dichotomous, although: polychotomous couplets may be very efficient but IF used, format them to make their distinction from dichotomy obvious.	Sharkey et al. 2021	--- -a¢
17. Put easily identified or common taxa early in the key	If a few taxa in the key are abundant and the rest are relatively rare, placing them early in the key will save users' time – I did not assess this formally as it was not possible to know which taxa were common/rare for all groups of insects assessed.	Packer et al. 2007	w--
18. Put taxa requiring complex manipulations late in the key	Faced with (for example) a key to 100 taxa in which the first couplet requires dissection of the genitalia, a newcomer to the group will likely decide to study something else. Not assessed: it was not always possible to know when complex manipulations were required (see 10 above).		w--
19. Diagnose all taxa that are keyed	A user can check their preliminary identification. It is best to include features that are in addition to those used in the identification key.	Gimmel and Leschen 2022	WA¢
20. Cite habitus images	As for 19, helps give users confidence and additional guidance. Almost all new genera were illustrated, so citing at least habitus figures in the key is easy and should be done.	Viswayjothi and Clark 2022	---
21.* Get naïve subjects to test the key	Those who write keys will understand what they mean, users might not. The best way to find out what parts are hard to follow is to get naïve subjects (i.e., not experts on the group) to test the key.		w--
22. Proofread the key particularly carefully	Some errors surely could not have been in the reviewed manuscript. Errors in couplet numbering and other formatting issues waste users' time.		w--
23. Format the key so that it stands out clearly	Most keys had a heading in an easy-to-detect font, some were in text boxes, others were well hidden.	§ e.g., Hsiao and Pollock 2022	---

2. If a key is to be placed in supplementary materials, reviewers and editors should ensure that its quality is as good as it would have been if in the main body of the paper: many years of editorial experience convinces me that neither reviewers nor editors (myself included) routinely check supplementary materials as rigorously as they do the main body of the text. It is noteworthy that simple errors of couplet numbering and lack of contrast for specific features (Castro-Huertas et al. 2021) and a complete lack of figures (Xu et al. 2021) were found in both papers where keys were relegated to supplementary materials. It is perhaps telling that both were published in Systematic Entomology, the mostly highly ranked journal for insect taxonomic/systematics research. This illustrates the balance between highlighting long space-hungry keys and the exigencies of publishing where the number of available pages is limited.

3. Make the keys easily accessible. This is essential – papers behind a paywall will be inaccessible to too many potentially interested users. Maximally useful would be freely available, online depositories of emendable keys that authors can modify as new taxa are described. While clearly desirable, I am under no illusions that this is likely to become a commonly applied approach.

8. There is a balance between putting in a single feature that might not be assessable from a specimen requiring identification and putting in so many features that use of the key becomes unnecessarily time consuming. If possible, monothetic couplets should be moved towards the end of the key, or at least not used as the first couplet. If the number of features included in a couplet is large, they should be sequenced such that the earlier ones are easier to evaluate, and it should be stated that agreement with any of the features in the lead are sufficient for making a decision (or the combinations that have to be agreed should be stated).

9. No key should contain any couplets comprised only of qualified or relative statements. If there are exceptions to a particular feature, additional information should be provided that explains how taxa possessing the exception can be identified. For example, "compound eyes usually divergent below in frontal view, exceptions have the thorax entirely black" versus "compound eyes parallel-sided or convergent below and thorax pale-coloured." Allied to this is the need not to leave alternatives implied – e.g., "distance between lateral ocelli wide (2× ocellar diameter)" versus "distance between lateral ocelli narrower" – state what the furthest apart the ocelli can be while still fitting the second option – is it 1.5× or 1.9×? If the latter, then the distinction might not be easy to make. Similarly, statements such as "carina between lateral ocelli present" are not useful unless the alternative is stated in the positive: "carina between lateral ocelli absent" might imply that this area is smooth, but a ridge between them or an area that is strongly sculptured might also be interpreted as being carinate. In both cases illustrations will help.

10. All branches of entomological taxonomy have their own terminologies, often inconsistent among different subgroups within individual higher-level taxa (e.g., use of the term scrobe by melittologists – it's on the mesopleuron - versus its use by chalcidologists – it's on the face) or even by different taxonomists studying exactly the same organisms. I made no attempt to assess how readily comprehensible the terminologies were as that would require familiarity with the words in standard usage in the description of most of the world's biota. Nonetheless, it was abundantly clear that taxon-specific language was the norm and that despite my experience of using entomological keys for almost 50 years and teaching insect family level identification for more than 30, a frustratingly large proportion of keys contained couplets that I found incomprehensible without recourse to a glossary which was rarely provided or cited. However, some papers stood out for going beyond due diligence to make the work readily comprehensible. For example, Esteves and Fisher (2021) included detailed explanations of ant anatomy with all important features, including surface sculpture and setation, illustrated. Any interested novice should be able to use this key successfully. If not included in the paper, a glossary should be cited that explains the terminology being used, preferably one that is both readily available and with images to assist comprehension. Furthermore, authors should check that they are indeed using the terminology consistently with the cited reference. For example, it is common for entomologists to cite Harris (1979) when dealing with surface sculpture (1874 citations as of May 2024). Yet most melittologists use the term "striate" to refer to raised linear features whereas Harris (1979) clearly states that striae are depressed. Such deviations from defined usage should be stated explicitly.

11. Habitus images were ubiquitous, surely some features are shown in many of them such that they could be cited in the key. It is also useful to add a line pointing out where the key feature is, different colours can be used if multiple features are being shown in the same image. Indeed, it should be possible to produce language-neutral, image-driven identification keys (those in Marshall's books on various insect orders, e.g., Marshall 2012, approach this, as do the keys of Sharkey et al. 2021, 2022).

12. Placing the images right next to the relevant couplet would frequently result in multiple copies of the same image arising in the paper. Thus, hyperlinking is likely the best option, especially when different images can come up on the screen simultaneously. Failing either of these options, placing all images that illustrate a key in one place (such as at the end of the paper, e.g., Yeshwanth and Konstantinov 2021) would be sensible as users can have two copies of the paper on the screen simultaneously and flip between the key in one and the images in the other.

14. Make keys as fan shaped as possible. This is relatively easy to do from a data matrix, such as one prepared for phylogenetic analysis or matrix-based key for which numerous automated procedures are available. Walter and Winterton (2007) listed 22 available early in 2006, noting that the list might not have been exhaustive even then. It seems that most of these are not in common use, nonetheless none of the papers surveyed used matrix keys.

In the absence of a matrix, it is possible to make a key more fan-like as follows (Packer et al. 2016). When there are couplets where one lead goes to one or a few taxa while the other goes to a much larger number, remove that couplet and see where the smaller number of taxa end up in the rest of the key and emend the downstream couplets accordingly. This process can be repeated as desired. Rigorous adherence to this recommendation is likely to take a lot of time for the researcher.

21. Authors will understand their key, reviewers are likely experts on the same or a similar group and will understand the key far better than will the average person that might want to use it. Colleagues or students who work with different taxonomic groups should be able to provide useful advice as to which parts of a key are problematic, where images are most essential and whether images that are provided point out the necessary morphological feature(s) clearly enough. This was Walter and Winterton's (2007) recommendation #10. I did not assess this because it would not be possible to tell either whether anyone who was acknowledged for "commenting upon the manuscript" might have tested the key or whether they would be considered naïve users.

Concluding remarks

Taxonomy is hard work and taxonomists are poorly funded (Britz et al. 2020), inadequately cited (Packer et al. 2018; Monckton et al. 2020), and negatively impacted by use of evaluation metrics that are not appropriate for the field (Krell 2000, 2002). Those that use the results of taxonomic research are also generally overworked and inadequately resourced. With the growth of activities such as citizen science (e.g., Gardiner and Roy 2022) and all-taxon biodiversity inventories (e.g., Ichter et al. 2022) an ever-increasing number of people are likely to want to identify a wide range of different insect taxa, but variance in their level of expertise will be considerable. While there are simple options for obtaining identifications, such as iNaturalist (e.g., Prudic et al. 2023), even those experts who perform research-quality determinations will generally have learned their skills by using keys. For new taxa, the paper describing them will be the only means of identification for some time. This suggests that whenever new taxa are described, the paper should include keys that are easily accessible, readily comprehensible, and easy to use. Yet my survey reveals that a minority of

new genus descriptions were associated with a key to facilitate identification and, when provided, the keys rarely followed what should be standard protocols (Walter and Winterton 2007) to make them both usable and user friendly.

Some of the recommendations made above would be very time-consuming to implement (e.g., attempting to ensure a fan-shaped key structure) and others likely impossible (such as rigorous enforcement of non-monothetic couplets). Some are costly, for example page charges and/or journal production costs discourage duplication of images for ease of use in different parts of a manuscript. However, other issues associated with keys are extremely easy to deal with and are cost free: there is no reason to avoid making retracing in a key possible, there is no reason to have couplets that are misnumbered (or not numbered at all), there is no reason not to cite images in a key when they are already elsewhere in the manuscript.

Not all these problems are necessarily the responsibility of authors: journals will discourage repeating an image in a key when the same, or similar, image is also associated with a diagnosis or other aspects of the description of a new taxon. Sometimes a recommended component of a key is disallowed by a journal (e.g., editorial removal of information permitting retracing – Gibbs pers. comm. 1 May 2024; Onuferko, pers. comm. 4 July 2024). Sometimes the production team makes errors and/or authors are not given the opportunity to check the proofs (I have been the victim of this in a paper where one couplet was unreachable and one figure was empty white space because of production errors and the proofs being sent elsewhere).

Indeed, the potential for journals to improve the utility of taxonomy through outlining best practices for key construction in their instructions to authors seems entirely unrealized. For the six journals which published the largest number of papers describing new genera (Austral Entomology, EJT, SE, ZJLS, ZK, ZT) no guidelines on how to construct a key were provided. Three did not mention keys at all, one stated a condition where keys to species would be required while also noting that keys would be published with “high priority”, one stated where in the taxonomic section the key should be placed and a third stated that typesetting keys is difficult and showed how they should be written to make it easier for the production team. I have found only one journal that requires a key to be included when new taxa are described (the search among journals was not exhaustive). The same journal, the Canadian Entomologist, also had some information on how to construct a key (Canadian Entomologist 2024). Ironically, this journal published no new genera during the time period I considered.

It is illustrative to compare the complete absence of guidelines on key construction to the enormous amount of space used instructing authors how to format references, a situation where all formats are likely equally comprehensible to any user. Guidance on how to construct a key is clearly a more pressing problem given that all keys fell foul of at least some of the issues noted above. Journals should add guidelines for key construction to their instructions to authors. Requirements that descriptions of new taxa should be accompanied by a key should be standard editorial practice, keys should be reviewed as carefully as possible to ensure they follow best practices and, unless hyperlinking to figures occurs, publishers should permit the formatting that is necessary to make keys easy to use even if this means that some figures are duplicated and/or some pages have extra empty space.

Acknowledgements

This paper was partly prompted by an invitation to speak at a symposium on bee taxonomy organized by Hollis Woodard and Michael Orr, to whom I am grateful. I thank all authors who sent me pdfs when their work was not available to me through normal online or library channels. I am grateful to Clement Kent for deriving equation 2, to James Woolley for bringing the use of the term scrobe in chalcidology to my attention, to Natalie Do for amalgamating the data on the accessibility of the papers surveyed, and Ilo-Katryn Maimets and Adam Taves for assistance with library resources. The manuscript was improved as a result of comments I gratefully received from Eduardo Almeida, Chris Darling, Jason Gibbs, Tiago Belintani, Shaun Winterton, and Fedor Konstantinov. I would also like to express my gratitude to Denis Brothers who, as an initially anonymous reviewer, explained to me in detail how to construct a good key (along with additional excellent advice) more than a decade ago.

Additional information

Conflict of interest

The author has declared that no competing interests exist.

Ethical statement

No ethical statement was reported.

Funding

This work was supported by the Natural Sciences and Engineering Research Council of Canada.

Author contributions

The author solely contributed to this work.

Author ORCIDs

Laurence Packer https://orcid.org/0000-0002-1711-8203

Data availability

All of the data that support the findings of this study are available in the main text or Supplementary Information.

References

Allsopp PG (2022) Australian Melolonthini (Coleoptera: Scarabaeidae: Melolonthinae): reclassification of eight species to *Antitrogus* Burmeister, 1855 and *Barryfilius* new genus. Zootaxa 5213: 513–545. https://doi.org/10.11646/zootaxa.5213.5.3

An J, Du Y, Hong P, Zhang L, Weng X (2023) Insect recognition based on complementary features from multiple views. Scientific Reports 13: 2966. https://doi.org/10.1038/s41598-023-29600-1

Anderson R, Bermudez-Higinio MF (2022). *Koreguajus antennatus* Anderson and Bermudez-Higinio, a new genus and new species of Sphenophorina (Coleoptera:

Curculionidae: Drophthatlminael Rhynchophorini) from Colombia. Zootaxa 5190: 595–600. https://doi.org/10.11646/zootaxa.5190.4.10

Ardila-Camacho A, Rivera-Gasperín SL, Martins CC, Contreras-Ramos A (2021) A reappraisal of the taxonomy of Neotropical Sialidae (Insecta: Megaloptera): with the description of a new genus from Cuba. European Journal of Taxonomy 782: 21–54. https://doi.org/10.5852/ejt.2021.782.1587

Austral Entomology (2024) Instructions to authors: Austral Entomology (wiley.com) [accessed 21.ii.2024]

Benda D, Pohl H, Nakase Y, Beutel R, Straka J (2022) A generic classification of Xenidae (Strepsiptera) based on the morphology of the female cephalothorax and male cephalotheca with a preliminary checklist of species. ZooKeys 1093: 1–134. https://doi.org/10.3897/zookeys.1093.72339

Bocakova M, Campello-Gonçalves L, Da Silveira LFL (2022) Phylogeny of the new subfamily Cladodinae: neotenic fireflies from the Neotropics (Coleoptera: Lampyridae). Zoological Journal of the Linnean Society 195: 1181–1199. https://doi.org/10.1093/zoolinnean/zlab091

Borkent A (2021) Diagnosing diagnoses – can we improve our taxonomy? ZooKeys 1071: 43–48. https://doi.org/10.3897/zookeys.1071.72904

Britz R, Hundsdörfer A, Fritz U (2020) Funding, training, permits – the three big challenges of taxonomy. Megataxa 1: 49–52. https://doi.org/10.11646/megataxa.1.1.10

Brunke AJ (2021) New relictual genera in Cyrtoquediini and Indoquediini (Coleoptera: Staphylinidae: Staphylininae). ZooKeys 1076: 109–124. https://zookeys.pensoft.net/article/73103/

Camacho GP, Franco W, Branstetter MG, Pie MR, Longino JT, Schultz TR, Feitosa RM (2022) UCE phylogenomics resolves major relationships among ectaheteromorph ants (Hymenoptera: Formicidae: Ectatomminae, Heteroponerinae): a new classification for the subfamilies and the description of a new genus. Insect Systematics and Diversity 6: 1–20. https://doi.org/10.1093/isd/ixab026

Canadian Entomologist (2024) Author instructions. Preparing your materials. https://www.cambridge.org/ [accessed 26.v.2024]

Castro-Huertas V, Forero D, Grazia J (2021) Evolution of wing polymorphism and genital asymmetry in the thread-legged bugs of the tribe Metapterini Stål (Hemiptera, Reduviidae, Emesinae) based on morphological characters. Systematic Entomology 46: 28–43. https://doi.org/10.1111/syen.12445

Colombo WD, Tribull CM, Waichert C, Azevedo CO (2022) Integrative taxonomy solves taxonomic impasses: a case study from Epyrinae (Hymenoptera, Bethylidae). Systematic Entomology 47: 504–529. https://doi.org/10.1111/syen.12544

Cumming RT, Le Tirant S (2022) Three new genera and one new species of leaf insect from Melanesia (Phasmatodea, Phylliidae). ZooKeys 1110: 151–200. https://doi.org/10.3897/zookeys.1110.80808

Cumming RT, Bank S, Bresseel J, Constant J, Le Tirant S, Dong Z, Sonet G, Bradler S (2021) *Cryptophyllium*, the hidden leaf insects–descriptions of a new leaf insect genus and thirteen species from the former celebicum species group (Phasmatodea, Phylliidae). ZooKeys 1018: 1–179. https://doi.org/10.3897/zookeys.1018.61033

Ćurčić S, Pavićević D, Vesović N, Vrbica M, Kuraica M, Marković Đ, Petković M, Lazović V, Pantelić D, Bosco F (2021) On the diversity of subterranean beetles of the Dinarides: new leiodid taxa (Coleoptera: Leiodidae) from Serbia. European Journal of Taxonomy 782: 55–81. https://doi.org/10.5852/ejt.2021.782.1589

David KJ, Hancock DL, Han HY, Gracy GR, Sachin K, Swathi RS (2021) A new genus in the tribe Acidoxanthini (Diptera: Tephritidae: Trypetinae) from India, with a discussion of its phylogenetic relationships. Journal of Asia-Pacific Entomology 24: 1194–1201. https://doi.org/10.1016/j.aspen.2021.06.010

Davidian GE (2022) A new weevil genus closely related to *Dactylotinus* Korotyaev, 1996 (Coleoptera, Curculionidae: Entiminae) with new species from the Sino-Tibetan Mountains. Entomological Review 101: 992–1003. https://doi.org/10.1134/S0013873821070150

Didham RK, Barbero F, Collins CM, Forister ML, Hassall C, Leather SR, Packer L, Saunders ME, Stewart AJ (2020) Spotlight on insects: trends, threats and conservation strategies. Insect Conservation and Diversity 13: 99–102. https://doi.org/10.1111/icad.12409

Engel MS, Nguyen LTP, Tran NT, Truong TA, Motta AFH (2022) A new genus of minute stingless bees from Southeast Asia (Hymenoptera, Apidae). ZooKeys 1089: 53–72. https://doi.org/10.3897/zookeys.1089.78000

Esteves FA, Fisher BL (2021) *Corrieopone nouragues* gen. nov., sp. nov., a new Ponerinae from French Guiana (Hymenoptera, Formicidae). ZooKeys 1074: 83–173. https://doi.org/10.3897/zookeys.1074.75551

Fujisawa T, Noguerales V, Meramveliotakis E, Papadopoulou A, Vogler AP (2023) Image-based taxonomic classification of bulk insect biodiversity samples using deep learning and domain adaptation. Systematic Entomology 48: 387–401. https://doi.org/10.1111/syen.12583

Gaimari SD, Havill NP (2021) A new genus of Chamaemyiidae (Diptera: Lauxanioidea) predaceous on Adelgidae (Hemiptera), with a key to chamaemyiid species associated with Pinaceae-feeding Sternorrhyncha. Zootaxa 5067: 1–39. https://doi.org/10.11646/zootaxa.5067.1.1

Gardiner MM, Roy HE (2022) The role of community science in entomology. Annual Review of Entomology 67: 437–456. https://doi.org/10.1146/annurev-ento-072121-075258

Gilasian E, Ziegler J, Tóthová A, Parchami-Araghi M (2021) A new genus and species of tachinid flies from Iran (Diptera, Tachinidae, Goniini). European Journal of Taxonomy 746: 162–185. https://doi.org/10.5852/ejt.2021.746.1331

Gimmel ML, Leschen RA (2022) Revision of the genera of Picrotini (Coleoptera: Cryptophagidae: Cryptophaginae). Acta Entomologica Musei Nationalis Pragae 62: 61–109. https://doi.org/10.37520/aemnp.2022.006

Gleason JE, Hanner RH, Cottenie K (2023) Hidden diversity: DNA metabarcoding reveals hyper-diverse benthic invertebrate communities. BMC Ecology and Evolution 23: 19. https://doi.org/10.1186/s12862-023-02118-w

Gostel MR, Kress WJ (2022) The expanding role of DNA barcodes: Indispensable tools for ecology, evolution, and conservation. Diversity 14: 213. https://doi.org/10.3390/d14030213

Harris RA (1979) A glossary of surface sculpturing. Occasional Papers in Entomology 28: 1–36.

He Z, Zhang T, Ma L (2021) Crickets of subfamily Nemobiinae Saussure, 1877 (Orthoptera: Grylloidea; Trigonidiidae) from China with descriptions of new genera and new species. Zootaxa 5011: 1–70. https://doi.org/10.11646/zootaxa.5011.1.1

Hsiao, Y, Pollock DA (2022) Morphology-based phylogeny of oval palm and flower beetles (Coleoptera: Mycteridae: Eurypinae), with descriptions of new genera and species from Australia. Zoological Journal of the Linnean Society 196: 677–703. https://doi.org/10.1093/zoolinnean/zlab122

Huo QB, Du Y-Z (2021) A new genus of Isoperlinae (Plecoptera: Perlodidae) from Tibet. Zootaxa 4996: 343–352. https://doi.org/10.11646/zootaxa.4996.2.8

Huo KK, Zhao L, Mengual X, Li G, Liu X, Zhao LJ, Chen ZN (2022) *Biema* Huo & Zhao gen. nov., a new flower fly genus (Diptera, Syrphidae) from China. European Journal of Taxonomy 852: 98–116. https://doi.org/10.5852/ejt.2022.852.2015

Ichter J, Gargominy O, Leccia MF, Robert S, Poncet L (2022) The first large-scale All Taxa Biodiversity Inventory in Europe: description of the Mercantour National Park ATBI datasets. Biodiversity Data Journal 10: e85901. https://doi.org/10.3897/BDJ.10.e85901

Jałoszyński P (2021) *Sinonichnus* gen. n. for *Scydmoraphes yunnanensis* Jałoszyński, and description of *Sinonichnus leiodicornutus* sp. n. (Coleoptera, Staphylinidae, Scydmaeninae). Zootaxa 4938: 487–496. https://doi.org/10.11646/zootaxa.4938.4.7

Jałoszyński P (2024) *Palposcydmus* gen. n. from India, with a preliminary key to world genera of Stenichnini (Coleoptera, Staphylinidae, Scydmaeninae). Zootaxa 5428: 549–570. https://doi.org/10.11646/zootaxa.5428.4.5

Jeannel R (1924) Monographie des Bathysciinae. Archives de Zoologie Expérimentale et Générale 63: 1–434.

Kirejtshuk AG, Kovalev AV (2022) Monograph on the Cillaeinae (Coleoptera: Nitidulidae) from the Australian Region with comments on the taxonomy of the subfamily. Zootaxa 5103: 1–133. https://doi.org/10.11646/zootaxa.5103.1.1

Kluge NJ, Vasanth M, Balasubramanian C, Sivaramakrishnan KG (2022) Review of the Kimminsula-complex (Ephemeroptera, Leptophlebiidae). Zootaxa 5212: 1–140. https://doi.org/10.11646/zootaxa.5212.1.1

Krell FT (2000) Impact factors aren't relevant to taxonomy. Nature 405: 507–508. https://doi.org/10.1038/35014664

Krell FT (2002) Why impact factors don't work for taxonomy. Nature 415: 957–957. https://doi.org/10.1038/415957a

Löbl I, Klausnitzer B, Hartmann M, Krell FT (2023) The silent extinction of species and taxonomists—An appeal to science policymakers and legislators. Diversity 15: 1053. https://doi.org/10.3390/d15101053

López-Pérez S, Zaragoza-Caballero S (2021) Two new genera of Telegeusidae (Coleoptera) from Mexico. Revista Mexicana de Biodiversidad 92: 1–10. https://doi.org/10.22201/ib.20078706e.2021.92.3613

Lucañas CC (2021) *Bundoksia* gen. nov. (Dictyoptera: Blattodea: Blattidae), a new sexually dimorphic cockroach from the Philippines. Journal of Natural History 55: 1009–1020. https://doi.org/10.1080/00222933.2021.1928317

MacPhail VJ, Gibson SD, Hatfield R, Colla SR (2020) Using Bumble Bee Watch to investigate the accuracy and perception of bumble bee (*Bombus* spp.) identification by community scientists. PeerJ 8: e9412. https://doi.org/10.7717/peerj.9412

Marshall SA (2012) Flies: The Natural History and Diversity of Diptera. Firefly Books, Richmond Hill, Canada, 616 pp.

Monckton SK, Johal S, Packer L (2020) Taxonomic validation in Zoology. Canadian Journal of Zoology 98: 533–542. https://doi.org/10.1139/cjz-2020-0027

Namaki-Khameneh R, Khaghaninia S, Disney RHL, Maleki-Ravasan N (2021a) Nine new species of scuttle flies, including one new genus (Diptera: Phoridae) from Iran. Biologia 76: 2895–2912. https://doi.org/10.1007/s11756-021-00762-5

Namaki-Khameneh R, Khaghaninia S, Disney RHL, Maleki-Ravasan N (2021b) The scuttle flies (Diptera: Phoridae) of Iran with the description of *Mahabadphora aesthespho-ra* as a new genus and species. PLoS ONE 16: e0257899. https://doi.org/10.1371/journal.pone.0257899

Nieves-Aldrey JL (2022) Description of *Fumariphilus* Nieves-Aldrey, gen. nov., a new genus of herb gall wasps, with a key to genera of the tribe Aulacideini (Hymenoptera: Cynipidae). Zootaxa 5155: 393–413. https://doi.org/10.11646/zootaxa.5155.3.5

Pacheco TL, Monné ML, Ahrens D (2022) Morphology-based phylogenetic analysis of South American Sericini chafers (Coleoptera, Scarabaeidae) contrasts patterns of morphological disparity and current classification. Zoologischer Anzeiger 302: 43–57. https://doi.org/10.1016/j.jcz.2022.11.004

Packer L, Genaro JA, Sheffield CS (2007) The bee genera of eastern Canada. Canadian Journal of Arthropod Identification 3: 1–32.

Packer L, Ali E, Dumesh S, Walker K (2016) The identification of pollinators: where are we and where should we go? In: Gemmill-Herren B (Ed.) Pollination Services to Agriculture: Sustaining and Enhancing a Key Ecosystem Service. Routledge, London and New York, 276 pp.

Packer L, Monckton SK, Onuferko TM, Ferrari RR (2018) Validating taxonomic identifications in entomological research. Insect Conservation and Diversity 11: 1–12. https://doi.org/10.1111/icad.12284

Polak S, Mulaomerović J (2021) *Rudogorites simonei* gen. nov. and sp. nov. from Central Bosnia (Coleoptera: Leiodidae: Cholevinae: Leptodirini). Zootaxa 5061: 545–558. https://doi.org/10.11646/zootaxa.5061.3.8

Prathapan KD, Konstantinov AS (2021) Revision of Oriental flea beetle genera with subparallel intercoxal ridges on the first abdominal ventrite (Coleoptera, Chrysomelidae, Galerucinae, Alticini). Journal of Natural History 55: 1521–1598. https://doi.org/10.1080/00222933.2021.1933229

Prudic KL, Zylstra ER, Melkonoff NA, Laura RE, Hutchinson RA (2023) Community scientists produce open data for understanding insects and climate change. Current Opinion in Insect Science 59: 101081. https://doi.org/10.1016/j.cois.2023.101081

Ratnasingham S, Hebert PDN (2013) A DNA-based registry for all animal species: the Barcode Index Number (BIN) system. PLoS ONE 8: e66213. https://doi.org/10.1371/journal.pone.0066213

Rheindt FE, Bouchard P, Pyle RL, Welter-Schultes F, Aescht E, Ahyong ST, Ballerio A, Bourgoin T, Ceríaco LM, Dmitriev D, Evenhuis N, Grygier MJ, Harvey MS, Kottelat M, Kluge N, Krell FT, Kojima J, Kullander SO, Lucinda P, Lyal CHC, Scioscia CL, Whitmore D, Yanega D, Zhang Z-Q, Zhou H-Z, Pape T (2023) Tightening the requirements for species diagnoses would help integrate DNA-based descriptions in taxonomic practice. PLOS Biology 21(8): p.e3002251. https://doi.org/10.1371/journal.pbio.3002251

Sánchez-Bayo F, Wyckhuys KA (2021) Further evidence for a global decline of the entomofauna. Austral Entomology 60: 9–26. https://doi.org/10.1111/aen.12509

Sharkey MJ, Janzen DH, Hallwachs W, Chapman EG, Smith MA, Dapkey T, Brown A, Ratnasingham S, Naik S, Manjunath R, Perez, K (2021) Minimalist revision and description of 403 new species in 11 subfamilies of Costa Rican braconid parasitoid wasps, including host records for 219 species. ZooKeys 1013: 1–666. https://doi.org/10.3897/zookeys.1013.55600

Sharkey MJ, Baker A, Manjunath R, Hebert PDN (2022) Description of *Chilearinus* Sharkey gen. nov. and status of Nearctic *Earinus* Wesmael, 1837 (Braconidae, Agathidinae) with the description of new species. ZooKeys 1099: 57–86. https://doi.org/10.3897/zookeys.1099.81473

Ślipiński A, Lawrence JF, Escalona HE (2021) The genera of Inopeplinae (Coleoptera: Salpingidae), world generic key, descriptions of four new genera and revision of the Australian fauna. Annales Zoologici 71: 701–735. https://doi.org/10.3161/00034541ANZ2021.71.4.002

Storozhenko SY (2021) On the exact position of the tribe Incolacridini in the modern classification of grasshoppers (Orthoptera: Acrididae). Zootaxa 4970: 106–118. https://doi.org/10.11646/zootaxa.4970.1.3

Sublett CA, Cook JL (2021) A comprehensive revision of the genus *Metaparia* Crotch, 1873 (Coleoptera: Chrysomelidae: Eumolpinae) and description of a new genus. The Coleopterists Bulletin 75: 779–811. https://doi.org/10.1649/0010-065X-75.4.779

Tshernyshev SE (2021) *Pectotibialis paghmanensis* Tshernyshev gen. nov. – a new genus and species of soft-winged flower beetle (Coleoptera, Cleroidea, Malachiidae) from Afghanistan. European Journal of Taxonomy 775: 1–14. https://doi.org/10.5852/ejt.2021.775.1539

Viswayjothi K, Clark SM (2022) New World genera of Galerucinae Latreille, 1802 (tribes Galerucini Latreille, 1802, Metacyclini Chapuis, 1875, and Luperini Gistel, 1848): an annotated list and identification key (Coleoptera: Chrysomelidae). European Journal of Taxonomy 842: 1–102. https://doi.org/10.5852/ejt.2022.842.1945

Wagner DL (2020) Insect declines in the Anthropocene. Annual Review of Entomology 65: 457–480. https://doi.org/10.1146/annurev-ento-011019-025151

Walter DE, Winterton S (2007) Keys and the crisis in taxonomy: extinction or reinvention? Annual Review of Entomology 52: 193–208. https://doi.org/10.1146/annurev.ento.51.110104.151054

Wheeler QD (2005) Losing the plot: DNA 'barcodes' and taxonomy. Cladistics 21: 405–407. https://doi.org/10.1111/j.1096-0031.2005.00075.x

Wood TJ, Patiny S, Bossert S (2022) An unexpected new genus of panurgine bees (Hymenoptera, Andrenidae) from Europe discovered after phylogenomic analysis. Journal of Hymenoptera Research 89: 183–210. https://doi.org/10.3897/jhr.89.72083

Xu Y, Dietrich CH, Zhang YL, Dmitriev DA, Zhang L, Wang YM, Lu SH Qin DZ (2021) Phylogeny of the tribe Empoascini (Hemiptera: Cicadellidae: Typhlocybinae) based on morphological characteristics, with reclassification of the Empoasca generic group. Systematic Entomology 46: 266–286. https://doi.org/10.1111/syen.12461

Yasunaga T, Chérot F, Schwartz MD (2021) New genera and species of the Oriental mirine plant bugs from Southeast Asia, with six new combinations (Insecta: Heteroptera: Miridae: Mirinae: Mirini). Raffles Bulletin of Zoology 69: 137–155.

Yeshwanth HM, Konstantinov FV (2021) Review of the plant bug tribe Eccritotarsini (Hemiptera: Heteroptera: Miridae) of India and Sri Lanka with description of two new genera and six new species. European Journal of Taxonomy 745: 1–69. https://doi.org/10.5852/ejt.2021.745.1311

Yin Z, Kurbatov SA (2022) *Schmidtinus annapurnensis*, a new genus and species of Batrisitae from Nepal (Coleoptera: Staphylinidae: Pselaphinae). Zootaxa 5169: 79–86. https://doi.org/10.11646/zootaxa.5169.1.7

Zettel H, Laciny A (2021) The taxonomy of some unusual Microveliinae (Hemiptera: Heteroptera: Veliidae) from India. Acta Entomologica Musei Nationalis Pragae 61: 517–527. https://doi.org/10.37520/aemnp.2021.029

Supplementary material 1

Complete list of papers that included keys used in the analyses

Authors: Laurence Packer

Data type: docx

Link: https://doi.org/10.3897/zookeys.1215.130416.suppl1

Supplementary material 2

Data extracted from assessed identification keys

Authors: Laurence Packer

Data type: xlsx

Link: https://doi.org/10.3897/zookeys.1215.130416.suppl2

ZooKeys 1215: 91–106 (2024)
DOI: 10.3897/zookeys.1215.133522

Research Article

Tenkana, a new genus of jumping spiders (Salticidae, Plexippina) from South Asia, with the new Indian species *Tenkana jayamangali*

Kiran Marathe[1,2*], John T. D. Caleb[3*], Wayne P. Maddison[4*], B. G. Nisha[5,6], Chinmay C. Maliye[7], Y. T. Lohit[8], Krushnamegh Kunte[2]

1 *Department of Zoology and Beaty Biodiversity Museum, University of British Columbia, 6270 University Boulevard, Vancouver, British Columbia, V6T 1Z4, Canada*
2 *National Centre for Biological Sciences, Tata Institute of Fundamental Research, GKVK Campus, Bengaluru, 560065, India*
3 *Department of Anatomy, Saveetha Medical College & Hospitals, Saveetha Institute of Medical and Technical Sciences, Saveetha University, Chennai 602105, Tamil Nadu, India*
4 *Departments of Zoology and Botany and Beaty Biodiversity Museum, University of British Columbia, 6270 University Boulevard, Vancouver, British Columbia, V6T 1Z4, Canada*
5 *Chilipili, 4th Main 5b Right cross Jayanagar West, Tumakuru, 572102, Karnataka, India*
6 *Wildlife Aware Nature Club, Tumakuru 572101, Karnataka, India*
7 *146, Sunkalpalya, Bengaluru 560060 Karnataka, India*
8 *Renusri Nilaya, 2nd 'A' cross, CSI layout, Tumakuru 572102, Karnataka, India*
Corresponding authors: Kiran Marathe (marathe12@gmail.com); John T. D. Caleb (caleb87woodgate@gmail.com)

Abstract

We describe a new plexippine genus, *Tenkana* **gen. nov.**, supported by phylogenomic data from ultraconserved elements (UCEs), Sanger sequences of four genes, and morphological evidence. The type species, *Tenkana manu* (Caleb, Christudhas, Laltanpuii & Chitra, 2014), **comb. nov.** is transferred from *Colopsus*, as is *Tenkana arkavathi* (Caleb, 2022), **comb. nov.** The phylogenomic data places *Tenkana* among the plexippines near *Hyllus* C.L. Koch, 1846 and *Telamonia* Thorell, 1887, while the constrained four-gene phylogeny indicates that *Tenkana* is distinct from *Colopsus*. Additionally, we describe a new species, *Tenkana jayamangali* **sp. nov.**

Key words: Araneae, biodiversity research, classification, new combination, phylogenomics, systematics, taxonomy, ultraconserved elements

Academic editor: Shuqiang Li
Received: 30 July 2024
Accepted: 12 September 2024
Published: 11 October 2024

ZooBank: https://zoobank.org/EFDA3644-EC1B-4160-8773-6FF0B575437D

Citation: Marathe K, Caleb JTD, Maddison WP, Nisha BG, Maliye CC, Lohit YT, Kunte K (2024) *Tenkana*, a new genus of jumping spiders (Salticidae, Plexippina) from South Asia, with the new Indian species *Tenkana jayamangali*. ZooKeys 1215: 91–106. https://doi.org/10.3897/zookeys.1215.133522

Introduction

The current composition of the jumping spider genus *Colopsus* Simon, 1902 is questionable due to morphological inconsistency among species. The genus now holds two disparate groups: (i) the *cancellatus* species group, consisting of vegetation-dwelling forest species mostly known from Sri Lanka, recognizable by the male palp lacking a tegular lobe and the body glossy and elongate; and (ii) the *manu* species group, consisting of ground-dwelling species found in Sri Lanka and relatively drier regions of southern India, recognizable by a conspicuous tegular lobe and a more compact body, neither glossy nor elongate. The type species, *Colopsus cancellatus* Simon, 1902, is in the first group. When Kanesharatnam and Benjamin (2021) revived the genus *Colopsus*, previously

* These authors contributed equally to this work.

synonymized with *Evarcha* Simon, 1902 (Prószyński 1984), they described three glossy species in the *cancellatus* group. However, they also placed in *Colopsus* a non-glossy compact-bodied species, *C. cinereus*, based on a male. They had molecular evidence to place the glossy species phylogenetically, but not *C. cinereus*, whose inclusion in *Colopsus* was considered provisional due to the lack of female morphology and molecular evidence. Subsequently, Caleb et al. (2022) transferred *Hyllus manu* (Caleb, Christudhas, Laltanpuii & Chitra, 2014) to *Colopsus* and synonymized *C. cinereus* with *C. manu*. Thus, currently, *Colopsus arkavathi* Caleb, 2022 and *C. manu* (Caleb, Christudhas, Laltanpuii & Chitra, 2014) represent the *manu* group, and *C. cancellatus*, *C. ferruginus* Kanesharatnam & Benjamin, 2021, *C. magnus* Kanesharatnam & Benjamin, 2021, and *C. tenuesi* Kanesharatnam & Benjamin, 2021 represent the *cancellatus* group.

Our goal here is to resolve the phylogenetic placement of the two groups. We used ultraconserved element (UCE) data from the *manu* group to test its monophyly and to explore its relationships among plexippines. UCE data is unavailable for the type species of *Colopsus* and other Sri Lankan species, but Kanesharatnam and Benjamin (2021) obtained data for four genes from them. We combined their data with data for the same genes obtained as bycatch from UCE work, in order to determine the placement of the *cancellatus* species group relative to the *manu* species group.

The molecular, morphological, and ecological evidence we present justify establishing a new genus comprising ground-dwelling species of southern India and Sri Lanka. We describe, diagnose, and illustrate a new species within this genus.

Materials and methods

Materials examined

The Indian specimens examined in this study are deposited in two repositories. (i) The male holotype (I/SP-48) and a female paratype (I/SP-49) in the Southern Regional Centre, Zoological Survey of India (**ZSIC**), Chennai, Tamil Nadu, India and (ii) three paratypes (1 ♂ and 2 ♀♀) in the Biodiversity Lab Research Collections of the National Centre for Biological Sciences (**NCBS**), Bengaluru, India (http://biodiversitycollections.in/). Individual specimens deposited in NCBS are identified by three-digit voucher codes prefixed with "IBC-BX". Non-Indian specimens are deposited in the University of British Columbia Spencer Entomological Collection.

Morphology

We examined and photographed 70% ethanol-preserved specimens using a Leica MC190 HD camera attached to a Leica SAPO stereomicroscope automatically using the Leica Application Suite (LAS) v. 4.13. We examined and photographed the genitalia using a Leica MC190 HD camera attached to a Leica DM3000 LED compound microscope and prepared the drawings by digitally tracing the photographs. We photographed the living spiders with a Tamron 90 mm macro lens attached to a Nikon Z6 camera and a Godox flash covered with a Radiant Diffuser.

Descriptions of colour patterns are based on ethanol-preserved specimens. The male genitalic description is based on the left palp. Carapace length is measured from the base of the anterior median eyes to the posterior margin of the carapace medially, while abdomen length is measured from the anterior to the end of the anal tubercle. All measurements are in millimetres. Leg measurements are represented as follows: total length (femur, patella, tibia, metatarsus, and tarsus). Abbreviations used here are as follows: **ALE**, anterior lateral eye; **ECP**, epigynal coupling pocket; **PME**, posterior median eye; **RTA**, retrolateral tibial apophysis.

Taxon sampling for phylogenomic analysis

The morphology (conspicuous tegular lobe and two ECPs) of the species of *Tenkana* is consistent with their current placement among the plexippines. Therefore, we gathered molecular data for *T. arkavathi*, *T. jayamangali*, and *T. manu* and appended it to (Marathe et al. 2024b) plexippine-biased UCE phylogenomic dataset, which included 16 plexippines, five outgroups (three harmochirines, one salticine, and one chrysilline). We also included cf. *Colopsus* sp. from Lin et al. (2024) to allow cf. *Colopsus*, along with *Pancorius* from the Marathe et al. (2024b) dataset, a chance to capture *Tenkana* in the phylogenomic analysis. The total set of 25 species comprising 20 plexippines and five outgroups used in the phylogenomic analysis, with their taxonomic authorities indicated, is listed in Table 1.

Taxon sampling for the four-gene phylogenetic analysis

To test *Tenkana*'s placement relative to the type species of *Colopsus* and others from Sri Lanka, we constructed matrices of mitochondrial cytochrome oxidase I (COI) and nuclear 28S, 18S and Histone 3 (H3) from publicly available data for *Colopsus* from Kanesharatnam and Benjamin's (2021) study. We appended bycatch data for the same four gene regions present among the sequence capture genomic assemblies from the UCE dataset to the four gene matrices of *C. cancellatus*, *C. ferruginus*, and *C. magnus*. We followed a bycatch protocol similar to that described by Maddison et al. (2020), constructing local BLAST databases from SPAdes (Nurk et al. 2013) assemblies of each taxon in the UCE dataset. These assemblies were queried with publicly available COI, 28S, 18S, and H3 sequences from seven different salticid species (*Aelurillus* cf. *ater* (Kroneberg, 1875), *Bianor maculatus* (Keyserling, 1883), *Colopsus cancellatus*, *Colopsus ferruginus*, *Hyllus treleaveni* Peckham & Peckham, 1902, *Pancorius athukoralai* Kanesharatnam & Benjamin, 2021, and *Salticius scenicus* (Clerck, 1757)). Thus, the total set of 31 taxa (25 UCE bycatch and six Sri Lankan *Colopsus* of three species) are used in the four-gene phylogenetic analysis. The accession numbers are listed in Table 3.

Ultraconserved element (UCE) data

Molecular data was gathered for UCE loci using target enrichment sequencing methods (Faircloth 2017), using the RTA_v3 probeset (Zhang et al. 2023) and following the protocols of Marathe et al. (2024a).

Table 1. Specimens used in UCE phylogenomic and four-gene phylogenetic analysis. The sex, latitude, and longitude information for 'IFS_SAL_#' vouchers are inferred from Kanesharatnam and Benjamin (2021).

Species	Voucher	Sex	Locality	Lat, long
Anarrhotus fossulatus Simon, 1902	AS19.1319	♂	Singapore	1.379, 103.816
Artabrus erythrocephalus (C.L. Koch, 1846)	AS19.2205	♂	Singapore	1.355–7, 103.774–5
Baryphas ahenus Simon, 1902	d536	♂	South Africa	-25.95, 30.56
Bianor maculatus (Keyserling, 1883)	NZ19.9864	♂	New Zealand	-42.1691, 172.8090
Carrhotus sp.	AS19.4650	♂	India	12.2145, 75.653–4
cf. *Colopsus* sp.	JXZ795	♀	China	21.910897, 101.283422
Colopsus cancellatus	IFS_SAL_360	♀	Sri Lanka	6.843333, 80.677778
Colopsus cancellatus	IFS_SAL_797	?	Sri Lanka	7.746111, 80.131667
Colopsus ferruginus	IFS_SAL_233	?	Sri Lanka	7.859444, 80.674444
Colopsus ferruginus	IFS_SAL_248	♂	Sri Lanka	7.298333, 80.641389
Colopsus magnus	IFS_SAL_832	♂	Sri Lanka	7.145833, 80.698056
Colopsus magnus	IFS_SAL_906	?	Sri Lanka	6.766667, 80.6
Chysilla volupe (Karsch, 1879)	AS19.6089	♂	India	12.223, 76.627
Epeus sp.	DDKM21.055	♂	Singapore	1.355, 103.78
Evacin bulbosa (Żabka, 1985)	AS19.2123	♂	Singapore	1.406, 103.971
Evarcha falcata (Clerck, 1757)	RU18-5264	♂	Russia	53.721, 77.726
Ghatippus paschima Marathe & Maddison, 2024	IBC-BP833	♂	India	12.220–1, 75.657–8
Habronattus hirsutus (Peckham & Peckham, 1888)	IDWM.21018	♂	Canada	48.827, -123.265
Hyllus keratodes (van Hasselt, 1882)	DDKM21.028	♂	Malaysia	3.325, 101.753
Hyllus semicupreus (Simon, 1885)	AS19.4415	♂	India	12.2156, 75.6606
Iranattus rectangularis Prószyński, 1992	DDKM21.091	juv.	India	26.28, 70.40
Pancorius dentichelis (Simon, 1899)	SWK12-0042	♂	Malaysia	1.605–6, 110.185–7
Pancorius alboclypeus Kanesharatnam & Benjamin, 2021	IFS_SAL_1145	♂	Sri Lanka	7.338611, 80.850833
Pancorius altus Kanesharatnam & Benjamin, 2021	IFS_SAL_1074	?	Sri Lanka	—
Pancorius athukoralai Kanesharatnam & Benjamin, 2021	IFS_SAL_1048	♂	Sri Lanka	7.145833, 80.698056
Pancorius petoti Prószyński & Deeleman-Reinhold, 2013	SWK12-0195	♂	Malaysia	1.603–4, 110.185
Pellenes limbatus Kulczyński, 1895	RU18-5679	♂	Russia	50.0501, 89.3878
Plexippus paykulli (Audouin, 1826)	AS19.7337	♂	India	12.825–6, 78.252–3
Ptocasius weyersi Simon, 1885	DDKM21.069	♂	Singapore	1.36, 103.78
Telamonia festiva Thorell, 1887	DDKM21.048	♂	China	21.8105, 107.2925
Tenkana arkavathi (Caleb, 2022)	IBC-BX509	♂	India	13.327, 77.657
Tenkana jayamangali **gen et. sp. nov.**	IBC-BX511	♀	India	13.3843, 77.2069
Tenkana manu (Caleb, Christudhas, Laltanpuii & Chitra, 2014)	IBC-BX510	♀	India	12.0305, 79.8483
Thyene imperialis (Rossi, 1846)	AS19.6443	♂	India	12.216, 76.625

Raw demultiplexed reads were processed with PHYLUCE v. 1.6 (Faircloth 2016), quality control and adapter removal were performed with Illumiprocessor wrapper (Faircloth 2013), and assemblies were created with SPAdes v. 3.14.1 (Nurk et al. 2013) using options at default settings. The UCE loci were recovered using RTA_v3 probeset (Zhang et al. 2023). The recovered loci were aligned with MAFFT using L-INS-i option (Katoh and Standley 2013). The

aligned UCE loci were then trimmed with Gblocks (Castresana 2000; Talavera and Castresana 2007) using –b1 0.5, –b2 0.7, –b3 8, –b4 8, –b5 0.4 setting within Mesquite v. 3.81 (Maddison and Maddison 2023b). As in the analysis of Maddison et al. (2020), loci suspected to include paralogies were deleted based on branch lengths in RAxML (Stamatakis 2014) inferred gene trees. Loci represented in fewer than 10 taxa total were deleted.

UCE phylogenomic analysis

Maximum-likelihood phylogenetic and bootstrap analyses were performed with IQ-TREE v. 2.3.4 (Minh et al. 2020) using the Zephyr v. 3.31 package (Maddison and Maddison 2023a) in Mesquite v. 3.81 (Maddison and Maddison 2023b) on the concatenated, unpartitioned UCE dataset with 25 taxa. For the phylogenetic tree inference, the option -m TEST (standard model selection followed by tree inference, edge-linked partition model, no partition-specific rates) was used with 10 search replicates. For the bootstrap analysis, a single IQ-TREE search was used for each of the 1000 search replicates.

Four-gene phylogenetic analysis

The loci were aligned using MAFFT with the L-INS-i option, partitioned by locus, assigned codon positions to minimize stop codons for H3 and COI, and then concatenated in Mesquite v. 3.81. Maximum-likelihood phylogenetic and standard bootstrap analyses were performed with IQ-TREE v. 2.3.4 on the concatenated dataset using the Zephyr v. 3.31 package in Mesquite v. 3.81. The option -m MFP+MERGE (find the best partition scheme including FreeRate heterogeneity followed by tree inference, edge-linked partition model (-spp), with partition-specific rates) was used with 10 search replicates. For the bootstrap analysis, a single IQ-TREE search was used for each of 1000 search replicates. For both, four partitions were provided. IQ-TREE found the best partition scheme (Chernomor et al. 2016) and best fitting models (Kalyaanamoorthy et al. 2017) for phylogenetic tree inference: GTR+F+I+R2 model for 28S+H3 merged partition, GTR+F+I+G4 for 18S and COI separate partitions. Two trees were obtained: (1) unconstrained tree for 34 taxa, followed by standard bootstrap analysis (Fig. 3). (2) A constrained tree for the same dataset, followed by standard bootstrap analysis with an additional option of -g to specify (*Tenkana*, (*Hyllus*, *Telamonia*)) as the topological constraint (Fig. 2).

Data availability

The raw sequence reads obtained from UCE capture are stored within the Sequence Read Archive (BioProject: PRJNA1145028, https://www.ncbi.nlm.nih.gov/bioproject/PRJNA1145028), and their accession numbers are listed in Table 2. The sequences obtained through UCE bycatch are available from the nucleotide database of the National Center for Biotechnology Information (NCBI, https://www.ncbi.nlm.nih.gov/), and their accession numbers are listed in Table 3. Concatenated UCE and legacy Sanger four-gene matrices used for phylogenetic and bootstrap analysis, along with trees, are available on the Dryad data repository (https://doi.org/10.5061/dryad.b8gtht7np).

Table 2. Specifics of molecular data used for this phylogenomic analysis. Molecular data was generated based on RTA_v2 probeset. "**SRA"** is Sequence Read Archive accession number available through NCBI; "**Reads pass QC"** is the number of reads after the removal of adapter-contamination and low-quality bases using Illumiprocessor; "**Total UCE loci"** is the total number of UCE loci recovered with RTA_v2 probeset; **"After paralogy filter"** is the number of UCE loci after deletion of suspected paralogous loci based on branch length ratios; "**In at least 10 taxa"** is the number of UCE loci in at least 10 or more taxa after branch length criteria; "**Filtered UCE sequence length"** is the concatenated sequence length of filtered UCE loci; **"Total loci"** is the number of UCE loci represented among all taxa. An asterisk besides cf. *Colopsus* sp. indicates that the SPAdes assembly was obtained from the senior author of Lin et al. (2024).

Species	Voucher	SRA	Reads pass QC	Total UCE loci	After paralogy filter	In at least 10 taxa	Filtered UCE sequence length
Anarrhotus fossulatus	AS19.1319	SRR27728361	15542927	2525	2442	2359	1937986
Artabrus erythrocephalus	AS19.2205	SRR27728359	14903498	2839	2753	2705	2160708
Baryphas ahenus	d536	SRR27728358	2653688	2256	2183	2171	940794
Bianor maculatus	NZ19.9864	SRR27728369	7914005	2963	2871	2764	2228134
Carrhotus sp.	AS19.4650	SRR27728370	5272657	2922	2834	2751	2179446
*cf. *Colopsus* sp.	JXZ795	SRR27541609	NA	2566	2478	2421	1977579
Chrysilla volupe	AS19.6089	SRR28802507	4968344	2878	2787	2692	2154458
Epeus sp.	DDKM21.055	SRR27728357	13896435	2898	2809	2743	2252399
Evacin bulbosa	AS19.2123	SRR27728356	10851810	2767	2683	2598	2014108
Evarcha falcata	RU18-5264	SRR27728355	11538276	2763	2676	2629	2064600
Ghatippus paschima	IBC-BP833	SRR27728354	7881860	2893	2806	2748	2249548
Habronattus hirsutus	IDWM.21018	SRR27728360	6581974	2821	2734	2647	2046288
Hyllus keratodes	DDKM21.028	SRR27728353	11349372	2926	2831	2749	2233053
Hyllus semicupreus	AS19.4415	SRR27728368	9874003	2942	2852	2784	2249371
Iranattus rectangularis	DDKM21.091	SRR28802508	14825117	2927	2839	2767	1863497
Pancorius dentichelis	SWK12-0042	SRR27728367	6025337	3092	3003	2931	2167369
Pancorius petoti	SWK12-0195	SRR27728366	5116119	2980	2891	2820	2147865
Pellenes limbatus	RU18-5679	SRR28802506	4288156	2661	2577	2522	1876069
Plexippus paykulli	AS19.7337	SRR27728365	7445183	2931	2839	2764	2048859
Ptocasius weyersi	DDKM21.069	SRR27728364	9926900	2880	2796	2739	2166828
Telamonia festiva	DDKM21.048	SRR27728363	7908436	2950	2856	2797	2281787
Tenkana arkavathi	IBC-BX509	SRR30215970	3427028	2723	2639	2618	2126265
Tenkana jayamangali	IBC-BX511	SRR30215969	2496709	2829	2740	2714	2230595
Tenkana manu	IBC-BX510	SRR30215968	3553397	2692	2600	2578	1979121
Thyene imperialis	AS19.6443	SRR27728362	7797854	2893	2802	2733	2232707
			Average:	2820.68	2732.84	2669.76	2072377.36
			Minimum:	2256	2183	2171	940794
			Maximum:	3092	3003	2931	2281787
			Total loci:	3404	3302	3043	2557548

Results

Phylogenetic results

Table 2 lists the sequence data recovered from the 25 taxa. 3404 UCE loci were initially recovered. Of these, 3302 remained after removing those suspected to include paralogies on branch lengths, and 3043 remained after removing those represented in fewer than 10 taxa. These were concatenated into the final matrix whose aligned length is 2557548 base pairs, in which each taxon had on average ~2 million base pairs of sequence data (min. 940794, max. 2281787). Table 3 lists sequence data for four genes for 34 taxa, including bycatch sequence data for 25 UCE taxa and *Colopsus* spp. gathered from NCBI.

Table 3. Accession numbers of nuclear 28S, 18S, H3, and mitochondrial COI fragments used in the four-gene phylogenetic analysis. An asterisk beside species indicates that the data for those were downloaded from NCBI and NA in cells indicate that data is not available.

Species	Voucher	28S	18S	H3	COI
Anarrhotus fossulatus	AS19.1319	PQ278946	PQ278921	PQ273890	PQ305882
Artabrus erythrocephalus	AS19.2205	PQ278958	PQ278933	PQ273902	PQ305894
Baryphas ahenus	d536	PQ278949	PQ278924	PQ273893	PQ305885
Bianor maculatus	NZ19.9864	PQ278944	PQ278931	PQ273888	PQ305892
Carrhotus sp.	AS19.4650	PQ278960	PQ278935	PQ273904	PQ305896
cf. *Colopsus* sp.	JXZ795	PQ278963	PQ278938	PQ273907	NA
Chrysilla volupe	AS19.6089	PQ278959	PQ278934	PQ273903	PQ305895
**Colopsus cancellatus*	IFS_SAL_360	MN888680.1	MN888692.1	MN895432.1	MN895417.1
**Colopsus cancellatus*	IFS_SAL_797	MN888677.1	MN888691.1	NA	MN895414.1
**Colopsus ferruginus*	IFS_SAL_233	MN888672.1	MN888689.1	MN895429.1	MN895411.1
**Colopsus ferruginus*	IFS_SAL_248	MN888673.1	MN888690.1	MN895431.1	MN895409.1
**Colopsus magnus*	IFS_SAL_832	MN888671.1	MN888687.1	NA	MN895408.1
**Colopsus magnus*	IFS_SAL_906	MN888670.1	MN888686.1	NA	MN895407.1
Epeus sp.	DDKM21.055	PQ278945	PQ278920	PQ273889	PQ305881
Evacin bulbosa	AS19.2123	NA	PQ278927	PQ273896	PQ305888
Evarcha falcata	RU18-5264	PQ278955	PQ278930	PQ273899	PQ305891
Ghatippus paschima	IBC-BP833	PQ278962	PQ278937	PQ273906	PQ305897
Habronattus hirsutus	IDWM.21018	PQ278948	PQ278923	PQ273892	PQ305884
Hyllus keratodes	DDKM21.028	PQ278942	PQ278917	PQ273887	PQ305879
Hyllus semicupreus	AS19.4415	PQ278947	PQ278922	PQ273891	PQ305883
Iranattus rectangularis	DDKM21.091	PQ278953	PQ278928	PQ273897	PQ305889
**Pancorius alboclypeus*	IFS_SAL_1145	MN888667	MN888685	MN895424	MN895404
**Pancorius altus*	IFS_SAL_1074	MN888666	NA	MN895422	MN895403
**Pancorius athukoralai*	IFS_SAL_1048	MN888663	MN888683	MN895421	MN895401
Pancorius dentichelis	SWK12-0042	PQ278957	PQ278932	PQ273901	PQ305893
Pancorius petoti	SWK12-0195	PQ278939	PQ278914	PQ273884	PQ305876
Pellenes limbatus	RU18-5679	PQ278940	PQ278915	PQ273885	PQ305877
Plexippus paykulli	AS19.7337	PQ278941	PQ278916	PQ273886	PQ305878
Ptocasius weyersi	DDKM21.069	PQ278961	PQ278936	PQ273905	NA
Telamonia festiva	DDKM21.048	PQ278954	PQ278929	PQ273898	PQ305890
Tenkana arkavathi	IBC-BX509	PQ278950	PQ278925	PQ273894	PQ305886
Tenkana jayamangali	IBC-BX511	PQ278943	PQ278918	NA	NA
Tenkana manu	IBC-BX510	PQ278956	PQ278919	PQ273900	PQ305880
Thyene imperialis	AS19.6443	NA	PQ278926	PQ273895	PQ305887

The phylogenetic results are shown in Figs 1–3. In the UCE phylogeny (Fig. 1), the broader phylogenetic structure and the structure within Plexippina are consistent with (Marathe et al. 2024a, 2024b) and show generally high bootstrap values at the nodes as expected for high volume data. The constrained four-gene phylogeny (Fig. 2) respects the constraint used for tree search. Thus, the relationship of *Tenkana* is recovered similarly to the UCE phylogeny as (*Tenkana*, (*Hyllus*, *Telamonia*)), showing high bootstrap values. However, the general relationships among plexippines in unconstrained and constrained four-gene phylogeny are less reliable, as reflected in the low bootstrap values.

Tenkana is nestled well within Plexippina as expected and recovered as the sister group to *Hyllus* C.L. Koch, 1846, and *Telamonia* Thorell, 1887 in clade 3 of the UCE phylogeny (see Fig. 1): (*Tenkana*, (*Hyllus*, *Telamonia*)). The type species

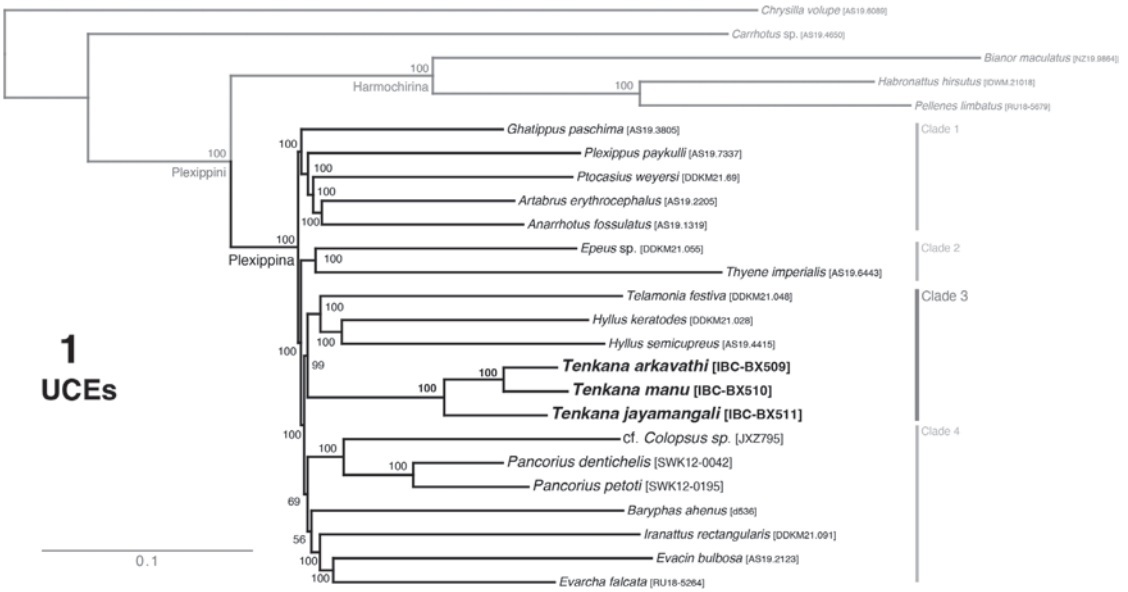

Figure 1. Maximum-likelihood tree from IQ-TREE analysis (best of 10 replicates) of a concatenated dataset of 3043 UCE loci. Numbers at the nodes are the percentage recovery of the clade based on 1000 bootstrap replicates. *Tenkana* is recovered as a sister genus to *Hyllus* and *Telamonia* in clade 3 and distantly from cf. *Colopsus* and *Pancorius* of clade 4.

of *Colopsus* and other members of the *cancellatus* group were found to be closely related to *Pancorius* Simon, 1902 (similarly to Kanesharatnam and Benjamin 2021). The *manu* species group is not closely related, however, to *Pancorius* and *Colopsus*. In the UCE phylogeny, it is recovered distantly from *Pancorius* and cf. *Colopsus* of clade 4 (see Fig. 1), while in unconstrained and constrained four-gene phylogenies, it is distant from *Pancorius*, cf. *Colopsus*, and the true *Colopsus* from Sri Lanka (Figs 2, 3). Their phylogenetic distance helps to explain the morphological differences between the *manu* group (non-glossy, non-elongate-bodied, tegulum with tegular lobe, medially located two ECPs) and the *cancellatus* group (glossy, elongate-bodied, without tegular lobe, laterally placed two ECPs).

Therefore, we propose *Tenkana* as a new genus to contain two species of the *manu* group currently placed within *Colopsus* and the new species described below.

Taxonomic results

Family Salticidae Blackwall, 1841
Subfamily Salticinae Blackwall, 1841
Tribe Plexippini Simon, 1901
Subtribe Plexippina Simon, 1901

***Tenkana* Marathe, Maddison & Caleb, gen. nov.**
https://zoobank.org/DE907A64-1CEC-4AE0-8976-929CCC31553D
Kannada: ತೆಂಕಣ; Telugu: తెంకణ; Tamil: தென்கண; Malayalam: ടെൻകണ; Devanagari: तेंकण

Type species. *Hyllus manu* Caleb, Christudhas, Laltanpuii & Chitra, 2014.

Species included. *Tenkana arkavathi* (Caleb, 2022), comb. nov.; *Tenkana jayamangali* gen. et sp. nov.; *Tenkana manu* (Caleb, Christudhas, Laltanpuii & Chitra, 2014), comb. nov.

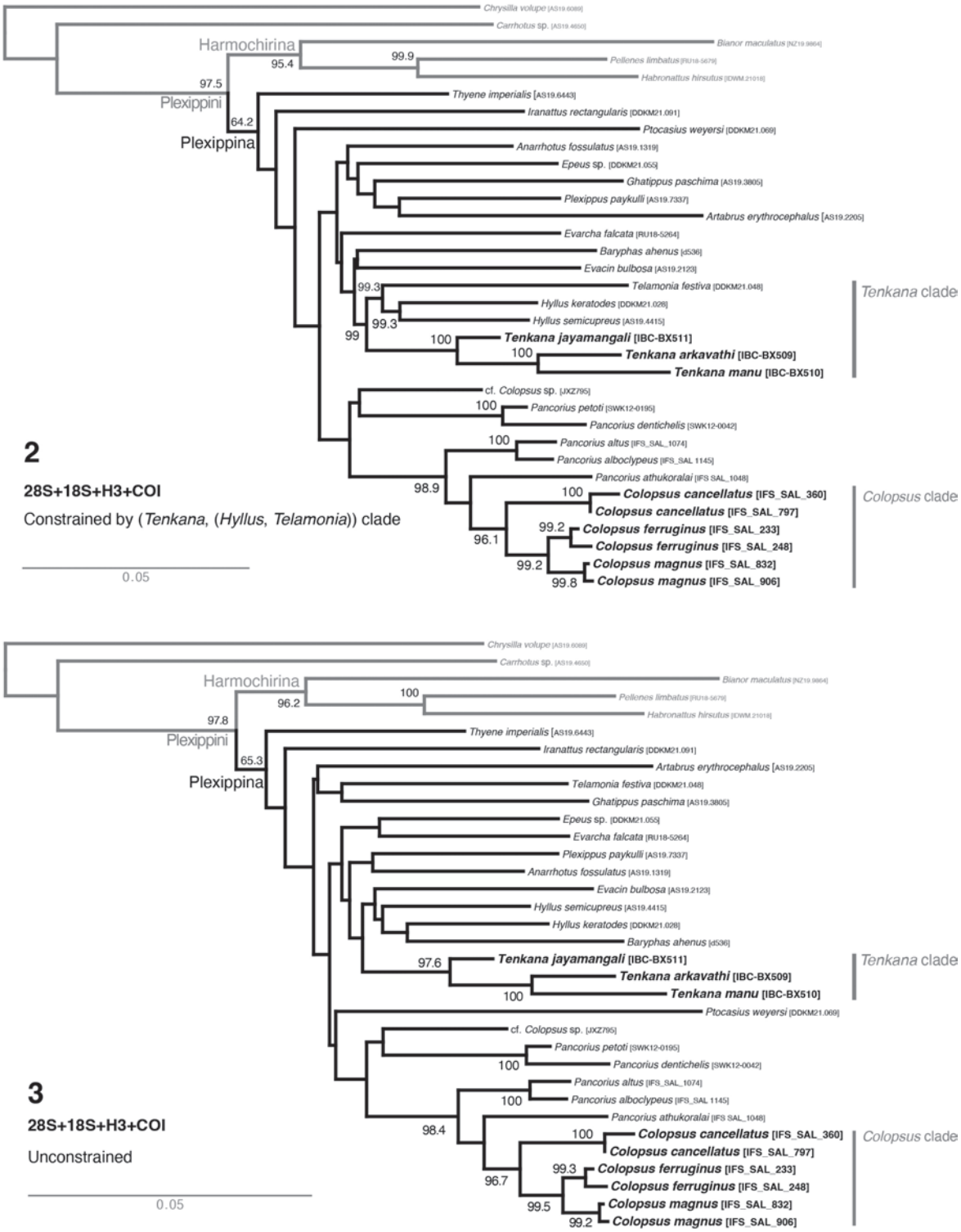

Figures 2, 3. 2 Maximum-likelihood tree from IQ-TREE analysis (best of 10 replicates) constrained for Tenkana clade (using clade 3 of the UCE tree, see Fig. 1) **3** Maximum-likelihood tree from IQ-TREE analysis (best of 10 replicates) without the constraint. The trees are inferred from a gene partitioned, concatenated nuclear 28S, 18S, H3 and mitochondrial COI genes. Numbers at the nodes are the percentage recovery of the clade based on 1000 bootstrap replicates and nodes without numbers suggests that those clades were not recovered in bootstrap analysis. *Tenkana* is recovered distantly (see *Tenkana* clade) from the type species of *Colopsus*, *Colopsus cancellatus* and other Sri Lankan *Colopsus* (see *Colopsus* clade) in both constrained and unconstrained trees.

Etymology. 'Tenkana' is a Kannada word meaning 'south'. The name acknowledges that all known species of the genus are found in the southern part of the Indian subcontinent. The gender of the name is to be treated as feminine. The transliterations to different Indian languages are meant only for accessibility and do not represent required pronunciations or transliterations.

Diagnosis. The phylogeny implies genetic diagnosability. Morphologically, *Tenkana* is a ground-dwelling plexippine with very robust first legs, recognisable by conspicuous pale bands under the ocular area ridge, often covering the entire surface and narrowing posteriorly on a rounded carapace. The teardrop-shaped abdomen has a broad median pale band. The stubby, non-glossy body of *Tenkana* distinguishes it from elongate, glossy *Colopsus* and from its closest relatives, glossy *Hyllus* and elongate *Telamonia*.

Tenkana may resemble *Hyllus* in sharing rounded body form, hair tufts behind ALEs, and membrane-accompanied embolus, but differs in epigyne (two ECPs in *Tenkana* vs none or reduced in *Hyllus*), and RTA (relatively delicate, narrow, short with pointed tip vs robust, broad with serrated broad tip). *Tenkana* can be confused with *Colopsus*, but they differ in embolus (membrane-accompanied in *Tenkana* vs membrane-lacking in *Colopsus*), tegular lobe (pronounced vs unpronounced or lacking), epigyne (medially located ECPs vs laterally located ECPs), and chelicerae (simple vs exaggerated).

Distribution. The southern states of India (Andhra Pradesh, Karnataka, Kerala, Tamil Nadu, and Telangana) and the northern region of Sri Lanka.

Natural history. *Tenkana* appears to be an exclusively ground-dwelling group. It is often found among relatively complex microhabitats of shaded short grasses with dry leaf litter in groves or relatively simpler microhabitats in open, sunny, sparse short grasses associated with rocky outcrops in relatively dry habitats. Its movements are reminiscent of those of the unrelated ground-dwelling *Stenaelurillus* jumping spiders (Aelurillini, Aelurillina).

***Tenkana jayamangali* Caleb & Marathe, sp. nov.**

https://zoobank.org/C4C0B4D7-20BF-4566-959B-C015940AF4E6

Figs 4–24

Kannada: ತೆಂಕಣ ಜಯಮಂಗಲಿ; Devanagari: तेंकण जयमंगलि

Materials examined. India • Karnataka, Tumakuru; 13.3843°N, 77.2069°E; 987 m a.s.l.; 23 April 2023; coll. Y.T. Lohit & B.G. Nisha. ***Holotype*:** • ♂ (I/SP-48) in ZSIC, ***Paratypes*:** • 1 ♀ (I/SP-49) in ZSIC; • 1 ♂ (IBC-BX512); • 1 ♀ (IBC-BX513) in NCBS. ***Paratype*:** • 1 ♀ (IBC-BX511) in NCBS, 16 December 2023; coll. B.G. Nisha.

Etymology. The specific epithet 'jayamangali', a noun in apposition, is the name of a river originating in Devarayanadurga, Tumakuru, where this species was observed for the first time.

Diagnosis. The phylogenies recover *Tenkana jayamangali* as a sister species to *T. arkavathi* and *T. manu*. In the males of *T. jayamangali*, pale hairs occupy most of carapace surface area leaving small bald patch posteriorly, while in *T. arkavathi* and *T. manu*, pale hairs are gentler on carapace forming narrower bands on carapace laterally, tapering posteriorly. Ocular area of *T. jayamangali* covered with white hairs uniformly, while *T. arkavathi* has distinctive V-shaped bands and

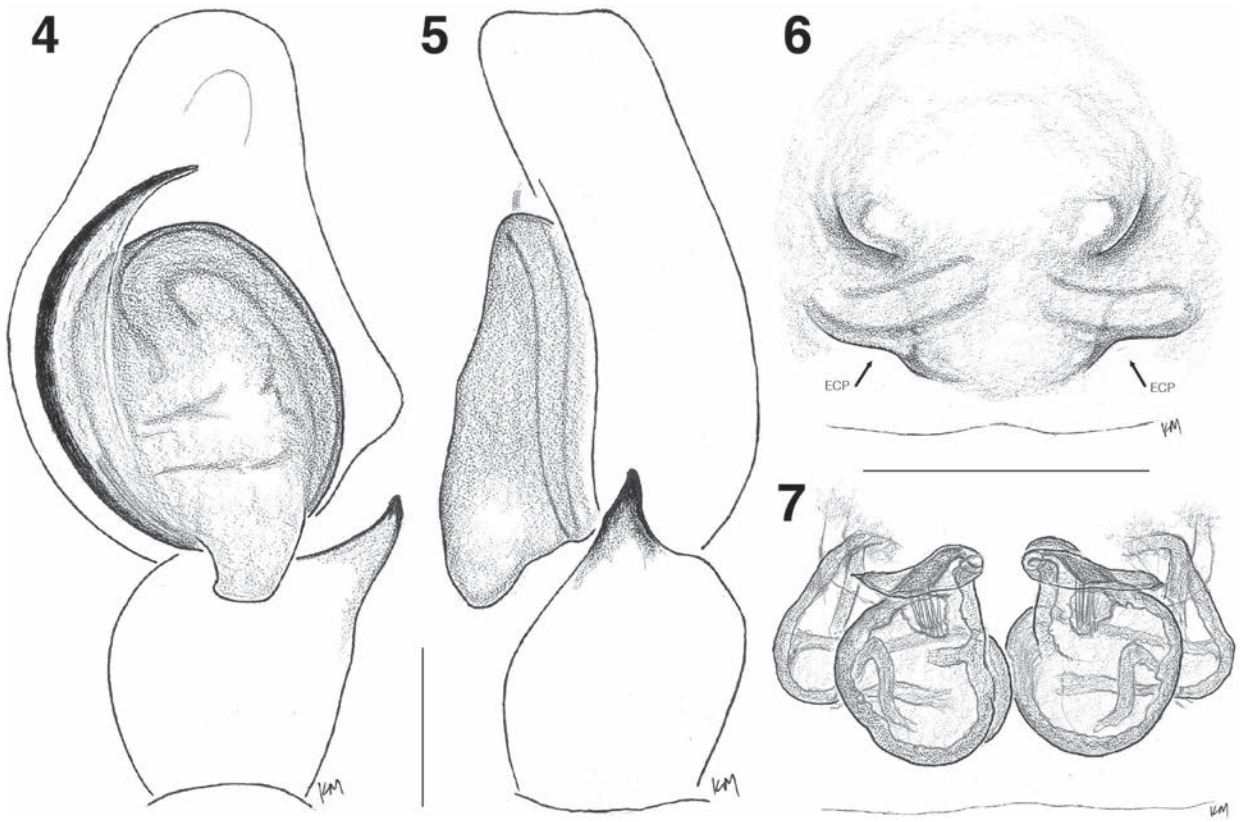

Figures 4–7. Genitalia of *Tenkana jayamangali* sp. nov. **4** male left palp, ventral view (holotype I/SP-48) **5** ditto, retrolateral view (holotype I/SP-48) **6** epigyne, ventral view (paratype IBC-BX511) **7** vulva, dorsal view (paratype IBC-BX511). Scale bars: 0.2 mm. **ECP**, epigynal coupling pocket.

T. manu has bald ocular area. From ventrally, RTA can be seen extending much more laterally with slight bend sub-apically in *T. jayamangali*, while *T. arkavathi* with relatively short with prominent bend and *T. manu* with longer with no bend. Short sperm duct loop arising at 11 o'clock in *T. jayamangali*, while much longer sperm duct arising at 10 o'clock in *T. arkavathi* and *T. manu*). ECPs laterally placed *T. jayamangali*, while ECPs medially in *T. arkavathi* and *T. manu*).

Description. ♂ (I/SP-48 in ZSIC). Total length 5.18; carapace 2.66 long, 2.09 wide; abdomen 2.52 long, 1.77 wide. ***Carapace***, brown, white hairs laterally traversing posteriorly. In life, white hairs cover most of its surface area leaving small patch of bald black integument on thoracic slope. Tufts of thick bunch of hairs ('eye lashes') behind ALEs and below PMEs. In life, reddish-orange small hairs along the circumference of anterior eyes. ***Clypeus*** brown, length 0.19. ***Chelicerae*** brown. ***Legs*** brown, robust. Leg I and II ventrally fringed thickly with black hairs, but less densely on leg II. White leaf-like hairs interspersed prolaterally on patella and tibia of leg I; similar white hairs retrolaterally on femora of leg I and II and distal end and proximal and distal ends of leg III and IV femora. Leg measurements: I 5.66 (1.68, 1.16, 1.38, 0.88, 0.56); II 4.86 (1.62, 0.89, 1.05, 0.77, 0.53); III 5.54 (1.94, 0.94, 1.06, 0.95, 0.65); IV 5.56 (1.77, 0.76, 1.13, 1.19, 0.71). Leg formula 1432. ***Palp*** (Figs 4, 5, 8, 9) medium long membrane-accompanied embolus arising at 6 o'clock. Ovoid tegulum with prominent tegular lobe. RTA short, simple (Figs 5, 9). ***Abdomen*** brown and black mottlings on yellow integument, which is pronounced medially with band like appearance. Chevronous markings posteriorly. In life, bright orange coloured. Spinnerets brown, somewhat long.

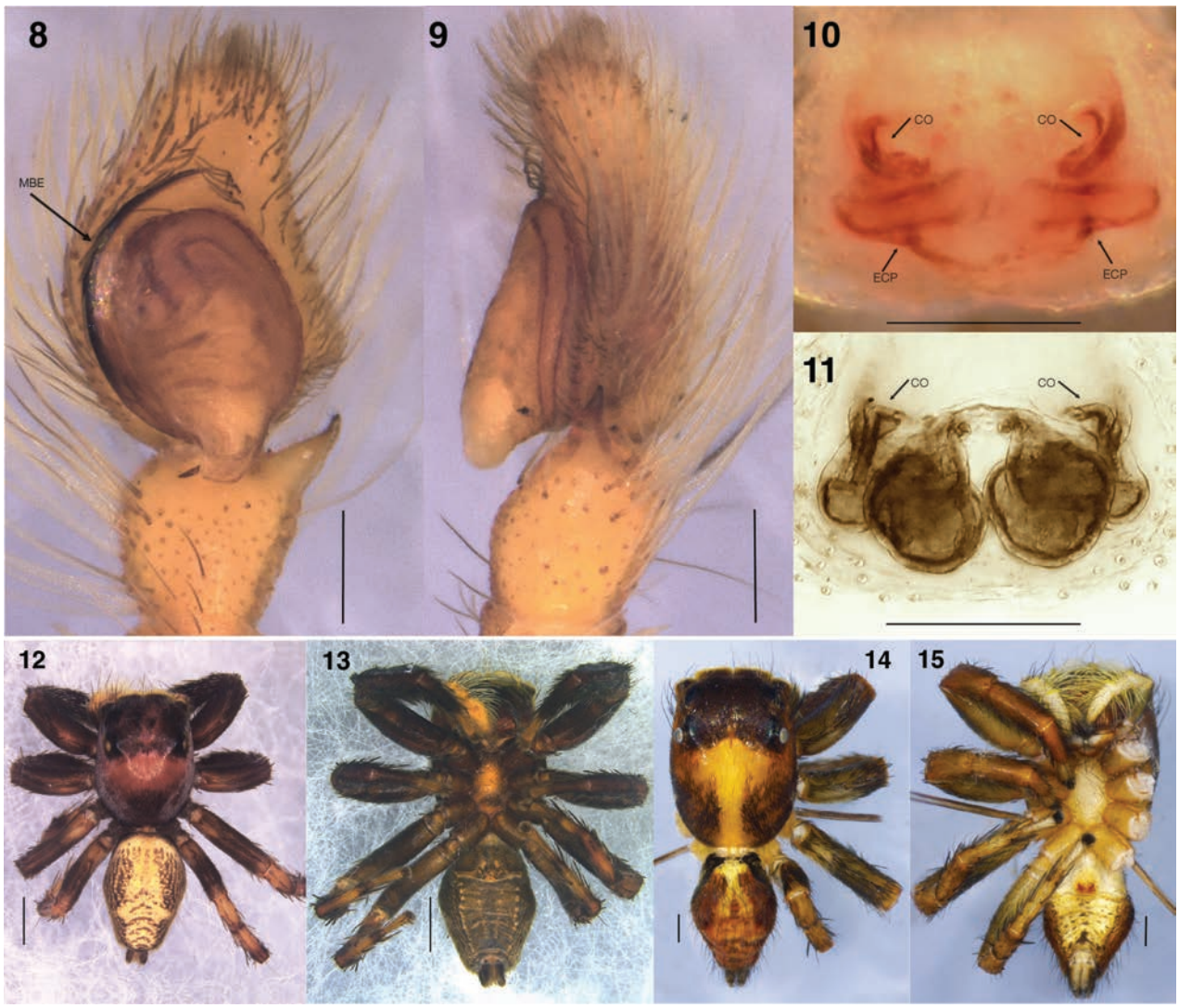

Figures 8–15. Photographs of genitalia and preserved bodies of *Tenkana jayamangali* sp. nov. Genitalia **8** male left palp, ventral view (holotype I/SP-48) **9** ditto, retrolateral view (holotype I/SP-48) **10** epigyne, ventral view (paratype IBC-BX511) **11** vulva, dorsal view (paratype IBC-BX511). Bodies: **12** male (holotype I/SP-48), dorsal view **13** ditto, ventral view **14** female (paratype IBC-BX511), dorsal view; 15, ditto, ventral view. Scale bars: 0.2 mm for genitalia; 1.0 mm for bodies. **CO**, copulatory opening; **ECP**, epigynal coupling pocket; **MBE**, membrane-bearing embolus.

♀ (IBC-BX511 in NCBS). Total length 5.24; carapace 2.53 long, 2.19 wide; abdomen 2.71 long, 1.83 wide. ***Carapace*** brown, more or less bald. White pale stripe posteriorly on thoracic slope. Tufts of thick bunch of hairs ('eye lashes') behind ALEs and below PMEs. In life, reddish-orange small hairs along the circumference of anterior eyes. ***Clypeus*** brown, length 0.16. ***Chelicerae*** brown. ***Legs*** brown, robust, largely bald. Leg measurements: I 5.36 (1.66, 1.05, 1.23, 0.85, 0.57); II 4.85 (1.60, 0.94, 0.97, 0.80, 0.54); III 5.68 (2.00, 1.02, 1.06, 0.98, 0.62); IV 5.57 (1.78, 0.82, 1.09, 1.21, 0.67). Leg formula 3412. ***Abdomen*** comparable as in male. In life, medial yellowish band surrounded by yellow and black mottlings. ***Epigyne*** (Figs 6, 7, 10, 11) medially located shallow two ECPs flanked by crescent shaped copulatory openings. Lamellar copulatory ducts join simple spermatheca ventrally.

Distribution. In addition to the type locality, iNaturalist observations (e.g. Mohan 2024; Raj 2024) appearing to represent this species are recorded around Bengaluru, Karnataka.

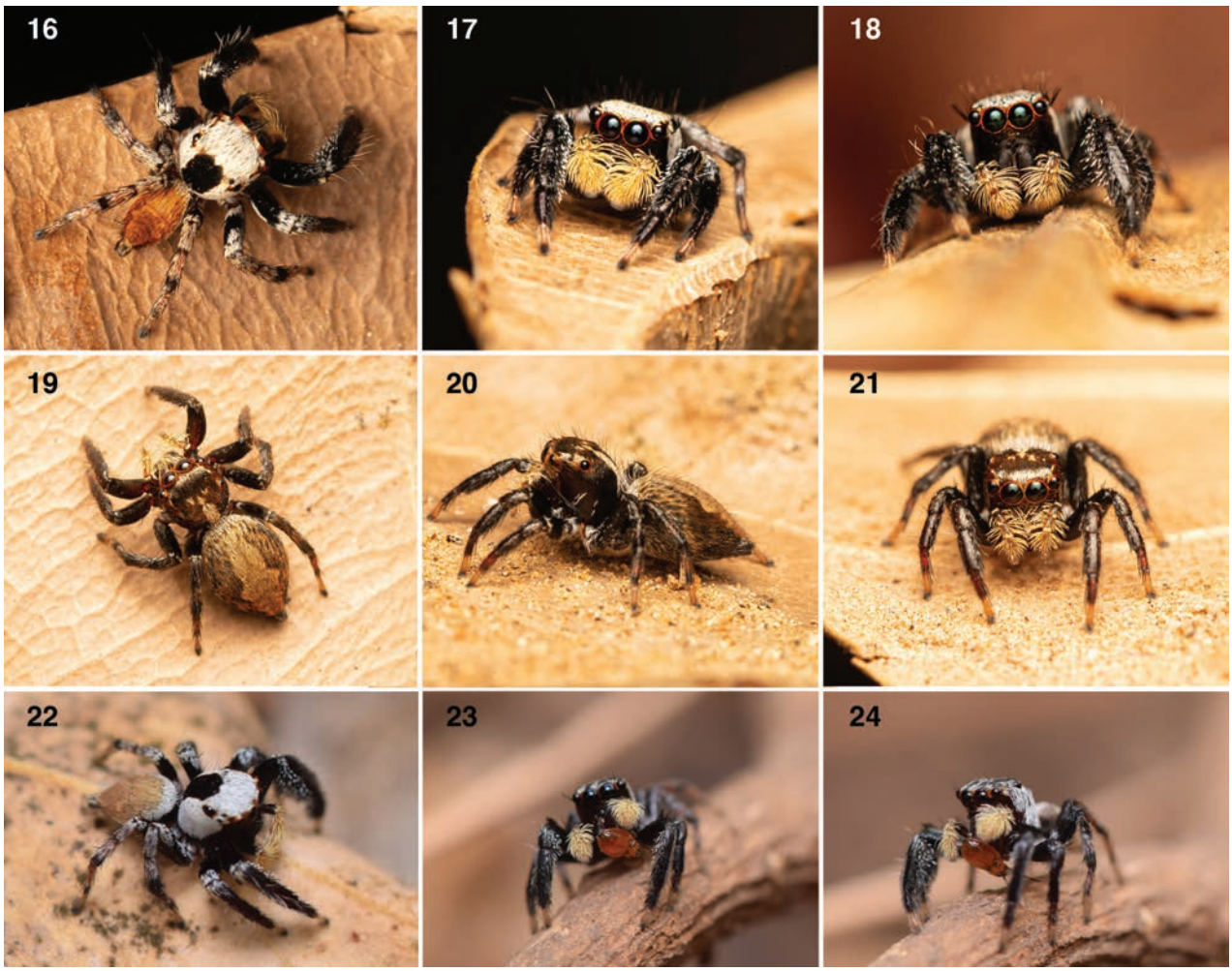

Figures 16–24. Habitus of *Tenkana jayamangali* sp. nov. **16–18** male **19–21** female **22** male **23–24** subadult male feeding on a bug nymph. Photo credit: Nisha B.G. (**16–21**) and Lohit Y.T. (**22–24**).

Natural history. *Tenkana jayamangali* was observed commonly in May; however, given the collecting of a female in December and iNaturalist observations, they may be adult year-round. *Tenkana jayamangali* were collected among dry leaf litter on the ground. A subadult was observed feeding on a bug nymph (Figs 23, 24).

Discussion. With *Tenkana*, the subtribe Plexippina now contains 36 genera; for India, the number of plexippines is 48 species in 19 genera (Maddison 2015; Marathe et al. 2024b; World Spider Catalog 2024). We continue to include *Colopsus* in the list of Indian plexippine genera, represented by *Colopsus peppara* Sudhin, Sen & Caleb, 2023. *Colopsus peppara* resembles *Tenkana* and *Pancorius* in body form; however, the features of the male palp could be attributed to *Colopsus* and *Pancorius* (simple round tegulum lacking tegular lobe and short embolus). What makes it puzzling is its epigyne, which has a medially located single ECP and does not match any of the three genera. The puzzling morphological features of *C. peppara*, along with a lack of clear synapomorphies for *Colopsus*, *Tenkana*, and *Pancorius*, compound the challenge of placing *C. peppara* definitively within a plexippine genus. Therefore, we propose maintaining the status quo until we can determine its placement using molecular data.

Acknowledgements

JTDC thanks Dr K.A. Subramanian, Officer-in-Charge, Southern Regional Centre, Zoological Survey of India, for kindly allowing the use of the microscope facility and Dr Deepak Nallaswamy Veeraiyan, the Director of Academics, SIMATS, Saveetha University, Chennai for necessary permissions to carry out the work. BGN, CCM, and YTL thank T.B. Dinesh and IruWay Hola (Janastu) for the place and sample collected from their land. Shashi Kumar, Darshan, S. Asha and Arun Kumar are thanked for their kind support during fieldwork. KM thanks Viraj Nawge (Biodiversity Lab, NCBS) for assisting in the field. KM and WPM thank Carol Ritland and Allyson Miscampbell of the Genetic Data Centre at the University of British Columbia for assistance with lab facilities. We thank Galina Azarkina and Junxia Zhang for reviewing the manuscript and providing useful comments.

Additional information

Conflict of interest

The authors have declared that no competing interests exist.

Ethical statement

No ethical statement was reported.

Funding

Funding to WPM was provided by an NSERC Canada Discovery Grant. Museum and lab work in NCBS was supported by an NCBS research grant to KK.

Author contributions

KM, BGN, CCM, and YTL participated in the fieldwork. KM, JTDC and KK managed specimens. KM did the molecular work. KK provided space and resources for molecular work. KM and WPM planned the molecular phylogenetic study, processed the data, and performed the phylogenetic analyses. KM and JTDC studied the morphology of *T. jayamangali*. JTDC made decisions about new species. KM did the drawings of *T. jayamangali* genitalia. KM, WPM, and JTDC made decisions about the new genus. KM studied the other *Tenkana* spp. morphologically for generic diagnosis and description. KK helped with microscopy. KM wrote the first draft of the manuscript, excluding the species description. JTDC wrote the first draft of the species description. KM and WPM finalized the first draft. All other authors assisted with additions and corrections to the manuscript.

Author ORCIDs

Kiran Marathe https://orcid.org/0000-0002-7364-3475
John T. D. Caleb https://orcid.org/0000-0002-9471-9467
Wayne P. Maddison https://orcid.org/0000-0003-4953-4575
B.G. Nisha https://orcid.org/0009-0006-7603-0785
Chinmay C. Maliye https://orcid.org/0009-0002-4050-9197
Y.T. Lohit https://orcid.org/0009-0007-8866-2226
Krushnamegh Kunte https://orcid.org/0000-0002-3860-6118

Data availability

All of the data that support the findings of this study are available in the main text.

References

Caleb JT, Lohit YT, Abhijith AP, Packiam SM (2022) A new species and new synonym in the genus *Colopsus* Simon, 1902 (Araneae: Salticidae: Plexippina) from India. Arthropoda Selecta 31: 470–476. https://doi.org/10.15298/arthsel.31.4.07

Castresana J (2000) Selection of Conserved Blocks from Multiple Alignments for Their Use in Phylogenetic Analysis. Molecular Biology and Evolution 17: 540–552. https://doi.org/10.1093/oxfordjournals.molbev.a026334

Chernomor O, Von Haeseler A, Minh BQ (2016) Terrace Aware Data Structure for Phylogenomic Inference from Supermatrices. Systematic Biology 65: 997–1008. https://doi.org/10.1093/sysbio/syw037

Faircloth BC (2013) illumiprocessor: a trimmomatic wrapper for parallel adapter and quality trimming. https://doi.org/10.6079/J9ILL

Faircloth BC (2016) PHYLUCE is a software package for the analysis of conserved genomic loci. Bioinformatics 32: 786–788. https://doi.org/10.1093/bioinformatics/btv646

Faircloth BC (2017) Identifying conserved genomic elements and designing universal bait sets to enrich them. Methods in Ecology and Evolution 8: 1103–1112. https://doi.org/10.1111/2041-210X.12754

Kalyaanamoorthy S, Minh BQ, Wong TKF, Von Haeseler A, Jermiin LS (2017) ModelFinder: fast model selection for accurate phylogenetic estimates. Nature Methods 14: 587–589. https://doi.org/10.1038/nmeth.4285

Kanesharatnam N, Benjamin SP (2021) Phylogenetic relationships and systematics of the jumping spider genus *Colopsus* with the description of eight new species from Sri Lanka (Araneae: Salticidae). Journal of Natural History 54: 2763–2814. https://doi.org/10.1080/00222933.2020.1869335

Katoh K, Standley DM (2013) MAFFT Multiple Sequence Alignment Software Version 7: Improvements in Performance and Usability. Molecular Biology and Evolution 30: 772–780. https://doi.org/10.1093/molbev/mst010

Lin L, Yang Z, Zhang J (2024) Revalidation of the jumping spider genus *Cheliceroides* Żabka, 1985 based on molecular and morphological data (Araneae, Salticidae). ZooKeys 1196: 243–253. https://doi.org/10.3897/zookeys.1196.117921

Maddison WP (2015) A phylogenetic classification of jumping spiders (Araneae: Salticidae). The Journal of Arachnology 43: 231. https://doi.org/10.1636/arac-43-03-231-292

Maddison DR, Maddison WP (2023a) Zephyr: a Mesquite package for interacting with external phylogeny inference programs. http://zephyr.mesquiteproject.org

Maddison WP, Maddison DR (2023b) Mesquite: a modular system for evolutionary analysis. http://www.mesquiteproject.org/ [August 18, 2023]

Maddison WP, Beattie I, Marathe K, Ng PYC, Kanesharatnam N, Benjamin SP, Kunte K (2020) A phylogenetic and taxonomic review of baviine jumping spiders (Araneae, Salticidae, Baviini). ZooKeys 1004: 27–97. https://doi.org/10.3897/zookeys.1004.57526

Marathe K, Maddison WP, Kunte K (2024a) *Ghatippus paschima*, a new species and genus of plexippine jumping spider from the Western Ghats of India (Salticidae, Plexippini, Plexippina). ZooKeys 1191: 89–103. https://doi.org/10.3897/zookeys.1191.114117

Marathe K, Tripathi R, Sudhikumar AV, Maddison WP (2024b) Phylogenomic placement and revision of *Iranattus* Prószyński, 1992 jumping spiders (Salticidae, Plexippini, Plexippina). Zoosystematics and Evolution 100: 531–542. https://doi.org/10.3897/zse.100.122034

Minh BQ, Schmidt HA, Chernomor O, Schrempf D, Woodhams MD, Von Haeseler A, Lanfear R (2020) IQ-TREE 2: New Models and Efficient Methods for Phylogenetic Inference in the Genomic Era. Teeling E (Ed.). Molecular Biology and Evolution 37: 1530–1534. https://doi.org/10.1093/molbev/msaa015

Mohan D (2024) Genus *Colopsus*. https://www.inaturalist.org/observations/215877785 [September 9, 2024]

Nurk S, Bankevich A, Antipov D, Gurevich A, Korobeynikov A, Lapidus A, Prjibelsky A, Pyshkin A, Sirotkin A, Sirotkin Y, Stepanauskas R, McLean J, Lasken R, Clingenpeel SR, Woyke T, Tesler G, Alekseyev MA, Pevzner PA (2013) Assembling Genomes and Mini-metagenomes from Highly Chimeric Reads. In: Deng M, Jiang R, Sun F, Zhang X (Eds) Research in Computational Molecular Biology. Lecture Notes in Computer Science. Springer Berlin Heidelberg, Berlin, Heidelberg, 158–170. https://doi.org/10.1007/978-3-642-37195-0_13

Prószyński J (1984) Atlas rysunków diagnostycznych mniej znanych Salticidae (Araneae). Zeszyty Naukowe Wyższej Szkoły Rolniczo-Pedagogicznej w Siedlcach 2: 1–777.

Raj K B (2024) Genus *Colopsus*. https://www.inaturalist.org/observations/220917937 [September 9, 2024]

Stamatakis A (2014) RAxML version 8: a tool for phylogenetic analysis and post-analysis of large phylogenies. Bioinformatics 30: 1312–1313. https://doi.org/10.1093/bioinformatics/btu033

Talavera G, Castresana J (2007) Improvement of Phylogenies after Removing Divergent and Ambiguously Aligned Blocks from Protein Sequence Alignments. Kjer K, Page R, Sullivan J (Eds) Systematic Biology 56: 564–577. https://doi.org/10.1080/10635150701472164

World Spider Catalog (2024) World Spider Catalog. https://wsc.nmbe.ch/ [July 1, 2024]

Zhang J, Li Z, Lai J, Zhang Z, Zhang F (2023) A novel probe set for the phylogenomics and evolution of RTA spiders. Cladistics 39: 116–128. https://doi.org/10.1111/cla.12523

ZooKeys 1215: 107–125 (2024)
DOI: 10.3897/zookeys.1215.123624

Research Article

Description of *Ixodes lanigeri* sp. nov., a new hard tick species (Acari, Ixodidae) collected from mouse-eared bats (Vespertilionidae, *Myotis*) in Vietnam

Sándor Hornok[1,2], Jenő Kontschán[3,4], Ai Takano[5], Yasuhiro Gotoh[6], Alexandre Hassanin[7], Vuong Tan Tu[8,9]

1 *Department of Parasitology and Zoology, University of Veterinary Medicine, Budapest, Hungary*
2 *HUN-REN-UVMB Climate Change: New Blood-sucking Parasites and Vector-borne Pathogens Research Group, Budapest, Hungary*
3 *Plant Protection Institute, HUN-REN Centre for Agricultural Research, Budapest, Hungary*
4 *Department of Plant Sciences, Albert Kázmér Faculty of Mosonmagyaróvár, Széchenyi István University, Mosonmagyaróvár, Hungary*
5 *Department of Veterinary Medicine, Joint Faculty of Veterinary Medicine and The United Graduate School of Veterinary Science, Yamaguchi University, Yamaguchi, Japan*
6 *Department of Bacteriology, Faculty of Medical Sciences, Kyushu University, Fukuoka, Japan*
7 *Institut Systématique Evolution Biodiversité, Sorbonne Université, Muséum national d'Histoire naturelle, Paris, France*
8 *Institute of Ecology and Biological Resources, Vietnam Academy of Science and Technology, Hanoi, Vietnam*
9 *Graduate University of Science and Technology, Vietnam Academy of Science and Technology, Hanoi, Vietnam*

Corresponding author: Sándor Hornok (hornok.sandor@univet.hu)

Abstract

Historically, for more than one and a half centuries, only one so-called "long-legged bat tick" species, i.e., *Ixodes vespertilionis* Koch was known to science. However, during the past decade, it was recognized on a molecular basis that long-legged ixodid ticks associated with bats may represent at least six species. Of these, until recently, five have been morphologically described. In this study, *Ixodes* ticks were collected from two *Myotis* species in southeastern Asia, Vietnam. Based on the morphological and molecular characteristics of the female, nymph and larva, *Ixodes lanigeri* Hornok, **sp. nov.** is described here. The male is unknown. Like other members of the *Ixodes ariadnae* complex, *I. lanigeri* Hornok apparently shows a preference for vesper bats as its typical hosts. In this context, host-association and geographical separation may explain the evolutionary divergence of *I. lanigeri* Hornok from its closest relative occurring on *Murina hilgendorfi* Peters in East Asia, Japan, because no *Myotis* or *Murina* spp. have overlapping distribution between Vietnam and the main islands of Japan. On the other hand, supposing that (similarly to *I. ariadnae*) *I. lanigeri* Hornok probably occurs on other myotine bats and knowing that several *Myotis* species indigenous in Vietnam have a broad geographical range in southern and southeastern Asia, the new tick species most likely has a widespread distribution in this area.

Key words: Chiroptera, *Myotis alticraniatus*, *Myotis laniger*, new species, *Pholeoixodes*, Southeast Asia, taxonomy

Academic editor: Dmitry Apanaskevich
Received: 21 March 2024
Accepted: 26 August 2024
Published: 14 October 2024

ZooBank: https://zoobank.org/A5630974-77AF-41EC-B0D2-222378EE1124

Citation: Hornok S, Kontschán J, Takano A, Gotoh Y, Hassanin A, Tu VT (2024) Description of *Ixodes lanigeri* sp. nov., a new hard tick species (Acari, Ixodidae) collected from mouse-eared bats (Vespertilionidae, *Myotis*) in Vietnam. ZooKeys 1215: 107–125. https://doi.org/10.3897/zookeys.1215.123624

Introduction

Hard ticks (Acari: Ixodidae) are haematophagous arthropods that affect their vertebrate hosts in multiple ways, causing skin lesions, blood loss, and, most importantly, transmitting tick-borne pathogens (Jongejan and Uilenberg 2004). Although ixodid ticks (as arachnids in general) cannot fly, their association with flying vertebrate hosts, such as birds and bats, make them capable of travelling large geographical distances (de la Fuente et al. 2015).

In the context of Eurasia, latitudinal (west-to-east/southeast) connectedness of tick populations via flying vertebrate hosts shows significant differences depending on whether they associate with birds or bats. Bird migration allows unrestricted gene flow, as reflected by the near genetic identity of conspecific hard ticks collected from avian hosts in Central Europe and the Far East, Japan (Hornok et al. 2016a). On the other hand, while a similar phenomenon was observed among bat soft ticks (Acari: Argasidae) between Central Europe and Central Asia (Hornok et al. 2017a), populations of taxonomically closely related bat-associated hard ticks (Acari: Ixodidae) in Europe and Southeast Asia show remarkable morphological and genetic differences and appear to be reproductively isolated. This can explain why long-legged ixodid ticks collected from horseshoe bats (Rhinolophidae) in Europe and Southeast Asia (Vietnam) were recognized to belong to different species, from the latter region described under the name *Ixodes collaris* Hornok, 2016 (Hornok et al. 2016b).

Most recently, the detailed morphological and genetic analyses of ixodid ticks collected from bats in Japan (i.e., in the Far East) revealed that these are different from those in Europe and deserve taxonomic status as separate species (Takano et al. 2023). While one of the two long-legged bat tick species discovered in Japan (*Ixodes nipponrhinolophi* Hornok & Takano, 2023: a member of the *I. vespertilionis* complex) was also shown to be different from its sibling species in Southeast Asia (*I. collaris*, occurring in Vietnam), the second long-legged species (*Ixodes fujitai* Hornok & Takano, 2023: member of the *Ixodes ariadnae* Hornok, 2014 complex) was not compared in a similar context. The typical hosts of the latter group of ticks are vesper bats (Vespertilionidae), most notably *Myotis* and *Murina* species. The aim of this study was to compensate for the lack of data on members of the *I. ariadnae* complex in Vietnam, i.e., to characterize long-legged bat ticks collected from *Myotis* spp. in this country with both morphological and molecular biological methods.

Material and methods

Sample collection

Ticks were removed from two species of mouse-eared bats (*Myotis* spp.) at three locations in northern Vietnam (Fig. 1). The type material is described below. After collection, the ticks were stored individually in vials containing 96% ethanol.

Molecular-phylogenetic and morphological analyses

DNA was extracted from two larvae collected with and showing the same morphological characters as paratype #2. From one of these larvae, the complete mitogenome was amplified as reported (Takano et al. 2023). From the other

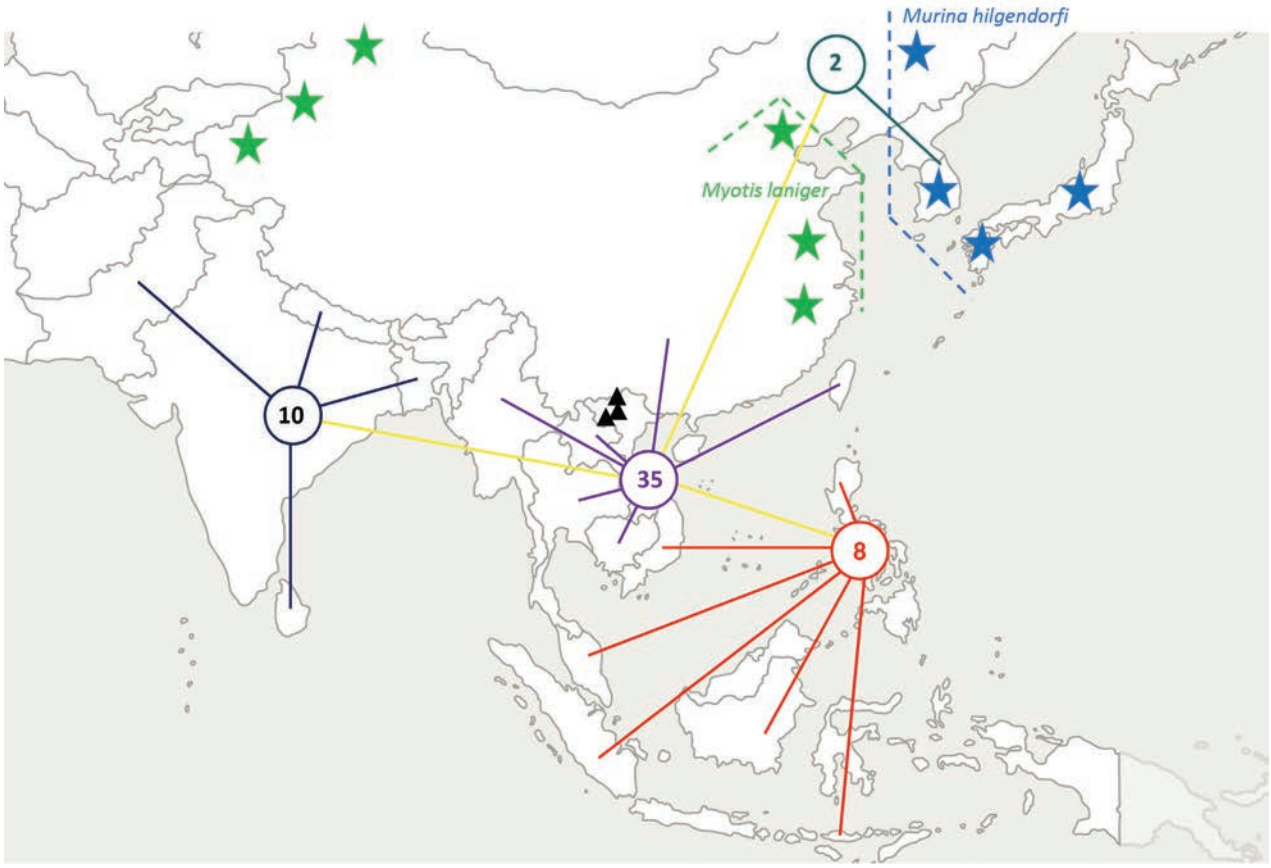

Figure 1. Map of Southeast and East Asia showing the number of *Myotis* and Murininae species indigenous in Vietnam and also occurring (1) in four countries (connected with dark blue lines) of the Himalayan and Indian subregions (*N* = 10 bat species), (2) in six countries (connected with purple lines) of the Indochinese (*N* = 35 bat species) subregion, as well as (3) in six countries (connected with red lines) of the Sundaic, Wallacean and Philippine (*N* = 8 bat species) subregions and (4) only two *Myotis* species from Vietnam occurring in and near the Korean Peninsula (blue line). For further details and references see Suppl. material 1. Black triangles show the collection sites of type material in northern Vietnam; green stars mark the eastern and western distribution limits of *Myotis laniger*; blue stars show the southernmost range of *Murina hilgendorfi*. The list of the species according to the above four categories: (1) *My. altarium* Thomas, 1911; *My. annectans* (Dobson, 1871); *My. hasseltii* (Temminck, 1840); *My. laniger* (Peter, 1871); *My. muricola* (Gray, 1846); *My. formosus* (Hodgson, 1835); *Harpiocephalus harpia* (Temminck, 1840); *Mu. cyclotis* Dobson, 1872; *Mu. huttoni* (Peters, 1872); *Mu. leucogaster* Milne-Edwards, 1872. (2) *My. altarium* Thomas, 1911; *My. ancricola* Kruskop et al., 2018; *My. annatessae* Kruskop & Borisenko, 2013; *My. annamiticus* Kruskop & Tsytsulina, 2001; *My. annectans* (Dobson, 1871); *My. ater* (Peters, 1866); *My. chinensis* (Tomes, 1857); *My. hasseltii* (Temminck, 1840); *My. horsfieldii* (Temminck, 1840); *My. indochinensis* Son et al., 2013; *My. laniger* (Peters, 1871); *My. montivagus* (Dobson, 1874); *My. muricola* (Gray, 1846); *My. phanluongi* Borisenko et al. 2008; *My. pilosus* (Peters, 1869); *My. rosseti* (Oey, 1951); *My. siligorensis* (Horsfield, 1855); *My. formosus* (Hodgson, 1835); *My. rufoniger* Tomes 1858; *Harpiocephalus harpia* (Temminck, 1840); *Harpiola isodon* Kuo et al., 2006; *Mu. annamitica* Francis & Eger, 2012; *Mu. beelzebub* Son et al., 2011; *Mu. chrysochaetes* Eger & Lim, 2011; *Mu. cyclotis* Dobson, 1872; *Mu. eleryi* Furey et al., 2009; *Mu. feae* (Thomas, 1891); *Mu. fionae* Francis & Eger, 2012; *Mu. harpioloides* Kruskop & Eger, 2008; *Mu. harrisoni* Crosba & Bates, 2005; *Mu. huttoni* (Peters, 1872); *Mu. kontumensis* Son et al., 2015; *Mu. leucogaster* Milne-Edwards, 1872; *Mu. lorelieae* Eger & Lim, 2011; *Mu. walstoni* Furey et al., 2011. (3) *My. ater* (Peters, 1866); *My. hasseltii* (Temminck, 1840); *My. horsfieldii* (Temminck, 1840); *My. muricola* (Gray, 1846); *My. siligorensis* (Horsfield, 1855); *Harpiocephalus harpia* (Temminck, 1840); *Mu. cyclotis* Dobson, 1872; *Mu. huttoni* (Peters, 1872). (4) *My. pilosus* (Peters, 1869); *My. rufoniger* Tomes 1858.

larva, as well as from one leg of the female holotype and two legs of the nymph paratype#1, an approx. 710-bp-long part of the cytochrome *c* oxidase subunit I (*cox*1) gene and a 450-bp-long part of the 16S rRNA gene were amplified and sequenced as reported (Hornok et al. 2014). The latter sequences were used

for phylogenetic analysis. Phylogenetic analysis was performed with MEGA 7 (Kumar et al. 2016), using 1000 bootstrap replicates and the Neighbor-Joining method, p-distance model. Measurements were performed and pictures were taken with a VHX-5000 digital microscope (Keyence Co., Osaka, Japan). The sizes in the descriptions below are provided in millimetres.

Taxonomic account

Family Ixodidae Koch
Genus *Ixodes* Latreille
Subgenus *Pholeoixodes* Schulze

***Ixodes lanigeri* Hornok, sp. nov.**
https://zoobank.org/F5F38340-44E4-45B0-8BFF-90C150548DD2
Figs 2–5

Diagnosis. Medium size, light brown prostriate tick with drop shape body of the female. Legs long. Basis capituli dorsally pentagonal, palps short and hypostome medium length. Scutum reverse pentagonal, broadest at mid-length, posteriorly rounded, with long, deep and curved cervical grooves.

Material examined. *Holotype*: • female from a female Himalayan whiskered bat (*Myotis alticraniatus* Osgood), collected in Vietnam (340 m a.s.l., Tho Than Cave, Xuan Son NP, Phu Tho Province: 21.138613°N, 104.939903°E) by Vuong Tan Tu on December 7, 2020. ***Paratype*** #1: • nymph from a male Chinese water myotis (*Myotis laniger* Peter), collected in Vietnam (1530 m a.s.l., Ta Phin # 1 Cave, Lao Cai Province: 22.402822°N, 103.836787°E) by Vuong Tan Tu on December 3, 2020. ***Paratype*** #2: • larva from a male Chinese water myotis (*M. laniger*), collected in Vietnam (1400 m a.s.l., Co Ma # 1 Cave, Co Ma Commune, Thuan Chau, Son La Province: 21.361139°N, 103.507718°E) by Vuong Tan Tu on December 17, 2020.

All above specimens are stored in ethanol and deposited at the Department of Parasitology, University of Veterinary Medicine, Budapest, Hungary (holotype and paratype #1) and the Institute of Ecology and Biological Resources, Hanoi, Vietnam (paratype #2).

Morphology. Female (engorged). Length of the idiosoma (from the half point between scapular apices to the middle of posterior margin) 3.38, width 2.74, ratio of idiosomal length/width 1.23 (Fig. 2).

Scutum reverse pentagonal, broadest at half-length, posteriorly rounded (Fig. 3G).

Length of scutum 1.26, maximum width 1.05, ratio length/width 1.2. On the scutum long, deep and curved cervical grooves, central and marginal rugosities and scattered punctuations visible (Fig. 3G). Caudolateral edge straight, with slight concavity where cervical grooves terminate. Scutal setae few, more evident laterally (length: 0.035).

Alloscutum with sparse hair covering dorsally. Length of centrodorsal setae 0.13, marginodorsal setae 0.1. Idiosoma with dense hair covering ventrally. Genital aperture flat W-shaped, with posterior concavity along its mid-line, situated slightly posterior to 2nd intercoxal space. Genital groove diverging backwards, with concavity at the level of 4th coxae. Spiracular plates asymmetrical,

Figure 2. Dorsal habitus of *Ixodes lanigeri* sp. nov. female.

pear-shape, length 0.4, position of opening submarginal, surrounding aeropyles (around a gap of 0.06) in 2–7 rows (Fig. 3D). Anal valves with setae measuring 0.1. Anal groove slightly converging from mid-length.

Length of gnathosoma (from palpal apices to posterior margin of basis capituli) 0.6, width of basis capituli dorsally 0.5. Ratio of gnathosomal length to basis capituli width 1.2. Length of basis capituli (from base of hypostome to posterior margin of basis capituli) 0.33, ratio of length to width of basis capituli 0.66. Basis capituli shape pentagonal, its sides parallel, anteriorly converging (Fig. 3A). Caudolateral corner oblique, slightly rounded, without cornuae and continuing as a dark brown lane of sclerotization along the relatively straight posterior margin. Areae porosae very large, elliptical (with their longitudinal axes perpendicular to each other), their breadth 0.18, interval narrow (0.06). Ventrally on basis capituli prominent, caudolaterally projecting auriculae, bearing two longitudinal ridges, posteriorly tapering (Fig. 4A). Behind auriculae constriction (“waist”). Posterior edge of ventral basis medially less, laterally strongly sclerotized and caudolaterally angled (Fig. 4A), its width shorter than distance between palpal articles I, laterally with a single hair (0.03).

Palps (dorsal view) short, club shape, edge curved medially, relatively straight laterally, length 0.63, maximum width 0.22, ratio length/width 2.9. Palpal hairs few (i.e., 4–6) medially, more numerous (as many as 12–14) laterally, shortest (measuring 0.02) anteriorly, longest (measuring 0.08) posteriorly. Palpal segment I with slight anterior protuberance, ventrally with two setae (0.05) and longitudinal ridge. Palpal segment II 0.33 long, anteriorly broadening, with a strongly sclerotized longitudinal ridge ventrally, both medial and lateral concavity (fovea) near mid-length, and a lateral protuberance near the junction with segment III (Fig. 3A). Two caudolateral hairs of palpal segment II, in and near the lateral concavity, have medium length (0.05). Palpal segment III 0.26 long, laterally concave, medially convex (Fig. 3A). Hypostome slightly lanceolate,

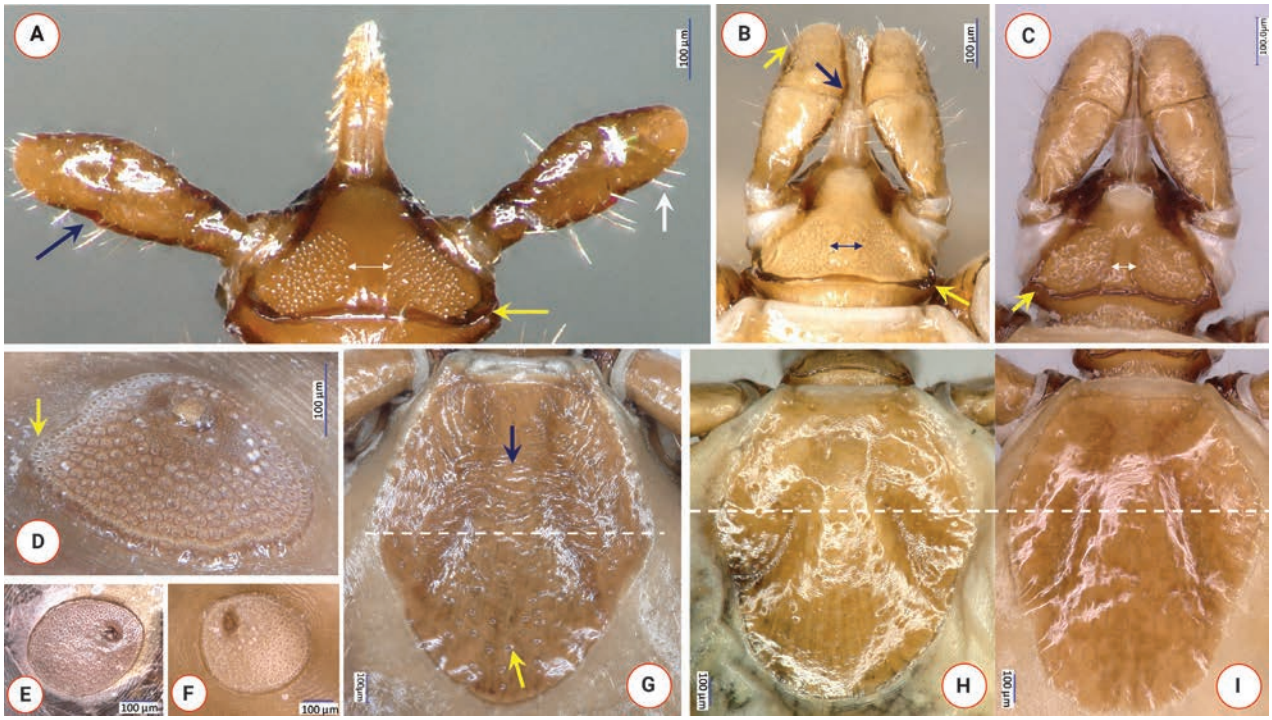

Figure 3. Key morphologic characters of *Ixodes lanigeri* sp. nov. female, in comparison with *I. fujitai* and *I. ariadnae* **A–C** dorsal view of basis capituli of **A** *I. lanigeri* sp. nov. (blue arrow: lateral protuberance of palpal segment II; white arrow: longest hair on palpal segment III; yellow arrow: caudolateral corner of basis; double white arrow: interval between porose areas) **B** *I. fujitai* (blue arrow: medial protuberance of palpal segment III; white arrow: longest hair on palpal segment III; yellow arrow: caudolateral corner of basis; double blue arrow: interval between porose areas) and **C** *I. ariadnae* (yellow arrow: caudolateral corner of basis; double white arrow: interval between porose areas) **D–F** Peritremes of **D** *I. lanigeri* sp. nov. (yellow arrow: narrowing) **E** *I. fujitai* and **F** *I. ariadnae* **G–I** scutum of **G** *I. lanigeri* sp. nov. (yellow arrow: relatively dense punctuations, blue arrow: rugosities) **H** *I. fujitai* and **I** *I. ariadnae* (the dashed line indicates the maximum width of the scutum). Collection data of samples used for comparison: *I. fujitai* female was removed from *Murina hilgendorfi* in Shiga (Japan) on April 22, 2016; *I. ariadnae* female was collected from the wall of Legény Cave (Pilis Mountains, Hungary) on March 5, 2017.

length 0.27, width 0.1, ratio length/width 2.7. Dental formula 2/2 (mid-length), in six rows (but apical part missing) (Fig. 4A).

Legs long, longer than 5 (Fig. 2). Coxae I asymmetrically trapezoid, coxae II rectangular, all coxae without spines or spurs but caudomedial angle of coxae I strongly sclerotized, with a slight protuberance laterally to it (Fig. 4A). A single coxal hair posterolaterally long (0.22), anterolaterally shorter (up to 0.1), except on coxae III where these two equal in length. Highest number of hair ($N > 5$) on coxae IV. Tarsus I. length 1.2, maximum diameter 0.1, length to diameter ratio 12. Haller's organ open, with six anterior pit sensillae arranged as a group of three, and another three in line.

Nymph (engorged). Length of the idiosoma 2.95 (Fig. 5A). Scutum broad, reverse pentagonal, broadest close to half-length (Fig. 5C). Length of scutum 0.61, maximum width 0.56, ratio length/width 1.1. On the scutum straight scapular groove measuring 0.1, and a relatively straight cervical groove reaching caudolateral margin at its middle, with a concavity. The surface has fine reticulate pattern. Punctuations not visible. Lateral scutal seta 0.04 long.

Alloscutum has few 0.08 long hair dorsally. Idiosoma has sparse hair covering ventrally (length: 0.04–0.05 between coxae, 0.1 in mid region and behind). Spiracular plates subcircular in shape, diameter 0.14, within marginal row

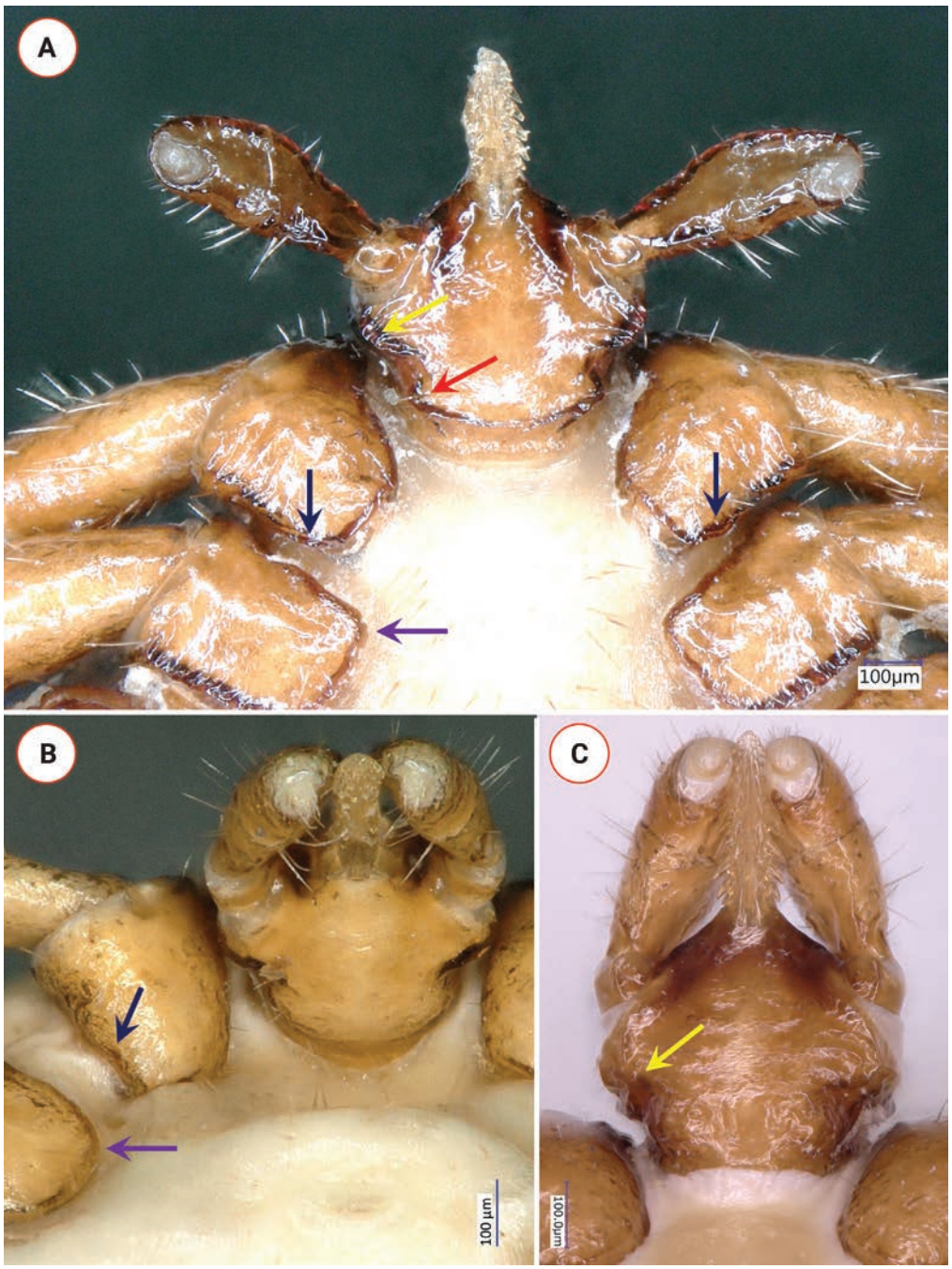

Figure 4. Key ventral morphological characters of *Ixodes lanigeri* sp. nov. female, in comparison with *I. fujitai* and *I. ariadnae* **A** ventral view of *I. lanigeri* sp. nov. (blue arrow: rectangular coxa II; black arrow: sclerotized caudal protuberance of coxae I; yellow arrow: auriculae; red arrow: angled caudolateral corner of ventral basis) **B** ventral view of *I. fujitai* (blue arrow: rounded coxa II; black arrow: caudal concavity of coxa I) **C** ventral view of *I. ariadnae* (yellow arrow: auricular ridge).

scattered aeropyles in 1–3 rows, position of opening subcentral. Anal valves with four 0.06–0.07 long setae. Anal grooves nearly parallel.

Length of basis capituli (from base of hypostome to posterior margin of basis capituli) 0.13, width of basis capituli dorsally 0.22, ratio of length to width of basis capituli 0.6 (Fig. 5B). Basis capituli shape pentagonal, its sides slightly then (anterior to palpal basis) abruptly converging toward the hypostome, dorsally broadest at its caudolateral corners which are perpendicular, lacking cornuae. Posterior margin nearly straight. Three isolated pores observable in

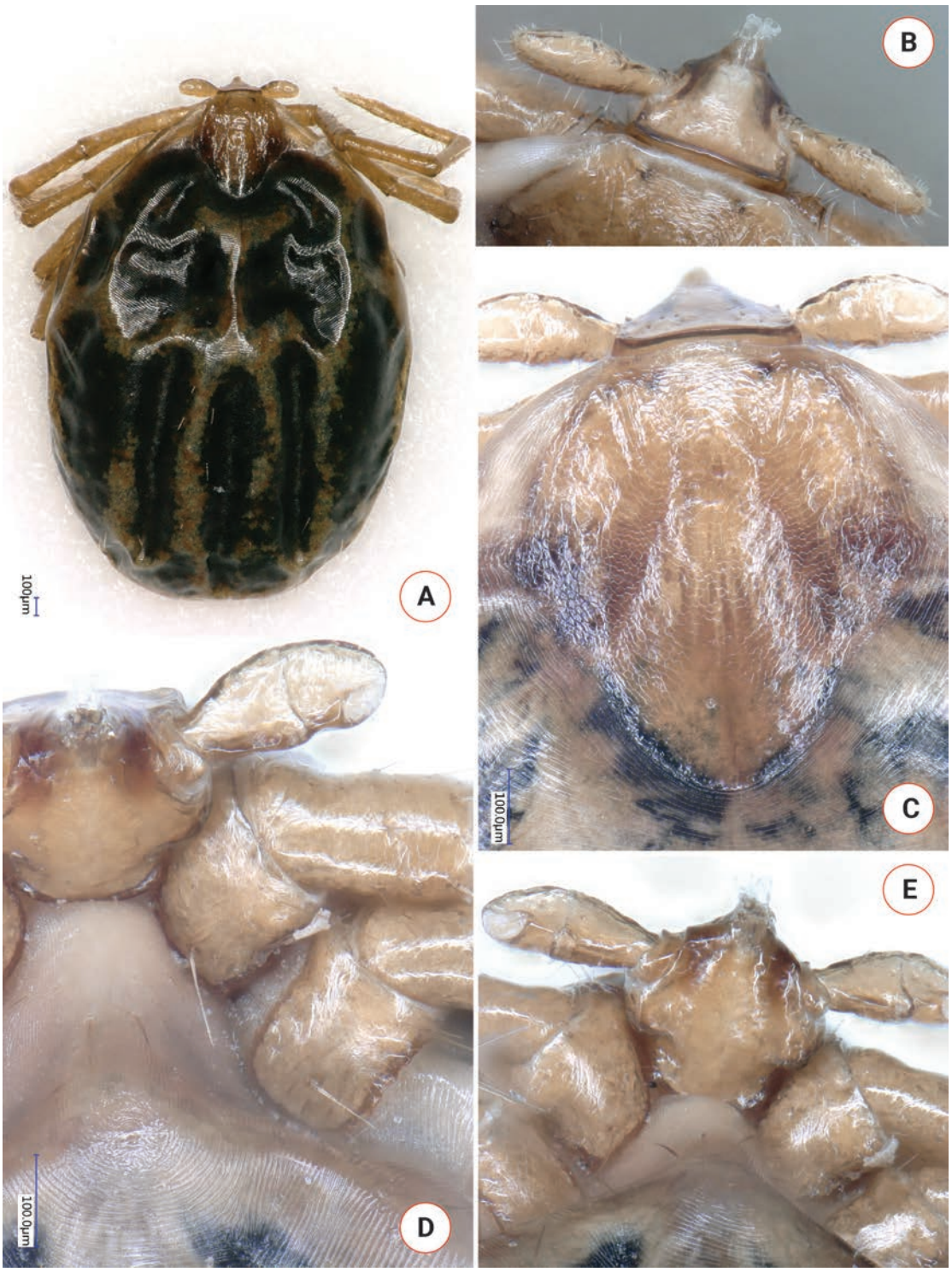

Figure 5. Key morphological characters of *Ixodes lanigeri* sp. nov. nymph **A** habitus, dorsal view **B** basis capituli **C** scutum and palps **D** coxae I-II **E** ventral view of basis and palps.

place of areae porosae. Ventrally on the basis triangular, sclerotized auriculae, with almost perpendicular lateral and caudal edges (Fig. 5E).

Palps (dorsal view) short, medial edge curved, lateral edge nearly straight (Fig. 5C), length 0.23, maximum width 0.095, ratio length/width 2.4. Palpal hairs longest (0.04) laterally on palpal segment II (*N* = 3) and slightly shorter

(0.03) medially (*N* = 2). Palpal segment II and III 0.12 and 0.1 long, respectively (Fig. 5B). Palpal segment III narrower than palpal segment II at their junction, forming a laterally concavity. Palpal segment III with dorsal deepening (fovea), and laterally with five short (0.02) and anteriorly with shorter (0.01) hairs. Hypostome missing from paratype #2.

Legs long and slender. Coxae I trapezoid, their caudomedial corner perpendicular-angled, coxae II rectangular (Fig. 5D). Coxae II-IV rounded, without spines or spurs. Coxae I and II with long hair (0.11 and 0.09, respectively) medially at mid-length (Fig. 5D), all coxae with prominent hair of similar length (0.05–0.11) caudolaterally. Tarsus I. length 0.81, maximum diameter 0.09, length to diameter ratio 9.

Larva (engorged). Length of idiosoma 1.12, breadth 0.8, ratio idiosomal length/breadth 1.4 (Fig. 6A, B).

Scutum reverse pentagonal, posteriorly rounded, broadest at its half-length (Fig. 6C). Length of scutum 0.34, breadth 0.39, ratio length/breadth 0.87. Surface reticulate, with slight rugosities. Cervical grooves narrow, terminating close to deepest point of the pronounced concavity along curved caudolateral scutal margin (Fig. 6C). Between carinae and cervical grooves posterolaterally directed, anteriorly convex deepening. In the caudal field of scutum two parallel grooves with length of 0.08 and interval of 0.05 (Fig. 6C). Scutal setae few (Sc2: 0.024, Sc4: 0.036), some further dorsal and ventral setae also missing. Alloscutal setae longest around mid-length; central dorsal setae (Cd1-2: 0.05) shorter than marginal dorsal setae (Md1-3: 0.07, Md5: 0.08, Md6: 0.07, Md8: 0.04). Ventrally, sternal setae (St1: 0.033, St2: 0.044; St3: 0.07) mostly shorter than marginal ventral setae (Mv1: 0.067, Mv2: 0.086, Mv3: 0.073).

Gnathosoma: length from base of hypostome to posterior margin of basis 0.094, width of basis capituli dorsally 0.17, ratio of length to width 0.55. Basis capituli dorsally triangular, with straight posterior margin and rounded, oblique caudolateral corner, both showing a dark brown lane (<0.01) of sclerotization. Ventrally on the basis capituli elevated, blunt and triangular auriculae with sclerotized edge (Fig. 6D). Posterior margin rounded. Palps short, club-shaped, medially curved, laterally slightly convex with prominent dorsal fovea and lateral outward bulging of segment II near the junction with segment III (Fig. 6C). Dorsally, palpal length 0.15, breadth 0.07, ratio length/breadth 2.2. Segments I-III measure 0.01, 0.08 and 0.06, respectively. Palpal setae longest (0.015) apically and close to junction of II-III segments. Ventrally on palpal segment II porous elevation at the junction with segment III. Hypostome conical, short (0.11), with dental formula 2/2.

Legs long. Haller's organ elongated, longer than maximum breadth (diameter) of tarsus I. Tarsus I length: 0.4, breadth: 0.058. Coxae without spines or spurs. Coxa I trapezoid, with caudomedial corner as elevated, perpendicular angle of dark sclerotization appearing as a short internal spur. Coxae II-III rounded.

Differential diagnosis. *Ixodes lanigeri* sp. nov. can be distinguished from *I. simplex* Neumann and *I. fuliginosus* Hornok & Takano based on its long legs (tarsus I: length to maximum diameter ratio above 8), and from members of the *I. vespertilionis* complex (*I. vespertilionis*, *I. collaris*, *I. nipponrhinolophi*) based on its short palps, relevant to all known developmental stages.

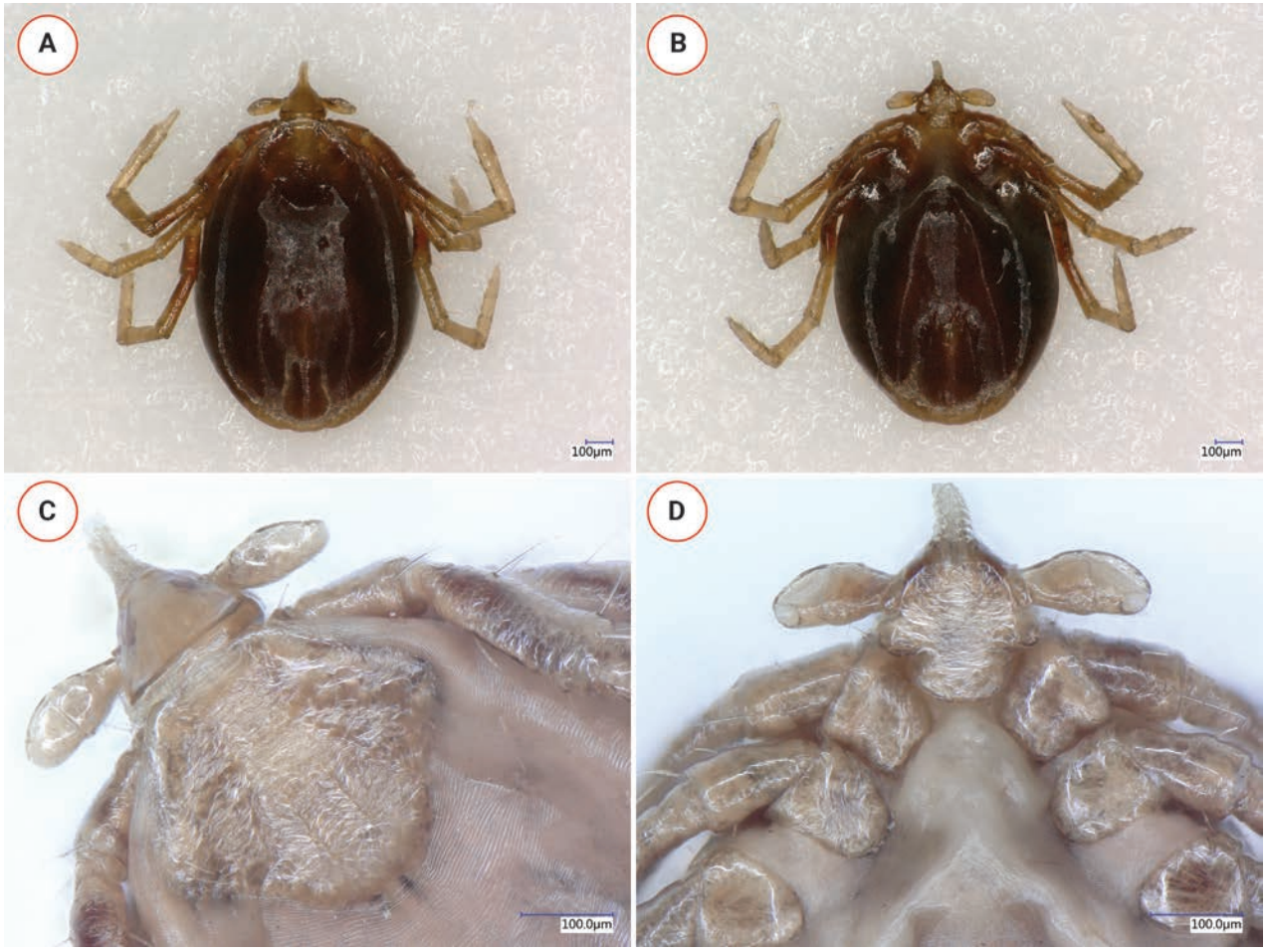

Figure 6. Key morphological characters of *Ixodes lanigeri* sp. nov. larva **A** habitus, dorsal view **B** habitus, ventral view **C** scutum, dorsal view of basis capituli and palps **D** coxae, ventral view of basis capituli and palps.

Within the *I. ariadnae* complex, the female of *I. lanigeri* sp. nov. is different from *I. fujitai* based on the following characters of the latter: (1) scarce punctuations in the anterior and posterior fields of scutum (Fig. 3H) (*vs* denser in *I. lanigeri* sp. nov.); (2) subcircular spiracular plates (Fig. 3E) (*vs* asymmetrical, pear-shape in case of *I. lanigeri* sp. nov.); (3) gnathosoma approximately 30% longer than broad (*vs* only approximately 20% longer than broad in *I. lanigeri* sp. nov.); (4) angled, thickened and protruding caudolateral corners of basis capituli (Fig. 3B) (*vs* rounded and blunt, oblique in *I. lanigeri* sp. nov.); (5) subtriangular areae porosae with a broader interval of 0.08 (Fig. 3B), ratio of width-to-interval 2:1 (*vs* broad elliptical areae porosae, with their longitudinal axes perpendicular to each other and a narrower interval of 0.06 in *I. lanigeri* sp. nov., with a 3:1 ratio of width-to-interval); (6) lack of sagittal rim anteriorly on palpal article I (Fig. 4B) (*vs* observable in *I. lanigeri* sp. nov.); (7) lack of strongly sclerotized longitudinal ridge ventrally at the basis of palpal article II (Fig. 4B) (*vs* present in *I. lanigeri* sp. nov.), and the two caudolateral hairs of palpal segment II, in and near the lateral concavity, are long (0.1) in *I. fujitai* (Fig. 4B) (*vs* short, 0.05 in *I. lanigeri* sp. nov.); (8) slightly elevated and sclerotized auricular ridge (Fig. 3B) (*vs* prominent auriculae in *I. lanigeri* sp. nov.); (9) rounded posterior margin of ventral basis (Fig. 4B) (*vs* caudolaterally angled posterior margin of *I. lanigeri* sp. nov.); and (10) rounded coxae, especially coxae II (Fig. 4B) and IV (*vs* rectangular coxae II in *I. lanigeri* sp. nov.).

Differences in comparison with females of *I. ariadnae* include the following characters. In *I. ariadnae* the scutum is slightly more elongated (Fig. 3I) (ratio length/width above 1.25 *vs* 1.2 in *I. lanigeri* sp. nov.) and has its maximum width at approximately one-third of its length (*vs* close to half-length in *I. lanigeri* sp. nov.). The straight portion is in the middle of the cervical grooves in *I. ariadnae* (Fig. 3I), but posteriorly in *I. lanigeri* sp. nov. The number of pores is low in the caudal region of the scutum of *I. ariadnae* (Fig. 3I) *vs* higher in *I. lanigeri* sp. nov. The spiracular plates of *I. ariadnae* are subcircular (Fig. 3F), with straight portions of its edges (*vs* asymmetrically pear-shaped in *I. lanigeri* sp. nov.), diameter smaller (0.33 *vs* 0.4 in *I. lanigeri* sp. nov.). Aeropyles occupy up to 10 rows in *I. ariadnae* (*vs* up to 7 in *I. lanigeri* sp. nov.), with narrower margin than the diameter of their opening (*vs* broad margin in *I. lanigeri* sp. nov.). Gnathosoma approximately 30% longer than broad (*vs* only approximately 20% longer than broad in *I. lanigeri* sp. nov.). Dorsally, basis capituli with straight oblique caudolateral corner and wavy edge including that of posterior margin which is strongly concave in middle (Fig. 3C), *vs* rounded corner and straight posterior margin in *I. lanigeri* sp. nov. Shape of areae porosae subtriangular in *I. ariadnae* (Fig. 3C) *vs* elliptical in *I. lanigeri* sp. nov. Palps of *I. ariadnae* broader, with length-to-width ratio of 2.4 (Fig. 3C) (*vs* 2.9 in *I. lanigeri* sp. nov.). Ratio of palpal segments II:III 1.6 in *I. ariadnae vs* 1.27 in *I. lanigeri* sp. nov. Palpal segment II is laterally concave at its basis in *I. ariadnae* (Fig. 3C) (*vs* close to its mid-length both laterally and medially in *I. lanigeri* sp. nov.). Surface of palpal segment III convex both laterally and medially in *I. ariadnae* (Fig. 3C) (*vs* laterally concave, medially convex in *I. lanigeri* sp. nov.). Ventrally on the basis capituli of *I. ariadnae* "waist" (narrowing) and sclerotized posterior edge less evident, unangled and inconspicuous auricular ridges have convex, rounded anterior margin (Fig. 4C) (*vs* concave anterior margin surrounding palpal article I. in *I. lanigeri* sp. nov.). Coxae II-IV of *I. ariadnae* are symmetrically rounded *vs* asymmetrically trapezoid or rectangular in *I. lanigeri* sp. nov.

In comparison with *I. collaris* nymph: palps slender, elongated, 0.45 (*vs* short, 0.23 in *I. lanigeri* sp. nov.) and the scutum is also more elongated (shape index is 1.5 *vs* 1.1 in *I. lanigeri* sp. nov.). Within the *I. ariadnae* complex, the nymph of *I. fujitai* is unknown. The nymph of *I. lanigeri* sp. nov. is different from that of *I. ariadnae* based on the following characters of the latter. The scutum is longer, as indicated by the shape index of 1.2, and broadest at its anterior third (Fig. 7A) (*vs* 1.1 in *I. lanigeri* sp. nov., maximum width close to half-length in *I. lanigeri* sp. nov.). The ratio of palpal segments II:III 1.7 (Fig. 7B) (*vs* 1.2 in *I. lanigeri* sp. nov.). Ventrally, on the basis of *I. ariadnae* nymph, less elevated auricular ridges are visible (Fig. 7D). Spiracular plates oval, with irregular outline in *I. ariadnae* nymph but subcircular in *I. lanigeri* sp. nov. Coxae of *I. ariadnae* nymph are all rounded (Fig. 7C).

Within the *I. ariadnae* complex, the larva of *I. fujitai* is unknown. The larva of *I. lanigeri* sp. nov. is different from that of *I. ariadnae* (Fig. 8A, B) based on the following characters of the latter. Scutum broadest anteriorly to its half-length; its caudolateral edge with only slight concavity (Fig. 8C) (*vs* deep in *I. lanigeri* sp. nov). Cervical grooves not apparent, reaching posterolateral margin of scutum behind its deepest point of concavity. Scutal setae shorter (0.02–0.03) than in *I. lanigeri* sp. nov. (0.05). Caudal alloscutal setae longer in *I. ariadnae* larva (0.15 *vs* 0.04–0.08 in *I. lanigeri* sp. nov.). Marginal ventral setae longer in

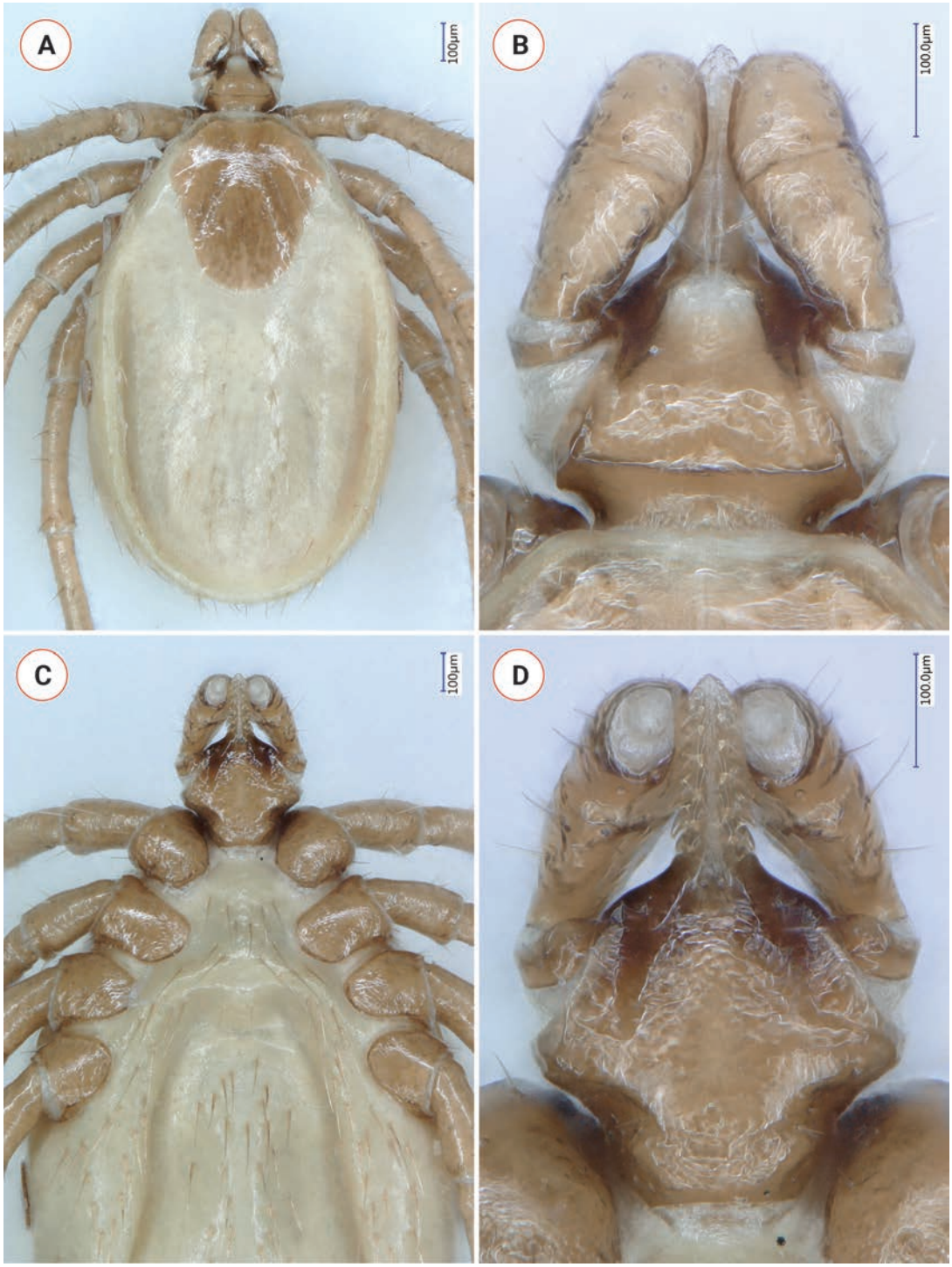

Figure 7. Key morphologic characters of *Ixodes ariadnae* nymph **A** habitus, dorsal view **B** dorsal view of basis capituli and palps **C** coxae and ventral view of gnathosoma **D** ventral view of basis and palps. This sample was collected from the cave wall of Szopláki Ördöglyuk (Pilis Mountains, Hungary) on April 10, 2016.

I. ariadnae larva (0.12–0.14 vs 0.06–0.09 in *I. lanigeri* sp. nov.). Palps of *I. ariadnae* larva laterally straight, with small fovea and dark outline (Fig. 8C) (*vs* laterally convex, with prominent fovea in *I. lanigeri* sp. nov.), but shape index is 2.2 in both species. Palpal setae longer in *I. ariadnae* (up to 0.05) than in *I. lanigeri* sp. nov. (0.015). Ventrally, on the basis, capituli auricular ridges of *I. ariadnae* are less apparent/elevated (Fig. 8D) than the auriculae in *I. lanigeri* sp. nov.

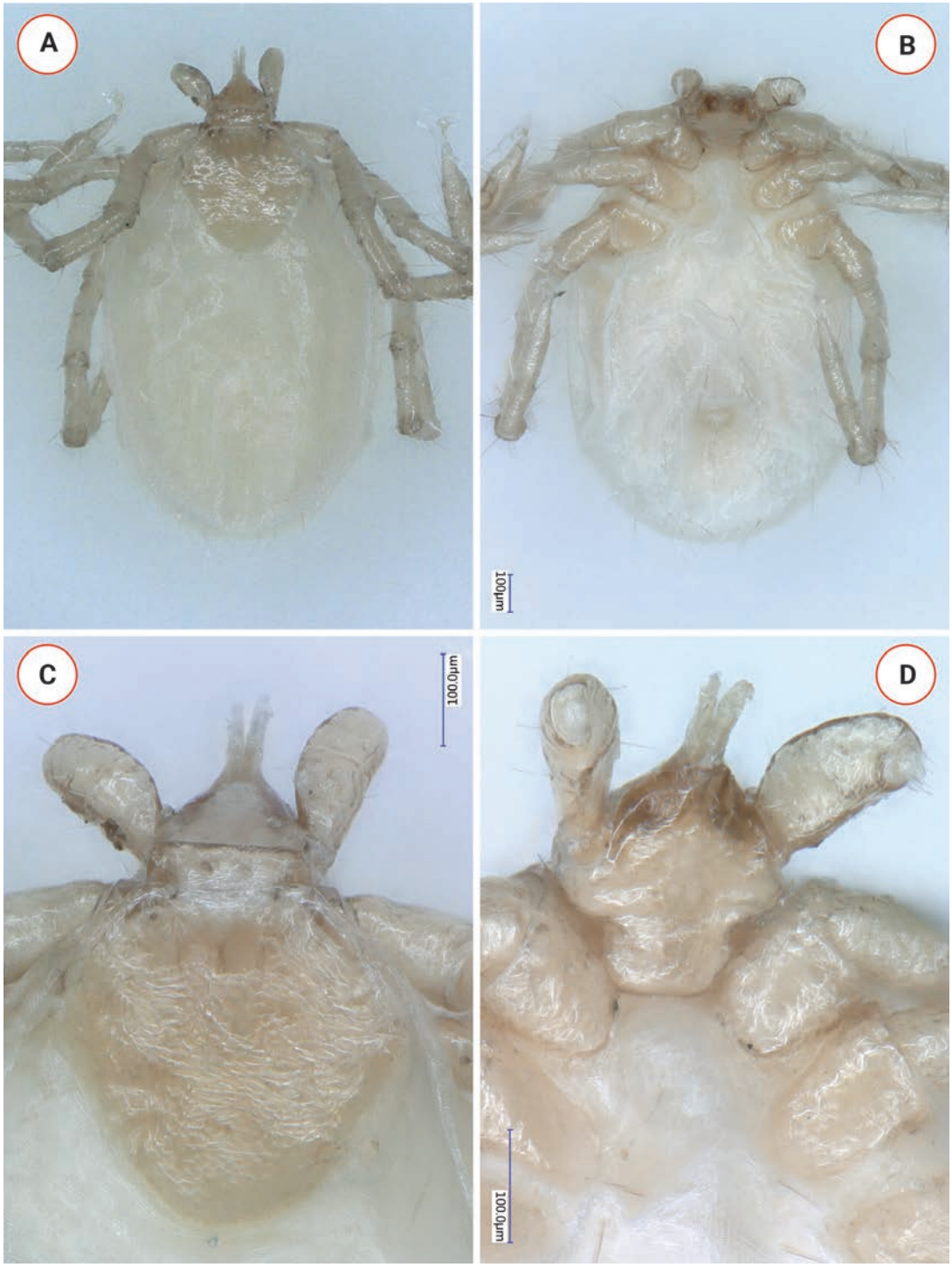

Figure 8. Key morphological characters of *Ixodes ariadnae* larva **A** habitus, dorsal view **B** habitus, ventral view **C** scutum, dorsal view of basis capituli and palps **D** coxae I-II, ventral view of basis capituli and palps. This sample was collected from the cave wall of Szopláki Ördöglyuk (Pilis Mountains, Hungary) on April 10, 2016.

GenBank data. Complete mitochondrial genome sequence from one larva is available in GenBank (LC797956). Sequences of the amplified parts of the *cox*1 and 16S rRNA genes of *I. lanigeri* sp. nov. from another larva (collected with paratype#2), the nymph (paratype#1) and the female (holotype) are found under the accession numbers PP079465, PP503326, PP503327 and PP081435, PP505539, PP505540 respectively.

Molecular and phylogenetic analyses. Pairwise comparison of *I. lanigeri* sp. nov. indicated 5.1% *cox*1 and 2.9% 16S rRNA gene sequence differences from *I. fujitai*, and 11.18% *cox*1 and 5.7% 16S rRNA gene sequence difference from *I. ariadnae* (Table 1). There were up to only 2 bp differences in the amplified part of the *cox*1 and 16S rRNA genes between the larvae, the nymph and female of *I. lanigeri* sp. nov. The complete mitogenome of *I. lanigeri* sp. nov. was 95.4% (13899/14570 bp) identical to that of *I. fujitai* (LC769934). The phylogenetic relationships of the new tick species from Vietnam are shown in Fig. 9.

Host records and distribution. Known host species: *Myotis alticraniatus*, *M. laniger*. Known geographical range: northern Vietnam.

Etymology. The name of the new species refers to the host species, the Chinese water myotis (*M. laniger*) from which the first specimen of the new species was collected.

Table 1. Pairwise nucleotide differences between (a) *cox*1 and (b) 16S rRNA gene sequences of species belonging to the *Ixodes ariadnae* complex, according to GenBank accession numbers. Asian and European data are indicated with light blue and grey background color, respectively.

(a) *cox*1 gene	***I. lanigeri* (PP079465: Vietnam)**	***I. fujitai* (LC036330: Japan)**	***I. ariadnae* (KJ490306: Hungary)**
***I. lanigeri* (PP079465: Vietnam)**	–	94.9% (603/635)	88.9% (560/630)
***I. fujitai* (LC036330: Japan)**	94.9% (603/635)	–	89.7% (565/630)
***I. ariadnae* (KJ490306: Hungary)**	88.9% (560/630)	89.7% (565/630)	–
(b) 16S rRNA gene	***I. lanigeri* (PP081435: Vietnam)**	***I. fujitai* (LC036330: Japan)**	***I. ariadnae* (KJ490306: Hungary)**
***I. lanigeri* (PP081435: Vietnam)**	–	97.1% (398/410)	94.3% (398/422)
***I. fujitai* (LC036330: Japan)**	97.1% (398/410)	–	93% (385/414)
***I. ariadnae* (KJ490306: Hungary)**	94.3% (398/422)	93% (385/414)	–

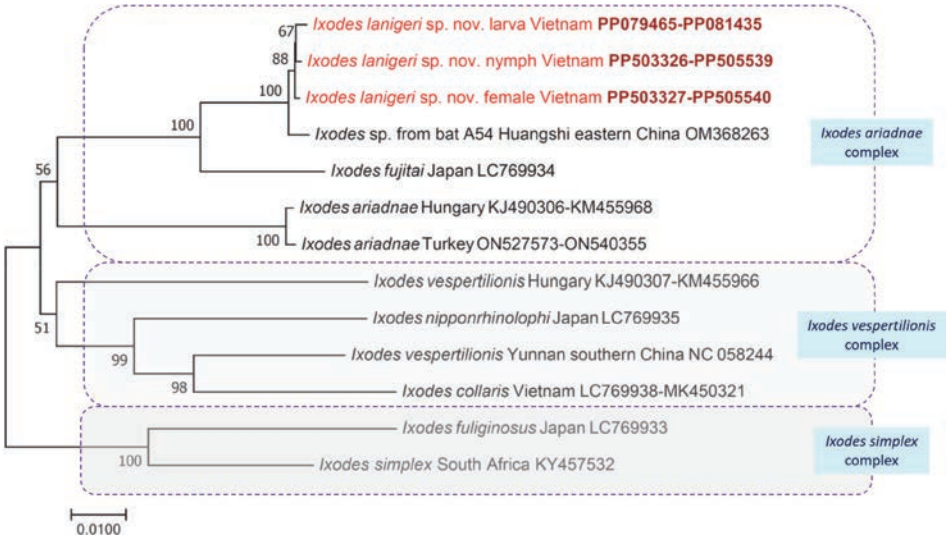

Figure 9. Phylogenetic tree of bat-associated ticks based on concatenated *cox*1 and 16S rRNA gene sequences. In each row of individual sequences, the region/country of origin and the GenBank accession number are shown after the species name. Rows of sequences from this study are indicated with red fonts and bold accession numbers. The evolutionary history was inferred by using the Neighbor-Joining method and p-distance model. The percentage of trees in which the associated taxa clustered together is shown next to the branches. Branch lengths are measured in the number of substitutions per site. The analysis involved 13 nucleotide sequences, and there were a total of 1020 positions in the final dataset.

Discussion

Bat-associated ixodid ticks are considered to belong to three species complexes: the *I. simplex* group characterized by the normal length of legs, and two complexes of the so-called long-legged bat tick species, *I. vespertilionis* and *I. ariadnae* (Hornok et al. 2014; Hornok et al. 2015; Takano et al. 2023). Although until the discovery of the latter species, only one long-legged bat-associated ixodid tick species was known in the Old World, later these were recognized to probably represent at least six species in Eurasia, as suspected on a molecular-phylogenetic basis (Hornok et al. 2015). This was later confirmed by the description of new long-legged bat tick species in Vietnam (*Ixodes collaris*: Hornok et al. 2016b) and in Japan (*Ixodes nipponrhinolophi* and *I. fujitai*: Takano et al. 2023). Thus, with the description of *I. lanigeri* sp. nov. in this study from Vietnam, the list and description of six species which were expected to exist among "long-legged bat ticks" became complete.

Hitherto, *I. lanigeri* was probably misidentified as *I. vespertilionis* in Southeast Asia. Among bat-associated ticks of the subgenus *Pholeoixodes* (formerly *Escathocephalus*: Hornok et al. 2017b), *I. lanigeri* belongs to the phylogenetic group of the *I. ariadnae* complex (Takano et al. 2023) and is most closely related to *I. fujitai* with East Asian occurrence, and also to *I. ariadnae* from Europe and Asia Minor (Hekimoglu et al. 2022). For these reasons, the differential diagnosis focused on the latter two species. Morphological comparisons in this context fully supported the taxonomic status of *I. lanigeri* sp. nov. as a separate species.

Myotis-associated ticks collected previously in Vietnam belonged to the *I. ariadnae* complex and were thus called *I. ariadnae*-like (Hornok et al. 2015). Based on two mitochondrial genetic markers, the clustering of *I. ariadnae*-like species from Vietnam, separately from *I. ariadnae* and *I. fujitai* was moderately (77–83%) or highly (94–100%) supported, respectively (Hornok et al. 2015; Takano et al. 2023). This was confirmed here, i.e. the clustering of *I. lanigeri* sp. nov. and *I. fujitai* received high (100%) support (Fig. 9). Interestingly, the phylogenetic position and evolutionary distance of a tick reported from southern China (MW411447: Lu et al. 2021) suggest that further, taxonomically undescribed, species of the *I. vespertilionis* complex might exist in southeastern Asia (Fig. 9).

In the present study, pairwise comparisons indicated 5.1% *cox*1 and 2.9% 16S rRNA gene sequence differences from the closest related species, *I. fujitai*. Although this is lower than the average sequence divergence between closely related species (6.1% and 5.2%, respectively: Lv et al. 2014), other well-established ixodid species are known with even lower degrees of interspecific differences (e.g., *Ixodes turdus* Nakatsudi and *Ixodes frontalis* (Panzer) differing by only 2.7% in their 16S rRNA gene sequences: Xu et al. 2003).

At the same time, there are shortcomings which originate from the rarity of *Myotis*-associated bat ticks in southeastern Asia, i.e., that the description of the new species is based on morphological analyses of a single individual of each developmental stage, and not on a representative number of specimens from a population. Considering the genetic differences between *I. lanigeri* sp. nov. and a previously reported specimen from *Myotis* sp. in Vietnam (KR902767, KR902770: Hornok et al. 2015) it is possible to assume that further (perhaps sibling) species of the *I. ariadnae* complex might also exist in this geographical region, and it will be necessary to address this in future studies.

Ixodid ticks associated with bats infrequently occur beyond the range of their typical hosts; thus, host spectra of these tick species reflect family-level adaptations. The typical hosts of the *I. vespertilionis* and *I. simplex* groups are bat species from the families Rhinolophidae and Miniopteridae, respectively (Hornok et al. 2015). Regarding the third group of bat-associated tick species, the *I. ariadnae* complex, they most frequently occur on vesper bats (family Vespertilionidae): *I. ariadnae* is the most common on *Myotis* species (Hornok et al. 2014), and *I. lanigeri* sp. nov. was only reported so far from bats of this genus, whereas *I. fujitai* only from *Murina hilgendorfi* (Takano et al. 2023). It is important to note that although both genera, *Myotis* and *Murina*, belong to Vespertilionidae, they are not sister-genera and are generally placed into two distinct subfamilies, Myotinae and Murininae (Jargalsaikhan et al. 2022). Apart from their distinct geographical range (see below), this may have contributed to, and may in part explain, the speciation events that most likely resulted in the divergent evolution of *I. lanigeri* sp. nov. and *I. fujitai*.

Among bat species of genera *Myotis* and *Murina*, the typical hosts of *I. lanigeri* sp. nov. and *I. fujitai* are geographically separated between south and southeastern and East Asia (Fig. 1). In particular, the majority of *Myotis* and *Murina* species indigenous in Vietnam (i.e., the expected hosts of *I. lanigeri* sp. nov.) have a south-southeastern Asian distribution: their geographical range including the Himalayan and Indian subregions (*N* = 10 bat species), the Indochinese (*N* = 35 bat species) subregion, as well as the Sundaic, Wallacean and Philippine (*N* = 7 bat species) subregions. However, only two of the Vietnamese *Myotis* species occur in Palearctic East Asia, and none of them on the five main islands of Japan where *I. fujitai* was reported from its type host, *Mu. hilgendorfi* (Fig. 1).

On the other hand, it has to be noted that the type host of *I. lanigeri* sp. nov., *My. lanigeri* is known to roost in sympatry with *My. fimbriatus* and *My. altarium* (Hu et al. 2012); therefore, the new tick species almost certainly has a larger geographical range, including China and other countries in south-southeastern Asia, where these bat species occur. This was reflected by the clustering of a long-legged bat tick species (reported recently from Eastern China: Tian et al. 2022) with *I. lanigeri* sp. nov. (Fig. 9).

By contrast, typical bat host species (Miniopteridae) of the *I. simplex* group show considerable overlapping in their geographical distribution in East and Southeast Asia. For example, the most important host species of *I. fuliginosus* described recently in Japan (i.e., *Miniopterus fuliginosus*) also occurs in Vietnam, and *Miniopterus magnater* from which a phylogenetically divergent genetic variant of *I. simplex* was reported from India (Hornok et al. 2015) is also found in Vietnam (Kusuminda et al. 2022). Therefore, due to this connectedness and in the absence of clear geographical separation, it is likely that so-called “short-legged bat ticks” of the *I. simplex* group in South, Southeast and East Asia probably belong to the same species, *I. fuliginosus*.

Acknowledgements

The authors thank Nóra Takács for performing PCRs. We also thank the management board of Xuan Son National Park, the local authorities of Ta Phin and Co Ma communes, and the directorate of the Institute of Ecology and Biological Resources) for their research permits and support during the field surveys.

Additional information

Conflict of interest

The authors have declared that no competing interests exist.

Ethical statement

No ethical statement was reported.

Funding

This study was supported by the Office for Supported Research Groups, Hungarian Research Network (HUN-REN), Hungary (Project No. 1500107) for SH and JK, the "Agence nationale de la recherche" (AAP RA-COVID-19, grant number ANR-21-CO12-0002) to AH and VTT, and the Vietnam Academy of Science and Technology (Project No: KHCBTĐ.02/22–24) to VTT.

Author contributions

Sándor Hornok: conceptualization, writing, data curation, methodology. Jenő Kontschán: data curation, methodology. Ai Takano: data curation, methodology. Yasuhiro Gotoh: data curation, methodology. Alexandre Hassanin: supervision. Vuong Tan Tu: conceptualization, data curation, methodology, writing.

Author ORCIDs

Sándor Hornok https://orcid.org/0000-0002-1125-5178
Jenő Kontschán https://orcid.org/0000-0001-8274-4238
Ai Takano https://orcid.org/0000-0002-5919-3738
Alexandre Hassanin https://orcid.org/0000-0002-4905-8540
Vuong Tan Tu https://orcid.org/0000-0002-5915-865X

Data availability

All of the data that support the findings of this study are available in the main text or Supplementary Information.

References

de la Fuente J, Estrada-Peña A, Cabezas-Cruz A, Brey R (2015) Flying ticks: anciently evolved associations that constitute a risk of infectious disease spread. Parasites & Vectors 8: 538. https://doi.org/10.1186/s13071-015-1154-1

Hekimoglu O, Elverici M, Yorulmaz T (2022) A survey of hard ticks associated with cave dwelling mammals in Turkey. Ticks and Tick-borne Diseases 13: 102008. https://doi.org/10.1016/j.ttbdis.2022.102008

Hornok S, Kontschán J, Kováts D, Kovács R, Angyal D, Görföl T, Polacsek Z, Kalmár Z, Mihalca AD (2014) Bat ticks revisited: *Ixodes ariadnae* sp. nov. and allopatric genotypes of *I. vespertilionis* in caves of Hungary. Parasites & Vectors 7: 202. https://doi.org/10.1186/1756-3305-7-202

Hornok S, Estrada-Peña A, Kontschán J, Plantard O, Kunz B, Mihalca AD, Thabah A, Tomanović S, Burazerović J, Takács N, Görföl T, Estók P, Tu VT, Szőke K, Fernández de Mera IG, de la Fuente J, Takahashi M, Yamauchi T, Takano A (2015) High degree of mitochondrial gene heterogeneity in the bat tick species *Ixodes vespertilionis*, *I. ariadnae* and *I. simplex* from Eurasia. Parasites & Vectors 8: 457. https://doi.org/10.1186/s13071-015-1056-2

Hornok S, Flaisz B, Takács N, Kontschán J, Csörgő T, Csipak Á, Jaksa BR, Kováts D (2016a) Bird ticks in Hungary reflect western, southern, eastern flyway connections and two genetic lineages of *Ixodes frontalis* and *Haemaphysalis concinna*. Parasites & Vectors 9: 101. https://doi.org/10.1186/s13071-016-1365-0

Hornok S, Görföl T, Estók P, Tu VT, Kontschán J (2016b) Description of a new tick species, *Ixodes collaris* n. sp. (Acari: Ixodidae), from bats (Chiroptera: Hipposideridae, Rhinolophidae) in Vietnam. Parasites & Vectors 9: 332. https://doi.org/10.1186/s13071-016-1608-0

Hornok S, Szőke K, Görföl T, Földvári G, Tu VT, Takács N, Kontschán J, Sándor AD, Estók P, Epis S, Boldogh S, Kováts D, Wang Y (2017a) Molecular investigations of the bat tick *Argas vespertilionis* (Ixodida: Argasidae) and *Babesia vesperuginis* (Apicomplexa: Piroplasmida) reflect "bat connection" between Central Europe and Central Asia. Experimental and Applied Acarology 72: 69–77. https://doi.org/10.1007/s10493-017-0140-z

Hornok S, Sándor AD, Beck R, Farkas R, Beati L, Kontschán J, Takács N, Földvári G, Silaghi C, Meyer-Kayser E, Hodžić A, Tomanović S, Abdullah S, Wall R, Estrada-Peña A, Duscher GG, Plantard O (2017b) Contributions to the phylogeny of Ixodes (Pholeoixodes) canisuga, I. (Ph.) kaiseri, I. (Ph.) hexagonus and a simple pictorial key for the identification of their females. Parasites & Vectors 10: 545. https://doi.org/10.1186/s13071-017-2424-x

Hu KL, Yang J, Tan LJ, Zhang LB (2012) Dietary differences and niche partitioning in three sympatric *Myotis* species. Zoological Research 2: 177–181. [in Chinese, with English abstract] https://doi.org/10.3724/SP.J.1141.2012.02177

Jargalsaikhan A, Ariunbold B, Dalannast M, Purevee E, Paek WK, Tsagaan K, Ganbold O (2022) Molecular phylogenetic analysis of bats in the family Vespertilionidae in Mongolia. Journal of Asia-Pacific Biodiversity 3: 329–335. https://doi.org/10.1016/j.japb.2022.04.006

Jongejan F, Uilenberg G (2004) The global importance of ticks. Parasitology 129 Suppl: S3–14. https://doi.org/10.1017/S0031182004005967

Kumar S, Stecher G, Tamura K (2016) MEGA7: Molecular Evolutionary Genetics Analysis Version 7.0 for Bigger Datasets. Molecular Biology and Evolution 33: 1870–1874. https://doi.org/10.1093/molbev/msw054

Kusuminda K, Mannakkara A, Ukuwela KDB, Kruskop SV, Amarasinghe CJ, Saikia U, Venugopal P, Karunarathna M, Gamage R, Ruedi M, Csorba G, Yapa WB, Patterson BD (2022) DNA barcoding and morphological analyses reveal a cryptic species of *Miniopterus* from India and Sri Lanka. Acta Chiropterologica 24: 1–17. https://doi.org/10.3161/15081109ACC2022.24.1.001

Lu X, Zuo X, Jiang D, Yang X (2021) The complete mitochondrial genome of *Ixodes vespertilionis* (Acari: Ixodidae). Mitochondrial DNA part B: Resources 6: 3001–3003. https://doi.org/10.1080/23802359.2021.1976686

Lv J, Wu S, Zhang Y, Chen Y, Feng C, Yuan X, Jia G, Deng J, Wang C, Wang Q, Mei L, Lin X (2014) Assessment of four DNA fragments (COI, 16S rDNA, ITS2, 12S rDNA) for species identification of the Ixodida (Acari: Ixodida). Parasites & Vectors 7: 93. https://doi.org/10.1186/1756-3305-7-93

Takano A, Yamauchi T, Takahashi M, Shimoda H, Gotoh Y, Mizuno J, Natsume M, Kontschán J, Kováts D, Tu VT, Hornok S (2023) Description of three new bat-associated species of hard ticks (Acari, Ixodidae) from Japan. Zookeys 1180: 1–26. https://doi.org/10.3897/zookeys.1180.108418

Tian J, Hou X, Ge M, Xu H, Yu B, Liu J, Shao R, Holmes EC, Lei C, Shi M (2022) The diversity and evolutionary relationships of ticks and tick-borne bacteria collected in China. Parasites & Vectors 15: 352. https://doi.org/10.1186/s13071-022-05485-3

Xu G, Fang QQ, Keirans JE, Durden LA (2003) Molecular phylogenetic analyses indicate that the *Ixodes ricinus* complex is a paraphyletic group. Journal of Parasitology 89: 452–457. https://doi.org/10.1645/0022-3395(2003)089[0452:MPAITT]2.0.CO;2

Supplementary material 1

Simplified geographical range of *Myotis* and *Murina* species

Authors: Sándor Hornok, Vuong Tan Tu

Data type: pdf

Explanation note: Simplified geographical range of *Myotis* and *Murina* species (Chiroptera: Vespertilionidae) found in Vietnam and Laos (based on IUCN (2023), Wilson & Mittermeier (2019) and selected references listed below). Species found only in Vietnam are indicated with red fonts. Known hosts of the new bat tick species are indicated with yellow background.

Link: https://doi.org/10.3897/zookeys.1215.123624.suppl1

ZooKeys 1215: 127–138 (2024)
DOI: 10.3897/zookeys.1215.130564

Research Article

Description of two new species of the genus *Trachelas* L. Koch, 1872 and the male of *T. gaoligongensis* Jin, Yin & Zhang, 2017 from China (Araneae, Trachelidae)

Gang Tang[1], Wen-long Yan[1], Yi Zhao[1], Xian-jin Peng[1]

1 *College of Life Sciences, Hunan Normal University, Changsha, Hunan 410081, China*
Corresponding author: Xian-jin Peng (xjpeng@126.com)

Abstract

Two new spider species of the genus *Trachelas* L. Koch, 1872 are described from China: *Trachelas kavanaughi* **sp. nov.** (♀) and *Trachelas ventriosus* **sp. nov.** (♀). The male of *Trachelas gaoligongensis* Jin, Yin & Zhang, 2017 is described for the first time. Illustrations of the body and copulatory organs and a distribution map are provided.

Key words: Morphology, spider, taxonomy, trachelids, Yunnan

Academic editor: Dimitar Dimitrov
Received: 27 June 2024
Accepted: 2 September 2024
Published: 14 October 2024

ZooBank: https://zoobank.org/19536B03-4F83-435F-A0EB-B29CAF39BBFE

Citation: Tang G, Yan W-l, Zhao Y, Peng X-j (2024) Description of two new species of the genus *Trachelas* L. Koch, 1872 and the male of *T. gaoligongensis* Jin, Yin & Zhang, 2017 from China (Araneae, Trachelidae). ZooKeys 1215: 127–138. https://doi.org/10.3897/zookeys.1215.130564

Introduction

The subfamily Tracheleae Simon, 1897 was originally treated as a member of the family Corinnidae Karsch, 1880. Ramírez (2014) separated it from Corinnidae and elevated it to its own family, Trachelidae. This family currently contains 290 species in 25 genera, of which nine genera and 38 species are distributed in China. *Trachelas* L. Koch, 1872 is the most species-rich genus in Trachelidae, with 91 species distributed worldwide, including 13 species in China (mainly distributed in southwest China) (WSC 2024). There have been seven new species of *Trachelas* described and one new record reported in China recently (Zhang et al. 2009; Jin et al. 2017; Liu et al. 2024).

During the examination of spider specimens collected from Yunnan Province in 2007, two new species, *Trachelas ventriosus* sp. nov. (♀), *T. kavanaughi* sp. nov. (♀), and the males of *T. gaoligongensis* Jin, Yin & Zhang, 2017 were discovered. Descriptions and photomicrographs of the habitus and copulatory organs and distribution map are provided.

Material and methods

Specimens were stored in 75% ethanol. The female genitalia were cleared with lactic acid before examination and photography. Specimens were photographed using a Kuy Nice E3IS PM digital camera attached to an Olympus BX53 compound microscope and examined and measured with a Leica M205C stereomicroscope. Photographs were taken by placing specimens on

alcohol-soaked cotton in a Petri dish. Focus-stacked images were composited using Helicon Focus ver. 7.0 and then modified in Adobe Photoshop CS6. All measurements are in millimeters (mm). Leg measurements are as follows: total length (femur, patella+tibia, metatarsus, tarsus). All specimens are deposited at the College of Life Sciences, Hunan Normal University (**HNU**), Changsha, Hunan Province, China.

The following abbreviations are used in the text and figures: **ALE** anterior lateral eyes, **AME** anterior median eyes, **ATR** atrium, **CD** copulatory duct, **CnD** connecting duct, **CO** copulatory opening, **RTA** retrolateral tibial apophysis, **E** embolus, **FD** fertilization duct, **MOA** median ocular area, **PLE** posterior lateral eyes, **PME** posterior median eyes, **RPA** retrolateral patellar apophysis, **SD** sperm duct, **ST** subtegulum, **ST1** primary spermatheca, **ST2** secondary spermatheca, **TA** tegular apophysis, **VFG** ventral femoral groove.

Taxonomy

Family Trachelidae Simon, 1897

Genus *Trachelas* L. Koch, 1872

Type species. *Trachelas minor* O. Pickard-Cambridge, 1872.

***Trachelas gaoligongensis* Jin, Yin & Zhang, 2017**
Figs 1–4

Trachelas gaoligongensis Jin, Yin & Zhang, 2017: 42, figs 16A–G, 18A, B (♀).

Material examined. • 4 ♂, 1 ♀(HNU-20071010); China, Yunnan Prov., Longyang County, Mangkuan Baihualing; 25.30366°N, 98.80032°E; 1624 m a.s.l.; 10 October 2007; Xian-jin Peng leg. • 2 ♀ (HNU-Tang-04-12); China, Yunnan Prov., Gongshan County, Cikai Township, Heiwadi Village; 27.47101°N, 98.35533°E; 1850 m a.s.l.; 13–16 November. 2004; Guo Tang leg. • 2 ♀ (HNU-DHK-2004-082); China, Yunnan Prov., Gongshan County, Dulongjiang Township, 0.2 km S of confluence of Dulongjiang with Muke Wang [river]; 27.84125°N, 98.32979°E; 1450 m a.s.l.; 11 November 2004; D. H. Kavanaugh leg. • 1 ♀ (HNU-VFL-04-0027); China, Yunnan Prov., Gongshan County, Bingzhongluo Township, west side of bridge NW of Stone Gate; 28.06670°N, 98.58890°E; 1500 m a.s.l.; 11 December 2004; V. F. Lee leg.

Etymology. The species name "gaoligongensis" refers to the Gaoligong mountain range where the type locality is found, adjective.

Diagnosis. The male of *Trachelas gaoligongensis* (Figs 2, 4A–C) resembles that of *T. bomiensis* Jin & Mi, 2024 (see Liu et al. 2024, fig. 2A–D) in having a hook-shaped sperm duct and a protruding genital bulb but differs as follows: (1) the embolus is enlarged at the base and elongated at the tip in retrolateral view (vs. elongated at the base and with two spirals at the tip); (2) the retrolateral tibial apophysis points to the dorsal side of the cymbium in prolateral view (vs. absent); and (3) the retrolateral patellar apophysis is longitudinally bar-shaped, distally covered with feathery setae in retrolateral view (vs. distal

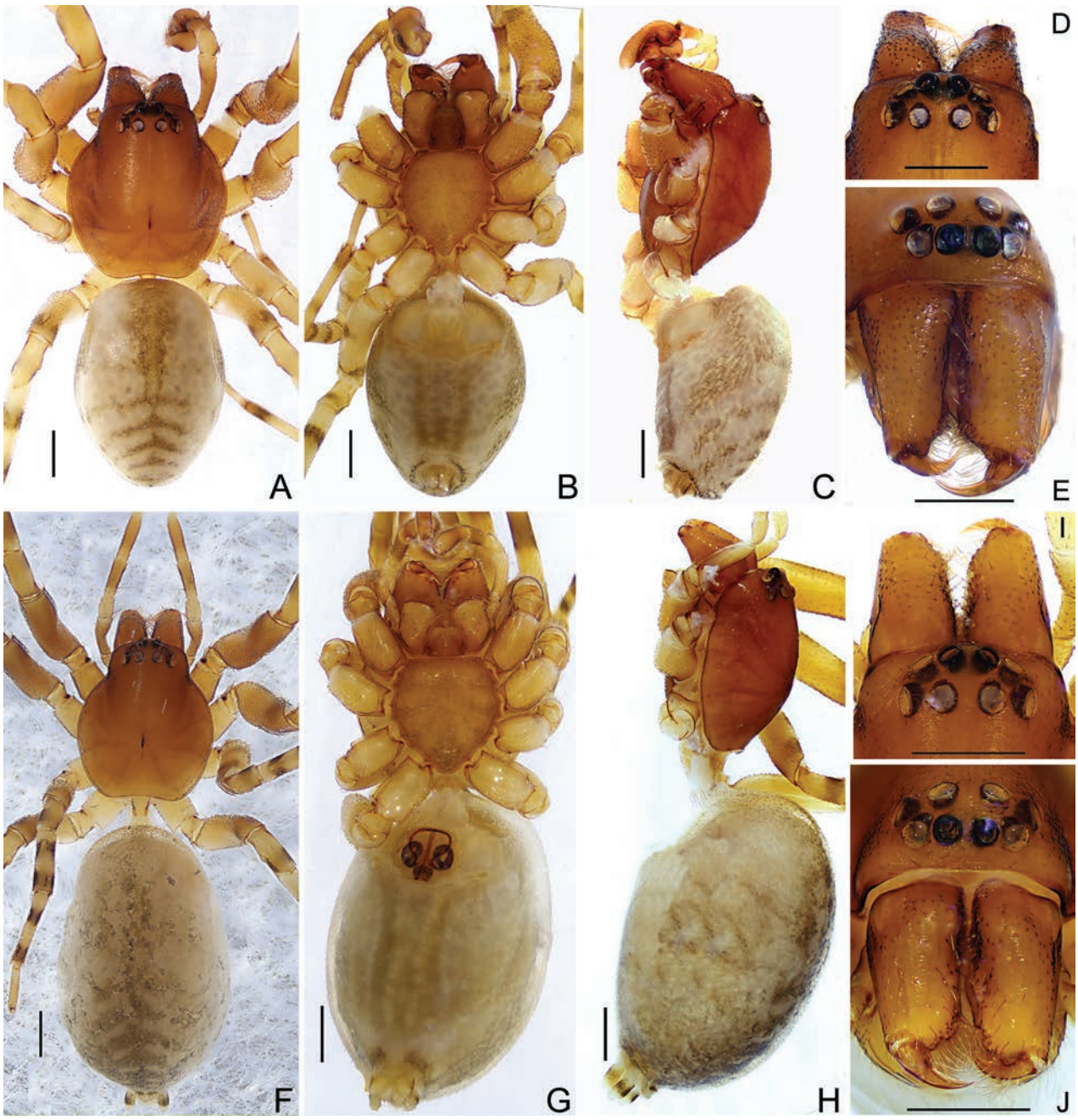

Figure 1. *Trachelas gaoligongensis* Jin, Yin & Zhang, 2017 (HNU-20071010). Male (**A–E**) **A** habitus, dorsal view **B** ditto, ventral view **C** ditto, lateral view **D** ocular area, dorsal view **E** carapace, frontal view. Female (**F–J**) **F** habitus, dorsal view **G** ditto, ventral view **H** ditto, lateral view **I** ocular area, dorsal view **J** carapace, frontal view. Scale bars: 0.5 mm.

portion transversely bent toward tibia and without feathery setae). The female of *T. gaoligongensis* (Figs 3, 4D, E) resembles that of *T. kavanaughi* sp. nov. (see Figs 5E, F, 7A, B) in the shape of the atrium and secondary spermathecae, but differs as follows: (1) the atrium is about as long as wide in ventral view (vs. wider than long); (2) the copulatory openings are posteriorly located on the genitalia in ventral view (vs. anteriorly located on the genitalia); (3) the primary spermathecae are oval in dorsal view (vs. round); and (4) the interdistance of the secondary spermathecae is more than twice the width of the primary spermathecae in dorsal view (vs. narrower than the width of the primary spermathecae).

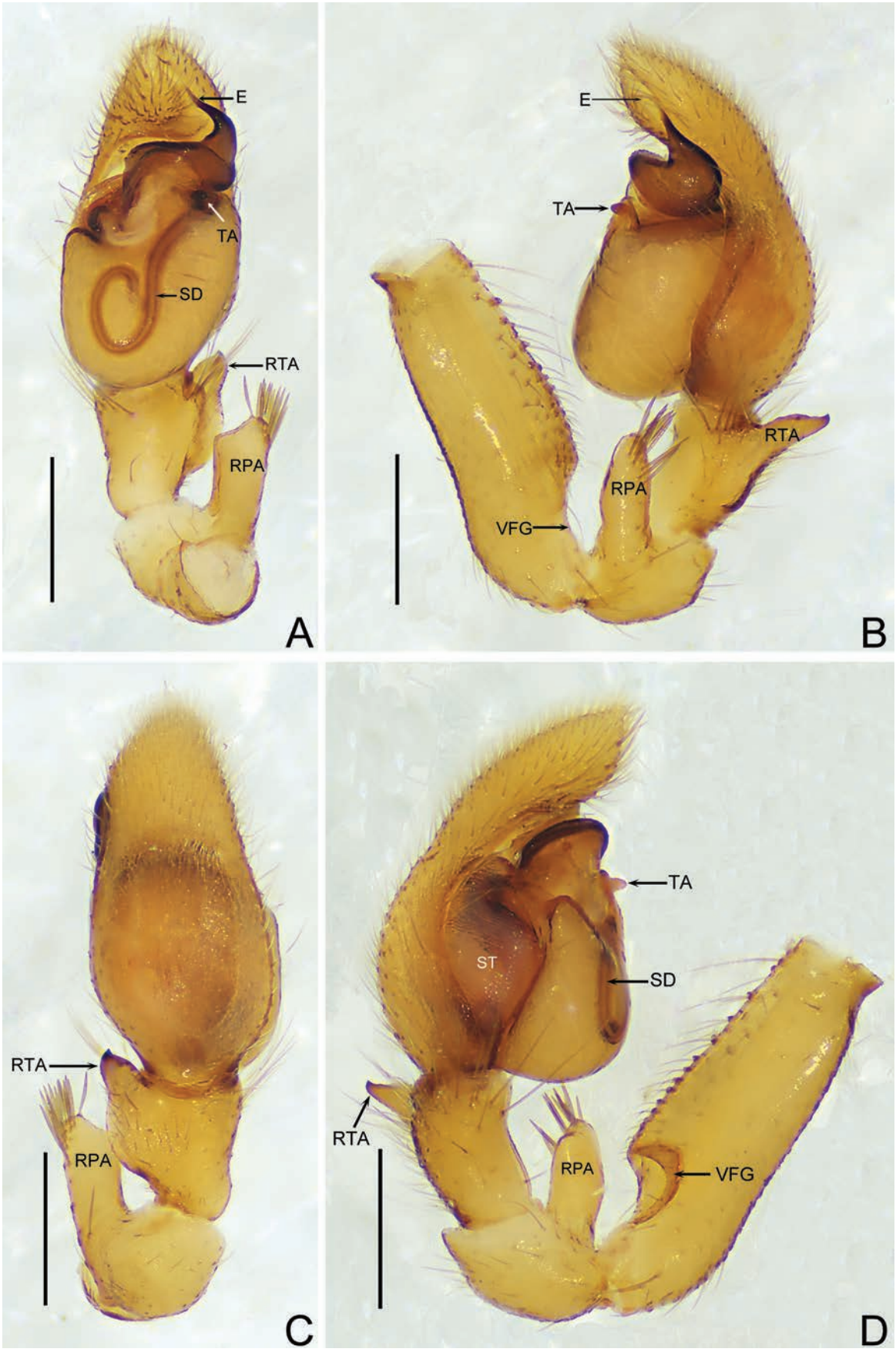

Figure 2. *Trachelas gaoligongensis* Jin, Yin & Zhang, 2017 (HNU-20071010) **A** male left palp, ventral view **B** ditto, retrolateral view **C** ditto, dorsal view **D** ditto, prolateral view. Scale bars: 0.3 mm.

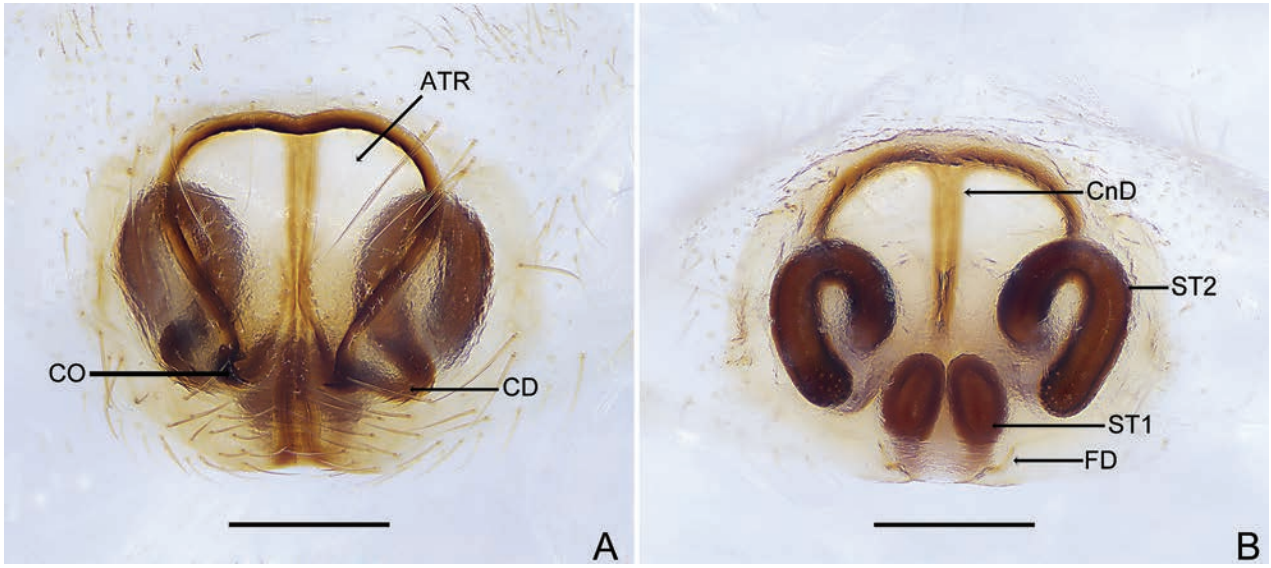

Figure 3. *Trachelas gaoligongensis* Jin, Yin & Zhang, 2017 (HNU-20071010) **A** genitalia, ventral view **B** ditto, dorsal view. Scale bars: 0.3 mm.

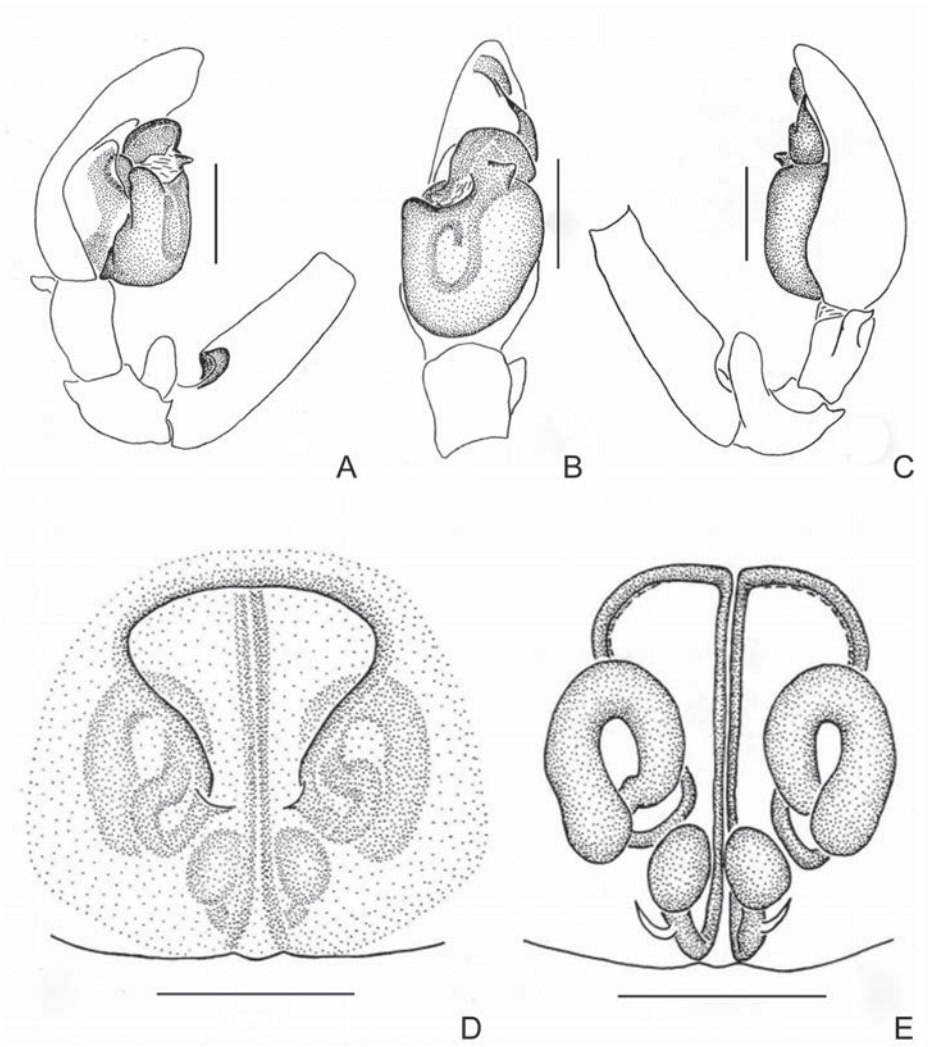

Figure 4. *Trachelas gaoligongensis* Jin, Yin & Zhang, 2017 **A** male left palp, prolateral view **B** ditto, ventral view **C** ditto, retrolateral view **D** genitalia, ventral view **E** ditto, dorsal view. Scale bars: 0.3 mm.

Description. Male. (one of HNU-20071010) (Fig. 1A–E). Total length 4.06. Carapace 2.05 long, 1.64 wide; abdomen 2.30 long, 1.65 wide. Carapace brown, fovea thin and black, cervicle and radial grooves distinct. Chelicerae and labium brown, three promarginal and two retromarginal teeth. Sternum and endites yellowish brown, truncated margin of sternum with distinct crescent-shaped depression. Eye sizes and interdistances: AME 0.14, ALE 0.14, PME 0.14, PLE 0.11, AME–AME 0.06, AME–ALE 0.02, PME–PME 0.11, PME–PLE 0.10, ALE–PLE 0.08. MOA 0.34 long, anterior width 0.28, posterior width 0.36. Clypeus height 0.12. Legs yellowish brown, with black rings. Leg measurements: leg I 5.38 (1.68, 2.19, 0.92, 0.59), II 5.24 (1.61, 2.13, 0.87, 0.63), III 3.15 (0.87, 0.90, 0.94, 0.44), IV 5.60 (1.74, 1.83, 1.45, 0.58). Leg formula: 4123. Abdomen oval, apricot-white; anterior half of dorsum with two black-brown longitudinal stripes; posterior half with five black-brown chevrons decreasing in size from anterior to posterior; venter with three dark longitudinal stripes. Spinnerets with parenthesis-shaped marks laterally.

Palp (Figs 2, 4A–C). Retrolateral patellar apophysis finger-like, as long as patella, distally covered with feathery setae; retrolateral tibial apophysis spur-like, as long as tibia, pointed distally; genital bulb oval, embolus short, with base broad and spiralled, apex constricted and spinelike. Sperm duct distinct and hook-shaped.

Female. (HNU-20071010) (Fig. 1F–J). Total length 4.95. Carapace 1.70 long, 1.39 wide; abdomen 2.84 long, 1.79 wide. Eye sizes and interdistances: AME 0.09, ALE 0.09, PME 0.11, PLE 0.11, AME–AME 0.08, AME–ALE 0.02, PME–PME 0.10, PME–PLE 0.09, ALE–PLE 0.08. MOA 0.28 long, anterior width 0.24, posterior width 0.32. Clypeus height 0.11. Leg measurements: leg I 4.81(1.50, 1.80, 0.89, 0.62), II 4.57 (1.44, 1.63, 0.91 0.59), III 3.73 (1.19, 1.12, 0.91, 0.51), IV 5.47 (1.54, 1.91, 1.40, 0.62). Leg formula: 4123. Abdomen oblong, anterior half of dorsum with a black-brown longitudinal stripe and some irregular darker patches. Other characters as in male.

Epigyne (Figs 3, 4D, E). Atrium about as long as wide, copulatory openings pore-like, located at posterior of epigyne; copulatory ducts C-shaped, connected to n-shaped secondary spermathecae; connecting ducts slender, axisymmetric; primary spermathecae oval, connected to lightly sclerotized fertilization ducts.

Distribution. China (Yunnan) (Fig. 8).

***Trachelas kavanaughi* sp. nov.**

https://zoobank.org/6250BA11-335B-45DD-B0BB-F65CCE47FF41

Figs 5, 7A, B

Type material. ***Holotype*** • ♀ (HNU-DHK-2004-058); China, Yunnan Prov., Gongshan County, Dulongjiang Township, south of Dizhengdang Village along Silalong River; 28.07654°N, 98.32603°E; 1890 m a.s.l.; 28 October 2004; D. H. Kavanaugh leg.

Etymology. The species is named in honor of the type specimen collector, D. H. Kavanaugh, the curator emeritus at the California Academy of Sciences.

Diagnosis. The female of this new species (Figs 5E, F, 7A, B) resembles that of *Trachelas gaoligongensis* (see Figs 3, 4D, E) in the shape of the atrium and

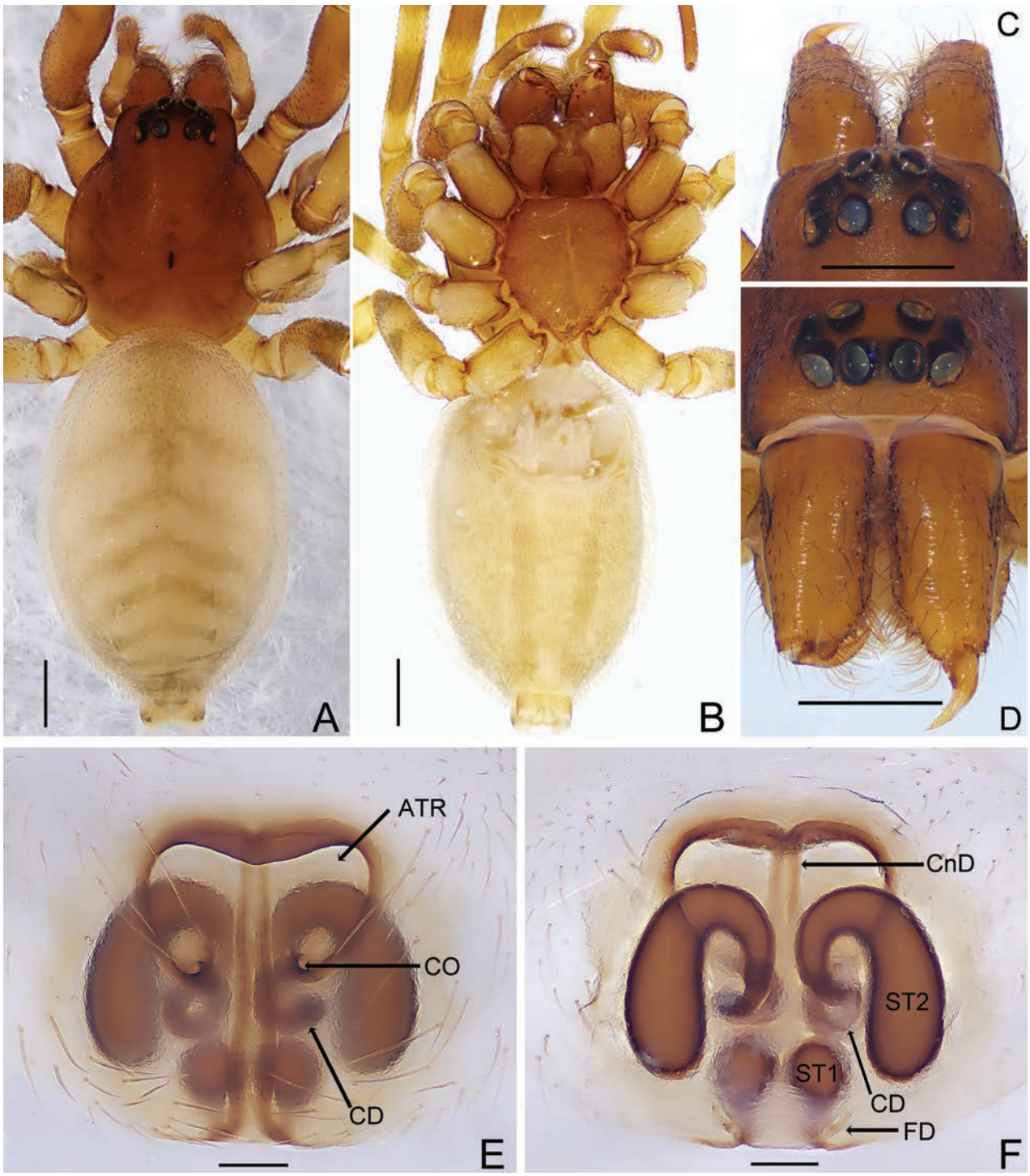

Figure 5. *Trachelas kavanaughi* sp. nov., female (holotype) **A** habitus, dorsal view **B** ditto, ventral view **C** ocular area, dorsal view **D** carapace, frontal view **E** genitalia, ventral view **F** ditto, dorsal view. Scale bars: 0.5 mm (**A–D**); 0.3 mm (**E, F**).

the secondary spermathecae but differs as follows: (1) the atrium is wider than long in ventral view (vs. about as long as wide); (2) the copulatory openings are located on the anterior of the genitalia in ventral view (vs. located on posterior); (3) the primary spermathecae are round in dorsal view (vs. oval); and (4) the interdistance of the secondary spermathecae is narrower than the width of the primary spermathecae in dorsal view (vs. more than the twice width of the primary spermathecae).

Description. Female (holotype) (Fig. 5A–D). Total length 4.45. Carapace 1.75 long, 1.61 wide; abdomen 2.68 long, 1.79 wide. Carapace brown, smooth, fovea black, small and distinct. Chelicerae brown, with three promarginal and two retromarginal teeth. Sternum and labium light brown, and truncated margin of sternum with distinct crescent-shaped depression. Eye sizes and interdistances: AME 0.13, ALE 0.13, PME 0.13, PLE 0.13, AME–AME 0.05, AME–ALE 0.02, PME–PME 0.10, PME–PLE 0.08, ALE–PLE 0.05. MOA 0.27 long, anterior width 0.30, posterior width 0.34. Clypeus height 0.12. Legs light brown alternating with dark brown. Leg measurements: leg I 5.53 (1.72, 2.02, 1.04, 0.75), II 5.30 (1.60, 1.93, 1.06, 0.71), III 4.20 (1.22, 1.43, 1.02, 0.53), IV 5.72 (1.66, 1.95, 1.46, 0.65). Leg formula: 4123. Abdomen oval, apricot-white; dorsum with five black-brown chevrons decreasing in size from anterior to posterior; venter with two blurry gray longitudinal stripes. Spinnerets yellowish.

Epigyne (Figs 5E, F, 7A, B). Atrium wider than long copulatory openings small, located at anterior of epigyne; copulatory ducts C-shaped, secondary spermathecae narrowest at junction with copulatory ducts, widening from copulatory openings to spermathecae; connecting ducts axisymmetric; primary spermathecae round, connected to lightly sclerotized fertilization ducts.

Male. Unknown.

Distribution. Known only from the type locality (Fig. 8).

***Trachelas ventriosus* sp. nov.**

https://zoobank.org/87DF29C7-02FA-411D-8A54-CBC9141565F7

Figs 6, 7C, D

Type material. ***Holotype*** • ♀ (HNU-Wang060528-1); China, Yunnan Prov., Tengchong County, Houqiao Township; 25.35391°N, 98.25488°E; 1785 m a.s.l.; 28 May 2006; Xin-Ping Wang, Peng Hu leg.

Etymology. The species name is derived from the Latin “ventriosus” (pot-bellied), referring to its large abdomen; adjective.

Diagnosis. The female of this new species (Figs 6E, F, 7C, D) resembles that of *Trachelas fasciae* Zhang, Fu & Zhu, 2009 (see Zhang et al. 2009, figs 21, 22) in having symmetrical connecting ducts and the primary spermathecae are near the genital groove but differs as follows: (1) the atrium occupies 3/4 of the genitalia in ventral view (vs. 1/3 of the genitalia); (2) the copulatory openings are posterior to the secondary spermathecae in ventral view (vs. anterior to the secondary spermathecae); (3) the secondary spermathecae are inverted V-shaped in dorsal view (vs. V-shaped); and (4) the primary and secondary spermathecae are far away from each other in dorsal view (vs. partially overlapping).

Description. Female (holotype) (Fig. 6A–D). Total length 4.47. Carapace 1.59 long, 1.33 wide; abdomen 2.87 long, 1.89 wide. Carapace brown, fovea black and slender, radial grooves distinct. Chelicerae light brown, with two promarginal and three retromarginal teeth. Sternum and labium light brown, partly covered with black setae. Eye sizes and interdistances: AME 0.12, ALE 0.12, PME 0.12, PLE 0.12, AME–AME 0.06, AME–ALE 0.01, PME–PME 0.10, PME–PLE 0.08, ALE–PLE 0.07. MOA 0.26 long, anterior width 0.24, posterior width 0.30. Clypeus height 0.11. Legs light brown alternating with dark brown. Leg measurements: leg I 4.56 (1.43, 1.65, 0.81, 0.67), II 4.82 (1.44, 1.62, 1.22, 0.54),

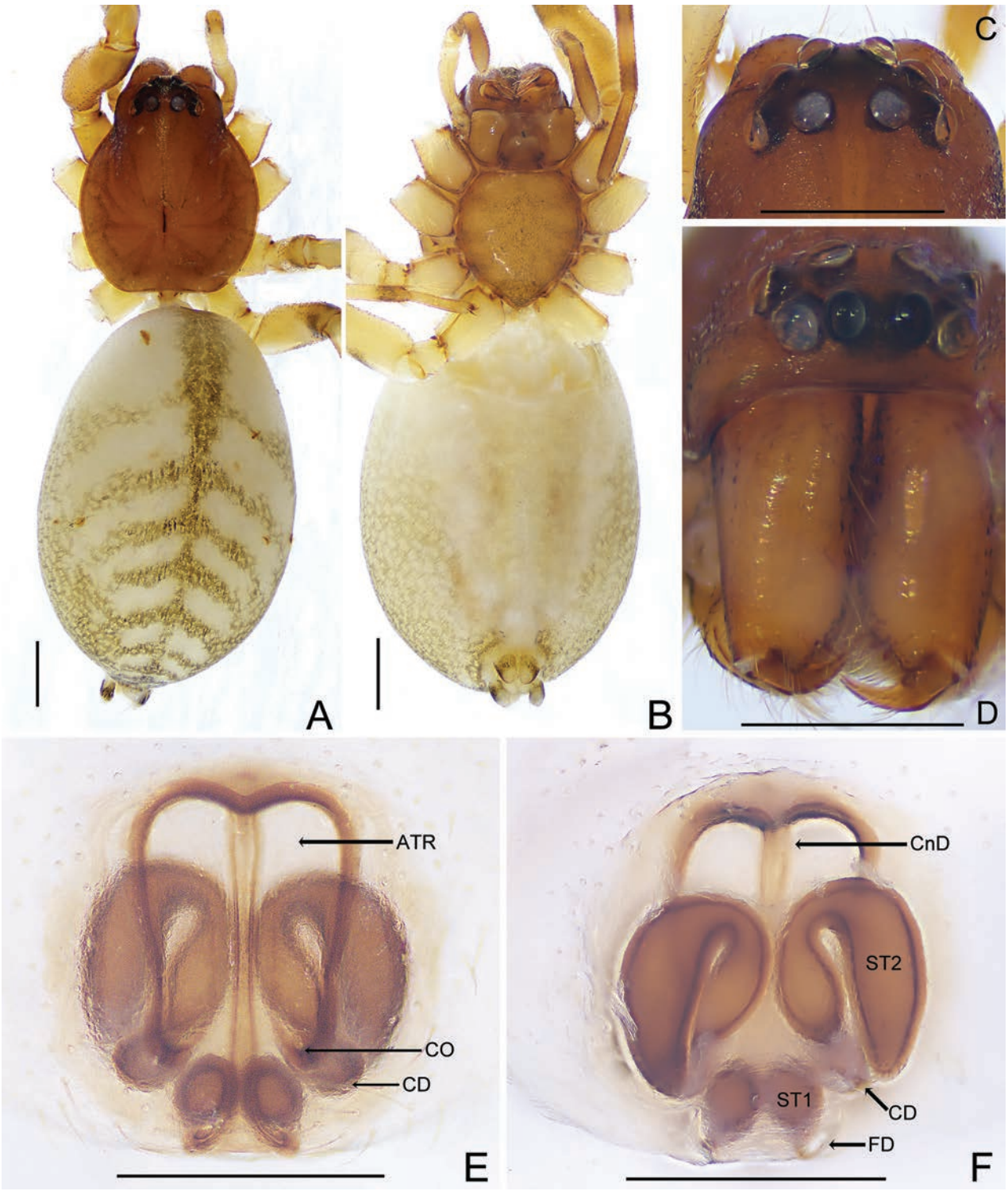

Figure 6. *Trachelas ventriosus* sp. nov., female (holotype) **A** habitus, dorsal view **B** ditto, ventral view **C** ocular area, dorsal view **D** carapace, frontal view **E** genitalia, ventral view **F** ditto, dorsal view. Scale bars: 0.5 mm (**A–D**); 0.3 mm (**E, F**).

III 3.02 (0.83, 1.05, 0.72, 0.42), IV 4.80 (1.32, 1.71, 1.23, 0.54). Leg formula: 2413. Abdomen oval, apricot-white; dorsum with eight black-brown chevrons decreasing in size from anterior to posterior, with a longitudinal black-brown stripe in middle, and several brown markings distributed irregularly; venter with two blurry gray longitudinal stripes. Spinnerets covered with black setae and parenthesis-shaped marks laterally.

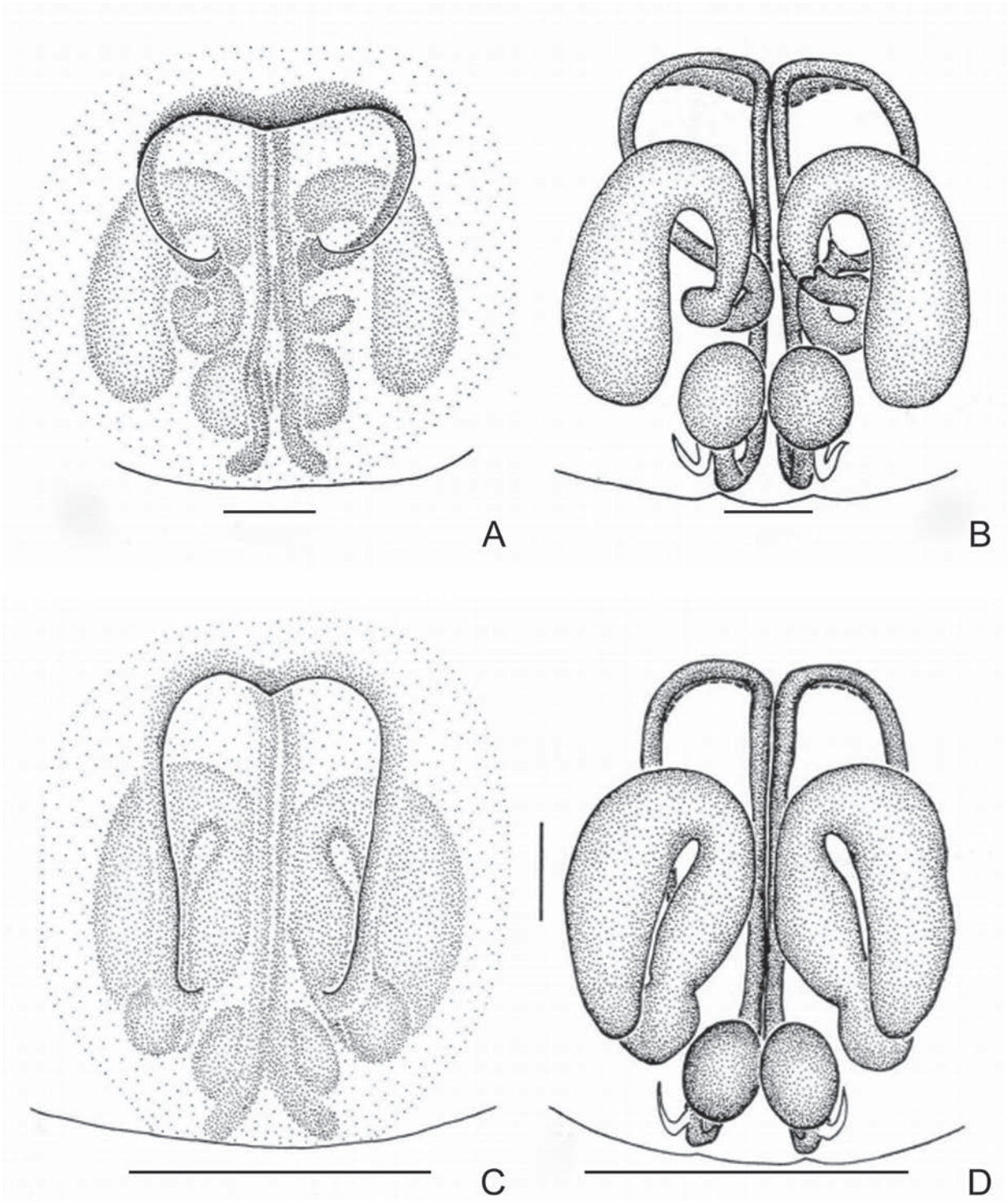

Figure 7. A, B *Trachelas kavanaughi* sp. nov. **C, D** *Trachelas ventriosus* sp. nov. **A** genitalia, ventral view **B** ditto, dorsal view **C** ditto, ventral view **D** ditto, dorsal view. Scale bars: 0.3 mm.

Epigyne (Figs 6E, F, 7C, D). Atrium longer than wide, copulatory openings located on posterior of epigyne; connecting ducts long and symmetrical; secondary spermathecae close to each other; primary spermathecae close to genital groove, connected by short fertilization ducts.

Male. Unknown.

Distribution. Known only from the type locality (Fig. 8).

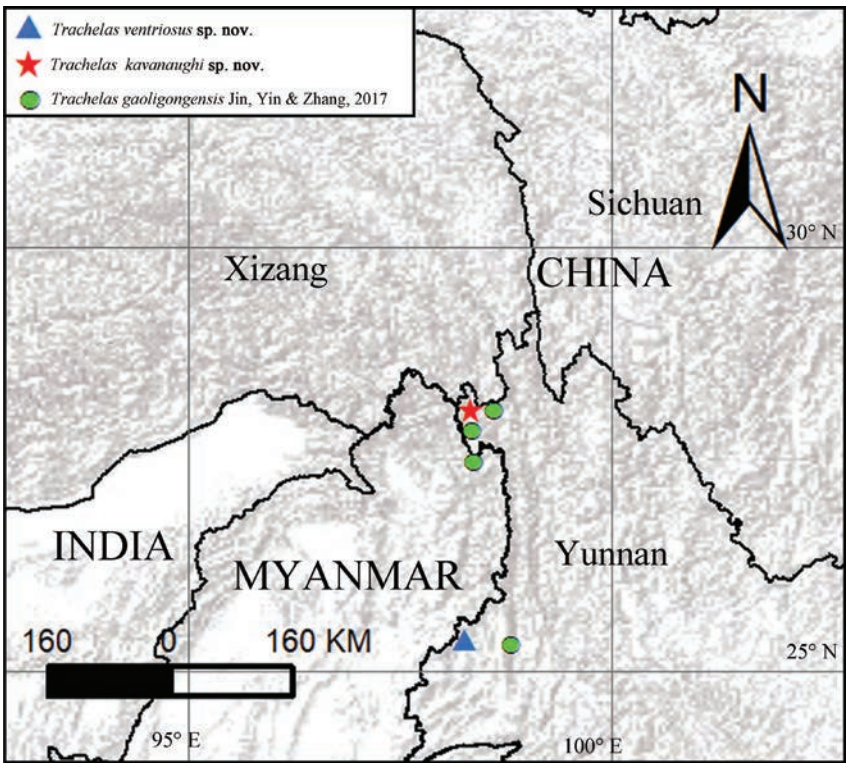

Figure 8. Collection localities of *Trachelas gaoligongensis* Jin, Yin & Zhang, 2017, *Trachelas kavanaughi* sp. nov. and *Trachelas ventriosus* sp. nov.

Acknowledgments

We are grateful to Guo Tang, Xin-Ping Wang, Peng Hu, D. H. Kavanaugh, and V. F. Lee for collecting specimens.

Additional information

Conflict of interest

The authors have declared that no competing interests exist.

Ethical statement

No ethical statement was reported.

Funding

This research was supported by the National Natural Sciences Foundation of China (NSFC-30970327, 31272271, 31272272, 31301861, 31660609).

Author contributions

Data curation: YZ. Methodology: WY. Writing - original draft: GT. Writing - review and editing: XP.

Author ORCIDs

Gang Tang https://orcid.org/0009-0009-6287-6706
Wen-long Yan https://orcid.org/0009-0001-9663-9436
Yi Zhao https://orcid.org/0009-0008-8804-5305
Xian-jin Peng https://orcid.org/0000-0002-2614-3910

Data availability

All of the data that support the findings of this study are available in the main text.

References

Jin C, Yin XC, Zhang F (2017) Four new species of the genus *Trachelas* L. Koch, 1872 and the first record of *T. vulcani* Simon, 1896 from south-west China (Araneae: Trachelidae). Zootaxa 4324(1): 23–49. https://doi.org/10.11646/zootaxa.4324.1.2

Koch L (1872) Apterologisches aus dem fränkischen Jura. Abhandlungen der Naturhistorischen Gesellschaft zu Nürnberg 5: 146–149.

Liu KZ, Liu JN, Zhang F, Li LT, Mi XQ, Jin C (2024) An update on the distribution of the genus *Trachelas* L. Koch, 1872 (Araneae, Trachelidae) in China, with description of a new species. Zootaxa 5453(4): 567–576. https://doi.org/10.11646/zootaxa.5453.4.7

Ramírez MJ (2014) The morphology and phylogeny of dionychan spiders (Araneae: Araneomorphae). Bulletin of the American Museum of Natural History 390: 342. https://doi.org/10.1206/821.1

Simon E (1897) Histoire naturelle des araignées. Deuxième édition, tome second. Roret, Paris, 1–192. https://doi.org/10.5962/bhl.title.51973

World Spider Catalog (2024) World Spider Catalog. Version version 25.0. Natural History Museum Bern. http://wsc.nmbe.ch [accessed on 19 June, 2024] https://doi.org/10.24436/2

Zhang F, Fu JY, Zhu MS (2009) A review of the genus *Trachelas* (Araneae: Corinnidae) from China. Zootaxa 2235: 40–58. https://doi.org/10.11646/zootaxa.2235.1.2

ZooKeys 1215: 139–149 (2024)
DOI: 10.3897/zookeys.1215.129623

Research Article

Distribution extension of a vent scale worm *Branchinotogluma bipapillata* (Polychaeta, Polynoidae) in the Indian Ocean

Won-Kyung Lee[1,2], Se-Joo Kim[1,3]

1 *Division of Biomedical Research, Korea Research Institute Bioscience and Biotechnology, Daejeon 34141, Republic of Korea*
2 *Division of EcoScience, Ewha Womans University, Seoul 03760, Republic of Korea*
3 *KRIBB School, University of Science and Technology, Daejeon, 34113, Republic of Korea*
Corresponding author: Se-Joo Kim (biosejoo@kribb.re.kr)

Abstract

Branchinotogluma Pettibone, 1985 is the most species-rich genus within the subfamily Lepidonotopodinae Pettibone, 1983, comprising 18 valid species from chemosynthesis-based ecosystems in the Pacific and Indian Oceans. Here, we report a new distributional record of *Branchinotogluma bipapillata* Zhou, Wang, Zhang & Wang, 2018, at the hydrothermal vent sites on the northern Central Indian Ridge (nCIR). This record represents the northernmost occurrence of *B. bipapillata* in the Indian Ocean. We conducted a comparative study of the nCIR population and other documented populations using distributional information, morphological traits, and genetic markers (two mitochondrial [*COI*, *16S* rRNA] and one nuclear [*18S* rRNA] genes). While most morphological characters of *B. bipapillata* were consistent with those found in the Southwest Indian Ridge (SWIR), variations were noted in the segment with the last branchiae. Molecular data revealed that all populations of *B. bipapillata* form a single clade, indicating a wide distribution from the SWIR to nCIR, covering ~4,000 km across various ridges in the Indian Ocean. This study presents extensive distribution of a vent species with well-connected populations throughout the Indian Ocean, distinguishing it from many other vent species affected by the dispersal barrier in the Indian Ocean.

Key words: *16S* rRNA, *18S* rRNA, *CO1*, deep-sea, hydrothermal vent, northern Central Indian Ridge, polynoids

Academic editor: Andrew Davinack
Received: 13 June 2024
Accepted: 2 September 2024
Published: 14 October 2024

ZooBank: https://zoobank.org/4A593809-AE76-458F-B085-0D34B29105CC

Citation: Lee W-K, Kim S-J (2024) Distribution extension of a vent scale worm *Branchinotogluma bipapillata* (Polychaeta, Polynoidae) in the Indian Ocean. ZooKeys 1215: 139–149. https://doi.org/10.3897/zookeys.1215.129623

Introduction

The subfamily Lepidonotopodinae Pettibone, 1983 consists of scale worms endemic to chemosynthesis-based ecosystems (Wu et al. 2023). Currently, seven species from the Indian Ocean are identified within this subfamily: three *Branchinotogluma*, two *Branchipolynoe*, and two *Levensteiniella* (Han et al. 2023). *Branchinotogluma* Pettibone, 1985, the most species-rich genus in the subfamily, comprises 18 species found in the Pacific and Indian Oceans (Han et al. 2023). Specifically, three *Branchinotogluma* species are distributed across different ridge systems in the Indian Ocean: *B. bipapillata* Zhou et al., 2018 in the Southwest Indian Ridge (SWIR) and southern Central Indian Ridge (sCIR), *B. jiaolongae* Han et al., 2023 in the SWIR and Carlsberg Ridge (CR), and *B. kaireiensis* Han et al., 2023 in the sCIR and CR (Zhou et al. 2018, 2022; Han et al. 2023).

Since the initial discovery of vent fields in the Indian Ocean in 2000, the Rodriguez Triple Junction, which links the SWIR, CIR, and Southeast Indian Ridge, was assumed to be a dispersal barrier for vent species within the Indian Ocean (Gamo et al. 2001; Chen et al. 2015). However, with the discovery of more vent fields and associated fauna, it now appears that the primary dispersal barriers lie within the ridge system itself, mainly due to ridge offsets, rather than between different ridge systems (Sun et al. 2020). For instance, the vent crab *Austinograea rodriguezensis* Tsuchida & Hashimoto, 2002 was absent from the southern SWIR (sSWIR) but was found in the northern SWIR (nSWIR) and showed panmixia with populations from other ridges like the sCIR. Similarly, the distribution of the hairy snail *Alviniconcha* species complex shows connectivity between different ridges, northern CIR (nCIR) and CR, but subdivisions between the sCIR and nCIR on the same CIR (Sun et al. 2020; Jang et al. 2023).

While *B. bipapillata* has been reported from vent fields on two ridge systems, the SWIR and CIR, morphological and genetic studies were previously only conducted on specimens from the sSWIR. In this study, we collected *Branchinotogluma* species from hydrothermal vent fields on the nCIR and compared morphological and molecular data with those from vent fields on the sSWIR.

Materials and methods

Specimens of *Branchinotogluma* were collected from hydrothermal vents in the nCIR during the 2023 KIOST expedition aboard the R/V *Isabu* (Fig. 1, Table 1) using a suction sampler and scoop mounted on the ROV ROPOS (Canadian Scientific Submersible Facility). Upon collection, a piece of elytron or parapodium from each specimen was dissected and preserved in 99% ethanol for molecular analysis. The entire body of the specimens was preserved in either 10% neutral buffered formalin or 70% ethanol for morphological studies.

For determination of morphological characters, all specimens were examined under a stereomicroscope (Stemi 508; Carl Zeiss, Germany). Specimen photographs were captured using a color camera (Axiocam 208 color; Carl Zeiss, Germany) and a DSLR camera (EOS 5D Mark IV; Canon, Tokyo, Japan). Images were processed with ZEN 3.3 blue edition (Carl Zeiss, Germany) and Helicon Focus software (Helicon Soft Ltd., Kharkov, Ukraine), and further edited using Adobe Photoshop 2022 (Adobe, San Jose, CA, USA). Specimen morphology was recorded following characters and states listed in Zhou et al. (2018).

A small piece of elytron or parapodium was used for total genomic DNA extraction using the AccuPrep® Genomic DNA Extraction Kit (Bioneer, Daejeon, South Korea), following the manufacturer's instructions. Partial cytochrome c oxidase subunit 1 (*CO1*) and *18S* rRNA (*18S*) sequences were amplified following the protocols in Lee et al. (2021) and Jimi et al. (2021), respectively. For *16S* rRNA (*16S*), the primers 16SA (5'-CGCCGTTTATCAAAAACAT-3') and 16Sbr (5'-CCGGTYTGAACTCAGATCAYG-3') (Palumbi et al. 1991; Palumbi 1996) were used. Polymerase chain reaction (PCR) was conducted using a SimpliAmp™ Thermal Cycler (Applied Biosystems, Life technologies) under the following conditions: initial denaturation at 94 °C for 2 min; 5 cycles at 95 °C for 10 s, 42 °C for 30 s, and 72 °C for 60 s; 35 cycles at 95 °C for 10 s, 48 °C for 30 s, and 72 °C for 60 s; with a final extension at 72 °C for 2 min. PCR products were sent to Macrogen (Seoul, Korea) for Sanger sequencing.

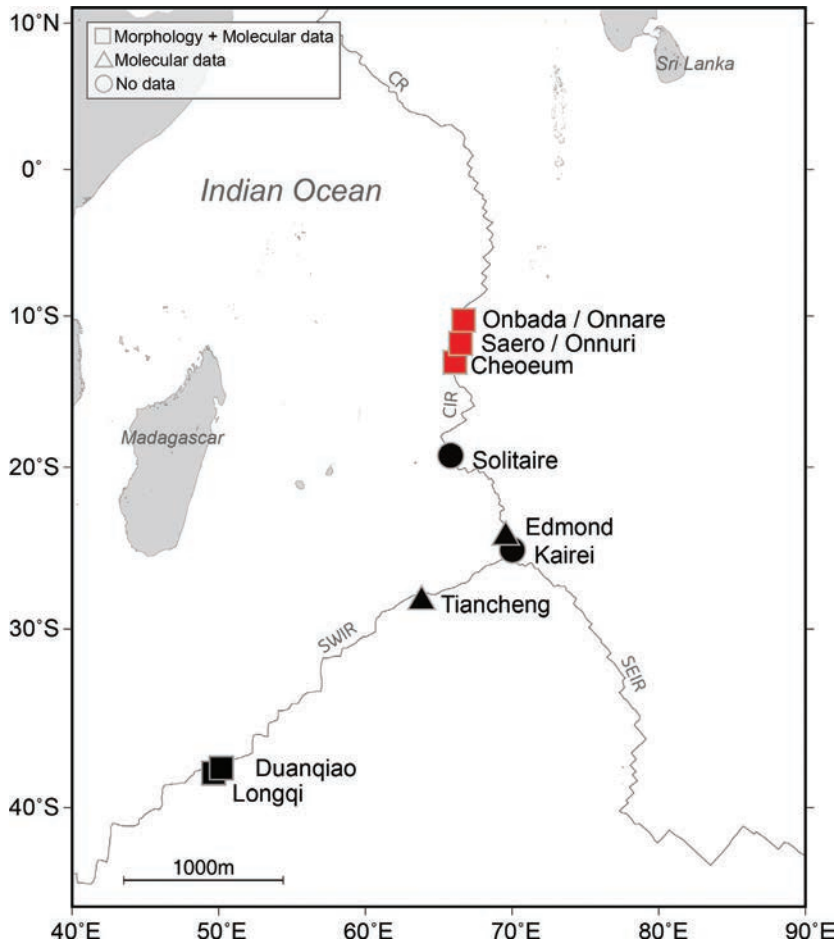

Figure 1. Map displaying the geographic distribution of *Branchinotogluma bipapillata* in the Indian Ocean. Red indicates sampling locations from this study and black indicates records of *B. bipapillata* from previous studies. Some closely situated sampling sites (< 10 km apart, such as Onbada and Onnare, Saero and Onnuri) are marked with a single square.

Table 1. Sampling information of newly obtained *Branchinotogluma bipapillata* specimens from the nCIR and their GenBank accession numbers sequenced in this study.

Voucher	Sampling site	Latitude (S), Longitude (E)	Depth (m)	GenBank Accession Numbers		
				CO1	*16S*	*18S*
KRIBB310101–KRIBB310102	Cheoeum	12°37.1'S, 66°7.6'E	3018	PP600168–PP600169	PP600150–PP600151	PP600184–PP600185
KRIBB310103–KRIBB310107	Onnuri	11°24.9'S, 66°25.4'E	2009	PP600170–PP600174	PP600152–PP600156	PP600186–PP600190
KRIBB310108–KRIBB310110	Onnare	9°47.4'S, 66°41.9'E	2993	PP600175–PP600177	PP600157–PP600159	PP600191–PP600193
KRIBB310111–KRIBB310112	Onbada	9°48.9'S, 66°40.6'E	2563	PP600178–PP600179	PP600160–PP600161	PP600194–PP600195
KRIBB310113–KRIBB310116	Saero	11°19.7'S, 66°26.9'E	3256	PP600180–PP600183	PP600162–PP600165	PP600196–PP600199

New sequences were aligned with those of other Lepidonotopodinae species from GenBank (Suppl. material 1: table S1) using Geneious Prime ver. 2023.0.1 (Biomatters, Auckland, New Zealand). Sequence divergence for the *CO1* and *16S* genes was calculated using the *p*-distance method in MEGA11 (Tamura et al. 2021). For phylogenetic analysis, the three genes were concatenated using

Geneious Prime. The best evolutionary model, GTR+I+G, was selected using jModelTest ver. 2.1.8 (Darriba et al. 2012). The phylogenetic tree was constructed using the maximum-likelihood method with raxmlGUI 2.0 (Edler et al. 2021).

All specimens used in this study are deposited at the Korea Research Institute of Bioscience and Biotechnology.

Results

Family Polynoidae Kinberg, 1856
Subfamily Lepidonotopodinae Pettibone, 1983

Genus *Branchinotogluma* Pettibone, 1985

Branchinotogluma bipapillata Zhou, Wang, Zhang & Wang, 2018: 528–533, figs 1–7; table 1.

Material examined. Indian Ocean • 2 ♂; Cheoeum; 12°37.1'S, 66°07.6'E; depth 3018 m; 28 Mar. 2023; W-K Lee leg.; hydrothermal vent; GenBank: PP600168– PP600169; KRIBB310101 to KRIBB310102 • 2 ♂, 2 ♀, 1 undetermined; Onnuri; 11°24.9'S, 66°25.4'E; depth 2009 m; 1–2 Apr. 2023; W-K Lee leg.; hydrothermal vent; GenBank: PP600170– PP600174; KRIBB310103 to KRIBB310107 • 1 ♀, 2 undetermined; Onnare; 9°47.4'S, 66°41.9'E; depth 2993 m; 3 Apr. 2023; W-K Lee leg.; hydrothermal vent; GenBank: PP600175– PP600177; KRIBB310108 to KRIBB310110 • 1 ♂, 1 ♀; Onbada; 9°48.9'S, 66°40.6'E; depth 2563 m; 4 Apr. 2023; W-K Lee leg.; hydrothermal vent; GenBank: PP600178– PP600179; KRIBB310111 to KRIBB310112 • 2 ♂, 2 ♀; Saero; 11°19.7'S, 66°26.9'E; depth 3256 m; 7 Apr. 2023; W-K Lee leg.; hydrothermal vent; GenBank: PP600180– PP600183; KRIBB310113 to KRIBB310116.

Description. Specimens relatively well preserved, with 21 segments, 12.0–51.0 mm in length and 5.0–16.6 mm in width. Body shape fusiform, tapered anteriorly and posteriorly (Fig. 2A, B, Table 2). Pairs of elytra on elytrophores on segments 2, 4, 5, 7, 9, 11, 13, 15, 17, and 19; elytra oval to subreniform, white, slightly transparent, with a smooth surface (Fig. 2C–E). Dorsal cirri on segments 3, 6, 8, 10, 12, 14, 16, 18, 20, and 21, extending beyond the tips of neurochaetae. Branchiae arborescent; grouped in two, one at base of the notopodia and another at base of dorsal tubercles or elytrophores; starting from segment 3 and ending between segments 18 or 21 (Table 2).

Prostomium bilobed, triangular anterior lobes with slender frontal filaments (Fig. 2F). Median antennae on anterior notch, with a cylindrical ceratophore and subulate style; palps thick, smooth, and end in subulate tips; lateral antennae and eyes absent (Fig. 2F). Tentacular segment fused to prostomium, with pair of tentacular cirri on each side, and a small acicular lobe at the base of tentaculophore; tentacular cirri slender (Fig. 2F).

First segment not distinct, fused to prostomium. Pharynx with five dorsal and four ventral papillae in one immature individual, but not seen in others (Fig. 2G). Second segment with first pair of elytrophores, ventral cirri, and biramous parapodia. Third segment with ventral cirri and first pair of branchiae. Fourth to last segments with ventral cirri and biramous parapodia. Notopodia smaller than neuropodia; notochaetae stout, few, arranged in radiating bundles; neurochaetae slender, numerous, forming a fan shape (Fig. 2H–K).

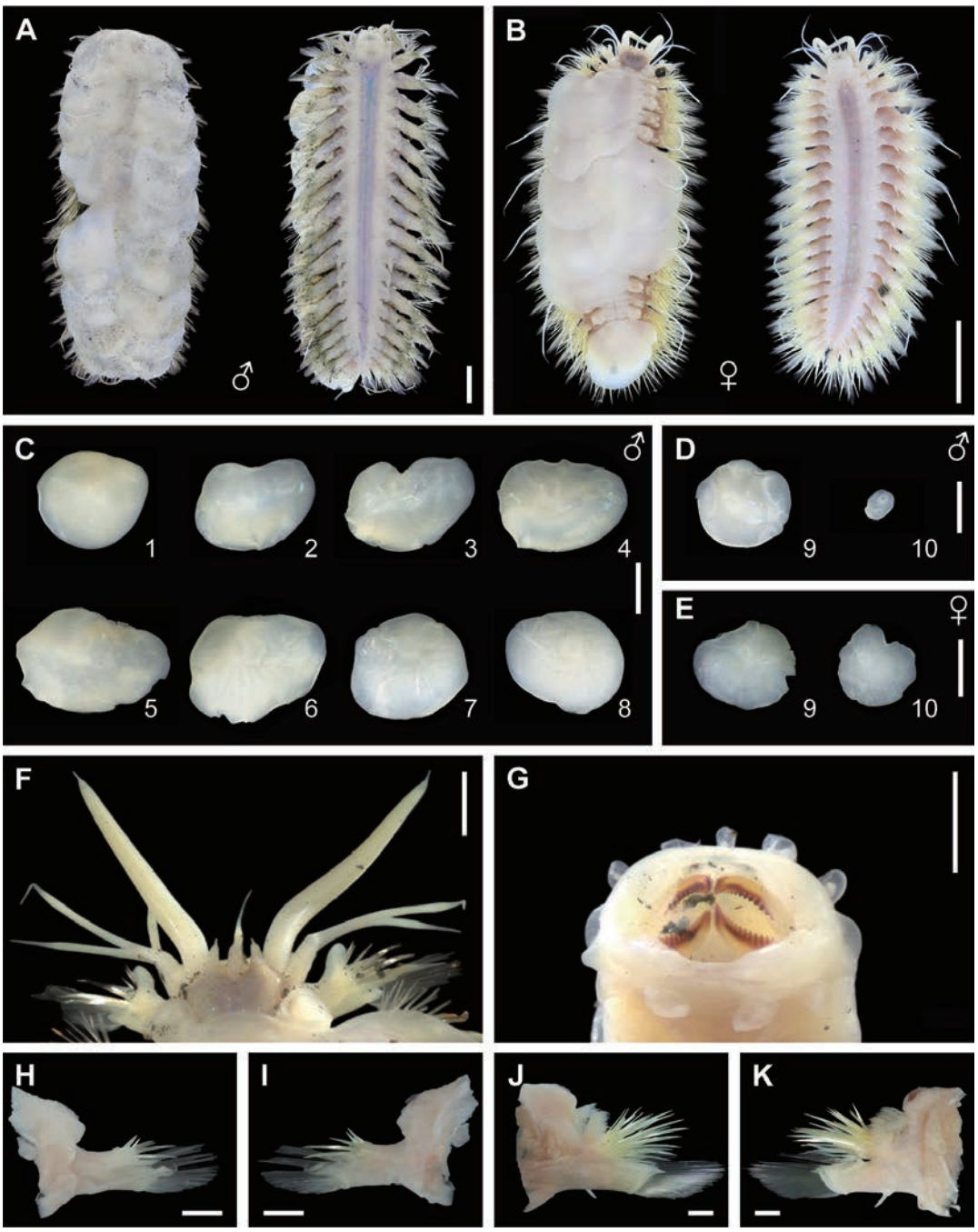

Figure 2. *Branchinotogluma bipapillata* specimens collected from the nCIR **A** dorsal and ventral views of male (KRIBB310116) **B** dorsal and ventral views of female (KRIBB310105) **C** 1st–8th left elytra **D** 9th–10th left elytra of male (KRIBB310103) E 9th–10th left elytra of female (KRIBB310110) **F** head featuring prostomium, palps, tentacular cirri, and first parapodia on segment 2 (KRIBB310112) **G** everted pharynx with dorsal and ventral papillae (KRIBB310108). Anterior and posterior views of left parapodia on (H-I) segment 2 and (J-K) segment 11 (KRIBB310106). Scale bars: 5 mm (**A–E**); 0.5 mm (**F, G**); 1 mm (**H–K**).

Sexual dimorphism evident. In males, posterior segments modified (Fig. 3A) with 10th elytra and elytrophores much smaller than 9th (Figs 2D, 3A, Table 2); ventral papillae present on segments 12–13, long, tapering, with slender tips extending to next segment; ventral lamellae on segments 14–17, round (Fig. 3B). In females, posterior segments not modified (Fig. 3C), with 10th elytra and elytrophores similar to 9th (Figs 2E, 3C, Table 2); ventral papillae present on segments 11–15, short and blunt (Fig. 3D).

Distribution. Indian Ocean (depth 1732–3256 m): Longqi and Duanqiao vent fields on the southern Southwest Indian Ridge; Tiancheng vent field on the northern Southwest Indian Ridge; Edmond vent field on the southern Central Indian Ridge; Onnare, Onbada, Saero, Onnuri, and Cheoeum vent fields on the northern Central Indian Ridge.

Remarks. Comparisons of key morphological characters between the geographically distant populations are present in Table 2. The key characters of the nCIR specimens of *B. bipapillata* largely correspond with those of the SWIR specimens (Zhang et al. 2018). However, the two populations differ in the last segment with branchiae in females (segment 19 in sSWIR compared with segment 18 or 21 in nCIR; Table 2).

Among the 16 specimens from the nCIR population, 10 specimens with body length greater than 20 mm were well-developed in all features indicating adult morphology, while characters of sexual dimorphism were not observed in 6 specimens shorter than 20 mm.

DNA barcoding and phylogenetic analysis. Partial sequences of *CO1*, *16S*, and *18S* were recovered from 16 specimens collected from the nCIR. As shown in Table 1, 48 newly obtained sequences have been deposited in GenBank.

In *CO1*, the mean intra-population variation was 0.56% for nCIR and 0.65% for SWIR, with an inter-population variation of 1.00% (Table 3). In *16S*, the mean intra-population variation was 0.27% for nCIR and 0.33% for SWIR, with an inter-population variation of 0.39%. In *18S*, the mean intra-population variation was 0.01% for nCIR and 0.00% for SWIR, with an inter-population variation of 0.004%.

The interspecific variation between *B. bipapillata* and other congeners ranged from 18.63% to 21.88% in *CO1*, and from 13.11% to 19.08% in *16S* (Suppl. material 1: table S2). In *18S*, the interspecific variation ranged from 1.69% to 3.80%.

Table 2. Morphological comparison of *Branchinotogluma bipapillata* from the nCIR and sSWIR.

Region	Length (mm)	Sex (# of ind.)	Last segment with branchiae	Number of dorsal/ventral papillae on pharynx	9th to 10th elytrophore diatmeter ratio	Reference
nCIR	24.4–48.0	Male (5)	18	Not observed	2.25–2.64	This study
	20.5–51.0	Female (8)	18 or 21		1.08–1.46	
	12.0–17.8	Undetermined (3)	18	5/4*	1.23–1.28	
SWIR	23.3–32.3	Male (1)	18	5/5	N/A	Zhou et al. 2018
		Female (2)	19		N/A	

*Observed in a single specimen (KRIBB310108; Fig. 2G).

Table 3. Sequence divergence (%) among three *Branchinotogluma bipapillata* populations based on partial *CO1* gene (553 bp).

Populations (# of ind.; intra)	nCIR	sCIR	SWIR
nCIR	–		
(16; 0.56)			
sCIR	0.70	–	
(1; NC*)	(0.20–1.18)		
SWIR	1.00	0.47	–
(5; 0.65)	(0.00–1.65)	(0.20–1.19)	

*not calculated.

The maximum likelihood phylogenetic tree, constructed with concatenated sequences of *CO1*, *16S*, and *18S* (Fig. 4), shows the SWIR and nCIR populations of *B. bipapillata* clustering together as a single clade, indicating no significant divergence between populations from different ridges. Within the *Branchinotogluma* genus, *B. bipapillata* is closely related to a clade including *B. kaireiensis*, *B. pettiboneae* Wu et al., 2019, and *B. robusta* Wu et al., 2023.

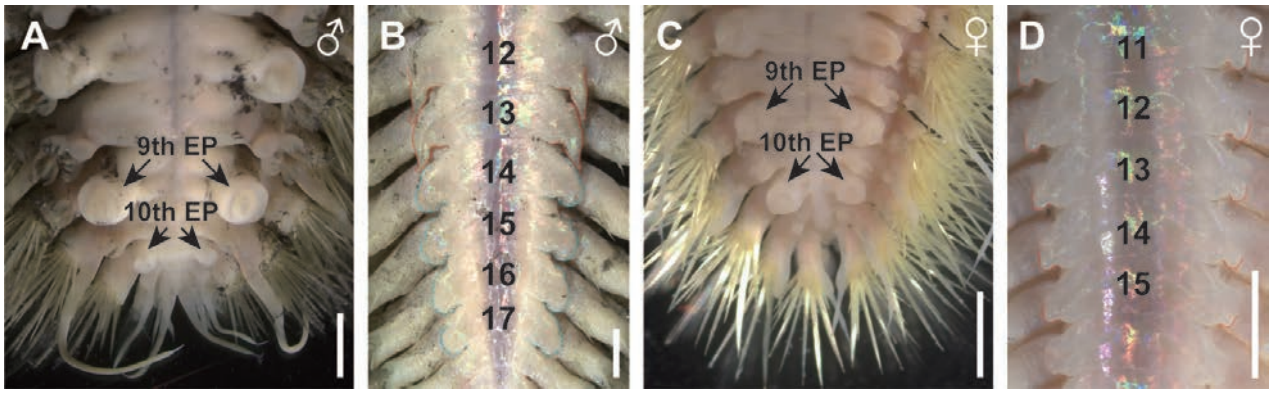

Figure 3. Sexually dimorphic characters of *Branchinotogluma bipapillata* **A** dorsal view of posterior segments **B** ventral view of segments 12–17 of male (KRIBB310116) **C** dorsal view of posterior segments **D** ventral view of segments 11–15 of female (KRIBB310105). Arrows point to 9th and 10th elytrophores (EP) pointed with arrows. Ventral papillae are outlined in red and ventral lamellae in blue. Scale bars: 2 mm (A, C); 1 mm (B, D).

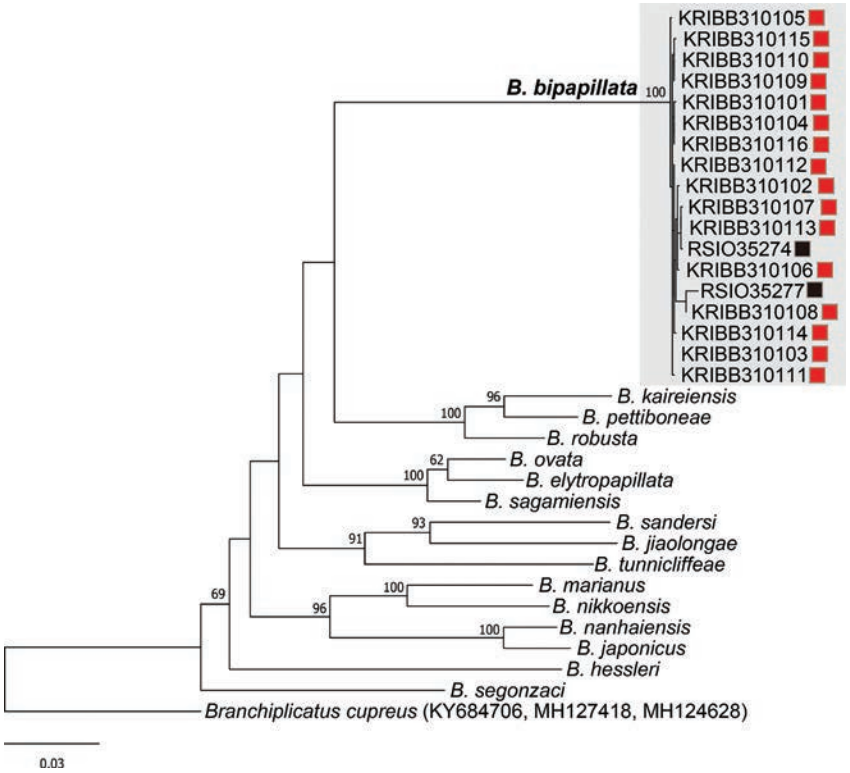

Figure 4. Maximum-likelihood phylogenetic tree of *Branchinotogluma* species based on concatenated sequences of the *CO1*, *16S*, and *18S* genes. *Branchinotogluma bipapillata* species are highlighted with a gray box. Red and black squares represent nCIR and sSWIR populations, respectively. GenBank accession numbers of the *CO1*, *16S* and *18S* genes of the outgroup are noted next to the species names. Maximum-likelihood bootstrap support values > 60 are displayed next to the nodes.

Discussion and conclusion

The vent scale worm *B. bipapillata* is widely distributed in the Indian Ocean, but comprehensive morphological and molecular data are lacking across all deep-sea oceanic ridges, and specimens are rarely reported at each sampling site (Fig. 1; only five specimens of *B. bipapillata* from the SWIR were barcoded with *CO1*, and only two sequences of *16S* and *18S* are available from SWIR specimens). In this study, 16 individuals, including female, male, and immature specimens of *B. bipapillata* from the nCIR were observed, enriching descriptions of features such as all elytra, and improving the molecular description of this species with both nuclear and mitochondrial gene sequences. Key morphological characters, such as the presence of an acicular lobe on the tentaculophore and the position of segmental ventral papillae, showed general congruence between the sSWIR and nCIR populations. Additionally, *CO1* barcode sequences revealed a mean intraspecific variation of 0.72% in *B. bipapillata*, which is within the variation range observed in other *Branchinotogluma* species (0.00–1.05%; Suppl. material 1: table S2).Thus, molecular data on genetic distances within and between populations showed no significant differences, and the phylogenetic analysis revealed a single clade of *B. bipapillata*, with no divergence between populations (Fig. 4, Table 3). Based on these morphological and molecular findings, the southernmost and northernmost populations appear to be well connected, forming a single genetic population with minimal morphological variability.

Other vent endemic species in the Indian Ocean, such as the mussel *Bathymodiolus marisindicus* Hashimoto, 2001, the snail *Chrysomallon squamiferum* Chen et al., 2015, the crab *A. rodriguezensis*, the barnacle *Neolepas marisindica* Watanabe et al., 2018, and the worm *Ophryotrocha jiaolongi* Zhang et al., 2017, all show a wide distribution range on the SWIR and CIR (Sun et al. 2020; Zhou et al. 2022). However, unlike the *B. bipapillata* populations in this study, most of these species exhibit low connectivity between populations, likely due to ridge offsets acting as dispersal barriers between the sSWIR and nSWIR, which do not seem to affect the connectivity of *B. bipapillata* (Sun et al. 2020; Zhou et al. 2022). Although the reproductive and larval development strategies of *B. bipapillata* are not fully understood, observations of other species within the same subfamily suggest that *B. bipapillata* likely have lecithotrophic larvae (Van Dover et al. 1999; Jollivet et al. 2000). This larval type, capable of traveling long distances in oligotrophic deep-sea environments, might partially explain the high connectivity of *B. bipapillata* populations across ~4,000 km of different ridges within the Indian Ocean.

Many studies have considered geological and hydrological features, along with the dispersal abilities of species, to explain the distribution of vent species (Slatkin 1987; Vrijenhoek 2010; Taylor and Roterman 2017; Perez et al. 2021). However, to fully understand the broad geographical distribution of these species, it is also crucial to consider their ability to adapt to diverse vent environments across different ridge systems. To further elucidate the strategies that enable species such as *B. bipapillata* to inhabit separate and geographically distant vent fields with no genetic differentiation, future studies should consider in vitro experiments for culturing as well as transcriptomic and genomic level data of populations.

Acknowledgements

We thank all scientists and crew members of the R/V *Isabu* from KIOST for their support in sampling and data collection.

Additional information

Conflict of interest

The authors have declared that no competing interests exist.

Ethical statement

No ethical statement was reported.

Funding

This work was supported by the Basic Science Research Program of the National Research Foundation of Korea, funded by the Ministry of Education (2021R1I1A2044998), the Korea Institute of Marine Science & Technology Promotion funded by the Ministry of Oceans and Fisheries, Korea (RS-2021-KS211514), and the Korea Research Institute of Bioscience and Biotechnology Research Initiative Program.

Author contributions

Conceptualization: SJK, WKL. Formal analysis: WKL. Funding acquisition: SJK. Supervision: SJK. Visualization: WKL. Writing - original draft: WKL. Writing - review and editing: SJK, WKL.

Author ORCIDs

Won-Kyung Lee https://orcid.org/0000-0001-7283-298X
Se-Joo Kim https://orcid.org/0000-0003-1653-072X

Data availability

All of the data that support the findings of this study are available in the main text or Supplementary Information.

References

Chen C, Copley JT, Linse K, Rogers AD (2015) Low connectivity between 'scaly-foot gastropod' (Mollusca: Peltospiridae) populations at hydrothermal vents on the Southwest Indian Ridge and the Central Indian Ridge. Organisms Diversity & Evolution 15: 663–670. https://doi.org/10.1007/s13127-015-0224-8

Darriba D, Taboada GL, Doallo Rn, Posada D (2012) jModelTest 2: more models, new heuristics and high-performance computing. Nature Methods 9: 772. https://doi.org/10.1038/nmeth.2109

Edler D, Klein J, Antonelli A, Silvestro D (2021) raxmlGUI 2.0: a graphical interface and toolkit for phylogenetic analyses using RAxML. Methods in Ecology and Evolution 12: 373–377. https://doi.org/10.1111/2041-210X.13512

Gamo T, Chiba H, Yamanaka T, Okudaira T, Hashimoto J, Tsuchida S, Ishibashi J-i, Kataoka S, Tsunogai U, Okamura K (2001) Chemical characteristics of newly discovered black smoker fluids and associated hydrothermal plumes at the Rodriguez Triple Junction, Central Indian Ridge. Earth and Planetary Science Letters 193: 371–379. https://doi.org/10.1016/S0012-821X(01)00511-8

Han Y, Zhou Y, Chen C, Wang Y (2023) Diversity and biogeography of scale worms in the subfamily Lepidonotopodinae (Annelida: Polynoidae) from Indian Ocean hydrothermal vents with descriptions of four new species. Zoological Journal of the Linnean Society 201: 290–304. https://doi.org/10.1093/zoolinnean/zlad140

Jang S-J, Cho S-Y, Li C, Zhou Y, Wang H, Sun J, Patra AK, Won Y-J (2023) Geographical subdivision of *Alviniconcha* snail populations in the Indian Ocean hydrothermal vent regions. Frontiers in Marine Science 10: 1139190. https://doi.org/10.3389/fmars.2023.1139190

Jimi N, Hookabe N, Moritaki T, Kimura T, Imura S (2021) First evidence of male dwarfism in scale worms: A new species of Polynoidae (Annelida) from hermit crab and molluscan shells. Journal of Zoological Systematics and Evolutionary Research 59: 801–818. https://doi.org/10.1111/jzs.12463

Jollivet D, Empis A, Baker M, Hourdez S, Comtet T, Jouin-Toulmond C, Desbruyeres D, Tyler P (2000) Reproductive biology, sexual dimorphism, and population structure of the deep sea hydrothermal vent scale-worm, *Branchipolynoe seepensis* (Polychaeta: Polynoidae). Journal of the Marine Biological Association of the United Kingdom 80: 55–68. https://doi.org/10.1017/S0025315499001563

Lee W-K, Lee GH, Ju S-J, Kim S-J (2021) Additional Records of the Hydrothermal Vent Scale Worm *Branchinotogluma segonzaci* (Polynoidae: Lepidonotopodinae) from the North Fiji Basin and Tonga Arc. Animal Systematics, Evolution and Diversity 37: 273–279. https://doi.org/10.5635/ASED.2021.37.4.027

Palumbi SR (1996) Nucleic Acids II: Polymerase Chain Reaction. In: Hillis D, Moritz C, Mable B (Eds) Molecular Systematic, 2nd edn. Sinauer Associates, Inc., Sunderland, 205–247.

Palumbi SR, Martin AP, Romano SL, McMillan WO, Stice L, Grabowski G (1991) The Simple Fool's Guide to PCR. Dept. of Zoology, University of Hawaii, Honolulu.

Perez Mv, Sun J, Xu Q, Qian P-Y (2021) Structure and connectivity of hydrothermal vent communities along the mid-ocean ridges in the West Indian Ocean: a review. Frontiers in Marine Science 8: 744874. https://doi.org/10.3389/fmars.2021.744874

Slatkin M (1987) Gene flow and the geographic structure of natural populations. Science 236: 787–792. https://doi.org/10.1126/science.3576198

Sun J, Zhou Y, Chen C, Kwan YH, Sun Y, Wang X, Yang L, Zhang R, Wei T, Yang Y (2020) Nearest vent, dearest friend: biodiversity of Tiancheng vent field reveals cross-ridge similarities in the Indian Ocean. Royal Society Open Science 7: 200110. https://doi.org/10.1098/rsos.200110

Tamura K, Stecher G, Kumar S (2021) MEGA11: Molecular Evolutionary Genetics Analysis version 11. Molecular Biology and Evolution 38: 3022–3027. https://doi.org/10.1093/molbev/msab120

Taylor M, Roterman C (2017) Invertebrate population genetics across Earth's largest habitat: The deep-sea floor. Molecular Ecology 26: 4872–4896. https://doi.org/10.1111/mec.14237

Van Dover CL, Trask J, Gross J, Knowlton A (1999) Reproductive biology of free-living and commensal polynoid polychaetes at the Lucky Strike hydrothermal vent field (Mid-Atlantic Ridge). Marine Ecology Progress Series 181: 201–214. https://doi.org/10.3354/meps181201

Vrijenhoek RC (2010) Genetic diversity and connectivity of deep-sea hydrothermal vent metapopulations. Molecular Ecology 19: 4391–4411. https://doi.org/10.1111/j.1365-294X.2010.04789.x

Wu X, Zhan Z, Xu K (2019) Two new and two rarely known species of *Branchinotogluma* (Annelida: Polynoidae) from deep-sea hydrothermal vents of the Manus Back-

Arc basin, with remarks on the diversity and biogeography of vent polynoids. Deep Sea Research Part I: Oceanographic Research Papers 149: 103051. https://doi.org/10.1016/j.dsr.2019.05.011

Wu X, Zhen W, Kou Q, Xu K (2023) Reevaluation of the systematic status of Branchinotogluma (Annelida, Polynoidae), with the establishment of two new species. Journal of Zoological Systematics and Evolutionary Research 2023: 1490800. https://doi.org/10.1155/2023/1490800

Zhang Y, Chen C, Qiu JW (2018) Sexually dimorphic scale worms (Annelida: Polynoidae) from hydrothermal vents in the Okinawa Trough: two new species and two new sex morphs. Frontiers in Marine Science 5: 112. https://doi.org/10.3389/fmars.2018.00112

Zhou Y, Wang Y, Zhang D, Wang C (2018) *Branchinotogluma bipapillata* n. sp., a new branchiate scale worm (Annelida: Polynoidae) from two hydrothermal fields on the Southwest Indian Ridge. Zootaxa 4482: 527–540. https://doi.org/10.11646/zootaxa.4482.3.5

Zhou Y, Chen C, Zhang D, Wang Y, Watanabe HK, Sun J, Bissessur D, Zhang R, Han Y, Sun D (2022) Delineating biogeographic regions in Indian Ocean deep-sea vents and implications for conservation. Diversity and Distributions 28: 2858–2870. https://doi.org/10.1111/ddi.13535

Supplementary material 1

Supplementary information

Authors: Won-Kyung Lee, Se-Joo Kim

Data type: docx

Explanation note: **table S1.** Sample information and accession numbers of the *Branchinotogluma* species used in this study (new sequences are highlighted in bold). **table S2.** Interspecific divergence (%) of mitochondrial *CO1* (below left) and 16S (upper right) genes of *Branchinotogluma* species. Mean intraspecific *CO1* distances are displayed in bold along the diagonal.

Link: https://doi.org/10.3897/zookeys.1215.129623.suppl1

ZooKeys 1215: 151–183 (2024)
DOI: 10.3897/zookeys.1215.134871

Research Article

The genus *Argopistes* Motschulsky from Japan and Taiwan, with descriptions of three new species from Taiwan (Coleoptera, Chrysomelidae, Galerucinae, Alticini)

Chi-Feng Lee[1], Ming-Yao Chiang[1], Haruki Suenaga[2]

1 *Applied Zoology Division, Taiwan Agricultural Research Institute, Taichung 413, Taiwan*
2 *Nakashima, 108-11, Kurashiki-shi, Okayama, 710-0803 Japan*
Corresponding author: Ming-Yao Chiang (mingyaw@tari.gov.tw)

Abstract

Four previously described species of *Argopistes* are recognized and redescribed from Japan and Taiwan: *A. biplagiatus* Motschulsky, 1860, *A. rufus* Chen, 1934, *A. tsekooni* Chen, 1934, and *A. unicolor* Jacoby, 1885. Three new species from Taiwan, *A. jungchani* **sp. nov.**, *A. tsoui* **sp. nov.**, and *A. yuae* **sp. nov.**, are described. Descriptions of species include illustrations of aedeagi, antennae, gonocoxae, abdominal ventrite VIII, and spermathecae. *Argopistes rufus* Chen, 1934, **stat. nov.** is raised to species status from a variety of *A. biplagiatus* Motschulsky, 1860. *Argopistes coccinelliformis* Csiki, 1940, **syn. nov.** and *A. ryukyuensis* Shigetoh & Suenaga, 2022, **syn. nov.** are proposed as junior synonyms of *A. rufus* Chen, 1934 Lectotypes are designated for *A. undecimmaculata* Jacoby, 1885, *A. unicolor* Jacoby, 1885, and *A. biplagiatus* var. *rufus* Chen, 1934.

Key words: *Chionanthus*, *Fraxinus*, *Jasminum*, *Ligustrum*, *Olea*, Oleaceae, *Osmanthus*, *Syringa*

OPEN ACCESS

Academic editor: Ron Beenen
Received: 16 August 2024
Accepted: 15 September 2024
Published: 15 October 2024

ZooBank: https://zoobank.org/C57CB315-F15F-4D98-868A-EFEA22BC64A3

Citation: Lee C-F, Chiang M-Y, Suenaga H (2024) The genus *Argopistes* Motschulsky from Japan and Taiwan, with descriptions of three new species from Taiwan (Coleoptera, Chrysomelidae, Galerucinae, Alticini). ZooKeys 1215: 151–183. https://doi.org/10.3897/zookeys.1215.134871

Introduction

The flea beetle genus *Argopistes* Motschulsky, 1860 contains 44 species recorded from Afrotropical, Australian, Neotropical, Oriental, and Palearctic regions (Blanco and Konstantinov 2013; Biondi et al. 2024). Four species were known from Japan and reviewed by Kimoto (1965) with emphasis on male aedeagi. A new species was also described from Ryukyu Islands and Daitô Islands (Shigetoh and Suenaga 2022). Chûjô (1936) was the first to record the genus from Taiwan as *A. biplagiatus* Mostschulsky, 1860, although Gressitt and Kimoto (1963) indicated that it was a misidentification of *A. coccinelliformis* Csiki, 1940. No other records have been reported from Taiwan since then.

Adults and larvae of *Argopistes* are oligophagous on Oleaceae (Jolivet and Hawkeswood 1995). A number of species of Oleaceae are ornamental trees popular in Japan, including *Osmanthus* × *fortunei* Carrière, *O. heterophyllus* (G. Don) P. S. Green, and *Ligustrum japonicum* Thunb. Although few insect pests are reported for these ornamental trees, *A. rufus* Chen, 1934 and *A. biplagiatus* Motschulsky, 1860 are major pests. Ecology of both species have been studied in this context (Inoue

and Shinkaji 1989a–c, 1990; Inoue 1990a, b, 1991a, b, 1992, 1993, 1994, 1996, 1998, 2001, 2014). In contrast, Chinese privet, *Ligustrum sinense* Lour., is one of the worst invasive plants in the U.S. *Argopistes tsekooni* Chen, 1934 was evaluated as a promising biological control agent of Chinese privet (Zhang et al. 2008a, b, 2009).

In Taiwan, *Chionanthus retusus* Lindley & Paxton (流蘇) (Fig. 1A–D, G), Chinese fringetree, and *Osmanthus fragrans* (Thunb.) Lour. (桂花), sweet osmanthus, are popular ornamental plants. They have been attacked by *Argopistes* species during recent years. This phenomenon also occurs on small islands, including Kinmen Island (Fig. 1E, F), Nangan Island (Fig. 1C, D), and Beigan Island (Fig. 1G, H). Taxonomic studies on *Argopistes* in Taiwan and Japan are needed to describe diagnostic characters in addition to male aedeagi.

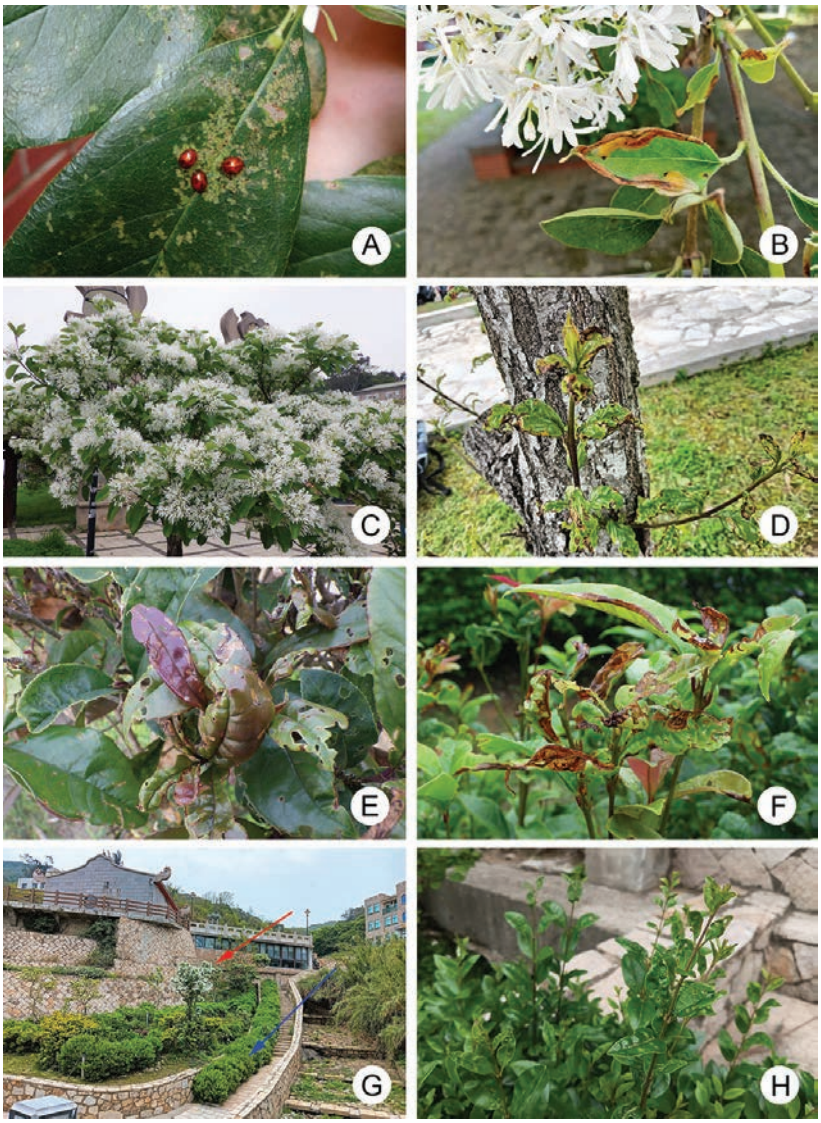

Figure 1. Field photographs of *Argopistes rufus* Chen **A** adults feeding on leaves of *Chionanthus retusus* surrounding Hsinchu City Government on April 23, 2021 **B** mature larvae mining leaves of the same tree **C** blooming *C. retusus* at Qingshui Village (清水村), Nangan Island (南竿島), on April 21, 2024 **D** larvae mining leaves near the ground of the same tree **E** larvae mining leaves of *Osmanthus fragrans* at Yingshan Temple (鶯山廟), Kinmen Island (金門島), on April 11, 2023 **F** larvae mining leaves of *Osmanthus fragrans* at the guesthouse, Jinhu Township (金湖鎮), Kinmen Island, on May 20, 2024 **G** *C. retusus* (red arrow) and *Ligustrum japonicum* (blue arrow) planting surrounding Chinbe Village (芹壁村), Beigan Island (北竿島) on 22 April 22 2024 **H** feeding marks caused by adults on leaves of *L. japonicum*.

Materials and methods

For taxonomic study, abdomens of adults were separated from the forebodies and boiled in 10% KOH solution, followed by washing in distilled water to prepare genitalia for illustrations. The genitalia were then dissected from the abdomens, mounted on slides in glycerin, and studied and drawn using a Leica M165 stereomicroscope. For detailed examinations, a Nikon ECLIPSE 50i microscope was used.

At least three males and females from each species were examined to delimit variability of diagnostic characters. For species collected from more than one locality or with color variations, at least one pair of each sex from each locality and color morph was examined. Length was measured from the anterior margin of the eye to the elytral apex, and width at the greatest width of the elytra. Nomenclature for morphological structures of adults follows Duckett and Daza (2004). Names of plant species follows the Taiwan Encyclopedia of Life (2024; TaiEOL).

Specimens studied herein are deposited at the following institutes and collections:

HAPC Private Collection of Haruki Suenaga, Okayama, Japan;
HIPC Private Collection of Hiroaki Shigetoh, Sapporo, Japan;
IZAS Institute of Zoology, Chinese Academy of Sciences, Beijing, China [Yongying Ruan];
NHMUK The Natural History Museum, London, UK [Michael F. Geiser, Maxwell V. L. Barclay];
SEHU The Laboratory for Systematic Entomology, Hokkaido University, Sapporo, Japan [Takuya Takemoto];
TAFI Forest Arthropod Collection of Taiwan, Taiwan Forestry Research Institute, Taipei City, Taiwan [Sheng-Shan Lu];
TARI Applied Zoology Division, Taiwan Agricultural Research Institute, Taichung, Taiwan [Chi-Feng Lee];
ZMMU Zoological Museum of Moscow State University, Moscow, Russia [Vladimir Savitsky].

Exact label data are cited for all type specimens of described species; a double slash (//) divides the data on different labels and a single slash (/) divides the data in different rows. Other comments and remarks are in square brackets: [p] – preceding data are printed, [h] – preceding data are handwritten, [w] – white label, [y] – yellow label, [g] – green label, [b] – blue label, and [r] – red label. Traditional Chinese fonts are added to the names of localities.

Taxonomic account

Argopistes biplagiatus Motschulsky, 1860

Figs 2A–F, 3, 4

Argopistes biplagiatus Motschulsky, 1860: 236 (Amur: Russian Far East and northeastern China); Csiki 1940: 523 (catalogue); Chûjô and Kimoto 1961: 174 (catalogue); Kimoto 1965: 436 (redescription); Lee and An 2001: 182 (South Korea); Lee and Cho 2006: 91 (host plants); Takizawa 2012: 38 (faunistics).

Argopistes flavitarsis Motschulsky, 1860: 137 (chromatic variation).
Argopistes limbatus Motschulsky, 1860: 137 (chromatic variation).
Argopistes suturalis Motschulsky, 1860: 137 (chromatic variation).
Argopistes undecimmaculata Jacoby, 1885: 738 (Japan: Sapporo); Chûjô 1936: 109 (catalogue); Csiki 1940: 524 (catalogue).

Type material examined. *Argopistes biplagiatus*. • 11 ***syntypes*** glued on the same card (ZMMU) (Fig. 2A–D): "type [h, w] // Amur [h, r] // Argopistes / biplagiatus / Amur. m. Motsch [h, w, with black border] // Syntypus [p, r] // Зоомузеň Mry (Mockba, POCCNR) / No ZMMU Col 03056 / Zool. Mus. Mosq. Univ. / (Mosquae, RUSSIA) / ex coll. V. I. Motschulsky [p, pink label]".

Argopistes undecimmaculata. ***Lectotype*** • (here designated, sex undetermined, NHMUK) (Fig. 2E, F): "Type / H.T. [p, w, circle label with red border] // SYN- / TYPE [p, w, circle label with blue border] // Sapporo / 5.VIII-16.VIII.80. [p, w] // Japan / G. Lewis. / 1910-320 [p, w] // Sap [h, w]". ***Paralectotypes*** • 1 (sex undetermined, NHMUK): "SYN- / TYPE [p, circle label with blue border] // Sapporo / 5.VIII-16. VIII.80. [p, w] // Japan/ G. Lewis. / 1910-320 [p, w] // Argopistes / 11maculata Jac [h, b]"; • 1♀ (TARI): "Sapporo [h] / JAPAN [p] / 10.VIII.1880 [h] / Col. G. LEWIS [p, w] // Argopistes / undecimmaculata / Jacoby [h] / DET. M. CHUJO [p, w] // CO / Type [p, w, circle label with yellow letters and border] / 1526 [p, w]".

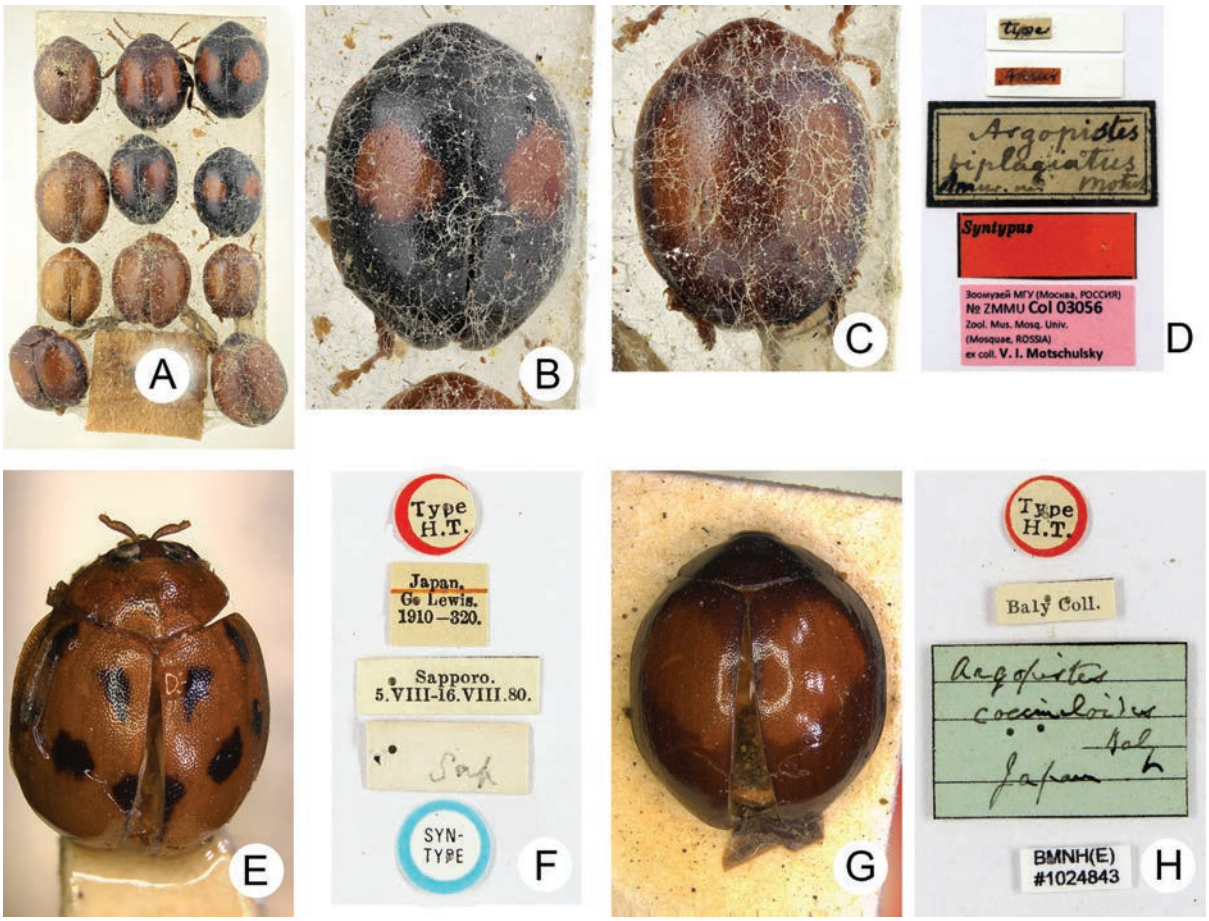

Figure 2. Type specimens and labels **A** *Argopistes biplagiatus* Motschulsky, 1860, syntypes **B** one syntype with typical color form **C** one syntype with enlarged red spots on elytra **D** labels pinned with syntypes **E** *A. undecimmaculata* Jacoby, 1885, lectotype **F** labels pinned with lectotype **G** *A. coccinelloides* Baly, 1874, holotype **H** labels pinned with holotype.

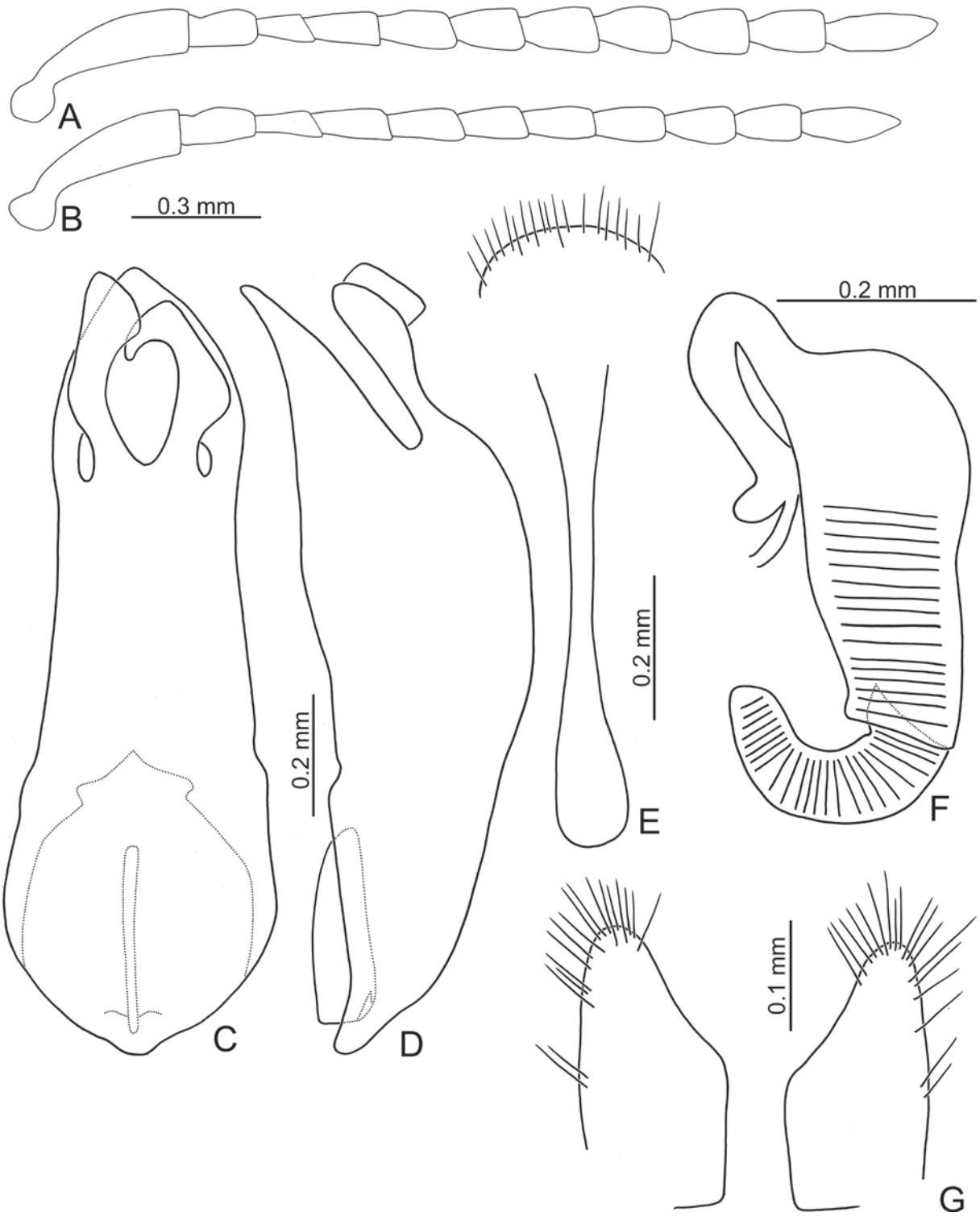

Figure 3. *Argopistes biplagiatus* Motschulsky **A** antenna, male **B** antenna, female **C** aedeagus, dorsal view **D** aedeagus, lateral view **E** abdominal ventrite VIII, female **F** spermatheca **G** gonocoxae.

Additional material examined. Japan. Hokkaido: • 1♀ (HAPC), Sapporo-shi, Hokkaido University, 15.X.2011, leg. H. Suenaga; Honshu. Aichi: • 1♂ (SEHU), Toyohashi-shi, Imou-shitsugen, 8.IV.1989, leg. Y. Komiya; Ibaraki: • 1♀ (HIPC), Daigo, Uenomiya, Mt. Yamizo-san, 28.V.2917, leg. H. Yoshitake; • 1♂ (SEHU), Sakura-mura, Sakura-gawa Riv., 1.VI.1986, leg. Y. Komiya; Ishikawa: • 1♀ (HAPC),

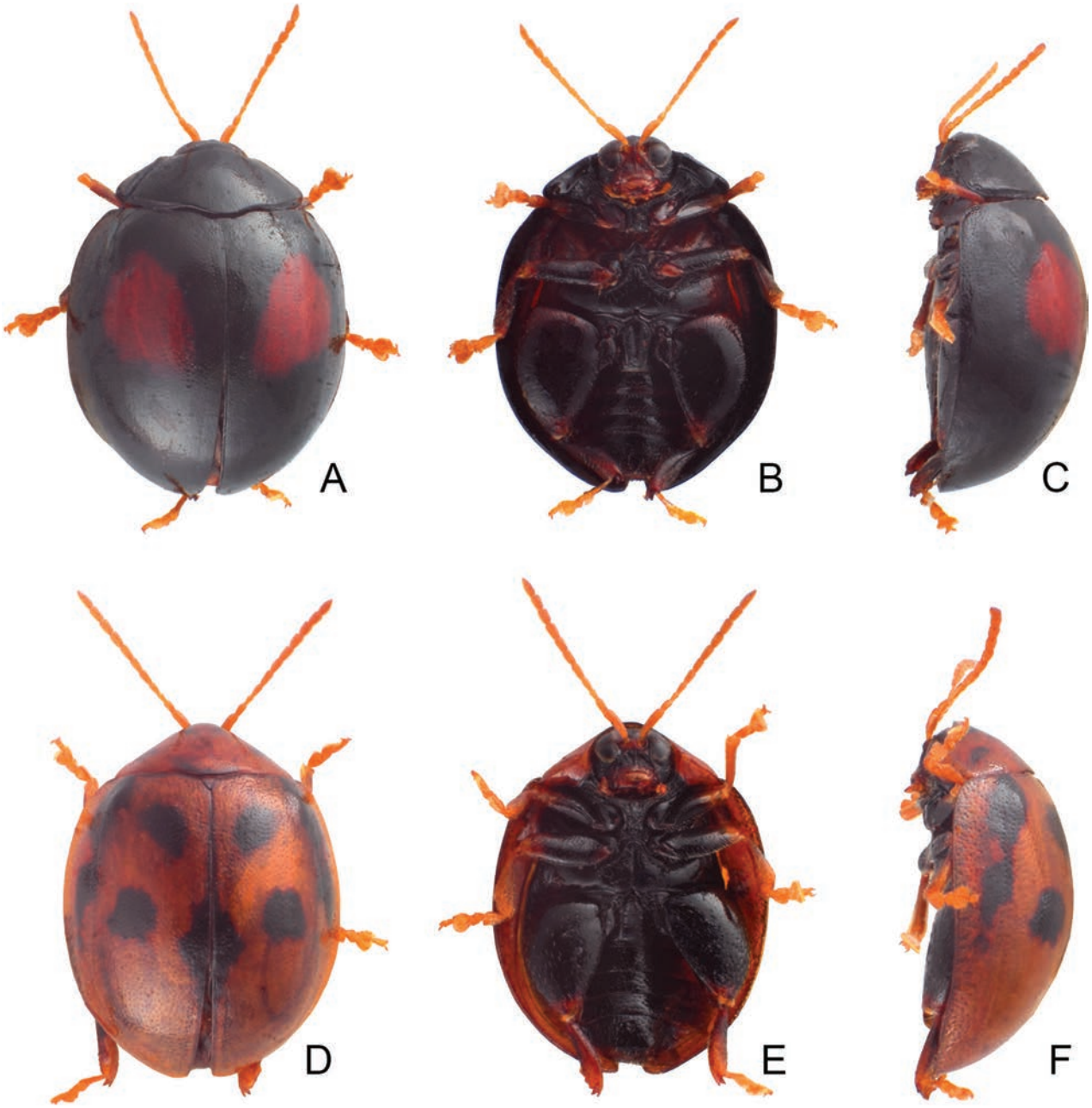

Figure 4. Habitus of *Argopistes biplagiatus* Motschulsky **A** typical color form, female, dorsal view **B** ditto, ventral view **C** ditto, lateral view **D** yellowish brown color form, female, dorsal view **E** ditto, ventral view **F** ditto, lateral view.

Mt. Haku-san, Betsuzan-dô, 21.V.2016, leg. H. Kawase; Shizuoka: • 1♂, 2♀ (SEHU), Izu-peninsula, Mt. Manzaburo-dake, 19.V.1980, leg. J. Okuma; • 1♀ (SEHU), Tagata-gum, Tohi, 4.V.1985, leg. Y. Komiya; Tokyo: • 1♂ (NHMUK), Katsushika-ku, Mizumoto Kôen Park, 8.V.2005, leg. Y. Komiya; Shikoku. Ehime: • 1♂ (HAPC), Kumakôgen-chô, Mt. Saragamine, 7.VI.2009, leg. H. Suenaga; • 1♂, 2♀ (HAPC), Matsuyama-shi, Mt. Takanawa-san, 12.V.2007, leg. S, Sejima; Kyushu. • 3♂, 1♀ (TARI), Mt. Hiko-san, 14.VIII.1941, leg. M. Chûjô; Fukuoka: • 2♂ (HAPC), Soeda-machi, Mt. Hiko-san, 8.VIII.2009, leg. S. Sejima; **Russian Far East.** Primorsky Krai: • 2♂ (NHMUK), Lazovski Zapovednik, 170 m E Vladivostok, Korpad, 28.V.-6.VI.2001, leg. M. Quest; • 1♂ (NHMUK), Odarkovskij, Zavod, 25.IV.1911, leg. A. Tsherskij; • 1♂ (NHMUK), Wladiwostok, leg. Herman Frieb.; **South Korea.**

• 1♀ (TARI), Sulgen, 15.VII.1932, leg. D. Okamoto; **Taiwan.** Taipei: • 1♂, 1♀ (TARI), Kueitzukeng (貴仔坑), 4.XII.2006, leg. H.-T. Cheng; • 1♀ (TARI), same but with "leg. H. Lee"; • 1♂ (TARI), same locality, 9.IX.2007, leg. M.-H. Tsou; • 1♀ (TARI), same but with "18.XI.2007"; • 2♀ (TARI), Tienmu (天母), 8.XII.2006, leg. S.-F. Yu.

Diagnosis. Adults of *Argopistes biplagiatus* are similar to those of *A. rufus* with similar color pattern but differing from *A. rufus* possessing line of punctures that are less coarse than those between the lines, sometimes confused (lines of punctures much coarser than those between lines in *A. rufus*) and a wider interspace between eyes. Genitalic characters are more diagnostic for both species. Those of *A. biplagiatus* possess pointed apices (Fig. 3C) and are wider in lateral view (Fig. 3D) (widely rounded apex (Fig. 5C) and narrow aedeagus in lateral view (Fig. 6D) in *A. rufus*); females have narrow, parallel-sided bases of gonocoxae (Fig. 3G) (medially widened gonocoxae (Fig. 5G) in *A. rufus*), and ventrite VIII evenly rounded and with dense setae on apical margin (Fig. 4E) (medially depressed and without setae on median area of apical margin of abdominal ventrite VIII (Fig. 5E) in *A. rufus*).

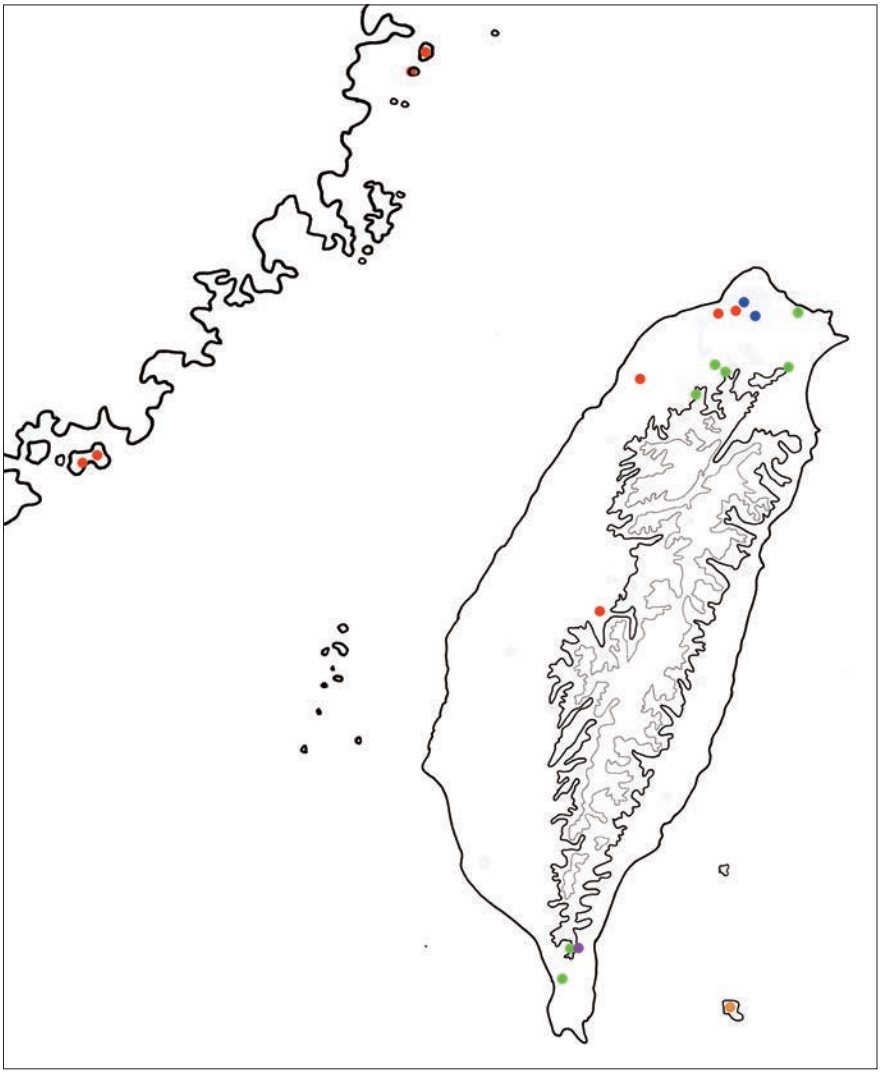

Figure 5. Distribution map of *Argopistes* species in Taiwan, solid line: 1000 m, broken line: 2000 m. Red dots *A. rufus* Chen; blue dots *A. biplagiatus* Motschulsky; green dots *A. tsoui* sp. nov.; orange dots *A. yuae* sp. nov.; purple dot *A. jungchani* sp. nov.

In addition, adults of *A. biplagiatus* in Taiwan are larger (4.7–4.9 mm) than those of *A. rufus* (3.8–4.3 mm). Moreover, distinct color patterns occur in both species respectively (black elytra with reddish brown at middle in *A. biplagiatus*; yellowish brown elytra with distinct arrangement of black spots in *A. rufus*).

Redescription. Length 4.4–4.9 mm, width 3.5–3.8 mm. Color variable (see below). Pronotum broad, convex, lateral margin narrowly explanate; 2.0–2.2 × wider than long, disc with dense coarse punctures; lateral margin rounded, anterior margin strongly concave, posterior margin moderately convex. Intercoxal prosternal process flattened and with coarse punctures, delimited by narrow ridge on apical and lateral margins, truncate or slightly rounded at apex. Elytra broadly oval, 1.1 × longer than wide, disc with dense, confused, coarse punctures. Abdominal ventrite I with intercoxal area 2.0 × as long as wide, widest at basal 1/5, disc glabrous, rounded by reversed U-shaped ridge, provided with a row of coarse punctures inside subparallel lateral ridges.

Male. Antenna filiform (Fig. 3A), antennomere I much longer than others, approximate ratios of length of antennomeres I–XI 1.0: 0.3: 0.2: 0.4: 0.4: 0.3: 0.4: 0.4: 0.4: 0.4: 0.6; approximate ratios of length to width of antennomeres I–XI 4.4: 1.9: 1.7: 2.4: 2.0: 1.6: 1.6: 1.8: 1.7: 1.7: 2.9. Aedeagus (Fig. 3C, D) apically and strongly narrowed from apical 1/5, slightly narrowed from apical 2/10–3/10, then slightly and basally widened towards basal 1/6, apex pointed; anterior opening very small, from apex to apical 3/10; tectum composed of one pair of sclerotized processes with apices twisted; extremely wide and straight in lateral view; paired processes straight in lateral view; endophallic sclerite laterally flattened, with small process near apex, and with basal processes membranous.

Female. Antenna (Fig. 3B) similar to males, ratios of length of antennomeres I–XI 1.0: 0.3: 0.2: 0.3: 0.3: 0.3: 0.3: 0.3: 0.3: 0.3: 0.6; ratios of length to width of antennomeres I–XI 4.5: 2.0: 1.7: 2.0: 1.9: 1.7: 1.5: 1.6: 1.3: 1.5: 2.4. Ventrite VIII (Fig. 3E) membranous, only apical margin sclerotized, T-shaped, with dense long setae along apical margin, apical margin widely rounded, spiculum long. Spermathecal receptaculum (Fig. 3F) much longer than pump, moderately swollen, curved in lateral view; pump slightly emarginated at inner side of base; spermathecal duct with long basal part, ramus rounded. Gonocoxae (Fig. 3G) wide and separated, base membranous, each gonocoxa longitudinal and asymmetric, apically narrowed from middle, with dense long setae along apical areas.

Color variation. In Japan, two distinct color patters of adults, typical color form (Fig. 4A–C): general color black, each elytron with one large red spot, lateral margin sometimes yellowish brown, legs dark brown but tarsi yellowish brown, head entirely black, or with one yellowish brown spot on vertex, or entirely yellowish brown except above eyes, abdominal ventrites yellowish brown but medially black; yellowish brown color form: general color yellowish brown (Fig. 4D–F; undecimmaculata form), pronotum with one pair of small lateral black spots, elytra with 11 black spots, two pairs arranged into transverse lines near base and middle, one transverse pair near suture at middle, others longitudinal, one additional transverse pair near apex, one spot along suture from basal 1/3 to apical 1/3, medially widened, head yellowish brown but black below eyes except mouthparts, thoracic and abdominal ventrites black but abdominal ventrites laterally yellowish brown, legs black but tarsi, pro- and mesotibiae yellowish brown.

At the type locality (Russian Far East and northeastern China), some individuals represent the typical form (Fig. 2B) but with yellowish margins of pronotum

and elytra, some with enlarged red spots on the elytra connected with each other, some with entirely yellowish-brown bodies (Fig. 2C).

In Taiwan, some specimens represent the typical form, but some have enlarged red spots on elytra that extend into the basal margin and connect with each other, and have reddish brown thoracic and abdominal ventrites.

Host plants. Inoue (1990a) recorded the following species as host plants: *Osmanthus* × *fortunei*, *O. heterophyllus*, *O. fragrans* (桂花), *O. fragrans* var. *aurantiacus* Makino, *Ligustrum japonicum* (日本女真), *L. ovalifolium* Hassk., *L. licidum* W. T. Aiton, *Syringa vulgaris* L., and *S. reticulata* (Blume) H. Hara. Chûjô and Kimoto (1961) recorded one additional host, *Fraxinus mandshurica* Rupr. var. *japonica* Maxim. Lee and Cho (2006) recorded *Ligustrum obtusifolium* Siebold & Zucc for Korean populations.

Biology. Various aspects of biology of *A. biplagiatus* were studied in Japan, including feeding habits, seasonal development, habitat selection, host plant preference, and adult diapause (Inoue 1990a, b, 1991b, 1992, 1993, 1994). Generally, the species has a univoltine life cycle. Eggs and/or larvae of this species are observed in the spring. Mature larvae fall from the host trees rather than crawling (Inoue 2014).

Remarks. Syntypes of *A. biplagiatus* Motschulsky display great color variation. Several names (*A. flavitarsis*, *A. limbatus*, and *A. suturalis*) have been proposed for different color patterns.

Distribution. China, Japan (Hokkaido, Honshu, Shikoku, Kyushu), Russian Far East, South Korea, and new to Taiwan (Fig. 5).

Argopistes rufus **Chen, 1934, stat. nov.**

Figs 1, 2G, H, 6, 7

Argopistes coccinelloides Baly, 1874 (nec Suffrian, 1868): 202 (Japan); Chûjô 1935a: 87 (Japan: Okinawa); Chûjô 1935b: 211 (catalogue).

Argopistes biplagiatus: Schönfeldt 1890: 175 (Japan: Loochoo); Chûjô 1936: 110 (Taiwan), misidentification (Gressitt and Kimoto 1963).

Argopistes biplagiatus var. rufus Chen, 1934a: 72 (China).

Argopistes coccinelliformis Csiki, 1940: 524 (new replacement name for *A. coccinelloides* Baly, 1874); Chûjô and Kimoto 1961: 174 (catalogue); Gressitt and Kimoto 1963: 812 (South China); Kimoto 1965: 436 (redescription); Takizwa, 2012: 38 (faunistics).

Argopistes ryukyuensis Shigetoh & Suenaga, 2022: 4 (Japan: Okinawa). syn. nov.

Type material examined. *Argopistes coccinelloides*. ***Holotype*** • (sex undetermined, NHMUK) (Fig. 2G, H): "Argopistes / coccinelloides / Baly / Japan [h, b] // Type / H.T. [p, circle label with red border] // Baly Coll. [h, w] // BMMH(E) / #1024843 [p, w]".

Argopistes biplagiatus var. rufus. ***Lectotype*** • ♀ (here designated, NHMUK): "China [p] // Bowring / 63•37* [p] // Argopistes coccinelliformis / Csiki, 1940 / det C.-F. Lee, 2023 [p] ♀ [h, w] // NHMUK 015998267 [with OR Code, p, w]". ***Paralectotypes*** • 3♀ (NHMUK), same as lectotype but with "0155998268–0155998270".

Argopistes ryukyuensis. ***Paratypes*.** Japan: Kitadaitô-jima Island (北大東島): • 1♂, 3♀ (HAPC), Kitadaitô-jima, 21.IV.2018, leg. H. Kawase; Okinawa-jima

Island: • 1♂ (HAPC), Tomigusuku-shi, Tomigusuku, 10.V.2020, leg. H. Shigetoh; 1 ♂, 1♀ (HAPC), same but with "11.III.2021"; Ou-jima Island: • 1♀ (HIPC), Nanjo-shi, Tamashiro-ou, 6.V.2019, leg. H. Shigetoh; • 3♂, 1♀ (1♂: HAPC; 2♂, 1♀: HIPC), same but with "2.III.2021"; Tonaki-jima Island: • 1♂, 1♀ (HIPC),

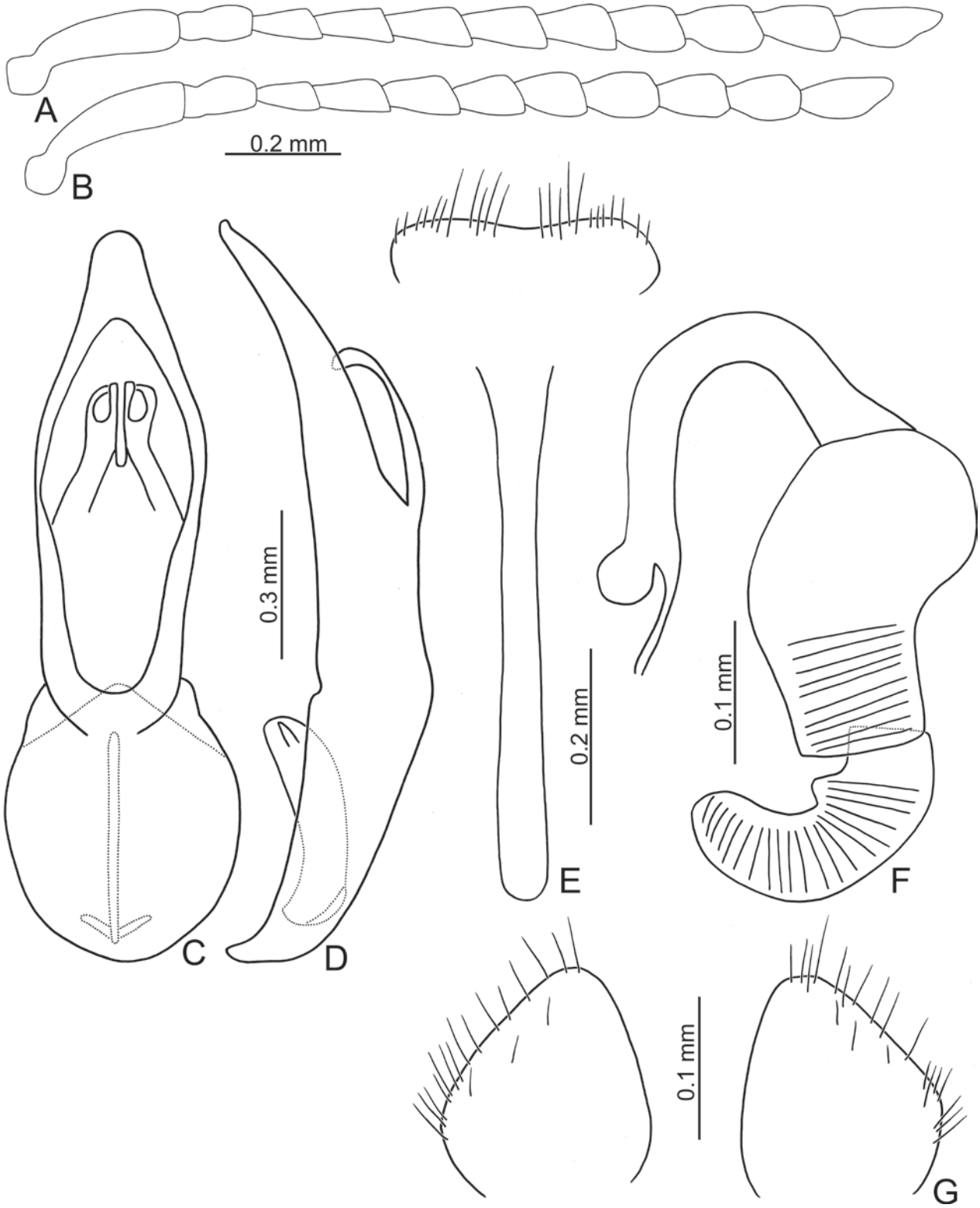

Figure 6. *Argopistes rufus* Chen **A** antenna, male **B** antenna, female **C** aedeagus, dorsal view **D** aedeagus, lateral view **E** abdominal ventrite VIII, female **F** spermatheca **G** gonocoxae.

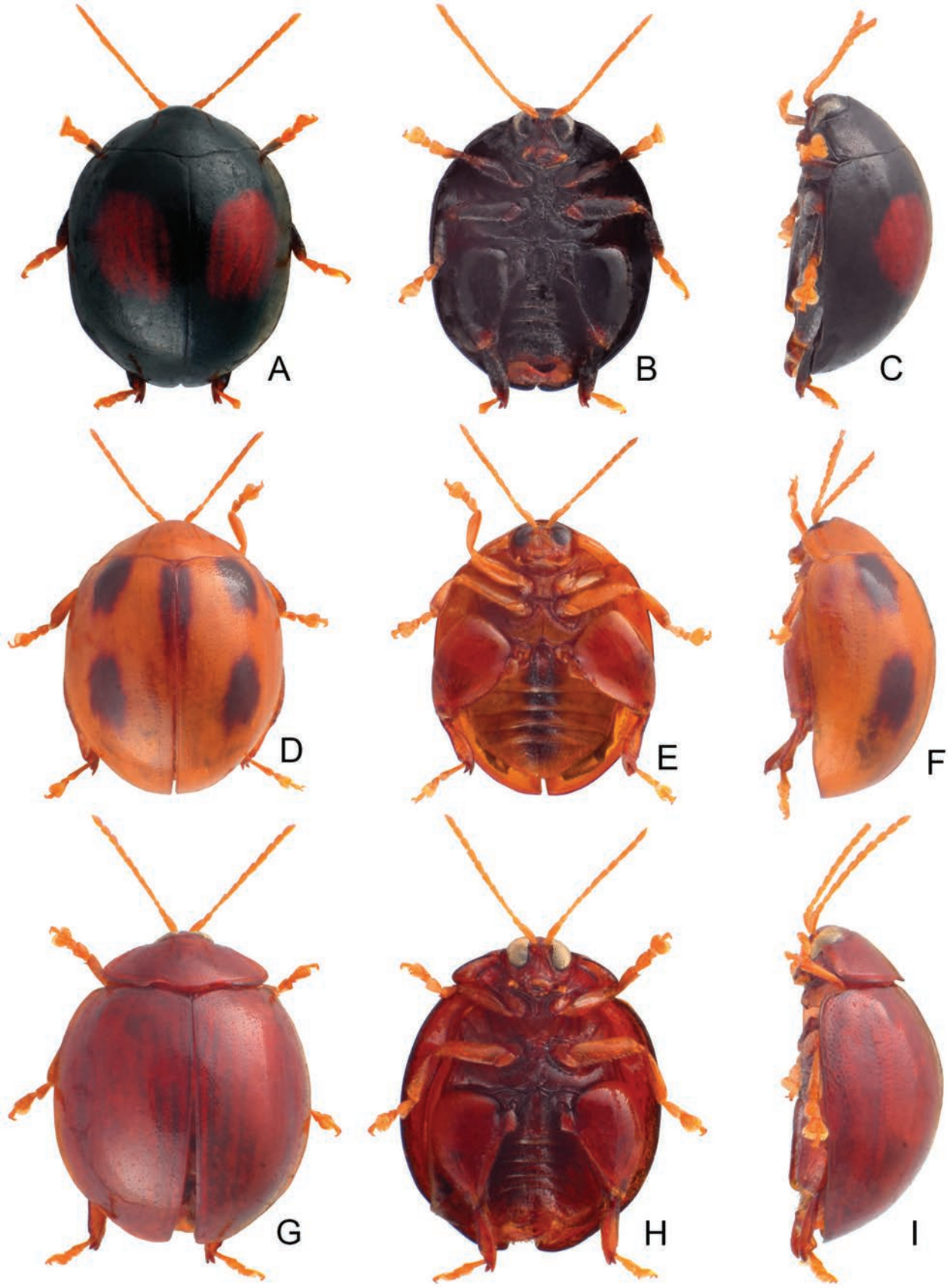

Figure 7. Habitus of *Argopistes rufus* Chen **A** typical color form, male, dorsal view **B** ditto, ventral view **C** ditto, lateral view **D** yellowish brown color form, female, dorsal view **E** ditto, ventral view **F** ditto, lateral view **G** reddish brown color form, male, dorsal view **H** ditto, ventral view **I** ditto, lateral view.

Tonaki-son, Uaki, 1.IX.2018, leg. H. Shigetoh; Tsuken-jima Island: • 1♀ (HAPC), Uruma-shi, Katsurentsuken, 14-16.VII.2020, leg. H. Shigetoh; Yonaguni-jima Island: • 1♂, 1♀ (HAPC), Kita-Bokujô, 28.III.2001, leg. S. Tsuyuki.

Additional material examined. China. Guandong: • 7♂, 6♀ (TARI), Yangtaishan (阳台山), 23.IV.2022, leg. Y.-Y. Ruan; • 13♂, 11♀ (TARI), Wutongshan (梧桐山), 5.IV.2023, leg. Y.-Y. Ruan; Hong Kong: • 2♂, 1♀ (NHMUK), 56 / 157, 894 / 7/8/63; • 1♂ (NHMUK), Walker Coll., 93—58; • 1♂ (NHMUK), Tailung National Park, 12.III.1963, leg. P. Y. So; **Japan.** Honshu. Gumma: • 1♀ (NHMUK), Maebashi-shi, Iwakami-chô, 18.IV.2003, leg. Y. Komiya; Okayama: • 1♀ (HAPC), Mimasaka-shi, Yono, 10.IV.2016, leg. H. Suenaga; • 1♂ (HAPC), Okayama-shi, Kita-ku, Kibi service area, 1.VII.2012, leg. O. Yamaji; • 2♂, 2♀ (HAPC), Tsuyama-shi, Yamakita, 3.IV.2014, leg. H. Suenaga; Tokyo: • 3♂, 3♀ (HIPC), Hachiôji-shi, Kinugaoka, 18.VI.2016, leg. H. Shigetoh; Hachijô-jima Island: • 2♂, 2♀ (SEHU), Okagô, 3.VIII.1963, leg. Y. Kamiya; Ogasawara Haha-jima Island: • 1♂ (SEHU), Funamidai, 24.VI.1987, leg. H. Akiyama; Kyushu. Fukuoka: • 1♀ (HAPC), Fukuoka-shi, Higashi-ku, Hakozaki Kyushu Univ., 7.VI.2008, leg. Y. Matsumura; • 1♀ (HAPC), Fukuoka-shi, Hakozaki, 16.VIII.2011, leg. H. Suenaga; Kagoshima: Koshiki-jima Island: • 1♀ (SEHU), Teuchi, 16.V.1965, leg. Y. Komiya; the Ryukyus. Okinawa: Kita-daitô-jima Island: • 2♂, 2♀ (HIPC), Kita-daitô-jima, 21.IV.2018, leg. H. Kawase; **Taiwan.** Hsinchu: • 3♂, 6♀ (TARI), Hsinchu (新竹市), 23.IV.2021, leg. C.-Y. Tsai; Kinmen: Kinmen Island (金門島): • 1♀ (TARI), Botanic Park (植物園), 12.VII.2023, leg. C.-F. Lee; • 3♂, 14♀ (TARI), Jinsha (金沙), 12.IV.2023, leg. C.-F. Lee; Matsu Islands: • 10♂, 11♀ (TARI), Beigan Island (北竿島), 12.IV.2024, leg. C.-F. Lee; • 6♂, 10♀ (TARI), Nangan Island (南竿島), 12.IV.2024, leg. C.-F. Lee; Nantou: • 4♂, 5♀ (TARI), Chichi (集集), 26.V.2023, leg. T.-W. Hsu; • 2♂ (TARI), Mingchien (名間), 14.VII.2022, leg. Y.-J. Tung; Taipei: • 1♂, 1♀ (TARI), Kuantu (關渡), 8.IV.2020, leg. M.-H. Tsou; • 4♂, 1♀ (TARI), same locality, 18.X.2010, leg. S.-F. Yu; • 1♀ (TARI), same but with "20.II.2011"; • 5♂, 6♀ (TARI), Kuanyinshan (觀音山), 21.III.2016, leg. H.-T. Cheng; • 2♂ (TARI), same locality, 20.V.2011, leg. H. Lee.

Diagnosis. Adults of *A. rufus* look similar to those of *A. biplagiatus* with a similar color pattern, but differ from *A. biplagiatus* in having lines of punctures much coarser than those between the lines (lined punctures slightly coarser than those between lines, sometime confused in *A. biplagiatus*) and a narrower interspace between eyes. Genitalic characters are diagnostic for both species. Those of *A. rufus* possess widely rounded apices (Fig. 6C) and the aedeagus is narrow in lateral view (Fig. 6D) (pointed apex (Fig. 3C) and wider aedeagus in lateral view (Fig. 3D) in *A. biplagiatus*); females have medially widened gonocoxae (Fig. 6G) (narrow and parallel-sided base of gonocoxae (Fig. 3G) in *A. biplagiatus*), and abdominal ventrite VIII medially depressed and without setae on median area (Fig. 6E) (evenly rounded and with dense setae on apical margin of abdominal ventrite VIII (Fig. 3E) in *A. biplagiatus*).

In addition, adults of *A. rufus* in Taiwan are smaller (3.8–4.3 mm) than those of *A. biplagiatus* (4.7–4.9 mm). Moreover, distinct color patterns occur to both species respectively (yellowish brown elytra with distinct arrangement of black spots in *A. rufus*; black elytra with reddish brown central area in *A. biplagiatus*).

Redescription. Length 3.6–4.3 mm, width 2.9–3.4 mm. Color variable (see below). Pronotum broad, convex, lateral margin narrowly explanate; 2.1–2.2 × wider than long, disc with dense fine punctures; lateral margin rounded, anterior margin strongly concave, posterior margin moderately convex. Elytra broadly

oval, 1.1 × longer than wide, disc with coarse punctures arranged into longitudinal striae and with dense fine punctures between striae.

Male. Antenna filiform (Fig. 6A), antennomere I much longer than others, approximate ratios of length of antennomeres I–XI 1.0: 0.4: 0.3: 0.4: 0.4: 0.4: 0.4: 0.4: 0.4: 0.4: 0.5; approximate ratios of length to width of antennomeres I–XI 4.3: 2.0: 2.0: 2.0: 2.0: 1.8: 1.5: 1.6: 1.7: 1.7: 2.7. Aedeagus (Fig. 6C, D) apically and strongly narrowed from apical 1/3, apex truncate; anterior opening large, ~ 0.52 as long as aedeagus, from apical 1/8–3/5; tectum composed of one pair of sclerotized processes with bifurcate apices, outer apex hooked, small, ~ 0.36 as long as anterior opening; narrow and slightly curved in lateral view; paired processes apically curved in lateral view; endophallic sclerite laterally flattened, with small process near apex, and with basal processes.

Female. Antenna (Fig. 6B) similar to males, ratios of length of antennomeres I–XI 1.0: 0.4: 0.3: 0.4: 0.4: 0.3: 0.3: 0.4: 0.4: 0.4: 0.5; ratios of length to width of antennomeres III–XI 4.4: 1.9: 2.0: 2.2: 1.8: 1.6: 1.4: 1.7: 1.6: 1.6: 2.3. Ventrite VIII (Fig. 5E) weakly sclerotized, T-shaped, with several setae along apical margin, apical margin medially depressed, spiculum long. Spermathecal receptaculum (Fig. 6F) longer than pump, moderately swollen, curved in lateral view; pump emarginate at inner side of base; spermathecal duct with long basal part, ramus rounded. Gonocoxae (Fig. 6G) wide and separated, base membranous, each gonocoxa asymmetric, apically narrowed from basal 1/3, with sparse long setae along apical areas.

Color variation. In Japanese populations, antennae yellowish brown; pronotum and elytra black, each elytron with one large red spot, sometimes widened and spots connected to each other, red spot reduced in some individuals; mesoventrite and abdominal ventrites reddish brown but medially black; femora blackish brown, tibiae dark brown, tarsi yellowish brown; few individuals have entirely reddish-brown bodies. In the Ryukyus, adults usually have larger red spots on the elytra and reddish-brown elytral margins (described as *A. ryukyuensis* Shigetoh & Suenaga, 2022).

On Taiwan Island, adults separate into two color forms. Typical form (Fig. 7A–C): black elytron with one large red spot, same as Japanese populations; yellowish brown color form (Fig. 7D–F): elytra with wide black stripe along suture, starting from base, apically narrowed and abbreviated at basal 1/3, with two pairs of black spots halfway between suture and lateral margin, anterior pair at base, posterior pair at apical 1/3, one wide black stripe along lateral margin, starting from base, apically narrowed, abbreviated at basal 1/3 or 1/4; abdominal ventrites medially darker. This color form is also found in Nangan Island.

In China and Kinmen Island, almost all adults belong to the typical form. A few specimens have entirely reddish-brown bodies (Fig. 7G–I). Three specimens collected from Hong Kong also have reddish bodies.

Host plants. Inoue (2014) recorded *Osmanthus* × *fortunei*, *O. heterophyllus*, *O. fragrans* (桂花), *O. fragrans* var. *aurantiacus*, *O. insularis* Koidz, *Ligustrum japonicum* (日本女真), *L. licidum*, *L. ovalifolium*, *L. obtusifolium*, *Syringa vulgaris*, *S. reticulata*, *Jasminum nudiflorum* Lindl., and *Olea europaea* L. as host plants in Japan. In Taiwan, larvae mine the leaves of the following plants: *Chionanthus retusus* (in Taiwan Island, Nangan, and Beigan islands), *Ligustrum japonicum* (in Beigan island), and *Osmanthus fragrans* (in Kinmen Island).

Biology. Various aspects of the biology of *A. rufus* were studied in Japan, including feeding habits, habitat selection, seasonal development, and developmental biology on various host trees, developmental success of larvae on two different host trees, seasonal trends of feeding and oviposition activities of adults, effects of food condition on oviposition, overwintering and oviposition ability of adults that emerge late in the season, effects of photoperiod and temperature on induction of reproductive diapause in newly emergence adults, and occurrence on olive trees (Inoue and Shinkaji 1989a–c, 1990; Inoue 1990b, 1991a, 1998, 2001, 2014).

The seasonal development of this species was studied in the field in southern Kantô, Central Japan (Inoue 1996). Overwintered adults appeared on host trees beginning mid-March, with a peak in mid-April to early May. Females began to deposit eggs from mid- to late April. The eggs were laid singly, embedded in young leaves, and coated with excrement. Leaf-mining larvae only developed in new leaves. Larvae underwent three larval instars and mature larvae crawled down to pupate in the upper layers of soil. Adults eclosed in mid-June, with a peak in later June-early July. They mainly fed on mature leaves. Adults passed the winter near the ground, mainly under fallen leaves. The egg, larval, prepupal, and pupal period took ~ 10, 20–30, 10–15, and 10–15 days respectively during spring to early summer. In Taiwan, larvae and adults can be found during April.

Remarks. *Argopistes biplagiatus* var. *rufus* was described by Chen (1934a) based on four reddish brown individuals (Fig. 7G–I) deposited in the NMHUK. We found the determination label: "Argopistes / biplagiatus / var. rufa", handwritten by Chen pinned with one typical form (Fig. 7A–C). Four adjacent females fit the original description (reddish brown body form) and bore two labels "China / Bowring" although no determination labels were found. Thus, those specimens were designated as lectotypes and paralectotypes. Bezděk and Konstantinov (2024) placed this name as a junior synonym of *A. coccinelliformis* Csiki, 1940. Actually, it is a distinct species and attributed to the oldest available name. Thus, the valid name is *Argopistes rufus* Chen, 1934, stat. nov.

Adults of *A. rufus* and *A. ryukyuensis* are not separable when Taiwanese and Chinese specimens are included. Aedeagi of both areas are intermediate between *A. rufus* and *A. ryukyuensis*. Moreover, one distinct color pattern (yellowish-brown elytra with black spots) occurs in Taiwanese populations. Thus, color patterns may not be considered as diagnostic characters. Other diagnostic characters provided by Shigetoh and Suenaga (2022) are not diagnostic for species delimitation. Thus *A. ryukyuensis* Shigetoh & Suenaga, 2022 is regarded as junior synonym of *A. rufus* Chen, 1934.

Distribution. China, Japan (Honshu, the Izu Isls., Ogasawara Isls., Shikoku, Kyushu, Okinoshima Is., Kashiwa-jima Is., the Koshiki-jima Isls., Yakushima Is., the Ryukyu Isls.), Taiwan including Kinmen Island and Matsu Islands (Beigan and Nangan Islands) (Fig. 5).

Argopistes tsekooni Chen, 1934

Figs 8A–C, 9

Argopistes tsekooni Chen, 1934b: 316 (China: Shanghai, Hangchow); Csiki 1940: 525 (catalogue); Chûjô and Kimoto 1961: 174 (China, Japan); Gressitt and Kimoto 1963: 813 (China: Jiangsu); Kimoto 1965: 437 (redescription);

Lee and An 2001: 183 (South Korea); Lee and Cho 2006: 91 (host plant); Takizwa, 2012: 38 (faunistics); Cho and An 2020: 15 (North Korea); Won et al. 2023: 9 (South Korea: Ulleungdo).

Argopistes biplagiatus: Baly 1874: 202 (misidentification).

Type material examined. One ***syntype*** • (sex undetermined, IZAS): "浙江 (= Zhejiang): 杭州 (= Hangchow) / 1934. [h] / 中国科學院 (= Chinese Academy of Sciences) [h, p] // 害水蜡樹 (attacking *Ligustrum obtusifolium*) [h, w] // Argopistes / tsekooni / Chen [h, w]". Although this specimen does not bear any type label, it should be regarded as type specimen since it fit the original description.

Additional material examined. Japan. • 1♀ (NHMUK): "Argopistes / biplagiatus / Motsch / Japan [h, w] // Baly Coll. [p, w]"; Honshu. Shizuoka: • 1♂ (SEHU), Tagata-gun, Tohi, 4.V.1985, leg. Y. Komiya; Tokyo: • 1♂ (HAPC), Komae-shi, Komai-machi, 10.VI.2021, leg. R. Seki; Yamaguchi: • 1♂ (NHMUK); Kyushu. Fukuoka: • 1♀ (HAPC), Fukuoka-shi, Higashi-ku, Shimobaru (alt. 100–360 m), 27.V.2009, leg. S. Sejima; • 1♀ (NHMUK), Mt. Mikazuki, 2.V.1954, leg. K. Morimoto; Nagasaki: • 1♂, 2♀ (SEHU), Sasebo-shi, Mt. Yahirodake, 14.IV.1981, leg. J. Okuma; • 1♂ (SEHU), same locality but with "21.IV.1981"; Oita: • 2♂, 3♀ (HAPC), Hita-shi, Miwa, Chikura, 11.IV.2016, leg. S. Sasaki.

Diagnosis. Adults of *A. tsekooni* are recognized easily by their small body sizes (< 3.5 mm; > 3.5 mm in others except *A. unicolor*), elongate ovate body shapes (elytra 1.2 × longer than wide; but 1.1 × longer than wide in others), and the combined red spots on elytra (usually separate red spots on the elytra in others); additionally, most genitalic characters are unique, such as the tube-like apex of the aedeagus (Fig. 9C); few setae on apical margin of abdominal ventrite VIII in females (Fig. 9E); and transverse gonocoxae with dense, long setae on the widely rounded apical margin (Fig. 9G).

Redescription. Length 2.8–3.2 mm, width 2.1–2.4 mm. Color (Fig. 8A–C) blackish brown, elytron with one transverse orange area at basal 1/3, and narrowed towards suture; tarsi and front tibiae yellow; antennae dark brown but seven basal antennomeres yellow. Pronotum broad, convex, lateral margin narrowly explanate; 2.0–2.1 × wider than long, disc with dense coarse punctures; lateral margin rounded, anterior margin strongly concave, posterior margin moderately convex. Elytra elongate oval, 1.2 × longer than wide, disc with confused, dense, coarse punctures.

Male. Antenna filiform (Fig. 9A), antennomere I much longer than others, approximate ratios of length of antennomeres I–XI 1.0: 0.4: 0.3: 0.5: 0.5: 0.5: 0.5: 0.5: 0.5: 0.5: 0.7; approximate ratios of length to width of antennomeres I–XI 3.1: 1.8: 2.0: 2.5: 2.3: 1.9: 1.8: 2.1: 2.1: 2.2: 2.9. Aedeagus (Fig. 9C, D) gradually widened from basal 1/9–1/2, then gradually narrowed to basal 1/2, strongly widened posterior–basal 1/2; anterior opening large, ~ 0.39 as long as aedeagus, from apex to apical 2/5; tectum composed of one pair of sclerotized processes, long, ~ 0.85 as long as anterior opening, wide and slightly curved from basal 2/4 to apex in lateral view, recurved near apex; endophallic sclerite laterally flattened, with base twisted.

Female. Antenna (Fig. 9B) similar to males, but antennomeres VII–X wider, ratios of length of antennomeres I–XI 1.0: 0.4: 0.3: 0.4: 0.4: 0.4: 0.4: 0.4: 0.4: 0.4: 0.6; ratios of length to width of antennomeres I–XI 3.8: 1.8: 2.0: 1.8: 1.9: 1.9: 1.6: 1.5: 1.5: 1.5: 2.4. Ventrite VIII (Fig. 9E) weakly sclerotized, only part of apical margin

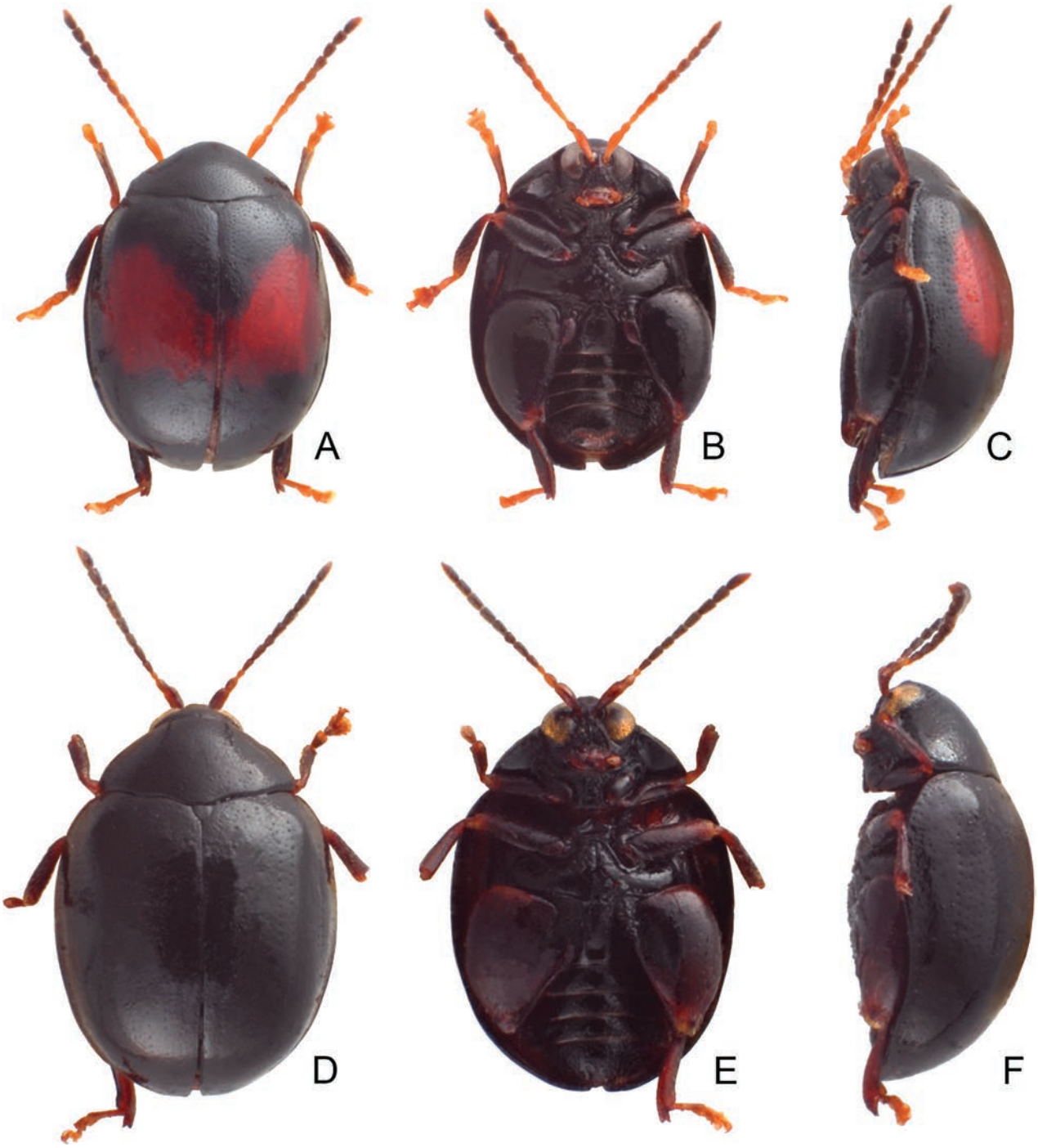

Figure 8. Habitus of *Argopistes* species **A** *A. tsekooni* Chen, male, dorsal view **B** ditto, ventral view **C** ditto, lateral view **D** *A. unicolor* Jacoby, female, dorsal view **E** ditto, ventral view **F** ditto, lateral view.

well sclerotized, with several setae along apical margin, spiculum long and base wider. Spermathecal receptaculum (Fig. 9F) longer than pump, moderately swollen, curved in lateral view; pump emarginated at inner side of base; spermathecal duct with long basal part, ramus truncate. Gonocoxae (Fig. 9G) wide and separated, base membranous, each gonocoxa asymmetric, apically narrowed from near base, with sparse setae along apical areas, setae longer at apical 1/2.

Color variation. One male has a black body and lacks transparent spots on elytra. Another male has an entire yellowish-brown body.

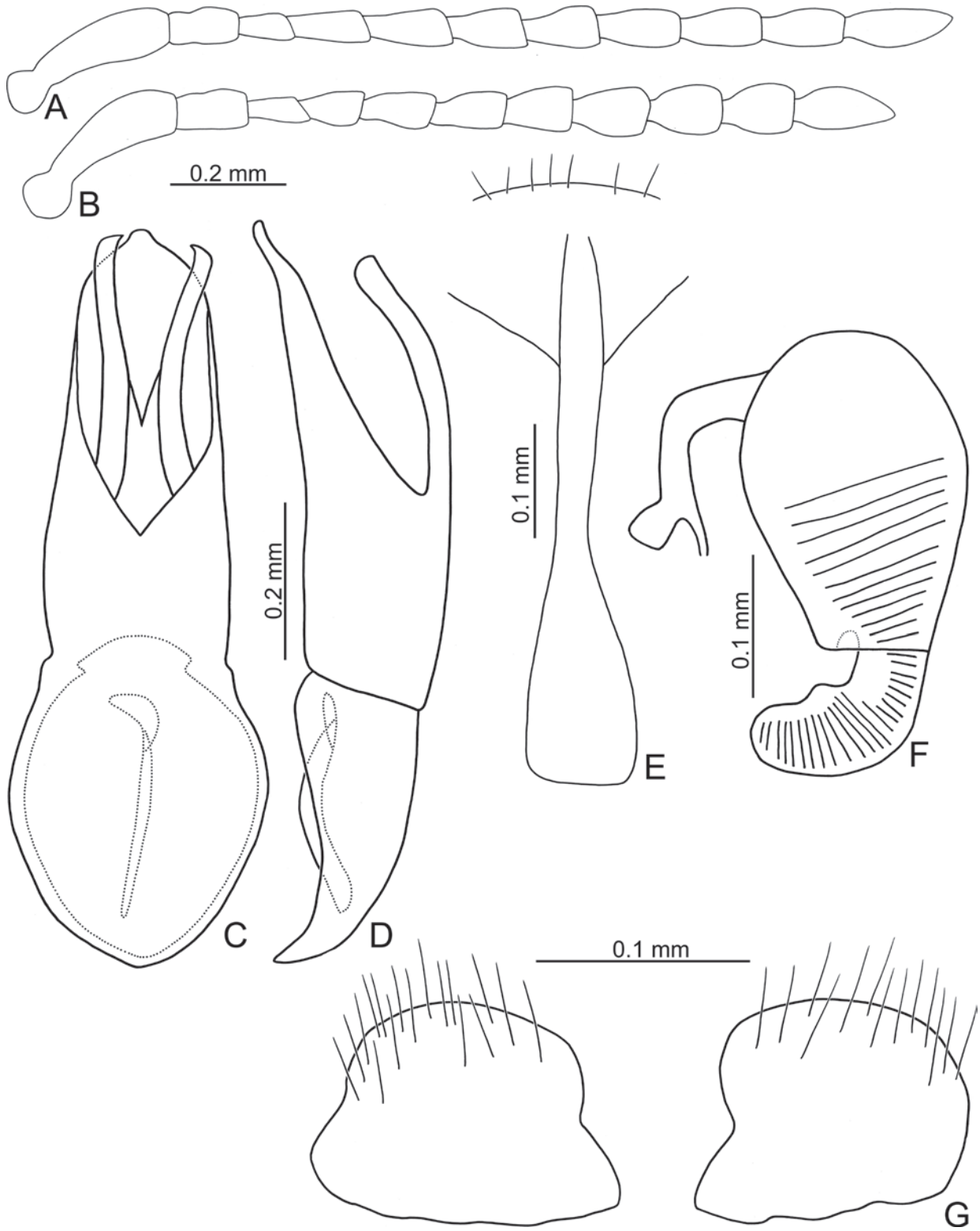

Figure 9. *Argopistes tsekooni* Chen **A** antenna, male **B** antenna, female **C** aedeagus, dorsal view **D** aedeagus, lateral view **E** abdominal ventrite VIII, female **F** spermatheca **G** gonocoxae.

Host plants. Oleaceae: *Ligustrum obtusifolium* (Chûjô & Kimoto, 1961); *Syringa oblata* Lindl., *L. japonicum*, *L. licidum*, and *L. sinense* (Zhang et al. 2008b).

Biology. The biology and life history of *A. tsekooni* were studied under laboratory and outdoor conditions in Huangshan City of Anhui Province, China (Zhang

et al. 2009). *Argopistes tsekooni* overwintered as adults and had three overlapping generations in Anhui Province.

Distribution. China, Japan (Honshu, Kyushu, the Goto Isls., Hirado-jima Is.Tsushima Is.), North Korea, South Korea.

Argopistes unicolor Jacoby, 1885

Figs 8D–F, 10

Argopistes unicolor Jacoby, 1885: 738 (Japan: Yuyama); Chûjô 1936: 109 (catalogue); Csiki 1940: 524 (catalogue); Chûjô and Kimoto 1961: 174 (catalogue); Kimoto 1965: 438 (redescription); Takizawa, 2012: 38 (faunistics).

Type material examined. ***Lectotype*** • ♂ (here designated, NHMUK): "(aedeagus glued on the transparent card) // Yuyama / 10.V.-14.V.81. [p, w] // Japan / G. Lewis. / 1910-320 [p, w] // Type / H.T. [p, w, circle label with red border] // Argopistes / unicolor. Jac. [h, b] // Argopistes unicolor JACOBY, / LECTOTYPUS 1885 / J. Král m. dit 1969! [h, w] // lecto- / typus [p, r]". ***Paralectotype*.** • 1♂ (TARI): "Yuyama [h] / Japan [p] / 10.V.1881 [h] / Col. G. LEWIS [p, w] // Argopistes / unicolor Jac. [h] / Det. T. Shiraki [p, w] // Co / Type [p, w, circle label with yellow letters and border] // Argopistes / unicolor Jacoby [h] // DET. M. CHUJO [p, w] // 1527 [p, w]".

Additional material examined. Japan. Kyushu. Nagasaki: • 3♂, 3♀ (SEHU), Shimbara-shi, Senbuki, 8.V.1984, leg. S. Imsaka; • 2♂, 2♀ (HAPC), same but with "Senfujiki", collected on *Ligustrum japonicum*.

Diagnosis. Adults of *A. unicolor* are recognized easily by their small body sizes (< 3.5 mm; > 3.5 mm in others except *A. tsekooni*), black antenna with three basal antennomeres paler (entirely yellowish-brown antennae in others except *A. tsekooni* with five dark apical antennomeres), and the entirely black elytra. Additionally, most genitalic characters are unique, including strongly curved aedeagus in lateral view (Fig. 10E), and anterior opening from apex to middle (Fig. 10C); straight apical margin of abdominal ventrite VIII in females (Fig. 10F) with setae reduced at medial area (other species with straight margin of abdominal ventrite VIII in female always with setae on median area); and longitudinally square gonocoxae (Fig. 10H).

Redescription. Length 3.2–3.4 mm, width 2.3–2.5 mm. Color (Fig. 8D–F) black; legs and mouthparts dark brown; antenna black but three basal antennomeres dark brown; abdominal ventrites yellowish brown but medially darkened. Pronotum broad, convex, lateral margins narrowly explanate; 1.9–2.0 × wider than long, disc with dense coarse punctures; lateral margin rounded, anterior margin strongly concave, posterior margin moderately convex. Elytra broadly oval, 1.1 × longer than wide, disc with coarse punctures arranged into longitudinal striae, and with fine punctures between striae.

Male. Antenna filiform (Fig. 10A), antennomere I much longer than others, approximate ratios of length of antennomeres I–XI 1.0: 0.4: 0.3: 0.4: 0.4: 0.4: 0.4: 0.4: 0.4: 0.5: 0.7; approximate ratio of length to width of antennomeres I–XI 3.8: 1.8: 1.8: 2.0: 1.8: 1.6: 1.6: 1.7: 1.5: 1.6: 2.7. Aedeagus (Fig. 10C–E) widest at apical 1/4, slightly narrowed at middle, apically narrowed from apical 1/4, apex broadly rounded; anterior opening large, ~ 0.45 as long as aedeagus, from apex to middle; tectum composed of one pair of sclerotized processes, long, ~ 0.78 as

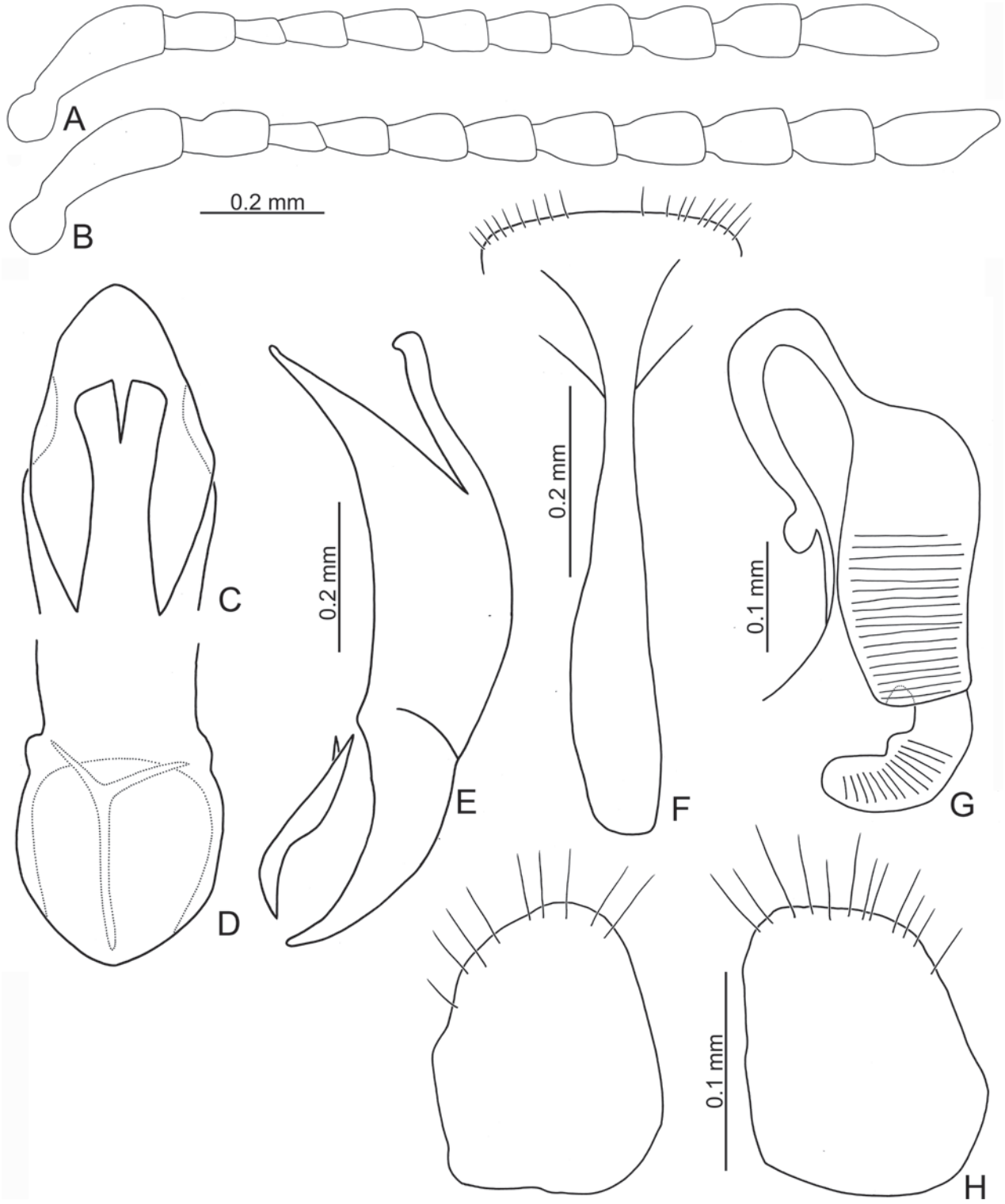

Figure 10. *Argopistes unicolor* Jacoby **A** antenna, male **B** antenna, female **C** apex of aedeagus, front view **D** base of aedeagus, dorsal view **E** aedeagus, lateral view **F** abdominal ventrite VIII, female **G** spermatheca **H** gonocoxae.

long as anterior opening, paired processes with apices recurved in lateral view; endophallic sclerite laterally flattened, with one pair of long apical processes.

Female. Antenna (Fig. 10B) similar to males, ratios of length of antennomeres I–XI 1.0: 0.4: 0.3: 0.3: 0.4: 0.3: 0.4: 0.4: 0.4: 0.4: 0.6; ratios of length to width of antennomeres III–XI 3.4: 1.9: 1.9: 1.9: 1.7: 1.5: 1.6: 1.7: 1.5: 1.6: 2.4.

Ventrite VIII (Fig. 10F) weakly sclerotized, T-shaped, with several pairs of setae along apical margin, spiculum long. Spermathecal receptaculum (Fig. 10G) longer and wider than pump, moderately swollen; pump emarginate at inner side of base; spermathecal duct with long basal part, ramus rounded. Gonocoxae (Fig. 10H) wide and separated, base membranous, each gonocoxa subquadrate, with sparse setae along apical areas.

Color variation. One male has a black body and lacks transparent spots on the elytra. Another male has an entire yellowish-brown body.

Host plants. Oleaceae: *Osmanthus heterophyllus* (= *Olea ilicifolia* Hassk.) (Chûjô and Kimoto 1961), *Ligustrum japonicum* (based on collecting data).

Biology. Unknown.

Distribution. Japan (Honshu, Kyushu, Hirado-jima Is.).

***Argopistes jungchani* sp. nov.**

https://zoobank.org/313C2711-2603-4D4D-A690-8E060F85480C

Figs 11A, B, 12

Type material examined. ***Holotype*** • ♂ (TARI). Taiwan. Pingtung: Jinshuiying (浸水營), 14.IV.2021, leg. J.-C. Chen. ***Paratype*** • 1♀ (TARI), same but with "27. VI.2012".

Diagnosis. Adults of this new species are easily recognized by their color pattern: black bodies with yellowish-brown lateral margins of pronotum and elytra; also, genitalic characters are diagnostic: tube-like apex of aedeagus similar to that of *A. tsekooni* but parallel-sided from near apex to middle (Fig. 12C) (apically narrowed from near apex to middle (Fig. 9C) in *A. tsekooni*), paired elongate tectum small, 0.76 as long as anterior opening (Fig. 12C) (paired elongate tectum long, 0.85 as long as anterior opening (Fig. 9C) in *A. tsekooni*), and anterior opening from apical 1/13–2/5 (Fig. 12C) (anterior opening from apex to apical 2/5 (Fig. 9C) in *A. tsekooni*); only two pair of long setae on apical margin of abdominal ventrite VIII (Fig. 12E) in females (more than two pair of setae on apical margin of abdominal ventrite VIII in females of other species), and cylindrical gonocoxae (Fig. 12G).

Description. Length 3.5–3.6 mm, width 2.7–2.9 mm. Color (Fig. 11A, B) blackish brown, sides of pronotum and elytra paled, tarsi, front femur and tibiae, and antennae yellowish brown. Pronotum broad, convex, lateral margin narrowly explanate; 2.3 × wider than long, disc with dense coarse punctures; lateral margin rounded, anterior margin strongly concave, posterior margin moderately convex. Elytra broadly oval, 1.1 × longer than wide, disc with fine punctures arranged into longitudinal lines, confused, dense, fine punctures present between longitudinal punctures.

Male. Antenna filiform (Fig. 12A), antennomere I much longer than others, approximate ratios of length of antennomeres I–XI 1.0: 0.5: 0.3: 0.5: 0.5: 0.5: 0.5: 0.5: 0.5: 0.5: 0.6; approximate ratios of length to width of antennomeres I–XI 4.4: 2.2: 1.9: 2.6: 2.3: 2.2: 1.9: 1.8: 1.7: 1.7: 2.6. Aedeagus (Fig. 12C, D) parallel-sided, strongly and subapically narrowed, apex tube-like and extremely small; anterior opening small, ~ 0.30 as long as aedeagus, from apical 1/13–2/5; tectum composed of one pair of sclerotized processes, large, ~ 0.76 as long as anterior opening; wide and slightly curved in lateral view; paired pro-

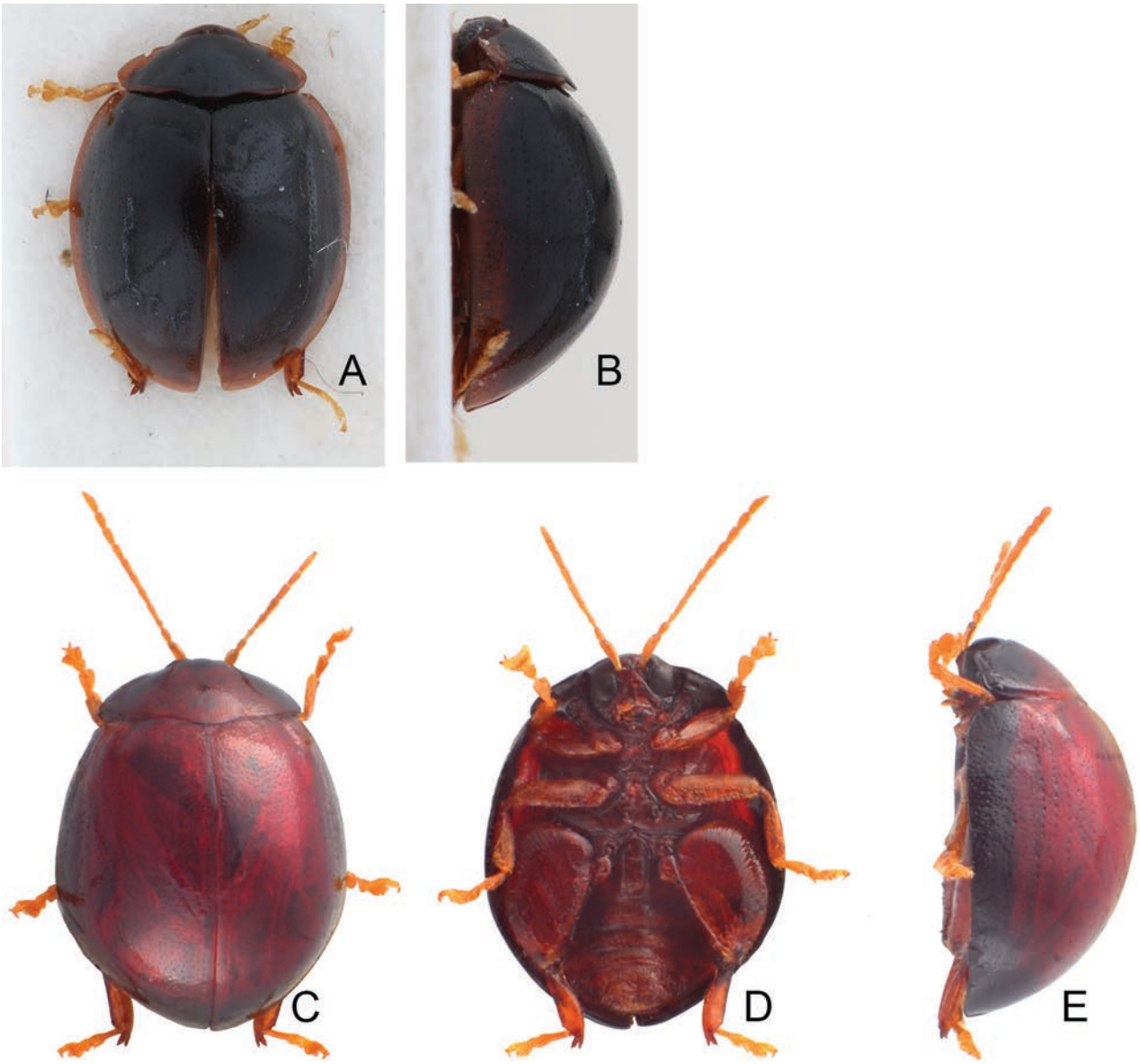

Figure 11. Habitus of *Argopistes* species **A** *A. jungchani* sp. nov., female, dorsal view **B** ditto, lateral view **C** *A. tsoui* sp. nov., male, dorsal view **D** ditto, ventral view **E** ditto, lateral view.

cesses apically curved in lateral view; endophallic sclerite laterally flattened, with basal processes slightly sclerotized.

Female. Antenna (Fig. 12B) much smaller than in males, ratios of length of antennomeres I–XI 1.0: 0.4: 0.3: 0.3: 0.3: 0.3: 0.3: 0.4: 0.4: 0.4: 0.6; ratios of length to width of antennomeres I–XI 4.2: 1.8: 1.8: 1.6: 1.7: 1.5: 1.5: 1.7: 1.6: 1.4: 2.3. Ventrite VIII (Fig. 12E) membranous, only apical margin sclerotized, T-shaped, with two pairs of short setae at sides of apical margin, apical margin truncate, spiculum long. Spermathecal receptaculum (Fig. 12F) much longer than pump, moderately swollen; pump slightly emarginate at inner side of base; spermathecal duct with long basal part, ramus rounded. Gonocoxae (Fig. 12G) cylindrical and separated, base membranous, each gonocoxa symmetric, with dense long setae along apical and outer margin.

Host plant. Unknown

Biology. Unknown.

Etymology. This new species is named for Jung-Chan Chen (陳榮章), the first person to collect specimens.

Distribution. Only known from the type locality (Fig. 5).

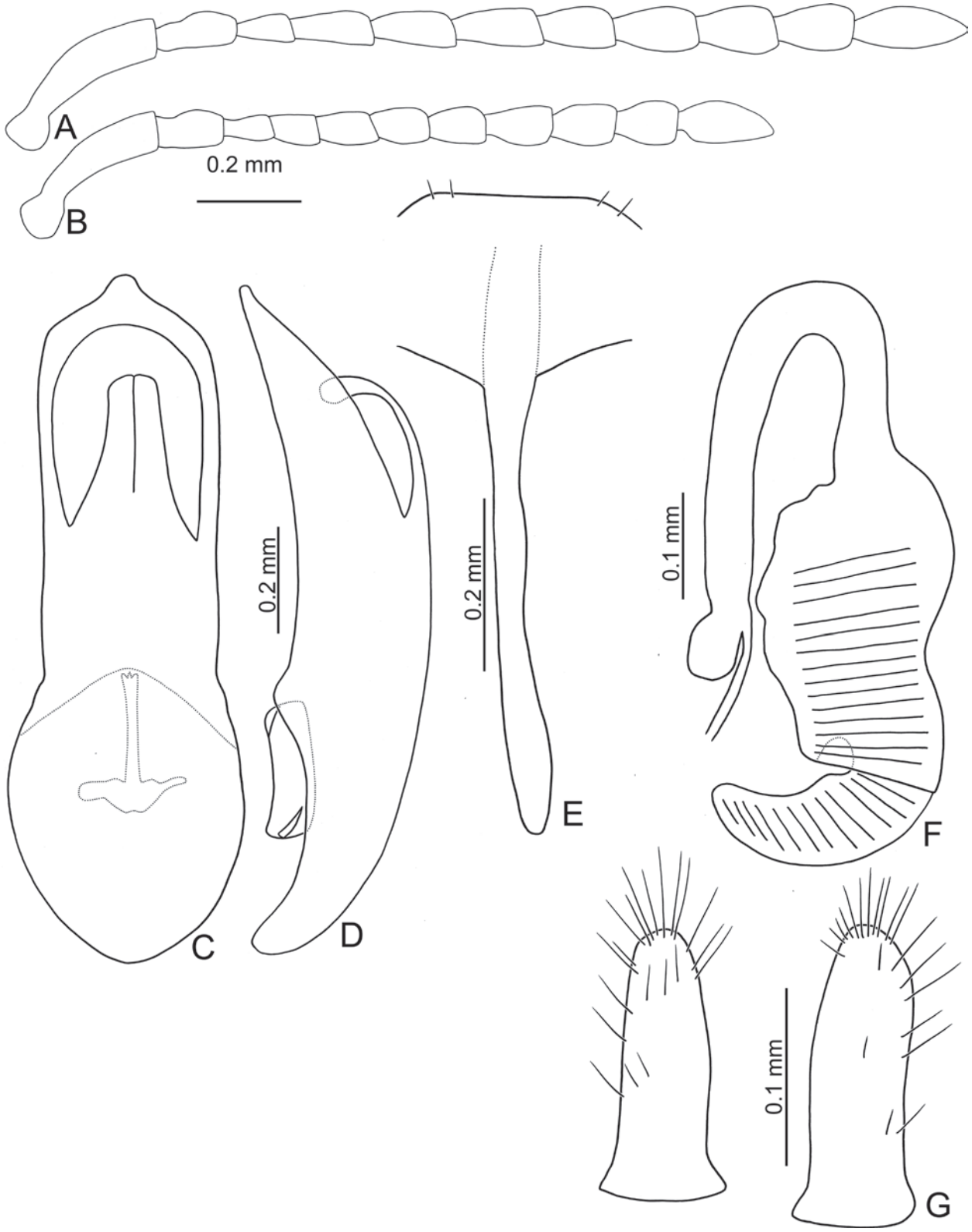

Figure 12. *Argopistes jungchani* sp. nov. **A** antenna, male **B** antenna, female **C** aedeagus, dorsal view **D** aedeagus, lateral view **E** abdominal ventrite VIII, female **F** spermatheca **G** gonocoxae.

***Argopistes tsoui* sp. nov.**
https://zoobank.org/7FA87DFC-55AB-45B2-AD05-A2EA64530D90
Figs 11C, D, 13, 14A, B

Type material examined. ***Holotype*** • ♂ (TARI). Taiwan. Hsinchu: Tahunshan (大混山), 24.II.2009, leg. S.-F. Yu. • ***Paratypes*** • 1♂, 1♀ (TARI), same as holotype; • 1♀ (TARI), same but with "8.IX.2009"; Ilan: • 3♂, 3♀ (TARI), Fushan (福山) Chihwuyan (植物園 = Botanic Park), 15.II.2009, leg. M.-H. Tsou; • 4♂, 6♀ (TARI), same locality, 8.VI.2023, leg. S.-S. Lu; • 1♂ (TAFI), same but with "27.XI.2023"; • 1♀ (TAFI), same but with "28.XI.2023"; • 1♂, 1♀ (TAFI), same but with "29.XI.2023"; • 1♂, 1♀ (TARI), same but with "5.XII.2023"; • 1♀ (TARI), same but with "7.XII.2023"; • 1♀ (TARI), same but with "18.XII.2023"; • 1♂ (TARI), same but with "11.I.2024"; • 1♂ (TARI), same but with "8.III.2024"; • 4♂, 3♀ (TARI), same but with "7.V.2024"; Keelung: • 1♂, 1♀ (TARI), Hungtanshan (紅淡山), 10.V.2008, leg. M.-H. Tsou; Pingtung: • 1♀ (TARI), Lilungshan (里龍山), 5.XI.2009, leg. M.-H. Tsou; • 1♀ (TARI), Tahanshan (大漢山), 22.I.2009, leg. S.-F. Yu; • 1♀ (TARI), same locality, 20.VIII.2022, leg. Y.-T. Chung; Taoyuan: • 2♂ (TARI), Tungyanshan (東眼山), 8.VII.2007, leg. M.-H. Tsou; • 1♀ (TARI), Yongfu (永福), 24.III.2014, leg. H. Lee.

Diagnosis. Adults of *A. tsoui* sp. nov. are similar to those of *A. biplagiatus* with reddish-brown elytra with wide black lateral margins, but differ from *A. biplagiatus* by the reddish-brown pronotum with wide black lateral margins (entirely black pronotum in *A. biplagiatus*). Diagnostic genitalic characters include pointed apex of aedeagus similar (Fig. 13C) to that of *A. biplagiatus* (Fig. 3C) but relatively narrower in lateral view (Fig. 13D) (relatively wider (Fig. 3D) in *A. biplagiatus*), longer, longitudinal paired sclerites of tectum (Fig. 13C) (short, curved paired sclerites of tectum (Fig. 3C) in *A. biplagiatus*), anterior opening from apical 1/10 to middle (Fig. 13C) (anterior opening from apex to apical 3/10 (Fig. 3C) in *A. biplagiatus*); triangular gonocoxae similar to those of *A. rufus* but expanding inwardly at basal 1/3 (Fig. 13G) (expanding outward at basal 1/3 (Fig. 6G) in *A. rufus*); dense setae along apical margin of abdominal ventrite VIII similar to those of *A. biplagiatus* but much denser and shorter (Fig. 13C) (less denser and longer setae on apical margin of abdominal ventrite VIII (Fig. 3E) in *A. biplagiatus*).

Description. Length 3.9–4.3 mm, width 3.2–3.5 mm. Color (Fig. 11C–E) reddish brown, sides of pronotum and elytra darker, tarsi and antennae yellow. Pronotum broad, convex, lateral margin narrowly explanate; 2.2 × wider than long, disc with dense coarse punctures; lateral margin rounded, anterior margin strongly concave, posterior margin moderately convex. Elytra broadly oval, 1.0–1.1 × longer than wide, disc with dense, confused, coarse punctures.

Male. Antenna filiform (Fig. 13A), antennomere I much longer than others, approximate ratios of length of antennomeres I–XI 1.0: 0.4: 0.3: 0.4: 0.4: 0.4: 0.4: 0.4: 0.4: 0.4: 0.6; approximate ratios of length to width of antennomeres I–XI 4.7: 2.1: 2.2: 2.4: 2.0: 2.0: 1.9: 1.9: 1.9: 1.7: 2.7. Aedeagus (Fig. 13B, C) strongly narrowed from apical 1/5 to apex, apex pointed; anterior opening small, ~ 0.35 as long as aedeagus, from apical 1/10 to middle; tectum composed of one pair of sclerotized processes with bifurcate apices, outer apex hooked, large, ~ 1.1 as long as anterior opening; narrow and slightly curved in lateral view; endophallic sclerite laterally flattened, with small process near apex, and with basal processes membranous.

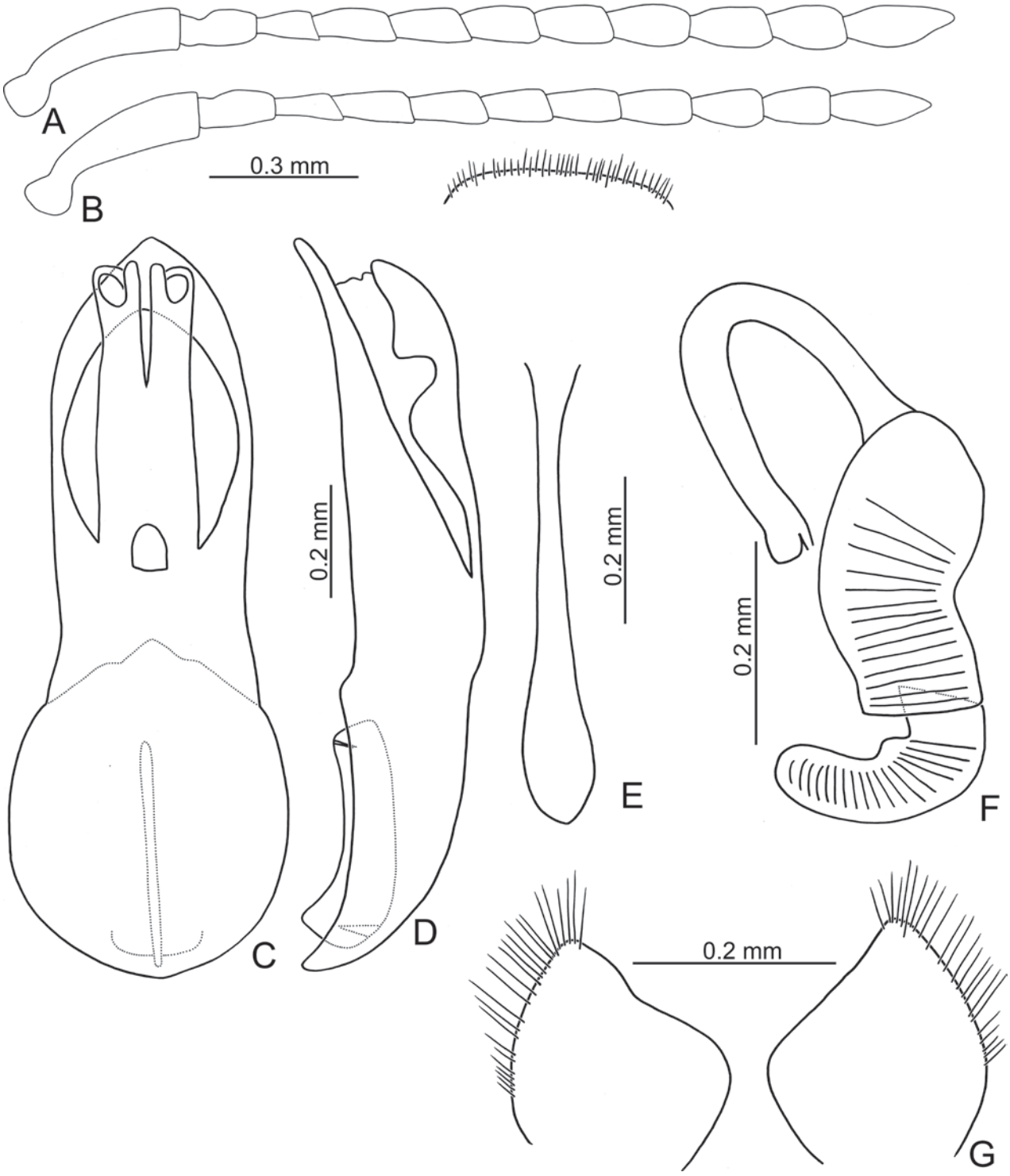

Figure 13. *Argopistes tsoui* sp. nov. **A** antenna, male **B** antenna, female **C** aedeagus, dorsal view **D** aedeagus, lateral view **E** abdominal ventrite VIII, female **F** spermatheca **G** gonocoxae.

Female. Antenna (Fig. 13B) similar to males, ratios of length of antennomeres I–XI 1.0: 0.4: 0.3: 0.4: 0.4: 0.3: 0.4: 0.4: 0.4: 0.4: 0.5; ratios of length to width of antennomeres III–XI 4.1: 2.2: 2.4: 2.4: 2.2: 1.9: 2.1: 2.0: 1.9: 1.8: 2.9. Ventrite VIII (Fig. 13E) membranous, only apical margin sclerotized, T-shaped, with dense short setae along apical margin, spiculum long. Spermathecal receptaculum (Fig. 13F) longer than pump, moderately swollen, curved in lateral

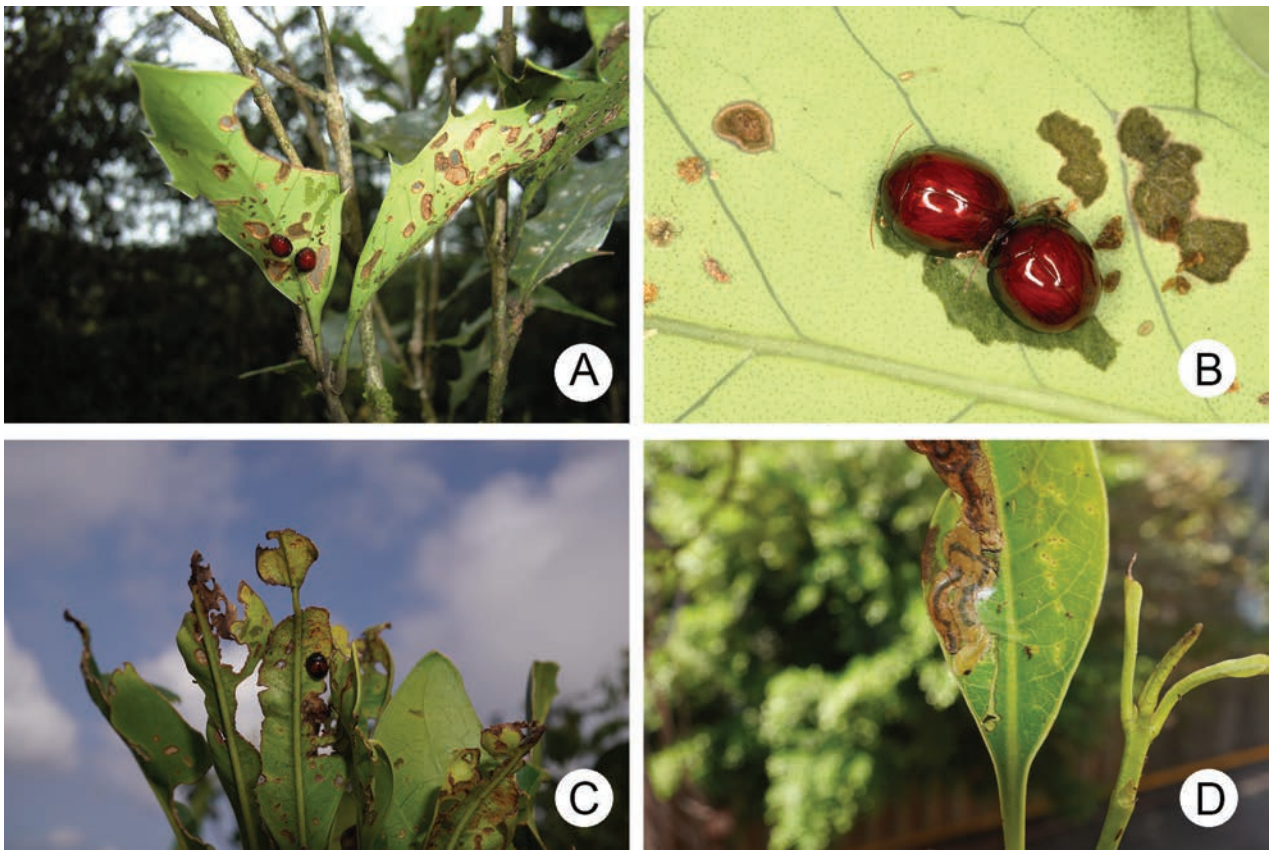

Figure 14. Field photographs of *Argopistes* species **A** adults of *A. tsoui* sp. nov. feeding on leaves of *Osmanthus heterophyllus* **B** close-up shot of adults of *A. tsoui* sp. nov. **C** adult of *A. yuae* sp. nov. resting on underside of leaf of *Chionanthus ramiflorus* **D** larva mining new leaf of *C. ramiflorus*.

view; pump emarginate at inner side of base; spermathecal duct with elongate basal part, ramus rounded. Gonocoxae (Fig. 13G) wide and separated, base membranous, each gonocoxa asymmetric, apically narrowed from apical 1/3, with dense long setae along apical areas.

Host plant. Oleaceae: *Osmanthus heterophyllus* (Fig. 13A, B), *O. kaoi* (T. S. Liu & J. C. Liao) S. Y. Lu, *O. enervius* Masam. & T. Mori, *O. fragrans*.

Biology. This species seems to be univoltine. The larvae were found only during late March.

Etymology. This new species is named for Mei-Hua Tsou (曹美華), the first person to collect specimens.

Distribution. This new species is widespread in lowlands of Taiwan (Fig. 5).

***Argopistes yuae* sp. nov.**

https://zoobank.org/D4D59AB2-7496-44F6-AD3B-C05251B4E355

Figs 14C, D, 15, 16

Type material examined. ***Holotype*** • ♂ (TARI). Taiwan. Taitung: Lanyu (蘭嶼), 16.IV.2023, leg. Y.-F. Hsu. ***Paratypes*** • 11♂, 7♀ (TARI), same data as holotype; • 10♂, 5♀ (TARI), same but with "20.III.2023"; • 8♂, 5♀ (TARI), same but with "17.VI.2023"; • 2♂, 3♀ (TARI), same island, 14.III.2023, leg. Y.-Y. Liu & Y.-F. Hsu; • 1♀ (TARI), same island, 28.IV.2022, leg. S-F. Yu; • 1♂ (TARI), same island, 4.IV.2016,

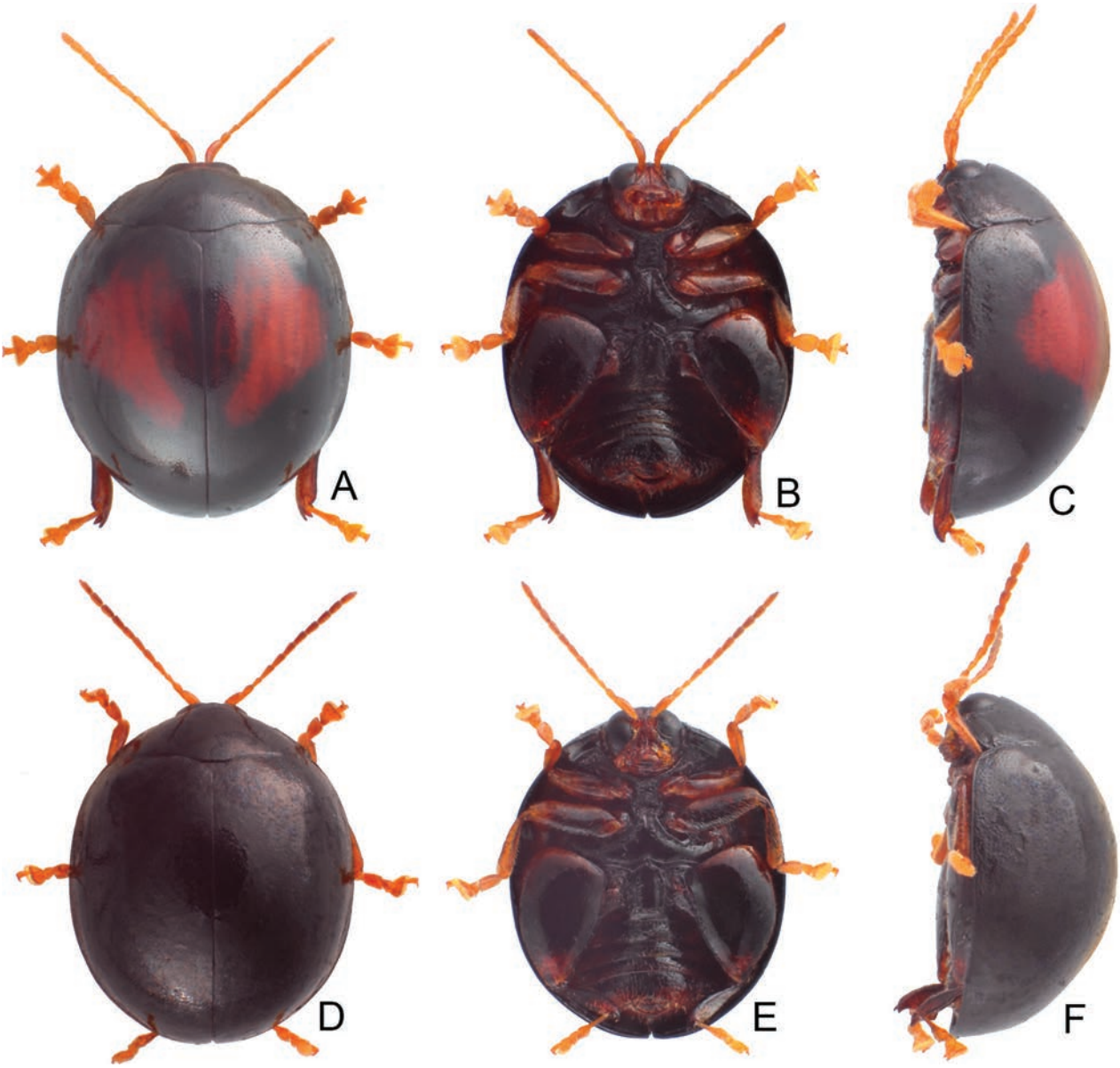

Figure 15. Habitus of *Argopistes yuae* sp. nov. **A** typical color form, male, dorsal view **B** ditto, ventral view **C** ditto, lateral view **D** Black color form, female, dorsal view **E** ditto, ventral view **F** ditto, lateral view.

leg. Y.-T. Chung; • 1♂ (TARI), same island, 14.IV.2013, leg. B.-X. Guo; • 1♂ (TARI), same island, 26.IV.2009, leg. U. Ong; • 3♂, 3♀ (TARI), same island, 18.III.2024, leg. Y.-F. Hsu; • 4♂, 3♀ (TARI), same island, 24.IV.2024, leg. J.-C. Chen; • 6♂, 3♀ (NHMUK), same island, Lanyu Weather Station (蘭嶼氣象站), 22°02.238'N, 121°33.287'E, 26.VII.2008, hand collecting, leg. M. V. L. Barclay & H. Mendel; • 2♂, 1♀ (TARI), same island, Tataienchih (大天池), 19.III.2024, leg. Y.-F. Hsu.

Diagnosis. Adults of this new species are not separable from those of *A. rufus* except by genitalic characters, including parallel-sided apex of aedeagus with anterior opening very close to apex of aedeagus, from apical 1/12–3/5 (Fig. 16C) (apically narrowed aedeagus with anterior opening not so close to apex of aedeagus, from apical 1/8–3/5 (Fig. 6C) in *A. rufus*); deeply notched apical margin of abdominal ventrite VIII (Fig. 16E) in females (shallowly notched apical margin of abdominal ventrite VIII (Fig. 6E) in females of *A. rufus*). In addition, this new species is restricted to Lanyu Island, and thus is isolated from other

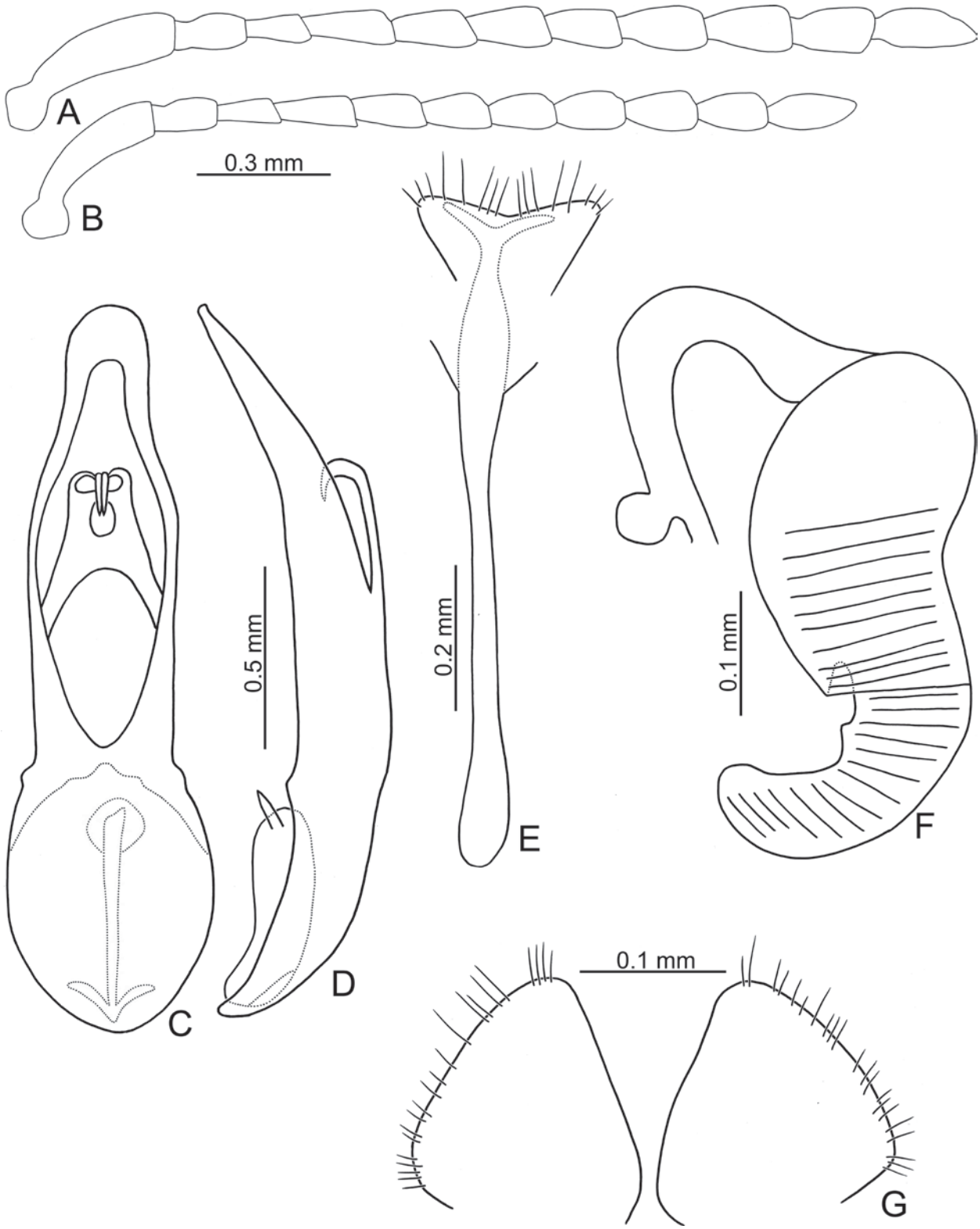

Figure 16. *Argopistes yuae* sp. nov. **A** antenna, male **B** antenna, female **C** aedeagus, dorsal view **D** aedeagus, lateral view **E** abdominal ventrite VIII, female **F** spermatheca **G** gonocoxae.

species geographically. Moreover, larvae and adults of this new species feed on leaves of *Chionanthus ramiflorus* Roxb. (Fig. 14C, D) but not those of *Osmanthus fragrans* based on laboratory rearing tests. Thus, both species are allopatric ecologically since *Osmanthus fragrans* is one of the host plants for *A. rufus*.

Description. Length 4.2–4.3 mm, width 3.5 mm. Color (Fig. 15A–C) blackish brown, elytron with one large transparent area at basal 1/3, near or connected with suture; tarsi and antennae yellowish brown. Pronotum broad, convex, lateral margin narrowly explanate; 2.3 × wider than long, disc with dense, coarse punctures; lateral margin rounded, anterior margin strongly concave, posterior margin moderately convex. Elytra broadly oval, 1.1 × longer than wide, disc with confused, dense, fine punctures.

Male. Antenna filiform (Fig. 16A), antennomere I much longer than others, approximate ratios of length of antennomeres I–XI 1.0: 0.4: 0.3: 0.5: 0.4: 0.4: 0.4: 0.5: 0.5: 0.4: 0.6; approximate ratios of length to width of antennomeres I–XI 3.8: 2.0: 2.0: 2.7: 2.0: 1.9: 1.9: 1.9: 1.8: 1.9: 2.8. Aedeagus (Fig. 16C, D) parallel-sided from basal 1/3–2/3, apically narrowed from apical 1/3–1/6, apex tube-like; anterior opening large, ~ 0.53 as long as aedeagus, from apical 1/12–3/5; tectum composed of one pair of sclerotized processes, small, ~ 0.43 as long as anterior opening; wide and slightly curved in lateral view; paired processes curved at apical 1/3 in lateral view; endophallic sclerite laterally flattened, with basal processes slightly sclerotized, and one pair of small processes near apex.

Female. Antenna (Fig. 16B) similar to males, ratios of length of antennomeres I–XI 1.0: 0.4: 0.3: 0.4: 0.4: 0.4: 0.4: 0.4: 0.4: 0.4: 0.5; ratios of length to width of antennomeres III–XI 4.9: 1.9: 2.3: 2.5: 2.0: 1.8: 1.9: 1.8: 1.8: 1.9: 2.5. Ventrite VIII (Fig. 15E) weakly sclerotized, T-shaped, with several pairs of setae along apical margin, setae smaller at sides, apical margin medially depressed, spiculum long. Spermathecal receptaculum (Fig. 16F) longer than pump, moderately swollen, curved in lateral view; pump emarginate at inner side of base; spermathecal duct with long basal part, ramus rounded. Gonocoxae (Fig. 16G) wide and separated, base membranous, each gonocoxa asymmetric, apically narrowed from near base, with sparse setae along apical areas, setae longer at apical 1/2.

Variation. A few specimens have black bodies and lack red spots on elytra (Fig. 14D–F).

Host plant. Oleaceae: *Chionanthus ramiflorus* Roxb.

Biology. This species seems to be univoltine. The larvae (Fig. 14D) were found only during late March.

Etymology. This new species is named for Su-Fang Yu (余素芳), the first person to collect specimens.

Distribution. Endemic to Lanyu Island (Fig. 5).

Key to Taiwanese species of *Argopistes*

Kimoto (1965) provided a key to Japanese species of *Argopistes*. We think that the key is appropriate for Japan but not other countries due to color variations or/and color patterns for species elsewhere. A key to Taiwanese species of *Argopistes* is provide as follows:

1 General color yellowish brown, elytra with black spots; aedeagus (Fig. 7C, D) apically narrowed, and apex widely rounded, apical margin of anterior opening far from (apical 1/8) apex of male aedeagus ..... ***A. rufus* Chen**

– General color black or reddish brown **2**

2 General color reddish brown, with black, wide margins along pronotum and elytra; aedeagus (Fig. 13B, C) strongly narrowed from apical 1/5 to apex, apex pointed; anterior opening from apical 1/10 to middle; narrow and slightly curved in lateral view ..... ***A. tsoui* sp. nov.**

– General color black, with or without yellowish brown margins along pronotum and elytra **3**

3 Elytra with one pair of red spots, but lacking yellowish brown margins along pronotum and elytra **4**

– Elytra without red spots, and with yellowish-brown margins on pronotum and elytra; aedeagus (Fig. 12C, D) parallel-sided, strongly subapically narrowed, apex tube-like and extremely small; anterior opening from apical 1/13–2/5; wide and slightly curved in lateral view..... ***A. jungchani* sp. nov.**

4 Only coarse punctures on elytra, wider interspace between eyes; aedeagus (Fig. 3C, D) apically and strongly narrowed from apical 1/5, apex pointed; anterior opening very small, from apex to apical 3/10; extremely wide in lateral view ..... ***A. biplagiatus* Motschulsky**

– Coarse and fine punctures confused on elytra, narrower interspace between eyes **5**

5 Aedeagus (Fig. 7C, D) apically narrowed, apex widely rounded, apical margin of anterior opening far from apex of male aedeagus (apical 1/8)..... ..... ***A. rufus* Chen**

– Aedeagus (Fig. 16C, D) apically narrowed, and apex parallel-sided, apex widely rounded, apical margin of anterior opening close to apex of male aedeagus (apical 1/12) ..... ***A. yuae* sp. nov.**

Discussion

Some Taiwanese species can be identified by their characteristic color patterns, including *A. tsoui* sp. nov., *A. jungchani* sp. nov., and the yellowish-brown form of *A. rufus* Chen. Male aedeagi are more diagnostic. Genital characters in females such as abdominal ventrite VIII, spermatheca, and gonocoxae are more or less diagnostic, but combinations of these morphological characters and biological information can form the basis for a sound taxonomy of the genus.

Although members of *Argopistes* are oligophagous or monophagous on Oleaceae, only *A. rufus* has established populations in small islands surrounding Japan, China, and Taiwan. Five islands (Beigan Island 北竿島, Nangan Island 南竿島, Dongju Island 東莒島, Xiju Island 西莒島, Dongyin Island 東引島) of the Matsu Islands were investigated during the spring 2024 field season. Populations of *A. rufus* were found on only Beigan Island and Nangan Island feeding on *Chionanthus retusus* and *Ligustrum japonicum*. *Chionanthus retusus* and *Ligustrum japonicum* were transported to both islands, the largest of the Matsu Islands, as ornamental trees. This supports the idea that *A. rufus* can be an invasive insect pest, invading islands as a result of exportation of ornamental trees of Oleaceae. In addition, populations of *A. rufus* expanded dramatically in Kinmen Island (金門島). One population was found at one locality of Jinsha township (金沙鎮) in the middle of April 2023 and one adult was collected at another locality (Botanical Park) at Jinhu township (金湖鎮) in the summer (July) of 2023. We have now found larvae attacking new leaves of *Osmanthus fragrans* at a guesthouse in Jinhu township (金湖鎮), in late May 2024.

Acknowledgements

We are grateful to the Taiwan Chrysomelid Research Team (TCRT) and citizen scientists, including Jung-Chan Chen (陳榮章), Hsing-Tzung Cheng (鄭興宗), Yi-Ting Chung (鍾奕霆), Yu-Feng Hsu (徐堉峰), Hsueh Lee (李雪), Sheng-Shan Lu (陸聲山), Mei-Hua Tsou (曹美華), and Su-Fang Yu (余素芳) for assistance in collecting material. We thank for Yi-Chia Chiu (邱奕家) and Chi-Lung Lee (李其龍) for photographs of specimens, Mei-Hua Tsou (曹美華) and Yu-Feng Hsu (徐堉峰) for field photography, and Chih-Kai Yang for identification of host plants. We would like to thank all curators for giving us the opportunity to study the specimens from their collections. We thank Messrs. Osaku Yamaji, Hiroaki Shigetoh, Ryôta Seki, and Shoma Sejima for providing valuable specimens, and Chang-Chin Chen (陳常卿) for assisting our study in various ways. We thank Chris Carlton for reading the draft and editing for American English style. Finally, we thank Maurizio Biondi for reviewing the manuscript, and Ron Beenen for editing the manuscript.

Additional information

Conflict of interest

The authors have declared that no competing interests exist.

Ethical statement

No ethical statement was reported.

Funding

This study was supported by the National Science and Technology Council NSTC 112-2313-B-055-001-MY3 and the Animal and Plant Health Inspection Agency, Ministry of Agriculture 113AS-5.5.4-VP-01.

Author contributions

Investigation: HS. Supervision: MYC. Writing - original draft: CFL.

Author ORCIDs

Chi-Feng Lee https://orcid.org/0000-0003-1996-0557
Ming-Yao Chiang https://orcid.org/0000-0002-1514-7086

Data availability

All of the data that support the findings of this study are available in the main text.

References

Baly JS (1874) VI. Catalogue of the phytophagous Coleoptera of Japan, with descriptions of the species new to science. Transactions of the Entomological Society of London 1874: 161–217. https://doi.org/10.1111/j.1365-2311.1874.tb00164.x

Bezděk J, Konstantinov AS (2024) Supertribe Alticitae. In: Bezděk J, Sekerka L (Eds) Catalogue of Palaearctic Coleoptera. Vol. 6/2. Updated and Revised 2nd edn. Chrysomeloidea (Orsodacnidae, Megalopodidae, Chrysomelidae). Brill, Leiden/Boston, 468–580. https://doi.org/10.1163/9789004707283

Biondi M, Iannella M, D'Alessandro P (2024) *Argopistes* Motschulsky from Madagascar with descriptions of six new species (Coleoptera, Chrysomelidae, Galerucinae, Alticini). ZooKeys 1202: 303–327. https://doi.org/10.3897/zookeys.1202.122977

Blanco J, Konstantinov A (2013) Review of the New World species of the genus *Argopistes* Motschulsky (Coleoptera: Chrysomelidae: Galerucinae: Alticini). Zootaxa 3626: 249–267. https://doi.org/10.11646/zootaxa.3626.2.3

Chen SH (1934a) On some species of Chrysomelidae (Col.) in the British Museum. Stylops 3: 66–72. https://doi.org/10.1111/j.1365-3113.1934.tb01547.x

Chen SH (1934b) Revision of the Halticinae (Col. Chrysomelidae) of Yunnan and Tonkin. Sinensia 5: 225–416.

Cho HW, An SL (2020) An annotated list of leaf beetles (Coleoptera: Chrysomelidae) of Korea, with comments and new records. Far Eastern Entomologist 404: 1–36. https://doi.org/10.25221/fee.404.1

Chûjô M (1935a) Chrysomelidae of Loo-choo Archipelago (I). Transactions of the Natural History Society of Formosa 25: 69–89.

Chûjô M (1935b) Chrysomelidae of Loo-choo Archipelago (II). Transactions of the Natural History Society of Formosa 25: 203–211.

Chûjô M (1936) Studies on the Chrysomelidae in the Japanese Empire (VIII). Subfamily Halticinae (6). Transactions of the Natural History Society of Formosa 26: 108–114.

Chûjô M, Kimoto S (1961) Systematic catalog of Japanese Chrysomelidae. Pacific Insects 3: 117–202.

Csiki E (1940) [new name. In: Heikertinger F, Csiki E: Pars 169.] Chrysomelidae: Halticinae. In: Schenkling S (Ed.) Coleopterorum Catalogus. W. Junk, s-Gravenhage, 337–635.

Duckett CN, Daza JD (2004) A new species of flea beetle in the genus *Alagoasa* Bechyné (Coleoptera: Chrysomelidae: Galerucinae) from highland Costa Rica. Coleopterists Bulletin 58(1): 84–96. https://doi.org/10.1649/608

Gressitt JL, Kimoto S (1963) The Chrysomelidae of China and Korea, Part 2. Pacific Insects Monograph 1B: 301–1026.

Inoue T (1990a) Feeding habits and seasonal development of the flea beetle *Argopistes biplagiatus* Motschulsky (Coleoptera: Chrysomelidae) in Chiba Prefecture, Central Japan. Japanese Journal of Applied Entomology and Zoology 34(2): 153–160. [in Japanese with English summary] https://doi.org/10.1303/jjaez.34.153

Inoue T (1990b) Habitat selection of two flea beetle species of the genus *Argopistes* (Coleoptera: Chrysomelidae) on their host trees. Japanese Journal of Applied Entomology and Zoology 34(3): 217–226. [in Japanese with English summary] https://doi.org/10.1303/jjaez.34.217

Inoue T (1991a) Studies on the life history of the flea beetle, *Argopistes coccinelliformis* Csiki (Coleoptera: Chrysomelidae). V. Effects of Food Conditions on Oviposition. Japanese Journal of Applied Entomology and Zoology 35(3): 213–220. [in Japanese with English summary] https://doi.org/10.1303/jjaez.35.213

Inoue T (1991b) Host plant preference of flea beetle *Argopistes biplagiatus* Motschulsky adults (Coleoptera: Chrysomelidae). Applied Entomology and Zoology 26(3): 403–406. https://doi.org/10.1303/aez.26.403

Inoue T (1992) Adult diapause of the flea beetle, *Argopistes biplagiatus* Motschulsky (Coleoptera: Chrysomelidae). I. Seasonal trends in feeding and oviposition activities. Japanese Journal of Applied Entomology and Zoology 36(3): 159–168. [in Japanese with English summary] https://doi.org/10.1303/jjaez.36.159

Inoue T (1993) Adult diapause of the flea beetle, *Argopistes biplagiatus* Motschulsky (Coleoptera: Chrysomelidae). II. Effects of photoperiodic condition on feeding and

oviposition activities. Applied Entomology and Zoology 28(3): 313–318. https://doi.org/10.1303/aez.28.313

Inoue T (1994) Adult diapause of the flea beetle, *Argopistes biplagiatus* Motschulsky (Coleoptera: Chrysomelidae). III. Effects of low temperatures on termination of winter diapause. Applied Entomology and Zoology 29(3): 433–436. https://doi.org/10.1303/aez.29.433

Inoue T (1996) Biology of two *Argopistes* (Chrysomelidae: Alticinae). In: Jolivet PHA, Cox ML (Eds) Chrysomelidae Biology, Vol. 3: General Studies, Academic Publishing, Amsterdam, 327–355.

Inoue T (1998) Studies on the life history of the flea beetle, *Argopistes coccinelliformis* Csiki (Coleoptera: Chrysomelidae). VI. Overwintering and oviposition abilities of adults which emerged late in the season. Applied Entomology and Zoology 33(1): 21–27. https://doi.org/10.1303/aez.33.21

Inoue T (2001) Studies on the life history of the flea beetle, *Argopistes coccinelliformis* Csiki (Coleoptera: Chrysomelidae). VII. Effects of photoperiod and temperature on induction of reproductive diapause in newly emerged adults. Applied Entomology and Zoology 36(1): 53–58. https://doi.org/10.1303/aez.2001.53

Inoue T (2014) Life history of the flea beetle, *Argopistes coccinelliformis* Csiki (Coleoptera: Chrysomelidae). VIII. Occurrence on olive tree. Japanese Journal of Environmental Entomology and Zoology 25(2): 71–73. https://doi.org/10.11257/jjeez.25.71

Inoue T, Shinkaji N (1989a) Studies on the life history of the flea beetle, *Argopistes coccinelliformis* Csiki (Coleoptera: Chrysomelidae). I. Feeding habits and seasonal development on various trees of Oleaceae. Japanese Journal of Applied Entomology and Zoology 33(4): 217–222. [in Japanese with English summary] https://doi.org/10.1303/jjaez.33.217

Inoue T, Shinkaji N (1989b) Studies on the life history of the flea beetle, *Argopistes coccinelliformis* Csiki (Coleoptera: Chrysomelidae). II. Developmental ability on various host trees. Japanese Journal of Applied Entomology and Zoology 33(4): 223–230. [in Japanese with English summary] https://doi.org/10.1303/jjaez.33.223

Inoue T, Shinkaji N (1989c) Studies on the life history of the flea beetle, *Argopistes coccinelliformis* Csiki (Coleoptera: Chrysomelidae). III. Developmental success of larvae on two different host plants. Japanese Journal of Applied Entomology and Zoology 33 (4): 262–263. [in Japanese with English summary] https://doi.org/10.1303/jjaez.33.262

Inoue T, Shinkaji N (1990) Studies on the life history of the flea beetle, *Argopistes coccinelliformis* Csiki (Coleoptera: Chrysomelidae). IV. Seasonal trends of feeding and oviposition activities of adults. Japanese Journal of Applied Entomology and Zoology 34: 55–62. [in Japanese with English summary] https://doi.org/10.1303/jjaez.34.55

Jacoby M (1885) Descriptions of the phytophagous Coleoptera of Japan obtained by Mr. George Lewis during his second journey, from February 1880 to September 1881. – Part II. Halticinae and Galerucinae. Proceedings of the Scientific Meetings of the Zoological Society of London 1885: 719–755. https://doi.org/10.1111/j.1096-3642.1885.tb02918.x

Jolivet P, Hawkeswood TJ (1995) Host-plants of Chrysomelidae of the World. Backhuys Publishers, Leiden, 281 pp.

Kimoto S (1965) The Chrysomelidae of Japan and the Ryukyu Islands. IX. Subfamily Aliticinae II. Journal of the Faculty of Agriculture, Kyushu University 13: 431–459. https://doi.org/10.5109/22730

Lee JE, An SL (2001) Family Chrysomelidae. Economic Insects of Kore 14. Insecta Koreana Supplement 21. National Institute of Agricultural Science and Technology, Suwon, 231 pp.

Lee JE, Cho HW (2006) Leaf beetles in the crops (Coleoptera: Chrysomelidae). Economic Insects of Korea 27. Insecta Koreana Supplement 34. National Institute of Agricultural Science and Technology, Suwon, 130 pp.

Motschulsky V de (1860) Coléoptères rapportés de la Sibérie orientale et notamment des pays situés sur le bords du fleuve Amour par MM. Schrenck, Maack, Ditmar, Voznessenski ect. In: Reisen und forschungen Petersburg ausgeführt und in Verbindung mit mehreren Gelehrten herausgegeben. Band II. Zweite Lieferung. Coleopteren. Eggers & Comp., St. Petersburg, 79–257.

Schönfeldt H von (1890) Ein Beitrag zur Coleopterenfauna der Liu-Kiu-Inseln. Entomologische Nachrichten 16: 168–175.

Shigetoh H, Suenaga H (2022) Description of a new species of the genus *Argopistes* Motschulsky (Coleoptera, Chrysomelidae, Galerucinae, Alticini) from the Ryukyu Islands and Daitô Islands, southwestern Japan, and redescription of *A. coccinelliformis* Csiki. Elytra, New Series, 12: 1–13.

Suffrian E (1868) Verzeichniss der von Dr. Gundlach auf der Insel Cuba gesammelten Chrysomelinen. Archiv fur Naturgeschichte 34(1): 163–252.

Taiwan Encyclopedia of Life (2024) TaiEOL. https://taieol.tw/ [accessed 3 July 2024]

Takizawa H (2012) Notes on biology of Chrysomelidae in Japan (6). Kanagawa-chûhô 177: 33–51. [in Japanese]

Won MH, Choi JW, Bang WJ, Lee DY, Moon MK, Kim YK, Kim DG, Kim DY, Suh SJ, Choi KS (2023) Insect fauna including unrecorded species in Ulleungdo, South Korea. Biodiversity Data Journal 11: e100783. https://doi.org/10.3897/BDJ.11.e100783

Zhang Y, Hanula J, Sun J (2008a) Survey for potential insect biological control agents of *Ligustrum sinense* (Scrophulariales: Oleaceae) in China. Florida Entomologist 91(3): 372–382. https://doi.org/10.1653/0015-4040(2008)91[372:SFPIBC]2.0.CO;2

Zhang Y, Hanula J, Sun J (2008b) Host specificity of *Argopistes tsekooni* (Coleoptera, Chrysomelidae), a potential biological control agent of Chinese privet. Journal of Economic Entomology 101(4): 1146–1151. https://doi.org/10.1603/0022-0493(2008)101[1146:HSOATC]2.0.CO;2

Zhang Y, Sun J, Hanula J (2009) Biology and life history of *Argopistes tsekooni* (Coleoptera: Chrysomelidae) in China, a promising biological control agent of Chinese privet. Annals of the Entomological Society of America 102: 508–516. https://doi.org/10.1603/008.102.0322

ZooKeys 1215: 185–208 (2024)
DOI: 10.3897/zookeys.1215.116624

Research Article

The seventh species of the newt genus *Tylototriton* in Thailand: a new species (Urodela, Salamandridae) from Tak Province, northwestern Thailand

Porrawee Pomchote[1], Parada Peerachidacho[2], Wichase Khonsue[1], Pitak Sapewisut[3], Axel Hernandez[4,5], Chitchol Phalaraksh[3], Parunchai Siriput[6], Kanto Nishikawa[7,8]

1 *Department of Biology, Faculty of Science, Chulalongkorn University, Bangkok 10330, Thailand*
2 *Research Institute for Languages and Cultures of Asia, Mahidol University, Nakhon Pathom 73170, Thailand*
3 *Department of Biology, Faculty of Science, Chiang Mai University, Chiang Mai 50200, Thailand*
4 *LASER, College of Biology & the Environment, Nanjing Forestry University, Nanjing 210000, China*
5 *Department of Environmental Sciences, Faculty of Sciences and Technics, University Pasquale Paoli of Corsica, Corte 20250, France*
6 *Department of National Parks, Wildlife and Plant Conservation, Bangkok 10900, Thailand*
7 *Graduate School of Global Environmental Studies, Kyoto University, Kyoto 606–8501, Japan*
8 *Graduate School of Human and Environmental Studies, Kyoto University, Kyoto 606–8501, Japan*

Corresponding author: Porrawee Pomchote (porrawee.p@chula.ac.th)

Abstract

A new species of the crocodile newt genus *Tylototriton* from Doi Soi Malai located at Mae Tuen Wildlife Sanctuary, Tak Province, northwestern Thailand is described based on molecular and morphological evidence, and named as *Tylototriton soimalai* **sp. nov.** The new species is the seventh recorded species of the genus *Tylototriton* reported in Thailand. It differs morphologically from its congeners by a combination of the following morphological characteristics: head longer than wide; snout blunt or truncate; sagittal ridge on head narrow, short and distinct; dorsolateral bony ridges on head pronounced and rough; parotoids distinct; vertebral ridge prominent, wide and not segmented; 14–16 distinct, rounded and isolated rib nodules but posterior nodules connected; tips of fore- and hind limbs overlapping when adpressed along the body. The body background color is black, while the color markings are orange. Molecular analysis indicated that *Tylototriton soimalai* **sp. nov.** is a distinct lineage and sister to *T. uyenoi* with a 4.1% genetic sequence divergence based on the mitochondrial NADH dehydrogenase subunit 2 gene. The new species is currently restricted to the hill evergreen forests of Doi Soi Malai. The implementation of a strategic plan is recommended to protect both the species and its habitat from anthropogenic activities.

Key words: Conservation, crocodile newt, morphology, phylogeny, *Tylototriton soimalai* sp. nov.

Academic editor: Annemarie Ohler
Received: 14 December 2023
Accepted: 4 September 2024
Published: 15 October 2024

ZooBank: https://zoobank.org/21ACA27D-7BB1-44C3-B170-8B0BB51488D0

Citation: Pomchote P, Peerachidacho P, Khonsue W, Sapewisut P, Hernandez A, Phalaraksh C, Siriput P, Nishikawa K (2024) The seventh species of the newt genus *Tylototriton* in Thailand: a new species (Urodela, Salamandridae) from Tak Province, northwestern Thailand. ZooKeys 1215: 185–208. https://doi.org/10.3897/zookeys.1215.116624

Introduction

The salamandrid genus *Tylototriton* Anderson, 1871, also known as crocodile newts, currently contains 40 nominal species with several unnamed taxa endemic to Southeast Asia and ranging across the eastern Himalayas, central to southern China (including Hainan island), and to the northern parts of Indochina (Wang et al. 2018; Pomchote et al. 2021b; Dufresnes and Hernandez

2022; Frost 2024). The genus has been divided into three subgenera: *Tylototriton*, *Yaotriton* Dubois & Raffaëlli, 2009, and *Liangshantriton* Fei, Ye & Jiang, 2012 (e.g., Nishikawa et al. 2013a; Pomchote et al. 2021b). This genus includes cryptic species that are difficult to distinguish based solely on external morphological characteristics (Pomchote et al. 2021b). Consequently, molecular phylogenetic methods, combined with extensive morphological investigations, are necessary to assess the taxonomic status of the genus *Tylototriton*. These approaches have led to the description of several new species of crocodile newts (Frost 2024).

In Thailand, six species of *Tylototriton* from the subgenera *Tylototriton* and *Yaotriton* are currently known: *T. verrucosus* Anderson, 1871; *T. uyenoi* Nishikawa, Khonsue, Pomchote & Matsui, 2013; *T. anguliceps* Le, Nguyen, Nishikawa, Nguyen, Pham, Matsui, Bernardes & Nguyen, 2015; *T. phukhaensis* Pomchote, Khonsue, Thammachoti, Hernandez, Suwannapoom & Nishikawa, 2020; *T. umphangensis* Pomchote, Peerachidacho, Hernandez, Sapewisut, Khonsue, Thammachoti & Nishikawa, 2021 (all belonging to the subgenus *Tylototriton*); and *T. panhai* Nishikawa, Khonsue, Pomchote & Matsui, 2013 (subgenus *Yaotriton*). Among these six species, *T. uyenoi* displays various phenotypes with allopatric distribution in scattered and isolated mountainous areas (Nishikawa et al. 2013a; Hernandez 2016; Hernandez and Pomchote 2021). In the past, this species was identified as *T. verrucosus* Type I based on coloration and distribution range (Pomchote et al. 2008). Subsequently, morphological and molecular evidence showed that the Type I could be separated into two groups, *T. uyenoi* (Nishikawa et al. 2013a) and *T. anguliceps* (Le et al. 2015). According to Nishikawa et al. (2013a), *T. uyenoi* was originally distributed in three mountains, Doi (meaning "mountain" in Thai) Ang Khang, Doi Inthanon, and Doi Suthep, all in Chiang Mai Province, in northern Thailand. Subsequently, this species has been reported in new distribution locations across northern to western parts of Thailand: Namtok Mae Surin National Park (NP), Mae Hong Son Province, northern region (Pomchote et al. 2020a); Chiang Dao Wildlife Sanctuary (WS) (Michaels 2014), Doi Mon Jong, and Doi Mak Lang (Hernandez et al. 2019), Chiang Mai Province, northern region; Doi Soi Malai in Mae Tuen WS, Tak Province, northwestern region (Hernandez 2017); Umphang in Tak Province, western region (Hernandez et al. 2019); Mae Wong NP, Kamphaeng Phet Province, western region (Pomchote et al. 2021a); and Khao Laem NP, Kanchanaburi Province, western region (Hernandez and Pomchote 2020b) (Fig. 1). However, among the aforementioned reports, only the study by Pomchote et al. (2020a) included morphological variations and molecular analyses of *T. uyenoi* based on ten specimens from Mae Hong Son Province. Additionally, the study by Pomchote et al. (2021b) collected four crocodile newts from Umphang, Tak Province, and examined their morphology and genetics. The results indicated that the crocodile newts from Umphang belong to a lineage distinct from the known *Tylototriton* species, and they were described as a new species, *T. umphangensis*. In the other studies, newts were identified as *T. uyenoi* based on external morphology of one individual and its distribution, due to several reasons such as lack of permission to collect specimens or tissues, or the newts being found accidentally.

On 16 July 2014, Hernandez found an adult male crocodile newt in a muddy water pond located in a dipterocarp and mixed deciduous forest on the top

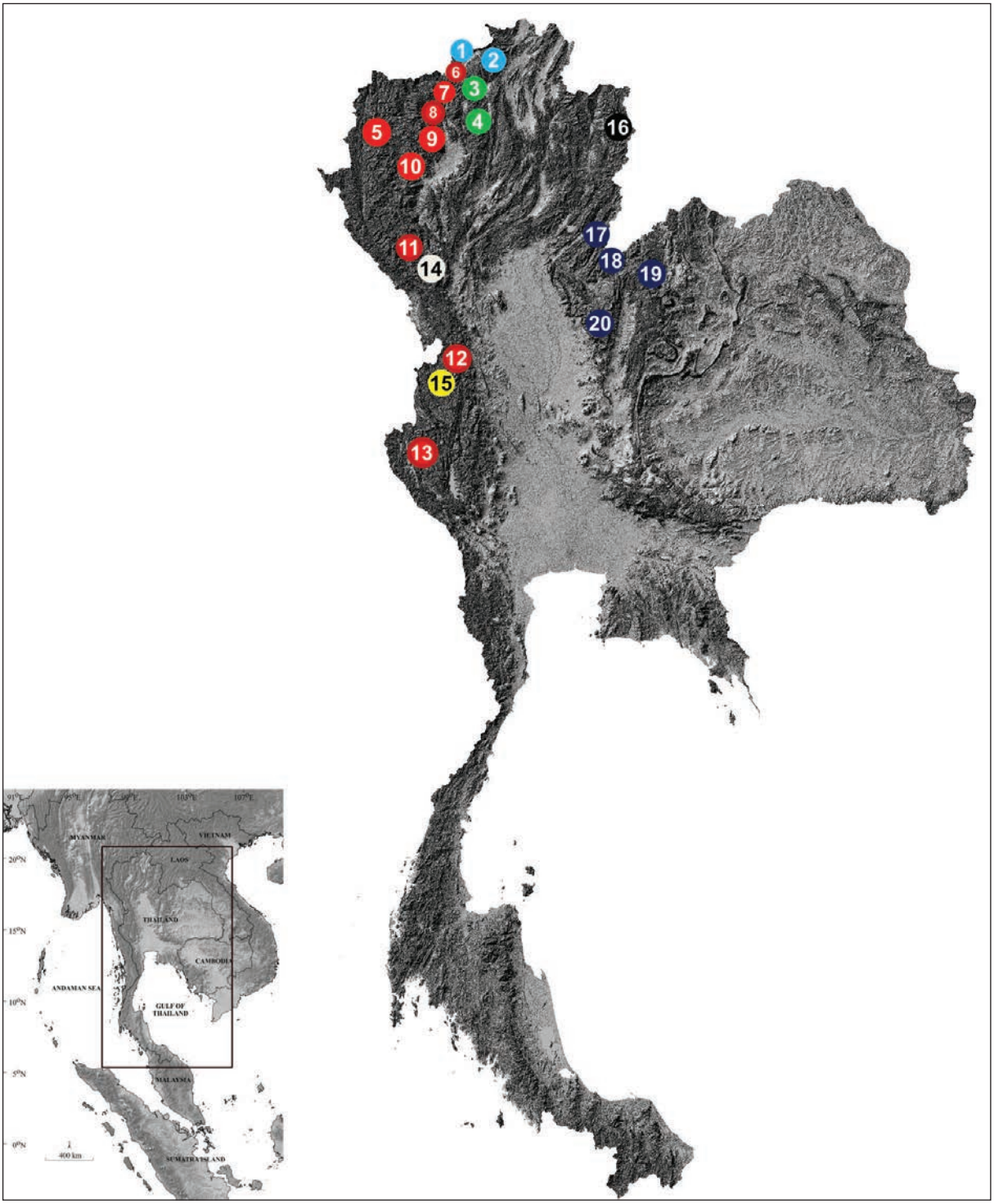

Figure 1. Current distribution of the genus *Tylototriton* in Thailand. *Tylototriton verrucosus* (pale blue): **1** Doi Pha Hom Pok NP, Chiang Mai Province **2** Doi Chang, Chiang Rai Province; *T. anguliceps* (green): **3** Si Dong Yen, Chiang Mai Province **4** Khun Chae NP, Chiang Rai Province; *T. uyenoi* (red): **5** Namtok Mae Surin NP, Mae Hong Son Province **7** Doi Ang Khang, Chiang Mai Province **9** Doi Suthep, Chiang Mai Province **10** Doi Inthanon, Chiang Mai Province; *T.* cf. *uyenoi* (red outlined with dark red): **6** Doi Mak Lang, Chiang Mai Province **8** Chiang Dao WS, Chiang Mai Province **11** Doi Mon Jong, Chiang Mai Province **12** Mae Wong NP, Kamphaeng Phet Province **13** Khao Laem NP, Kanchanaburi Province; *T. soimalai* sp. nov. (tan): **14** Doi Soi Malai, Mae Tuen WS, Tak Province; *T. umphangensis* (yellow): **15** Umphang WS, Tak Province; *T. phukhaensis* (black): **16** Doi Dong Ya Wai, Doi Phu Kha NP, Nan Province; and *T. panhai* (dark blue): **17** Phu Soi Dao NP, Uttaradit Province **18** Phu Suan Sai NP, Loei Province **19** Phu Luang WS, Loei Province **20** Phu Hin Rong Kla NP, Phitsanulok Province. NP = National Park and WS = Wildlife Sanctuary. The map is modified from https://www.mitrearth.org.

of Doi Soi Malai, at an elevation of approximately 1,500 m a.s.l., in Mae Tuen WS, Tak Province, and tentatively assigned the specimen as *T. uyenoi* without conducting a detailed study (see Hernandez 2017). However, the male crocodile newt shown in figure 1 of this publication showed some morphological differences from the original description of *T. uyenoi* (see Nishikawa et al. 2013a). For example, the shape of the midsagittal ridge in the former is narrow, short, and distinct, while in the latter, it is indistinct. Additionally, the rib nodules in the former are connected posteriorly, whereas they are separated posteriorly in the latter. Furthermore, in 2015, the Tourism Authority of Thailand (TAT) confirmed the presence of *Tylototriton* in this locality by publishing pictures and a short VDO clip on MGR Online. The crocodile newt was identified using the Thai local name Ka-taang or Kra-taang (meaning lizard), or Jing-jok Nam (meaning house gecko and water, respectively) without providing its scientific name.

Thus, the aforementioned data lead to new field surveys being conducted at Doi Soi Malai, Mae Tuen WS where a newt population was discovered in a mud puddle on the road near the summit of the mountain. Detailed phylogenetic and morphological analyses of this population were performed to clarify its taxonomic status, and revealed that the specimens from Doi Soi Malai, Mae Tuen WS belong to a distinct lineage within the subgenus *Tylototriton*. Herein, we describe this population as a new species, *Tylototriton soimalai* sp. nov.

Materials and methods

Sampling

The field survey was conducted on the 31 August 2022 at Mae Tuen WS, Tak Province, northwestern Thailand (Fig. 1, locality 14) using the visual encounter survey method (Heyer et al. 1994). Three newts were found during the daytime only in one mud puddle on the road through the highest peak of Doi Soi Malai, at ca 1,500 m a.s.l. Due to the turbid and muddy water, the newts were captured using an aquatic dip net and kept in plastic bags for examination. All newts were checked for sex and maturity, based on their cloacal characters (Pomchote et al. 2008). They were subsequently identified as breeding males. These male specimens were used for molecular and morphological analyses. Additionally, two larvae were discovered and photographed in this mud puddle (Fig. 2); however, while we were attempting to take morphological measurements, they managed to escape and hide in the puddle. Due to the discovery of the larvae, this mud paddle is considered a breeding site for the Mae Tuen WS newts.

Following previous studies (Pomchote et al. 2021b), live specimens were anesthetized by immersion in a solution of tricaine methanesulfonate (MS-222; 5 g/L) for ~ 5 min, then euthanized in a solution of chloretone (Heyer et al. 1994), and measured for morphometrics and body weight (BW) (see details below). The tissue samples (liver) of each specimen were taken, and subsequently stored in 95% (v/v) ethanol for molecular analysis prior to preservation. The voucher specimens were fixed in 10% buffered formalin, stored in 70% (v/v) ethanol, and then deposited in the Chulalongkorn University Museum of Natural History (**CUMZ**), Bangkok, Thailand.

Figure 2. The two larvae of *Tylototriton soimalai* sp. nov. in life.

Molecular analyses

Total DNA was extracted from the liver using a PureDireX™ genomic isolation kit (Bio-Helix, Taiwan). The mitochondrial NADH dehydrogenase 2 gene (ND2) was amplified using the polymerase chain reaction (PCR) with the SL-1 (5'–ATAGAGGTTCAAACCCTCTC–3') and SL-2 (5'–TTAAAGTGTCTGGGTTGCATTCAG–3') primers (Wang et al. 2018). Each PCR reaction consisted of 15 µL of OnePCR™ Ultra (GeneDirex, Taiwan), which is a premixed solution, 1.5 µL of each primer (10 µM), 9 µL of UltraPure™ DNase/RNase-Free distilled water (Invitrogen, USA), and 3 µL of DNA template. The thermal cycling was performed at 94 °C for 4 min, followed by 35 cycles of 94 °C for 30 s, 55 °C for 1 min, and 72 °C for 90 s (Wang et al. 2018). The PCR products were checked by agarose gel electrophoresis to confirm their size and estimate the concentration. The desired PCR products were purified and commercially sequenced by Bioneer Inc. in South Korea.

We combined the three new ND2 sequences of the Mae Tuen WS samples obtained in this study with those of the other related species available from GenBank (Table 1). We then constructed phylogenetic trees by Bayesian inference (BI) and maximum likelihood (ML) analyses using MrBayes v. 3.2.6 (Ronquist et al. 2012) and RAxML-NG v. 1.0.2 (Kozlov et al. 2019), respectively. The optimum substitution models were selected using Kakusan 4 (Tanabe 2011) for BI and ModelTest-NG v. 0.1.7 (Darriba et al. 2020) for ML. The codon-proportional model with the Hasegawa-Kishino-Yano-1985 (HKY85) model + Gamma (G) for each codon position for the BI and criterion used for model selection was AIC, with the codon-equal-rate model with the general time reversible model (GTR) + I + G being selected for ML. The BI analysis was performed as two independent runs of four Markov chains for 10 million generations, sampling one tree every 100 generations and calculating a consensus topology for 10,000 trees after discarding the first 25,001 trees (burn-in = 2,500,000). For the BI, we considered posterior

probabilities (bpp) of 95% or greater as significant support (Leaché and Reeder 2002). The robustness of the ML tree was tested using bootstrap analysis (Felsenstein 1985) with 1,000 replicates, and we accepted tree topologies with bootstrap support (bs) values of ≥ 70% to be significantly supported (Huelsenbeck and Hillis 1993). Pairwise comparisons of uncorrected sequence divergences (*p*-distance by 2,842 base pairs; bps) were calculated using MEGA v. 7 (Kumar et al. 2016).

Morphological examination

Morphometric comparisons and morphological differences between the Mae Tuen WS newts and *T. uyenoi* and *T. umphangensis* were examined using data from Pomchote et al. (2020a) for *T. uyenoi* and from Pomchote et al. (2021b) for *T. umphangensis* for three reasons. Firstly, the color pattern is rather similar between the Mae Tuen WS population and the two chosen *Tylototriton* species. Secondly, the genetic sequence divergences between the Mae Tuen WS newts and the two *Tylototriton* species were found to be lower than those observed in other pairs between Mae Tuen WS newts and the other species (%; as reported in this study). Thirdly, the distribution of the Mae Tuen WS population in the northeastern region (Fig. 1, locality 14) overlaps with the distribution ranges of *T. uyenoi* in its northern (Fig. 1, locality 11) and western (Fig. 1, localities 12 and 13) range, and with *T. umphangensis* in its western range (Fig. 1, locality 15). Moreover, previous studies identified a male newt found at Mae Tuen WS as *T. uyenoi* (Hernandez 2017). Note that the other four *Tylototriton* species present in Thailand (*T. verrucosus*, *T. anguliceps*, *T. phukhaensis*, and *T. panhai*) were not included in this morphometric study for two reasons. Firstly, the external morphology of *T. verrucosus*, *T. anguliceps*, and *T. phukhaensis* are clearly different from that of *Tylototriton* sp. from Mae Tuen WS (see details in Pomchote et al. 2020a, 2020b, 2022); however, morphological comparisons using the published literature were undertaken, as detailed in the morphological comparisons below. Secondly, *T. panhai* has a different color pattern from those of the other Thai *Tylototriton* species. It has a dark ground coloration, with the exception of the dorsal head, upper and lower lips, parotoids, vertebral ridge, rib nodules, tips of fingers and toes, margins of the cloacal slit, and the dorsal and ventral edges of the tail, which are yellow, orange, or reddish brown. In contrast, the other Thai *Tylototriton* species exhibit bright color markings on the head, dorsum, tail, or sides of the body (Nishikawa et al. 2013a; Phimmachak et al. 2015; Hernandez and Pomchote 2020a; Pomchote et al. 2020a, 2020b, 2021b, 2022; this study). Moreover, *T. panhai* is a member of the subgenus *Yaotriton* (Nishikawa et al. 2013a; Dufresnes and Hernandez 2022), while *Tylototriton* sp. from Mae Tuen WS is assigned to the subgenus *Tylototriton* (this study).

A total of 17 male specimens, including the three *Tylototriton* sp. from Mae Tuen WS (CUMZ-A-8253, -8254, and -8256) of this study, plus four specimens of *T. umphangensis* [using data from Pomchote et al. (2021b)] and ten of *T. uyenoi* [using data from Pomchote et al. (2020a)] were used for the morphometric comparison.

The 27 measurements taken for morphometric comparison followed Pomchote et al. (2020a), where the character definitions followed Nishikawa et al. (2011): **SVL** (snout-vent length); **HL** (head length); **HW** (head width); **MXHW** (maximum head width); **SL** (snout length); **LJL** (lower jaw length); **ENL** (eyelid-nostril length); **IND** (internarial distance); **IOD** (interorbital distance); **UEW** (upper eyelid width); **UEL** (upper eyelid length); **OL** (orbit length); **AGD** (axilla-groin

distance); **TRL** (trunk length); **TAL** (tail length); **VL** (vent length); **BTAW** (basal tail width); **MTAW** (medial tail width); **BTAH** (basal tail height); **MXTAH** (maximum tail height); **MTAH** (medial tail height); **FLL** (forelimb length); **HLL** (hind limb length); **2FL** (second finger length); **3FL** (third finger length); **3TL** (third toe length); and **5TL** (fifth toe length). All measurements were taken to the nearest 0.01 mm using a digital sliding caliper, and subsequently rounded to 0.1 mm. The **BWs** were recorded using a digital weighing scale to the nearest 0.1 gm.

The SVL, BW, and the other 26 ratio values to SVL (presented as the % SVL) were compared among the three Thai *Tylototriton* species. Due to the paucity of specimens, we did not conduct statistical tests. The relationships of all morphometric characters were examined using principal component analysis (PCA). All statistical analyses were performed using the SPSS v. 28 for Windows software.

For morphological comparisons, the data of the other related congeners were taken from previous works (Anderson 1871; Fang and Chang 1932; Nussbaum et al. 1995; Hou et al. 2012; Nishikawa et al. 2013a, 2014; Khatiwada et al. 2015; Le et al. 2015; Phimmachak et al. 2015; Fei and Ye 2016; Grismer et al. 2018, 2019; Zaw et al. 2019; Pomchote et al. 2020a, 2020b, 2021b, 2022; Dufresnes and Hernandez 2022; Decemson et al. 2023).

The skulls of each specimen from the new species of this study (CUMZ-A-8253), *T. umphangensis* [CUMZ-A-8246, details of this specimen were reported in Pomchote et al. (2021b)], and *T. uyenoi* [THNHM 13866, loaned from the Natural History Museum, National Science Museum, Thailand (**THNHM**)—details of this specimen were provided in Pomchote et al. (2021b)] were scanned using micro X-ray computerized tomography (micro-CT; Bruker SkyScan 1173; 80 kV and 100 A; distortion-free Flat Panel sensor 2,240 × 2,240 pixels). This scanning process was conducted at the Scientific and Technological Research Equipment Center (**STREC**), Chulalongkorn University, Thailand. The segmentation and 3D reconstruction were performed using 3D Slicer v. 4.11.20200930 (Fedorov et al. 2012).

Results

Molecular analyses

We obtained 452–1,035 bp sequences of the partial ND2 gene region for 20 specimens, including the outgroup (Table 1). The sequences of the three specimens from Mae Tuen WS (this study) were the same, and of the 2,804 nucleotide sites, 451 were variable and 158 were parsimony informative within the ingroup (sequence statistics available upon request from the senior author). The mean likelihood score of the BI analyses for all trees sampled at stationary was −7689.148. The likelihood value of the ML tree was −7652.488946.

Phylogenetic analyses employing the BI and ML criteria yielded nearly identical topologies and so we present only the BI tree in Fig. 3. Monophyly of the subgenus *Tylototriton* was fully supported in the BI and ML trees (bpp = 98% and bs = 96%). Within this subgenus, *T. kweichowensis* was first separated from the remaining lineages. The latter group was further divided into two clades: one including *T. shanorum*, *T. himalayanus*, and *T. kachinorum*; the other included the remaining lineages. The newts from Mae Tuen WS were nested in the latter clade and were clustered with *T. uyenoi* with significant support.

Table 1. Specimens of *Tylototriton* and other related species used for the molecular analyses in this study. CAS = California Academy of Sciences; CIB = Chengdu Institute of Biology; CUMZ (A) = Natural History Museum of Chulalongkorn University Section Amphibians; KIZ = Kunming Institute of Zoology; KUHE = Graduate School of Human and Environmental Studies, Kyoto University; MVZ = Museum of Vertebrate Zoology, University of California, Berkeley; NMNS = National Museum of Natural Science, Taiwan; VNMN = Vietnam National Museum of Nature; ZMMU = Zoological Museum of Moscow State University. *Topotype.

Sample no.	Species	Voucher no.	Locality	GenBank acc. no.	Source
Ingroup					
1	*Tylototriton soimalai* sp. nov.	CUMZ-A-8253	Mae Tuen Wildlife Sanctuary, Tak, Thailand	PQ218721	This study
2	*Tylototriton soimalai* sp. nov.	CUMZ-A-8254	Mae Tuen Wildlife Sanctuary, Tak, Thailand	PQ218722	This study
3	*Tylototriton soimalai* sp. nov.	CUMZ-A-8256	Mae Tuen Wildlife Sanctuary, Tak, Thailand	PQ218723	This study
4	*Tylototriton umphangensis**	CUMZ-A-8243	Umphang Wildlife Sanctuary, Tak, Thailand	OK092618	Pomchote et al. (2021b)
5	*Tylototriton uyenoi**	KUHE 19147	Doi Suthep, Chiang Mai, Thailand	AB830733	Nishikawa et al. (2013a)
6	*Tylototriton phukhaensis**	CUMZ-A-7719	Doi Phu Kha National Park, Nan, Thailand	MN912575	Pomchote et al. (2020b)
7	*Tylototriton anguliceps**	VNMN A.2014.3	Muong Nhe, Dien Bien, Vietnam	LC017832	Le et al. (2015)
8	*Tylototriton verrucosus**	KIZ 201306055	Husa, Yunnan, China	AB922818	Nishikawa et al. (2014)
9	*Tylototriton panhai**	No voucher	Phu Luang Wildlife Sanctuary, Loei, Thailand	AB830736	Nishikawa et al. (2013a)
10	*Tylototriton shanjing**	NMNS 3682	Jingdong, Yunnan, China	AB830721	Nishikawa et al. (2013a)
11	*Tylototriton pulcherrimus*	KUHE 46406	Yunnan, China	AB830738	Nishikawa et al. (2013a)
12	*Tylototriton podichthys*	KUHE 34399	Xam Neua, Houa Phan, Laos	AB830727	Nishikawa et al. (2013a)
13	*Tylototriton panwaensis**	CAS 245418	Panwa, Myitkyina, Myanmar	KT304279	Grismer et al. (2018)
14	*Tylototriton yangi*	KUHE 42282	Yunnan, China	AB769546	Nishikawa et al. (2013b)
15	*Tylototriton shanorum**	CAS 230940	Taunggyi, Shan, Myanmar	AB922823	Nishikawa et al. (2014)
16	*Tylototriton himalayanus*	MVZ no number	Nepal	DQ517854	Weisrock et al. (2006)
17	*Tylototriton kachinorum**	ZMMU A5953	Indawgyi, Kachin, Myanmar	MK097273	Zaw et al. (2019)
18	*Tylototriton kweichowensis*	MVZ 230371	Daguan, Yunnan, China	DQ517851	Weisrock et al. (2006)
19	*Tylototriton taliangensis*	KUHE 43361	Unknown, China	AB769543	Nishikawa et al. (2013b)
Outgroup					
20	*Echinotriton andersoni**	KUHE no number	Nago, Okinawa, Japan	AB769545	Nishikawa et al. (2013b)

The *p*-distances between each pair of a total 19 haplotypes recognized above ranged from 0.8% (between *Tylototriton* sp. specimens) to 11.7% (between *T. uyenoi* and *T. kachinorum*) (Table 2). The distance between the newts from Mae Tuen WS and its sister species *T. uyenoi* was 4.1–4.2%, which was less than and/or comparable (4.2% between *T. anguliceps* and *T. verrucosus*, and 4.3% between *T. anguliceps* and *T. phukhaensis*) to the 17 heterospecific combinations in this study.

Morphological examination

A total of 17 adult males were used for the morphometric comparisons and morphological differences, as shown in Table 3 and Table 4, respectively. The Mae Tuen WS samples, *T. uyenoi*, and *T. umphangensis* showed some similar morphological characteristics. For instance, the nostrils were visible from the dorsal view, the surface of the dorsolateral bony ridges was rough, the glandular skin was dense, particularly on the dorsum, and the tips of the fore- and hind limbs overlapped when adpressed along the body. However, there were morphological

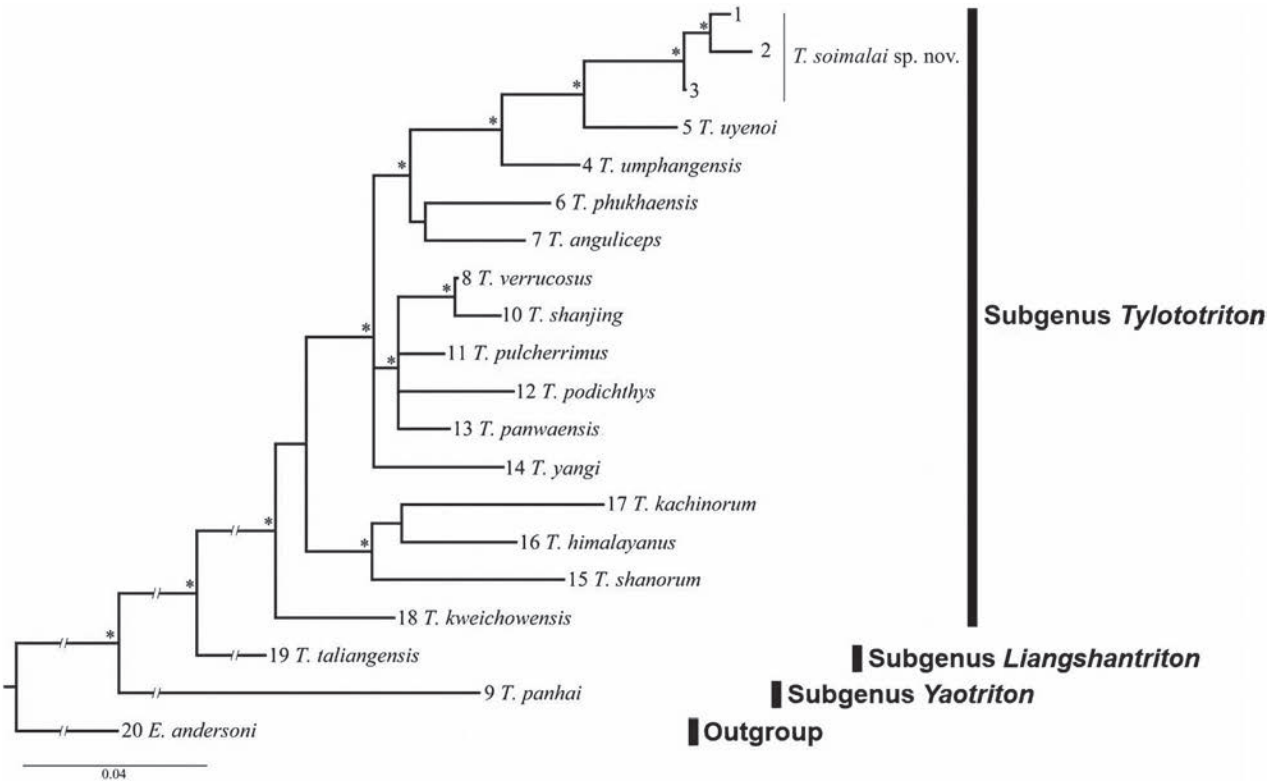

Figure 3. Bayesian inference tree based on the partial ND2 gene for the samples examined. Asterisks indicate nodes with bpp ≥ 0.95 and bs ≥ 70%. Numbers at branch tips are the sample numbers, as shown in Table 1. Scale bar: 0.04 substitutions/site.

differences between the Mae Tuen WS samples and the other two *Tylototriton* species. For example, in lateral view, the dorsolateral bony ridges of the Mae Tuen WS population were oriented rather parallel to body axis, while those of *T. uyenoi* and *T. umphangensis* were oriented obliquely upwards and curved upwardly at the posterior end. The vertebral ridge of the Mae Tuen WS population was not segmented, while those of *T. uyenoi* and *T. umphangensis* were segmented (see details in Table 4). Regarding coloration, they displayed rather similar color patterns. In life, *T. uyenoi* had a dark brown to black color background, while the Mae Tuen WS samples and *T. umphangensis* were black. The dorsal and ventral head, parotoids, vertebral ridge, rib nodules, limbs, vent, and tail were orange-brown in *T. umphangensis*, being dark orange-brown in *T. uyenoi*, but the Mae Tuen WS samples had a somewhat paler orange coloration. The ventral tail ridge had the brightest coloration among these three congeners. In preservative, the color pattern of *T. umphangensis* remained relatively similar to that observed in life after approximately two years. However, the background color of the *Tylototriton soimalai* sp. nov. samples was blackish brown, and the color markings shifted to a paler orange hue after one year in preservative.

The overall morphological differences between the *Tylototriton soimalai* sp. nov. population and the other two *Tylototriton* species included in the morphological study were examined using PCA. The first two principal components (PCs) accounted for 49.4% of the total variation. The two-dimensional PC1 vs PC2 plot showed that the *Tylototriton soimalai* sp. nov. population was clustered together and completely separated from its closely related species, *T. uyenoi* and *T. umphangensis* (Fig. 4).

Table 2. Uncorrected *p*-distance (%) of the ND2 region between samples examined in this study.

Sample no.	Species	Sample no.																		
		1	2	3	4	5	6	7	8	9	10	11	12	13	14	15	16	17	18	19
1	*Tylototriton soimalai* sp. nov.																			
2	*Tylototriton soimalai* sp. nov.	0.010																		
3	*Tylototriton soimalai* sp. nov.	0.008	0.010																	
4	*Tylototriton umphangensis*	0.057	0.058	0.057																
5	*Tylototriton uyenoi*	0.041	0.042	0.041	0.049															
6	*Tylototriton phukhaensis*	0.080	0.083	0.070	0.060	0.072														
7	*Tylototriton anguliceps*	0.068	0.069	0.068	0.050	0.073	0.043													
8	*Tylototriton verrucosus*	0.072	0.073	0.072	0.048	0.071	0.048	0.042												
9	*Tylototriton panhai*	0.137	0.138	0.137	0.139	0.142	0.128	0.130	0.124											
10	*Tylototriton shanjing*	0.075	0.076	0.075	0.053	0.075	0.054	0.045	0.009	0.124										
11	*Tylototriton pulcherrimus*	0.067	0.068	0.067	0.055	0.068	0.044	0.040	0.019	0.120	0.025									
12	*Tylototriton podichthys*	0.081	0.082	0.081	0.070	0.084	0.058	0.050	0.035	0.123	0.039	0.033								
13	*Tylototriton panwaensis*	0.076	0.079	0.066	0.054	0.076	0.053	0.044	0.022	0.126	0.031	0.026	0.034							
14	*Tylototriton yangi*	0.075	0.076	0.075	0.056	0.075	0.056	0.042	0.038	0.126	0.045	0.038	0.049	0.041						
15	*Tylototriton shanorum*	0.095	0.096	0.095	0.083	0.093	0.078	0.068	0.062	0.124	0.066	0.066	0.074	0.066	0.068					
16	*Tylototriton himalayanus*	0.091	0.095	0.080	0.079	0.086	0.067	0.067	0.062	0.123	0.061	0.063	0.067	0.064	0.065	0.052				
17	*Tylototriton kachinorum*	0.111	0.111	0.111	0.088	0.117	0.086	0.077	0.071	0.133	0.080	0.077	0.080	0.064	0.082	0.077	0.053			
18	*Tylototriton kweichowensis*	0.083	0.085	0.072	0.077	0.081	0.058	0.060	0.053	0.106	0.056	0.052	0.056	0.052	0.060	0.062	0.060	0.064		
19	*Tylototriton taliangensis*	0.097	0.098	0.097	0.093	0.100	0.086	0.085	0.073	0.106	0.070	0.072	0.078	0.077	0.078	0.083	0.076	0.073	0.063	
20	*Echinotriton andersoni*	0.181	0.180	0.181	0.172	0.181	0.168	0.166	0.159	0.155	0.161	0.157	0.161	0.149	0.160	0.159	0.157	0.188	0.152	0.148

Table 3. Morphometric comparisons of the examined specimens of *Tylototriton* [median SVL (in mm), BW (in g), and ratios of characters (R: % SVL), with the range in parentheses]. Data for *T. uyenoi* are derived from Pomchote et al. (2020a) and for *T. umphangensis* are derived from Pomchote et al. (2021b). For character abbreviations refer to the text.

	***T. soimalai* sp. nov.**	***T. umphangensis***	***T. uyenoi***
	3 males	**4 males**	**10 males**
SVL	66.5 (66.3–66.5)	73.5 (65.6–75.3)	71.1 (68.9–75.8)
BW	12.2 (10.8–12.7)	12.4 (10.2–13.3)	15.1 (11.2–17.0)
RHL	27.2 (27.1–27.4)	23.0 (22.0–25.2)	25.1 (24.2–26.3)
RHW	21.7 (21.4–23.0)	21.4 (19.4–22.7)	18.8 (17.5–19.3)
RMXHW	24.7 (24.4–24.9)	25.6 (25.0–26.9)	25.8 (24.5–26.4)
RSL	9.4 (8.2–9.5)	8.8 (8.2–9.8)	8.8 (8.1–9.4)
RLJL	24.3 (23.6–24.3)	22.8 (22.1–23.5)	22.0 (20.7–22.5)
RENL	5.9 (5.2–6.1)	5.8 (5.6–6.2)	6.8 (6.0–7.5)
RIND	5.5 (5.2–5.6)	6.2 (5.8–6.5)	6.8 (5.6–7.5)
RIOD	13.3 (12.7–13.7)	13.2 (12.9–13.7)	13.0 (12.6–14.4)
RUEW	3.5 (3.1–3.7)	2.5 (2.3–2.9)	3.1 (2.2–3.8)
RUEL	7.1 (6.3–7.3)	6.0 (5.5–6.4)	6.4 (5.8–7.1)
ROL	4.0 (3.7–4.3)	3.0 (2.7–3.3)	4.2 (3.5–4.8)
RAGD	50.6 (50.4–57.3)	53.7 (51.9–54.4)	49.9 (45.7–52.3)
RTRL	76.5 (74.1–80.0)	76.8 (75.4–77.4)	75.0 (71.8–98.0)
RTAL	101.5 (90.7–109.3)	104.7 (91.9–107.3)	98.0 (88.8–110.4)
RVL	9.7 (6.6–9.9)	8.0 (7.3–9.4)	12.4 (7.4–15.3)
RBTAW	12.1 (11.0–14.1)	14.5 (12.6–15.1)	5.8 (4.4–6.2)
RMTAW	3.0 (2.9–3.8)	2.3 (2.2–2.4)	3.7 (2.9–4.3)
RBTAH	11.9 (11.6–13.8)	15.0 (11.9–15.3)	12.1 (11.5–12.9)
RMXTAH	15.5 (14.6–16.7)	11.1 (8.8–12.1)	12.7 (11.0–14.2)
RMTAH	15.9 (14.2–16.2)	10.6 (7.9–12.0)	11.8 (11.0–13.3)
RFLL	41.4 (38.2–41.8)	37.0 (34.2–40.5)	43.7 (42.6–44.6)
RHLL	39.1 (37.1–39.5)	38.4 (35.2–41.9)	44.8 (42.3–48.1)
R2FL	6.3 (5.9–7.0)	7.1 (6.7–8.1)	5.5 (4.5–6.8)
R3FL	6.7 (6.5–7.6)	7.6 (5.6–8.9)	6.8 (5.5–7.4)
R3TL	9.5 (7.2–9.6)	9.3 (8.9–11.0)	8.3 (7.0–9.2)
R5TL	3.4 (2.8–4.4)	4.9 (4.8–5.7)	4.1 (2.8–6.1)

Table 4. Morphological comparisons between *Tylototriton soimalai* sp. nov. and *T. umphangensis* and *T. uyenoi*. Data for *T. uyenoi* are modified from Pomchote et al. (2020a), and *T. umphangensis* are modified from Pomchote et al. (2021b).

Characters	***T. soimalai* sp. nov.**	***T. umphangensis***	***T. uyenoi***
Number and sex	3 males	4 males	10 males
Snout in dorsal view	Blunt or truncate	Truncate	Rounded to blunt
Snout in lateral view	Projecting beyond lower jaw	Hardly projecting beyond lower jaw	Projecting beyond lower jaw
Sagittal ridge	Narrow, short	Wide	Wide
Dorsolateral bony ridges in dorsal view	Weakly or hardly curved medially at posterior end	Distinctly curved medially at posterior end	Weakly or rather curved medially at posterior end
Dorsolateral bony ridges in lateral view	Oriented rather parallel to body axis	Oriented obliquely upwards and curved upwardly at posterior end	Oriented obliquely upwards and curved upwardly at posterior end
Parotoids in lateral view	Oriented rather parallel to body axis and slightly or hardly curved upwardly at posterior end	Oriented rather parallel to body axis and curved upwardly at posterior end	Oriented obliquely downwardly or rather parallel to body axis and not curved or curved upwardly at posterior end
Vertebral ridge	Not segmented	Segmented	Segmented
Rib nodules	Distinct, rounded, isolated but connected posteriorly, 14–16	Indistinct, rounded anteriorly to irregularly shaped posteriorly, isolated, 14–15	Distinct, rounded, isolated, 12–16

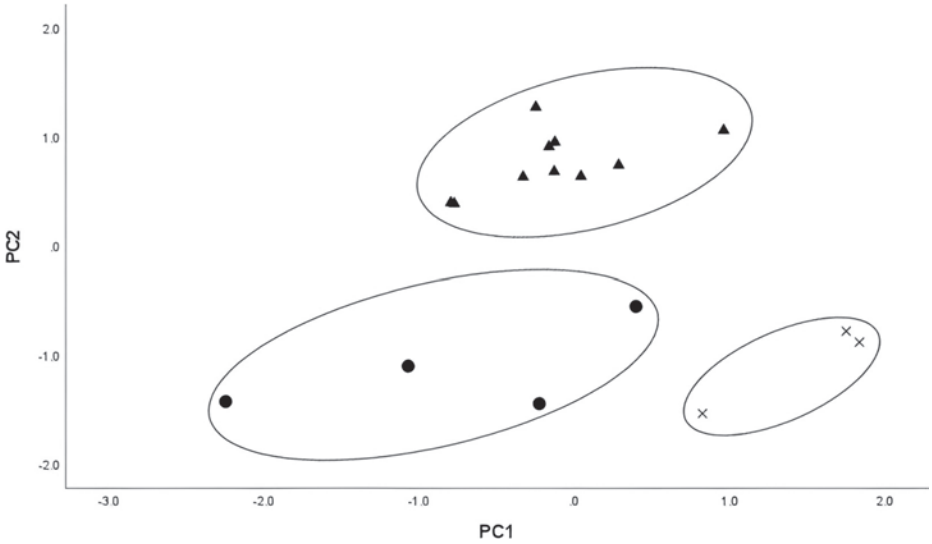

Figure 4. The PCA plots of PC1 versus PC2 for morphological parameters of the samples examined: **cross** *Tylototriton soimalai* sp. nov. **circle** *T. umphangensis* **triangle** *T. uyenoi*.

There are some differences in the skull morphology among *Tylototriton soimalai* sp. nov., *T. uyenoi*, and *T. umphangensis* (Fig. 5). For example, the distance between the nostrils was widest in *T. umphangensis*, followed by *Tylototriton soimalai* sp. nov. and *T. uyenoi*, respectively. The midsagittal ridge was more distinct in *Tylototriton soimalai* sp. nov. compared to *T. uyenoi* and *T. umphangensis*. Additionally, the density of secondary bony ridges was greater in *T. uyenoi* and *T. umphangensis* compared to *Tylototriton soimalai* sp. nov. However, the most prominently different character among the skull of the three species was the direction of the posterior ends of the dorsolateral bony ridges in the posterior view. In *Tylototriton soimalai* sp. nov., they were directed more upwards than those of *T. uyenoi*, while in *T. umphangensis*, they were directed downwards.

Based on the molecular and morphological evidence, we herein describe the *Tylototriton* sp. from Mae Tuen WS, Tak Province, northwestern Thailand as a new species, *Tylototriton soimalai* sp. nov.

Systematics

***Tylototriton soimalai* sp. nov.**
https://zoobank.org/8CB99CD2-A029-4FD4-928C-82AD853F9A04
Figs 2, 5–8
(Thai name: Ka Tang Nam Doi Soi Malai)
(English name: Doi Soi Malai Crocodile Newt)

Tylototriton uyenoi: Hernandez (2017): 110.

Type material. ***Holotype*** • CUMZ-A-8253, adult male, collected from Doi Soi Malai, Mae Tuen Wildlife Sanctuary, Tak Province, northwestern Thailand, at ca 1,500 m a.s.l., collected on the 31 August 2022 by Porrawee Pomchote and Pitak Sapewisut. Data regarding the specific location (geographical coordinates) of the new species cannot be publicly disclosed due to the need to prevent illegal hunting, which has been increasing dramatically in Thailand. However,

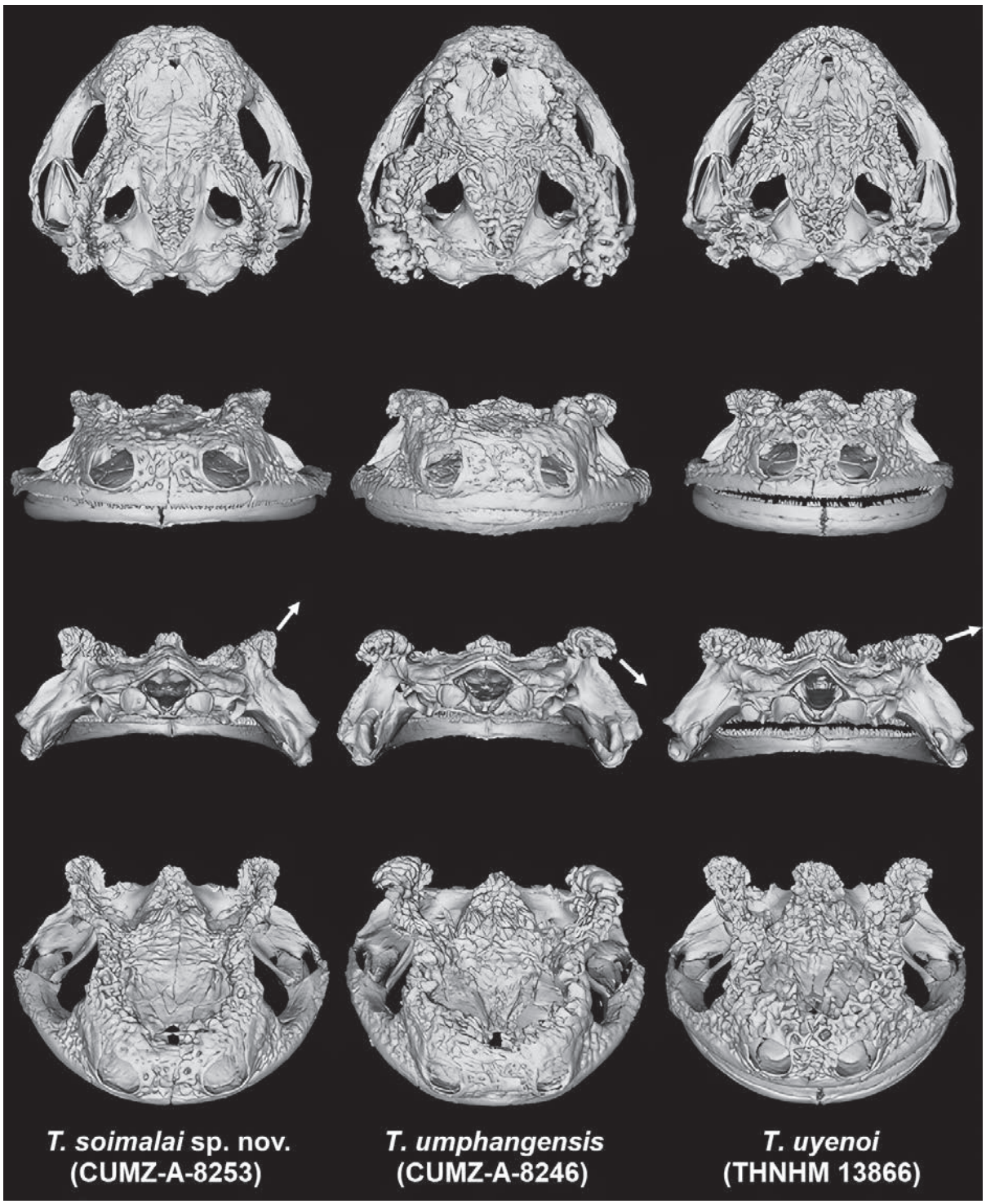

Figure 5. Three-dimensional model of the skull of *Tylototriton soimalai* sp. nov. (left), *T. umphangensis* (center), and *T. uyenoi* (right) based on micro-CT reconstruction. **Top** dorsal view **Second from the top** anterior view **Second from the bottom** posterior view **Bottom** anteriodorsal view. White arrows representing directions of posterior ends of dorsolateral bony ridges.

the data are available to the editors or reviewers if necessary. ***Paratypes*** • CUMZ-A-8254 and CUMZ-A-8256; two adult males, same data as the holotype.

Etymology. The specific epithet *soimalai* refers to Doi Soi Malai, Mae Tuen Wildlife Sanctuary, the type locality of the new species; it is a noun in apposition, thus invariable.

Diagnosis. *Tylototriton soimalai* sp. nov. is assigned to the genus *Tylototriton* by having a combination of dorsal granules present, dorsolateral bony ridges on head present, knob-like warts or rib nodules on dorsolateral body present, and quadrate spine absent. *Tylototriton soimalai* sp. nov. is distinguished from its congeners by a combination of the following morphological characters: (1) medium-sized, adult SVL 66.3–66.5 mm in males; (2) skin rough with fine granules; (3) head longer than wide; (4) snout blunt or truncate in dorsal view, and extending beyond the lower jaw in lateral view; (5) sagittal ridge on head narrow, short, and distinct; (6) dorsolateral bony ridges on head pronounced, with rough surface, posterior ends weakly or hardly curved medially in dorsal view, and oriented rather parallel to the body axis in lateral view; (7) parotoids distinct, oriented rather parallel to the body axis and posterior ends slightly or hardly curved upwards in lateral view; (8) vertebral ridge prominent, wide, and not segmented; (9) rib nodules distinct, rounded, and isolated but posterior nodules connected, 14–16 along each side of body; (10) limbs long, tips of forelimbs and hind limbs overlapping when adpressed along body; (11) tail laterally compressed, lacking lateral grooves, and tip pointed; (12) background coloration black; (13) dorsal, ventral, and lateral of head, parotoids, vertebral ridge, rib nodules, limbs, vent region, and whole tail with orange markings.

Description of holotype. Body slim and long (RTRL 80.0%); skin rough; fine granules dense on dorsum, dense on both sides of body and tail, and sparse on ventral trunk; head longer than wide (HW/HL 0.8), hexagonal in shape, depressed, and slightly oblique in profile; snout truncate in dorsal view, projecting beyond lower jaw in lateral view; eyes protrude from dorsolateral portion of head in dorsal view, and upper eyelids prominent in lateral view; nostrils close to snout tip, visible from dorsal view; sagittal ridge on head narrow, short, and distinct; dorsolateral bony ridges on head pronounced, rough, and posterior ends weakly curved proximally in dorsal view; labial fold absent; tongue oval, attached to anterior floor of mouth, free laterally and posteriorly; vomerine tooth series in an inverted V-shape, converging anteriorly, and reaching choanae; parotoids distinct, projecting posteriorly, posterior ends hardly curved medially in dorsal view, oriented rather parallel to body axis and hardly curved upwards in lateral view; gular fold present; costal folds absent; vertebral ridge prominent, wide, and not segmented, separated from sagittal ridge on head; rib nodules distinct, rounded, forming knob-like warts, 14 on left side and 16 on right side of body from axilla to base of tail; rib nodules isolated but posterior nodules connected; rib nodules slightly increasing in size from most anterior to third nodule, then decreasing posteriorly; forelimbs (41.8% SVL) longer than hind limbs (39.5% SVL); tips of forelimb and hind limb overlapping when adpressed along body; fingers and toes well developed, free of webbing; fingers four, comparative finger lengths 3 > 2 > 1 > 4; toes five, comparative toe lengths 3 > 4 > 2 > 5 > 1; tail laterally compressed, lacking lateral grooves, dorsal fin and ventral edge smooth, tip pointed; tail as long as body length (101.5% SVL); cloaca slightly swollen; vent slit longitudinal.

Color of holotype. In life, dorsal ground coloration is black, while the ventral color is dark grayish, paler than dorsum. Dorsal, ventral, and lateral of head, parotoids, vertebral ridge, rib nodules, limbs, vent region, and whole tail are orange. Tip of tail is slightly paler than dorsal and lateral sides of tail. Ventral side of head, part of pectoral and pubic region, limbs, and tail are paler than dorsum. The palest is the ventral edge of the tail. The paler region between the ventral

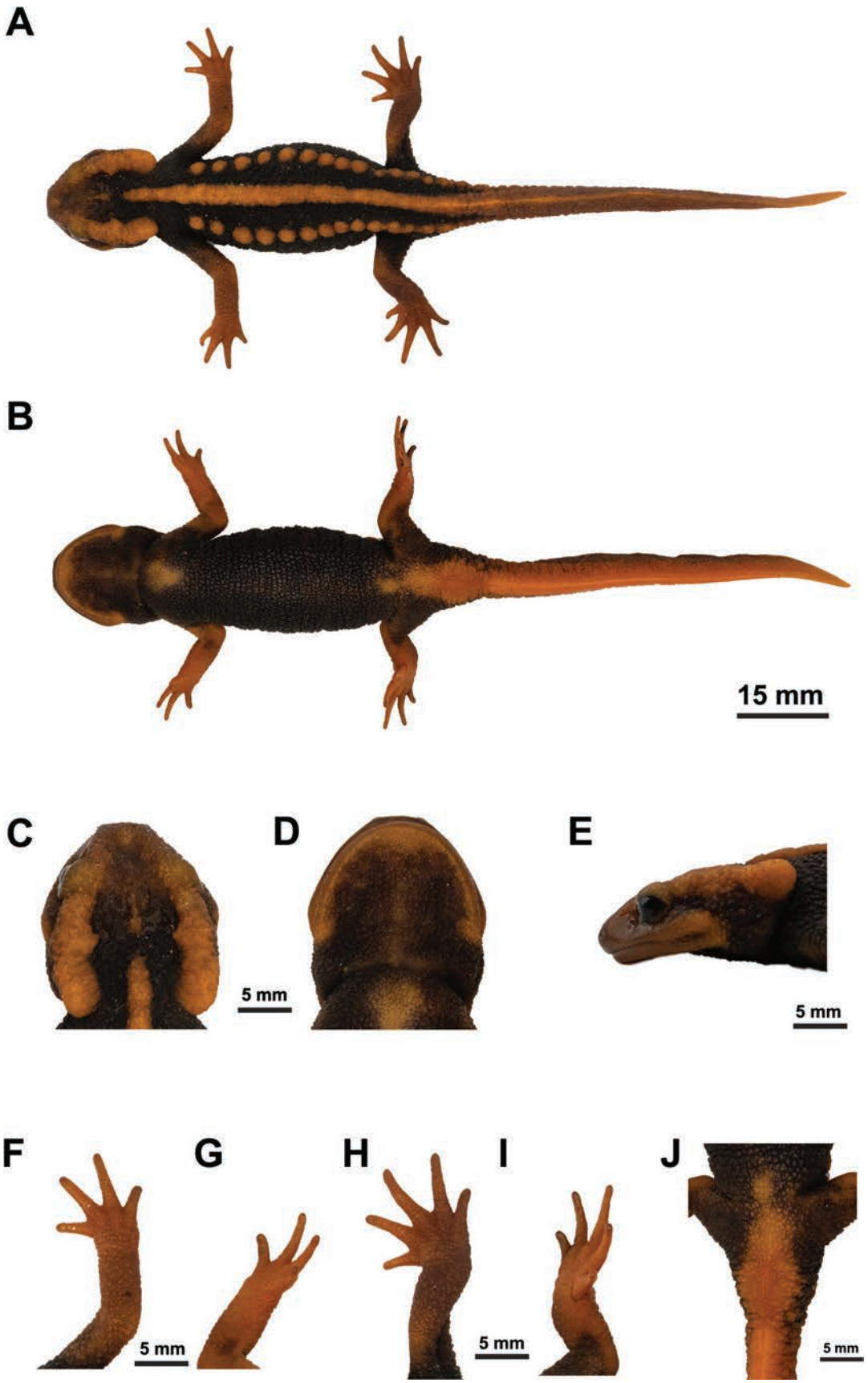

Figure 6. The male holotype of *Tylototriton soimalai* sp. nov. (CUMZ-A-8253) before preservation **A** dorsal view **B** ventral view **C** dorsal head **D** ventral head **E** lateral head **F** dorsal right hand **G** ventral right hand **H** dorsal right foot **I** ventral right foot **J** cloacal area.

edge of the tail and the area of the vent is connected. After preservation in ethanol for approximately one year, the background color is blackish brown, and the color markings are faded to pale orange.

Measurement of holotype (in mm). SVL 66.5; HL 18.0; HW 14.3; MXHW 16.6; SL 6.3; LJL 16.2; ENL 4.0; IND 3.7; IOD 8.9; UEW 4.2; UEL 2.1; OL 2.5; AGD 38.1; TRL 53.3; TAL 67.5; VL 6.5; BTAW 9.4; MTAW 2.5; BTAH 7.9; MXTAH 10.3; MTAH 10.6; FLL 27.8; HLL 26.3; 2FL 4.2; 3FL 5.1; 3TL 6.3; and 5TL 2.9.

Variation. All specimens generally exhibit a similar morphology and coloration; however, some differences were observed among the three specimens. The snout of the holotype is truncate, while those of two paratypes (CUMZ-A-8254 and CUMZ-A-8256) are blunt. The sagittal ridge is most distinct in the holotype, followed by CUMZ-A-8256 and CUMZ-A-8254, respectively. Dorsolateral bony ridges of the holotype and one paratype (CUMZ-A-8254) weakly curve medially in dorsal view, in contrast to the other paratype where they hardly curve medially in dorsal view. The posterior ends of parotoids in two paratypes slightly curve upwards in lateral view compared to the holotype that hardly curve upwards in lateral view. Rib nodules of the holotype are 14 on the left side and 16 on the right side of the body from axilla to base of tail, while the two paratypes have 14 on left side and 15 on right side (CUMZ-A-8254) or 15 on both left and right sides (CUMZ-A-8256). One paratype (CUMZ-A-8256) has five fingers on the left forelimb; moreover, all finger lengths on the left forelimb are short. The dorsal tail fin is smooth in the holotype, whereas in the other paratypes it is uneven with CUMZ-A-8256 exhibiting the most pronounced unevenness. The color marking on the dorsal side of the holotype is the palest compared to the two paratypes. The palest color marking on the ventral side of the head is clearly observed in one paratype (CUMZ-A-8254) followed by CUMZ-A-8256 and the holotype, respectively. The part of the ventral trunk of two paratypes exhibits a pale color marking, whereas there is no pale color marking on the ventral trunk of the holotype.

Larva. Two larvae one nearly double the size of the other (Fig. 2). Head large. Eyes well visible. Three pairs of external gills present. Body and tail laterally compressed. Skin smooth. Costal grooves of larger-sized larva rather distinct, but smaller-sized larva indistinct. Dorsal and ventral fins present. Background color of larger larva pale brown with scattered black pigments. Parts of lateral body, ventral fin, and around eyeballs silver-purple, while the smaller larva had a pale brown background with dense black pigments. Parts of lateral body, and around eyeballs silver-purple. External gills of both larvae red-brown.

Comparisons. *Tylototriton soimalai* sp. nov. is a member of the subgenus *Tylototriton* based on the molecular phylogenetic analyses. The new species can be distinguished from the other members of the subgenus *Tylototriton* as follows: from *T. anguliceps*, *T. phukhaensis*, *T. kachinorum*, and *T. shanorum* by having a narrow, short, and distinct sagittal ridge (vs prominent in *T. anguliceps*, narrow, long, and distinct in *T. phukhaensis*, very weak and almost indistinct in *T. kachinorum*, and absent in *T. shanorum*); from *T. verrucosus* and *T. podichthys* by having rough dorsolateral bony ridges (vs smooth in *T. verrucosus* and very rough in *T. podichthys*); from *T. zaimeng* by having an inverted V-shape of the vomerine tooth series (vs a bell-shape in *T. zaimeng*); from *T. panwaensis* by having a non-segmented vertebral ridge (vs weakly segmented in *T. panwaensis*); from *T. himalayanus* by lacking grooves on either side at the base of tail (vs present in *T. himalayanus*); from *T. shanjing* by having no sharp contrast between

Figure 7. Holotype (CUMZ-A-8253) and paratypes (CUMZ-A-8254 and CUMZ-A-8256) of *Tylototriton soimalai* sp. nov. before preservation **A** dorsal view **B** ventral view.

the orange crown of the head and black nape (vs sharp contrast in *T. shanjing*); from *T. yangi* by having uniformly orange parotoids (vs black coloration except for posterior end of parotoids with orange coloration in *T. yangi*); from *T. kweichowensis* by having isolated pale markings on rib nodules (vs connected markings forming continuous pale dorsolateral lines in *T. kweichowensis*); from *T. ngarsuensis* by having orange markings on parotoids, vertebral ridge, rib nodules, and limbs (vs dark-brown, nearly black coloration in *T. ngarsuensis*); from *T. houi* by having orange markings on the head, trunk, limbs, and tail (vs extensive orange-red markings in *T. houi*); and from *T. pulcherrimus* by lacking pale spots located ventrolaterally and on flanks (vs present in *T. pulcherrimus*).

Distribution. *Tylototriton soimalai* sp. nov. is currently known from only Doi Soi Malai, Mae Tuen Wildlife Sanctuary, Tak Province, northwestern Thailand. However, Doi Soi Malai-Mai Klay Pen Hin National Park, which is contiguous to Mae Tuen Wildlife Sanctuary, is also expected to be a habitat for this species.

Natural history. The new species were found during the midday, at ~ 12:00 h when the adult males came up to the water surface, and the two larvae lived in a single isolated mud puddle situated along the road to the top of Doi Soi Malai during the rainy season, which is the breeding season of *Tylototriton* species. The puddle had turbid water and the bottom was deposited with muddy sediment. The surrounding area of the puddle consisted of evergreen hill forests. The puddle size was approximately 1,000 cm long, 500 cm wide, and 35 cm in maximum depth. No fish were observed.

Conservation recommendation. The type locality of *Tylototriton soimalai* sp. nov. is a well-known destination for mountain biking and 4×4 road trips, particularly in the period following the late rainy season, starting from October onwards, when these activities extend to the summit of Doi Soi Malai. Although, the Department of National Parks, Wildlife and Plant Conservation (DNP) has imposed a ban on motor races in Thai NPs and WSs (The Nation 2019), some mountain biking and 4×4 road trips continue to violate these regulations by entering the Mae Tuen Wildlife Sanctuary (Park rangers, personal communications), likely due to the paved road that runs through the sanctuary, providing easy access (Pattanavibool and Dearden 2002). This could have adverse effects on the population of this new species, particularly during the larval stage, because the breeding site we found in this study is situated along the road leading to the summit of Doi Soi Malai. In nature, the breeding season of Thai *Tylototriton* species is around the end of April to August during the monsoon season (Pomchote et al. 2008; Hernandez and Pomchote 2020a, 2021). Aquatic larvae of *Tylototriton* inhabit the breeding water for several months and undergo complete metamorphosis before the efts start to move to land (Hernandez 2016). Based on data from Thai *Tylototriton* species in their natural habitat, larvae were found in the water bodies from August to November in *T. panhai* (Hernandez and Pomchote 2020a), from August to December in *T. uyenoi* (Nishikawa et al. 2013a; Pomchote, unpublished data), in December in *T. verrucosus* (Pomchote, unpublished data), and from December to March in *T. anguliceps* (Pomchote, unpublished data). Therefore, the breeding site should not be disturbed by any anthropogenic activities, especially road disturbances. We strongly recommend that the road to the summit of Doi Soi Malai be opened only after the breeding site has dried up, or alternatively, the road should be accessible during the winter and dry seasons, with walking to the peak as the preferred option.

Figure 8. The male holotype of *Tylototriton soimalai* sp. nov. (CUMZ-A-8253) observed at the type locality.

Based on our multiple surveys conducted across various locations at Mae Tuen Wildlife Sanctuary in all seasons, we encountered only a few newts during the most recent survey at a single location on the 31 August 2022, suggesting that the population of the new species is small. Moreover, in addition to the road disturbances mentioned earlier, both the areas surrounding and within Mae Tuen Wildlife Sanctuary have been heavily impacted by habitat alteration and deforestation, leading to forest fragmentation, primarily due to agricultural activities, especially cabbage cultivation (Pattanavibool and Dearden 2002). Due to the reasons mentioned above, we recommend that *Tylototriton soimalai* sp. nov. be listed as Endangered (EN) [IUCN Red List criteria B1ab(iii)+2ab(iii)] and, a conservation plan is urgently needed for this new species.

Discussion

The current study employed morphological evidence, including external morphology, morphometrics, skull morphology, and molecular data. Consequently, the newt population from Doi Soi Malai, Mae Tuen WS in Tak Province, northwestern Thailand, previously identified as *T. uyenoi* (Hernandez 2017), is described as a new species, *Tylototriton soimalai* sp. nov. Although the *T. uyenoi* specimens generally exhibit similarity in their morphology and color pattern, they display some morphological variations (Nishikawa et al. 2013a; Pomchote et al. 2020a) that may lead to confusion, particularly when attempting identification based on a limited number of individuals and external morphological characters without considering skull morphology or genetic analysis. Thus, conducting field surveys at the previously surveyed locations, voucher specimen collection, and both morphological and molecular analyses are essential for clarifying the taxonomic status and distri-

bution range of *T.* cf. *uyenoi*. This is particularly the case at Doi Mak Lang, Chiang Dao WS, and Doi Mon Jong at Chiang Mai Province (Fig. 1, localities 6, 8, and 11, respectively); Mae Wong NP at Kamphaeng Phet Province (Fig. 1, locality 12); and Khao Laem NP at Kanchanaburi Province (Fig. 1, locality 13). These efforts will also help to clarify the boundaries between *Tylototriton soimalai* sp. nov., *T.* cf. *uyenoi*, and *T. umphangensis* in order to manage a future conservation plan.

In summary, the genus *Tylototriton* currently comprises 41 nominal species, with seven of them occurring in Thailand: *T. verrucosus*, *T. uyenoi*, *T. anguliceps*, *T. phukhaensis* from the northern region, *T. panhai* from the northern and northeastern regions, *Tylototriton soimalai* sp. nov. from the northwestern region, and *T. umphangensis* from the western region (Fig. 1) (Nishikawa et al. 2013a; Le et al. 2015; Hernandez and Pomchote 2020a; Pomchote et al. 2020a, 2020b, 2021b, 2022; this study).

Acknowledgements

We are grateful to Mae Tuen Wildlife Sanctuary staff for facilitating the field support; Nuttakorn Taewcharoen for reconstructing the 3D skulls and for modifying figures; Asami Kimoto for helping molecular analysis; Santi Pailoplee for providing the elevation map of Thailand; and Keratika Boonkum for rechecking some data. We thank the Department of National Parks, Wildlife and Plant Conservation (DNP) for research permission. We also thank the Natural History Museum, National Science Museum, Thailand (THNHM) for allowing us to examine the specimens of *T. uyenoi*.

Additional information

Conflict of interest

The authors have declared that no competing interests exist.

Ethical statement

The experimental protocol was approved by the Animal Care and Use Committee of Faculty of Science, Chulalongkorn University (Protocol Review No. 2123012).

Funding

This research was supported by the Plant Genetic Conservation Project Under the Royal initiative of Her Royal Highness Princess Maha Chakri Sirindhorn (RSPG) responded by Chulalongkorn University to Porrawee Pomchote (GB_65_01_23_01) and partly supported by the Kyoto University Foundation in 2008, the Ministry of Education, Science and Culture, Japan (no. 18H03602), and JSPS Core-to-Core program B [to Kanto Nishikawa (coordinator: Masaharu Motokawa)].

Author contributions

Conceptualization: PP. Data curation: PP. Formal analysis: PP, KN. Funding acquisition: PP. Investigation: PP, PP. Methodology: PP. Project administration: PP. Resources: PS, KN, PP, PS, WK, CP. Supervision: PP. Validation: PP. Visualization: KN, PP, PP. Writing – original draft: WK, KN, PP, AH. Writing – review and editing: PP, KN.

Author ORCIDs

Porrawee Pomchote https://orcid.org/0000-0003-1035-5553
Wichase Khonsue https://orcid.org/0000-0002-3058-6378
Axel Hernandez https://orcid.org/0000-0003-3720-2856
Chitchol Phalaraksh https://orcid.org/0000-0002-7662-4931
Kanto Nishikawa https://orcid.org/0000-0002-6274-4959

Data availability

All of the data that support the findings of this study are available in the main text.

References

Anderson J (1871) Description of a new genus of newts from western Yunan. Proceedings of the Zoological Society of London 1871: 423–425.

Darriba D, Posada D, Kozlov AM, Stamatakis A, Morel B, Flouri T (2020) ModelTest-NG: a new and scalable tool for the selection of DNA and protein evolutionary models. Molecular Biology and Evolution 37(1): 291–294. https://doi.org/10.1093/molbev/msz189

Decemson H, Lalremsanga HT, Elangbam PS, Vabeiryureilai M, Shinde P, Purkayastha J, Arkhipov DV, Bragin AM, Poyarkov NA (2023) A new cryptic species of *Tylototriton* (Amphibia, Caudata, Salamandridae) from mysterious mountain lakes in Manipur, north-eastern India. Herpetozoa 36: 203–224. https://doi.org/10.3897/herpetozoa.36.e106614

Dufresnes C, Hernandez A (2022) Towards completing the crocodile newts' puzzle with all-inclusive phylogeographic resources. Zoological Journal of the Linnean Society 197(3): 620–640. https://doi.org/10.1093/zoolinnean/zlac038

Fang PW, Chang MLY (1932) Notes on *Tylototriton kweichowensis* sp. nov. and *asperrimus* Unterstein with synopsis to species. Sinensia 2(9): 111–122.

Fedorov A, Beichel R, Kalpathy-Cramer J, Finet J, Fillion-Robin J-C, Pujol S, Bauer C, Jennings D, Fennessy F, Sonka M, Buatti J, Aylward S, Miller JV, Pieper S, Kikinis R (2012) 3D Slicer as an image computing platform for the quantitative imaging network. Magnetic Resonance Imaging 30(9): 1323–1341. https://doi.org/10.1016/j.mri.2012.05.001

Fei L, Ye CY (2016) s.n. In: Amphibians of China. Vol. I. Science Press, Beijing, 266–320.

Felsenstein J (1985) Confidence limits on phylogenies: an approach using the bootstrap. Evolution 39(4): 783–791. https://doi.org/10.2307/2408678

Frost DR (2024) Amphibian Species of the World 6.2: an Online Reference. https://amphibiansoftheworld.amnh.org/index.php

Grismer LL, Wood Jr PL, Quah ESH, Thura MK, Espinoza RE, Grismer MS, Murdoch ML, Lin A (2018) A new species of Crocodile Newt *Tylototriton* (Caudata: Salamandridae) from Shan State, Myanmar (Burma). Zootaxa 4500(4): 553–573. https://doi.org/10.11646/zootaxa.4500.4.5

Grismer LL, Wood Jr PL, Quah ESH, Thura MK, Espinoza RE, Murdoch ML (2019) A new species of crocodile newt *Tylototriton* (Caudata: Salamandridae) from northern Myanmar (Burma). Journal of Natural History 53(7–8): 475–495. https://doi.org/10.1080/00222933.2019.1587534

Hernandez A (2016) Crocodile Newts, the Primitive Salamandridae of Asia (Genera *Echinotriton* and *Tylototriton*). Edition Chimaira, Frankfurt, 415 pp.

Hernandez A (2017) New localities for *Tylototriton panhai* and *Tylototriton uyenoi* Nishikawa, Khonsue, Pomchote and Matsui 2013 in northern Thailand. Bulletin de la Société Herpétologique de France 162: 110–112.

Hernandez A, Pomchote P (2020a) Habitat, distribution and life history of the polytypic Panha's Crocodile Newt, *Tylototriton panhai* in northeastern Thailand. Alytes 37(3–4): 25–46.

Hernandez A, Pomchote P (2020b) New southernmost record for the genus *Tylototriton* in Asia: *Tylototriton uyenoi* Nishikawa, Khonsue, Pomchote and Matsui 2013 discovered in Khao Laem National Park, Kanchanaburi province, western Thailand. Bulletin de la Société Herpétologique de France 175: 64–67.

Hernandez A, Pomchote P (2021) *Tylototriton uyenoi* Nishikawa, Khonsue, Pomchote & Matsui 2013 Uéno's crocodile newt. In: Grosse WR (Ed.) Threatened Newts and Salamanders, Volume 3: Captive Care Management. Edition Chimaira, Frankfurt, 206–211.

Hernandez A, Escoriza D, Pomchote P, Hou M (2019) New localities for *Tylototriton uyenoi*, *T. panhai* and *T. anguliceps* in Thailand with remarks on the southernmost distribution of the genus. The Herpetological Bulletin 147: 15–18. https://doi.org/10.33256/hb147.1518

Heyer WR, Donnelly MA, McDiarmid RW, Hayek L-AC, Foster MS (1994) Measuring and Monitoring Biological Diversity: Standard Methods for Amphibians. Smithsonian Institution Press, Washington DC, 384 pp.

Hou M, Li P, Lü S-Q (2012) Morphological research development of genus *Tylototriton* and primary confirmation of the status of four cryptic populations. Journal of Huangshan University 14(3): 61–65. [In Chinese]

Huelsenbeck JP, Hillis M (1993) Success of phylogenetic methods in the four-taxon case. Systematic Biology 42(3): 247–264. https://doi.org/10.1093/sysbio/42.3.247

Khatiwada JR, Wang B, Ghimire S, Vasudevan K, Paudel S, Jiang J (2015) A new species of the genus *Tylototriton* (Amphibia: Urodela: Salamandridae) from Eastern Himalaya. Asian Herpetological Research 6(4): 245–256. https://doi.org/10.16373/j.cnki.ahr.140097

Kozlov AM, Darriba D, Flouri T, Morel B, Stamatakis A (2019) RAxML-NG: a fast, scalable and user-friendly tool for maximum likelihood phylogenetic inference. Bioinformatics 35(21): 4453–4455. https://doi.org/10.1093/bioinformatics/btz305

Kumar S, Stecher G, Tamura K (2016) MEGA7: molecular evolutionary genetics analysis version 7.0 for bigger datasets. Molecular Biology and Evolution 33(7): 1870–1874. https://doi.org/10.1093/molbev/msw054

Le DT, Nguyen TT, Nishikawa K, Nguyen SLH, Pham AV, Matsui M, Bernardes M, Nguyen TQ (2015) A new species of *Tylototriton* Anderson, 1871 (Amphibia: Salamandridae) from northern Indochina. Current Herpetology 34(1): 38–50. https://doi.org/10.5358/hsj.34.38

Leaché AD, Reeder TW (2002) Molecular systematics of the eastern fence lizard (*Sceloporus undulatus*): a comparison of parsimony, likelihood, and Bayesian approaches. Systematic Biology 51(1): 44–68. https://doi.org/10.1080/106351502753475871

Michaels CJ (2014) Field observations, morphometrics and a new locality for *Tylototriton uyenoi* in Chiang Mai Province, Thailand. The Herpetological Bulletin 130: 26–27.

Nishikawa K, Jiang J-P, Matsui M (2011) Two new species of *Pachytriton* from Anhui and Guangxi, China (Amphibia: Urodela: Salamandridae). Current Herpetology 30(1): 15–31. https://doi.org/10.5358/hsj.30.15

Nishikawa K, Khonsue W, Pomchote P, Matsui M (2013a) Two new species of *Tylototriton* from Thailand (Amphibia: Urodela: Salamandridae). Zootaxa 3737(3): 261–279. https://doi.org/10.11646/zootaxa.3737.3.5

Nishikawa K, Matsui M, Nguyen TT (2013b) A new species of *Tylototriton* from northern Vietnam (Amphibia: Urodela: Salamandridae). Current Herpetology 32(1): 34–49. https://doi.org/10.5358/hsj.32.34

Nishikawa K, Matsui M, Rao D (2014) A new species of *Tylototriton* (Amphibia: Urodela: Salamandridae) from central Myanmar. Natural History Bulletin of the Siam Society 60(1): 9–22.

Nussbaum RA, Brodie Jr ED, Yang D (1995) A taxonomic review of *Tylototriton verrucosus* Anderson (Amphibia: Caudata: Salamandridae). Herpetologica 51(3): 257–268.

Pattanavibool A, Dearden P (2002) Fragmentation and wildlife in montane evergreen forests, northern Thailand. Biological Conservation 107(2): 155–164. https://doi.org/10.1016/S0006-3207(02)00056-3

Phimmachak S, Aowphol A, Stuart BL (2015) Morphological and molecular variation in *Tylototriton* (Caudata: Salamandridae) in Laos, with description of a new species. Zootaxa 4006(2): 285–310. https://doi.org/10.11646/zootaxa.4006.2.3

Pomchote P, Pariyanonth P, Khonsue W (2008) Two distinctive color patterns of the Himalayan newt *Tylototriton verrucosus* (Urodela: Salamandridae) found in Thailand and its implication on geographic segregation. The Natural History Journal of Chulalongkorn University 8(1): 35–43.

Pomchote P, Khonsue W, Sapewisut P, Eto K, Nishikawa K (2020a) Discovering a population of *Tylototriton verrucosus* (Caudata: Salamandridae) from Thailand: implications for conservation. Tropical Natural History 20(1): 1–15.

Pomchote P, Khonsue W, Thammachoti P, Hernandez A, Peerachidacho P, Suwannapoom C, Onishi Y, Nishikawa K (2020b) A new species of *Tylototriton* (Urodela: Salamandridae) from Nan Province, northern Thailand. Tropical Natural History 20(2): 144–161.

Pomchote P, Khonsue W, Thammachoti P, Sapewisut P, Hernandez A (2021a) Range extension of *Tylototriton uyenoi* discovered in Mae Wong National Park, Kamphaeng Phet province, western Thailand. Bulletin de la Société Herpétologique de France 178: 77–79.

Pomchote P, Peerachidacho P, Hernandez A, Sapewisut P, Khonsue W, Thammachoti P, Nishikawa K (2021b) A new species of the genus *Tylototriton* (Urodela, Salamandridae) from western Thailand. ZooKeys 1072: 83–105. https://doi.org/10.3897/zookeys.1072.75320

Pomchote P, Peerachidacho P, Sapewisut P, Hernandez A, Onishi Y, Nishikawa K (2022) Description of the Himalayan newt *Tylototriton verrucosus* (Urodela: Salamandridae) in northern Thailand with its phylogenetic relationships, distribution, and conservation status. Journal of Asia-Pacific Biodiversity 15(1): 30–39. https://doi.org/10.1016/j.japb.2021.10.006

Ronquist F, Teslenko M, van der Mark P, Ayres DL, Darling A, Höhna S, Larget B, Liu L, Suchard MA, Huelsenbeck JP (2012) MrBayes 3.2: efficient Bayesian phylogenetic inference and model choice across a large model space. Systematic Biology 61(3): 539–542. https://doi.org/10.1093/sysbio/sys029

Tanabe AS (2011) Kakusan4 and Aminosan: two programs for comparing nonpartitioned, proportional and separate models for combined molecular phylogenetic analyses of multilocus sequence data. Molecular Ecology Resources 11(5): 914–921. https://doi.org/10.1111/j.1755-0998.2011.03021.x

The Nation (2019) DNP confirms ban on motor races within wildlife sanctuaries. https://www.nationthailand.com/in-focus/30370861

Wang B, Nishikawa K, Matsui M, Nguyen TQ, Xie F, Li C, Khatiwada JR, Zhang B, Gong D, Mo Y, Wei G, Chen X, Shen Y, Yang D, Xiong R, Jiang J (2018) Phylogenetic surveys on the newt genus *Tylototriton sensu lato* (Salamandridae, Caudata) reveal cryptic diversity and novel diversification promoted by historical climatic shifts. PeerJ 6: e4384. https://doi.org/10.7717/peerj.4384

Weisrock DW, Papenfuss TJ, Macey JR, Litvinchuk SN, Polymeni R, Ugurtas IH, Zhao E, Jowkar H, Larson A (2006) A molecular assessment of phylogenetic relationships and lineage accumulation rates within family Salamandridae (Amphibia, Caudata). Molecular Phylogenetics and Evolution 41(2): 368–383. https://doi.org/10.1016/j.ympev.2006.05.008

Zaw T, Lay P, Pawangkhanant P, Gorin VA, Poyarkov Jr NA (2019) A new species of Crocodile Newt, genus *Tylototriton* (Amphibia, Caudata, Salamandridae) from the mountains of Kachin State, northern Myanmar. Zoological Research 40(3): 151–174. https://doi.org/10.24272/j.issn.2095-8137.2019.043

ZooKeys 1215: 209–234 (2024)
DOI: 10.3897/zookeys.1215.130669

Research Article

Four new species and four newly recorded species of *Omphale* Haliday (Hymenoptera, Eulophidae) from China, with a key to Chinese species

Ming-Rui Li[1], Jia-Sheng Wang[1], Ze-Ji Jing[1], Qing-Fan Meng[1], Hong-Rui Zhao[1], Xing-Peng Li[1], Sheng-Dong Liu[1], Cheng-De Li[2]

1 *Jilin Provincial Key Laboratory of Insect Biodiversity and Ecosystem Function of Changbai Mountains, Beihua University, Jilin, 132013, China*
2 *School of Forestry, Northeast Forestry University, Harbin, 150040, China*
Corresponding authors: Cheng-De Li (lichengde0608@sina.com); Qing-Fan Meng (qingfanmeng@163.com)

Abstract

In this paper, four species of *Omphale* Haliday, *O. longigena* Li & Li, **sp. nov.**, *O. longitarsus* Li & Li, **sp. nov.**, *O. rectisulcus* Li & Li, **sp. nov.**, and *O. xanthosoma* Li & Li, **sp. nov.**, are described as new to science; four species, *O. brevibuccata* Szelényi, *O. connectens* Graham, *O. melina* Yefremova & Kriskovich, and *O. obscura* (Förster) are reported from China for the first time; and the male of *O. melina* is reported for the first time in the world. A key to all known species of the genus *Omphale* in China is provided.

Key words: Chalcidoidea, Entedoninae, morphology, new species records, taxonomy

Academic editor: Zachary Lahey
Received: 27 June 2024
Accepted: 9 September 2024
Published: 15 October 2024

ZooBank: https://zoobank.org/80E4960E-18E5-40EA-AA0D-AB19434AC96A

Citation: Li M-R, Wang J-S, Jing Z-J, Meng Q-F, Zhao H-R, Li X-P, Liu S-D, Li C-D (2024) Four new species and four newly recorded species of *Omphale* Haliday (Hymenoptera, Eulophidae) from China, with a key to Chinese species. ZooKeys 1215: 209–234. https://doi.org/10.3897/zookeys.1215.130669

Introduction

Omphale Haliday, 1833 (Hymenoptera, Eulophidae, Entedoninae), containing 271 species worldwide (Noyes 2019; Jamali et al. 2022), is cosmopolitan in distribution and the second largest genus in the Entedoninae. Species of *Omphale* can be separated from other genera in Entedoninae by the following characters: head with frontal sulcus present; interantennal area and antennal scrobe more or less broadened; clypeus distinctly delimited by grooves at least laterally, quadrangular to semicircular, lower margin usually arcuately protruding; occipital median sulcus absent; mesoscutum and mesoscutellum with finely engraved reticulation; propodeum smooth; males usually with verticillate setae on flagellomeres.

The genus *Omphale* from America and Europe are well studied. Two-hundred three (203) species from America and Europe were divided into 18 species groups by Hansson (1996, 1997, 2004) and Hansson and Shevtsova (2012), respectively. Keys to Nearctic, Mexican, Costa Rican and European species were also given. Before this study, there were only eleven *Omphale* species known from China: two species (*O. longiventris* (Ling, 1994) and *O. pulchra* (Ling, 1994)) were described by Ling (1994); nine species (*O. gibsoni* Hansson, 2004, *O. longiseta* Hansson, 1996, *O. masneri* Hansson, 1996, *O. mellea* Hans-

son, 1996, *O. salicis* (Haliday, 1833), *O. stelteri* (Boucek, 1971), *O. straminea* Hansson, 1996, *O. sulciscuta* (Thomson, 1878), and *O. theana* (Walker, 1839)) were reported by Zhu and Huang (2001, 2002) and Zhang et al. (2007) during taxonomic studies on Eulophidae from Zhejiang, Guangxi, and Gansu provinces of China, respectively. Since then, there have been no further reports of *Omphale* from China.

This paper includes eight additional species, of which four, *O. longigena* sp. nov., *O. longitarsus* sp. nov., *O. rectisulcus* sp. nov., and *O. xanthosoma* sp. nov. are described as new to science; four species, *O. brevibuccata* Szelényi, *O. connectens* Graham, *O. melina* Yefremova & Kriskovich, and *O. obscura* (Förster) are recorded from China for the first time, and the male of *O. melina* is reported for the first time in the world. The species *O*. *sulciscuta* (Thomson) has new distribution data for China. Detailed descriptions and illustrations of the new species, diagnoses and illustrations of the five previously described species, and a key to all known species of *Omphale* in China are given.

Materials and methods

Specimens were collected by sweep nets, yellow-pan traps, and Malaise traps, and were mounted on triangular cards or in Canada Balsam on slides after dissection following methods described by Noyes (1982). Photographs were taken with an Aosvi AO-HK830-5870T digital microscope or a digital CCD camera attached to an Olympus BX51 compound microscope. The quality of these images was improved by using Helicon Focus 7 and Adobe Photoshop 2022. Measurements were made using the built-in software of Aosvi AO-HK830-5870T.

Terminology follows the Hymenoptera Anatomy Consortium (2024), and the following abbreviations are used:

F1–5 flagellomeres 1–5;
HE height of eye;
MS malar space;
MV marginal vein;
OOL minimum distance between a posterior ocellus and corresponding eye margin;
PMV postmarginal vein;
POL minimum distance between posterior ocelli;
SMV submarginal vein;
STV stigmal vein;
WM width of mouth opening.

Type material is deposited in the insect collections at Northeast Forestry University (**NEFU**), Harbin, China. Abbreviations for other depositories:

HDOU Hope Department, Oxford University, Oxford, England
HNHM Hungarian Natural History Museum, Budapest, Hungary
LUZN Zoological Museum, Lund University, Sweden
ZISP Zoological Institute, St Petersburg, Russia
NHMV Naturhistorisches Museum, Vienna, Austria

Results

Key to Chinese species of *Omphale* (females)

1 Fore wing with STV enlarged and circular (Fig. 6D); membrane around STV and base of MV infuscate ..... ***O. melina* Yefremova & Kriskovich**
– Fore wing with STV not enlarged; membrane hyaline or only infuscate below MV **2**
2 Body mainly yellow without metallic reflections; midlobe of mesoscutum with only 1 pair of setae **3**
– Body mainly brown, dark brown to black, with weak or strong metallic reflections; midlobe of mesoscutum with 2 pairs of setae **4**
3 Mesoscutum and mesoscutellum both with a brown longitudinal stripe along median part (Fig. 10C); fore wing hyaline, without any infuscate part; antenna with flagellum slender, F2 as long as F1 ..... ***O. xanthosoma* sp. nov.**
– Only scutellum occasionally with a median infuscate stripe along median line; fore wing with an infuscate part close to STV; antenna with flagellum stouter, F2 0.8 × as long as F1 ..... ***O. mellea* Hansson**
4 Mesoscutellum with a median groove (as in Fig. 9D, E) **5**
– Mesoscutellum without median groove **10**
5 Frontal sulcus straight (Fig. 8A, B); median groove on mesoscutellum shallow and narrow ..... ***O. rectisulcus* sp. nov.**
– Frontal sulcus at least curved slightly, mostly arcuate or V-shaped; median groove on mesoscutellum wide and deep **6**
6 Mesoscutum with a shallow but distinct median groove in posterior part; PMV at most 0.15 × as long as MV **7**
– Median groove on mesoscutum not obvious; PMV long, approximately 0.33 × as long as MV ..... ***O. pulchra* (Ling)**
7 Meshes of reticulation on mesoscutellum elongate (Fig. 7D, E) ..... ***O. obscura* (Förster)**
– Meshes of reticulation on mesoscutellum not elongate in posterior 1/2 at least **8**
8 Length of body 2.1 mm at least; gaster slender and long, 5.0 × as long as wide ..... ***O. longiventris* (Ling)**
– Length of body 1.8 mm at most; gaster stouter, 2.0 × as long as wide at most **9**
9 Antennae with F1 as long as F4, F4 ~ 3.0 × as long as wide (see Bouček, 1971: fig. 13 ..... ***O. stelteri* (Bouček)**
– Antennae with F1 1.15 × as long as F4, and at most 2.2 × as long as wide ..... ***O. sulciscuta* (Thomson)**
10 Fore wing with radial cell bare (as in Fig. 6D) **11**
– Fore wing with radial cell setose (as in Fig. 5F) **13**
11 Clypeus distinctly paler than surrounding parts of face, without metallic reflections ..... ***O. straminea* Hansson**
– Clypeus with more or less metallic reflections and with same color as surrounding parts of face **12**
12 All coxae dark brown with bluish green metallic reflections; all femora brown ..... ***O. salicis* (Haliday)**
– All coxae mainly yellowish white, pale brown at base only; all femora yellowish white, metafemur infuscate along dorsal margin ..... ***O. theana* (Walker)**

13 Lateral mesosoma yellowish white to yellowish brown, without metallic reflections **14**
– Lateral mesosoma dark brown, with bluish green metallic reflections ... **15**
14 Gena elongate, MS 0.4 × as long as HE (Fig. 4A, B); fore wing below MV with a wide infuscate band (Fig. 4I) ..... ***O. longigena* sp. nov.**
– Gena shorter, MS 0.2 × as long as HE; fore wing hyaline, without infuscate band ..... ***O. brevibuccata* Szelényi**
15 Legs with 4th tarsomere on all legs slender and elongate, half as long as whole tarsus (Fig. 5I–K)..... ***O. longitarsus* sp. nov.**
– Legs with 4th tarsomeres of protarsus and mesotarsus at most 0.4 × as long as the length of corresponding tarsus..... **16**
16 Head with frontal cross-ridge present (as in Hansson, 1996: fig. 1)..... **17**
– Head with frontal cross-ridge absent (as in Hansson, 1996: fig. 101) **18**
17 Setae on vertex and thoracic dorsum distinctly longer than in alternate, outermost seta on vertex as long as POL, hind pair of setae on mesoscutum longer than distance separating them ..... ***O. longiseta* Hansson**
– Setae on vertex and thoracic dorsum shorter, outermost seta on vertex at most 0.7 × as long as POL, hind pair of setae on mesoscutum at most half the distance separating them..... ***O. connectens* Graham**
18 Clypeus poorly delimited, more or less semicircular; antenna with scape dark brown except proximal 1/3 pale ..... ***O. masneri* Hansson**
– Clypeus distinctly delimited, quadrangular; antenna with scape predominantly pale to dark brown with a pale median spot ..... ***O. gibsoni* Hansson**

Species descriptions

***Omphale brevibuccata* Szelényi, 1978**
Figs 1A, 2A–I

Omphale brevibuccata Szelényi, 1978: 222, holotype ♀, Hungary, HNHM, not examined.

Material examined. • 14♀: 1♀ [NEFU; on card, right antenna and right wings on slide], China, Guangdong Province, Shaoguan City, Chebaling National Nature Reserve, 29–30.IV.2019, leg. Wen-Jian Li and Jun Wu, by yellow-pan trapping • 3♀ [NEFU; on cards], China, Shandong Province, Qingdao City, Laoshan Scenic Spot, Beijiushui, 8–10.VII.2014, leg. Hui Geng, Guo-Hao Zu, Zhi-Guang Wu, and Hai-Feng Bai, by yellow-pan trapping • 2♀ [NEFU; on cards], China, Shandong Province, Qingdao City, Jimo District, Mashan Park, 11.VII.2014, leg. Si-Zhu Liu, Guo-Hao Zu, and Zhi-Guang Wu, by sweep netting • 2♀ [NEFU; 1 on slide, 1 on card], China, Shandong Province, Qingdao City, Laoshan Scenic Spot, Beijiushui, 12.VII.2014, leg. Hui Geng, Guo-Hao Zu, Zhi-Guang Wu, and Hai-Feng Bai, by sweep netting • 4♀ [NEFU; on cards], China, Shandong Province, Qingdao City, Dazhushan, 13–14.VII.2014, leg. Ye Chen and Chao Zhang, by yellow-pan trapping • 2♀ [NEFU; on cards], China, Liaoning Province, Anshan City, Qianshan, 20.VIII.2015, leg. Hui Geng, Yan Gao, and Zhi-Guang Wu, by sweep netting.

Diagnosis. Female. Body length 1.2–1.8 mm. Vertex golden-green, face dark brown with golden or purple reflections; antenna with scape yellow to pale brown, pedicel and flagellum brown; mesoscutum dark brown, mesoscutellum with an-

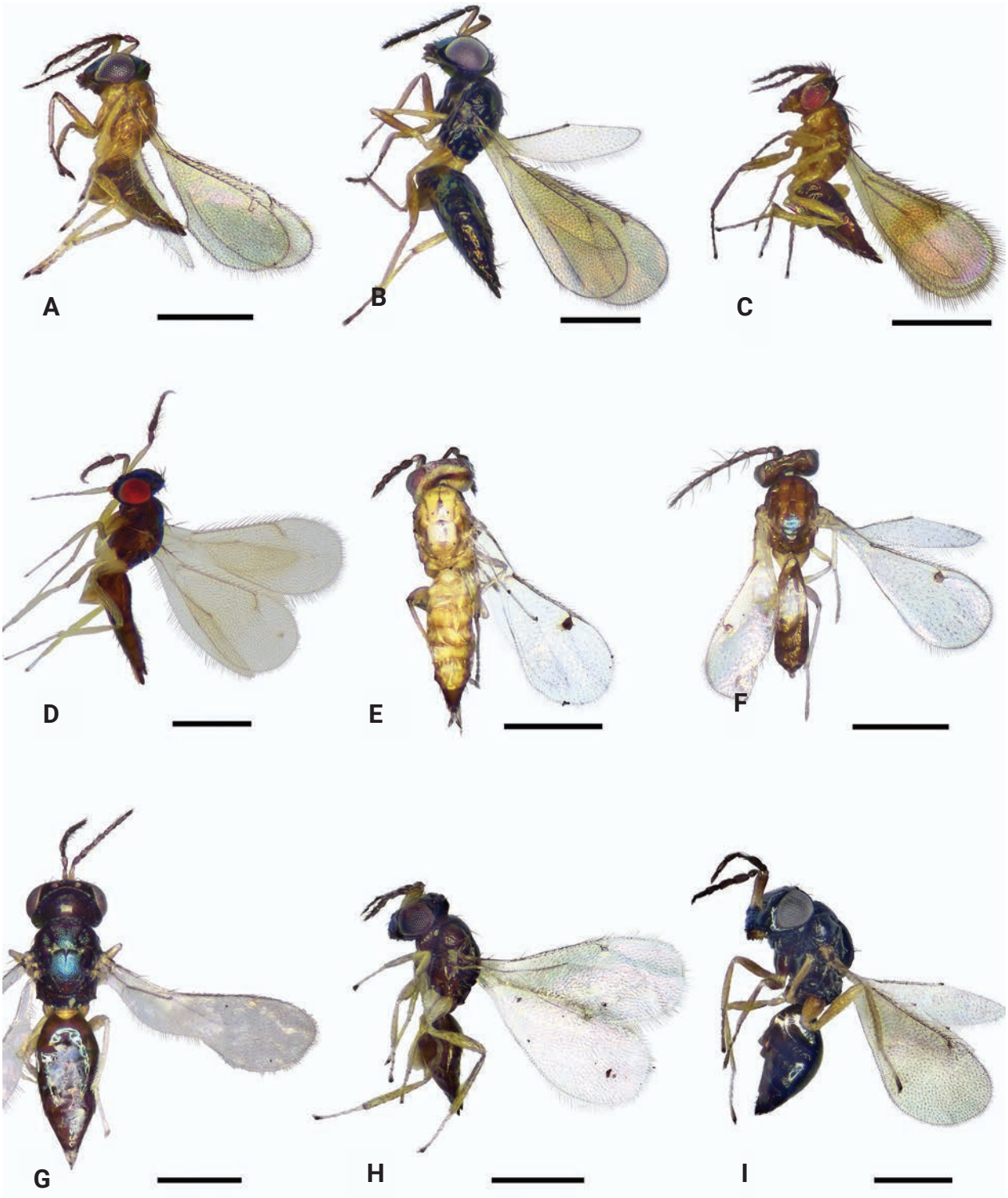

Figure 1. *Omphale* spp., habitus **A** *O. brevibuccata*, ♀, lateral **B** *O. connectens*, ♀, lateral **C** *O. longigena* sp. nov., holotype, ♀, lateral **D** *O. longitarsus* sp. nov., holotype, ♀, lateral **E** *O. melina*, ♀, dorsal **F** *O. melina*, ♂, dorsal **G** *O. rectisulcus* sp. nov., holotype, ♀, dorsal **H** *O. obscura*, ♀, lateral **I** *O. sulciscuta*, ♀, lateral. Scale bars: 500 μm.

terior 1/3–1/2 yellowish brown and remainder brown to dark brown; axillae with anterior 1/2 dark brown to brown, remainder yellowish brown to yellowish white; propodeum pale brown; other parts of mesosoma yellow to yellowish white (including legs); gaster dark brown. Head (Fig. 2A) with antennal scrobes meeting on the V-shaped frontal sulcus; frontal cross-ridge absent; gena very short,

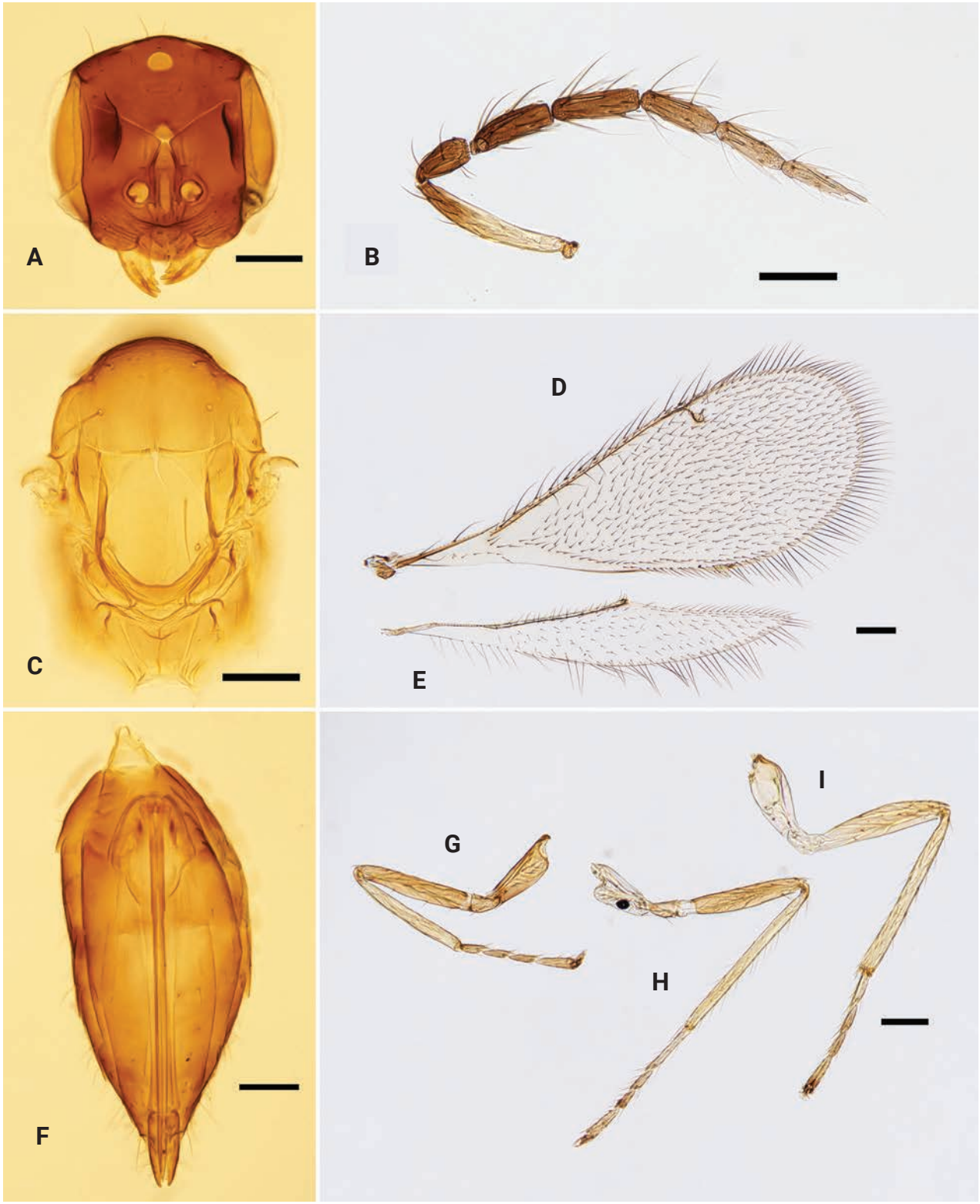

Figure 2. *Omphale brevibuccata*, ♀ **A** head, frontal view **B** antenna **C** mesosoma, dorsal view **D** fore wing **E** hind wing **F** metasoma, dorsal view **G–I** fore, mid and hind leg, respectively. Scale bars: 100 μm.

HE:MS:WM ~ 5.0:1.0:3.4; clypeus semicircular 1.7 × as wide as high; antenna (Fig. 2B) slender, with five flagellomeres separated from each other, F1 1.1 × as long as F2. Mesosoma (Fig. 2C) with mesoscutum and scutellum with weak reticulation; midlobe of mesoscutum with two pairs of setae; scutellum 1.0–1.2 ×

as long as wide, with anterior margin almost straight; propodeum smooth, with a weak median carina, and anteromedially with a fovea. Fore wing (Fig. 2D) speculum closed, with seven or eight admarginal setae arising from MV and membrane just behind MV, radial cell setose, PMV 1.8 × as long as STV. Metasoma (Fig. 2F), gaster 1.6 × as long as mesosoma, and nearly as long as head + mesosoma.

Male. Unknown.

Host. Unknown.

Distribution. China (Liaoning, Shandong, and Guangdong Provinces) (new record); Hungary (Szelényi 1978); United Kingdom (Askew 2003); Russia, Sweden, Netherlands, Bulgaria (Hansson and Shevtsova 2012); Romania (Hansson 2016).

Omphale connectens Graham, 1963

Figs 1B, 3A–K

Omphale connectens Graham, 1963: 261, holotype ♀, Berkshire, England, UK, HDOU, not examined.

Material examined. • 4♀: 2♀ [NEFU; 1 on card, 1 on slide], China, Chongqing City, Simian Mountain, Dawopu, 04.VIII.2018, leg. Guang-Xin Wang and Jun-Jie Fan, by sweep netting • 2♀ [NEFU; 1 on card, 1 on slide], China, Inner Mongolia, Ulanhot City, Sanhe Village, 12.VII.2021, leg. Yuan-Yuan Jin and Yue Qin, by sweep netting.

Diagnosis. Female. Body length 1.0–2.4 mm. Vertex and face bronze, golden green, golden blue to purple metallic; antenna with scape yellow, along dorsal edge dark brown, pedicel and flagellum dark brown; mesoscutum bluish green, bronze to purple metallic; scutellum with similar color to mesoscutum, sometime darker; propodeum bluish green to purple metallic; legs with procoxa dark brown, mesocoxa and metacoxa yellowish brown to yellow; femora yellowish brown to brown; tibiae yellow to yellowish brown; protarsus pale brown, mesotarsus and metatarsus yellow to yellowish brown; gaster with first tergite bluish green metallic, remainder dark brown metallic. Head (Fig. 3A, B) with face and vertex smooth to with very weak sculpture partly; antennal scrobes meeting on the nearly V-shaped frontal sulcus; frontal cross-ridge present; clypeus trapezoid to semicircular 1.4–1.6 × as wide as high; antenna (Fig. 3C) with 3-segmented funicle and 2-segmented clava, F1–3 with two sets of setae, one set attached closed to base and another attached subapically or medially on the flagellomere, F1 1.1 × as long as F2. Mesosoma (Fig. 3D, E) with mesoscutum and scutellum with shallow reticulation; midlobe of mesoscutum with two pairs of setae; scutellum 1.2 × as long as wide, with anterior margin almost straight or weakly curved forwards; propodeum smooth, without median carina. Fore wing (Fig. 3J) speculum closed, with 6–10 admarginal setae arising from MV and membrane just below MV, STV short, PMV 1.5–2.0 × as long as STV, radial cell small and setose, only along PMV bare. Metasoma (Fig. 3I), gaster 1.6–2.0 × as long as mesosoma, and longer than head + mesosoma (1.2:1.0).

Male. Not collected from China, see Hansson and Shevtsova (2012).

Host. Unknown.

Distribution. China (Inner Mongolia and Chongqing Provinces) (new record); United Kingdom (Graham 1963); Ireland (north and south) (Bouček and Askew

1968); France, Germany, Netherlands (Gijswijt 1976); Croatia, Serbia (Bouček 1977); Sweden (Hansson 1991); Czech Republic, Denmark, Hungary, Russia (Hansson and Shevtsova 2012); Romania (Hansson 2016).

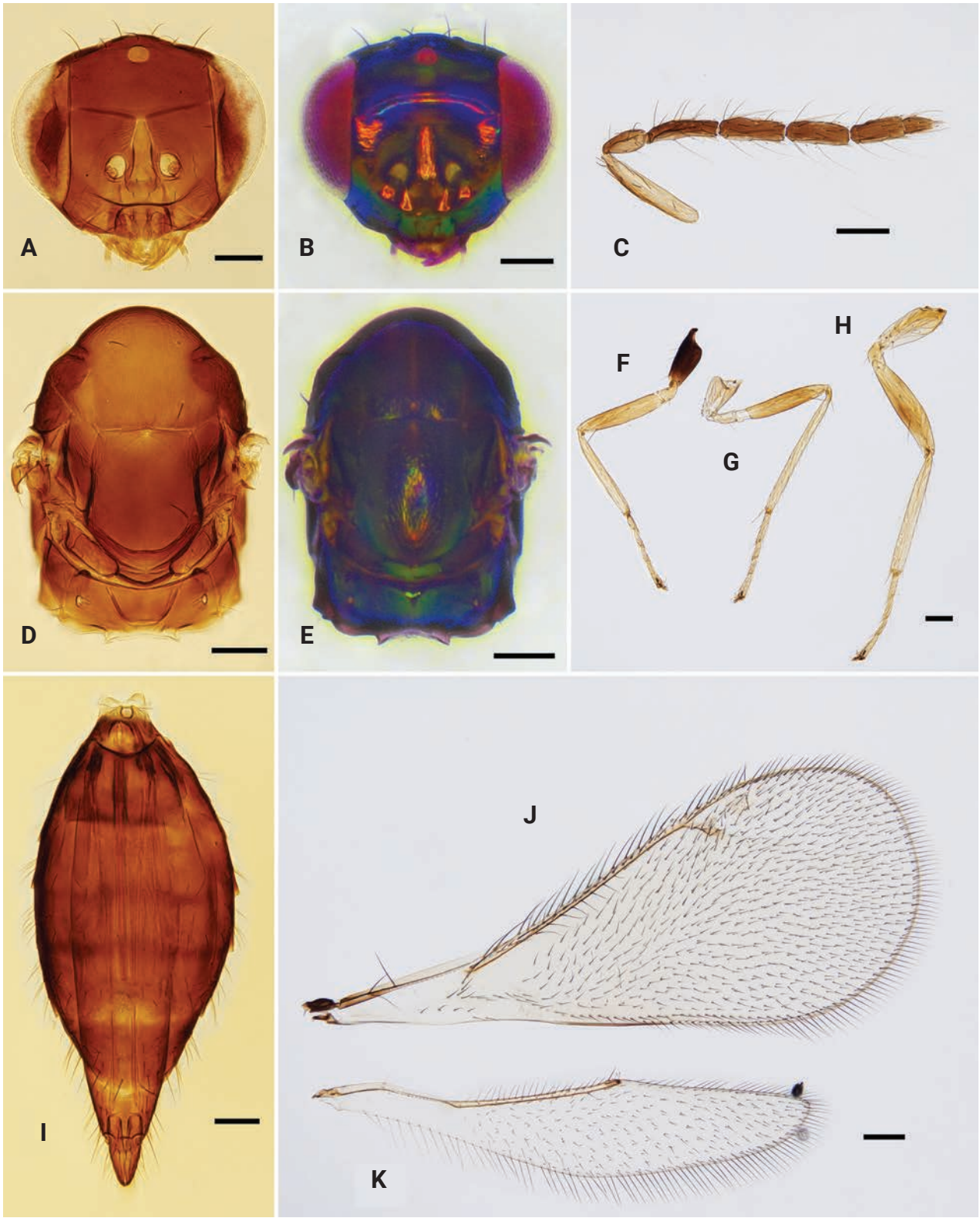

Figure 3. *Omphale connectens*, ♀ **A, B** head, frontal view **C** antenna **D, E** mesosoma, dorsal view **F–H** fore, mid and hind leg, respectively **I** metasoma, dorsal view **J** fore wing **K** hind wing. Scale bars: 100 μm.

***Omphale longigena* Li & Li, sp. nov.**
https://zoobank.org/4EEBF025-FB50-481A-AD26-E2BB7A85168F
Figs 1C, 4A–J

Material examined. *Holotype*: • ♀ [NEFU; on card], China, Shandong Province, Qingdao City, Jimo District, Mashan Park, 11.VII.2014, leg. Si-Zhu Liu, Guo-Hao Zu, and Zhi-Guang Wu, by sweep netting. ***Paratypes*:** • 12♀: 1♀ [NEFU; on slide], same data as the holotype • 2♀ [NEFU; on cards], China, Shandong Province, Qingdao City, Dahedong Village, 10.VII.2014, leg. Si-Zhu Liu, Ye Chen and Chao Zhang, by sweep netting • 3♀ [NEFU; on cards], China, Shandong Province, Qingdao City, Laoshan Scenic Spot, Beijiushui, 8–10.VII.2014, leg. Hui Geng, Guo-Hao Zu, Zhi-Guang Wu, and Hai-Feng Bai, by yellow-pan trapping • 2♀ [NEFU; 1 on card, 1 on slide], China, Guangdong Province, Shaoguan City, Chebaling National Nature Reserve, 29–30.IV.2019, leg. Wen-Jian Li and Jun Wu, by yellow-pan trapping • 4♀ [NEFU; on cards], China, Guangdong Province, Shaoguan City, Chebaling National Nature Reserve, 1–2.V.2019, leg. Wen-Jian Li and Jun Wu, by yellow-pan trapping.

Diagnosis. Female. Frontal sulcus slightly V-shaped; antennal scrobes meeting on frontal sulcus; antennal toruli situated completely below the level of lower eye margin; gena distinctly elongate, MS 0.4 × as long as HE; fore wing with a broad infuscate band below MV beyond speculum, extending to STV and posterior margin of wing; admarginal setae seven or eight, arising from both MV and membrane just below MV, and the most apical seta attached close to STV; PMV slightly shorter than STV.

Description. Female. Body length 1.0–1.2 mm. Upper face and vertex brown to dark brown with golden-green reflections, lower face yellowish brown, eyes dull red, clypeus with same color as surrounding parts of face, mandibles yellowish white with apex brown. Mesosoma with mid lobe of mesoscutum golden-green, mesoscutellum dark brown, remaining parts of mesosoma yellow to pale brown. Metasoma brown to dark brown except yellow petiole. Antenna with scape yellowish brown with dorsal margin dark brown, pedicel and flagellum brown to dark brown. All legs yellow, except dark brown tarsal claws. Fore wing with a broad infuscate band below MV beyond speculum, extending to STV and to posterior margin of wing.

Head (Fig. 4A, B) in frontal view 1.2 × as wide as high, usually collapsed after death; face and vertex smooth. POL:OOL ~ 1.5:1.0; frontal sulcus slightly V-shaped, reaching eye margin, the midpoint closer to median ocellus than to antennal toruli; antennal scrobes meeting on frontal sulcus; antennal toruli situated completely below the level of lower eye margin; frontal cross-ridge present, gena distinctly elongate, HE:MS:WM ~2.6:1.0:1.8; clypeus weakly delimited with lower margin distinctly protruding, 1.8–1.9 × as wide as high; mandible with two large teeth at apex and a row of smaller teeth at base. Antenna (Fig. 4C) slender, with all five flagellomeres separated from each other; scape 6.3 × as long as wide; pedicel 2.2 × as long as wide, and as long as F1; flagellomeres decreasing in width from F1 to F5, F1 1.0 × as long and 1.1 × as wide as F2.

Mesosoma (Fig. 4D) 1.4 × as long as wide; pronotum reduced and not visible in dorsal view; mesoscutum, mesoscutellum, metascutellum and propodeum smooth, without any sculpture; mid lobe of mesoscutum with two pairs of setae; notauli indicated only in anterior 1/3; mesoscutellum 1.2 × as long as wide, with one pair of setae located in median part; metascutellum smooth, nearly

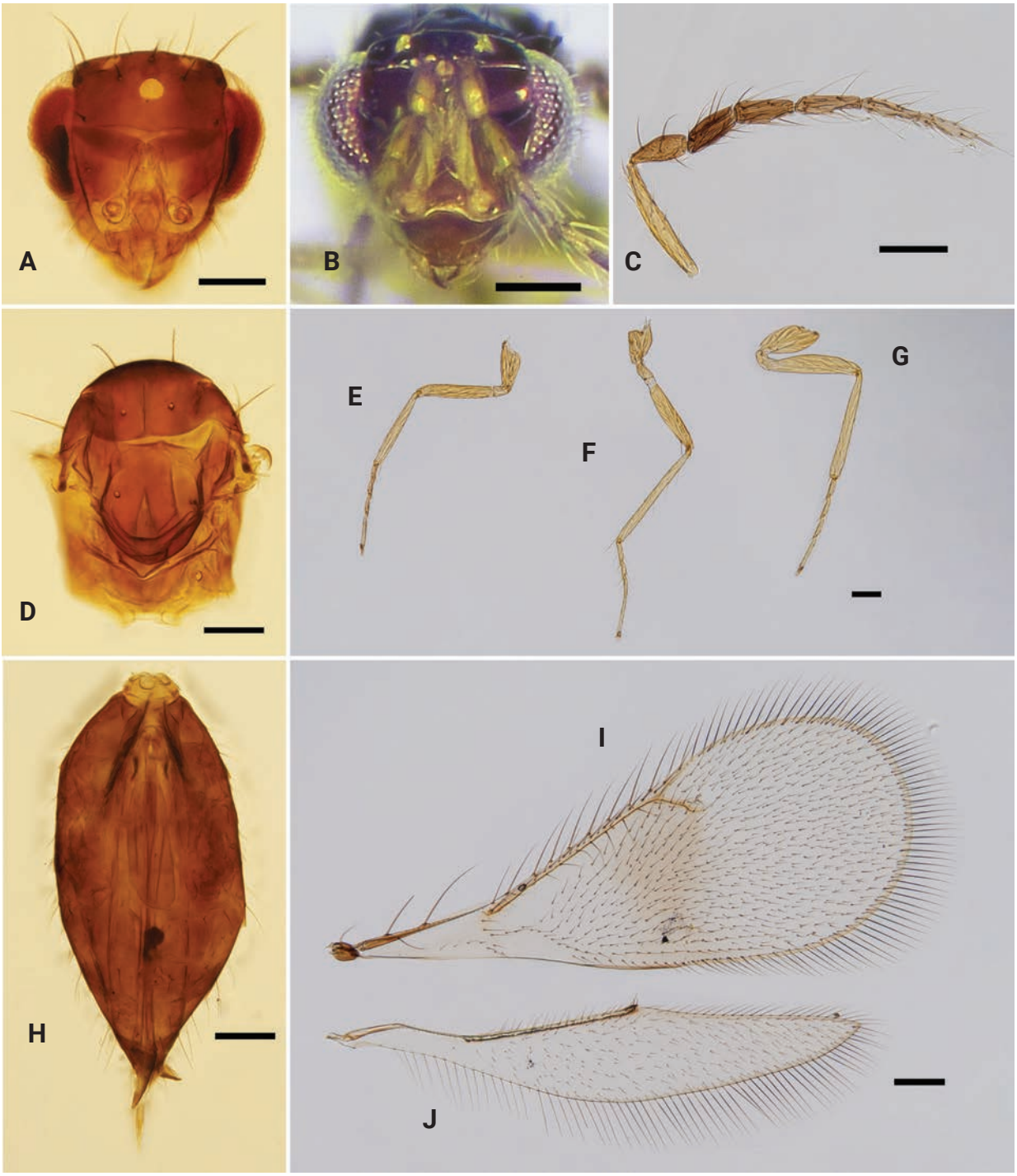

Figure 4. *Omphale longigena* sp. nov., paratype, ♀ **A, B** head, frontal view **C** antenna **D** mesosoma, dorsal view **E–G** fore, mid and hind leg, respectively **H** metasoma, dorsal view **I** fore wing **J** hind wing. Scale bars: 100 μm.

triangular, 0.4 × as long as wide, and 0.5 × as long as length of median propodeum; propodeum without median carina. Fore wing (Fig. 4I) 2.5 × as long as wide, speculum closed; with seven or eight admarginal setae arising from both MV and from membrane just below MV, with apical setae attached close to STV; PMV slightly shorter than STV, radial cell setose, ratio of SMV:MV:PMV:STV ~ 3.8:4.9:1.0:1.3. Hind wing (Fig. 4J) 5.4 × as long as wide, apex pointed. All legs (Fig. 4E–G) with 4th tarsomere slightly elongate, 0.3–0.4 × as long as whole tarsus; metatibial spur short, only reaching the middle of 1st tarsomere.

Metasoma (Fig. 4H) 2.0 × as long as wide; petiole short; gaster 1.4 × as long as length of mesosoma, and longer than head + mesosoma (1.2:1.0); ovipositor sheaths exserted beyond apex of gaster.

Male. Unknown.

Host. Unknown.

Etymology. The specific name refers to the elongate gena.

Distribution. China (Shandong and Guangdong Provinces).

Remarks. *Omphale longigena* sp. nov. is very similar to *O. litera* Jamali & Zeya, 2022. The two species share the following characteristics: head with gena elongate, MS 0.4 × as long as HE; flagellomeres decreasing in width from F1 to F5; fore wing with a broad infuscate band below MV beyond speculum, extending to STV and to posterior margin of disc; mesoscutum, mesoscutellum, metascutellum and propodeum smooth. *Omphale longigena* sp. nov. differs from *O. litera* in having the antennal torulus situated completely below the level of lower eye margin (vs above lower eye margin in *O. litera*); scape 6.3 × as long as wide (vs 4.2 × in *O. litera*), hind leg yellow, except dark brown tarsal claws (vs hind leg with coxa, femur basally three fourths and last tarsomere brown in *O. litera*). The figure in Jamali et al. (2022: fig. 2C) shows that the scape of the holotype of *O. litera* was damaged, and the color of the leg usually has variation, so the latter two differences may not be reliable characters for identification. The most reliable characteristic to distinguish these two species is the position of the antennal torulus.

Omphale longitarsus **Li & Li, sp. nov.**

https://zoobank.org/5A68F1ED-E168-479F-AAC0-F8378FA6EAEF

Figs 1D, 5A–K

Type material. ***Holotype*****:** • ♀ [NEFU; on card], China, Xizang Autonomous Region, Medog County, Damu Village, 22–29.VI.2017, leg. Zhaxi, by Malaise trapping. ***Paratypes*****:** • 2♀: 1♀ [NEFU; on slide], same data as the holotype • 1♀ [NEFU; on card], China, Xizang Autonomous Region, Medog County, Gedang Village, 31.V–5.VI.2021, leg. Jun-Jie Fan and Jun Wu, by yellow-pan trapping.

Diagnosis. Female. Frontal sulcus slightly curved, nearly straight, reaching eye margin; clypeus quadrangular with lower margin arcuately protruding, 1.9–2.0 × as wide as high; antenna slender, flagellomeres decreasing in width from F1 to F5; propodeum smooth and flat, with a narrow groove along anterior margin, without median carina; all legs with apical tarsomere slander and elongate, nearly as long as half the length of whole tarsus.

Description. Female. Body length 1.4–1.5 mm. Face and vertex bronze with golden-green reflections, eyes red, clypeus with same color as surrounding parts of face, mandibles yellowish white with base and apex brown. Mesosoma brown with weak golden-blue or golden-green reflections. Metasoma brown to dark brown, except yellow petiole. Antenna with scape yellowish white, pedicel and flagellum brown, gradually lighten towards apex, F5 yellowish white. All legs yellowish white except brown claws and fore coxae. Fore wings hyaline.

Head (Fig. 5A, B) in frontal view 1.3 × as wide as high. Face between frontal sulcus and frontal cross-ridge with weak and irregular sculpture, remainder of face and vertex smooth; POL:OOL ~ 1.8:1.0; frontal sulcus slightly curved, nearly straight, reaching eye margin, the midpoint closer to antennal torulus than me-

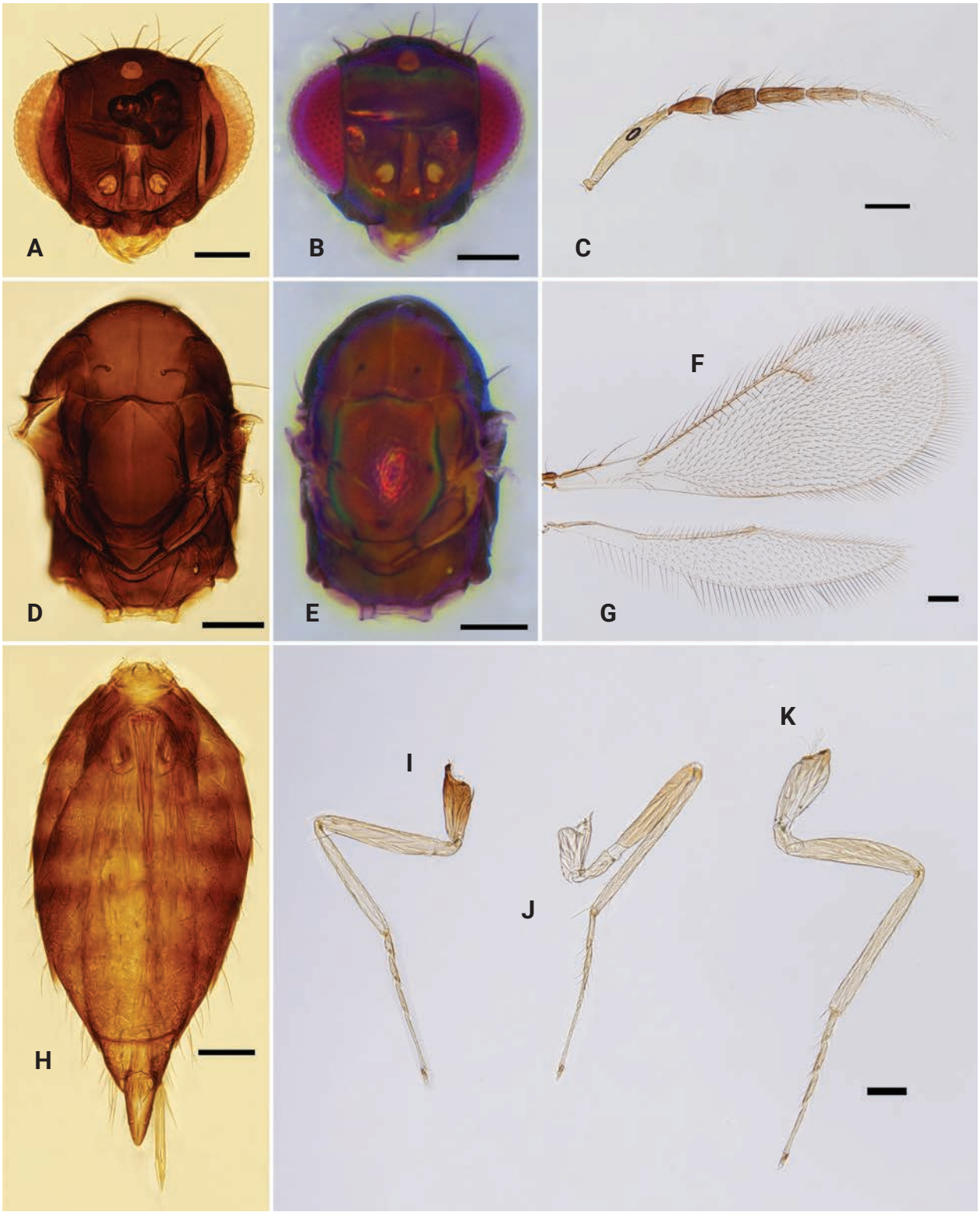

Figure 5. *Omphale longitarsus* sp. nov., paratype, ♀ **A, B** head, frontal view **C** antenna **D, E** mesosoma, dorsal view **F** fore wing **G** hind wing **H** metasoma, dorsal view **I–K** fore, mid and hind leg, respectively. Scale bars: 100 μm.

dian ocellus; antennal scrobes join frontal sulcus separately; subtorular grooves and frontal cross-ridge present; clypeus quadrangular with lower margin arcuately protruding, 1.9–2.0 × as wide as high; mandible with two large teeth at apex and a row of smaller teeth at base; HE:MS:WM ~ 2.8:1.0:1.2. Antenna (Fig.

5C) slender, with all five flagellomeres separated from each other; scape 6.5 × as long as wide; pedicel 2.4 × as long as wide, and 0.6 × as long as F1; flagellomeres decreasing in width from F1 to F5, F1 0.9 × as long and 1.5 × as wide as F2.

Mesosoma (Fig. 5D, E) 1.5 × as long as wide; pronotum reduced and not visible in dorsal view; mesoscutum smooth and flat, with two pairs of setae; notauli indicated only in anterior third; mesoscutellum flat, with very weak traces of reticulation, 1.4 × as long as wide, with one pair of setae located in the middle and close to lateral margin; axillae smooth; metascutellum smooth, nearly triangular, 0.4 × as long as wide, and 0.5 × as long as length of median propodeum. Lateral panels of metanotum smooth; propodeum smooth and flat, with a narrow groove along anterior margin, without median carina. Fore wing (Fig. 5F) 2.6 × as long as wide, with rather dense setae on membrane, speculum closed; with nine admarginal setae arising from MV; PMV shorter than STV, radial cell setose, ratio of SMV:MV:PMV:STV ~ 4.3:7.8:1.0:1.8. Hind wing (Fig. 5G) 5.5 × as long as wide, apex slightly pointed. All legs (Fig. 5I–K) with apical tarsomere slander and elongate, nearly half the length of whole tarsus; metatibial spur distinctly shorter than basal tarsomere, only reaching the middle of basal tarsomere.

Metasoma (Fig. 5H) 2.2 × as long as wide; petiole short; gaster 1.6 × as long as the length of mesosoma, and longer than head + mesosoma (1.2:1.0); ovipositor sheaths exserted beyond apex of gaster.

Male. Unknown.

Host. Unknown.

Etymology. The specific name refers to the elongate tarsus.

Distribution. China (Xizang Autonomous Region).

Remarks. *Omphale longitarsus* sp. nov. should belong to *Aetius* group, and can be separated from other species by having antenna slender, flagellomeres decreasing in width distinctly from F1 to F5, F1 0.9 × as long and 1.5 × as wide as F2; all legs with apical tarsomere slander and elongate, nearly half the length of whole tarsus.

Omphale melina Yefremova & Kriskovich, 1994

Figs 1E, F, 6A–G

Omphale melinum Yefremova & Kriskovich, 1994: 247, holotype ♀, Russia-Primorsky Krai, ZISP, not examined.

Omphale melina Yefremova & Kriskovich: Hansson and Shevtsova (2012): 139.

Material examined. • 6♀1♂: 2♀1♂ [NEFU; on cards, right antenna of ♂ on slide], China, Liaoning Province, Fushun City, Dahuofang Forestry Station, 18.VI.2012, leg. Hui Geng, Xiang-Xiang Jin, and Jiang Liu, by sweep netting • 1♀ [NEFU; on card], China, Liaoning Province, Fushun City, Yuanshuailin (Marshal Mausoleum), 18.VI.2012, leg. Hui Geng, Xiang-Xiang Jin, and Jiang Liu, by sweep netting • 1♀ [NEFU; on card], China, Liaoning Province, Anshan City, Qianshan, 21.VI.2015, leg. Hui Geng, Si-Zhu Liu, Yan Gao, and Zhi-Guang Wu, by sweep netting • 2♀ [NEFU; on cards], China, Liaoning Province, Anshan City, Qianshan, 23.VI.2015, leg. Hui Geng, Si-Zhu Liu, Yan Gao, and Zhi-Guang Wu, by sweep netting.

Diagnosis. Female. Body length 1.2–1.5 mm, mainly yellowish white, yellow to pale brown without metallic reflection; occiput with a brown transverse stripe; along median line of mesoscutum and scutellum dark brown; 7th tergite

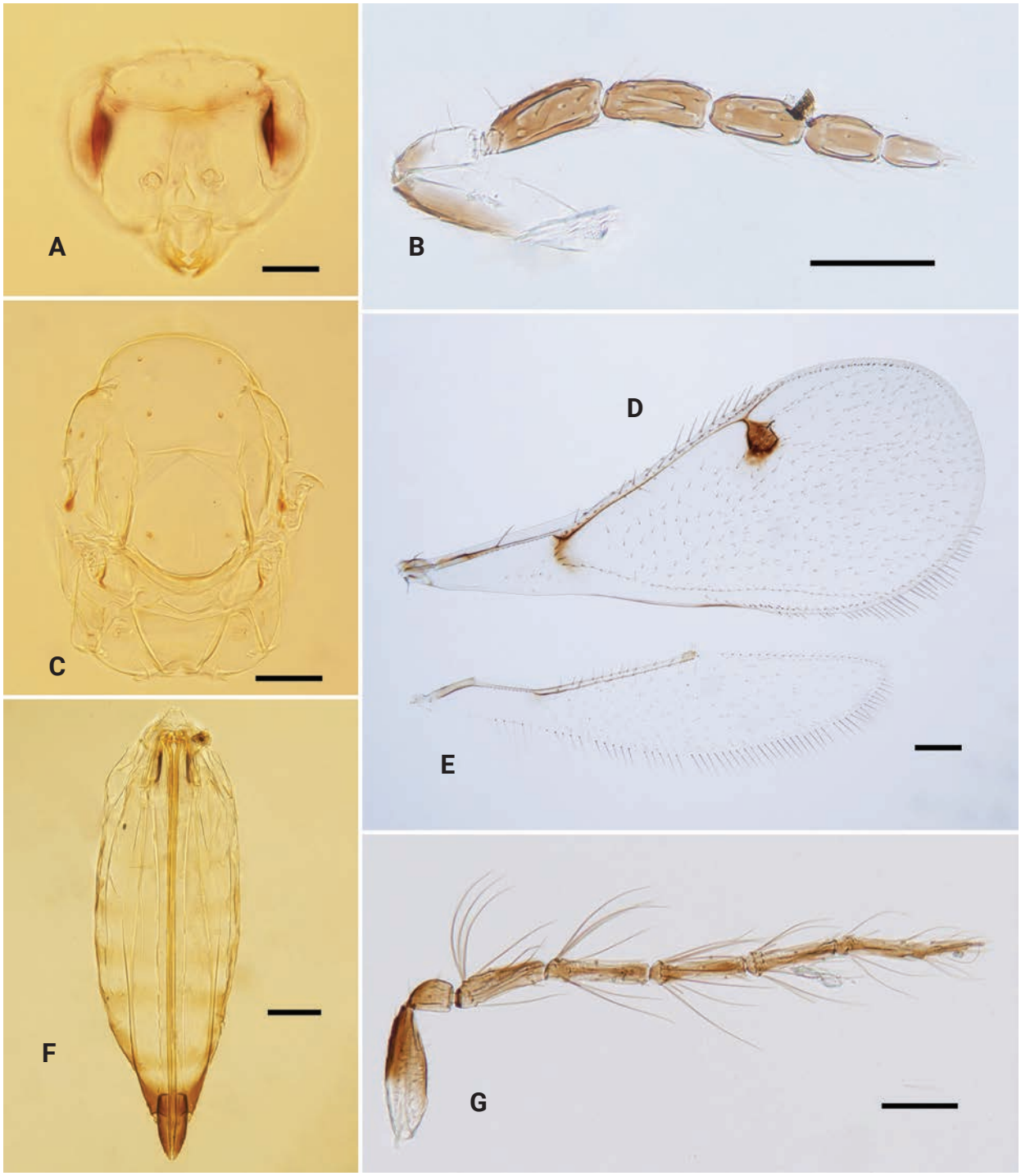

Figure 6. *Omphale melina* **A** head, frontal view, ♀ **B** antenna, ♀ **C** mesosoma, dorsal view, ♀ **D** fore wing, ♀ **E** hind wing, ♀ **F** metasoma, dorsal view, ♀ **G** antenna, ♂. Scale bars: 100 μm.

and apical parts of ovipositor sheaths dark brown to black; antenna with scape yellowish white, only dorsal part dark brown; pedicel yellowish white, brown at base; flagellum dark brown; fore wing hyaline, with infuscate around STV and base of MV; legs mainly yellow to yellowish white. Head (Fig. 6A) with face with weak sculpture; frontal sulcus nearly straight, antennal scrobes meeting on frontal sulcus; frontal cross-ridge absent; clypeus semicircular 1.3–1.4 × as wide as high; mandible tridentate. Antenna (Fig. 6B) with five flagellomeres separated from each other; scape slightly stout, 3.4 × as long as wide; pedicel 2.0 ×

as long as wide; flagellomeres decreasing in length distinctly from F1 to F5, F1 1.2 × as long and 1.1 × as wide as F2. Mesosoma (Fig. 6C) with mesoscutum and scutellum with shallow reticulation; midlobe of mesoscutum with two pairs of setae; scutellum 1.2 × as long as wide; propodeum smooth, without median carina. Fore wing (Fig. 6D) speculum closed; with 4–5 admarginal setae arising from MV and membrane just below MV; STV enlarged and subcircular, PMV 1.0–1.2 × as long as STV, radial cell bare. Metasoma (Fig. 6F), gaster elongate, 1.7 × as long as mesosoma, longer than head + mesosoma (1.4:1.0).

Male. Body length 1.2 mm, mainly brown and with weak metallic reflection; antenna brown, only basal 1/3 of scape yellowish white. Antenna (Fig. 6G) slender and longer than female, F1–4 with verticillate setae and the setae reaching beyond apex of flagellomere attached to; F1 0.9 × as long and 1.2 × as wide as F2. Gaster with an oval and transparent membranous region between 1st tergite and 4th tergite. Other features as in female.

Host. Unknown.

Distribution. China (Liaoning Province) (new record); Russia (Yefremova and Kriskovich 1994).

Remarks. The male of *Omphale melina* is recorded for the first time in the world. The color of females collected from China is distinctly lighter than in the paratype from Russia, while the male collected from China has similar color to the paratype female from Russia (Hansson and Shevtsova (2012: figs 468–470). Both sexes of *O. melina* can be easily separated from other species in *Omphale* through its enlarged stigmal vein and non-metallic body.

Omphale obscura (Förster, 1841)

Figs 1H, 7A–K

Elachestus obscurus Förster, 1841: 40, lectotype ♀, Germany, NHMV, not examined.
Holcopelte obscura (Förster): Förster, 1856: 81.
Holcopelte fulvipes Förster, 1861: 137, lectotype ♀, Switzerland, NHMV, not examined.
Horismenus obscurus (Förster): Schmiedeknecht 1909: 433.
Horismenus fulvipes (Förster): Schmiedeknecht 1909: 433.
Omphale obscura (Förster): Hansson and Shevtsova 2012: 113.

Material examined. • 12♀: 4♀ [NEFU; 3 on cards, 1 on slide], China, Liaoning Province, Anshan City, Qianshan, 21.VI.2015, leg. Hui Geng, Si-Zhu Liu, Yan Gao, and Zhi-Guang Wu, by sweep netting • 3♀ [NEFU; on cards], China, Liaoning Province, Huludao City, Jianchang county, Bailangshan National Nature Reserve, 04.VII.2012, leg. Si-Zhu Liu and Jiang Liu, by sweep netting • 2♀ [NEFU; 1 on card, 1 on slide], China, Xizang Autonomous Region, Medog County, Damu Village, 22–29.VI.2017, leg. Zhaxi, by Malaise trapping • 2♀ [NEFU; on cards], China, Xizang Autonomous Region, Medog County, Damu Village, 15–22.VI.2017, leg. Zhaxi, by Malaise trapping • 1♀ [NEFU; on card], China, Xizang Autonomous Region, Medog County, Gedang Village, 31.V–05.VI.2021, leg. Jun-Jie Fan and Jun Wu, by yellow-pan trapping.

Diagnosis. Female. Body length 1.2–1.4 mm, mainly brown to dark brown, face and vertex with bronze metallic tinges; eyes dull red; antenna with scape yellow

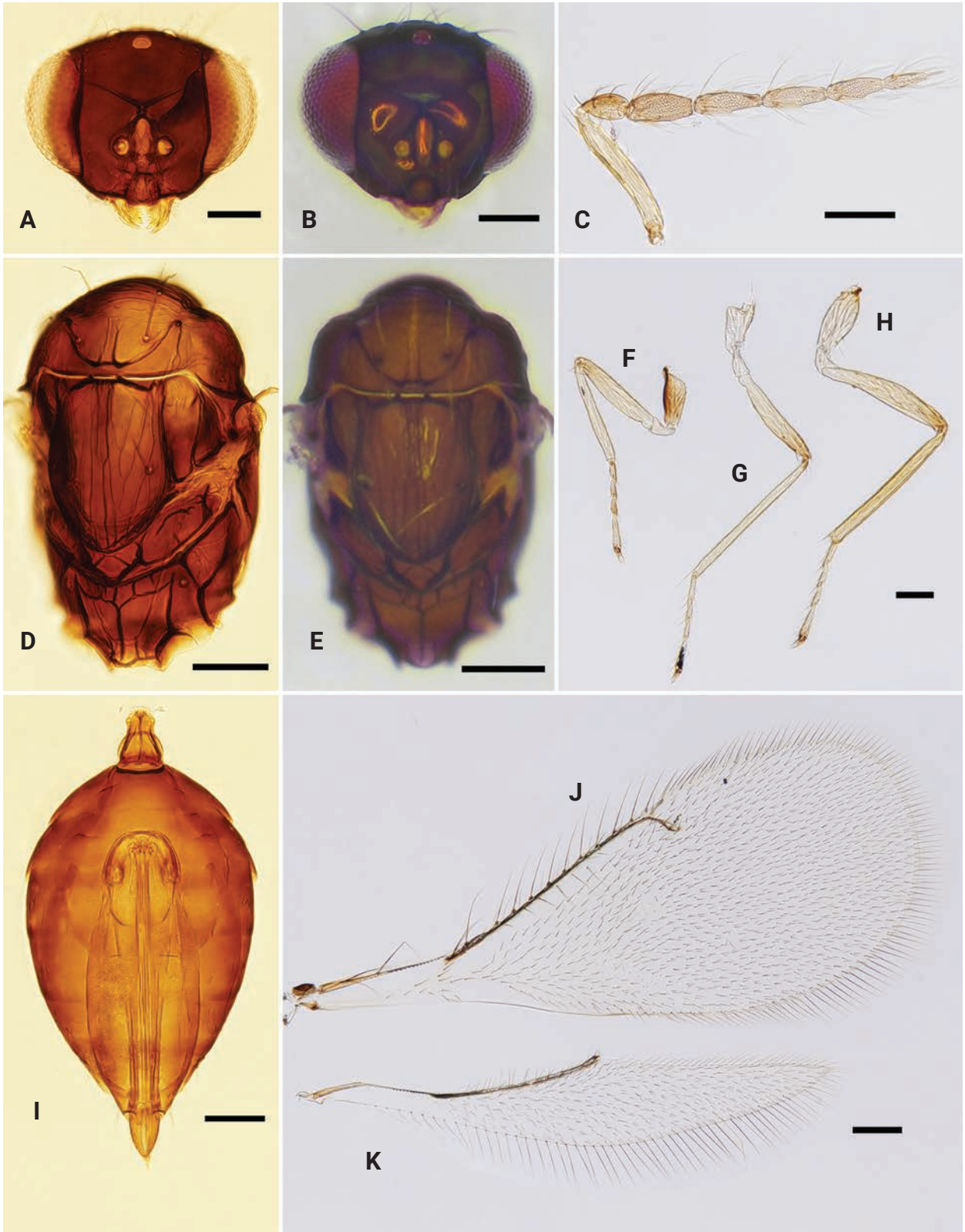

Figure 7. *Omphale obscura*, ♀ **A, B** head, frontal view **C** antenna **D, E** mesosoma, dorsal view **F–H** fore, mid and hind leg, respectively **I** metasoma, dorsal view **J** fore wing **K** hind wing. Scale bars: 100 μm.

to pale brown, pedicel and flagellum brown to dark brown; mandibles pale brown to yellow; legs yellow to yellowish white, except dark brown claws and brown fore coxa; wings hyaline. Head (Fig. 7A, B) not collapsed after death; face and ver-

tex smooth, without any reticulation; POL:OOL ~ 1.3:1.0; frontal sulcus V-shaped, reaching eye margin, the midpoint closer to antennal toruli than to median ocellus; antennal scrobes meeting just below frontal sulcus and connected to frontal sulcus by a short longitudinal suture; HE:MS:WM ~ 3.9:1.0:2.3; clypeus trapezoid to triangular, as high as the width at its lower margin, lower margin protruding and emarginate; mandible with two large and pointed teeth at apex and 3–4 smaller and obtuse teeth at base. Antenna (Fig. 7C) with all five flagellomeres separated from each other; scape 5.3 × as long as wide, longer than pedicel + F1; pedicel 1.8 × as long as wide; F1–5 with verticillate setae, setae on F1 reaching apex of F1, and setae on F2–5 reaching beyond apex of flagellomere attached to; F1 1.0 × as long and 1.4 × as wide as F2; F3 to F5 slightly decreasing in both length and width. Mesosoma (Fig. 7D, E), 1.6 × as long as wide; mesoscutum with sparse reticulation with transverse meshes, mid lobe with two pairs of setae, with a shallow median groove in posterior 1/3; notauli as subtriangular impressions in posterior 1/2; mesoscutellum 1.3 × as long as wide, with sparse and elongate reticulation or striation and one pair of setae, anterior 1/2 with an indistinct and shallow median groove; metascutellum with two foveae anterolaterally, 0.4 × as long as wide, 0.3 × as long as length of median propodeum; propodeum 0.5 × as long as mesoscutellum, smooth, with a distinct and complete median carina and a pair of plicae, as well as a wide groove along anterior margin, posteromedian part forms a short nucha. Fore wing (Fig. 7J) 2.8 × as long as wide, speculum closed; with six to ten admarginal setae arising from both MV and from membrane just below MV; STV long and slender, PMV shorter than STV, radial cell setose, ratio of SMV:MV:PMV:STV ~ 5.9:10.0:1.0:1.5. Hind wing (Fig. 7K) 6.3 × as long as wide, apex pointed. Legs (Fig. 7F–H) with metatibial spur very short, not reaching the middle of basal tarsomere. Metasoma (Fig. 7I) with petiole pyriform, 0.6 × as long as length of median propodeum; gaster 1.2 × as long as length of mesosoma, nearly as long as head + mesosoma; ovipositor sheaths exserted beyond apex of gaster.

Male. Not collected from China, see Hansson and Shevtsova (2012).

Host. *Dasineura viciae* (Diptera, Cecidomyiidae) (Bouček and Askew 1968).

Distribution. China (Xizang Autonomous Region and Liaoning Province) (new record); Germany (Förster 1841); Switzerland (Förster 1861); Hungary (Erdös 1956); Austria, Sweden, United Kingdom, Yugoslavia (Bouček and Askew 1968); Croatia (Bouček 1977); Czech Republic (Kalina 1989); Italy (De Stefani 1905); Netherlands (Gijswijt 2003); France, Russia (Hansson and Shevtsova 2012); Romania (Hansson 2016).

Remarks. The specimens collected from China have distinct propodeal plicae that almost reach the anterior margin of the propodeum, whereas the European specimens have irregular plicae that only reach half the length of the propodeum (Hansson and Shevtsova 2012: fig. 376).

Omphale rectisulcus **Li & Li, sp. nov.**

https://zoobank.org/4DC8D2ED-A242-4974-8A63-3FFF470CDC8F
Figs 1G, 8A–K

Type material. ***Holotype*****:** • ♀ [NEFU; on card], China, Jiangxi Province, Shangrao City, Yanshan County, Yejiachang Village, 7.VII.2013, leg. Chao Zhang, by sweep netting. ***Paratypes*****:** • 1♀ [NEFU; on slide], China, Sichuan Province,

Guangyuan City, Qingchuan County, 20.VIII.2015, leg. Ye Chen and Chao Zhang, by sweep netting.

Diagnosis. Female. Frontal sulcus straight, reaching eye margin, distance from frontal sulcus to median ocellus is as long as distance to toruli; antennal scrobes slightly wide and deep, as grooves rather than sulcus, meeting below frontal sulcus and connected to frontal sulcus by a short longitudinal suture; clypeus with both upper and lower margins arcuate, nearly oval-shaped, 2.0 × as wide as high; notauli step-shaped, indicated by smooth depressions; propodeum with a narrow groove along anterior margin, without median carina.

Description. Female. Body length 1.5–1.6 mm. Face and vertex dark brown with weak golden-green and bronze reflections; eyes dull red; clypeus with same color as surrounding parts of face; mandibles yellowish white with apex brown; mesosoma brown with golden-blue and golden-green reflections; metasoma brown to dark brown except yellow petiole; antenna with scape yellowish white, pedicel and flagellum brown; all legs yellowish white except fore coxae and fore tarsi, which are brown or yellowish brown; fore wings hyaline.

Head (Fig. 8A, B) in frontal view 1.2 × as wide as high; face and vertex smooth, only parts around antennal toruli with very weak reticulation and genae with weak transverse sculpture; occipital margin with a sharp edge; POL:OOL ~ 1.3:1.0; frontal sulcus straight, reaching eye margin, distance from frontal sulcus to median ocellus as long as distance to antennal toruli; antennal scrobes slightly wide and deep, meeting below frontal sulcus and connected to frontal sulcus by a short longitudinal suture; frontal cross-ridge slightly W-shaped and not reaching eye margin; clypeus with both upper and lower margins arcuate, nearly oval-shaped, 2.0 × as wide as high; mandible with two large teeth at apex and five smaller teeth at base; gena curved and slightly convex; HE:MS:WM ~ 5.7:1.0:4.7. Antenna (Fig. 8C) with all five flagellomeres separated from each other; scape 4.7 × as long as wide; pedicel 1.8 × as long as wide, and 0.75 × as long as F1; flagellomeres with F1, F2 and F3 almost equal in length, width of basal part of F1 equal to width of F2, but widest part of F1 1.5 × as wide as F2.

Mesosoma (Fig. 8D, E) 1.5 × as long as wide; pronotum reduced and not visible in dorsal view; mesoscutum with shallow polygonal reticulation, meshes of reticulation barely elongate or transverse; notauli step-shaped, indicated by smooth depressions; median part of mesoscutum with two pairs of setae, and posterior margin slightly emarginate; mesoscutellum 1.2 × as long as wide, with same reticulation as mesoscutum, anterior 1/4–1/3 with a weak median groove, anterior corners impressed, single pair of setae located in the lower middle of scutellum; axillae with weak reticulation; metascutellum smooth, 0.4 × as long as wide, and 0.5–0.6 × as long as length of median propodeum, with two foveae anterolaterally; lateral panels of metanotum smooth; propodeum smooth with a narrow groove along anterior margin, without median carina. Fore wing (Fig. 8J) 2.3 × as long as wide, speculum closed; with seven admarginal setae arising from both MV and from membrane just below MV; PMV distinctly longer than STV, radial cell bare; ratio of SMV:MV:PMV:STV ~ 4.2:7.5:2.1:1.0. Hind wing (Fig. 8K) 4.8 × as long as wide, apex rounded. Legs (Fig. 8F–H) with metatibial spur nearly reaching apex of basal tarsomere.

Metasoma (Fig. 8I) with petiole short and wide; gaster 1.9 × as long as length of mesosoma, and longer than head + mesosoma (1.2:1.0); ovipositor sheaths exserted beyond apex of gaster.

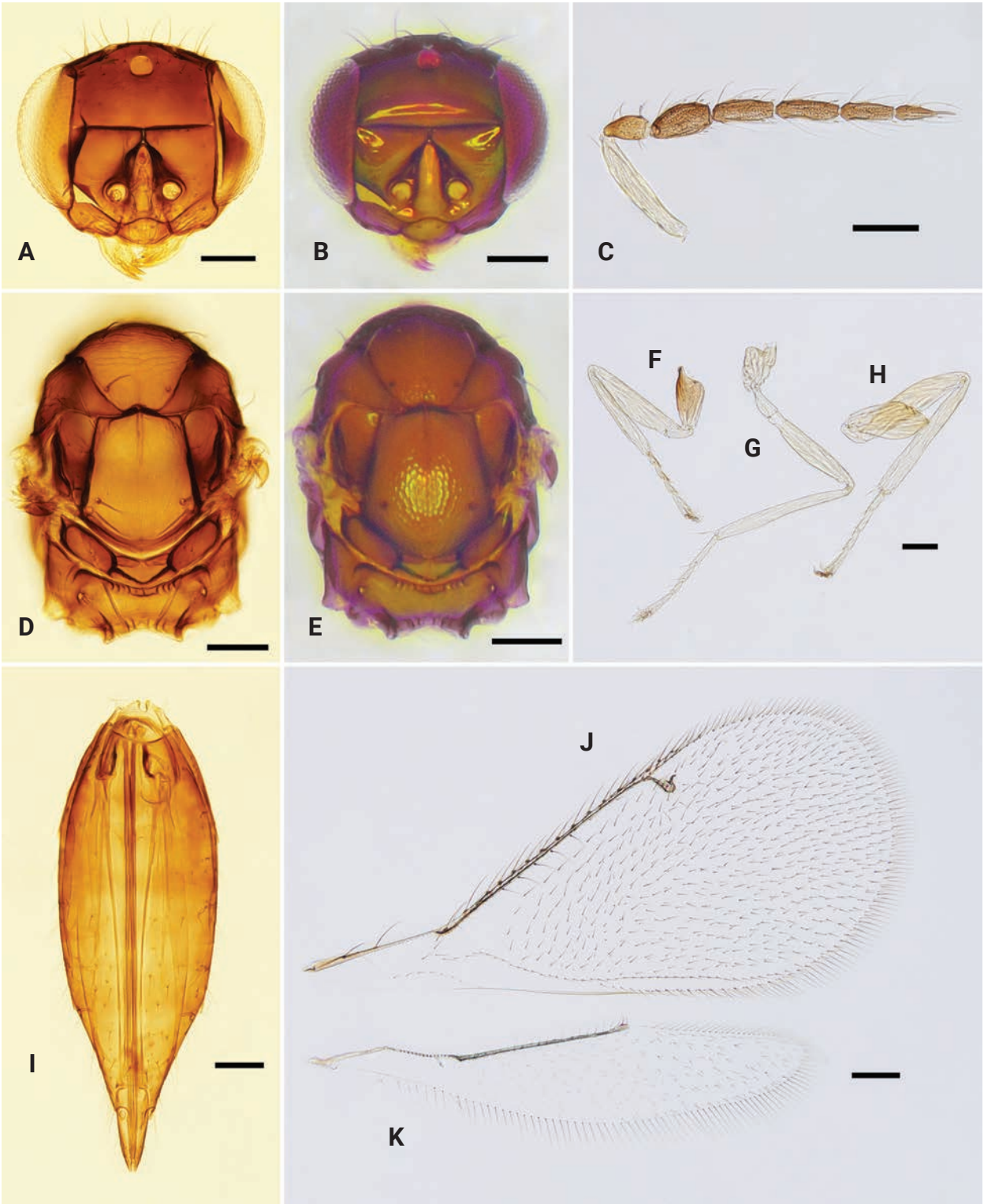

Figure 8. *Omphale rectisulcus* sp. nov., paratype, ♀ **A, B** head, frontal view **C** antenna **D, E** mesosoma, dorsal view **F–H** fore, mid and hind leg, respectively **I** metasoma, dorsal view **J** fore wing **K** hind wing. Scale bars: 100 μm.

Male. Unknown.

Host. Unknown.

Etymology. The specific name refers to the straight frontal sulcus (*recti-* is Latin for straight).

Distribution. China (Sichuan and Jiangxi Provinces).

Remarks. *Omphale rectisulcus* sp. nov. should belong to the *huggerti* group, and is closest to *O*. *aperta* Hansson, 2004. The two species share the following characteristics: frontal sulcus straight or nearly straight; antennal scrobes meeting below frontal sulcus and connected to frontal sulcus by a short longitudinal suture; metascutellum flat, with two foveae anterolaterally; petiole short and wide. *Omphale rectisulcus* sp. nov. differs from *O. aperta* in having the clypeus nearly oval-shaped (vs nearly semicircular in *O. aperta*); fore wing with seven admarginal setae arising from MV and membrane just below MV (vs six in *O. aperta*), speculum closed (vs open below in *O. aperta*), PMV distinctly longer than STV (vs shorter than in *O. aperta*); propodeum without median carina (vs with median carina in *O. aperta*).

Omphale sulciscuta (Thomson, 1878)

Figs 1I, 9A–K

Derostenus (*Holcopelte*) *sulciscuta* Thomson, 1878: 272, holotype ♀, Sweden, LUZN, not examined.
Horismenus sulciscuta (Thomson, 1878): Schmiedeknecht (1909): 433.
Holcopelte sulciscuta (Thomson, 1878): Bouček (1971): 541.
Omphale sulciscuta (Thomson, 1878): Hansson and Shevtsova (2012): 122.

Material examined. • 2♀: 1♀ [NEFU; on card], China, Heilongjiang Province, Yichun City, Dailing District, Liangshui National Nature Reserve, 26.VII.2015, leg. Si-Zhu Liu, Xing-Yue Jin, and Xin-Yu Zhang, by sweep netting • 1♀ [NEFU; on slide], China, Heilongjiang Province, Yichun City, Dailing District, Liangshui National Nature Reserve, 02.VIII.2015, leg. Si-Zhu Liu, Xing-Yue Jin, and Xin-Yu Zhang, by sweep netting.

Diagnosis. Female. Body length 1.1–1.7 mm, strongly sclerotized, mainly black to dark brown; antenna with scape yellowish brown to brown, pedicel and flagellum dark brown; fore wing hyaline. Head (Fig. 9A, B) with face and vertex smooth, frontal sulcus V-shaped, antennal scrobes meeting below meeting below frontal sulcus and connected frontal sulcus with longitudinal suture; clypeus trapezoid, 1.5 × as wide as high. Antenna (Fig. 9C) with five flagellomeres separated from each other; scape slightly stout, 5.2 × as long as wide; pedicel 1.5 × as long as wide; F1 1.0 × as long and 2.0 × as wide as F2; F1–5 with verticillate setae at base, the setae reaching or reaching beyond the apex of flagellomere attached to. Mesosoma (Fig. 9D, E) with mesoscutum and scutellum with distinct and sparse reticulation, meshes of reticulation mainly hexagonal; midlobe of mesoscutum with two pairs of setae and an incomplete shallow median groove; notauli as distinct deep grooves in posterior 1/2; scutellum 1.2 × as long as wide, with an incomplete median groove in anterior 1/2–2/3; metascutellum tongue like and without foveae anterolaterally; propodeum smooth, with a weak and narrow median carina, plica, between median carina and spiracular sulcus with a longitudinal carina, posterior part forming a short nucha; Fore wing (Fig. 9J) speculum closed, with 8–12 admarginal setae arising from MV and membrane just below MV; PMV shorter than STV, 0.7–0.8 × as long as STV, radial cell nearly bare (at least without setae along PMV). Metasoma (Fig. 9I), petiole quadratic to

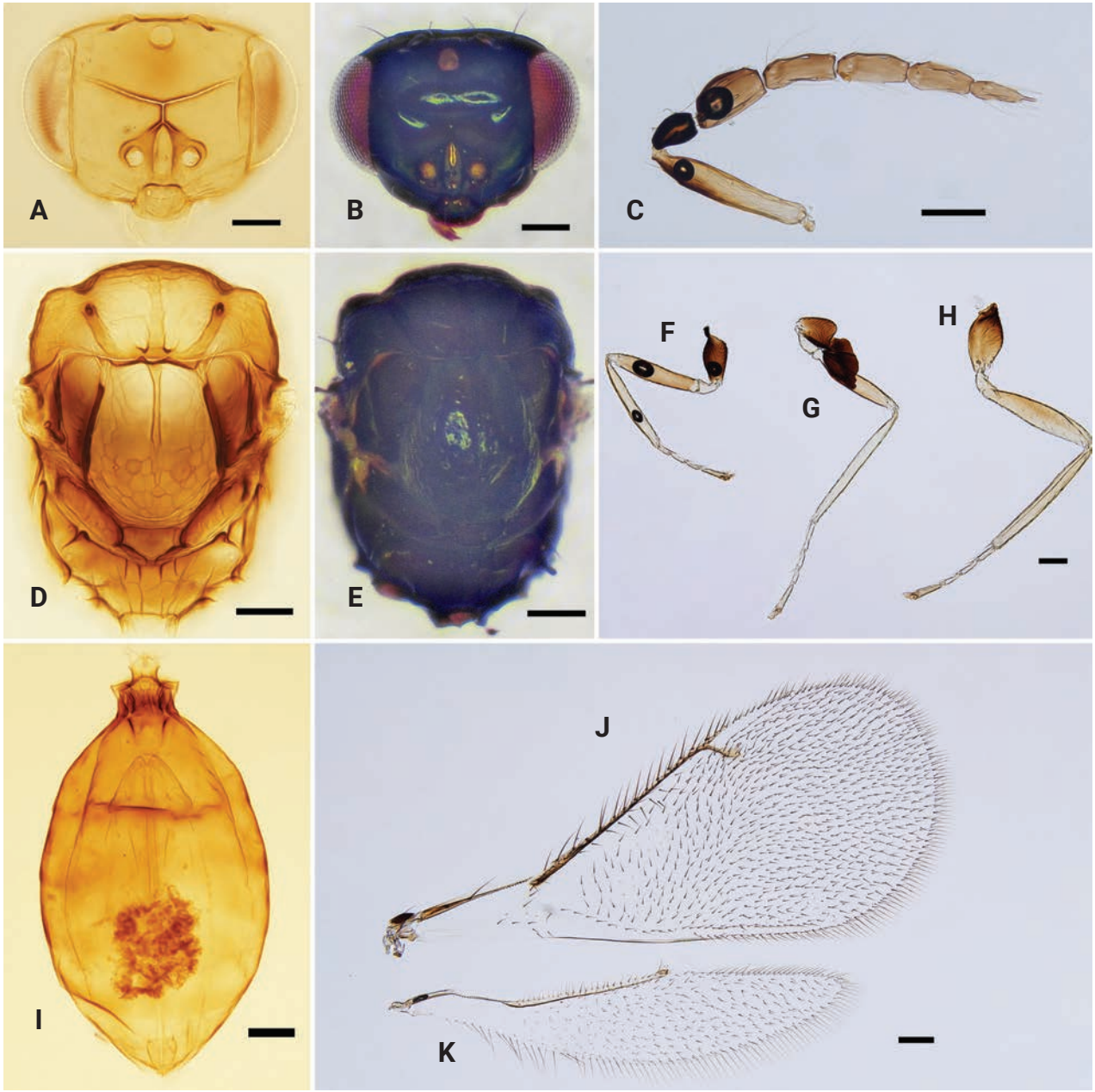

Figure 9. *Omphale sulciscuta*, ♀ **A, B** head, frontal view **C** antenna **D, E** mesosoma, dorsal view **F–H** fore, mid and hind leg, respectively **I** metasoma, dorsal view **J** fore wing **K** hind wing. Scale bars: 100 μm.

transverse, with anterior part drawn out to form a sharp margin that covers propodeal nucha; gaster 1.3 × as long as mesosoma, slightly longer than head + mesosoma (1.1:1.0).

Male. See Hansson and Shevtsova (2012).

Host. Unknown.

Distribution. China (Heilongjiang, Gansu, and Guangxi provinces); Armenia and Germany (Bouček and Askew 1968); Bulgaria (Boyadzhiev 2006); Croatia and Montenegro (Bouček 1977); Czech Republic (Bouček 1957); Denmark, France, and Russia (Hansson and Shevtsova 2012); Hungary (Erdös 1956); Moldova (Bouček 1965); Netherlands (Gijswijt 2003); Romania (Hansson 2016); Slovakia (Kalina 1989); Sweden (Thomson 1878); United Kingdom (Graham 1959).

***Omphale xanthosoma* Li & Li, sp. nov.**
https://zoobank.org/B9396418-A6D1-4B45-BA54-AF51AF74BD45
Fig. 10A–F

Material examined. *Holotype*: • ♀ [NEFU; on card, right antenna and right wings on slide], China, Hainan Province, Ledong Li Autonomous County, Jianfengling National Forest Park, 18.V.2021, leg. Ming-Rui Li and Gang Fu, by sweep netting.

Diagnosis. Female. Body mainly yellow without metallic reflections, mesoscutum and mesoscutellum with a brown median stripe, posterior margin of abdominal tergites and apical part of ovipositor sheaths brown to dark brown; mid lobe of mesoscutum with only one pair of setae; gaster lanceolate, 2.0 × as long as length of mesosoma, obviously longer than head + mesosoma (1.6:1.0); antenna with scape short, 4.0 × as long as wide; fore wing with ten admarginal setae, radial cell nearly bare, with a sparsely hairline from the middle part of radial cell.

Description. Female. Body length 1.4 mm, mainly yellow without metallic reflections, with a brown longitudinal stripe along median part of mesoscutum and mesoscutellum, posterior margin of abdominal tergites and apical part of ovipositor sheaths dark brown; eyes dull red; antenna with scape yellowish white, except apical 1/3 of dorsal edge brown, pedicel pale brown to brown, flagellum dark brown; mandibles with teeth dark brown; all legs yellow to yellowish white, except brown tarsal claws; wings hyaline.

Head (Fig. 10A) in frontal view 1.3 × as wide as high, slightly collapsed after death; face and vertex smooth; POL:OOL ~ 1.5:1.0; frontal sulcus arcuate, reaching eye margin, the midpoint closer to median ocellus than to antennal toruli; antennal scrobes join frontal sulcus separately; antennal toruli situated above level of lower eye margin; HE:MS:WM ~ 3.1:1.0:3.0; clypeus more or less semicircular, with upper margin weakly delimited and lower margin protruding, 2.2 × as wide as high; mandible with two large and pointed teeth at apex and one smaller and obtuse tooth at base. Antenna (Fig. 10B) with all five flagellomeres separated from each other; scape 4.0 × as long as wide; pedicel 1.4 × as long as wide; F1 1.0 × as long and 1.4 × as wide as F2; F3 to F5 slightly decreasing in both length and width.

Mesosoma (Fig. 10C) 1.4 × as long as wide; pronotum reduced and not visible in dorsal view; mesoscutum with fine reticulation, mid lobe with only one pair of black setae; notauli indicated in anterior third; mesoscutellum 1.1 × as long as wide, anterior 1/2 with fine reticulation, posterior 1/2 smooth, with one pair of black setae located in the middle part; metascutellum small and triangular; propodeum short medially, 0.2 × as long as mesoscutellum, smooth, without median carina or plica. Fore wing (Fig. 10D) 2.5 × as long as wide, speculum closed, with ten admarginal setae arising from both MV and from membrane just below MV, with apical setae attached close to STV; PMV longer than STV, radial cell nearly bare, with a sparsely hairline from the middle part of radial cell, ratio of SMV:MV:PMV:STV ~ 3.9:5.3:1.9:1.0. Hind wing (Fig. 10E) 5.3 × as long as wide, apex pointed. Legs (Fig. 10F)with hind femur with three distinct long setae on outer side.

Metasoma (Fig. 10C) 3.4 × as long as wide; petiole short; Gaster lanceolate, 2.0 × as long as length of mesosoma, obviously longer than head + mesosoma (1.6:1.0); ovipositor sheaths exserted beyond apex of gaster.

Male. Unknown.

Host. Unknown.

Etymology. The specific name refers to the yellow body of this new species.

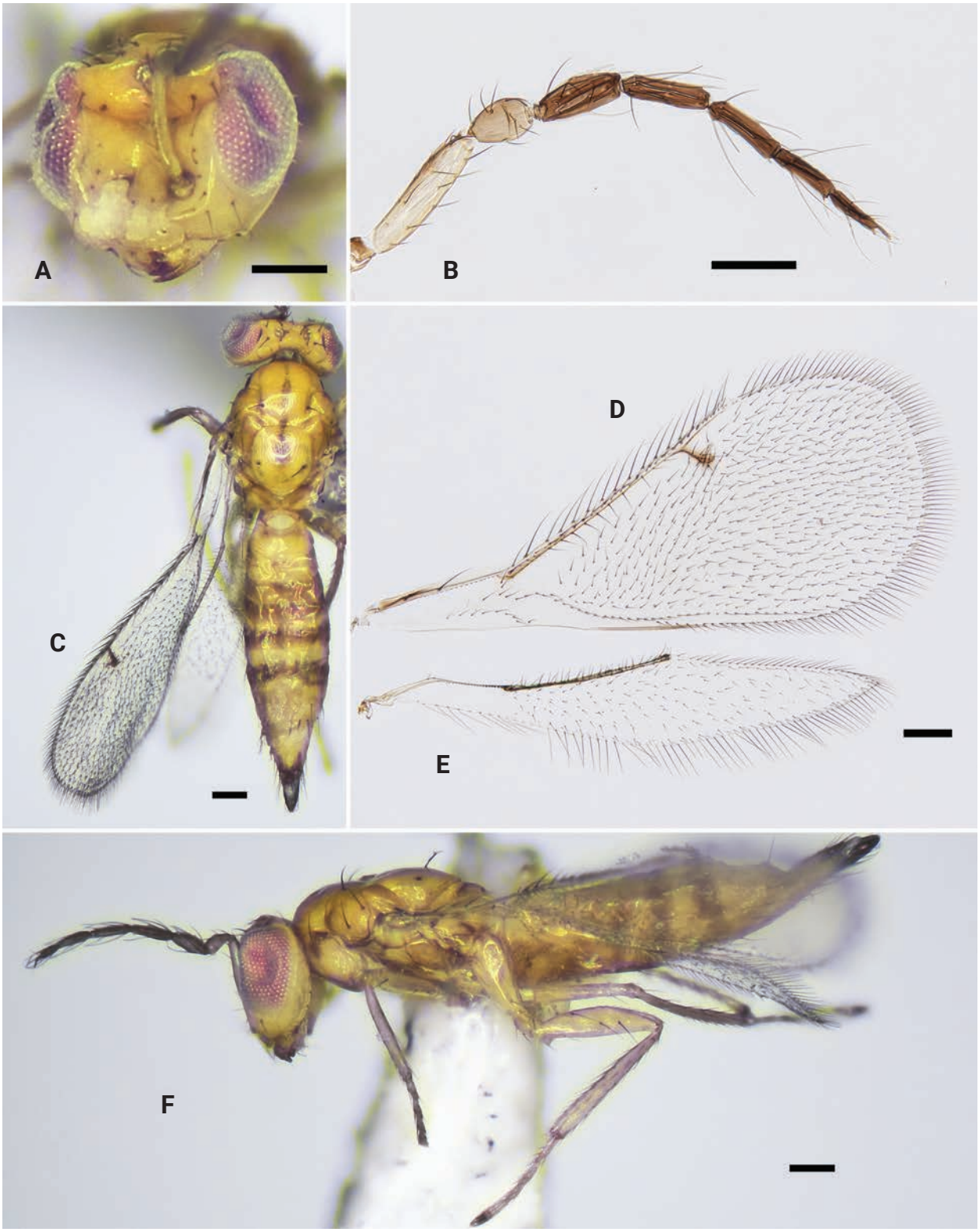

Figure 10. *Omphale xanthosoma* sp. nov., holotype, ♀ **A** head, frontal view **B** antenna **C** dorsal habitus, shows mesosoma and metasoma **D** fore wing **E** hind wing **F** lateral habitus, shows legs. Scale bars: 100 μm.

Distribution. China (Hainan Province).

Remarks. *Omphale xanthosoma* sp. nov. should belong to the *obscurinotata* group, and is similar to *Omphale mellea* Hansson. The two species share the following characteristics: body mostly yellow; antenna with scape mainly yel-

lowish white to yellow, flagellum dark brown; mid lobe of mesoscutum with only one pair of setae; metascutellum small; propodeum short medially; fore wing with radial cell nearly bare, with a sparsely hairline from the middle part of radial cell; gaster elongate. *Omphale xanthosoma* sp. nov. differs from *O. mellea* in having a brown longitudinal stripe along the median part of the mesoscutum and mesoscutellum (vs only scutellum occasionally with a median infuscate stripe in *O. mellea*); fore wing hyaline, without any infuscate part (hyaline, infuscate close to STV in *O. mellea*); antenna with flagellum slender, F2 and F3 both nearly as long as F1 (vs flagellum stouter, F2 and F3 both shorter than F1 in *O. mellea*). *Omphale xanthosoma* sp. nov. also looks similar to *O. melina* but can be easily separated from it through the one pair setae on the midlobe of the mesoscutum and the narrow STV (midlobe of mesoscutum with two pairs setae and STV enlarged in *O. melina*). *Omphale xanthosoma* sp. nov.is also similar to *O. ochra* Hansson & Shevtsova, 2012 and *O. rodopiensis* Yefremova, Yegorenkova & Boyadzhiev, 2017. Habitually, it can be easily separated from the latter two species through the mostly yellow and non-metallic mesoscutum and the long PMV, which 1.9 × as long as STV (mesoscutum with at least anterior 1/2 golden green, PMV 0.7–0.9 × as long as STV in both *O. ochra* and *O. rodopiensis*, see Yefremova et al. (2017)).

Acknowledgements

We would like to thank the above collectors for their contributions to the specimen collection and Chen Yang (University of Kent, UK) for proofreading. We are also grateful to Prof. Christer Hansson and Dr Alex Gumovsky for providing valuable comments and suggestions to improve the manuscript.

Additional information

Conflict of interest

The authors have declared that no competing interests exist.

Ethical statement

No ethical statement was reported.

Funding

This work was supported by Natural Science Foundation of Jilin Province (YDZJ202201ZYTS691), Jilin Provincial Science and Technology Programme (YDZJ202102CXJD032), and Scientific Research Foundation of Beihua University (No. 160324044).

Author contributions

Data curation: HRZ, XPL, MRL, QFM. Funding acquisition: SDL. Resources: CDL. Software: ZJJ, JSW. Writing - original draft: MRL. Writing - review and editing: CDL.

Author ORCIDs

Ming-Rui Li https://orcid.org/0000-0002-9143-1548
Qing-Fan Meng https://orcid.org/0009-0007-9729-7435
Sheng-Dong Liu https://orcid.org/0000-0002-4699-2469

Data availability

All of the data that support the findings of this study are available in the main text.

References

Askew RR (2003) Observations on some British *Omphale* Haliday (Hym., Eulophidae) with descriptions of two new species. Entomologists Monthly Magazine 139: 29–37.

Bouček Z (1957) Chalcidoidea. Klíc Zvíreny CSR [Key to the Fauna of Czechoslovakia] 2: 204–288.

Bouček Z (1965) A review of the Chalcidoid fauna of the Moldavian S.S.R., with descriptions of new species (Hymenoptera). Acta Faunistica Entomologica Musei National Pragae 11: 5–38.

Bouček Z (1971) Descriptive and taxonomic notes on ten, mainly new, species of West Palaearctic Eulophidae (Hymenoptera). Acta Entomologica Musei Nationalis Pragae 38: 525–543.

Bouček Z (1977) A faunistic review of the Yugoslavian Chalcidoidea (Parasitic Hymenoptera). Acta Entomologica Jugoslavica 13(Supplement): 1–145.

Bouček Z, Askew RR (1968) Hym. Chalcidoidea. Palearctic Eulophidae (excl. Tetrastichinae). Index of Entomophagous Insects 3. Le François, Paris, 260 pp.

Boyadzhiev P (2006) Eulophidae (Hymenoptera: Chalcidoidea) of the Western Rhodopes (Bulgaria). In: Beron P (Ed.) Biodiversity of Bulgaria. 3. Biodiversity of Western Rhodopes (Bulgaria and Greece) I. Pensoft & National Museum of Natural History, Sofia, 561–580.

De Stefani T (1905) Contributo all'entomofauna del cecidii. Marcellia 3: 36–40, 113–114.

Erdös J (1956) Additamente ad cognitionem faunae Chalcidoidarum in Hungaria et regionibus finitimis VI 19 Eulophidae. Folia Entomologica Hungarica (s.n.) 9: 1–64.

Förster A (1841) Beiträge zur Monographie der Pteromalinen Nees. Aachen, 46 pp. https://doi.org/10.5962/bhl.title.66014

Förster A (1856) Hymenopterologische Studien. 2. Chalcidiae und Proctotrupii. Aachen, 152 pp.

Förster A (1861) Ein Tag in den Hoch-Alpen. Programm der Realschule zu Aachen 1860/61, 43 pp.

Gijswijt MJ (1976) Notes on biology and distribution of the genus *Omphale* Haliday, 1833, with descriptions of two new species (Insecta, Hymenoptera, Eulophidae). Bulletin Zoologische Museum, Universiteit van Amsterdam 5(10): 77–84.

Gijswijt MJ (2003) Naamlijst van de Nederlandse bronswespen (Hymenoptera: Chalcidoidea). Nederlandse Faunistische Mededelingen 18: 17–79.

Graham MWR de V (1959) Keys to the British genera and species of Elachertinae, Eulophinae, Entedontinae and Euderinae (Hym., Chalcidoidea). Transactions of the Society for British Entomology 13(10): 169–204.

Graham MWR de V (1963) Additions and corrections to the British list of Eulophidae (Hym., Chalcidoidea), with descriptions of some new species. Transactions of the Society for British Entomology 15(9): 167–275.

Haliday AH (1833) An essay on the classification of the parasitic Hymenoptera of Britain, which correspond with the *Ichneumones minuti* of Linnaeus. Entomologists Magazine 1: 333–350.

Hansson C (1991) A catalogue of Chalcidoidea described by C.G. Thomson, with a checklist of Swedish species. Entomologica Scandinavica Supplement 38: 1–70.

Hansson C (1996) Taxonomic revision of the Nearctic species of *Omphale*. Entomologica Scandinavica Supplement 49: 1–78.

Hansson C (1997) Mexican species of the genus *Omphale* Haliday (Hymenoptera: Eulophidae), a taxonomic study. Journal of Hymenoptera Research 6: 107–151.

Hansson C (2004) Eulophidae of Costa Rica, 2. Memoirs of the American Entomological Institute 75: 1–537.

Hansson C (2016) New records of Eulophidae (Hymenoptera: Chalcidoidea) from Romania, including two new species. Travaux du Muséum d'Histoire Naturelle 'Grigore Antipa', Bucuresti 59(1): 53–72. https://doi.org/10.1515/travmu-2016-0017

Hansson C, Shevtsova E (2012) Revision of the European species of *Omphale* Haliday (Hymenoptera, Chalcidoidea, Eulophidae). ZooKeys 232(Special Issue): 1–157. https://doi.org/10.3897/zookeys.232.3625

Hymenoptera Anatomy Consortium (2024) Hymenoptera Anatomy Ontology Portal. http://glossary.hymao.org [accessed 1 June 2024]

Jamali MM, Zeya SB, Andrabi SAH (2022) The genus *Omphale* Haliday (Hymenoptera, Chalcidoidea, Eulophidae) from India with description of four new species. Journal of Insect Biodiversity and Systematics 8(2): 229–243. https://doi.org/10.52547/jibs.8.2.229

Kalina V (1989) Checklist of Czechoslovak Insects III (Hymenoptera). Chalcidoidea. Acta Faunistica Entomologica Musei Nationalis Pragae 19: 1–194.

Ling ZP (1994) Two new species of *Holcopelte* from China (Hymenoptera: Eulophidae). Acta Zootaxonomica Sinica 19(3): 357–361.

Noyes JS (1982) Collecting and preserving chalcid wasps (Hymenoptera: Chalcidoidea). Journal of Natural History 16(3): 315–334. https://doi.org/10.1080/00222938200770261

Noyes JS (2019) Universal Chalcidoidea Database. World Wide Web electronic publication. http://www.nhm.ac.uk/chalcidoids [accessed 1 May 2024]

Schmiedeknecht O (1909) Hymenoptera Fam. Chalcididae. Genera Insectorum 97: 1–550.

Szelényi G (1978) Four new eulophid wasps from Hungary (Hymenoptera: Chalcidoidea). Acta Zoologica Academiae Scientiarum Hungaricae 24(1/2): 219–224.

Thomson CG (1878) Hymenoptera Scandinaviae. Lundae 5: 1–307.

Walker F (1839) Monographia Chalciditum I. Ballière, London, 330 pp. https://doi.org/10.5962/bhl.title.67725

Yefremova ZA, Yegorenkova EN, Stojanova AM, Boyadzhiev PS (2017) A New Species of *Omphale* Haliday, 1833 (Hymenoptera, Eulophidae) from Bulgaria. Acta Zoologica Bulgarica Supplement 8: 119–122.

Yefremova ZA, Kriskovich MV (1994) A new species of the genus *Omphale* (Hymenoptera, Eulophidae) from the Far East. Entomological Review 74(2): 245–248.

Zhang YZ, Ding L, Huang HR, Zhu CD (2007) Eulophidae fauna (Hymenoptera, Chalcidoidea) from south Gansu and Quinling mountain areas, China. Acta Zootaxonomica Sinica 32(1): 6–16.

Zhu CD, Huang DW (2001) A taxonomic study on Eulophidae from Zhejiang, China (Hymenoptera: Chalcidoidea). Acta Zootaxonomica Sinica 26(4): 533–547.

Zhu CD, Huang DW (2002) A taxonomic study on Eulophidae from Guangxi, China (Hymenoptera: Chalcidoidea). Acta Zootaxonomica Sinica 27(3): 583–607.

ZooKeys 1215: 235–257 (2024)
DOI: 10.3897/zookeys.1215.130919

Research Article

A new species of the pill millipede genus *Rhopalomeris* Verhoeff, 1906 (Diplopoda, Glomerida, Glomeridae) from Myanmar, and notes on *Rhopalomeris carnifex* (Pocock, 1889)

Natdanai Likhitrakarn[1], Sergei I. Golovatch[2], Ruttapon Srisonchai[3], Parin Jirapatrasilp[4], Pichsinee Sapparojpattana[5], Ekgachai Jeratthitikul[5], Somsak Panha[4,6], Chirasak Sutcharit[4]

1 *Program of Agriculture, Faculty of Agricultural Production, Maejo University, Chiang Mai 50290, Thailand*
2 *Institute of Ecology and Evolution, Russian Academy of Sciences, Leninsky pr. 33, Moscow 119071, Russia*
3 *Department of Biology, Faculty of Science, Khon Kaen University, Khon Kaen 40002, Thailand*
4 *Animal Systematics Research Unit, Department of Biology, Faculty of Science, Chulalongkorn University, Bangkok 10330, Thailand*
5 *Animal Systematics and Molecular Ecology Laboratory, Department of Biology, Faculty of Science, Mahidol University, Bangkok 10400, Thailand*
6 *Academy of Science, The Royal Society of Thailand, Bangkok 10300, Thailand*
Corresponding author: Chirasak Sutcharit (jirasak4@yahoo.com; chirasak.s@chula.ac.th)

Abstract

The taxonomy of the pill millipede genus *Rhopalomeris* Verhoeff, 1906, which is restricted to Indochina and currently comprises six described species, is refined and updated. An integrative taxonomic approach was employed that combines morphological examination with DNA barcoding using the cytochrome *c* oxidase subunit I (COI) gene for species identification and delineation. The first objective was to confirm the identity of *Rhopalomeris carnifex* (Pocock, 1889), a charismatic species known as the "candy pill millipede" due to its vivid coloration, based on specimens collected near the type locality in Myanmar. The second objective was to describe a new species, *Rhopalomeris nigroflava* Likhitrakarn, **sp. nov.**, discovered in Linno Gu, Kayin State, Myanmar. This new species is distinguished by its small body size (5.1–9.7 mm long) and yellow body with contrasting brown to blackish markings on certain terga. In addition, the position of the telopod syncoxital lobe relative to the lateral syncoxite horns separates it from other *Rhopalomeris* species. The interspecific divergence between *R. nigroflava* Likhitrakarn, **sp. nov.** and other congeners ranges from 10.85% to 16.13%, based on uncorrected COI p-distances, while the intraspecific divergence was 0%–7.44%. A distribution map of and a revised identification key to all known species of *Rhopalomeris* are also provided.

Key words: Biodiversity, candy pill millipede, key, systematics, taxonomy

Academic editor: Pavel Stoev
Received: 1 July 2024
Accepted: 29 August 2024
Published: 16 October 2024

ZooBank: https://zoobank.org/63D44DED-AB0D-4762-99A9-CC64B9EB8AE4

Citation: Likhitrakarn N, Golovatch SI, Srisonchai R, Jirapatrasilp P, Sapparojpattana P, Jeratthitikul E, Panha S, Sutcharit C (2024) A new species of the pill millipede genus *Rhopalomeris* Verhoeff, 1906 (Diplopoda, Glomerida, Glomeridae) from Myanmar, and notes on *Rhopalomeris carnifex* (Pocock, 1889). ZooKeys 1215: 235–257. https://doi.org/10.3897/zookeys.1215.130919

Introduction

The Oriental genus *Rhopalomeris* Verhoeff, 1906 consists of only six species, all of which are restricted to Indochina (Golovatch et al. 2011; Golovatch 2017). The distribution range of this genus extends from the southern peninsular regions (Malaysia and Myanmar) to the North, encompassing Thailand and reaching as far as northern Vietnam (Fig. 1). All species except for *R. carnifex*

(Pocock, 1889) show narrow distributions, while *R. carnifex* has been reported from a broader area that includes both Myanmar and Thailand (Fig. 1).

The genus *Rhopalomeris* belongs to the family Glomeridae. A total of 43 species of Glomeridae have so far been identified in Indochina and classified into six genera: *Annameris* Verhoeff, 1915 (two species), *Hyleoglomeris* Verhoeff, 1910 (23 species), *Hyperglomeris* Silvestri, 1917 (eight species), *Rhopalomeris* Verhoeff, 1906 (six species), *Peplomeris* Silvestri, 1917 and *Tonkinomeris* Nguyen, Sierwald & Marek, 2019 (one species each) (Likhitrakarn et al. 2014, 2023a, 2023b, 2024; Golovatch 2017; Golovatch and Semenyuk 2016; Nguyen et al. 2019, 2021).

Two unique morphological characters could be used to distinguish *Rhopalomeris* from the other glomerid genera: (1) antennomere 6 conspicuously enlarged, axe-shaped, exceeding the size of antennomeres 3–5 combined; (2) antennomere 7 also wide, topped by a disc-shaped antennomere 8 with numerous sensory cones, vs usually only four apical cones in other genera (except *Peplomeris*).

A well-known *Rhopalomeris* species is *R. carnifex*, commonly referred to as the "candy pill millipede" or "rainbow candy pill millipede" because of its striking and vibrant patterns (Fig. 2). This characteristic has contributed to its popularity among exotic pet traders worldwide (https://www.reddit.com/r/millipedes/comments/xdrsr0/candy_pill_millipede/; https://undergroundreptiles.com/product/candy-pill-millipede/; https://www.exotic-pets.co.uk/candy-red-pill-bug.html; https://thespidershop.co.uk/product/rhopalomeris-carnifex/).

The present study employs an integrative taxonomic approach, combining both traditional morphological examinations and DNA barcodes derived from a fragment of the COI gene. The aims of this study are to re-evaluate the taxonomy of *R. carnifex* by examining specimens collected from Koh Kala, Tanintharyi Division, Myanmar, and to describe a new species discovered at Linno Gu, Kayin State, Myanmar. We also provide a comprehensive distribution map and a revised identification key to all species currently recognized in this genus.

Material and methods

Morphological studies

The new material was collected in Myanmar in 2015 and 2016 by SP and members of the Animal Systematics Research Unit, Chulalongkorn University, as well as by a French collecting team led by Louis Deharveng, of the Muséum national d'Histoire naturelle (MNHN), Paris, France. The locations of the collecting sites were recorded by GPS using a Garmin GPSMAP 60 CSx based on the WGS 84 datum, and all coordinates and elevations were double-checked using Google Earth. The collected specimens were euthanized using a two-step method following the AVMA Guidelines for the Euthanasia of Animals (AVMA 2013) and preserved in 90% (v/v) ethanol for morphological and molecular studies. After 24 h, the ethanol was replaced with 95% (v/v) ethanol to prevent defensive chemicals from interfering with DNA extraction.

The holotype and most paratypes are housed in the Museum of Zoology, Chulalongkorn University (**CUMZ**), Bangkok, Thailand. A few paratype duplicates have been deposited in the MNHN, Paris, France. The specimens were

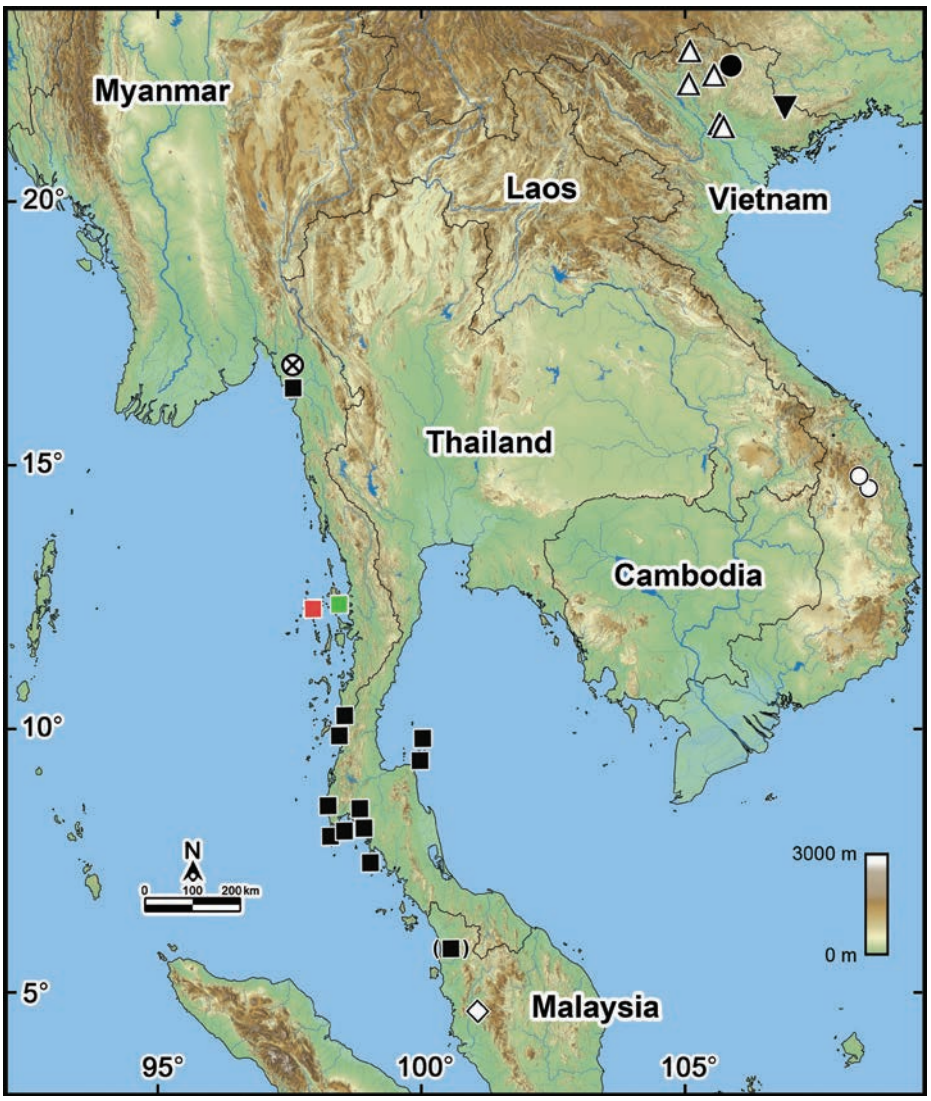

Figure 1. Distributions of all seven currently known *Rhopalomeris* species. Open triangles *Rhopalomeris sauda* Nguyen, Sierwald & Marek, 2019; filled circle *Rhopalomeris nagao* Nguyen, Nguyen & Eguchi, 2021; inverted filled triangle *Rhopalomeris tonkinensis* Silvestri, 1917; crossed circle *Rhopalomeris nigroflava* sp. nov.; filled squares *Rhopalomeris carnifex* (Pocock, 1889); red square Elphinstone Island; green square Kala Island; open circle *Rhopalomeris variegata* Golovatch, 2016; open diamond *Rhopalomeris monacha* Silvestri, 1917.

examined, measured, and photographed using a Nikon SMZ 745T trinocular stereo microscope equipped with a Canon EOS 5DS R digital SLR camera. Digital photographs were processed and modified using Adobe Photoshop CS5. The line drawings were based on photographs captured under a stereo microscope equipped with a digital SLR camera.

The terminology used to describe the morphological structures is consistent with that applied in the most recent publications (Golovatch et al. 2006; Golovatch 2017; Likhitrakarn et al. 2024).

In the catalogue sections, **D** stands for the original description and subsequent descriptive notes; **K** for the appearance in a key; **L** for the appearance in a species list; **M** for a mere mention; **MI** for molecular information; and **R** for new subsequent records.

DNA extraction, PCR amplification, and sequencing

Total genomic DNA was extracted from the legs and part of the thoracic tissues using a DNA extraction kit for animal tissue (NucleoSpin Tissue Extraction Kit, Macherey-Nagel, Germany) following the standard procedure. The mitochondrial cytochrome *c* oxidase subunit I gene (COI: 660 bp) fragments were amplified using the primers LCO1490 and HCOoutout (Folmer et al. 1994; Schulmeister et al. 2002) or LoboF1 and LoboR1 (Lobo et al. 2013) using a T100™ thermal cycler (BIO-RAD) with a final volume 30 µL, DNA template 5 µL (15 µL EmeraldAmp GT PCR Master Mix, 1.5 µL each primer, 10 ng template DNA, and distilled water up to 20 µL total volume). Thermal cycling was performed at initial denaturation at 94 °C for 3 min, followed by 35 cycles of 94 °C for 30 s, annealing at 46 °C for 60 s in both primer sets, extension at 72 °C for 90 s, and final extension at 72 °C for 5 min. Amplification of the PCR products was confirmed by 1.5% (w/v) agarose gel electrophoresis before purification using MEGAquick-spinTM plus (Fragment DNA purification kit) and sequenced in both directions (forward and reverse) using an automated sequencer (ABI prism 3730XL).

All nucleotide sequences obtained in this study have been deposited in the GenBank Nucleotide sequence database under the accession numbers PQ219547–PQ219550. The collecting localities and GenBank accession numbers for each nominal species are listed in Table 1.

Phylogenetic analyses

The sequences were aligned using MEGA7 (Kumar et al. 2016). The final aligned dataset included 660 bp of the 61 COI sequences. The dataset included four sequences of *Rhopalomeris* that were newly obtained in this study and 57 sequences retrieved from the GenBank database, including all available sequences of *Rhopalomeris* species from Vietnam and other countries, and species of other genera in the Glomeridae (*Eupeyerimhoffia* Brölemann, 1913, *Glomeris* Latreille, 1802, *Hyperglomeris* Silvestri, 1917, *Peplomeris* Silvestri, 1917, *Hyleoglomeris* Verhoeff, 1910, *Tonkinomeris* Nguyen, Sierwald & Marek, 2019, and *Trachysphaera* Heller, 1858) (Table 1). *Sphaerobelum* Verhoeff, 1924 and *Zephronia* Gray, 1832 (order Sphaerotheriida, family Zephroniidae) were used as distant outgroups.

The best-fit substitution model was determined using PartitionFinder2 v. 2.3.4 (Lanfear et al. 2016) and used in subsequent phylogenetic analyses. The selected best-fit models for the three COI codon positions were SYM+I+G, GTR+I, and GTR+G, respectively. Phylogenetic relationships were reconstructed using two methods, maximum likelihood (ML) and Bayesian inference (BI) analysis, and through the online CIPRES Science Gateway (Miller et al. 2010). The ML analysis was calculated in IQ-TREE 2.2.2.7 (Minh et al. 2020) with 10,000 replicates of ultrafast bootstrap approximation to assess topology bootstrap support (BS). The BI analysis was estimated in MrBayes 3.2.7 (Ronquist et al. 2012) using the Markov chain Monte Carlo technique (MCMC). The BI trees were run for 10 million generations using a random starting tree. The resultant trees were sampled every 1,000 generations and the values were used to estimate the consensus tree topology, bipartition posterior probability (bpp), and branch lengths, after discarding the first 25% of the obtained trees as burn-in. The average effective sample size (ESS) from the MCMC analysis were > 1,800

Table 1. List of the species used for molecular phylogenetic analyses and their relevant information. * = paratype.

Species	Voucher number	Locality	GenBank accession number COI	Reference
Rhopalomeris carnifex	GLO016-1; GLO016-2	Myanmar	PQ219547; PQ219548	This study
Rhopalomeris nigroflava sp. nov.	GLO093-1*; GLO093-2*	Myanmar	PQ219549; PQ219550	This study
Rhopalomeris sauda	IEBR-801; IEBR-706; IEBR-654; IEBR-533	Vietnam	MT749398; MT749400; MT749401; MT749404	Nguyen et al. 2021
Rhopalomeris nagao	IEBR-852; IEBR-854	Vietnam	MT749411; MT749392	Nguyen et al. 2021
Hyleoglomeris tongkerdae	MUMNH-GLO071-1*	Thailand	P493218	Likhitrakarn et al. 2024
Hyleoglomeris bomba	MUMNH-GLO096-1*	Thailand	PP493219	Likhitrakarn et al. 2024
Hyleoglomeris suwannakhuhensis	MUMNH-GLO039*	Thailand	PP493220	Likhitrakarn et al. 2024
Hyleoglomeris nigromaculata	MUMNH-GLO019-1*; MUMNH-GLO019-2*; MUMNH-GLO019-3*	Thailand	PP493221; PP493222; PP493223	Likhitrakarn et al. 2024
Hyleoglomeris dracosphaera	MUMNH-GLO001-1*; MUMNH-GLO001-2*; MUMNH-GLO001-3*; MUMNH-GLO035-M2*; MUMNH-GLO035-F4*; MUMNH-GLO035-M1*; MUMNH-GLO035-F3*	Thailand	PP493224; PP493225; PP493226; PP493227; PP493228; PP493229; PP493230	Likhitrakarn et al. 2024
Hyleoglomeris krasoon	MUMNH-GLO059*	Thailand	PP493231	Likhitrakarn et al. 2024
Hyleoglomeris hongkhraiensis	MUMNH-GLO029-2*; MUMNH-GLO029-3*; MUMNH-GLO031-3*	Thailand	PP493232; PP493233; PP493234	Likhitrakarn et al. 2024
Hyleoglomeris awaumi	EG20210711-227-01; EG20210711-227-03; KS20210513-04; KS20210513-07	Japan	LC713407; LC713409; LC713416; LC713419	Kuroda et al. 2022b
Hyleoglomeris insularum	EG20201213-09	Japan	LC713421	Kuroda et al. 2022b
Hyleoglomeris japonica	MS20210617-01; MS20210617-02; MS20210617-03	Japan	LC713422; LC713423; LC713424	Kuroda et al. 2022b
Hyleoglomeris lucida	EG20210718-240-01; MS20210426-11	Japan	LC713425; LC713426	Kuroda et al. 2022b
Hyleoglomeris sulcata	MS20210521B-05	Japan	LC713428	Kuroda et al. 2022b
Hyleoglomeris uenoi	ST20211028	Japan	LC713429	Kuroda et al. 2022b
Hyleoglomeris halang	IEBR-Myr898P; IEBR-Myr926	Vietnam	ON704753; ON704754	Kuroda et al. 2022a
Hyleoglomeris lobus	SVE-204; IEBR-653; IEBR-678	Vietnam	MT749391; MT749402; MT749406	Nguyen et al. 2021
Hyperglomeris bicaudata	CUMZ-GLO004*; CUMZ-GLO007*	Laos	OQ661871; OQ661872	Likhitrakarn et al. 2023a
Hyperglomeris inkhavilayi	CUMZ-GLO095/1*; CUMZ-GLO095/2*	Laos	OQ661873; OQ661874	Likhitrakarn et al. 2023a
Hyperglomeris simplex	IEBR-605; SVE-102	Vietnam	MT749403; MT749410	Nguyen et al. 2021
Peplomeris magna	IEBR-677; IEBR-656	Vietnam	MT749405; MT749408	Nguyen et al. 2021

Species	Voucher number	Locality	GenBank accession number COI	Reference
Tonkinomeris napoensis	IEBR-804b; IEBR-804a	Vietnam	MT749396; MT749397	Nguyen et al. 2021
Trachysphaera costata	Tcost8-MK	Slovakia	KX467622	Mock et al. 2016
Glomeris marginata	ZFMK-TIS-18977; ZFMK-TIS-2517216	France	MG892125; MG892167	Reip and Wesener 2018
Trachysphaera lobata	ZFMK:MYR TW01	United; Kingdom	KJ408484	Wilbrandt et al. 2015
Trachysphaera schmidtii	ZFMK:MYR BGIMyr16	Croatia	KJ408481	Wilbrandt et al. 2015
Eupeyerimhoffia archimedis	ZFMK:MYR1876	Italy	KP205574	Oeyen and Wesener 2015
Sphaerobelum truncatum	CUMZ:2010.18	Thailand	JN885184	Wongthamwanich et al. 2012
Zephronia laotica	ZFMK:MYR3502	Laos	MK330977	Wesener 2019

for all parameters. The resulting tree was examined and edited using FigTree v. 1.4.3 (http://tree.bio.ed.ac.uk/software/figtree/, accessed on 28 February 2024). A clade was considered well supported if the ultrafast BS was ≥ 95% and Bayesian bipartition posterior probability was ≥ 0.95 (San Mauro and Agorreta 2010; Hoang et al. 2018).

Intraspecific genetic distances within taxa that contained more than one individual and interspecific genetic distances based on the COI sequences were also calculated using uncorrected p-distances, as implemented in MEGA7 (Kumar et al. 2016).

Taxonomy

Descriptions

Family Glomeridae Leach, 1815

Genus *Rhopalomeris* Verhoeff, 1906

Rhopalomeris Verhoeff, 1906: 188 (D).

Rhopalomeris – Silvestri 1917: 140 (D); Jeekel 1971: 17 (L); Mauriès 1971: 435 (M); 2007: 243 (M); Hoffman 1980: 68 (L); Golovatch et al. 2011: 1 (D); Golovatch and Semenyuk 2016: 413 (D, K); Nguyen et al. 2019: 292 (D, K); 2021: 259 (D).

Diagnosis. The genus *Rhopalomeris* could be recognized through numerous apical sensory cones on the antennal tip, and antennomere 6 being particularly enlarged and rather strongly curved. In addition, the posterior telopods are rather strongly enlarged and stout, supplied with both prefemoral and femoral trichosteles. The femur has a distinctive and particular distocaudal process. The body is relatively large, with adults ranging from 11 to 20 mm in length. The body coloration is variable, but often useful for species identification.

Type species. *Glomeris carnifex* Pocock, 1889, fixed under Art. 70.3 (ICZN 1999) in Golovatch et al. (2011), misidentified as *Rhopalomeris bicolor* (Wood, 1865) in the original designation by Verhoeff (1906).

Other species included. *Rhopalomeris monacha* Silvestri, 1917; *R. tonkinensis* Silvestri, 1917; *R. variegata* Golovatch & Semenyuk, 2016; *R. sauda* Nguyen, Sierwald & Marek, 2019; and *R. nagao* Nguyen, Nguyen & Eguchi, 2021.

Remarks. The genus *Rhopalomeris* was originally typified by Verhoeff (1906) through the designation of *Glomeris bicolor* Wood, 1865 as the type species. However, this designation was based on specimens from Salanga Island (presently known as Phuket Island, Thailand) housed in the Berlin Museum (currently Museum für Naturkunde Berlin; ZMB), and these specimens had been previously identified by F. Karsch as *G. bicolor*. Although the type locality of *G. bicolor* is in Hong Kong (Wood 1865), Verhoeff (1906) followed Karsch's identification, and refrained to introduce a new name to those specimens.

Furthermore, Verhoeff (1906) compared the specimens from Phuket Island with *G. carnifex*, noting that several characteristics were similar to his specimens. He admitted that both might be two distinct species because of possible distinctions in telopods and the number of apical sensory cones on the antennae. Verhoeff also suggested to reclassify *G. carnifex* under the genus *Rhopalomeris*.

Subsequently, Silvestri (1917) examined relevant material probably housed in the Zoological Survey of India, (formerly the Indian Museum). He synonymized *G. bicolor* sensu Verhoeff (1906) with *R. carnifex* var. *pallida* (Pocock, 1889) from Elphinstone Island, Mergui Archipelago, Myanmar, and redesignated *R. carnifex* from Tenasserim, Myanmar, as the type species.

Finally, Golovatch et al. (2011) studied the specimens of *G. bicolor* sensu Verhoeff (1906), from Salanga Island housed in the ZMB, and confirmed the identification of these specimens as *R. carnifex*. Golovatch et al. (2011) also synonymized the variety *pallida* with *R. carnifex* given the reason that the variety *pallida* was simply a color morph of *R. carnifex*, and validated that *R. carnifex* is the type species of *Rhopalomeris*, fixed under Art. 70.3 (ICZN 1999). Therefore, the millipede genus *Rhopalomeris* is currently known only from Myanmar, Thailand, Malaysia, and Vietnam, with a total of six nominal species involved (Fig. 1).

Peplomeris was originally described as a subgenus of *Rhopalomeris* (Silvestri, 1917). However, it was later raised to a genus level by Mauriès (1971), who assigned this genus to the tribe Haploglomerini, whereas *Rhopalomeris* belongs to the tribe Trachysphaerini (Mauriès, 1971). Nguyen et al. (2019) provided a comprehensive comparison among these two genera, highlighting key morphological differences among five Vietnamese glomerid genera. *Peplomeris* is characterized by simple, elongated telopods, the presence of a prefemoral trichostele, and a reduced to missing femoral trichostele. In contrast, *Rhopalomeris* has antennomere 6 that is unusually large, and trichosteles present in both prefemur and femur of the telopods. The antennae of *Rhopalomeris* also have numerous apical sensory cones like in *Peplomeris*.

Rhopalomeris carnifex **(Pocock, 1889)**

Figs 2, 3

Glomeris carnifex Pocock, 1889: 290 (D). Type locality: Tenasserim.

Glomeris carnifex var. *pallida* Pocock, 1889: 290 (D). Type locality: Elphinstone Island.

Glomeris carnifex – Pocock 1890: 385 (R); Attems 1914: 138 (L); Hoffman 1980: 65 (M).

Glomeris carnifex var. *pallida* – Attems 1914: 138 (L); Silvestri 1917: 143 (D).

"Glomeris" bicolor [non Wood, 1865] – Verhoeff 1910: 241 (M); Silvestri 1917: 143 (M); Hoffman 1980: 65 (M).

Rhopalomeris carnifex – Silvestri 1917: 142 (D); Attems 1936: 194 (R); Enghoff 2005: 88 (R); Decker 2010: 24 (R); Golovatch et al. 2011: 6 (D); Golovatch and Semenyuk 2016: 411 (M, K); Likhitrakarn et al. 2017: 6 (L); Nguyen et al. 2019: 292 (M); 2021: 259 (M).

Rhopalomeris carnifex var. *pallida* – Silvestri 1917: 143 (D); Attems 1936: 194 (L).

Records in the literature. Myanmar, south Tenasserim (Pocock 1889); Malwoon in Tenasserim (Pocock 1890); Elphinstone Island (Pocock 1889); Moulmein (Attems 1936); Taninthay Division, Tanintharyi Region, 9°56'20″N, 98°32'22″E, Thatay Kyun (= Pulo Ru, Ko Son) (Decker 2010). Thailand, Phuket Province, Salanga Island (= Phuket Island) (Verhoeff 1906; Enghoff 2005); Mueang Phuket District, Ko Siray, 7°53'7″N, 98°26'14″E, 20–50 m a.s.l. (Decker 2010); Krabi Province, Krabi District, Nai Chong (Enghoff 2005); Ao Luk, 8°10'54″N, 98°50'30″E, 70 m; Ban Khlong Jilat, 8°05'18″N, 98°52'56″E, 60 m a.s.l.; near Saengphet Cave, 8°9'46″N, 98°53'12″E, 80 m; Ko Lanta District, Ko Lanta Island, 80 m a.s.l.; Phang Nga Province, Ko Yao District, Ko Yao Noi, 8°9'53″N, 98°37'20″E, 150 m a.s.l.; Thap Put District, Had Lek Beach, 8°37'N, 98°13'E, 10 m a.s.l.; Khao Lak-Lamru National Park, 8°37'N, 98°14'E, 30–40 m; Surat Thani Province, Ko Samui District, Samui Island, Khao Phlu, 10–500 m a.s.l.; Nam Tok Na Muang Forest Park, 30 m a.s.l.; Ko Pha Ngan District, Phangan Island, Than Sadet-Ko Phangan National Park, 9°44'7″N, 100°1'10″E, 320 m a.s.l. (Decker 2010). Malaysia, neighboring the Malay Peninsula (Verhoeff 1906).

New material examined. Myanmar – Tanintharyi Division • 2 ♂; Myeik, Kala Island; elev. 5 m a.s.l.; 12°29'38"N, 98°30'53"E; 5 Apr. 2016; C. Sutcharit, W. Siriwut, R. Srisonchai leg.; CUMZ-GLO016-1, 16-2.

Description. Body length of unrolled specimens, 17.5–17.9 mm (♂), width 8.9–9.1 (♂).

Color faded after 15 years of preservation in alcohol (Fig. 2A–C): body blackish, with contrasting light yellow to yellow, broad to narrow bands at posterior edges of each of terga 2–11; axial stripe yellow, short, starting from behind caudal edge, not reaching 1/5–1/6 length of each tergite (Fig. 2A); in lateral view, terga 2–11 each with a large, reddish or carmine to red orange band each side, ~ 1/4–2/3 height of each tergum (Fig. 2B). Thoracic shield with a very large, lateral, reddish to red orange band each side at lateral edges, ~ 2/3–3/4 height of tergum in lateral view (Fig. 2A–C); anal shield (= pygidium) with a reddish to red-orange band at the lateral and posterior edges, ~ 2/3–3/4 height of tergum (Fig. 2B). Head, collum and antennae black to dark brown, only labrum and Tömösváry's organ brownish (Fig. 2C), venter and legs brownish to pale yellowish (Fig. 2C).

Labrum sparsely setose (Fig. 2C). Gnathochilarium with 2+2 palps subequal in length. Eyes blackish, with 8–11+1 ommatidia, cornea convex and translucent. Antennomere 6 long, ~ 2.3–2.5× as long as its height, dorsal margin strongly curved (Figs 2C, 3A). Disk of antennomere 7 beset with 55–62 small sensory cones apically (♂) (Figs 2C, 3A). Organ of Tömösváry typical, horseshoe-shaped, suboval, elongate, ~ 1.5–1.6× as long as broad.

Collum as usual, with two transverse striae. Thoracic shield with a small hyposchism field not projecting past rear tergal margin (Fig. 2B); 7–9 mostly

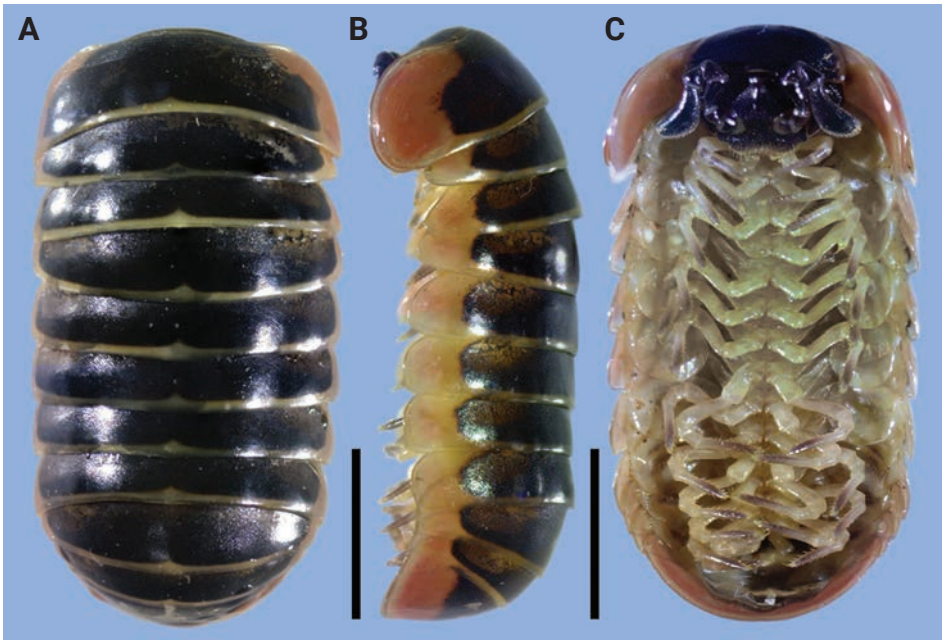

Figure 2. *Rhopalomeris carnifex* (Pocock, 1889), ♂ specimen from Kala Island **A–C** dorsal, lateral, and ventral views. Scale bars: 5 mm.

superficial striae, only lower two or three lying in front of schism, one or two level to schism, remaining 2–4 behind schism, 6 and 7 complete striae, crossing the dorsum. Terga 3 and 4 relatively broadly rounded laterally (Fig. 2B). Following terga in front of pygidium faintly concave medially at caudal edge and with three or four striae starting above lateral edge, sometimes first and second stria fading away towards midway. Pygidium slightly concave medially at caudal edge.

♂ legs 17 (Fig. 3B) simple, rather strongly reduced, with a rather low to medium-sized, often rounded, coxal lobe and a 4-segmented telopodite. Tarsus with 4–10 strong median and 1–3 strong apical spines (Fig. 3B).

♂ legs 18 (Fig. 3C) simple, slightly reduced, without any evident outgrowths; syncoxite membranous, with a small, broad, arch-shaped syncoxite notch and a 4-segmented telopodite. Tarsus with a small, but strong apical spine.

Telopods (= ♂ legs 19) (Fig. 3D–F) with a rather large and roundly pentagonal syncoxite lobe, this being flanked by two short, spiniform, acuminate and setose syncoxite horns, the latter being evidently lower than syncoxite lobe (Fig. 3F). Telopodite 4-segmented, with a spine apically. Prefemur (Fig. 3D, E) subtrapeziform, with a conspicuous, elongated, robust, tuberculiform, distomesal prefemoral trichostele with a rounded tip, extending to about half or distal boundary of femur (Fig. 3D, E). Femur (Fig. 3D, E) subtrapeziform, with a stout, relatively short femoral trichostele in anterior view, extending apically to ~ 1/2–3/4 prefemoral trichostele, in posterior view with a rounded, slightly narrowed, subtrapeziform femoral process, this being strongly curved anterolaterally and gently tapering into an acuminate and pointed tip (Fig. 3D). Tibia stout, gently tapering distad and curved apicobasad towards femoral process, with an evident, distolateral tibial process, this being strongly curved mesad (Fig. 3E). Tarsus the smallest, subcylindrical, moderately sigmoid, strongly curved, narrowly rounded apically, with a robust and small terminal seta (Fig. 3D).

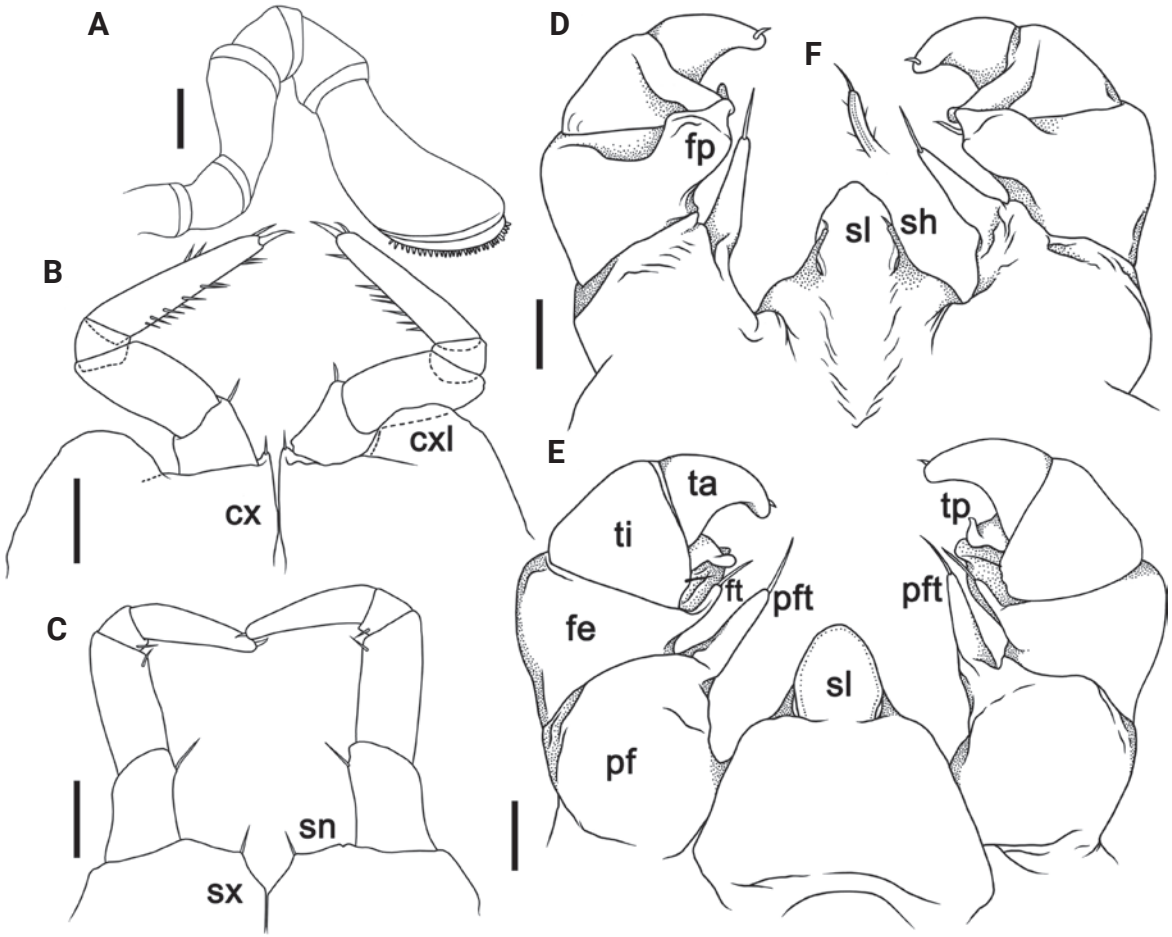

Figure 3. *Rhopalomeris carnifex* (Pocock, 1889), ♂ specimen from Kala Island **A** antenna, anterior view **B** leg 17, anterior view **C** leg 18 anterior view **D, E** telopod, anterior and posterior views **F** tip of syncoxital lobes (without scaling). Scale bars: 0.5 mm. Abbreviations: cx coxa, cxl coxal lobe, fe femur, fp femoral process, ft femoral trichostele, pf prefemur, pft prefemoral trichostele of telopod, sh syncoxital horn of telopod, sl syncoxital lobe of telopod, sn syncoxite notch, sx syncoxite, ta tarsus, ti tibia, tp tibial process.

Remarks. The taxonomic status of *R. carnifex* presents a challenge. Pocock (1889) originally described both *Glomeris carnifex* and *G. carnifex* var. *pallida* in the same paper. However, the original description of *G. carnifex* lacked details, focusing solely on body coloration and a vague collection locality (south Tenasserim, Myanmar). Pocock (1890) subsequently provided more information regarding the precise sampling locations, viz. south Tenasserim and Malwoon (= Maliwan, Kawthoung, Tanintharyi, Myanmar; Likhitrakarn et al. 2017).

In contrast, the description of *G. carnifex* var. *pallida* from Elphinstone Island contained far more detail. Pocock (1889) provided information on the number of specimens (male and female individuals), body characteristics, the 18th pair of legs and the telopod structure, all accompanied by clear illustrations. Notably, *G. carnifex* and *G. carnifex* var. *pallida* differ only slightly in coloration, showing a central, longitudinal, carmine line and large, lateral, carmine spots on each tergite.

Subsequently, Silvestri (1917) provided a more detailed description, accompanied by comprehensive illustrations, while still treating *R. carnifex* and *R. carnifex* var. *pallida* as two different taxa. He also treated *G. bicolor* sensu Verhoeff (1906) as a synonym with *R. carnifex* var. *pallida* (Pocock, 1889). In a recent study, Golovatch et al. (2011) formally synonymized *R. carnifex* var. *pallida* with *R. carnifex*.

However, our recently obtained specimens from Kala Island, Myanmar (Fig. 1, green square) closely resemble the original description of *G. carnifex* var. *pallida* from Elphinstone Island (Fig. 1, red square) both in color pattern (Fig. 2) and morphological characters, especially the structure of their legs and telopod (Fig. 3) as described by Pocock (1889). These two geographically distant populations (ca 50 km apart) (Fig. 1) share these similarities, indicating that they probably belong to the same taxon. As *R. carnifex* var. *pallida* is now synonymized under *R. carnifex* (Golovatch et al. 2011), we currently identify these specimens from Kala Island, Myanmar as *R. carnifex*.

Although there were previous reports of *R. carnifex* from several localities in southern Thailand, preliminary analyses of a number of *R. carnifex* specimens from this area reveal notable intraspecific variation in coloration, morphology, and molecular genetics, suggesting an occurrence of cryptic species (unpublished data). Therefore, a comprehensive redescription of newly retrieved male specimens from Kala Island, Myanmar in this study, comparing them with the original description of *G. carnifex* var. *pallida* from the nearby Elphinstone Island, is essential before any taxonomic revisions of other Thai specimens can be proposed. Furthermore, the morphological redescription of *R. carnifex* above is thus based only on these Myanmarese specimens.

Rhopalomeris monacha Silvestri, 1917

Rhopalomeris (*s.s.*) *monacha* Silvestri, 1917: 143 (D).
Rhopalomeris monacha – Golovatch et al. 2011: 6 (M); Golovatch and Semenyuk 2016: 414 (M, K); Nguyen et al. 2019: 292 (M); 2021: 259 (M).

Remarks. This species was described from Perak State, western Malaysia (Silvestri 1917). The species remains known only from a female holotype (Silvestri 1917). Endemic to Malaysia.

Rhopalomeris tonkinensis Silvestri, 1917

Rhopalomeris (*s.s.*) *tonkinensis* Silvestri, 1917: 144 (D).
Rhopalomeris tonkinensis – Attems 1936: 194 (L); Golovatch 1983: 180 (L); Enghoff et al. 2004: 31 (L); Golovatch et al. 2011: 6 (M); Golovatch and Semenyuk 2016: 414 (M, K); Nguyen et al. 2019: 263 (L, M); 2021: 259 (M).

Remarks. This species was described from Tonkin, Montes Mauson, 2,000–3,000 ft. a.s.l., Lang Son Province, northern Vietnam (Silvestri 1917). The species is likewise known only from a female holotype (Silvestri 1917). Endemic to Vietnam.

Rhopalomeris variegata Golovatch & Semenyuk, 2016

Rhopalomeris variegata Golovatch & Semenyuk, 2016: 411 (D, K).
Rhopalomeris variegata – Golovatch 2017: 199 (D, R); Nguyen et al. 2019: 263 (L, M); 2021: 259 (M).

Remarks. This species was described from Vietnam, Gia Lai Province, Kon Chu Rang Nature Reserve, 14°30'54"N, 108°32'47"E, ca 1,000 m a.s.l. (Golovatch and Semenyuk 2016) and later reported from Kon Tum Province, Kon Plong District, Bak Khe River, 14°43.450'N, 108°18.882'E, ca 1,000–1,260 m a.s.l. (Golovatch 2017). Endemic to Vietnam.

Rhopalomeris sauda Nguyen, Sierwald & Marek, 2019

Rhopalomeris sauda Nguyen et al., 2019: 292 (D, K).
Rhopalomeris sauda – Nguyen et al. 2021: 259 (R, M, MI).

Remarks. This species was described from Vietnam, Bac Kan Province, Ba Be National Park, 400–500 m a.s.l.; Vinh Phuc Province, Phuc Yen Town, Ngoc Thanh Commune, Me Linh Station for Biodiversity, 21.385°N, 105.7119°E; Tam Dao district, Tam Dao National Park, 21.460945°N, 105.647021°E (Nguyen et al. 2019); Tuyen Quang province, Cham Chu Nature Reserve; Ha Giang Province, Khau Ca Nature Reserve (Nguyen et al. 2021). Endemic to Vietnam.

Rhopalomeris nagao Nguyen, Nguyen & Eguchi, 2021

Rhopalomeris nagao Nguyen et al., 2021: 259 (D, K, MI).

Remark. This species was described from Vietnam, Cao Bang Province, Pia Oac – Pia Den National Park, 22.5540°N, 105.8622°E, 850–1,600 m a.s.l. (Nguyen et al. 2021). Endemic to Vietnam.

Rhopalomeris nigroflava Likhitrakarn, sp. nov.

https://zoobank.org/6D8B6CCE-FED1-49C9-9E20-ADD3FD6AF618
Figs 4–6

Material examined. *Holotype*: Myanmar – Kayin State • ♂; Linno Gu (Lateral small cave); 16°50'52.9"N, 097°36'37.7"E; 25 Nov. 2015; F. Bréhier leg.; MY15-13/01-CUMZ-GLO093. ***Paratypes*:** Myanmar – Kayin State • 7 ♂♂ 5 ♀♀; same locality as holotype; MY15-13/01-CUMZ-GLO093) • 2 ♂♂ 2 ♀♀; same locality as holotype; MNHN-MY15-13/01.

Diagnosis. Differs from other species of *Rhopalomeris* by the yellowish body with contrasting brown to blackish markings on terga 4–9 (Fig. 4A–F). Additionally, characterized by the smallest body sizes (5.1–9.7 mm in length and 2.6–4.7 mm in width), coupled with the telopod syncoxital lobe being slightly lower than lateral syncoxite horns. For further details, see key below.

Description. Body length of unrolled holotype,7.3 mm, width 4.1 mm. Body length of unrolled paratypes, 5.6–9.3 mm (♂), 5.1–9.7 mm (♀), width 3.1–4.8 (♂), 2.6–4.7 mm (♀).

Color faded after nine years of preservation in alcohol (Fig. 4A–F): body yellowish to brown yellowish, with contrasting brown to blackish markings on terga 4–9 (Fig. 4A, B, D, E); lateral sides of terga 10, 11, and anal shield sometimes

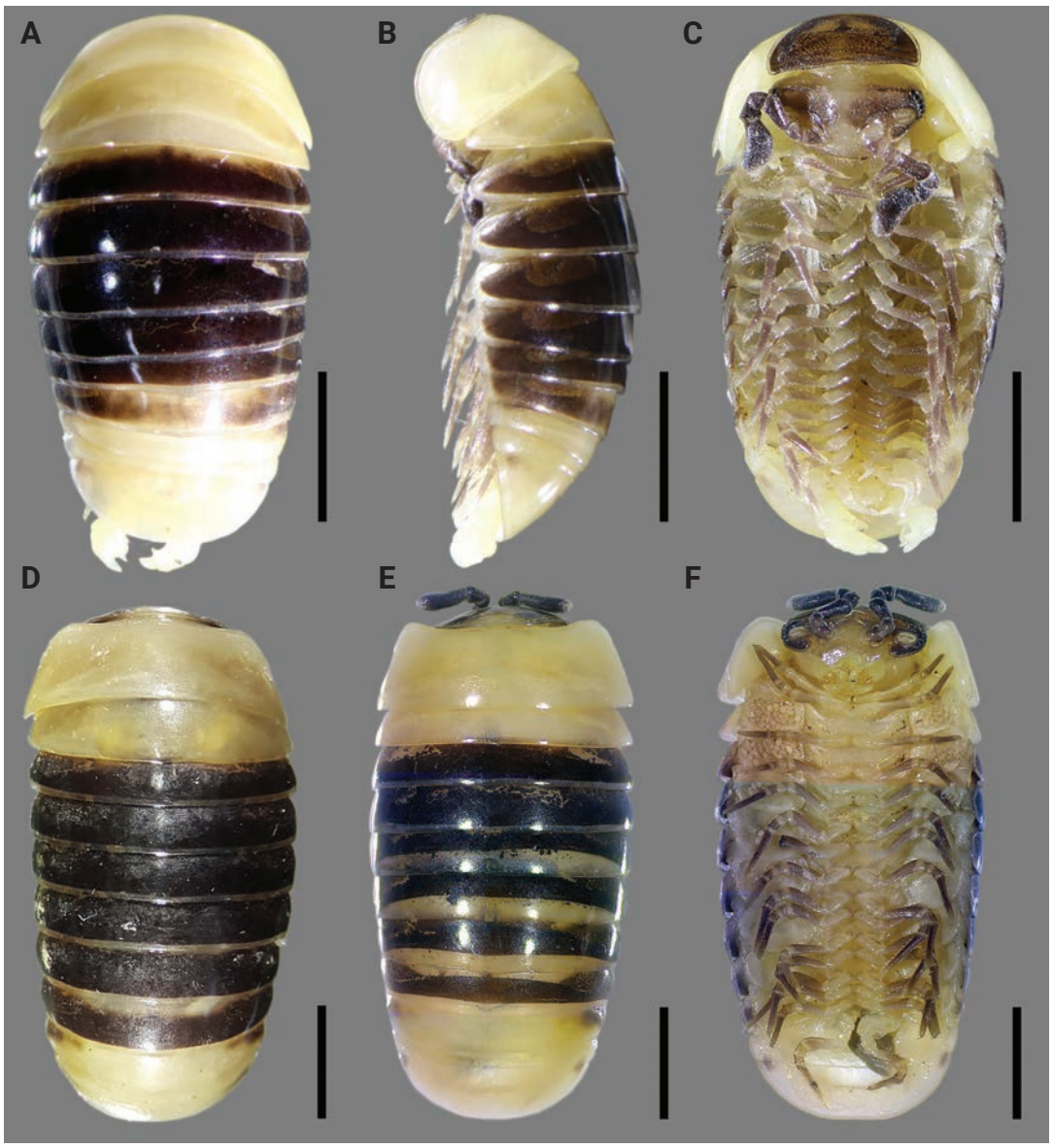

Figure 4. *Rhopalomeris nigroflava* sp. nov., **A–C** ♂ holotype in **A** dorsal **B** lateral and **C** ventral views **D–F** ♂ paratypes **D, E** dorsal and **F** ventral views. Scale bars: 0.2 mm.

with a pair of small, faint, dark paramedian spots, these reaching neither caudal nor lateral edges (Fig. 4A, B, D, E); head, antennae and collum brown to dark brownish, only labrum, vertex and Tömösváry's organ light brown; venter yellow brown to light yellowish; legs pale brown to brownish, with basal part of each podomere whitish (Fig. 4C, F).

Labrum sparsely setose (Figs 4C, F, 5A). Gnathochilarium with 2+2 palps subequal in length. Eyes blackish, with 6(7)+1 (♂) ommatidia (Fig. 5A), 6–(9)+1 ommatidia (♀), cornea convex and translucent. Antennomere 6 rather short, ~ 1.7–1.8× as long as its height, dorsal margin only slightly curved (Figs 4C, 5A, C). Disk of antennomere 7 beset with 22–28 small sensory cones apically (Fig. 5A, C), 16–26 small sensory cones apically (♀). Tömösváry's organ typical, horse-shoe-shaped, oblong-oval, elongate, ~ 1.6–1.7× as long as broad (Fig. 5A, C).

Collum as usual, with two transverse striae (Fig. 5A). Thoracic shield with a small hyposchism field not projecting past rear tergal margin (Fig. 5B).

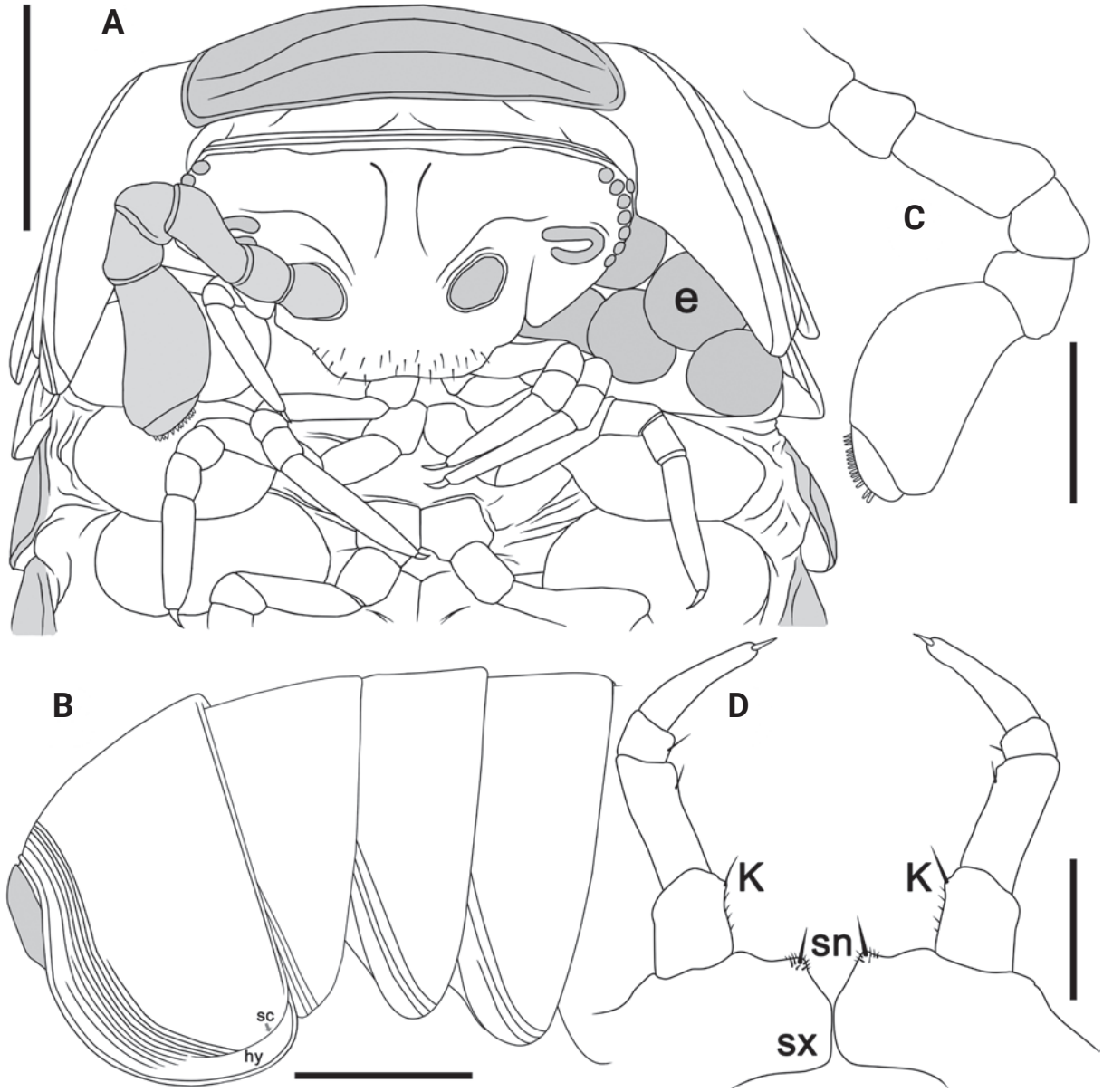

Figure 5. *Rhopalomeris nigroflava* sp. nov., ♂ holotype **A** head and anterior part of body, ventral view **B** thoracic shield, lateral view **C** left antenna, frontal view **D** leg 18, anterior view. Scale bars: 1 mm (**A, B**), 0.2 mm (**C**), 0.4 mm (**D**). Abbreviations: cxl coxal lobe, e eggs, hy hyposchism field, K caudomedial tubercle, sc schism, sn syncoxite notch, sx syncoxite.

7–9 mostly superficial striae, only lower 4 or 5 lying above schism, one level to schism, remaining 3 or 4 below schism, 6 or 7 complete, crossing the dorsum (Fig. 5B). Terga 3–7 rather broadly rounded laterally, with two or three striae starting above lateral edge, sometimes middle stria fading away mid-dorsally (Fig. 5B). Following terga in front of pygidium concave medially at caudal edge and with one or two striae starting above lateral edge. Male pygidium faintly concave medially at caudal edge (Fig. 4A, D, E).

♂ legs 17 (Fig. 6A–C) particularly strongly reduced, with a rather small to medium-sized, often irregularly rounded coxal lobe and a 4-segmented telopodite. Tarsus with 2–4 strong apical spines.

♂ legs 18 (Fig. 5D) rather strongly reduced, with a rounded ogival syncoxital notch and a 4-segmented telopodite. Femur with a small, setose, caudomedial tubercle near apex. Tarsus with a small apical spine.

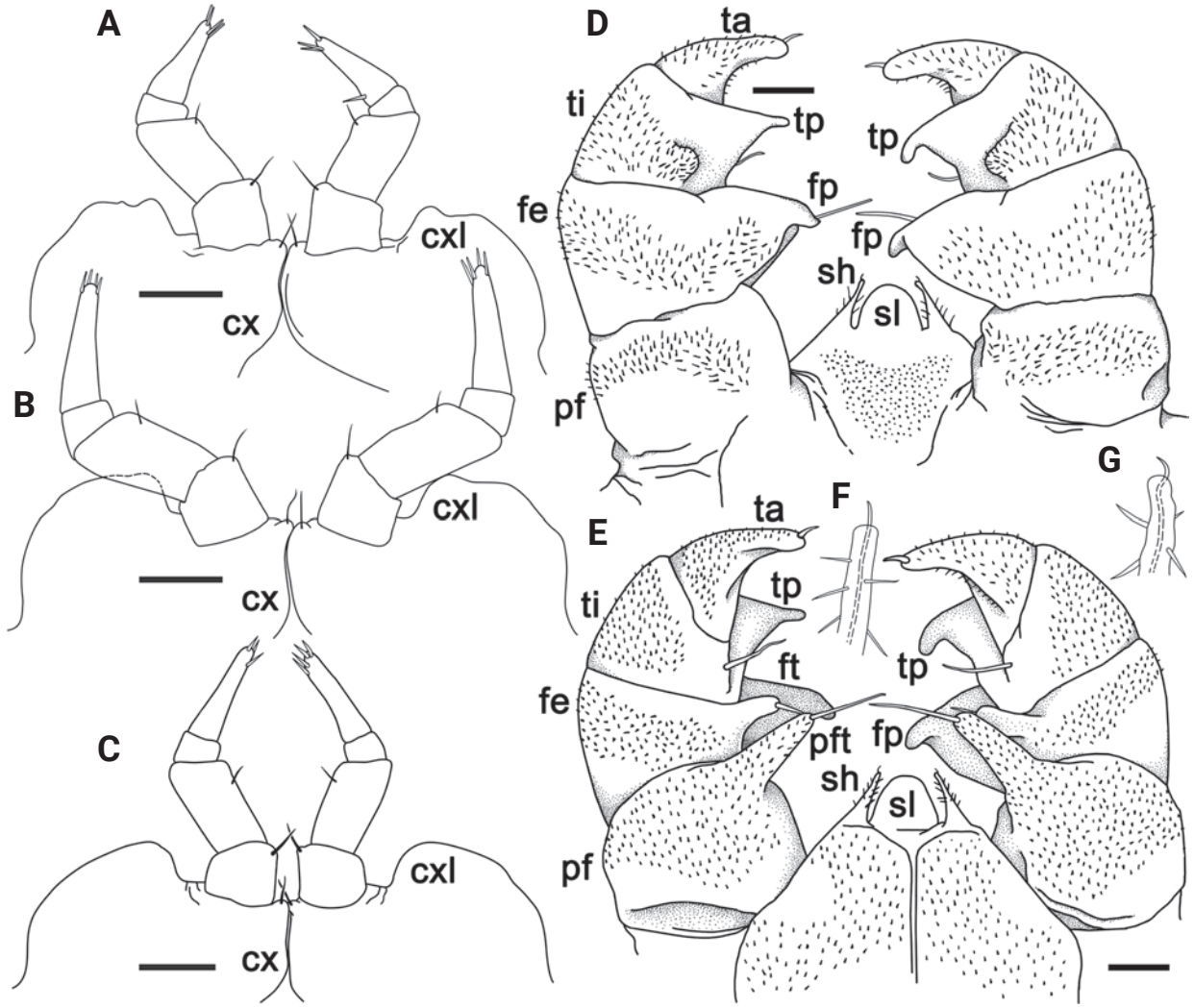

Figure 6. *Rhopalomeris nigroflava* sp. nov., **A, B** ♂ paratypes **C–F** ♂ holotype **A–C** leg 17, anterior view **D, E** telopod, posterior and anterior views, respectively **F, G** tip of syncoxital lobes (without scaling). Scale bars: 0.2 mm. Abbreviations: cx coxa, cxl coxal lobe, fe femur, fp femoral process, ft femoral trichostele, pf prefemur, pft prefemoral trichostele of telopod, sh syncoxital horn of telopod, sl syncoxital lobe of telopod, ta tarsus, ti tibia, tp tibial process.

Telopods (= ♂ legs 19) (Fig. 6D–G) with a small subtrapeziform, narrowly and roundly emarginated syncoxital lobe, this being flanked by two setose syncoxite horns, each of the latter higher than syncoxital lobe (Fig. 6D, E) and crowned by a subapical setoid filament (Fig. 6F, G). Telopodite 4-segmented. Prefemur (Fig. 6E) rectangular, with a conspicuous, elongated, robust, tuberculiform, distomesal prefemoral trichostele; in anterior view, with a rounded tip, extending to about half or distal boundary of femur (Fig. 6E). Femur (Fig. 6D, E) rectangular, with a prominent, stout, relatively short femoral trichostele in anterior view, extending apically to ~ 1/2–3/4 prefemoral trichostele, in posterior view with a rounded, subtriangular femoral process, this being curved anterolaterally and gently tapering into an acuminate rounded tip distally (Fig. 6D, E). Tibia stout, gently tapering distally and curved apicobasally towards femoral process, with a rather large, distolateral tibial process strongly curved mesad (Fig. 6D, E), with a strong anterior seta in anterior view (Fig. 6D) near base of tibial process. Tarsus the smallest, subcylindrical, moderately sigmoid, strongly curved, narrowly rounded apically, with a robust and small terminal seta (Fig. 6D, E).

Remarks. It seems noteworthy that a female and two male (Fig. 5C) specimens were found guarding a clutch of eggs near its head, beneath the thoracic shield. This behavior deviates from the typical reproductive strategy so far known in the entire order Glomerida, where females deposit eggs in specialized clay chambers and leave them to develop independently (Thomas et al. 1970; Janssen 2013). This is the first instance of paternal brood care observed in Glomerida. Therefore, this newly discovered species presents fascinating traits worthy of a dedicated future study.

Etymology. The specific epithet *nigroflava* is derived from the Latin *niger* meaning black and *flavus* meaning yellow, in reference to the dark bands on a yellowish dorsum, adjective in feminine gender.

Key to known species of *Rhopalomeris*, based on adults, modified from Golovatch (2017)

1 Thoracic shield yellowish or yellowish brown, contrasting to dark body background **2**
– Thoracic shield dark, variegated **3**
2 Body larger, ~ 12 mm in length and 6 mm in width. Head, collum and thoracic shield light yellowish, body mostly blackish with a light, rather broad, axial stripe. Perak State, western Malaysia ..... ***R. monacha***
– Body the smallest, 5.1–9.7 mm in length and 2.6–4.7 mm in width. Body yellowish to yellowish brown-, contrasting to brown to blackish terga 4–9 (Fig. 4A, B, D, E). Head and collum brown to dark brownish (Fig. 5C, E, F). Kayin State, Myanmar ..... ***R. nigroflava* sp. nov.**
3 Body large-sized, ~ 20 mm in length and 11 mm in width (♀). Dorsum: mostly blackish, not variegated. Mount Mau Son, Lang Son Province, northern Vietnam..... ***R. tonkinensis***
– Body < 20 mm in length and 11 mm in width. Dorsum: with a varied color pattern or contrasting colors **4**
4 Dorsum mostly dark, lateral edges of terga contrasting reddish or carmine. Telopod syncoxital lobe clearly higher than lateral syncoxite horns (Fig. 3D), each latter with a tiny filament on top (Fig. 3D, F). Southern Thailand and southern Myanmar (Fig. 1) ..... ***R. carnifex****
– Dorsum dark or light, sometimes variegated, lateral edges of terga neither reddish nor carmine. Telopod syncoxital lobe clearly shorter than lateral syncoxite horns, each latter without filament on top. Vietnam **5**
5 Body almost entirely dark with contrasting four yellow lateral spots on each of terga 3–11. Telopods with a medially slightly concave syncoxite lobe. Prefemoral trichostele short, not extending to about half the distal boundary of femur. Femoral process (**fp**) long, narrow, erect, acute at tip. Tibial process short and lobuliform ..... ***R. nagao***
– Body color variegated. Telopods with a medially slightly convex syncoxite lobe. Prefemoral trichostele long, extending to about half or distal boundary of femur. Femoral process large, subtrapeziform, rounded at tip. Tibial process long and sigmoid mesally **6**

* The current key does not take the variation of *R. carnifex* from southern Thailand into consideration, see Remarks under *R. carnifex* above.

6 Body light brown to blackish, with variegated, marbled, brown-yellow to yellowish markings. Body larger, 15–18 mm in length and 7–8 mm in width. Antennomere 6 slightly shorter, ~ 2.0× as long as high. Thoracic shield with 8–10 striae. Central Vietnam..... ***R. variegata***

– Body blackish, with contrasting yellowish, lateral, oval bands on each of terga 2–11. Body smaller, 11 mm in length and 6 mm in width. Antennomere 6 longer, 2.5–3× as long as high. Thoracic shield with 2–3 striae. Northern Vietnam..... ***R. sauda***

Phylogenetic analysis

The COI alignment (Table 1) was 660 bp in length and contained 61 individuals, including 29 taxa from the Glomeridae as ingroup and two taxa from the Zephroniidae as outgroup. The tree shows that all 29 pill millipede species from the eight genera of Glomeridae form a monophyletic group that is evidently separated from the outgroup, with strong support values (100% BS for ML and 1 bpp for BI) (Fig. 7). However, most of the relationships at the generic level among glomerid species still remained unresolved.

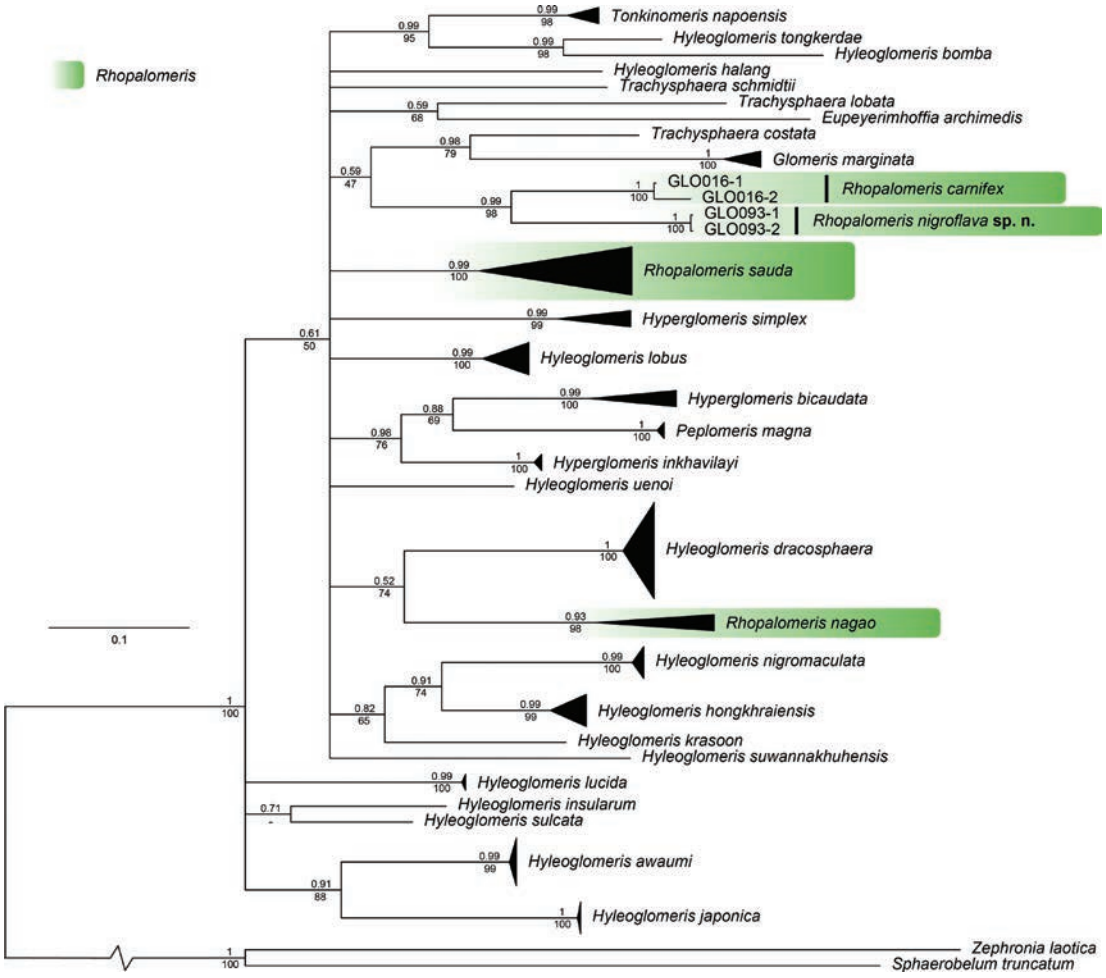

Figure 7. Bayesian inference tree (BI) of pill millipedes in the family Glomeridae based on 660 bp of COI gene. Clades of *Rhopalomeris* species in this study are highlighted in green. Numbers above branches indicate bipartition posterior probability (bpp) from Bayesian inference analysis (BI) and numbers below branches are Bootstrap Support (BS) values from the ML analysis.

The COI tree revealed a sister relationship between *R. carnifex* and *R. nigroflava* sp. nov., forming a well-supported clade 98% BS for ML and 0.99 bpp for BI. However, all *Rhopalomeris* species, including *R. sauda* and *R. nagao*, were not retrieved together as monophyletic (Fig. 7).

The interspecific divergences based on COI uncorrected p-distance among the glomerid species in this study ranged from 9.74 to 19.87%, with an average of 14.87% (data not show). The interspecific divergences among *Rhopalomeris* species ranged from 10.85 to 16.13%, with an average of 13.32% (Table 2). This analysis also demonstrates that the intraspecific divergence for *Rhopalomeris nigroflava* sp. nov. is 0%, vs 1.75% for *R. carnifex*.

Table 2. Matrix of the average interspecific genetic divergence (uncorrected p-distance) for the 660 bp barcoding region of the COI gene between *Rhopalomeris* species.

Taxa	***Rhopalomeris sauda***	***Rhopalomeris nagao***	***Rhopalomeris carnifex***	***Rhopalomeris nigroflava* sp. nov.**
Rhopalomeris sauda	**0.0744**			
Rhopalomeris nagao	0.1289	**0.0521**		
Rhopalomeris carnifex	0.1613	0.1397	**0.0175**	
Rhopalomeris nigroflava sp. nov.	0.1376	0.1235	0.1085	**0**

Discussion and conclusions

Currently, the genus *Rhopalomeris* comprises seven species distributed across Vietnam (four species), Myanmar (two species), Thailand and Malaysia (one species each), with a notable absence of documented sympatry of species. The distribution patterns (Fig. 1), particularly the higher species diversity in Vietnam compared to the neighboring countries, suggest still a high probability of discovering new *Rhopalomeris* species in Cambodia and southern Thailand through future surveys.

Rhopalomeris species occur at elevations ranging between 5 and 1,600 meters above sea-level. Apparently, most are narrow endemics restricted to their type localities and are only rare to be encountered. The exceptions are *R. sauda* which boasts a wider distribution of roughly 180 kilometers, and *R. carnifex* that demonstrates a remarkably extensive range exceeding 1,200 kilometers and stretching from southern Myanmar through Thailand to northern Malaysia (Fig. 1).

It seems noteworthy that our preliminary surveys of millipede diversity in southern Thailand have yielded a high level of variation in the shape and coloration of *R. carnifex*, and high genetic diversity, suggesting a high-level intraspecific variation or the occurrence of cryptic species (unpublished data). This observation underscores the need for further research to comprehensively understand the extent of this variation, ultimately paving the way for future studies to definitively identify the *R. carnifex* complex.

The interspecific divergence based on COI uncorrected p-distance among the *Rhopalomeris* species in this study ranged between 10.85–16.13%, aligning with previous findings for European *Glomeris* species (11.5–17.1%; Wesener 2015), Vietnamese glomeridan genera (13–15.8%; Nguyen et al. 2021), *Hyperglomeris* species (8.81–12.48%, Likhitrakarn et al. 2023a), and *Hyleoglomeris* species (9.12–16.92%; Likhitrakarn et al. 2024).

This consistency suggests that COI proves effective in identifying species-level differentiation within Glomeridae. Even such species as *R. carnifex* and

R. nigroflava sp. nov. that are very closely related and form a well-supported clade show a significant p-distance of 10.85%. This indicates that there can be considerable variability in the COI gene even among closely related glomerid species.

This study investigates the intraspecific COI divergence within Glomeridae millipedes. The low genetic intraspecific differences observed in *Rhopalomeris carnifex* (1.75%) and the newly described *R. nigroflava* sp. nov. (0%) are consistent with previous reports on *Peplomeris magna* (0.2%; Nguyen et al. 2021), some *Hyleoglomeris* (0–1.19%; Likhitrakarn et al. 2024) and *Hyperglomeris* species (0.45–5.30%; Likhitrakarn et al. 2023a).

Analyzing the COI gene sequence is highly valuable in determining species boundaries and enabling precise classifications of glomerid species. Unsurprisingly, most recent taxonomic studies on millipedes frequently employ this technique to distinguish between taxa. Unfortunately, the phylogenetic relationships in this study appear insufficient to resolve genus-level relationships within the family, as shown in this study and others (Nguyen et al. 2019, 2021; Liu and Golovatch 2020; Likhitrakarn et al. 2023a, 2024). Subsequent research should include other genetic markers, such as 16S and 28S ribosomal RNA genes, as well as more advanced techniques, such as transcriptomic and phylogenomic data in clarifying phylogenetic relationships (Means et al. 2021; Benavides et al. 2023; Likhitrakarn et al. 2023a). Nevertheless, it is necessary to conduct these investigations combined with analyzing morphological, distributional, and ecological characteristics in order to obtain a more integrative comprehension of the evolutionary relationships among glomerid species, particularly regarding the intraspecific variation observed in the *R. carnifex* complex.

Acknowledgements

We thank the members of the Animal Systematics Research Unit for their invaluable assistance in the field. We owe an obligation of gratitude to Henrik Enghoff, Duc-Anh Nguyen, and Thomas Wesener, the reviewers, whose constructive comments, grammatic corrections, and assistance have significantly improved the paper.

Additional information

Conflict of interest

The authors have declared that no competing interests exist.

Ethical statement

No ethical statement was reported.

Funding

This study was funded by the Thailand Science Research and Innovation Fund of Chulalongkorn University (grant number DIS66230007) and the TRF (Thailand Research Fund) Senior Research Scholar.

Author contributions

NL, RS, PJ, PS, EJ, SP, and CS collected and prepared specimens in the field. SP and CS provided financial and intellectual support. NL, RS, and EJ prepared specimens and

wrote the manuscript. NL, RS, PJ, EJ, and CS conceived, designed, supervised the study, prepared figures, and approved and edited the final manuscript. SIG and SP reviewed, advised, and approved the final manuscript.

Author ORCIDs

Natdanai Likhitrakarn https://orcid.org/0000-0002-1306-317X
Sergei I. Golovatch https://orcid.org/0000-0001-7159-5484
Ruttapon Srisonchai https://orcid.org/0000-0002-7142-0999
Parin Jirapatrasilp https://orcid.org/0000-0002-5591-6724
Pichsinee Sapparojpattana https://orcid.org/0009-0005-9134-4910
Ekgachai Jeratthitikul https://orcid.org/0000-0002-3477-9548
Somsak Panha https://orcid.org/0000-0002-4431-2458
Chirasak Sutcharit https://orcid.org/0000-0001-7670-9540

Data availability

All of the data that support the findings of this study are available in the main text.

References

Attems C (1914) Die indo-australischen Myriopoden. Archiv für Naturgeschichte 80A, 1–398.

Attems C (1936) Diplopoda of India. Memoirs of the Indian Museum 11(4): 133–323.

AVMA (2013) AVMA guidelines for the euthanasia of animals. https://www.avma.org/KB/Policies/Documents/euthanasia.pdf [Accessed on: 2024-8-21]

Benavides LR, Edgecombe GD, Giribet G (2023) Re-evaluating and dating myriapod diversification with phylotranscriptomics under a regime of dense taxon sampling. Molecular Phylogenetics and Evolution 178: e107621. https://doi.org/10.1016/j.ympev.2022.107621

Decker P (2010) Contributions to the myriapod fauna of Thailand—New records of millipedes and centipedes from Thailand (Myriapoda: Diplopoda, Chilopoda). Schubartiana 4: 23–34.

Enghoff H (2005) The millipedes of Thailand (Diplopoda). Steenstrupia 29(1): 87–103.

Enghoff H, Golovatch SI, Nguyen DA (2004) A review of the millipede fauna of Vietnam (Diplopoda). Arthropoda Selecta 13(1–2): 29–43.

Folmer O, Black M, Hoeh W, Lutz R, Vrijenhoek R (1994) DNA primers for amplification of mitochondrial cytochrome c oxidase subunit I from diverse metazoan invertebrates. Molecular Marine Biology and Biotechnology 3(5): 294–299.

Golovatch SI (1983) [Millipedes (Diplopoda) in the fauna of Vietnam]. In: Sokolov VE (Ed.) Fauna i ekologiya zhivotnykh Vietnama [Fauna and animal ecology of Vietnam]. Moscow, Nauka Publ., 178–186. [in Russian]

Golovatch SI (2017) Another two new species of the millipede family Glomeridae from Vietnam, with a new record of *Rhopalomeris variegata* Golovatch et Semenyuk, 2016 from southern Vietnam (Diplopoda: Glomerida). Russian Entomological Journal 26(2): 195–202. https://doi.org/10.15298/rusentj.26.2.10

Golovatch SI, Semenyuk II (2016) Two new species of the millipede family Glomeridae from Vietnam (Diplopoda: Glomerida). Russian Entomological Journal 25(4): 411–416. https://doi.org/10.15298/rusentj.25.4.11

Golovatch SI, Geoffroy JJ, Mauriès JP (2006) Review of the millipede genus *Hyleoglomeris* Verhoeff, 1910 (Diplopoda, Glomerida, Glomeridae), with descriptions of new species from caves in Southeast Asia. Zoosystema 28(4): 887–915.

Golovatch SI, Hoffman RL, Chang HW (2011) Identity of *Glomeris bicolor* Wood, 1865, and the status of the generic names *Hyleoglomeris* Verhoeff, 1910 and *Rhopalomeris* Verhoeff, 1906 (Diplopoda, Glomeridae). Tropical Natural History 11(1): 1–8.

Hoang DT, Chernomor O, von Haeseler A, Minh BQ, Vinh LS (2018) UFBoot2: Improving the ultrafast bootstrap approximation. Molecular Biology and Evolution 35: 518–522. https://doi.org/10.1093/molbev/msx281

Hoffman RL (1980) Classification of the Diplopoda. Muséum d'Histoire Naturelle, Genève, Switzerland, 237 pp.

International Commission on Zoological Nomenclature (1999) International Code of Zoological Nomenclature, 4th edn. The International Trust for Zoological Nomenclature, London.

Janssen R (2013) A curious abnormally developed embryo of the pill millipede *Glomeris marginata* (Villers, 1789). ZooKeys 276: 67–75. https://doi.org/10.3897/zookeys.276.4767

Jeekel CAW (1971) Nomenclator generum et familiarum Diplopodorum: A list of the genus and family-group names in the Class Diplopoda from the 10th edn of Linnaeus, 1758, to the end of 1957. Monografieën van de Nederlandse Entomologische Vereniging 5: 1–412.

Kumar S, Stecher G, Tamura K (2016) MEGA7: Molecular Evolutionary Genetics Analysis version 7.0 for bigger datasets. Molecular Biology and Evolution 33(7): 1870–1874. https://doi.org/10.1093/molbev/msw054

Kuroda M, Eguchi K, Oguri E, Nguyen AD (2022a) Two new cave *Hyleoglomeris* species (Glomerida, Glomeridae) from northern Vietnam. ZooKeys 1108: 161–174. https://doi.org/10.3897/zookeys.1108.85423

Kuroda M, Susukida M, Sakamoto K, Tsukamoto S, Nguyen AD, Oguri E, Eguchi K (2022b) A new species of the genus *Hyleoglomeris* Verhoeff 1910 from Central Japan (Diplopoda: Glomerida: Glomeridae). Acta Arachnologica 71(2): 115–124. https://doi.org/10.2476/asjaa.71.115

Lanfear R, Frandsen PB, Wright AM, Senfeld T, Calcott B (2016) Partition Finder 2: New methods for selecting partitioned models of evolution for molecular and morphological phylogenetic analyses. Molecular Biology and Evolution 34(3): 772–773. https://doi.org/10.1093/molbev/msw260

Likhitrakarn N, Golovatch SI, Panha S (2014) A checklist of the millipedes (Diplopoda) of Laos. Zootaxa 3754(4): 473–482. https://doi.org/10.11646/zootaxa.3754.4.8

Likhitrakarn N, Golovatch SI, Jirapatrasilp P, Panha S (2017) A checklist of the millipedes (Diplopoda) of Myanmar, with an updated list of Leonardo Fea's collecting localities. Zootaxa 4350(1): 1–46. https://doi.org/10.11646/zootaxa.4350.1.1

Likhitrakarn N, Srisonchai R, Siriwut W, Jirapatrasilp P, Jeratthitikul E, Panha S, Sutcharit C (2023a) Review of the pill millipede genus *Hyperglomeris* Silvestri, 1917 (Diplopoda, Glomerida, Glomeridae) with description of two new species from Laos. ZooKeys 1163: 177–198. https://doi.org/10.3897/zookeys.1163.103950

Likhitrakarn N, Srisonchai R, Golovatch SI (2023b) An updated catalogue of the millipedes (Diplopoda) of Thailand. Tropical Natural History, Supplement 7: 51–92.

Likhitrakarn N, Jeratthitikul E, Sapparojpattana P, Siriwut W, Srisonchai R, Jirapatrasilp P, Seesamut T, Poolprasert P, Panha P, Sutcharit C (2024) Six new species of pill millipede genus *Hyleoglomeris* Verhoeff, 1910 (Diplopoda, Glomerida, Glomeridae) in Thailand revealed by DNA-barcoding. Contributions to Zoology 93: 289–323. https://doi.org/10.1163/18759866-bja10062

Liu W, Golovatch S (2020) The first representatives of the millipede family Glomeridellidae (Diplopoda, Glomerida) recorded from China and Indochina. ZooKeys 954: 1–15. https://doi.org/10.3897/zookeys.954.54694

Lobo J, Costa PM, Teixeira MA, Ferreira MS, Costa MH, Costa FO (2013) Enhanced primers for amplification of DNA barcodes from a broad range of marine metazoans. bmc Ecology 13(1): 34. https://doi.org/10.1186/1472-6785-13-34

Mock A, Tajovský K, Žurovcová M, Jarošová A, Kocourek P, Gruber J, Angyal D, Spelda J (2016) *Hungarosoma bokori* Verhoeff, 1928 (Diplopoda: Chordeumatida): new insights into its taxonomy, systematics, molecular genetics, biogeography and ecology. Zootaxa 4178(2): 234–256. https://doi.org/10.11646/zootaxa.4178.2.4

Mauriès JP (1971) Diplopodes épigés et cavernicoles des Pyrénées espagnoles et des Monts Cantabriques. VII. Glomerides. Essai de classification des Glomeroidea. Bulletin de la Société d'histoire naturelle de Toulouse 107: 423–436.

Means JC, Hennen DA, Tanabe T, Marek PE (2021) Phylogenetic systematics of the millipede family Xystodesmidae. Insect Systematics and Diversity 5(2): 1–26. https://doi.org/10.1093/isd/ixab003

Miller M, Pfeiffer W, Schwartz T (2010) Creating the CIPRES Science Gateway for inference of large phylogenetic trees. Proceedings of the Gateway Computing Environments Workshop (GCE), 14 November 2010, New Orleans, LA, 1–8. https://doi.org/10.1109/GCE.2010.5676129

Minh BQ, Schmidt HA, Chernomor O, Schrempf D, Woodhams MD, von Haeseler A, Lanfear R (2020) IQ-TREE 2: new models and efficient methods for phylogenetic inference in the genomic era. Molecular Biology and Evolution 37: 1530–1534. https://doi.org/10.1093/molbev/msaa015

Nguyen AD, Sierwald P, Marek PE (2019) The pill millipedes of Vietnam: A key to genera and descriptions of five new species (Diplopoda: Glomerida: Glomeridae). Raffles Bulletin of Zoology 67: 260–297. https://doi.org/10.26107/RBZ-2019-0020

Nguyen AD, Nguyen SG, Eguchi K (2021) A new *Rhopalomeris* species (Diplopoda: Glomerida: Glomeridae), and notes on the phylogenetic relationships between glomeridans in Vietnam. Zootaxa 4927(2): 257–264. https://doi.org/10.11646/zootaxa.4927.2.5

Oeyen JP, Wesener T (2015) Steps towards a phylogeny of the pill millipedes: non-monophyly of the family Protoglomeridae, with an integrative redescription of *Eupeyerimhoffia archimedis* (Diplopoda, Glomerida). Zookeys 510:49–64. https://doi.org/10.3897/zookeys.510.8675

Pocock RI (1889) Contributions to the fauna of Mergui and its archipelago, Volume 1: Myriopoda. Zoological Journal of the Linnean Society 21(132): 287–303. https://doi.org/10.1111/j.1096-3642.1889.tb00980.x

Pocock RI (1890) On the myriapods of Burma. Pt. 1. Report on the Oniscomorpha collected by Sig. L. Fea, by Mr. L. W. Oates and by the late Sig. G.B. Comotto. Annali del Museo Civico di Storia Naturale di Genova, Series 2, 10: 399–432.

Reip HS, Wesener T (2018) Intraspecific variation and phylogeography of the millipede model organism, the Black Pill Millipede *Glomeris marginata* (Villers, 1789) (Diplopoda, Glomerida, Glomeridae). In: Stoev P, Edgecombe GD (Eds) Proceedings of the 17th International Congress of Myriapodology, Krabi, Thailand. ZooKeys 741: 93–131. https://doi.org/10.3897/zookeys.741.21917

Ronquist F, Teslenko M, van der Mark P, Ayres DL, Darling A, Höhna S, Larget B, Liu L, Suchard MA, Huelsenbeck JP (2012) MrBayes 3.2: Efficient Bayesian phylogenetic inference and model selection across a large model space. Systematic Biology 61(3): 539–542. https://doi.org/10.1093/sysbio/sys029

San Mauro D, Agorreta A (2010) Molecular systematics: A synthesis of the common methods and the state of knowledge. Cellular & Molecular Biology Letters 15: 311–341. https://doi.org/10.2478/s11658-010-0010-8

Schulmeister S, Wheeler WC, Carpenter JM (2002) Simultaneous analysis of the basal lineages of Hymenoptera (Insecta) using sensitivity analysis. Cladistics 18: 455–484. https://doi.org/10.1111/j.1096-0031.2002.tb00287.x

Silvestri F (1917) Contributions to a knowledge of the Oriental Diplopoda Oniscomorpha, I. The family Glomeridae. Records of the Indian Museum 13(3, 9): 103–151. https://doi.org/10.26515/rzsi/v13/i3/1917/163604

Thomas E, Zahler SA, Carrel JE, Brown DJ (1970) Absence of antimicrobial substances in the egg capsules of millipedes. Nature 225: 661. https://doi.org/10.1038/225661a0

Verhoeff KW (1906) Über Diplopoden. 4.(24). Aufsatz: Zur Kenntnis der Glomeriden (zugleich Vorläufer einer *Glomeris*-Monographie). (Beiträge zur Systematik, Geographie, Entwicklung, vergleichenden Morphologie und Biologie). Archiv für Naturgeschichte 72: 107–226

Verhoeff KW (1910) Über Diplopoden. 41. Aufsatz: Indomalayische Glomeriden. Sitzungsberichte der Gesellschaft Naturforschender Freunde zu Berlin 1910(5): 240–249.

Wesener T (2015) No millipede endemics north of the Alps? DNA-barcoding reveals *Glomeris malmivaga* Verhoeff, 1912 as a synonym of *G. ornata* Koch, 1847 (Diplopoda, Glomerida, Glomeridae). Zootaxa 3999(4): 571–580. https://doi.org/10.11646/zootaxa.3999.4.7

Wesener T (2019) The oldest pill millipede fossil: a species of the Asiatic pill millipede genus *Hyleoglomeris* in Baltic amber (Diplopoda: Glomerida: Glomeridae). Zoologischer Anzeiger 283: 40–45. https://doi.org/10.1016/j.jcz.2019.08.009

Wilbrandt J, Lee P, Read H, Wesener T (2015) A first integrative study of the identity and origins of the British Dwarf Pill Millipede populations, *Trachysphaera* cf. *lobata* (Diplopoda, Glomerida, Glomeridae). Biodiversity Data Journal 3: e5176. https://doi.org/10.3897/BDJ.3.e5176

Wongthamwanich N, Panha S, Sierwald P, Wesener T, Thirakhupt K (2012) A new species of the giant pill-millipede genus *Sphaerobelum* Verhoeff, 1924 from northern Thailand, with an extensive description and molecular characters (Diplopoda: Sphaerotheriida: Zephroniidae). Zootaxa 3220(1): 29–43. https://doi.org/10.11646/zootaxa.3220.1.2

Wood HC (1865) New Polyzoniidae, Gervais. Proceedings of the Academy of Natural Sciences of Philadelphia 1865: 172–173.

ZooKeys 1215: 259–288 (2024)
DOI: 10.3897/zookeys.1215.128603

Research Article

Review of the Palaearctic species of *Apsilocera* Bouček, 1956 (Chalcidoidea, Pteromalidae), with descriptions of the eight new species

Ekaterina V. Tselikh[1], Jaehyeon Lee[2], Michael Haas[3], Mircea-Dan Mitroiu[4], Deok-Seo Ku[5]

1 *Zoological Institute, Russian Academy of Sciences, St. Petersburg 199034, Russia*
2 *Department of Plant Medicine, Gyeongsang National University, Jinju 52828, Republic of Korea*
3 *Department of Entomology, State Museum of Natural History, Stuttgart, Germany*
4 *Faculty of Biology, Alexandru Ioan Cuza University, Iasi, Romania*
5 *The Science Museum of Natural Enemies, Geochang 50147, Republic of Korea*

Corresponding author: Ekaterina V. Tselikh (tselikhk@gmail.com)

Abstract

Palaearctic species of the genus *Apsilocera* Bouček, 1956 are reviewed. Twelve Palaearctic species are recognized based on females, of which eight new species are described: *Apsilocera bradburyi* Tselikh, Lee & Ku, **sp. nov.** (Republic of Korea), *A. budai* Tselikh, Lee & Ku, **sp. nov.** (Republic of Korea), *A. eleganta* Tselikh, Haas & Ku, **sp. nov.** (Republic of Korea, Sweden), *A. grandistigma* Tselikh, Lee & Ku, **sp. nov.** (Republic of Korea), *A. jejuensis* Tselikh, Lee & Ku, **sp. nov.** (Republic of Korea), *A. marina* Tselikh, Lee & Ku, **sp. nov.** (Republic of Korea), *A. totoroi* Tselikh, Haas & Ku, **sp. nov.** (Germany, Japan, Sweden), and *A. triapitzini* Tselikh, Haas & Ku, **sp. nov.** (Russia, Republic of Korea, Sweden). The female of *A. verticillata* Bouček, 1956 is described for the first time. *Apsilocera dupla* Mitroiu & Achterberg, 2013 and *A. elongata* Mitroiu & Achterberg, 2013 are recorded from the Palaearctic region for the first time. An identification key to females of all Palaearctic species of *Apsilocera* is given.

Key words: Description, key, new record, new species, parasitoid, Pteromalinae, redescription

Academic editor: Jonah M. Ulmer
Received: 30 May 2024
Accepted: 9 July 2024
Published: 17 October 2024

ZooBank: https://zoobank.org/73344A05-B2C1-4FBC-A67A-5F1E29B3BB2A

Citation: Tselikh EV, Lee J, Haas M, Mitroiu M-D, Ku D-S (2024) Review of the Palaearctic species of *Apsilocera* Bouček, 1956 (Chalcidoidea, Pteromalidae), with descriptions of the eight new species. ZooKeys 1215: 259–288. https://doi.org/10.3897/zookeys.1215.128603

Introduction

The pteromalid genus *Apsilocera* Bouček, 1956 (type species *Apsilocera verticillata* Bouček, 1956) belongs to the family Pteromalidae, subfamily Pteromalinae (Burks et al. 2022), and is distributed in the Nearctic, Palaearctic, Oriental and Australian regions. Until present, it comprised nineteen species, with only *A. bramleyi* Graham, 1966 and *A. verticillata* Bouček, 1956 being found in the Palaearctic region (Bouček 1956; Graham 1966; UCD Community 2023). Another one species *A. breviscapus* Bouček, 1993 is distributed in the Nearctic region (Bouček 1993; UCD Community 2023). Thirteen other species *A. acuticristata* Mitroiu & Achterberg, 2013, *A. bicristata* Mitroiu & Achterberg, 2013, *A. brevivena* Xiao & Huang, 2001, *A. cornuta* Mitroiu & Achterberg, 2013, *A. dentata* Mitroiu & Achterberg, 2013, *A. dupla* Mitroiu & Achterberg, 2013, *A. elongata* Mitroiu &

Achterberg, 2013, *A. fulvipennis* Mitroiu & Achterberg, 2013, *A. longicornis* Mitroiu & Achterberg, 2013, *A. maculata* Mitroiu & Achterberg, 2013, *A. obtusicristata* Mitroiu & Achterberg, 2013, *A. palliclava* Mitroiu & Achterberg, 2013, and *A. tuberculata* Mitroiu & Achterberg, 2013 are distributed in the Oriental region (Xiao and Huang 2001; Mitroiu and Achterberg 2013; UCD Community 2023). Three species, *A. australis* Bouček, 1988, *A. bidens* (Bouček, 1988) and *A. brevis* (Bouček, 1988) are distributed in the Australian region (UCD Community 2023).

Unfortunately, the biology of most *Apsilocera* species is unknown, but most were collected near dead trees in forests. Only *A. bramleyi* is known to parasitize small dipterans of the family Cecidomyiidae: *Cecidomyia* sp. and *Mycocecis ovalis* Edwards, 1922 (Graham 1969; Ghahari and Huang 2012).

The aim of this work is to describe eight new species of *Apsilocera* from Palaearctic region. An identification key to females of all Palaearctic species of *Apsilocera* is also provided.

Materials and methods

The specimens examined in this study are deposited in the collections of the National Institute of Biological Resources (Incheon, Republic of Korea; **NIBR**), the Science Museum of Natural Enemies (Geochang, Republic of Korea; **SMNE**), the National Museum in Prague (Prague, Czech Republic; **NMPC**), the State Museum of Natural History Stuttgart (Stuttgart, Germany; **SMNS**), the Swedish Museum of Natural History (Stockholm, Sweden; **NRM**), and the Zoological Institute of the Russian Academy of Sciences (St Petersburg, Russia; **ZISP**), the Entomological Laboratory of the Hokkaido University (Sapporo, Japan; **EIHU**), the Rijksmuseum Natuurlijke (Leiden, Netherlands; **RNHL**).

Morphological terminology, including sculpture and wing venation, follows Bouček and Rasplus (1991), Gibson (1997), and Burks et al. (2022). The flagellum consists of two anelli, six funicular segments, and the four-segmented clava. The antennal formula includes the number of segments: scapus, pedicellus, anelli, funicular segments, claval segments. The following abbreviations are used: **POL** – posterior ocellar line, the minimum distance between the posterior ocelli; **OOL** – ocello-ocular line, the minimum distance between a posterior ocellus and compound eye; **C1–C4** – claval segments; **M** – marginal vein; **S** – stigmal vein; **PM** – postmarginal vein; **F1–F6** – funicular segments; **Mt2–Mt8** – metasomal tergites (**Mt1** – petiole). The scape is measured without the radicle; the pedicel is measured in lateral view. The distance between the clypeal lower margin and the toruli is measured from the lower margins of the toruli. Eye height is measured as the maximum diameter, eye length as the minimum diameter. The mesosoma and metasoma are measured in lateral view, the latter including the ovipositor sheaths.

Specimens were examined using Olympus SZX12 and Nikon SMZ745T microscopes. Photographs were taken with a Canon EOS 70D digital camera mounted on an Olympus SZX10 microscope (IZAS, SMNE and ZISP specimens), and a Leica DFC500 digital camera attached to a Leica M205A automated research stereomicroscope (RNHL specimens). The acquired images were then processed with Helicon Focus.

Taxonomic account

Class Hexapoda Blainville, 1816
Order Hymenoptera Linnaeus, 1758
Family Pteromalidae Dalman, 1820
Subfamily Pteromalinae Ashmead, 1904

Genus *Apsilocera* Bouček, 1956

Apsilocera Bouček, 1956: 319–121. Type species *Apsilocera verticillata* Bouček, 1956, by monotypy.

Buloloa Bouček, 1988: 425–426. Type species: *B. bidens* Bouček, 1988, by monotypy. Synonymy by Mitroiu and Achterberg 2013: 449.

Kratinka Bouček, 1988: 428–429. Type species: *K. brevis* Bouček, 1988, by monotypy. Synonymy by Mitroiu and Achterberg 2013: 449, 450.

Bulolosa Bouček, 1990: 87. Replacement name for *Buloloa* Bouček, 1988. Synonymy by Mitroiu and Achterberg 2013: 449.

Diagnosis. Head with (Figs 1, 53, 61, 69, 100, 101, 105) or without (Figs 11, 20, 27, 36, 42, 78, 85, 94, 103) ornamentation; without occipital carina. Gena usually moderately to strongly receding towards mouth, hollowed of not hollowed at mouth corner; gena lamina absent. Lower margin of clypeus with one small tooth (Fig. 91), with two small teeth (Figs 13, 27, 75), convex (Fig. 45), produced and emarginate medially (Figs 19, 35, 84), with small median projection (Fig. 105), weakly emarginate (Fig. 1), rounded (Fig. 58). Antennal formula 11264; anelli small, F1–F6 longer than broad or quadrate, with one or two rows of sensilla, antennal clava not large, symmetrical, micropilose area small. Antennal toruli situated above level of lower edges of eyes (Figs 11, 20, 27, 36, 42, 53, 69, 78, 85, 94, 100, 101, 103), sometimes on level of upper edges of eyes (Figs 1, 61); antennal protuberance and scrobes absent. Mandible formula 3:4 (Figs 11, 91) or 4:4 (Figs 35, 68).

Mesosoma short, moderately depressed or arched. Pronotum narrower than mesoscutum, with collar margin carinate (Figs 21, 28, 37, 43). Notauli incomplete (Figs 4, 10, 25, 33, 41, 49, 57, 65, 82, 90). Scutellum moderately depressed (Figs 2, 24, 89, 102, 104, 106) or arched (Figs 16, 40, 48, 64, 81, 97), without conspicuous sublateral grooves, with distinct reticulate frenal area, but without frenal groove. Metapleuron entirely smooth. Propodeum finely reticulate (Figs 49, 74), weakly alutaceous (Figs 33, 41, 57, 65, 82), smooth and shiny (Figs 4, 9, 90), plicae present; without costula and with median carina, nucha short or absent; propodeal spiracles near to front margin of sclerite. Fore wing hyaline or with infumation, with distinct speculum; M not widened proximally; M longer than S (Figs 14, 22, 30, 38, 46, 54, 62, 71, 79, 87, 95). Hind coxa dorsally bare; hind tibia with one spur.

Metasoma sessile, short, ovate (Figs 39, 55, 72, 80, 96) to acuminate (Figs 7, 15, 23, 31, 47, 63, 88), as long as or shorter than combined length of mesosoma and head. Cerci with setae subequal in length. Ovipositor not much protruding.

Distribution. Nearctic, Palaearctic, Oriental and Australian regions.

Key to Palaearctic species of *Apsilocera* based on females

1 Vertex with only regular sculpture (Figs 11, 20, 27, 36, 42, 78, 85, 94, 103)...**2**
– Vertex with various ornamentations distinctly raised above regular sculpture (Figs 1, 53, 61, 69, 100, 101, 105) ...**11**
2 Clypeal margin with one small tooth (Fig. 91) or broadly convex (Fig. 45)...**3**
– Clypeal margin with two small teeth (Figs 13, 27, 75) or produced and emarginate medially (Figs 19, 35, 84)...**5**
3 Clypeal margin broadly convex (Fig. 45). POL 1.70–1.85 × OOL. Stigma of fore wing elongate (Fig. 46)...***A. elongata* Mitroiu & Achterberg**
– Clypeal margin with one small tooth (Fig. 91). POL 1.2–1.5 × OOL. Stigma of fore wing less elongate (Fig. 95) ...**4**
4 Head in dorsal view 2.55–2.60 × as broad as long (Fig. 93) and in frontal view 1.48–1.50 × as broad as high (Fig. 94). Fore wing with M 2.10–2.20 × as long as S (Fig. 95). Antenna with scape, pedicel and F1–F6 yellowish brown, clava brown (Fig. 92)...***A. verticillata* Bouček**
– Head in dorsal view 2.10–2.25 × as broad as long and in frontal view 1.30–1.45 × as broad as high (Fig. 103). Fore wing with M 2.4–2.5 × as long as S (Fig. 104). Antenna with scape and pedicel yellowish brown, funicle and clava brown (Fig. 104) ..... ***A. maculata* Mitroiu & Achterberg**
5 Clypeal margin produced and emarginate medially (Figs 19, 35, 84).....**6**
– Clypeal margin with 2 small teeth (Figs 13, 27, 75) ...**9**
6 Fore wing with M 1.50 × as long as S. Eye height 4.00 × as long as malar space...***A. brevivena* Xiao & Huang**
– Fore wing with M 1.85–2.20 × as long as S (Figs 22, 38, 87). Eye height 1.76–2.10 × as long as malar space...**7**
7 Mandible formula 4:4 (Fig. 35). F1 with many unevenly arranged sensilla (Fig. 34). Clypeal margin narrowly emarginate (Fig. 35)..... ..... ***A. eleganta* Tselikh, Haas & Ku, sp. nov.**
– Mandible formula 3:4. F1 with sparse, uniformly arranged sensilla (Figs 18, 83). Clypeal margin widely emarginate (Figs 19, 84)...**8**
8 Head and mesosoma finely reticulate (Figs 17, 20). Head in dorsal view not curved (Fig. 21). Spiracles of propodeum narrow (Fig. 17) ....***A. bramleyi* Graham**
– Head and mesosoma grossly reticulate (Figs 82, 85). Head in dorsal view curved (Fig. 86). Spiracles of propodeum not narrow (Fig. 82) ....***A. triapitzini* Tselikh, Haas & Ku, sp. nov.**
9 Propodeum with reticulate sculpture (Fig. 74). Fore coxae black or dark brown (Fig. 73). Scutellum finely reticulate (Fig. 74) ....***A. totoroi* Tselikh, Haas & Ku, sp. nov.**
– Propodeum smooth (Figs 9, 25). Fore coxa yellowish brown (Fig. 24) or basally brown, apically yellowish brown (Fig. 8). Scutellum grossly reticulate (Figs 9, 25)...**10**
10 Mandible formula 4:4. Distance between antennal toruli and lower margin of clypeus 2.00–2.30 × distance between antennal toruli and median ocellus.....***A. dupla* Mitroiu & Achterberg**
– Mandible formula 3:4 (Fig. 11). Distance between antennal toruli and lower margin of clypeus 3.00–3.20 × distance between antennal toruli and median ocellus ..... ***A. bradburyi* Tselikh, Lee & Ku, sp. nov.**

11 Vertex normal, not high, with a row of teeth originating near eye and ending near posterior ocellus (Fig. 69, 105). Head in frontal view 1.40–1.60 × as broad as high (Fig. 69, 105) **12**
– Vertex high (Figs 1, 53, 61, 100, 101), with one (Figs 1, 61, 100) or two (Fig. 53, 101) crests or elevations between posterior ocelli and anterior ocellus. Head in frontal view 1.00–1.19 × as broad as high (Figs 1, 53, 61, 100, 101) **13**
12 Clypeal margin with small median projection (Fig. 105). Eye height 1.14 × eye length (Fig. 106) and 2.00 × as long as malar space ..... ***A. tuberculata* Mitroiu & Achterberg**
– Clypeal margin with two teeth (Fig. 66). Eye height 1.31–1.35 × eye length and 1.60–1.67 × as long as malar space..... ***A. marina* Tselikh, Lee & Ku, sp. nov.**
13 Vertex with two distinct crests not composed of small sharp teeth, leaving a depression in middle (Fig. 53, 101) **14**
– Vertex with one continuous crest composed of small sharp teeth, leaving no depression in middle (Figs 1, 61, 100) **15**
14 POL 1.70–1.85 × OOL. Antenna with scape 1.37 × as long as eye length. Propodeum smooth. Fore wing with M 1.93 × as long as S, stigma small (Fig. 102) ..... ***A. bicristata* Mitroiu & Achterberg**
– POL 1.45 × OOL. Antenna with scape 1.03 × as long as eye length. Propodeum finely reticulate (Fig. 49). Fore wing with M 1.50 × as long as S, stigma enlarged (Fig. 54) ..... ***A. grandistigma* Tselikh, Lee & Ku, sp. nov.**
15 Crest of vertex moderately high (Fig. 99, 100). Distal tooth of mandible blunt. POL 1.08 × OOL ..... ***A. acuticristata* Mitroiu & Achterberg**
– Crest of vertex very high (Figs 1, 61). Distal tooth of mandible not blunt (Figs 1, 61). POL 0.77–0.85 × OOL **16**
16 Crest height 0.80 × eye length (Fig. 1). Clypeal margin weakly emarginate (Fig. 1). Distance between antennal toruli and lower margin of clypeus 3.40 × distance between antennal toruli and median ocellus. Head grossly reticulate (Fig. 1) ..... ***A. budai* Tselikh, Lee & Ku, sp. nov.**
– Crest height 0.50 × eye length (Fig. 61). Clypeal margin rounded (Fig. 58). Distance between antennal toruli and lower margin of clypeus 4.00–4.15 × distance between antennal toruli and median ocellus. Head finely reticulate (Fig. 61) ..... ***A. jejuensis* Tselikh, Lee & Ku, sp. nov.**

***Apsilocera bradburyi* Tselikh, Lee & Ku, sp. nov.**
https://zoobank.org/592086BF-94C3-489C-9B0D-3B04D9C4CA6A
Figs 8–15

Type material. ***Holotype*** • female, Republic of Korea: "Gyeongsangbuk-do, Andong-si, Bukhu-myeon, Dahyeon-ri, Malaise trap, coll. Kwon Gi-myon" (NIBR). ***Paratypes*** • 3 females, "Jeju-do, Jeju-si, Geumak-ri, Hanllim-eup, 16.VI–14.VII.2021, 16.VII–13.X.2021, Malaise trap, coll. Y.H. Park, M.H. Kim, D.H. Park, J.Y. Kim (1 female in ZISP, 2 females in SMNE) • 1 female, "Jeju-do, Jeju-si, Jocheon-eup, Gyorae Natual Recreate, 33°26'28"N, 126°39'53"E, 13.VII.2023, coll. E. Tselikh" (ZISP).

Description. Female. Body length 1.50–1.70 mm; fore wing length 1.40–1.50 mm.

***Coloration*.** Head black; antenna with scape, pedicel, and anelli yellow, F1–F6 yellowish brown, clava brown. Mesosoma black, but propodeum dorsally dark blue with metallic diffuse luster; fore coxa basally brown, apically yellowish brown, mid and hind coxae yellowish brown, all femora yellowish brown, tibiae and tarsi yellow. Fore wing hyaline, venation yellowish brown. Metasoma dorsally brown, laterally and ventrally yellowish brown; ovipositor sheaths brown.

***Sculpture*.** Head reticulate; clypeus radially striate. Mesosoma reticulate; propodeum smooth. Metasoma weakly alutaceous and shiny.

***Head*.** Head in dorsal view 2.50–2.53 × as broad as long and 1.31–1.36 × as broad as mesoscutum; in frontal view 1.42–1.45 × as broad as high. Vertex with regular sculpture. POL 1.13–1.25 × as long as OOL. Eye height 1.29–1.33 × eye length and 2.00–2.10 × as long as malar space. Distance between antennal toruli and lower margin of clypeus 2.90–3.15 × distance between antennal toruli and median ocellus. Antenna with scape 0.90–0.95 × as long as eye height and 1.09–1.16 × as long as eye length; pedicel 1.57–1.66 × as long as broad; combined length of pedicel and flagellum 1.04–1.10 × breadth of head; F1–F6 longer than broad, with 1 row of sensilla; clava 2.88–3.16 × as long as broad, with small micropilose area on each C3 and C4. Clypeal margin with two small teeth. Mandible formula 3:4.

***Mesosoma*.** Mesosoma 1.22–1.31 × as long as broad. Scutellum moderately arched, 0.82 × as long as broad, frenal area indistinct. Propodeum 0.37–0.41 × as long as scutellum; nucha short. Fore wing 2.13–2.22 × as long as its maximum width; basal cell with several hairs near basal vein; basal vein pilose; speculum partly closed below; M 0.85–0.87 × as long as PM and 2.17–2.20 × as long as S; stigma small.

***Metasoma*.** Metasoma 1.73–2.03 × as long as broad, 1.50–1.55 × as long as mesosoma. Petiole strongly transverse. Ovipositor sheath projecting slightly beyond apex of metasoma.

Male. Unknown.

Etymology. The species is named in honor of the famous writer Ray Douglas Bradbury.

Distribution. Korean Peninsula.

Comments. *Apsilocera bradburyi* sp. nov. belongs to a group of species that have a vertex with regular sculpture. This species is very similar to *A. dupla*; the differences between these species are given in the key.

Apsilocera bramleyi Graham, 1966

Figs 16–23

Apsilocera bramleyi Graham, 1966: 301–304. Holotype female (HDOU, not examined).

Additional material examined. Japan • 1 female, "Yokohama, Kanagawa Pref., 11.VI.2002, coll. K. Kubo" (EIHU). Russia • 1 female, "Krasnodar Reg., Sochi, Lazarevskoe, VIZR, 21.VII.1975, coll. V. Triapitzin" (ZISP). Germany • 1 female (SMNS_Hym_Pte_001795), "D, Sachsen, Lkr. Bautzen, Luppa,

51.278N, 14.403183E, 164 m, Sweep net, coll. L. Krogmann, T. Kothe", Sample ID: SMNS_38858 (SMNS). Sweden • 1 female (SMNS_Hym_Pte_006119), "Sweden, Mörbylånga, Lilla Vickleby Lunds NR (#115/2014), old oak forest, 27.VI–30.VII.2014, Malaise trap, 56.567331N, 16.441516E, coll. M. Jaschhof, C. Jaschhof", Sample ID: SMNS_48289 (SMNS); • 1 female (SMNS_Hym_Pte_005876), "Sweden, Mörbylånga, Lilla Vickleby Lunds NR (#137/2014), old oak forest, 31.VII–29.VIII.2014, Malaise trap, 56.567331N, 16.441516E, coll. M. Jaschhof, C. Jaschhof", Sample ID: SMNS_48046 (SMNS).

Biology. Primary parasitoid of *Cecidomyia* sp. and *Mycocecis ovalis* Edwards, 1922 (Diptera, Cecidomyiidae) (Graham 1969; Ghahari and Huang 2012).

Distribution. France, Germany, Iran, Japan, Russia, Serbia, Sweden, United Kingdom.

Comments. *Apsilocera bramleyi* belongs to a group of species that have a vertex with regular sculpture. This species is very similar to *A. triapitzini* sp. nov.; the differences between these species are given in the key.

Apsilocera budai Tselikh, Lee & Ku, sp. nov.

https://zoobank.org/2C0500D4-3403-4AF9-B5CA-1A0C06F2110E
Figs 1–7

Type material. ***Holotype*** • female, Republic of Korea: "Gyeongsangnam-do, Goseong-gun, Hail-myeon, Suyang-ri, 34°58'34.8"N, 128°12'08.3"E, 18.VI.2022, coll. E. Tselikh" (NIBR).

Description. Female. Body length 1.40 mm; fore wing length 1.30 mm.

***Coloration*.** Head black, in frontal view dark green with metallic diffuse luster; antenna yellowish brown. Mesosoma black, but propodeum dorsally dark blue-green with metallic diffuse luster; all coxa, all femora and tibiae yellowish brown, all tarsi yellow. Fore wing hyaline, venation yellowish brown. Metasoma dark brown with metallic green, diffuse coppery luster; ovipositor sheaths dark brown.

***Sculpture*.** Head grossly reticulate; clypeus radially striate, but near clypeal margin smooth. Mesosoma grossly reticulate; propodeum smooth. Metasoma weakly alutaceous and shiny.

***Head*.** Head in dorsal view 2.39 × as broad as long and 1.27 × as broad as mesoscutum; in frontal view 1.00 × as broad as high. Vertex with one continuous crest composed of small sharp teeth, leaving no depression in middle; crest height 0.80 × eye length. POL 0.77 × as long as OOL. Eye height 1.31 × eye length and 1.79 × as long as malar space. Distance between antennal toruli and lower margin of clypeus 3.46 × distance between antennal toruli and median ocellus. Antenna with scape 1.18 × as long as eye height and 1.54 × as long as eye length; pedicel 1.31 × as long as broad; combined length of pedicel and flagellum 1.26 × breadth of head; F1–F6 longer than broad, with 1 row of sensilla; clava 2.63 × as long as broad, with small micropilose area on each C3 and C4. Clypeal margin produced and weakly emarginate medially.

***Mesosoma*.** Mesosoma 1.30 × as long as broad. Scutellum moderately depressed, 0.96 × as long as broad, frenal area indistinct. Propodeum 0.38 × as long as scutellum; nucha short. Fore wing 2.24 × as long as its maximum width; basal cell with several hairs near submarginal vein; basal vein pilose; speculum partly closed below; M 0.98 × as long as PM and 2.17 × as long as S; stigma small.

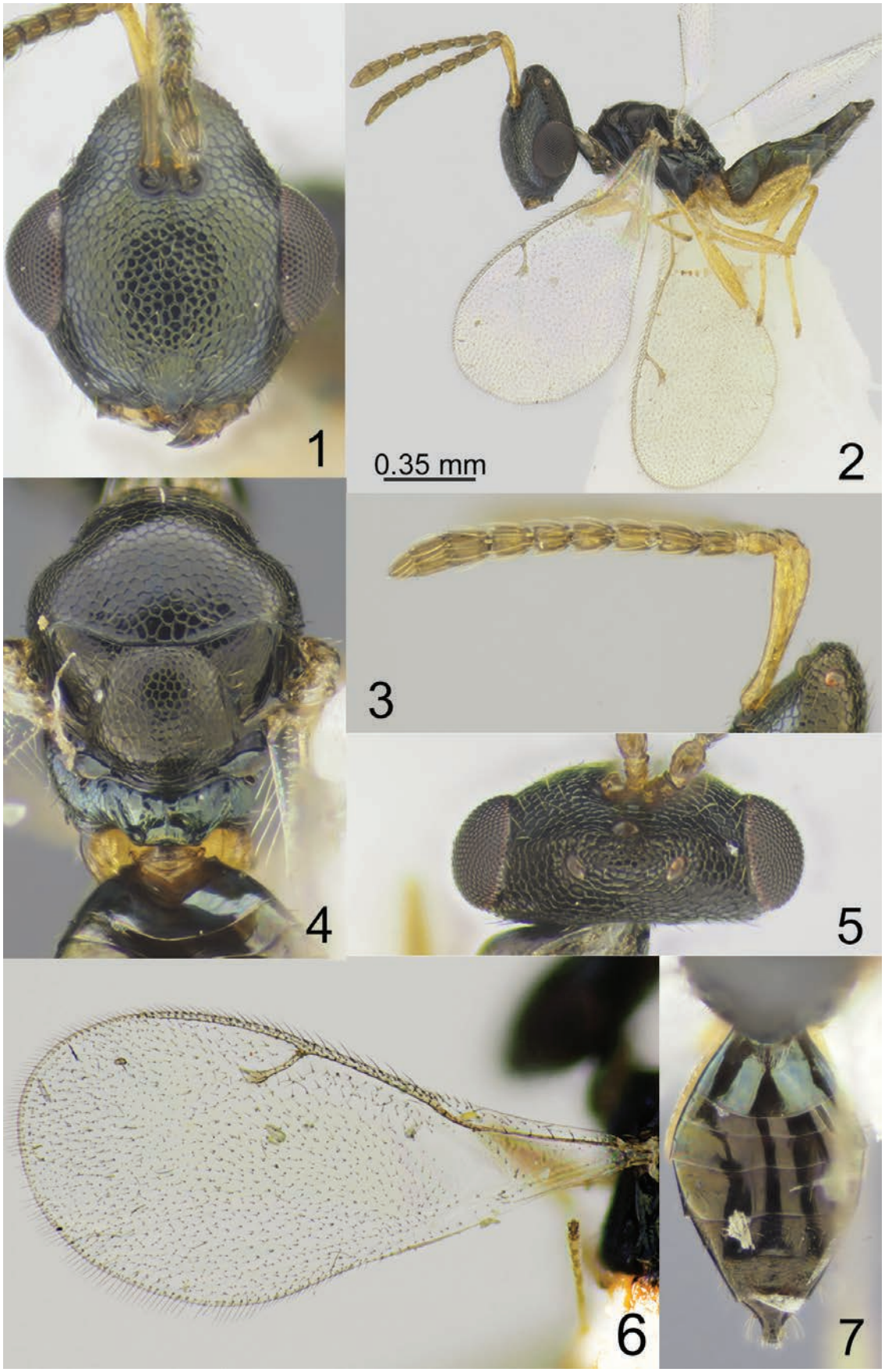

Figures 1–7. *Apsilocera budai* sp. nov., female, holotype **1** head, frontal view **2** habitus, lateral view **3** antenna **4** mesosoma, dorsal view **5** head, dorsal view **6** fore wing **7** metasoma, dorsal view.

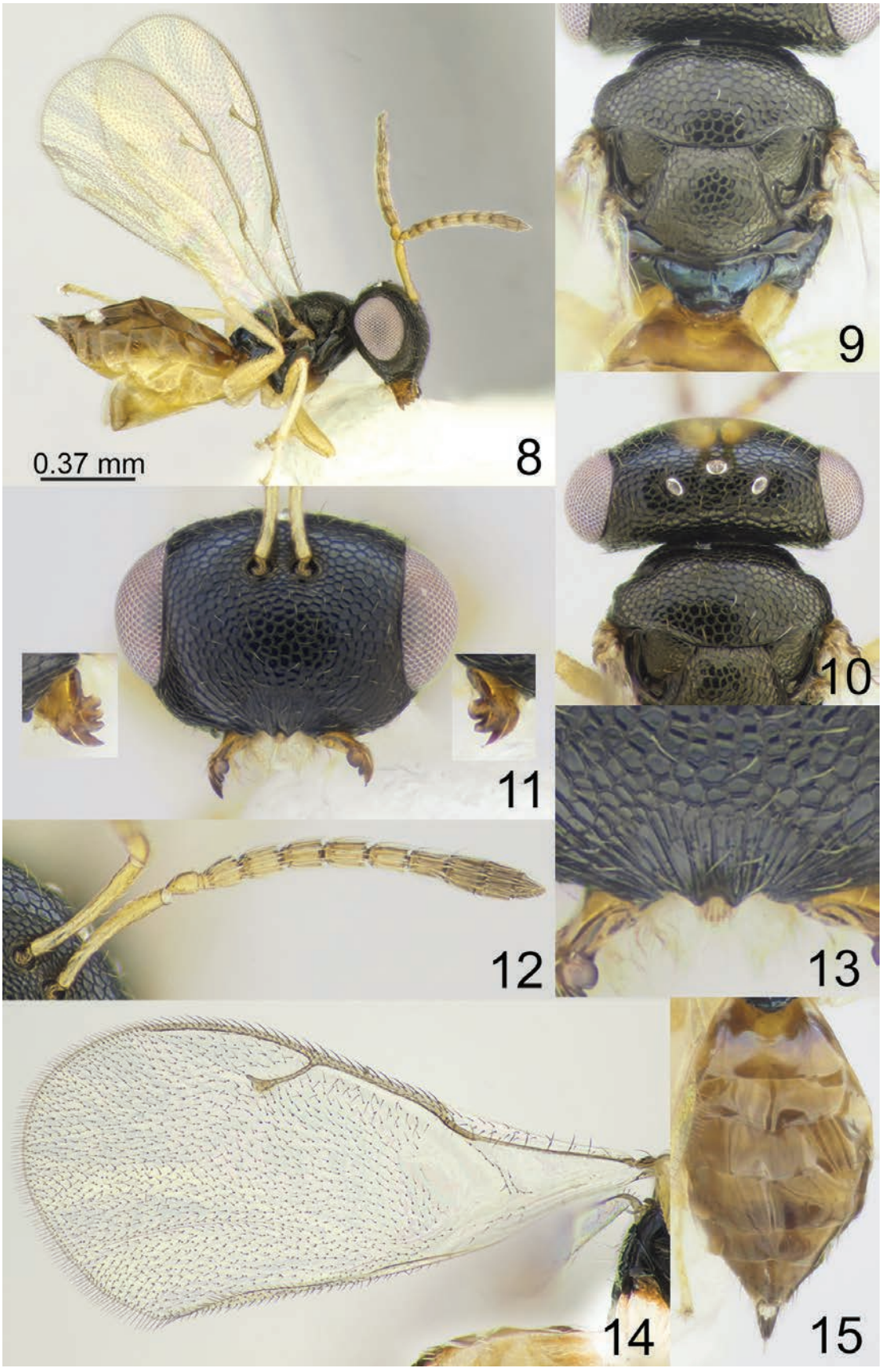

Figures 8–15. *Apsilocera bradburyi* sp. nov., female, holotype **8** habitus, lateral view **9** mesosoma, dorsal view **10** head, pronotum and mesoscutum, dorsal view **11** head, mandible, frontal view **12** antenna **13** clypeus **14** fore wing **15** metasoma, dorsal view.

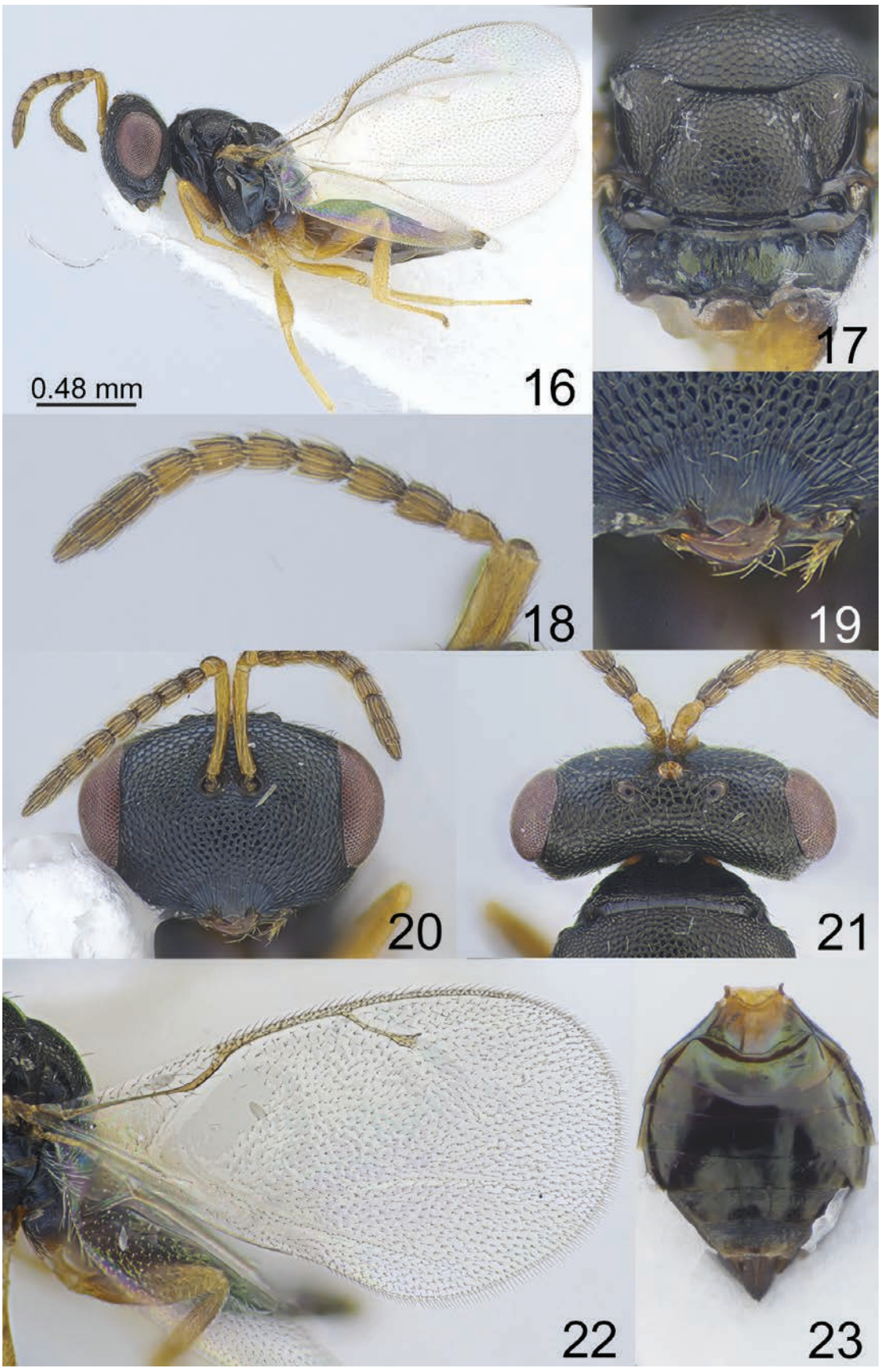

Figures 16–23. *Apsilocera bramleyi* Graham, 1966, female, not type **16** habitus, lateral view **17** scutellum and propodeum, dorsal view **18** antenna **19** clypeus **20** head, frontal view **21** head and pronotum, dorsal view **22** fore wing **23** metasoma, dorsal view.

***Metasoma*.** Metasoma 1.63 × as long as broad, 1.19 × as long as mesosoma. Petiole strongly transverse. Ovipositor sheath projecting slightly beyond apex of metasoma.

Male. Unknown.

Etymology. The species is named in honor of the large golden statue of Buddha in the type locality.

Distribution. Korean Peninsula.

Comments. *Apsilocera budai* sp. nov. belongs to a group of species that have a vertex with one continuous crest composed of small sharp teeth. This species is very similar to *A. jejuensis* sp. nov.; the differences between these species are given in the key.

Apsilocera dupla Mitroiu & Achterberg, 2013

Figs 24–31

Apsilocera dupla Mitroiu & Achterberg, 2013: 451, 461–462. Holotype female (RNHL, examined).

Type material. ***Holotype*** • female, Vietnam: "N. VIETNAM: Hoa Binh, Hang Kia Pà Cò N.R., 1329 m, 20°44'36"N, 104°53'45"E, 2.III–15.IV.2011, Mal. tr. 5, C. v. Achterberg, RMNH'11" (RMNH).

Additional material examined. Republic of Korea • 2 females, 1 male, "Gyeongsangbuk-do, Yeongyang-gun, Irwol-myeon, Mt. Ilwolsan, 36°48'29"N, 129°05'25"E, 7.VII.2015, coll. E. Tselikh" (ZISP) • 1 female, "Jeollanam-do, Goheung-gun, Geumsan-myeon, Eojeon-ri, 3.VIII–16.VIII.2020, Malaise trap, coll. D.S. Ku, J.H. Lee" (NIBR) • 2 females, "Gyeongsangnam-do, Jinju-si, Ilbanseong-myeon, Changchon-ri, 4.VI–20.VI.2022, 25.VI–16.VII.2022, Malaise trap, coll. An Tae-Ho" (SMNE) • 5 females, "Gyeongsangnam-do, Geoje-si, Hacheong-myeon, Eoon-ri, 34°59'24.6"N, 128°38'27"E, 2.VII.2023, coll. E. Tselikh (ZISP).

Distribution. Indonesia, Vietnam, Korean Peninsula.

Comments. *Apsilocera dupla* belongs to a group of species that have a vertex with regular sculpture. This species is very similar to *Apsilocera bradburyi* sp. nov.; the differences between these species are given in the key.

Apsilocera eleganta Tselikh, Haas & Ku, sp. nov.

https://zoobank.org/FEFF5EEE-761D-4D06-890B-DB485B647AC2

Figs 32–39

Type material. ***Holotype*** • female, Republic of Korea: "Gyeonggi-do, Pocheon-si, Soheul-eup, Jikdong-ri, Malaise trap, 30.X.2009, coll. S.Y. Park" (NIBR). ***Paratypes*** • 1 female (NHRS-HEVA000022836), "Sweden Öl, Mörbylånga kommun, Västerstads almlunds naturreservat., Old elm forest (3002 Trap ID, 3053 Event ID), 10.VI–9.VII.2014, Malaise trap, 56.427648N, 16.421110E, leg. Swedish Malaise Trap Project", Sample ID: SMNS_50686 (NRM) • 1 female (SMNS_Hym_T00802), "Sweden Sm, Nybro kommun, Alsterbro/Alsterån, Mixed forest (1008 Trap ID, 2000 Event ID), 5.IX–13.X.2006, Malaise trap, 56.936536N, 15.920167E,

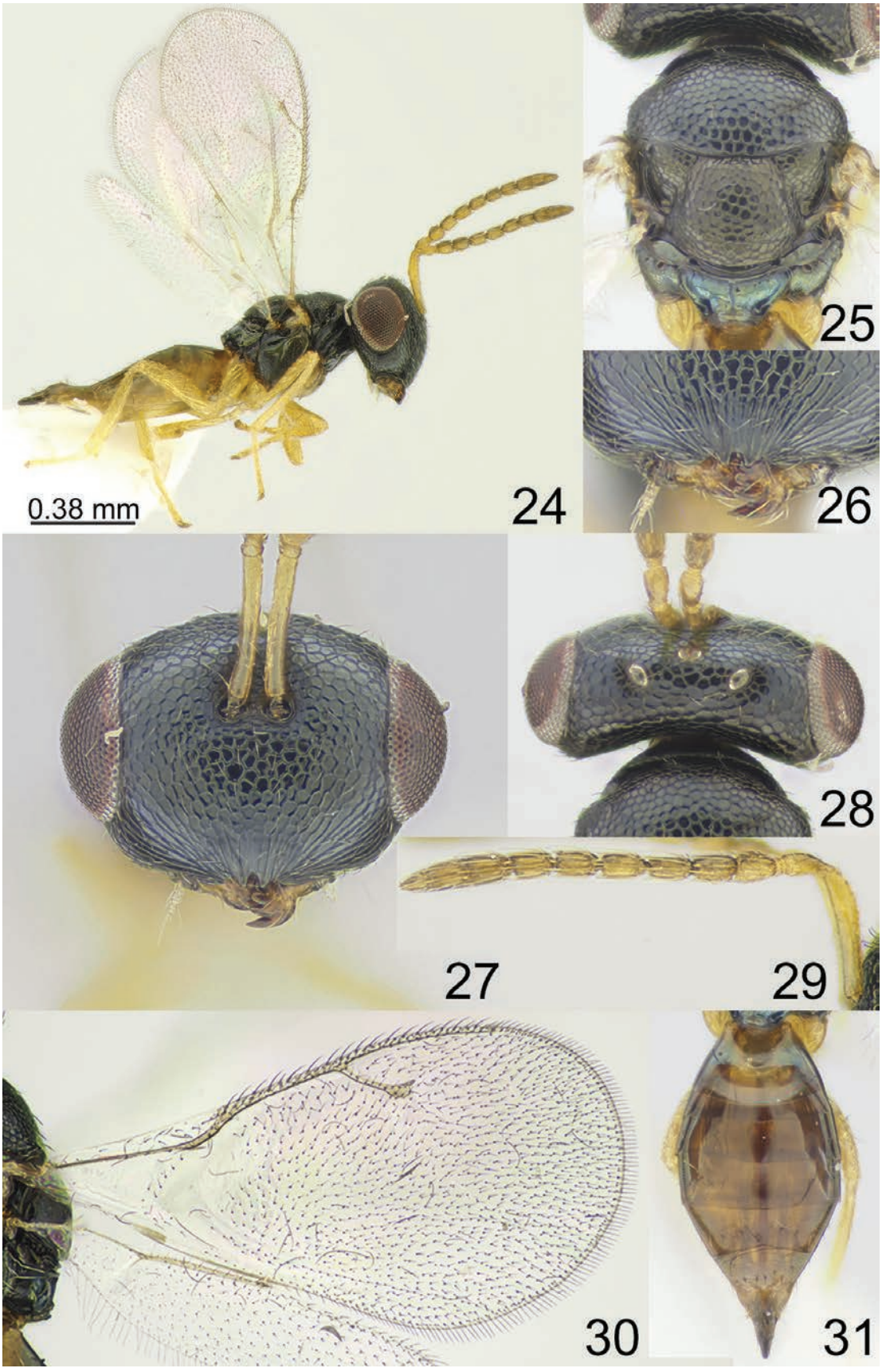

Figures 24–31. *Apsilocera dupla* Mitroiu & Achterberg, 2013, female, not type **24** habitus, lateral view **25** mesosoma, dorsal view **26** clypeus **27** head, frontal view **28** head and pronotum, dorsal view **29** antenna **30** fore wing **31** metasoma, dorsal view.

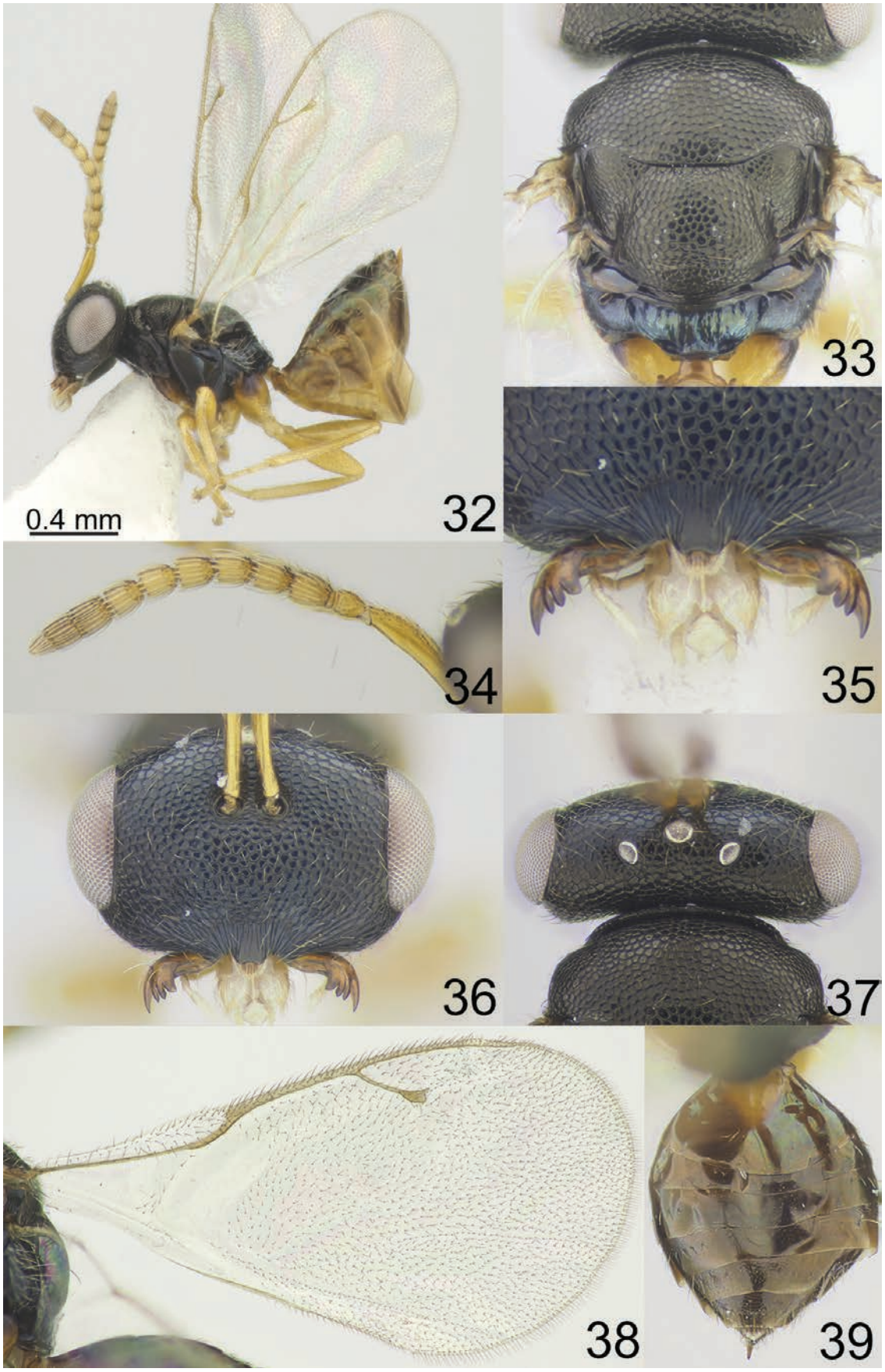

Figures 32–39. *Apsilocera eleganta* sp. nov., female, holotype **32** habitus, lateral view **33** mesosoma, dorsal view **34** antenna **35** clypeus **36** head, frontal view **37** head and pronotum, dorsal view **38** fore wing **39** metasoma, dorsal view.

leg. Swedish Malaise Trap Project", Sample ID: SMNS_115563 (SMNS); • 1 female (NHRS-HEVA000022837), "Sweden Sm, Nybro kommun, Alsterbro/Alsterån, Mixed forest (1008 Trap ID, 1746 Event ID), 8.VIII–19.VIII.2006, Malaise trap, 56.936536N, 15.920167E, leg. Swedish Malaise Trap Project" (NRM).

Description. Female. Body length 1.60–2.82 mm; fore wing length 1.65–2.11 mm.

***Coloration*.** Head black; antenna yellowish brown. Mesosoma black, but propodeum dorsally dark blue with metallic diffuse luster; all coxae basally metallic blue, apically yellowish brown; all femora, tibiae and tarsi yellowish brown. Fore wing hyaline, venation yellowish brown. Metasoma dorsally brown, laterally and ventrally yellowish brown; ovipositor sheaths yellowish brown.

***Sculpture*.** Head reticulate; clypeus radially striate, but near clypeal margin smooth. Mesosoma reticulate; propodeum alutaceous. Metasoma weakly alutaceous and shiny.

***Head*.** Head in dorsal view 2.43–2.65 × as broad as long and 1.27–1.32 × as broad as mesoscutum; in frontal view 1.49–1.58 × as broad as high. Vertex with regular sculpture. POL 1.14–1.19 × as long as OOL. Eye height 1.37–1.40 × eye length and 1.76–2.00 × as long as malar space. Distance between antennal toruli and lower margin of clypeus 2.50–2.61 × distance between antennal toruli and median ocellus. Antenna with scape 0.92–0.95 × as long as eye height and 1.28–1.31 × as long as eye length; pedicel 1.50–1.66 × as long as broad; combined length of pedicel and flagellum 0.94–0.98 × breadth of head; F1, F2 longer than broad, F3–F6 subquadrate, with single row of sensilla; clava 2.85–3.18 × as long as broad, with small micropilose area on each C3 and C4. Clypeal margin produced and emarginate medially. Mandible formula 4:4.

***Mesosoma*.** Mesosoma 1.23–1.34 × as long as broad. Scutellum moderately depressed, 0.78 × as long as broad, frenal area indistinct. Propodeum 0.37–0.43 × as long as scutellum. Fore wing 1.94–2.01 × as long as its maximum width; basal cell with several hairs; basal vein pilose; speculum partly closed below; M 0.72–0.89 × as long as PM and 1.73–2.06 × as long as S; stigma small.

***Metasoma*.** Metasoma 1.19–1.50 × as long as broad and 1.05–1.20 × as long as mesosoma.

Male. Unknown.

Etymology. From the Latin *elegans*, referring to the elegant habitus of this species.

Distribution. Korean Peninsula, Sweden.

Comments. *Apsilocera eleganta* sp. nov. belongs to a group of species that have a vertex with regular sculpture. This species is very similar to *A. bramleyi* and *A. triapitzini* sp. nov.; the differences between these species are given in the key.

Apsilocera elongata Mitroiu & Achterberg, 2013

Figs 40–47

Apsilocera elongata Mitroiu & Achterberg, 2013: 451, 462. Holotype female (RNHL, examined).

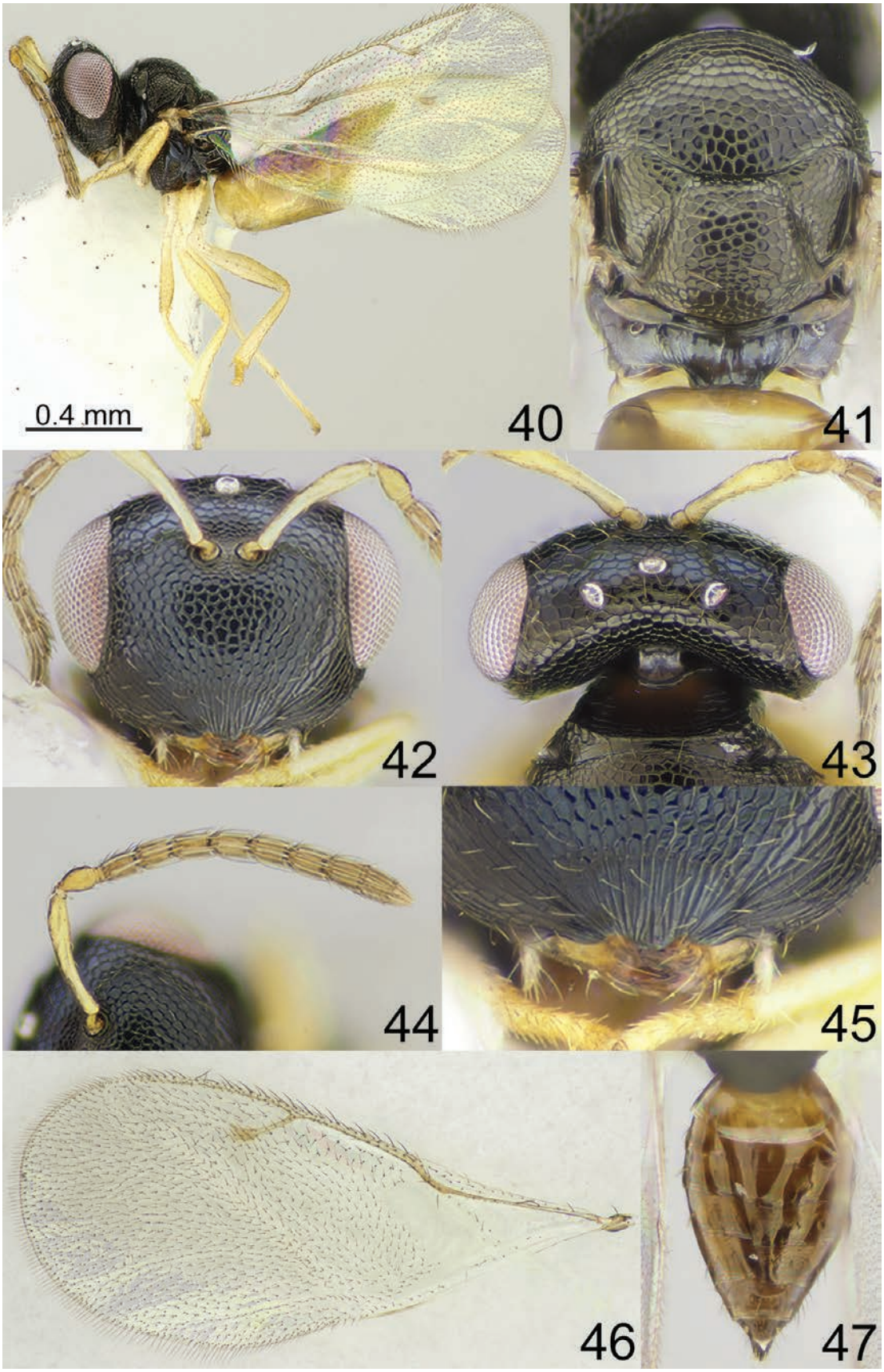

Figures 40–47. *Apsilocera elongata* Mitroiu & Achterberg, 2013, female, not type **40** habitus, lateral view **41** mesosoma, dorsal view **42** head, frontal view **43** head and pronotum, dorsal view **44** antenna **45** clypeus **46** fore wing **47** metasoma, dorsal view.

Type material. ***Holotype*** • female, Vietnam: "N. VIETNAM: Ninh Binh, Cuc Phuong N.P., nr centre (I), c 225 m, 20.XII.1999–10.II.2000, Mai Phu Quy, RMNH'00" (RMNH).

Additional material examined. Republic of Korea • 1 female, "Gyeongsangbuk-do, Ulijn-gun, Geumgangsong-myeon, Sogwang-ri, Malaise trap, 17.VIII.2016, coll. H.K. Lee" (NIBR).

Distribution. Korean Peninsula, Vietnam.

Comments. *Apsilocera elongata* sp. nov. belongs to a group of species that have a vertex with regular sculpture. This species is very similar to *A. verticillata* and *A. maculata*; the differences between these species are given in the key.

Apsilocera grandistigma **Tselikh, Lee & Ku, sp. nov.**

https://zoobank.org/844D223D-603C-4F56-8131-74805087F4B1

Figs 48–55

Type material. ***Holotype*** • female, Republic of Korea: "Gyeonggi-do, Pocheon-si, Soheul-eup, 37°45'01.6"N, 127°08'34.9"E, 24.V–12.VI.2017, coll. Kim, Kim, Nam" (NIBR).

Description. Female. Body length 1.40 mm; fore wing length 1.40 mm.

Coloration**.** Head black; antenna with scape, pedicel, and anelli yellowish brown, F1–F6 and clava brown. Mesosoma black; fore and mid coxa black, hind coxae basally black, apically yellowish brown, all femora yellowish brown, all tibiae and tarsi yellow. Fore wing hyaline, venation yellowish brown. Metasoma and ovipositor sheaths brown.

Sculpture**.** Head reticulate; clypeus radially striate. Mesosoma reticulate; propodeum finely reticulate. Metasoma weakly alutaceous and shiny.

Head**.** Head in dorsal view 2.26 × as broad as long and 1.21 × as broad as mesoscutum; in frontal view 1.13 × as broad as high. Vertex with two distinct crests not composed of small sharp teeth, leaving a depression in middle. POL 1.45 × as long as OOL. Eye height 1.27 × eye length and 1.75 × as long as malar space. Distance between antennal toruli and lower margin of clypeus 1.36 × distance between antennal toruli and median ocellus. Antenna with scape 0.80 × as long as eye height and 1.03 × as long as eye length; pedicel 1.88 × as long as broad; combined length of pedicel and flagellum 1.18 × breadth of head; F1–F6 longer than broad, with 1 row of sensilla; clava 3.50 × as long as broad, with small micropilose area on each C3 and C4. Clypeal margin with one tooth.

Mesosoma**.** Mesosoma 1.46 × as long as broad. Scutellum moderately depressed, 1.00 × as long as broad, frenal area indistinct. Propodeum 0.34 × as long as scutellum; nucha short. Fore wing 2.02 × as long as its maximum width; basal cell with several hairs; basal vein pilose; speculum partly closed below; M 0.75 × as long as PM and 1.50 × as long as S; stigma enlarged.

Metasoma**.** Metasoma 1.40 × as long as broad, 1.00 × as long as mesosoma. Petiole strongly transverse. Ovipositor sheath projecting slightly beyond apex of metasoma.

Male. Unknown.

Etymology. From the Latin *grandis* and *stigma*, referring to the wide stigma of fore wing of this species.

Distribution. Korean Peninsula.

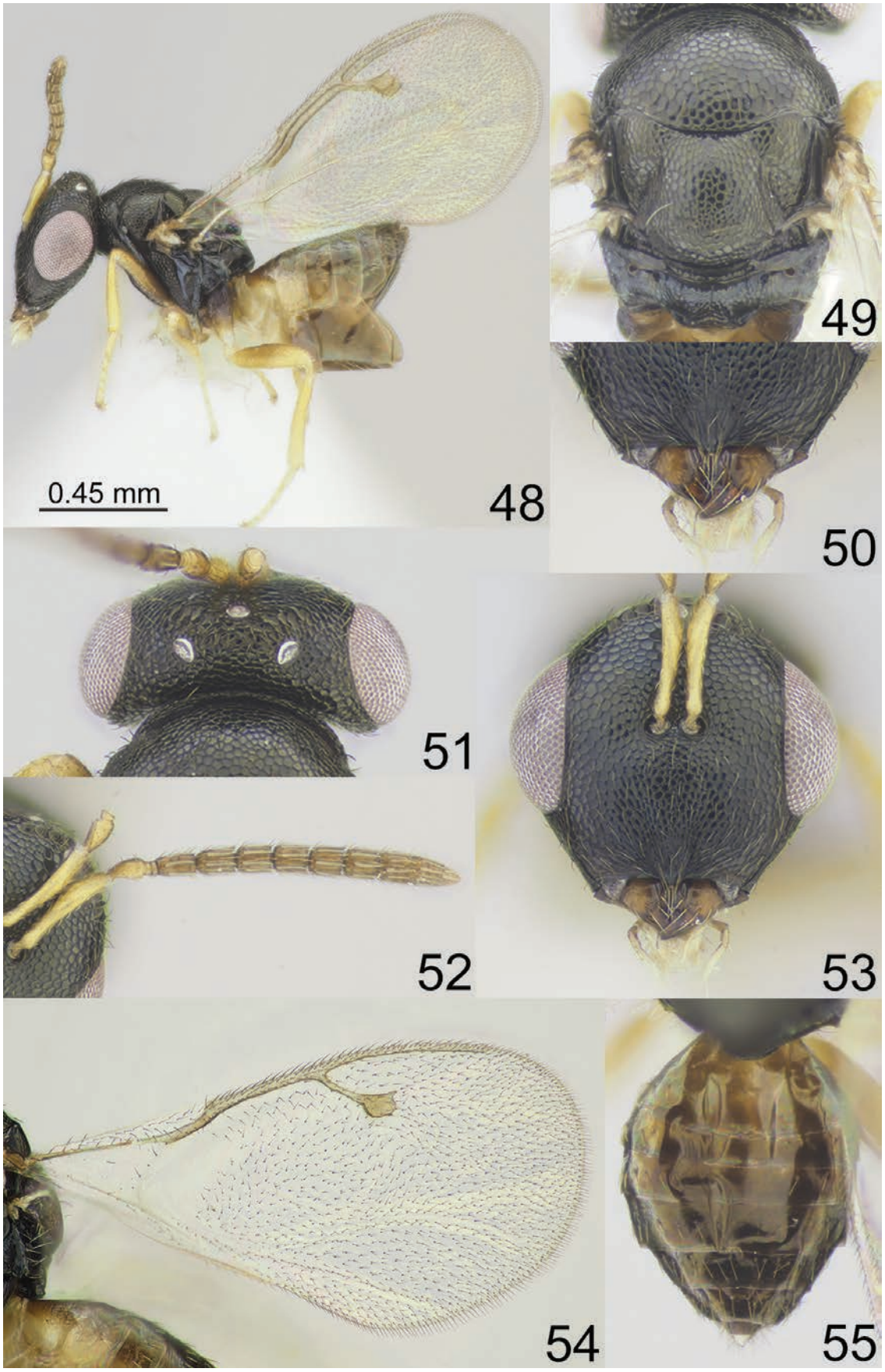

Figures 48–55. *Apsilocera grandistigma* sp. nov., female, holotype **48** habitus, lateral view **49** mesosoma, dorsal view **50** clypeus **51** head and pronotum, dorsal view **52** antenna **53** head, frontal view **54** fore wing **55** metasoma, dorsal view.

Comments. *Apsilocera grandistigma* sp. nov. belongs to a group of species that have a vertex with two distinct crests not composed of small sharp teeth, leaving a depression in middle. This species is very similar to *A. bicristata*; the differences between these species are given in the key.

***Apsilocera jejuensis* Tselikh, Lee & Ku, sp. nov.**

https://zoobank.org/55F61397-C5FE-41F7-8A22-B90FA6F3B6F9

Figs 56–63

Type material. ***Holotype*** • female, Republic of Korea: "Jeju-do, Jeju-si, Hanllim-eup, Geumak-ri, 16.VII–13.X.2021, Malaise trap, coll. Y.H. Park, M.H. Kim, D.H. Park, J.Y. Kim" (NIBR). ***Paratype*** • 1 female, "Jeju-do, Jeju-si, Jocheon-eup, Gyorae Nat. Recreat., forest, 33°26'28"N, 126°39'53"E, 13.VII.2023, coll. E. Tselikh" (ZISP).

Description. Female. Body length 1.50–1.55 mm; fore wing length 1.43–1.50 mm.

***Coloration*.** Head black in dorsal view and dark blue-green with metallic diffuse luster in frontal view; antenna with scape yellowish brown; pedicel, anelli, F1–F6, and clava brown. Mesosoma black, but propodeum dorsally dark blue-green with metallic diffuse luster; fore and mid coxa black, hind coxae basally black, apically yellowish brown, all femora yellowish brown, all tibiae and tarsi yellow. Fore wing hyaline, venation yellowish brown. Metasoma dark brown with metallic green, diffuse coppery luster; ovipositor sheaths dark brown.

***Sculpture*.** Head finely reticulate; clypeus radially striate, but near clypeal margin smooth. Mesosoma finely reticulate; propodeum weakly alutaceous. Metasoma Mt2 and Mt3 smooth, Mt4–Mt8 weakly alutaceous and shiny.

***Head*.** Head in dorsal view 2.30–2.36 × as broad as long and 1.31–1.33 × as broad as mesoscutum; in frontal view 0.90–1.11 × as broad as high. Vertex with one continuous crest composed of small sharp teeth, crest height 0.50 × eye length. POL 0.85–0.87 × as long as OOL. Eye height 1.37–1.40 × eye length and 1.95–2.10 × as long as malar space. Distance between antennal toruli and lower margin of clypeus 4.40–4.15 × distance between antennal toruli and median ocellus. Antenna with scape 1.09–1.12 × as long as eye height and 1.44–1.53 × as long as eye length; pedicel 1.35–1.45 × as long as broad; combined length of pedicel and flagellum 0.95–0.98 × breadth of head; F1–F6 longer than broad, with 1 row of sensilla; clava 3.70–3.84 × as long as broad, with small micropilose areas on each C3 and C4. Clypeal margin rounded.

***Mesosoma*.** Mesosoma 1.30–1.36 × as long as broad. Scutellum moderately depressed, 0.77–0.81 × as long as broad, frenal area indistinct. Propodeum 0.45–0.48 × as long as scutellum; nucha short. Fore wing 2.24–2.28 × as long as its maximum width; basal cell with several hairs; basal vein pilose; speculum open below; M 0.90 × as long as PM and 2.10–2.22 × as long as S; stigma small.

***Metasoma*.** Metasoma 1.40–1.45 × as long as broad, 1.20–1.25 × as long as mesosoma. Petiole strongly transverse. Ovipositor sheath projecting slightly beyond apex of metasoma.

Male. Unknown.

Etymology. The species is named in honor of the type locality, Jeju Island.

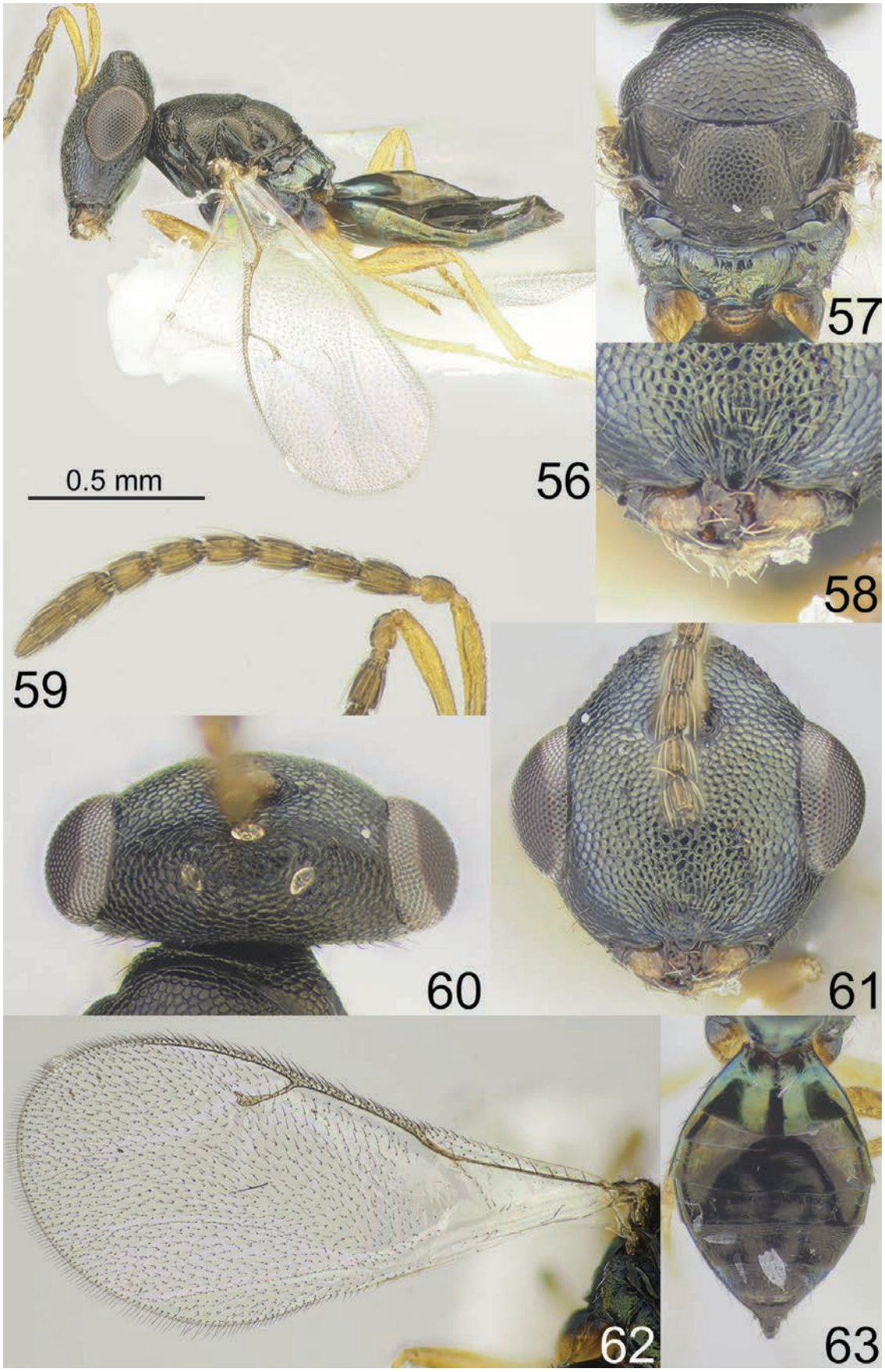

Figures 56–63. *Apsilocera jejuensis* sp. nov., female, holotype **56** habitus, lateral view **57** mesosoma, dorsal view **58** clypeus **59** antenna **60** head and pronotum, dorsal view **61** head, frontal view **62** fore wing **63** metasoma, dorsal view.

Distribution. Korean Peninsula.

Comments. *Apsilocera jejuensis* sp. nov. belongs to a group of species that have a vertex with one continuous crest composed of small sharp teeth. This species is very similar to *A. budai* sp. nov.; the differences between these species are given in the key.

***Apsilocera marina* Tselikh, Lee & Ku, sp. nov.**

https://zoobank.org/0C2D724C-E018-49FE-9ABB-B80F8B51DA23

Figs 64–72

Type material. ***Holotype*** • female, Republic of Korea: "Jeollanam-do, Goheung-gun, Bongnae-myeon, Oenarodo, Malaise trap, 16–29.VIII.2020, coll. D.S. Ku, J.H. Lee" (NIBR). ***Paratype*** • 1 female, "Jeju-do, Jeju-si, Hanllim-eup, Geumak-ri, 16.VI–14.VII.2021, Malaise trap, coll. Y.H. Park, M.H. Kim, D.H. Park, J.Y. Kim" (ZISP).

Description. Female. Body length 1.30–1.35 mm; fore wing length 1.40–1.45 mm.

***Coloration*.** Head black in dorsal view and dark blue in frontal view; antenna with scape yellowish brown; pedicel, anelli, F1–F6, and clava brown. Mesosoma black, but propodeum dorsally dark blue-green with metallic diffuse luster; fore and hind coxa black with metallic diffuse violet luster, mid coxae yellowish brown, all femora yellowish brown, all tibiae and tarsi yellow. Fore wing hyaline, venation yellowish brown. Metasoma dark brown with metallic green, diffuse coppery luster, laterally and ventrally brown; ovipositor sheaths dark brown.

***Sculpture*.** Head finely reticulate; clypeus radially striate. Mesosoma reticulate; propodeum alutaceous. Metasoma smooth and shiny.

***Head*.** Head in dorsal view 2.36–2.43 × as broad as long and 1.31–1.34 × as broad as mesoscutum; in frontal view 1.36–1.38 × as broad as high. Vertex with a row of teeth originating near eye and ending near posterior ocellus. POL 1.20–1.33 × as long as OOL. Eye height 1.31–1.35 × eye length and 1.60–1.67 × as long as malar space. Distance between antennal toruli and lower margin of clypeus 3.68–3.70 × distance between antennal toruli and median ocellus. Antenna with scape 1.00 × as long as eye height and 1.30–1.33 × as long as eye length; pedicel 1.48–1.50 × as long as broad; combined length of pedicel and flagellum 1.00 × breadth of head; F1–F6 longer than broad, with single row of sensilla; clava 2.60–2.85 × as long as broad, with small micropilose area on each C3 and C4. Clypeal margin with two teeth. Mandible formula 4:4.

***Mesosoma*.** Mesosoma 1.24–1.26 × as long as broad. Scutellum arched, 0.86–0.88 × as long as broad, frenal area indistinct. Propodeum 0.44 × as long as scutellum; nucha short. Fore wing 2.10–2.22 × as long as its maximum width; basal cell with two or three hairs; basal vein pilose; speculum partly open; M 0.85–0.87 × as long as PM and 1.80–1.86 × as long as S; stigma moderate enlarged.

***Metasoma*.** Metasoma 1.03–1.20 × as long as broad, 0.82–0.88 × as long as mesosoma. Petiole strongly transverse. Ovipositor sheath projecting slightly beyond apex of metasoma.

Male. Unknown.

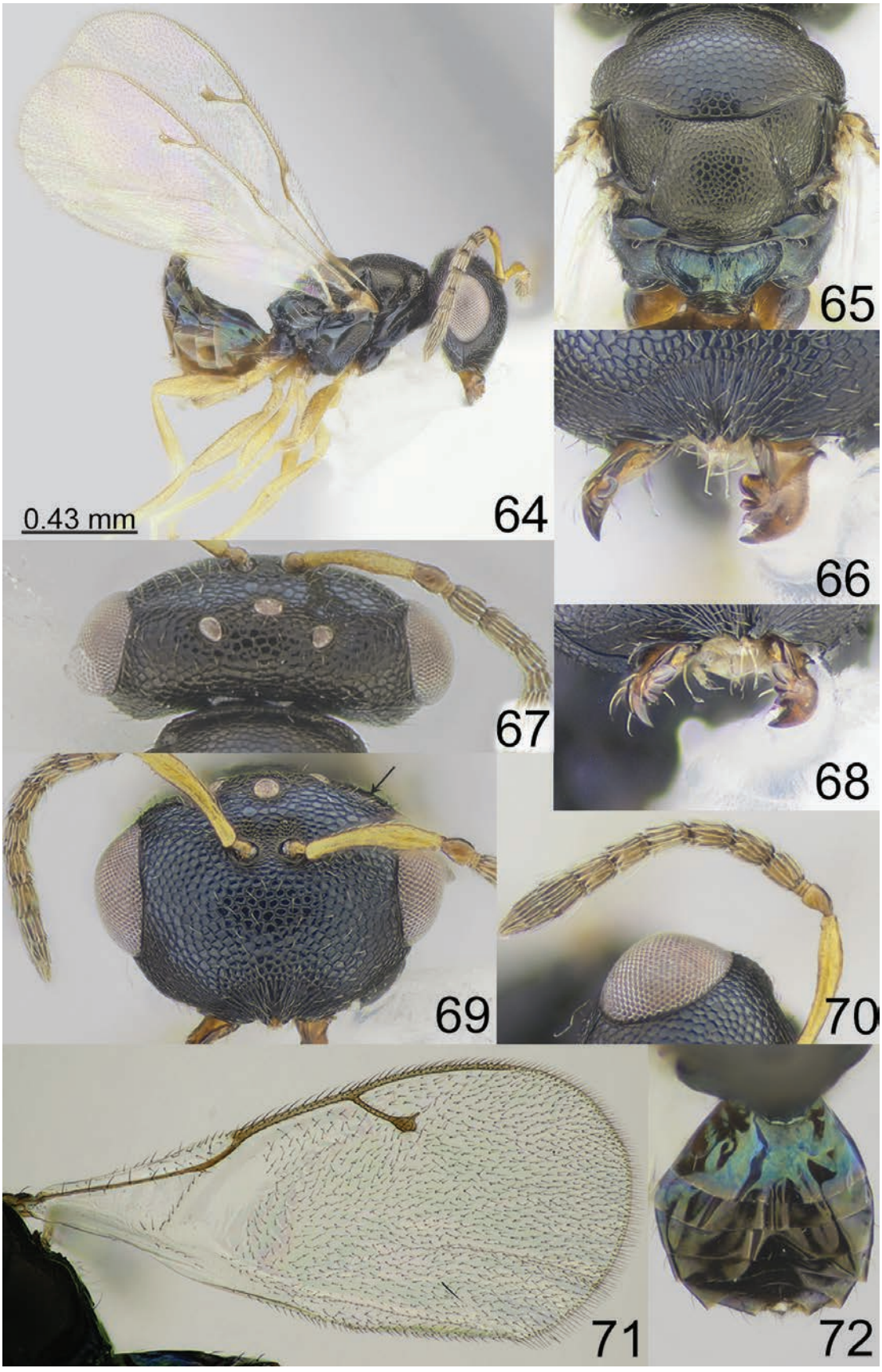

Figures 64–72. *Apsilocera marina* sp. nov., female, holotype **64** habitus, lateral view **65** mesosoma, dorsal view **66** clypeus **67** head and pronotum, dorsal view **68** mandible **69** head, frontal view **70** antenna **71** fore wing **72** metasoma, dorsal view.

Etymology. The species is named in honor of the senior author's sister, Marina (Tselikh) Kopylova.

Distribution. Korean Peninsula.

Comments. *Apsilocera marina* sp. nov. belongs to a group of species that have a vertex with a row of teeth originating near eye and ending near posterior ocellus. This species is very similar to *A. tuberculata* Mitroiu & Achterberg; the differences between these species are given in the key.

***Apsilocera totoroi* Tselikh, Haas & Ku, sp. nov.**

https://zoobank.org/5E49E91F-0A53-4490-A810-EEECB758FA84

Figs 73–80

Type material. ***Holotype*** • female, Japan: "Honshu, Fukushima Pref., HinoemataVill., 16–18.VIII.1999, coll. S. Belokobylskij" (ZISP). ***Paratypes*** • 1 female (SMNS_Hym_T00799), "Sweden, Mörbylånga, Kalkstad NR (#136/2014), mixed deciduous forest, 31.VII–27.VIII.2014, Malaise trap, 56.609569N, 16.503726E, coll. M. Jaschhof, C. Jaschhof", Sample ID: SMNS_47998 (SMNS) • 2 females (SMNS_Hym_T00800 & SMNS_Hym_T00801), "Germany, Baden-Württemberg, Lkr. Rems-Murr-Kreis, Aspach bei Backnang, Forest, 15.VII–8.VIII.2013, Malaise trap, 48.998972N, 9.419746E, leg. L. Krogmann, J. Holstein, T. Kothe", Sample ID: SMNS_50181 & SMNS_50214 (SMNS).

Description. Female. Body length 1.50–1.99 mm; fore wing length 1.36–1.76 mm.

***Coloration*.** Head black; antenna with scape, pedicel, and anelli yellowish brown, F1–F6 and clava brown. Mesosoma black, but propodeum dorsally dark blue with metallic diffuse luster. Fore coxae black or dark brown, mid and hind coxae yellowish brown; all femora and tibiae yellowish brown, all tarsi yellow. Fore wing hyaline, venation yellowish brown. Metasoma dorsally dark brown, but Mt2 dorsally dark metallic blue-green; laterally and ventrally brown; ovipositor sheaths brown.

***Sculpture*.** Head reticulate; clypeus radially striate. Mesosoma with propodeum reticulate. Metasoma weakly alutaceous and shiny.

***Head*.** Head in dorsal view 2.33–2.53 × as broad as long and 1.23–1.37 × as broad as mesoscutum; in frontal view 1.40–1.67 × as broad as high. Vertex with regular sculpture. POL 1.13–1.29 × as long as OOL. Eye height 1.24–1.38 × eye length and 1.80–1.95 × as long as malar space. Distance between antennal toruli and lower margin of clypeus 1.92–2.10 × distance between antennal toruli and median ocellus. Antenna with scape 0.96–1.07 × as long as eye height and 1.30–1.38 × as long as eye length; pedicel 1.50–1.67 × as long as broad; combined length of pedicel and flagellum 0.91–1.10 × breadth of head; F1–F6 longer than broad, with a row of sensilla; clava 3.00–3.40 × as long as broad, with small micropilose area on each C3 and C4. Clypeal margin with two small teeth. Mandible formula 4:4.

***Mesosoma*.** Mesosoma 1.29–1.48 × as long as broad. Scutellum moderately depressed, 0.92 × as long as broad, frenal area indistinct. Propodeum 0.44–0.53 × as long as scutellum. Fore wing 1.96–2.12 × as long as its maximum width; basal cell bare; basal cell with 0–4 hairs; basal vein pilose; speculum partly closed below; M 0.96–1.00 × as long as PM and 2.27–2.33 × as long as S, stigma small.

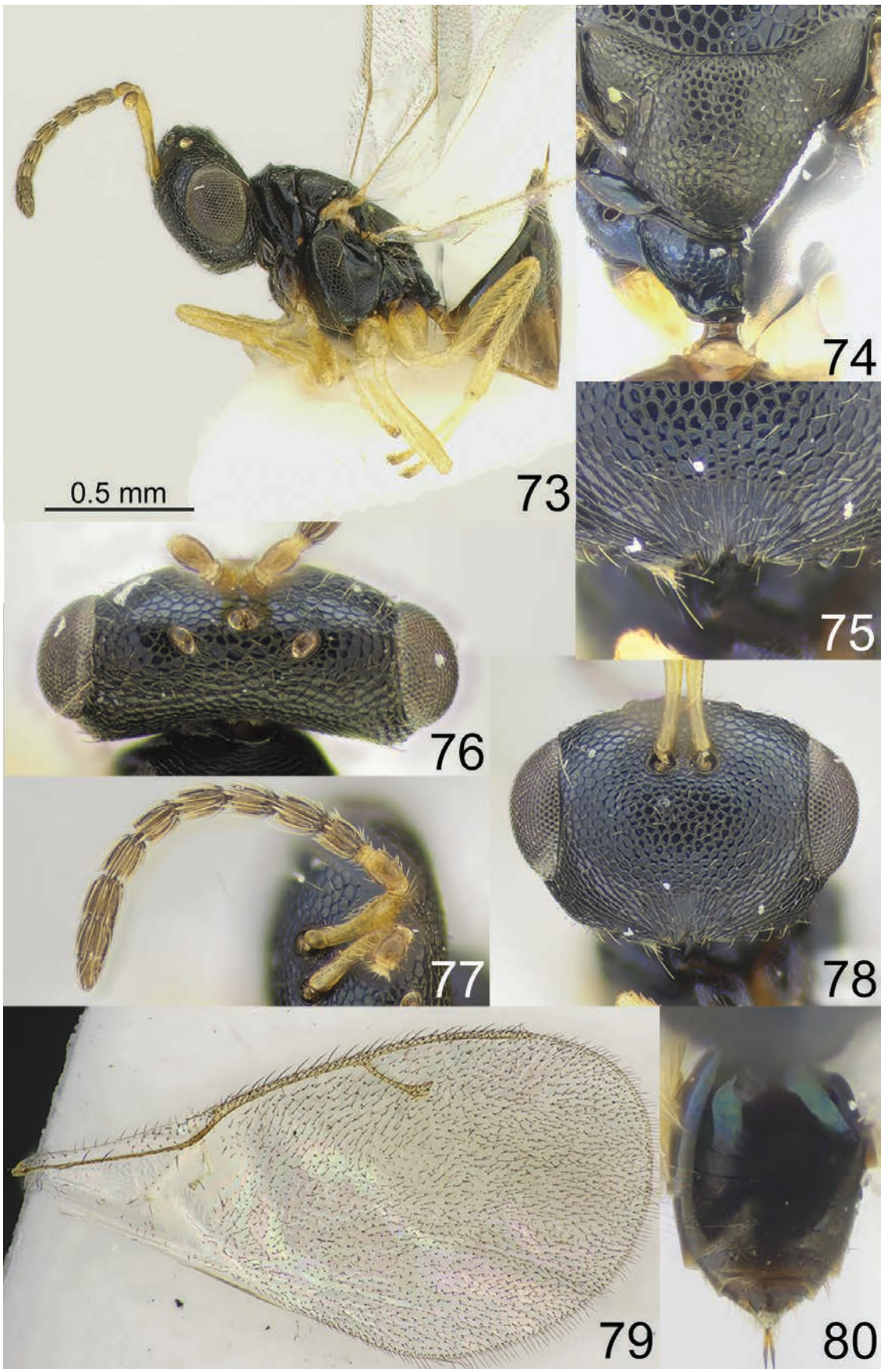

Figures 73–80. *Apsilocera totoroi* sp. nov., female, holotype **73** habitus, lateral view **74** scutellum and propodeum, dorsal view **75** clypeus **76** head, dorsal view **77** antenna **78** head, frontal view **79** fore wing **80** metasoma, dorsal view.

***Metasoma*.** Metasoma 1.45–1.82 × as long as broad and 0.85–1.28 × as long as mesosoma. Petiole strongly transverse. Ovipositor sheath projecting slightly beyond apex of metasoma.

Male. Unknown.

Etymology. The species is named in honor of the "My Neighbor Totoro" character – "Totoro" of Hayao Miyazaki.

Distribution. Germany, Japan, Sweden.

Comments. *Apsilocera totoroi* sp. nov. belongs to a group of species that have a vertex with regular sculpture. This species is very similar to *A. bramleyi* and *A. triapitzini* sp. nov.; the differences between these species are given in the key.

***Apsilocera triapitzini* Tselikh, Haas & Ku, sp. nov.**

https://zoobank.org/DB674A4F-0616-4300-A2D9-42BA3BF5547E

Figs 81–88, 98

Type material. ***Holotype*** • female, Republic of Korea: "Gyeongsangnam-do, Goseong-gun, Hail-myeon, Suyang-ri, 34°58'34.8"N, 128°12'08.3"E, 18.VI.2022, coll. E. Tselikh" (NIBR). ***Paratypes*** • 1 male, same labels as holotype (SMNE) • 1 female, "Gyeongsangnam-do, Geochang-gun, Mari-myeon, Yeongseung-ri, 35.714060N, 127.876007E, 06.VII.2023, coll. E. Tselikh" (ZISP) • 1 female, "Russia, Primirskii Reg., Lazovsky Reserve, Preobrazhenie Vill., 18–19.VIII.2010, coll. E. Tselikh" (ZISP) • 1 female (SMNS_Hym_T00798), "Sweden, Mörbylånga, Kalkstad (#114/2014), mixed deciduous forest, 27.VI–30.VII.2014, Malaise trap, 56.609569N, 16.503726E, coll. M. Jaschhof, C. Jaschhof", Sample ID: 48265 (SMNS) • 1 female (NHRS-HEVA000022838), "Sweden Öl, Mörbylånga kommun, Västerstads almlunds naturreservat., Old elm forest (3002 Trap ID, 3053 Event ID), 10.VI-9.VII.2014, Malaise trap, 56.427648N, 16.421110E, leg. Swedish Malaise Trap Project", Sample ID: SMNS_50682 (NRM).

Description. Female. Body length 1.20–1.61 mm; fore wing length 1.05–1.36 mm.

***Coloration*.** Head black; antenna with scape yellowish brown; pedicel, anelli, F1–F6, and clava brown. Mesosoma black, but propodeum dorsally dark blue with metallic diffuse luster. Fore coxae metallic blue, mid coxae yellowish brown, hind coxae basally metallic blue, apically yellowish brown; all femora and tibiae yellowish brown, all tarsi yellow. Fore wing hyaline, venation yellowish brown. Metasoma dorsally brown with metallic green diffuse coppery luster, laterally and ventrally yellowish brown; ovipositor sheaths brown.

***Sculpture*.** Head grossly reticulate; clypeus radially striate, but near clypeal margin smooth. Mesosoma grossly reticulate; propodeum alutaceous. Metasoma weakly alutaceous and shiny.

***Head*.** Head in dorsal view 2.15–2.32 × as broad as long and 1.24–1.34 × as broad as mesoscutum; in frontal view 1.37–1.52 × as broad as high. POL 1.22–1.50 × as long as OOL. Eye height 1.24–1.33 × eye length and 1.94–2.05 × as long as malar space. Distance between antennal toruli and lower margin of clypeus 1.87–2.21 × distance between antennal toruli and median ocellus. Antenna with scape 0.90–0.97 × as long as eye height and 1.12–1.28 × as long as eye length; pedicel 1.33–1.45 × as long as broad; combined length of pedicel

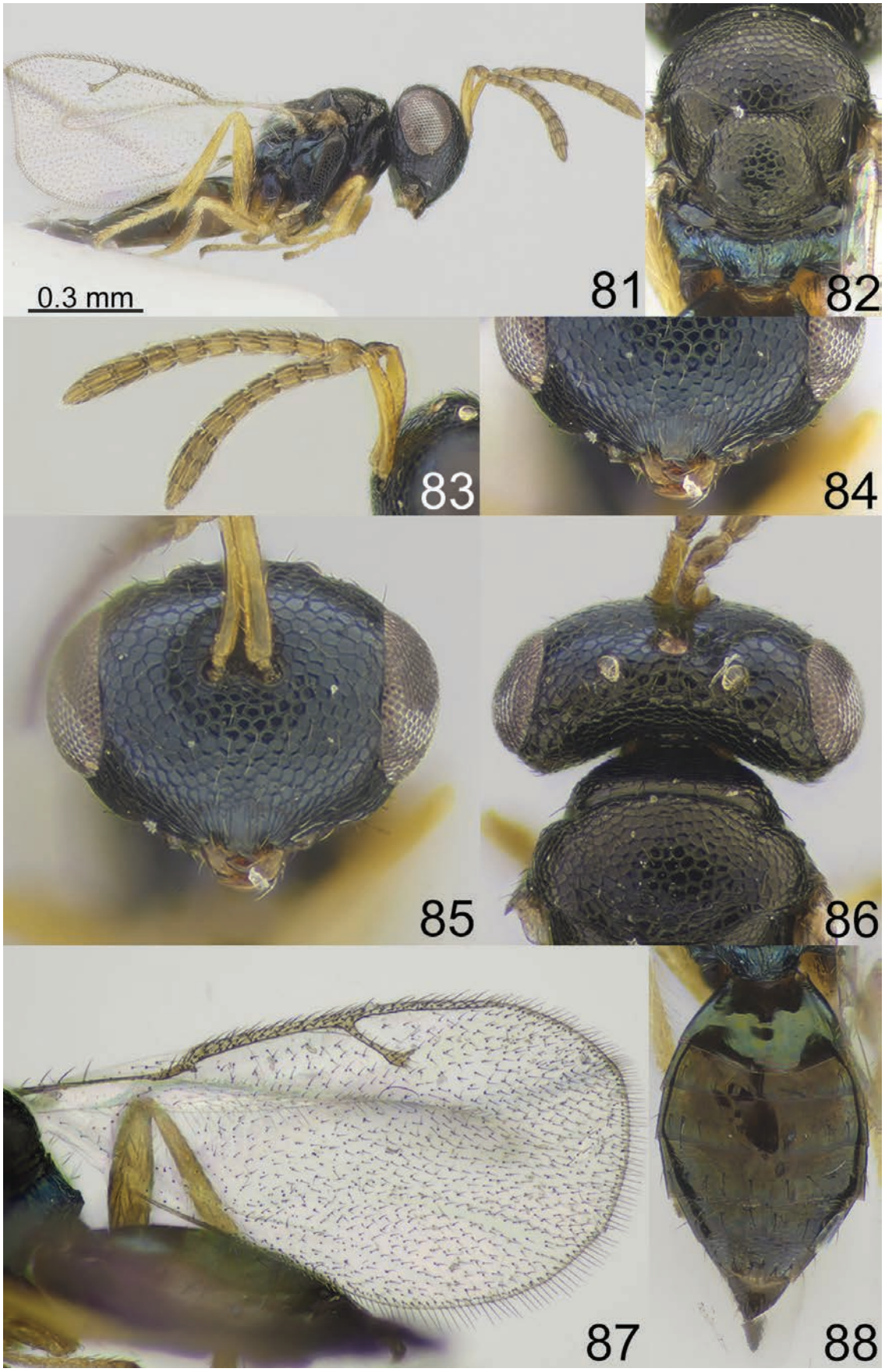

Figures 81–88. *Apsilocera triapitzini* sp. nov., female, holotype **81** habitus, lateral view **82** mesosoma, dorsal view **83** antenna **84** clypeus **85** head, frontal view **86** head and pronotum, dorsal view **87** fore wing **88** metasoma, dorsal view.

and flagellum 0.99–1.15 × breadth of head; F1–F4 longer than broad, F5, F6 subsquare, with single row of sensilla; clava 2.70–3.23 × as long as broad, with small micropilose area on each C3 and C4. Clypeal margin produced and emarginate medially. Mandible formula 3:4.

***Mesosoma*.** Mesosoma 1.30–1.42 × as long as broad. Scutellum arched, 0.77 × as long as broad, frenal area indistinct. Propodeum 0.39–0.50 × as long as scutellum. Fore wing 2.02–2.09 × as long as its maximum width; basal cell bare; basal vein pilose; speculum partly closed below; M 0.93–1.13 × as long as PM and 2.20–2.38 × as long as S, stigma small.

***Metasoma*.** Metasoma 1.53–1.77 × as long as broad and 1.22–1.35 × as long as mesosoma. Petiole strongly transverse. Ovipositor sheath projecting slightly beyond apex of metasoma.

Male. Body length 0.95 mm; fore wing length 0.90 mm. Eye height 2.46 × as long as malar space. Distance between antennal toruli and lower margin of clypeus 3.16 × distance between antennal toruli and median ocellus. Antenna with pedicel 1.60 × as long as broad; clava 5.60 × as long as broad; combined length of pedicel and flagellum 1.29 × breadth of head. Metasoma 2.30 × as long as broad and 0.97 × as long as mesosoma. Otherwise, similar to female.

Etymology. The species is named in honor of the prominent entomologist, an expert on Encyrtidae (Hymenoptera), Dr., Prof. Vladimir A. Trjapitzin.

Distribution. Russia, Republic of Korea, Sweden.

Comments. *Apsilocera triapitzini* sp. nov. belongs to a group of species that have a vertex with regular sculpture. This species is very similar to *A. bramleyi*; the differences between these species are given in the key.

Apsilocera verticillata Bouček, 1956

Figs 89–97

Apsilocera verticillata Bouček, 1956: 319. Holotype male (NMPC, examined).

Type material. ***Holotype*** • male, Slovakia: "Slov. mer.: Gbelce 29.7.55 Bouček", "Holotypus", "Mus. Nat. Pragae Inv. 3086", "*Apsilocera verticillata* ♂ Bčk. Det Z. Bouček, 1955" (RMNH).

Additional material examined. Japan • 1 female, 1 male, "Chiba Pref., Ichinomiya-Machi, 25.X.2002, coll. K. Kubo" (EIHU). Russia • 1 female, "Primorskii Reg., Spassk-Dal'niy Vill., 2–4.VII.2011, coll. S. Belokobylskij" (ZISP). Republic of Korea • 1 female, "Gyeongsangnam-do, Namhae-gun, Sangiu-myeon, Sangiu-ri, 13.VIII.2022, coll. D.S Ku, J.H. Lee, H.J. Jeong" (NIBR) • 1 female, "Gyeongsangnam-do, Geochang-gun, Namsang-myeon, Jeoncheok-ri, 35°37'15.3"N, 127°57'51.4"E, 22.VI. 2023, coll. S. Belokobylskij" (ZISP) • 5 females, "Gyeongsangbuk-do, JuWangSan-myeon, Cheongsong-gun, JuWangSan SW, 21.IV.2023, 3.V.2023, 31.V.2023, 18.VII.2023, coll. J.H. Lee (SMNE).

Description. Female. Body length 1.18–1.25 mm; fore wing length 0.98–1.05 mm.

***Coloration*.** Head black; antenna with scape, pedicel, anelli, and F1–F6 yellowish brown, clava brow. Mesosoma black, but propodeum dorsally dark blue-green with metallic diffuse luster. All coxae yellowish brown; all femora, tibiae and tarsi yellow. Fore wing hyaline, venation yellowish brown.

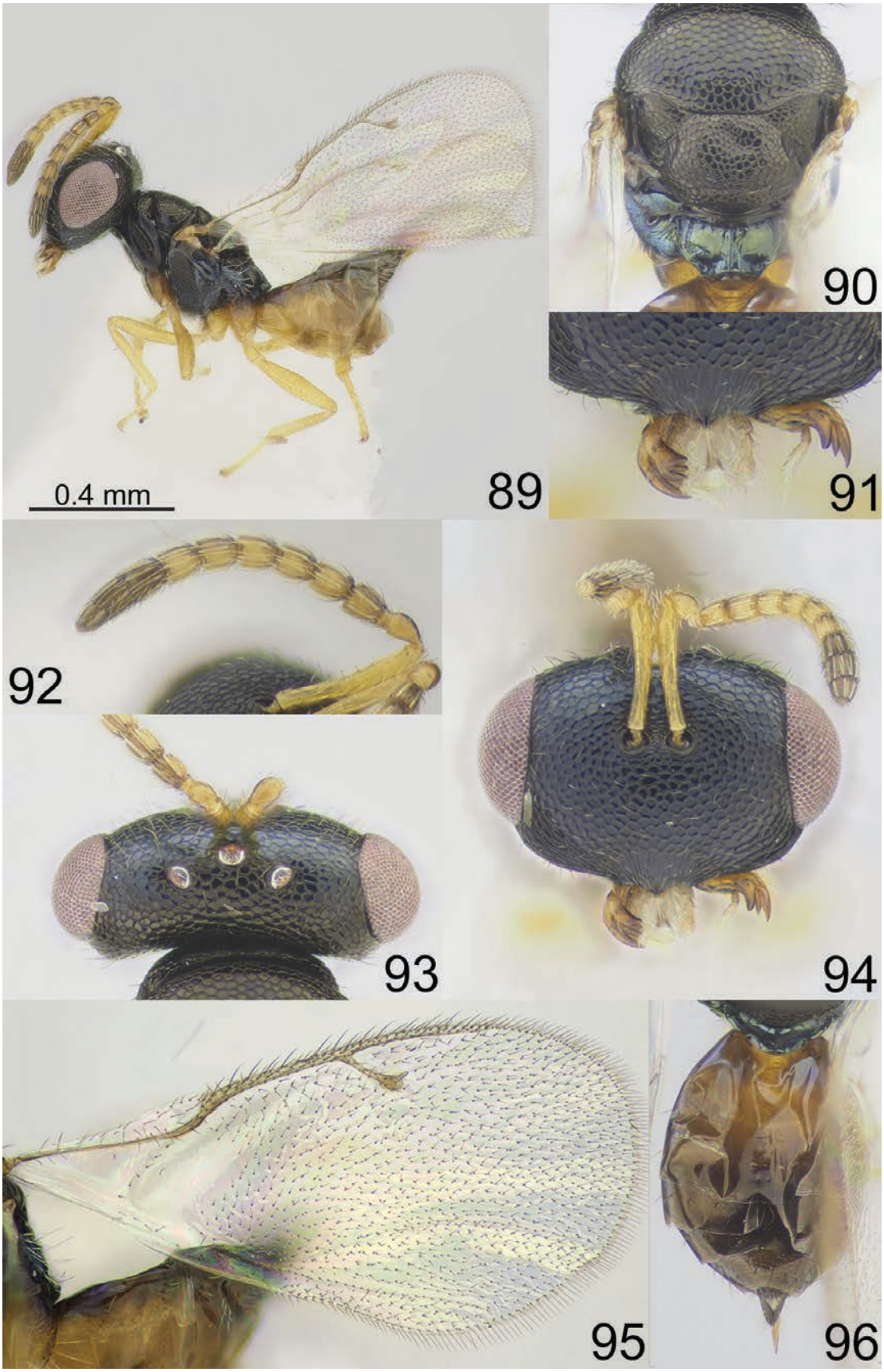

Figures 89–96. *Apsilocera verticillata* Bouček, 1956, female, not type **89** habitus, lateral view **90** mesosoma, dorsal view **91** clypeus and mandible **92** antenna **93** head and pronotum, dorsal view **94** head, frontal view **95** fore wing **96** metasoma, dorsal view.

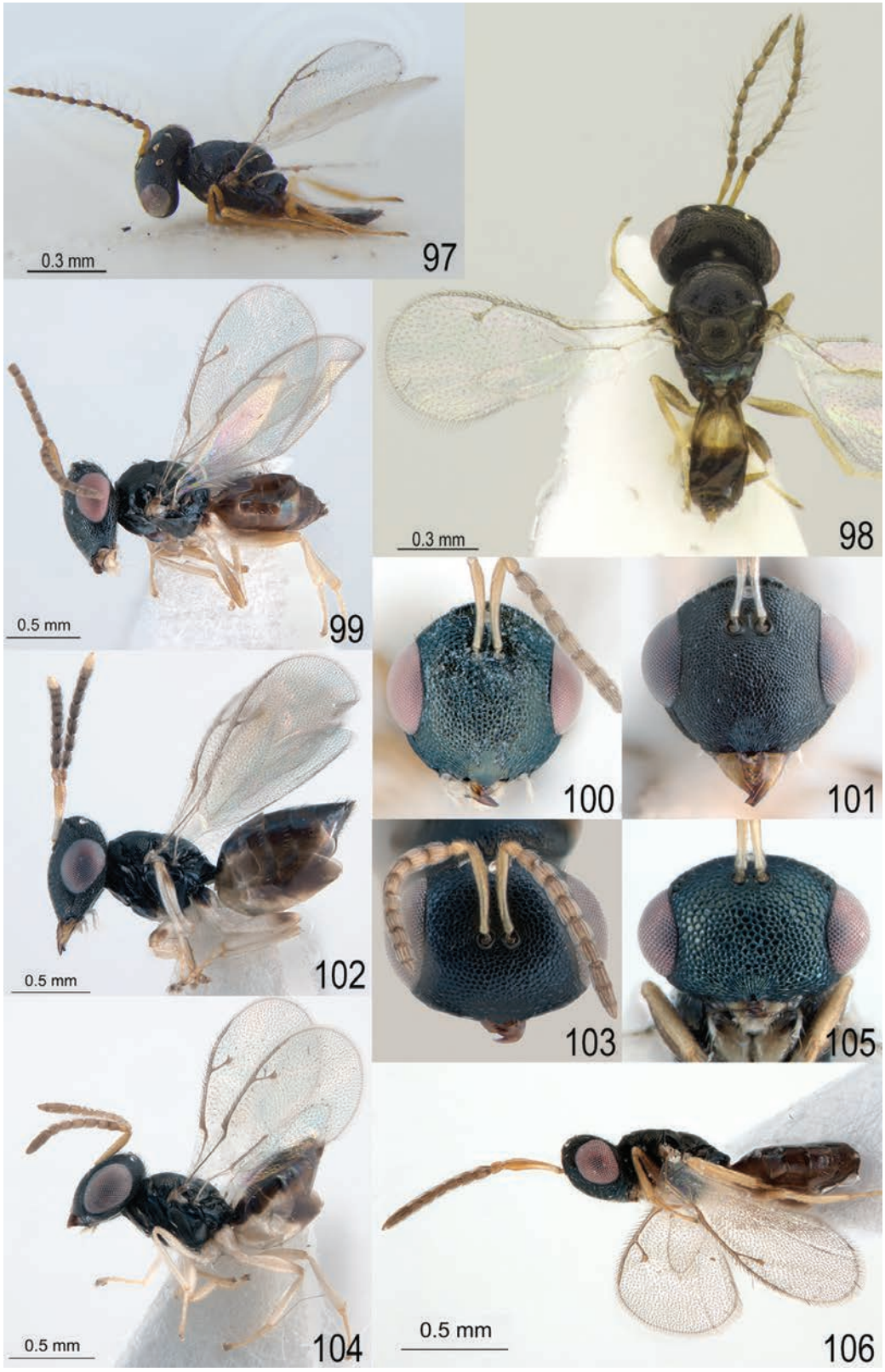

Figures 97–106. 97 *Apsilocera verticillata* Bouček, 1956, male, holotype habitus, lateral view **98** *Apsilocera triapitzini* sp. nov., male, paratype habitus, dorsal view **99, 100** *Apsilocera acuticristata* Mitroiu & Achterberg, 2013, female, holotype **99** habitus, lateral view **100** head, frontal view **101, 102** *Apsilocera bicristata* Mitroiu & Achterberg, 2013, female, holotype **101** head, frontal view **102** habitus, lateral view **103, 104** *Apsilocera maculata* Mitroiu & Achterberg, 2013, female, holotype **103** head, frontal view **104** habitus, lateral view **105, 106** *Apsilocera tuberculata* Mitroiu & Achterberg, 2013, female, holotype **105** head, frontal view **106** habitus, lateral view.

Metasoma dorsally brown, laterally and ventrally yellowish brown; ovipositor sheaths yellowish brown.

***Sculpture*.** Head reticulate; clypeus radially striate. Mesosoma reticulate; propodeum smooth and shiny. Metasoma smooth and shiny, but Mt7 weakly alutaceous and shiny.

***Head*.** Head in dorsal view 2.55–2.60 × as broad as long and 1.37–1.49 × as broad as mesoscutum; in frontal view 1.48–1.50 × as broad as high. Vertex with regular sculpture. POL 1.20–1.30 × as long as OOL. Eye height 1.34–1.36 × eye length and 2.10–2.36 × as long as malar space. Distance between antennal toruli and lower margin of clypeus 1.98–2.00 × distance between antennal toruli and median ocellus. Antenna with scape 0.90–0.95 × as long as eye height and 1.29–1.32 × as long as eye length; pedicel 1.40–1.46 × as long as broad; combined length of pedicel and flagellum 0.90–0.92 × breadth of head; F1–F6 longer than broad with a row of sensilla; clava 2.89–3.30 × as long as broad, with small micropilose area on each C3 and C4. Clypeal with one small tooth. Mandible formula 3:4.

***Mesosoma*.** Mesosoma 1.30–1.32 × as long as broad. Scutellum moderately depressed, 0.70–0.73 × as long as broad, frenal area indistinct. Propodeum 0.51–0.54 × as long as scutellum. Fore wing 2.07–2.12 × as long as its maximum width; basal cell bare; basal vein pilose; speculum partly closed below; M 1.03–1.17 × as long as PM and 2.10–2.20 × as long as S, stigma small.

***Metasoma*.** Metasoma 1.41–1.43 × as long as broad and 1.00–1.04 × as long as mesosoma. Petiole strongly transverse. Ovipositor sheath projecting slightly beyond apex of metasoma.

Male. Body length 1.25–1.30 mm; fore wing length 1.10–1.15 mm. Head in dorsal view 2.30–2.35 × as broad as long. POL 1.40–1.55 × as long as OOL. Combined length of pedicel and flagellum 1.30–1.35 × breadth of head. Metasoma 1.65–1.73 × as long as broad. Otherwise, similar to female.

Distribution. Czech Republic, Japan, Moldova, Netherlands, Republic of Korea, Russia, Slovakia, Sweden.

Comments. *Apsilocera verticillata* Bouček belongs to a group of species that have a vertex with regular sculpture. This species is very similar to *A. maculata* Mitroiu & Achterberg; the differences between these species are given in the key.

Additional information

Conflict of interest

The authors have declared that no competing interests exist.

Ethical statement

No ethical statement was reported.

Funding

This work was supported by a grant from the National Institute of Biological Resources (NIBR), funded by the Ministry of Environment (MOE) of the Republic of Korea (NIBR202304203, NIBR202402202). And it was partially funded by Russian State Research (project No. 122031100272-3).

Author contributions

All authors have contributed equally.

Author ORCIDs

Ekaterina V. Tselikh https://orcid.org/0000-0002-9184-043X
Jaehyeon Lee https://orcid.org/0000-0002-3666-6029
Michael Haas https://orcid.org/0000-0001-6869-6698
Mircea-Dan Mitroiu https://orcid.org/0000-0003-1368-7721
Deok-Seo Ku https://orcid.org/0000-0002-6274-6479

Data availability

All of the data that support the findings of this study are available in the main text.

References

Bouček Z (1956) Chalcidologické poznamky III, Torymidae, Pteromalidae, Perilampidae a Eucharitidae. Acta Entomologica Musei Nationalis Pragae 30(462): 305–330.

Bouček Z (1988) Australasian Chalcidoidea (Hymenoptera). A biosystematic revision of genera of fourteen families, with a reclassification of species. CAB International, Wallingford, Oxon/Cambrian News Ltd., Aberystwyth, Wales, 832 pp.

Bouček Z (1993) New taxa of North American Pteromalidae and Tetracampidae (Hymenoptera), with notes. Journal of Natural History 27: 1239–1313. https://doi.org/10.1080/00222939300770741

Bouček Z, Rasplus J-Y (1991) Illustrated key to West-Palaearctic genera of Pteromalidae (Hymenoptera: Chalcidoidea). Institut National de la Recherche Agronomique, Paris, 140 pp.

Burks R, Mitroiu M-D, Fusu L, Heraty JM, Janšta P, Heydon S, Dale-Skey Papilloud N, Peters RS, Tselikh EV, Woolley JB, Noort S, Baur H, Cruaud A, Darling Ch, Haas M, Hanson P, Krogmann L, Rasplus J-Y (2022) From hell's heart I stab at thee! A determined approach towards a monophyletic Pteromalidae and reclassification of Chalcidoidea (Hymenoptera). Journal of Hymenoptera Research 94: 13–88. https://doi.org/10.3897/jhr.94.94263

UCD Community (2023) Universal Chalcidoidea Database (UCD) curated in TaxonWorks. 1143 https://sfg.taxonworks.org/api/v1/ [accessed on 11 April 2023]

Ghahari H, Huang J (2012) A study of the Pteromalidae (Hymenoptera: Chalcidoidea) from Western and Northwestern Iran. Archives of Biological Sciences 64(1): 353–357. https://doi.org/10.2298/ABS1201353G

Gibson G (1997) Morphology and Terminology. In: Gibson GAP, Huber JT, Woolley JB (Eds) Annotated Keys to the Genera of Nearctic Chalcidoidea (Hymenoptera). NRC Research Press, Ottawa, 16–44.

Graham MWR de V (1966) A new species of *Apsilocera* (Hym., Pteromalidae) from England, parasitizing a fungus gall-midge. Entomologist 99(1239): 301–304.

Graham MWR de V (1969) The Pteromalidae of North-Western Europe (Hymenoptera: Chalcidoidea). Bulletin of the British museum (Natural history) Entomology, Supplement 16: 1–908. https://doi.org/10.5962/p.258046

Mitroiu M-D, Achterberg C (2013) Revision of the Oriental species of *Apsilocera* Bouček (Hymenoptera, Pteromalidae), with description of twelve new species. Zootaxa 3717(4):448–468. https://doi.org/10.11646/zootaxa.3717.4.2

Xiao H, Huang DW (2001) Three new species of Pteromalidae (Hymenoptera) from Fujian Province, China. Entomologia Sinica 8(1): 8–12.

ZooKeys 1215: 289–309 (2024)
DOI: 10.3897/zookeys.1215.125043

Research Article

Discovery of a new species of the subgenus *Japonigekko* (Squamata, Gekkonidae, *Gekko*) from the Hengduan Mountains, southwestern China: the best *Japonigekko* mountaineer

Shun Ma[1,2], Sheng-Chao Shi[1,3], Cheng Shen[1], Li-Ming Chang[1], Jian-Ping Jiang[1,2,4]

1 *Chengdu Institute of Biology, Chinese Academy of Sciences, Chengdu 610041, China*
2 *University of Chinese Academy of Science, Beijing 100049, China*
3 *Hubei Engineering Research Center for Protection and Utilization of Special Biological Resources in the Hanjiang River Basin, School of Life Science, Jianghan University, Wuhan 430056, China*
4 *Mangkang Biodiversity and Ecological Station, Xizang Ecological Safety Monitor Network, Changdu 854500, Xizang, China*

Corresponding author: Jian-Ping Jiang (jiangjp@cib.ac.cn)

Abstract

A new *Gekko* (subgenus *Japonigekko*) species, *Gekko alpinus* **sp. nov.**, is described from the Jinsha River Basin in southwestern China, between the border of Mangkang County, Xizang Autonomous Region and Batang County, Sichuan Province, according to the integrative taxonomic results combining molecular data and morphological characters obtained from the type series comprising 11 specimens. Our molecular phylogeny inferred from the mitochondrial *16S* and *ND2* gene fragments indicated that this new species is most closely related to *Gekko jinjiangensis*, but a considerable amount of genetic divergence exists between them (*p*-distance: 3.6%-4.1% (*16S*) and 7.1%–9.1% (*ND2*)). The new species can be distinguished from its congeners via a combination of series morphological characters. The discovery of this new species marks the highest altitudinal range (2400 to 2542 m a.s.l.) recorded for the subgenus *Japonigekko* and also represents a new provincial record for the genus in Xizang Autonomous Region.

Key words: *Gekko alpinus* sp. nov., *Gekko jinjiangensis*, Gekkonidae, molecular phylogeny, morphological characters, new provincial genus record

OPEN ACCESS

Academic editor: Thomas Ziegler
Received: 9 April 2024
Accepted: 28 August 2024
Published: 17 October 2024

ZooBank: https://zoobank.org/5EAB81EF-326D-4884-B046-5ECEE3DAEC26

Citation: Ma S, Shi S-C, Shen C, Chang L-M, Jiang J-P (2024) Discovery of a new species of the subgenus *Japonigekko* (Squamata, Gekkonidae, *Gekko*) from the Hengduan Mountains, southwestern China: the best *Japonigekko* mountaineer. ZooKeys 1215: 289–309. https://doi.org/10.3897/zookeys.1215.125043

Introduction

The gekkonid genus *Gekko* Laurenti, 1768 is widely distributed across eastern and southeastern Asia, Northwest Oceania, and Melanesia. Currently, this genus contains 88 known gecko species and has been divided into seven subgenera: *Archipelagekko*, *Balawangekko*, *Gekko*, *Japonigekko*, *Lomatodactylus*, *Ptychozoon*, and *Rhacogekko* (Wood et al. 2020; Wang et al. 2024; Uetz et al. 2024). Amongst these, *Japonigekko* comprises 33 species, accounting for one-third of the species within the genus. Members of this subgenus are distributed across East Asia, with the majority found in China (20/33), of which the members present the following characters: size moderate; nare usually touching rostral; nasals two or three; dorsal tubercles 0–21 rows; precloacal pores

0–32; postcloacal tubercles 1–4; lateral folds without tubercles (Wood et al. 2020; Hou et al. 2021; Wang et al. 2024; Uetz et al. 2024).

During our field work in the Jinsha River Basin, along the border between Mangkang County of Xizang Autonomous Region and Batang County of Sichuan Province, China, a series of *Gekko* (*Japonigekko*) specimens was collected (Fig. 1). This discovery marks the first recorded occurrence of genus *Gekko* in Xizang Autonomous Region (Che et al. 2020). Phylogenetic analysis revealed a significant genetic differentiation between these specimens and their closest relative, *G. jinjiangensis* Hou, Shi, Wang, Jiang & Xie, 2021. Upon closer examination, we found that these specimens are morphologically distinct from *G. jinjiangensis* by having a relatively narrower head, more supralabials and infralabials, more interorbitals and dorsal tubercle rows at the midbody in females, fewer scales in a line from the mental to the front of the cloacal slit, and fewer scale rows at the mid-body. Hence, we describe these specimens as a new species.

Materials and methods

Specimen preparation

A total of 11 specimens, two specimens (one adult male and one adult female) from Zhubalong Village, Mangkang County, Xizang Autonomous Region collected in July, 2022, and nine specimens (three adult males, four adult females and two subadult females) from Zhubalong Village, Batang County, Sichuan Province in June, 2020 (Fig. 1), were preserved in 75% ethanol and deposited in Chengdu Institute of Biology, Chinese Academy of Sciences (**CIB, CAS**), with their liver tissue samples separately preserved in 95% ethanol for molecular analyses.

Molecular data and phylogenetic analysis

Total genomic DNA was extracted by Vazyme FastPure Blood/Cell/Tissue/Bacteria DNA Isolation Mini Kit (Vazyme Biotech Co., Ltd, Nanjing, China) from the liver tissue samples of each specimen. Two mitochondrial gene fragments of partial 16S ribosomal RNA gene (*16S*) and partial NADH dehydrogenase subunit 2 gene (*ND2*) were respectively amplified by primers L3975 (5'-CGCCTGTTTACCAAAAACAT-3') and H4551 (5'-CCGGTCTGAACTCAGATCACGT-3') for *16S* (Simon et al. 1994), and rMet-3L (5'-ATACCCCGACAATGTTGG-3') and rAla-1H (5'-GCCTTAGCTTAATTAAAGTG-3') for *ND2* (Jonniaux and Kumazawa 2008). The polymerase chain reaction (PCR) was performed in 25 μl reactant with the following cycling conditions: first an initial denaturing step at 95 °C for 5 min; then 35 cycles of denaturing at 95 °C for 40 s, annealing at 53 °C for 40 s and extending at 72 °C for 60 s; last a final extending step at 72 °C for 10 min. PCR products were sequenced by Beijing Qingke New Industry Biotechnology Co., Ltd.

For our phylogenetic analysis, DNA sequences of 49 specimens were used (Table 1), amongst which *ND2* (of specimens No. 1–11, 49) and *16S* (of specimens No. 1–11, 13–17, 44, 49) were sequenced in this study and others were obtained from GenBank. *Gehyra mutilata* (Wiegmann, 1834) (No. 49) was

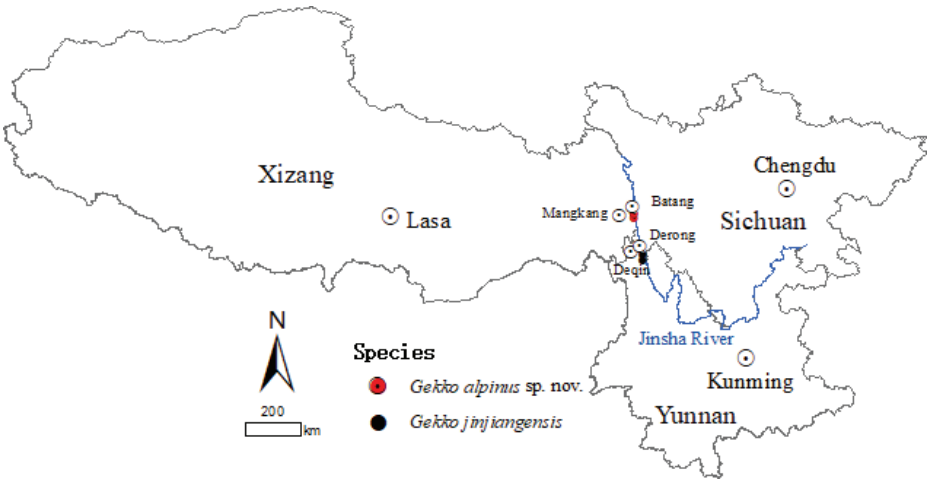

Figure 1. Distribution of *Gekko alpinus* sp. nov. and its sister taxon *G. jinjiangensis*.

used as the outgroup (Pyron et al. 2013). All *16S* (569 bp) and *ND2* (1011 bp) sequences were input in MEGA11 (Tamura et al. 2021) respectively and aligned by MUSCLE (Edgar 2004). Then we calculated the uncorrected pairwise distances (*p*-distance) for each data matrix in MEGA11. Then the concatenation sequences (1580 bp) were prepared for the phylogenetic analysis. The Maximum Likelihood (ML) analysis was performed in IQ-TREE 1.6.12 (Nguyen et al. 2015) based on the best-fit model TIM2+F+I+G4 for the 1st and 3rd codons of *ND2* and all three codons of *16S* and HKY+F+I+G4 for the 2nd codon of *ND2* were computed by ModelFinder for IQ-Tree in PhyloSuite 1.2.3 according to Bayesian Information Criterion (BIC) (Kalyaanamoorthy et al. 2017; Zhang et al. 2020). Ultrafast Bootstrap Approximation (UFB) nodal support was assessed via using ten thousand ultrafast bootstrap replicates and when the value (UFB, %) is ≥ 95, it would be considered as significantly supported (Hoang et al. 2018). The single branch tests were conducted by SH-like approximate likelihood ratio test (SH-aLRT) by 1000 replicates and when the nodal support (SH, %) is ≥ 80, it would also be considered well supported (Stephane et al. 2010). The Bayesian Inference (BI) analysis was conducted via MrBayes 3.2.1 (Ronquist et al. 2012) under the best-fit model GTR+F+I+G4 for the 1st and 3rd codons of *ND2* and all three codons of *16S* and HKY+F+I+G4 for the 2nd codon of *ND2*, which was calculated according to BIC as well by ModelFinder for MrBayes in PhyloSuite 1.2.3. The BI analysis program worked through two independent runs with a four-chain run calculated for 20 million generations using the Markov Chain Monte Carlo (MCMC), sampling every 1000 with the first 25% of samples discarded as burn-in and resulting in a potential scale reduction factor (PSRF) of < 0.005. The nodal support Bayesian posterior probabilities (BI, %) ≥ 95 were considered significantly supported.

Morphological comparisons and statistical analysis

Morphological data were obtained from the 11 *Gekko alpinus* sp. nov. (four males, four adult females, and three subadult females). The terminology and methods of mensural characters and meristic features followed Zhao et al. (1999) and Rösler et al. (2011). Bilateral morphological characters measurements and scale counts were given as left/right.

Table 1. Information and references for *16S* and *ND2* used in this study.

No.	Species	Localities	Voucher ID.	*16S* GenBank Accession No.	*ND2* GenBank Accession No.	Reference
1	*Gekko* alpinus sp. nov.	Mangkang, Xizang, China	CIB 121656	PQ255976	PQ303494	This study
2			CIB 121657	PQ255977	PQ303495	
3		Batang, Sichuan, China	CIB 121658	PQ255978	PQ303496	
4			CIB 121659	PQ255979	PQ303497	
5			CIB 121660	PQ255980	PQ303498	
6			CIB 121661	PQ255981	PQ303499	
7			CIB 121662	PQ255982	PQ303500	
8			CIB 121663	PQ255983	PQ303501	
9			CIB 121664	PQ255984	PQ303502	
10			CIB 121665	PQ255985	PQ303503	
11			CIB 121666	PQ255986	PQ303504	
12	*G. jinjiangensis*	Deqin, Yunan, China	CIB 5334220115	–	MT449431	Hou et al. 2021, this study
13			CIB 5334220088	PQ255987	MT449432	
14			CIB 5334220089	PQ255988	MT449433	
15			CIB 5334220090	PQ255989	MT449434	
16			CIB 5334220100	PQ255990	MT449435	
17			CIB 5334220114	PQ255991	MT449436	
18		Derong, Sichuan, China	CIB 5133380017	–	MT449437	
19			CIB 5133380019	–	MT449438	
20			CIB 5133380021	–	MT449439	
21			CIB 5133380024	–	MT449440	
22			CIB 5133380025	–	MT449441	
23			CIB 5133380026	–	MT449442	
24			CIB 5133380047	–	MT449443	
25	*G. adleri*	Jingxi, Guangxi, China	SYS r001400	MW451654	OR902178	Lyu et al. 2021; Wang et al. 2024
26	*G. auriverrucosus*	Yuncheng, Shanxi, China	NNU Z20050801.004	–	JN019062	Rösler et al. 2011
27	*G. bonkowskii*	Khammouane, Laos	VFU R.2014.10	–	KT266818	Luu et al. 2015
28	*G. chinensis*	Hong Kong, China	SYS r001211	MW451644	OR902183	Lyu et al. 2021; Wang et al. 2024
29	*G. cib*	Chengdu, Sichuan, China	AMB 6567	–	JN019063	Rösler et al. 2011
30	*G. cib*	Hejiang, Sichuan, China	SYS r001489	MW451655	OR902165	Lyu et al. 2021; Wang et al. 2024
31	*G. hokouensis*	Jinzhai, Anhui, China	NNU Z20050902.001	–	JN019060	Rösler et al. 2011
32	*G. hokouensis*	Wuyishan, Fujian, China	SYS r001290	MW451647	OR902173	Lyu et al. 2021; Wang et al. 2024
33	*G. japonicus*	Zhoushan, Zhejiang, China	NNU Z20050801.004	–	JN019059	Rösler et al. 2011
34	*G. japonicus*	Wuyishan, Fujian, China	SYS r000672	MW451628	OR902176	Lyu et al. 2021; Wang et al. 2024
35	*G. khunkhamensis*	Khammouane, Laos	VNUF R.2021.23	–	OL416111	Sitthivong et al. 2021
36	*G. kwangsiensis*	Wuming, Guangxi, China	SYSr 001195	MW451642	OR902175	Lyu et al. 2021; Wang et al. 2024
37	*G. melli*	Dongguan, Guangdong, China	SYS r001742	MW451661	OR902169	Lyu et al. 2021; Wang et al. 2024
38	*G. nadenensis*	Khammouane, Laos	ZFMK 98741	–	KY421618	Luu et al. 2017
39	*G. palmatus*	Zhaoqing, Guangdong, China	SYS r002797	OR903156	OR902179	Wang et al. 2024
40	*G. paucituberculatus*	Baise, Guangxi, China	SYS r002806	OR903154	OR902163	Wang et al. 2024
41	*G. scientiadventura*	Quang Binh, Vietnam	IEBR A.2014.7	–	KP205392	Luu et al. 2014
42	*G. sengchanthavongi*	Khammouane, Laos	VFU R2014.14	–	KT266816	Luu et al. 2015
43	*G. similignum*	Wuzhishan, Hainan, China	SYS r001597	MW451658	OR902185	Lyu et al. 2021; Wang et al. 2024
44	*G. scabridus*	Yanbian, Sichuan, China	CIB YN201909199	PQ255992	MT449429	Hou et al. 2021; this study
45	*G. subpalmatus*	Fenghua, Zhejiang, China	SYS r001762	MW451662	OR902167	Lyu et al. 2021; Wang et al. 2024
46	*G. swinhonis*	Zunhua, Hebei, China	SYS r001814	MW451666	OR902171	Lyu et al. 2021; Wang et al. 2024
47	*G. thakhekensis*	Thakhek, Khammouane, Laos	IEBR A.2014.6	–	KP205396	Luu et al. 2014
48	*G. truongi*	Khanh Hoa, Vietnam	IEBR A.2011.1	–	KP205398	Luu et al. 2014
49	*Gehyra mutilata*	Xishuangbanna, Yunnan, China	CIB R201711	PQ255993	PQ303505	this study

The mensural characters were measured to the nearest 0.01 mm using a Deli Caliper (DL92150): (1) snout-vent length (**SVL:** from tip of snout to anterior margin of cloaca); (2) tail length (**TaL:** from posterior margin of cloaca to tip of tail); (3) axilla-groin distance (**AGD:** distance between axilla and groin); (4) head length (**HL:** maximum head length from tip of snout to posterior margin of auricular opening); (5) head width (**HW:** maximum head width measured at the angle of the jaws); (6) head height (**HH:** maximum head height from the top of the head posterior to the eyes to the bottom of the lower jaw); (7) snout length (**SL:** from snout tip to anterior corner of eye); (8) eye-ear distance (**EED:** distance between posterior margin of eye to posterior margin of ear opening) (9) maximum eye diameter (**ED**); (10) maximum ear opening diameter (**EOD**); (11) maximum rostral width (**RW**); (12) maximum rostral height (**RH**); (13) maximum mental width (**MW**); (14) maximum mental length (**ML**); (15) forelimb length (**FlL**: length from the base of the palm to the elbow); (16) hindlimb length (**HlL**: distance from the base of heel to the knee).

All mensural characters except for TaL, FIL, and HIL, which were lacking for *G. jinjiangensis*, were statistically analyzed using R v. 4.3.2, and sexes were separated for subsequent comparisons among the samples due to sexual dimorphism within geckos. For analyses, all measurements were ln-transformed to normalize and reduce the variance, and then scaled to remove allometric effects of body size using the following equation: $X_a = X_{ln} - \beta \cdot (SVL_{ln} - SVL_m)$, where X_a = adjusted value; X_{ln} = ln-transformed measurements; β = unstandardized regression coefficient for each species; SVL_{ln} = ln-transformed SVL; and SVL_m = overall average SVL_{ln} of all samples. This project was performed under *GroupStruct* R package (Thorpe 1975, 1976, 1983; Reist 1985; Lleonart et al. 2000; Chan and Grismer 2021). Principal component analysis (PCA) was performed to cluster the morphometrics except SVL, TaL, FIL, HIL related to each species using *prcomp* R function and *factoextra* R package.

The meristic features were taken as the followings: (1) supralabials (**SPL:** number of scales from commissure of jaw to the rostral scale); (2) infralabials (**IFL:** number of scales from commissure of jaw to the mental scale); (3) interorbitals (**IO:** number of scales in a line between anterior corners of eyes); (4) postmentals (**PM:** scales bordering the mental); (5) dorsal tubercles row at midbody (**DTR**); (6) scales in a line from mental to the front of cloacal slit (**SMC**); (7) scale rows at midbody (**SR**); (8) ventral scales at midbody from one ventrolateral fold to the other (**V**); (9) subdigital lamellae under entire first finger (**LF1**); (10) subdigital lamellae under entire fourth finger (**LF4**); (11) subdigital lamellae under entire first toe (**LT1**); (12) subdigital lamellae under entire fourth toe (**LT4**); (13) precloacal pores (**PP**); (14) postcloacal tubercles (**PAT**).

One-way analysis of variance (ANOVA) test was used to evaluate significant differences in the mensural and meristic characteristics between the newly collected specimens and *G. jinjiangensis*, with significant different variances (p-values < 0.05 in the Levene's test) using the *aov* R function.

Morphological information of *G. jinjiangensis* were obtained from Hou et al. (2021), and for other species, morphological data were taken from the literature (Stejneger 1907; Zhou et al. 1982; Song 1985; Zhao et al. 1999; Goris and Maeda 2004; Rösler et al. 2005, 2011; Toda et al. 2008; Zhou and Wang 2008; Phung and Ziegler 2011; Nguyen et al. 2013; Luu et al. 2014; Ngo et al. 2015; Yang 2015; Luu et al. 2015, 2017; Hou et al. 2021; Lyu et al. 2021; Sitthivong et al. 2021; Zhang et al. 2023; Wang et al. 2024).

Results

Phylogenetic analysis

The new *Gekko* (*Japonigekko*) *alpinus* sp. nov. specimens formed a well-supported sister lineage (SH 100/UFB 100/BI 100) to *G. jinjiangensis* (SH 98/UFB 100/BI 100) with considerable evolutionary differentiation (Fig. 2). The uncorrected pairwise divergences amongst some species of the subgenus *Japonigekko* studied in this work inferred from the mitochondrial *16S*/*ND2* gene fragments range from 2.2% (*G. chinensis* (Gray, 1842) vs *G. similignum* Smith, 1923) / 5.4% (*G. chinensis* vs *G. similignum*) to 18.4% (*G. chinensis* vs *G. swinhonis* Günther, 1864, and *G. similignum* vs *G. swinhonis*) / 26.5% (*G. melli* (Vogt, 1922) vs *G. similignum*), while the genetic distances amongst *Gekko alpinus* sp. nov. with its congeners range from 3.6% (vs *G. jinjiangensis*) to 14.0% (vs *G. swinhonis*) for *16S* and 7.1% (vs *G. jinjiangensis*) to 24.1% (vs *G. similignum*) for *ND2* (Tables 2, 3), indicating that *Gekko alpinus* sp. nov. have distinct interspecific genetic differentiation from its congeners. Based on the molecular results, these *Gekko alpinus* sp. nov. are supported as representing a new taxon.

Morphological analysis

Morphological characters of 11 *Gekko* (*Japonigekko*) *alpinus* sp. nov. specimens are presented in Table 4, which can be easily distinguished from all other known congeners (Table 5). By tubercles existing on dorsal body,

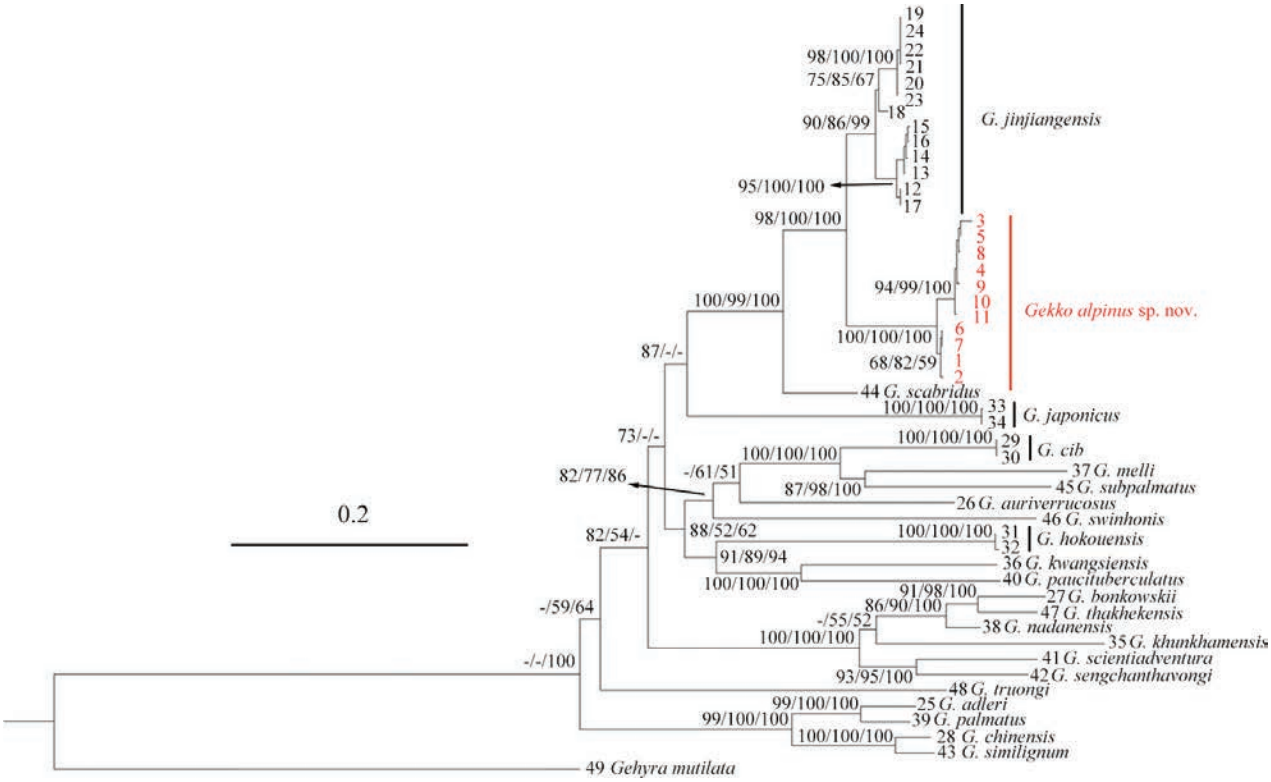

Figure 2. Maximum Likelihood tree topology of *Japonigekko* inferred from the concatenated *16S* and *ND2* gene fragments (1580 bp). The support values of each node present on the tree: SH / UFB / BI (the ones lower than 50 are displayed as "-"). The ID numbers of *Gekko alpinus* sp. nov. are noted in red.

Table 2. Uncorrected *p*-distance (%) of some species in the subgenus *Japonigekko* based on the partial mitochondrial *16S* gene sequences. Numbers refer to specimens listed in Table 1.

Species	1–11	13–17	25	28	30	32	34	36	37	39	40	43	44	45
1–11 *Gekko* alpinus sp. nov.	0–0.5													
13–17 *G. jinjiangensis*	3.6–4.1	0–0.6												
25 *G. adleri*	12.6–13.5	12.9–13.3												
28 *G. chinensis*	11.7–12.4	11.4–11.9	7.2											
30 *G. cib*	8.9–9.4	9.2–9.8	13.5	11.9										
32 *G. hokouensis*	11.3–12.2	9.8–10.5	13.6	12.9	13.3									
34 *G. japonicus*	9.8–11.0	9.8–10.5	15.3	14.3	13.7	11.1								
36 *G. kwangsiensis*	11.7–12.8	10.8–11.5	15.6	15.0	11.9	11.9	14.5							
37 *G. melli*	8.9–9.4	9.8–10.4	14.2	13.8	6.0	12.1	13.0	15.0						
39 *G. palmatus*	11.9–12.9	12.5–12.8	3.5	5.0	12.7	14.2	12.8	12.9	10.9					
40 *G. paucituberculatus*	9.8–10.6	9.8–10.5	13.2	12.1	12.0	11.1	13.0	9.8	11.9	14.4				
43 *G. similignum*	11.9–12.7	11.6–12.1	7.4	2.2	12.9	13.6	14.5	16.2	14.2	5.2	13.2			
44 *G. scabridus*	4.7–5.5	4.7–5.4	12.8	12.1	9.7	10.2	10.4	12.4	10.3	11.7	9.7	12.8		
45 *G. subpalmatus*	9.5–9.9	10.9–11.3	16.3	15.9	7.1	13.2	14.1	15.1	10.1	12.8	13.7	16.7	11.3	
46 *G. swinhonis*	13.2–14.0	14.0–14.6	17.2	18.4	11.7	13.4	15.3	17.4	15.3	14.6	14.9	18.4	14.6	15.7

forelimbs, hindlimbs, and tails, *Gekko alpinus* sp. nov. can be distinguished from the following 26 species: *G. aaronbaueri* Tri, Thai, Phimvohan, David & Teynié, 2015; *G. adleri* Nguyen, Wang, Yang, Lehmann, Le, Ziegler & Bonkowski, 2013; *G. bonkowskii* Luu, Calame, Nguyen, Le & Ziegler, 2015; *G. canhi* Rösler, Nguyen, Van, Doan, Ho, Nguyen & Ziegler, 2010; *G. chinensis*; *G. cib* Lyu, Lin, Ren, Jiang, Zhang, Qi & Wang, 2021; *G. guishanicus* Lin & Yao, 2016; *G. hokouensis* Pope, 1928; *G. khunkhamensis* Sitthivong, Lo, Nguyen, Ngo, Khotpathoom, Le, Ziegler & Luu, 2021; *G. kwangsiensis* Yang, 2015; *G. liboensis* Zhou, Liu & Li, 1982; *G. melli*; *G. nadenensis* Luu, Nguyen, Le, Bonkowski & Ziegler, 2017; *G. palmatus* Boulenger, 1907; *G. paucituberculatus* Wang, Qi, Zhou & Wang, 2024; *G. scientiadventura* Rösler, Ziegler, Vu, Herrmann & Böhme, 2004; *G. sengchanthavongi* Luu, Calame, Nguyen, Le & Ziegler, 2015; *G. shibatai* Toda, Sengoku, Hikida & Ota, 2008; *G. similignum*; *G. subpalmatus* (Günther, 1864); *G. tawaensis* Okada, 1956; *G. thakhekensis* Luu, Calame, Nguyen, Le, Bonkowski & Ziegler, 2014; *G. truongi* Phung & Ziegler, 2011; *G. vertebralis* Toda, Sengoku, Hikida & Ota, 2008; *G. wenxianensis* Zhou & Wang, 2008; *G. yakuensis* Matsui & Okada, 1968. By having 4–7 precloacal pores in the male, *Gekko alpinus* sp. nov. differs from *G. kaiyai* Zhang, Wu & Zhang, 2023 (9–12) and *G. scabridus* Liu & Zhou, 1982 (10–15). By having 13–15 subdigital lamellae on fourth toes, *Gekko alpinus* sp. nov. is different from *G. swinhonis* Günther, 1864 (6–9) and *G. taibaiensis* Song, 1985 (7–8). *Gekko alpinus* sp. nov. can be differed from *G. japonicus* (Schlegel, 1836) by having fewer interorbitals (IO 22–28 vs 32–35), fewer scale rows at midbody (SR 92–114 vs 130–144) and fewer ventral scales at midbody (32–39 vs 39–44).

Table 3. Uncorrected *p*-distance (%) of some species in the subgenus *Japonigekko* based on the partial mitochondrial *ND2* gene sequences. Numbers refer to specimens listed in Table 1.

Species	1–11	12–24	25	26	27	28	29–30	31–32	33–34	35	36	37	38	39	40	41	42	43	44	45	46	47	48
1–11 *Gekko* alpinus sp. nov.	0–2.9																						
12–24 *G. jinjiangensis*	7.1–9.1	0–3.5																					
25 *G. adleri*	22.8–23.8	20.3–21.6																					
26 *G. auriverrucosus*	21.2–22.9	20.1–20.8	24.9																				
27 *G. bonkowskii*	18.8–19.4	18.0–19.1	24.6	21.7																			
28 *G. chinensis*	21.8–23.3	20.7–22.2	14.5	24.4	21.2																		
29–30 *G. cib*	22.6–23.7	20.3–20.9	26.3	20.7	19.3	24.2	0																
31–32 *G. hokouensis*	20.7–22.3	18.7–21.1	25.4–25.5	21.5–21.7	20.3	25.0	23.7–23.8	0.3															
33–34 *G. japonicus*	19.8–21.2	17.0–18.1	26.2–26.4	21.0–21.2	19.7–19.9	25.0–25.2	22.8–22.9	22.6–23.0	0.1														
35 *G. khunkhamensis*	21.3–21.7	20.9–21.7	26.0	24.3	15.2	24.6	21.1	24.2	22.6–22.8														
36 *G. kwangsiensis*	22.0–23.5	19.2–19.6	24.3	22.5	21.0	23.2	20.6	21.7–21.8	22.8–23.1	21.5													
37 *G. melli*	23.1–23.6	20.1–21.1	25.3	23.5	21.8	25.3	19.0	24.7	23.8–24.0	23.4	23.8												
38 *G. nadenensis*	18.4–19.4	17.1–18.4	23.3	20.4	6.9	21.2	20.3	21.8–22.1	20.1–20.5	13.8	20.6	21.4											
39 *G. palmatus*	21.4–22.8	21.1–21.6	6.5	23.9	23.6	14.5	26.3	24.6–24.7	25.0–25.2	26.2	23.6	26.1	23.3										
40 *G. paucituberculatus*	20.0–21.7	17.5–18.3	25.5	21.2	19.1	25.6	21.0	21.7	21.6–21.8	21.5	18.9	25.3	18.6	24.6									
41 *G. scientiadventura*	18.4–18.8	17.8–18.6	24.4	20.6	13.9	22.5	20.5	21.4–21.6	21.1–21.2	14.8	21.0	21.6	13.5	23.5	18.6								
42 *G. sengchanthavongi*	19.8–20.3	19.1–19.7	23.8	20.2	14.3	22.1	21.6	22.5–22.9	21.0–21.3	15.7	21.6	22.5	12.0	23.5	18.9	10.5							
43 *G. similignum*	22.8–24.1	21.1–22.6	15.0	25.4	23.1	5.4	25.5	25.1	25.1–25.2	25.0	23.7	26.5	22.7	14.4	25.1	23.1	22.7						
44 *G. scabridus*	11.2–11.8	10.1–10.6	18.5	19.1	19.9	20.3	21.3	17.2	17.2–17.5	21.7	20.1	20.7	19.1	19.2	17.9	17.6	18.4	20.3					
45 *G. subpalmatus*	21.9–23.1	19.2–20.7	25.1	21.8	20.6	24.2	18.0	23.3–23.5	23.3–23.5	22.6	22.3	18.5	18.8	25.6	22.4	20.5	20.6	25.2	20.0				
46 *G. swinhonis*	22.0–23.4	19.4–20.7	25.3	20.8	21.2	25.9	22.0	22.4–22.6	21.9–22.0	23.6	21.8	23.6	21.4	24.5	23.9	22.5	22.1	25.6	19.8	21.7			
47 *G. thakhekensis*	18.8–19.6	18.2–19.5	21.8	20.8	6.8	19.9	20.3	20.8	19.1–19.4	15.9	20.5	20.6	6.8	22.9	18.0	13.1	13.1	21.0	18.9	20.1	23.1		
48 *G. truongi*	20.2–20.6	19.7–20.8	20.5	24.5	22.1	20.8	21.8	22.3	22.0–22.2	22.2	23.1	21.4	22.1	21.8	21.2	22.3	22.0	21.8	18.2	21.6	24.0	20.5	

Table 4. The measurements (in mm) and meristic characters of the type series of *Gekko alpinus* sp. nov. ("H/P" = holotype and paratype respectively; "F/M" = the gender female and male respectively; "#" = subadult; "*" = the length of regenerated tail; "-" = data unavailable; "+" = tail is broken).

ID	CIB 121663	CIB 121661	CIB 121664	CIB 121658	CIB 121659	CIB 121662	CIB 121666	CIB 121660	CIB 121665	CIB 121656	CIB 121657	Range Mean ± SD
Type	H	P	P	P	P	P	P	P	P	P	P	
Sex	M	M	M	F	F	F	F	F#	F#	M	F#	
SVL	74.16	68.28	65.68	66.76	59.02	66.22	64.34	51.58	50.56	56.44	50.74	50.56–74.16 61.25 ± 7.67
TaL	68.02	54.52*	72.06	59.10	59.16*	61.18*	49.22*	59.32	20.28(+)	6.88(+)	39.46*	68.02–72.06 70.04 ± 2.02
AGD	27.70	32.34	30.62	34.78	21.16	29.88	31.44	18.62	24.46	24.24	23.72	18.62–34.78 27.18 ± 4.86
HL	18.44	17.82	17.22	20.80	16.12	17.42	15.84	15.24	14.92	17.24	19.92	14.92–20.80 17.36 ± 1.76
HW	13.26	12.62	12.68	13.24	11.42	12.56	12.56	10.34	10.28	12.22	10.18	10.18–13.26 11.94 ± 1.13
HH	6.78	6.74	6.58	5.76	5.14	5.38	5.72	5.12	4.34	7.10	5.44	4.34–7.10 5.83 ± 0.82
SL	7.62/7.68	7.12/7.22	6.98/7.16	7.42/7.64	6.72/6.72	7.06/7.16	6.90/6.92	5.82/5.86	5.72/5.74	6.90/6.96	5.78/5.80	5.72–7.68 6.77 ± 0.66
EED	5.72/5.66	6.26/6.30	5.62/5.52	5.64/5.72	5.02/5.04	5.78/5.72	5.36/5.46	4.24/4.38	4.64/4.62	5.76/5.76	4.42/4.42	4.24–6.30 5.32 ± 0.61
ED	4.36/4.26	3.96/3.98	3.84/3.76	3.94/3.96	3.36/3.38	3.98/3.94	3.26/3.28	2.96/3.02	2.90/2.94	4.24/4.22	3.38/3.40	2.90–4.36 3.65 ± 0.46
EOD	1.18/1.12	1.06/1.08	0.74/0.86	1.02/0.98	1.24/1.16	1.14/1.26	0.86/0.88	0.94/0.96	0.86/0.82	1.24/1.24	0.64/0.70	0.64–1.26 1.00 ± 0.18
RW	2.12	3.02	2.08	2.52	3.04	2.08	2.92	1.62	1.86	1.56	2.40	1.56–3.04 2.29 ± 0.51
RH	1.22	1.42	1.12	1.32	1.44	0.82	1.40	0.84	1.12	1.18	1.18	0.82–1.44 1.19 ± 0.20
MW	2.22	2.04	1.66	1.82	1.64	1.42	1.60	1.38	1.86	1.62	1.42	1.38–2.22 1.70 ± 0.25
ML	1.62	1.54	1.52	1.48	1.32	1.28	1.52	1.18	1.28	1.82	1.62	1.18–1.82 1.47 ± 0.18
FIL	6.86/6.70	7.52/7.34	7.58/7.64	7.58/7.74	6.82/6.88	7.42/7.56	6.42/6.36	5.82/5.98	6.32/6.02	7.98/8.00	6.14/6.16	5.82–8.00 6.95 ± 0.69
HIL	8.56/8.48	8.62/8.84	8.72/8.62	8.60/8.58	9.06/9.02	8.72/8.84	7.42/7.64	6.44/6.48	7.34/7.38	7.18/7.22	6.92/7.04	6.44–9.06 7.99 ± 0.85
SPL	11/11	10/9	10/10	9/9	10/10	11/12	10/10	10/11	10/10	13/11	10/10	9–13 10.32 ± 0.92
IFL	10/10	8/8	9/9	10/10	9/9	9/9	9/9	9/9	.10/9	9/10	9/9	8–10 9.18 ± 0.57
IO	27	23	25	24	28	23	28	22	25	24	25	22–28 25.00 ± 2.00
PM	2	2	2	2	2	2	2	2	2	2	2	2 2.00 ± 0
DTR	15	16	12	17	17	17	15	14	15	17	17	12–17 15.64 ± 1.55
SMC	165	175	173	158	162	162	179	163	169	189	181	158–189 170.55 ± 9.25
SR	114	109	112	106	101	101	104	101	92	98	95	92–114 103.00 ± 6.54
V	33	36	35	34	34	38	36	32	36	38	39	32–39 35.55 ± 2.10
LF1	10/10	10/11	10/10	11/11	10/10	11/10	10/9	9/9	9/9	8/9	9/9	8–11 9.45 ± 1.34
LT1	11/10	10/10	11/11	10/10	10/10	11/10	10/10	-/9	10/10	9/8	10/9	8–11 9.95 ± 0.72
LF4	13/13	13/12	14/13	12/13	14/14	12/13	12/13	13/13	14/12	12/12	13/13	12–14 12.86 ± 0.69
LT4	15/14	14/15	14/12	14/14	15/15	14/14	14/14	-/15	15/15	13/14	13/14	12–15 14.14 ± 0.77
PP	7	6	4	0	0	0	0	0	0	5	0	4–7 5.50 ± 1.12
PAT	1/1	1/1	1/1	2/2	1/1	2/2	1/1	1/1	1/1	2/2	1/1	1–2 1.30 ± 0.46

Table 5. Morphological characters of *Japonigekko* ("*" = species distributed in China; "-" = data unavailable; bold = difference between the new species).

No.	Species	SVLmax	SPL	IFL	IO	DTR	SMC	SR	V	LT1	LT4	Web	Fore tubercles	Hind tubercles	Tail tubercles	PP
1*	*Gekko alpinus* sp. nov.	74.16	9–13	8–10	22–28	12–17	158–189	92–114	32–39	8–11	13–15	0	1	1	1	4–7
2	*G. aaronbaueri*	**80**	13–14	10–11	**34–37**	**0**	–	98–104	**39–43**	**14–17**	14–16	–	**0**	**0**	**0**	3–4
3*	*G. adleri*	75.3	10–15	9–13	**27–36**	**7–11**	168–190	**123–144**	35–44	11–14	11–15	**1**	**0**	1	1	**17–21**
4*	*G. auriverrucosus*	**69**	9–11	9–11	26–27	16–20	–	–	–	6–8	**6–8**	0	1	1	1	**8–11**
5	*G. bonkowskii*	**69.2**	12–14	10–11	**49–50**	**0**	154–169	**117**	37–40	11–13	15	**1**	**0**	**0**	**0**	6
6	*G. canhi*	**99.2**	**14**	10–12	**49–50**	11–12	168–170	**205–227**	**49–51**	**13–16**	14–17	0	**0**	1	**0**	5
7*	*G. chinensis*	72	10–14	9–13	**35–48**	**10**	156–167	**118–140**	37–39	8–10	9–12	**1**	**0**	1	1	**17–27**
8*	*G. cib*	**66.4**	10–12	10–14	**28–36**	**0**	171–196	**128–149**	37–45	9–13	9–17	**1**	**0**	**0**	**0**	7–9
9*	*G. guishanicus*	**64**	–	–	–	**0**	–	–	–	8–10	**8–10**	0	**0**	**0**	**0**	6–8
10*	*G. hokouensis*	70	10–14	8–11	**30–33**	12–18	153–174	**119–130**	36–43	8–11	15–18	0	**0**	**0**	1	5–9
11*	*G. japonicus*	74	9–13	8–13	**32–35**	9–14	169–188	**130–144**	**39–44**	10–12	14–16	0	1	1	1	4–9
12*	*G. jinjiangensis*	**61.6**	7–10	6–9	20–24	12–16	146–169	**111–149**	31–47	8–11	11–15	0	1	1	1	4–5
13*	*G. kaiyai*	**64.99**	9–12	9–13	22–33	11–18	157–209	99–121	30–43	8–9	**7–11**	0	1	1	1	**9–12**
14	*G. khunkhamensis*	75.2	9–10	9–10	**31–32**	**0**	181–185	**127–138**	**42–45**	**13–14**	14–15	**1**	**0**	**0**	**0**	**0**
15*	*G. kwangsiensis*	**69.7**	10–12	**11–13**	**29–31**	**9–11**	**185–208**	**143–156**	**41–45**	11–13	13–18	**1**	**0**	**0**	1	**9–11**
16*	*G. liboensis*	**85**	12	**11**	**40**	**10**	–	–	–	8	**9**	0	**0**	**0**	–	–
17*	*G. melli*	**80.3**	10–13	9–12	**34–40**	**0**	171–192	**148–160**	**44–46**	10–12	11–14	**1**	**0**	**0**	**0**	**9–11**
18	*G. nadenensis*	77.1	12–14	10–12	**28–30**	**0**	175–185	**123–140**	38–40	**13–15**	14–16	**1**	**0**	**0**	**0**	6
19*	*G. palmatus*	79.7	11–15	9–13	27–36	4–12	160–191	**116–147**	36–47	10–13	10–16	**1**	**0**	**0**	1	**23–30**
20*	*G. paucituberculatus*	**85.9**	11	9–10	**37**	**4**	**189–192**	**136–140**	**42–44**	11	11–13	0	**0**	**0**	**0**	**12**
21	*G. scientiadventura*	73	12–14	9–13	**41–51**	**0**	**118–140**	**139–143**	**38–48**	**12–15**	14–17	**1**	**0**	**0**	1	**23–30**
22*	*G. scabridus*	**64**	9–11	9–11	**30**	17–21	–	–	–	6–9	**7–9**	0	1	1	1	**10–15**
23	*G. sengchanthavongi*	77.3	8–10	6–7	**28–32**	0	175–184	**120–135**	35–43	11–14	13–17	**1**	**0**	**0**	**0**	4–5
24	*G. shibatai*	70.9	10–13	10–14	**37–52**	5–14	–	**114–134**	–	–	9–16	0	**0**	**0**	1	**0–3**
25*	*G. similignum*	**58.9**	12–14	**11**	**46–48**	**11**	–	**144–153**	–	11–13	12–14	**1**	**0**	**0**	1	**17**
26*	*G. subpalmatus*	**65.8**	8–12	7–12	**28–37**	**0**	144–190	**129–156**	**39–46**	9–12	11–14	**1**	**0**	**0**	**0**	5–9
27*	*G. swinhonis*	**66**	7–12	7–11	23–24	**6–8**	–	–	**40**	6–9	**6–9**	0	1	1	–	7–9
28*	*G. taibaiensis*	**69**	9–10	8–10	28	–	–	–	–	**6–7**	**7–8**	–	–	–	–	4–6
29	*G. tawaensis*	71	**15**	**13**	–	**0**	–	–	–	10	**12**	0	**0**	**0**	**0**	**0**
30	*G. thakhekensis*	79.2	12–14	10–11	22–26	**0**	165–174	110–116	32–40	11–13	14–15	**1**	**0**	**0**	**0**	1–5
31	*G. truongi*	**95.9**	13–15	**11–13**	**45–48**	**0**	160–172	**131–143**	35–36	11–13	15–17	0	**0**	**0**	**0**	**10–11**
32	*G. vertebralis*	**69.2**	10–15	10–15	**35–50**	2–12	–	**112–139**	–	–	9–17	0	**0**	**0**	**0**	**0–1**
33*	*G. wenxianensis*	59	12	**11**	–	**10**	–	–	**42–44**	**6**	**9**	0	**0**	1	–	6–8
34	*G. yakuensis*	72	12–13	9–13	–	–	–	–	–	10	15	0	**0**	**0**	1	6–8

The results of the ANOVA indicated that *Gekko alpinus* sp. nov. is significantly different from its sister taxon *G. jinjiangensis* (Table 6) in the following characters: (1) male: HL, HW, SL, ED, SPL, IFL, SMC, SR, LF4; (2) female: AGD, HL, HW, HH, SL, EOD, SPL, IFL, IO, DTR, SMC, SR, LF4, and LT4. In the PCA analysis (Table 7), the first four principal components explained 97.96% of the total variation in the males, where PC1, PC2, PC3, and PC4 eigenvectors accounted for 45.77%, 20.84%, 17.51%, and 13.86% of the total variance respectively, and similarly, the first four principal components occupied a considerable proportion in the females, 76.82% of the total, whereas the PC1, PC2, PC3, and PC4 eigenvectors accounted for 33.42%, 18.13%, 15.47%, and 9.80% of the total variance respectively. As illustrated in the scatter plots of PC1 and PC2 (Fig. 3), regardless of sex, the samples of each species cluster together and do not overlap with each other. The results of the ANOVA and PCA indicated that *Gekko alpinus* sp. nov. was significantly different from the closely related *G. jinjiangensis*. As for morphological comparisons, *Gekko alpinus* sp. nov. can be distinguished from *G. jinjiangensis* by (1) relatively narrower head (HW/HL 0.72 ± 0.01 vs 0.83 ± 0.01 in males and 0.68 ± 0.08 vs 0.81 ± 0.05 in females); (2) more supralabials (SPL 10.63 ± 1.16 vs 8.00 ± 0.50 in males and 10.14 ± 0.74 vs 8.89 ± 0.50 in females) and infralabials (IFL 9.13 ± 0.83 vs 6.63 ± 0.48 in males and 9.21 ± 0.41 vs 7.33 ± 0.70 in females); (3) more interorbitals in females (IO 25 ± 2.14 vs 21.33 ± 1.63); (4) more dorsal tubercles row at midbody in females (DTR 16.00 ± 1.20 vs 13.67 ± 1.15); (5) fewer scales in a line from mental to the front of cloacal slit (SMC 175.50 ± 8.65 vs 155.25 ± 5.63 in males and 167.71 ± 8.34 vs 158.89 ± 6.61 in females); and fewer scale rows at midbody (SR 108.25 ± 6.18 vs 131.75 ± 10.03 in males and 100.00 ± 4.54 vs 123.78 ± 10.20 in females).

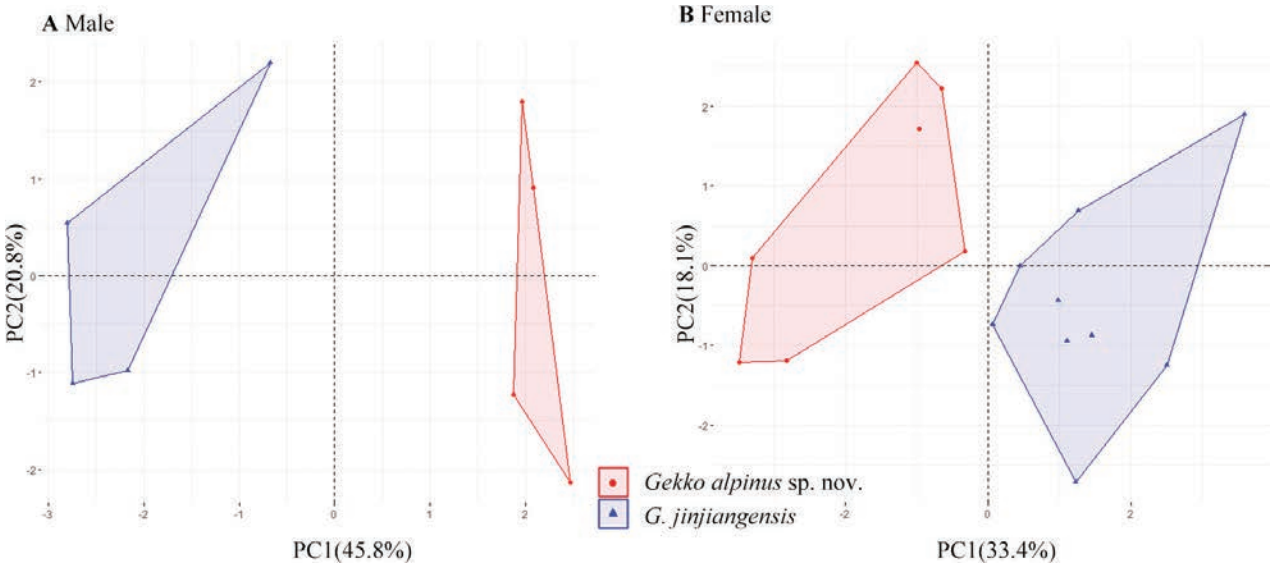

Figure 3. Principal component analysis performed for *Gekko alpinus* sp. nov. and *G. jinjiangensis* based on 12 commonly used morphological traits (except SVL, Tal, FIL, HIL). Numbers inside the brackets indicate the percentages of the total variance explained by each axis.

Table 6. Morphological comparisons of *Gekko alpinus* sp. nov. with *G. jinjiangensis*. "–" = data unavailable, "*" = *p*-values < 0.05, "**" = *p*-values < 0.01, "***" = *p*-values < 0.001.

	***Gekko alpinus* sp. nov. *n* = 4**	***G. jinjiangensis* *n* = 4**	***p*-values**	***Gekko alpinus* sp. nov. *n* = 7**	***G. jinjiangensis* *n* = 9**	***p*-values**
	Range Mean ± SD (males)	**Range Mean ± SD (males)**		**Range Mean ± SD (females)**	**Range Mean ± SD (females)**	
SVL	56.44–74.16 66.14 ± 6.39	50.2–61.6 56.25 ± 4.26	0.0672	50.56–66.76 58.46 ± 6.90	54.6–61.5 56.57 ± 2.02	0.477
AGD	24.24–32.34 28.73 ± 3.08	22.1–24.7 23.83 ± 1.04	0.0547	18.62–34.78 26.29 ± 5.43	20.2–26 24.29 ± 1.65	0.0262*
HL	17.22–18.44 17.68 ± 0.50	12.1–15.5 14.03 ± 1.24	0.0000***	14.92–20.80 17.18 ± 2.15	12.2–15.1 13.59 ± 0.89	0.0001***
HW	12.22–13.26 12.70 ± 0.37	11.1–12.9 11.65 ± 1.00	0.0047**	10.18–13.24 11.51 ± 1.19	9.2–12.3 11.01 ± 0.87	0.0082**
HH	6.58–7.10 6.80 ± 0.19	6.4–7 6.68 ± 0.22	0.144	4.34–5.76 5.27 ± 0.45	4.9–6.8 6.06 ± 0.52	0.0197*
SL	6.90–7.68 7.21 ± 0.29	5.4–7 5.98 ± 0.63	0.0012**	5.72–7.64 6.52 ± 0.68	5.2–6.2 5.70 ± 0.41	0.0009***
EED	5.52–6.30 5.83 ± 0.26	5.6–6.1 5.40 ± 0.53	0.143	4.24–5.78 5.03 ± 0.55	3.8–5.7 5.03 ± 0.54	0.722
ED	3.76–4.36 4.08 ± 0.18	3.3–3.8 3.58 ± 0.19	0.0021**	2.90–3.98 3.41 ± 0.38	3–3.9 3.36 ± 0.27	0.386
EOD	0.74–1.24 1.07 ± 0.16	0.6–1.3 0.85 ± 0.29	0.0833	0.64–1.26 0.96 ± 0.18	0.4–1 0.72 ± 0.20	0.0046**
RW	1.56–3.02 2.20 ± 0.53	1.7–2.1 1.95 ± 0.17	0.828	1.62–3.04 2.35 ± 0.49	1.9–2.5 2.18 ± 0.17	0.146
RH	1.12–1.42 1.24 ± 0.11	1.1–1.2 1.15 ± 0.05	0.339	0.82–1.44 1.16 ± 0.23	1–1.6 1.23 ± 0.20	0.616
MW	1.62–2.22 1.89 ± 0.25	1.6–1.9 1.75 ± 0.11	0.631	1.38–1.86 1.59 ± 0.18	1.1–2.1 1.51 ± 0.28	0.319
ML	1.52–1.82 1.63 ± 0.12	1.4–1.8 1.68 ± 0.16	0.995	1.18–1.62 1.38 ± 0.15	1.2–2 1.54 ± 0.24	0.202
FIL	6.70–8.00 7.45 ± 0.47	–	–	5.82–7.74 6.66 ± 0.65	–	–
HIL	7.18–8.84 8.28 ± 0.66	–	–	6.44–9.06 7.82 ± 0.92	–	–
SPL	9–13 10.63 ± 1.16	7–10 8.00 ± 0.50	0.0001***	9–12 10.14 ± 0.74	8–10 8.89 ± 0.50	0.0000***
IFL	8–10 9.13 ± 0.83	6–7 6.63 ± 0.48	0.0000***	9–10 9.21 ± 0.41	6–9 7.33 ± 0.70	0.0000***
IO	23–27 25.00 ± 1.63	21–24 22.50 ± 1.12	0.0803	22–28 25 ± 2.14	20–24 21.33 ± 1.63	0.0027**
DTR	12–17 15.00 ± 1.87	13–16 14.25 ± 1.30	0.589	14–17 16.00 ± 1.20	12–15 13.67 ± 1.15	0.0024**
SMC	165–189 175.50 ± 8.65	146–161 155.25 ± 5.63	0.0145*	158–181 167.71 ± 8.34	146–169 158.89 ± 6.61	0.0444*
SR	98–114 108.25 ± 6.18	124–149 131.75 ± 10.03	0.0136*	92–106 100.00 ± 4.54	111–142 123.78 ± 10.20	0.0001***
V	33–38 35.50 ± 1.80	35–47 39.08 ± 4.70	0.14	32–39 35.57 ± 2.26	31–47 38.44 ± 4.52	0.172
LF1	8–11 9.75 ± 0.88	8–10 8.85 ± 0.66	0.0901	6–11 9.29 ± 1.53	8–10 8.94 ± 0.66	0.412
LT1	8–11 10.00 ± 0.99	8–10 9.31 ± 0.46	0.334	9–11 9.92 ± 0.47	8–10 9.17 ± 0.53	0.0003
LF4	12–14 12.75 ± 0.70	10–13 11.92 ± 0.83	0.0154*	12–14 12.93 ± 0.61	11–14 11.94 ± 0.83	0.0020**
LT4	12–15 13.88 ± 0.64	12–14 13.23 ± 0.89	0.067	13–15 14.31 ± 0.61	11–14 13.17 ± 0.85	0.0001***
PP	4–7 5.50 ± 1.12	4–5 4.50 ± 0.43	0.121	–	–	–
PAT	1–2 1.25 ± 0.45	1–2 1.25 ± 0.43	1	1–2 1.29 ± 0.45	1–2 1.11 ± 0.33	0.222

Table 7. Variable loadings with the first four principal components of *Gekko alpinus* sp. nov. and *G. jinjiangensis*, with morphometric characters corrected.

Mensural characteristics	Male				Female			
	PC1	PC2	PC3	PC4	PC1	PC2	PC3	PC4
AGD	0.2599	-0.4656	-0.0058	-0.0808	-0.1946	0.1391	-0.3604	0.5002
HL	0.4186	0.0068	0.0178	0.1257	-0.4724	0.0931	-0.0008	0.1661
HW	0.4042	0.1511	0.1207	-0.0109	-0.3806	-0.0953	-0.0450	-0.1095
HH	0.1810	-0.1023	-0.0092	0.6899	0.1077	-0.5288	0.2804	0.1429
SL	0.3534	-0.2054	0.2237	0.2483	-0.4333	0.0069	0.1578	-0.1221
EED	0.3066	0.2964	0.1377	-0.3658	-0.2573	-0.4521	0.3332	0.0167
ED	0.4202	0.0147	-0.0935	-0.0302	-0.2948	-0.0683	0.1355	0.2130
EOD	0.3339	0.2310	-0.1955	-0.2986	-0.3289	0.3158	0.1295	0.1447
RW	-0.0120	-0.3874	-0.4658	-0.3179	-0.2810	-0.3568	-0.2907	-0.0266
RH	0.2125	-0.1708	-0.5392	0.0107	-0.0212	-0.4456	-0.4152	-0.2448
MW	-0.0851	0.2069	-0.5609	0.3128	-0.1462	0.0650	-0.5343	-0.3276
ML	0.0396	0.5866	-0.2162	0.1305	0.1808	-0.2107	-0.2756	0.6636
Standard deviation	2.3435	1.5812	1.4494	1.2894	2.0027	1.4749	1.3626	1.0844
Percentage of total variance	45.766	20.836	17.506	13.855	33.424	18.128	15.472	9.799
Cumulative percentage	45.766	66.602	84.108	97.963	33.424	51.552	67.024	76.823

Taxonomic account

***Gekko alpinus* sp. nov.**

https://zoobank.org/CA4785F4-B8D1-4F62-AAF2-B8EB9CC093A3

Figs 4–7

Type materials. *Holotype*. • CIB 121663 (Figs 4, 5), an adult male, collected 26 June 2020 (29.615722°N, 99.02285°E; 2542 m a.s.l.), from Zhubalong Village, Batang County, Ganzi Zang Autonomous Prefecture, Sichuan Province, China by Sheng-Chao Shi, Cheng Shen, Xian-Guang Guo, and Jian-Ping Jiang. ***Paratypes*.** • One adult male: CIB 121661, four adult females: CIB 121658–60, and CIB 121664, and one subadult female: CIB 121662, with the same collection information as the holotype • One adult male: CIB 121665 and one subadult female: CIB QZ088 collected 29 June 2020 (29.731613°N, 99.002355°E; 2494 m a.s.l.), with the same collection locality and collectors' information • One adult male: CIB 121656 and one subadult female: CIB 121657 (Fig. 6) collected 7 July 2022 (29.758142°N, 99.005975°E; 2400 m a.s.l.), from Zhubalong Village, Mangkang County, Changdu City, Xizang Autonomous Region, China by Cheng Shen, Li-Ming Chang, and Qun-De Zhang.

Diagnosis. (1) body size moderate, SVL 56.44–74.16 mm in adults; (2) head relatively narrow, HW/HL 0.51–0.79; (3) midbody scale rows 92–114, 98–114 in males and 92–106 in females; (4) interorbital scales between anterior corners of the eyes 22–28; (5) ventral scale rows 32–39; (6) tubercles present on dorsal body, forelimbs, hindlimbs and tails; (7) precloacal pores 4–7 in males and absent in the females; (8) subdigital lamellae on first finger 8–11, on fourth finger 12–14, on first toe 8–11, on fourth toe 12–15, no webbing between the fingers and toes; (9) ventral scales between mental and cloacal slit 158–189; (10) nares in contact with rostral; (11) postcloacal tubercles one or two; (12) dorsal surface of body with six or seven large dark taupe bands between nape and sacrum.

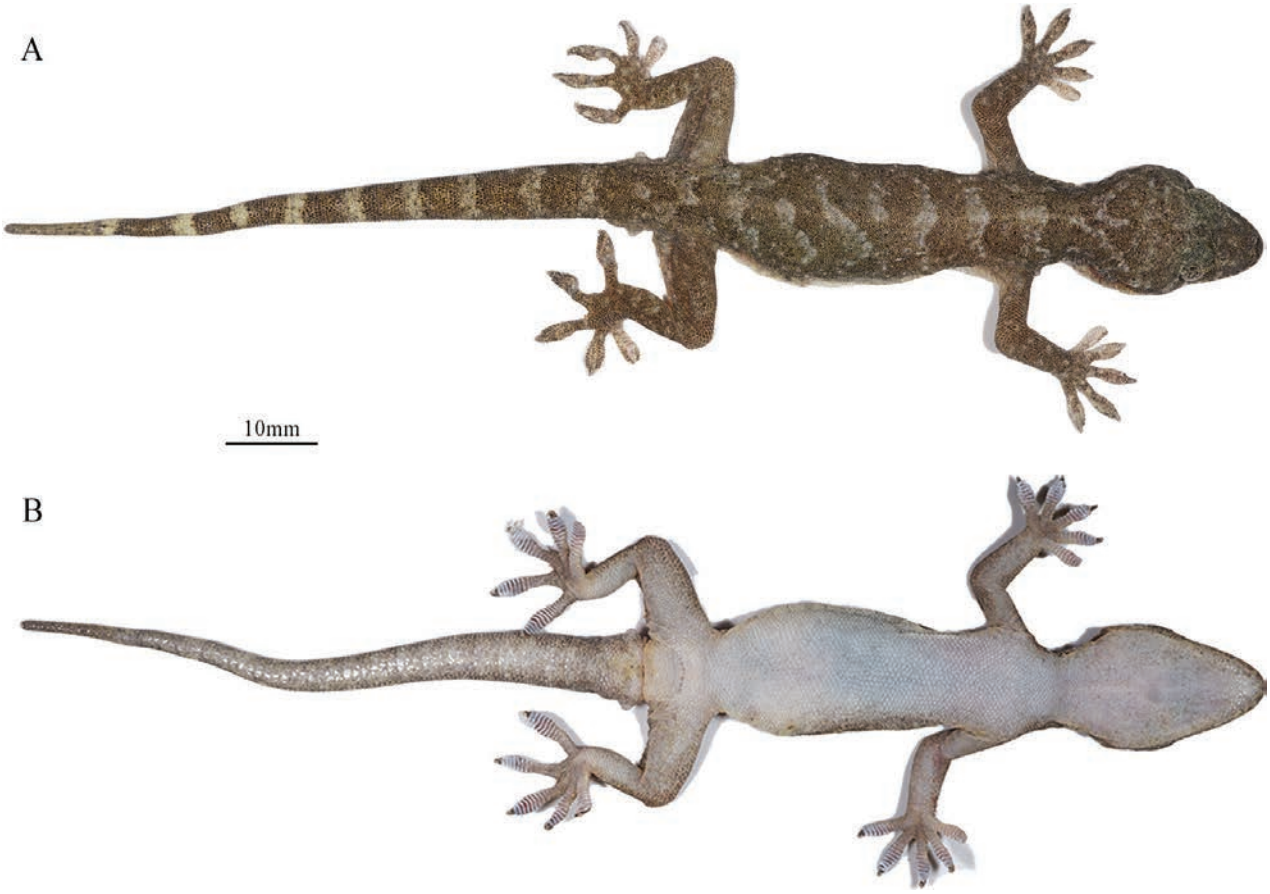

Figure 4. Holotype (CIB 121663, adult male) of *Gekko alpinus* sp. nov. **A** dorsal view of body **B** ventral view of body. Photographs by S-C Shi.

Description of holotype. (Figs 3, 4) An adult male, moderate size, SVL 74.16 mm; body slender and trunk relatively elongate (AGD/SVL 0.37); tail little broken at end, TaL 68.02 mm, slightly shorter than SVL.

Head depressed (HH/HL 0.37), length longer than width (HL/HW), distinct from neck. Snout rounded at top, elongate (SL/HL 0.41/0.42), larger than eye (SL/ED 1.75/1.80); rostral irregular polygon, wider than high (RW/RH 1.74) and slightly narrower than mental (RW/MW 0.95); rostral groove absent; rostral in contact with nostril, first supralabial and nasorostral; nares oval, touching rostral, first supralabial three nasals (nasorostral, supranasal, postnasal); one small internasal; snout region medially concave; preorbitals 12/12, preorbital region deeply concave; eye large (ED/HL 0.24/0.23), pupil vertical with crenulated margins; interorbital scales between anterior corners of eyes 27; ear opening oval, obliquely oriented, much smaller than eye (EOD/ED = 0.27/0.26); mental pentagon, width more than length (MW/ML = 0.73); two enlarged postmentals, hexagonal, twice as long as wide; postmentals in contact with mental and first infralabials anteriorly and five gular scales posteriorly; supralabials 11/11; infralabials 10/10; tubercles absent on dorsal head, granulars on anteriodorsal head larger than those on posterior.

Dorsal scales on body smooth, round or oval, granular, juxtaposed; dorsal tubercles 3–4 times the size of dorsal scales, smooth, round to oval, convex, surrounded by 8–10 dorsal scales; dorsal tubercles extending from occiput region to base of tail; tubercles in 15 regular rows at midbody; ventrolateral

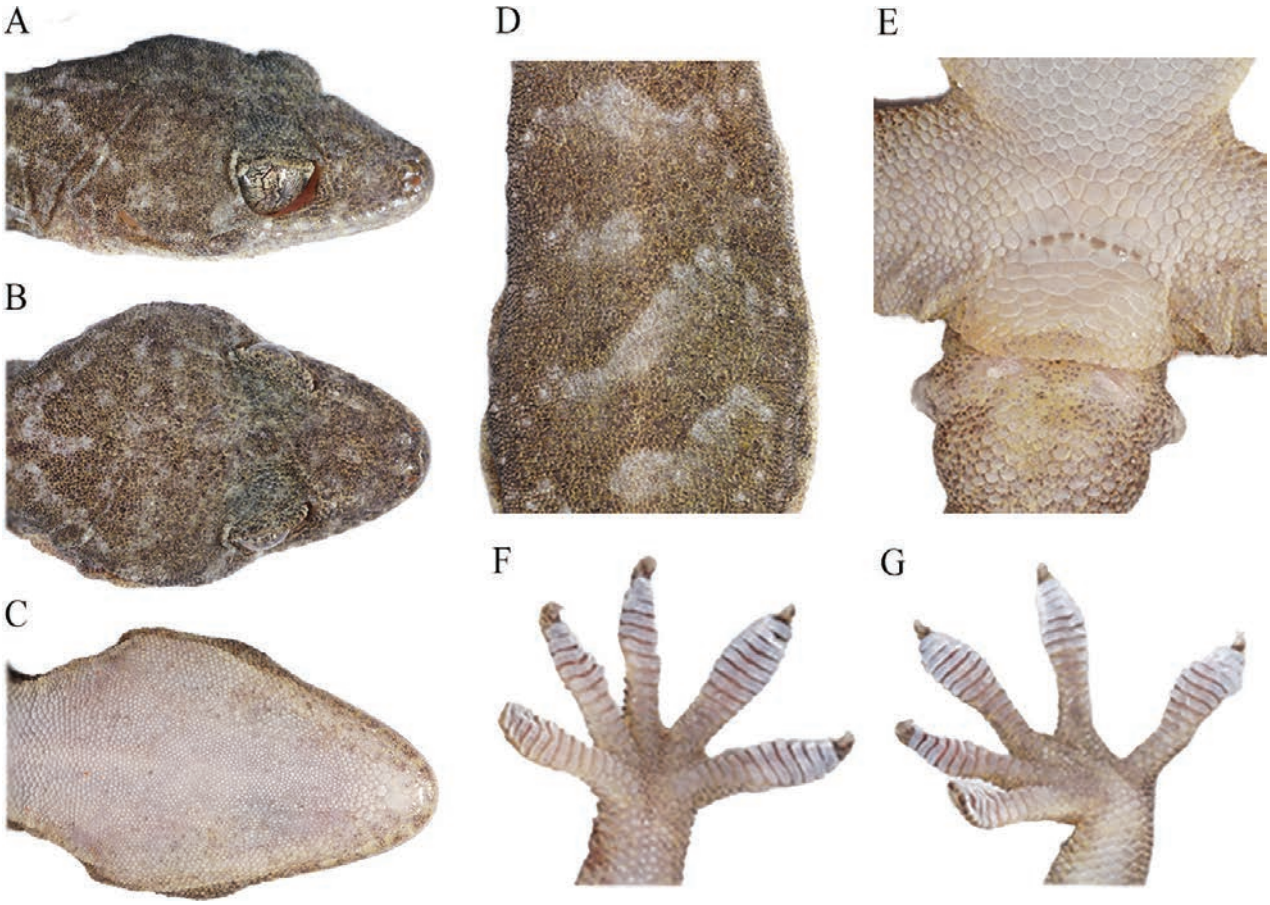

Figure 5. Holotype (CIB 121663, adult male) of *Gekko alpinus* sp. nov. **A** right lateral view of head **B** dorsal view of head **C** ventral view of body **D** dorsal view of middle body **E** ventral view of precloacal region **F** ventral view of left hand **G** ventral view of left foot. Photographs by S-C Shi.

fold weakly developed, without tubercles; ventrals distinctly larger than dorsal scales, smooth, imbricate and largest in middle of belly; ventral scale rows at midbody 33; scale rows around mid-body 114; ventral scales in a row between mental and cloacal slit 165; precloacal scales enlarged, but no enlarged scales on thighs; precloacal pores seven, in a continuous row.

Forelimbs and hindlimbs well developed, tubercles on fore and hind limbs are present, moderately long, slender; forearm and tibia moderately long, forearm shorter than tibia; digits moderately expanded, both first finger and first toe, clawless, others remaining digits clawed; webbing on fingers and toes absent; subdigital lamellae unnotched and undivided: 10/10-9/10-11/10-13/13-11/11 (manus) and 11/10-11/10-12/12-15/14-13/13 (pes). Relative length of fingers: IV > III > V > II > I; relative length of toes: IV > III > V > II > I.

Tail oval in section, swollen at base, gradually tapering; postcloacal tubercle 1/1, obviously large on tail base side; dorsal scales small, flat, smooth, with dorsal tubercles at the tail base dorsum; ventral scales much larger than dorsal, smooth, and imbricated, with enlarged subcaudal plates arranged into a longitudinal row formed ~ 1/6 TaL distance from the cloaca.

Coloration of holotype in life. (Figs 4, 5). Dorsal surfaces of head, neck and body dark taupe, irregularly scattered with some pale grey threads or blotches, alternatively ornamented with eight large pale grey and seven dark taupe wide bands from neck to the sacrum; an indistinct pale-colored vertebral line

Figure 6. Paratype (CIB 121657, subadult female) of *Gekko alpinus* sp. nov. **A** dorsal view of body **B** ventral view of body **C** dorsal view of head **D** ventral view of head **E** dorsal view of middle body **F** ventral view of precloacal region. Photos by S Ma.

is present from the nape to the tail base; dorsal surfaces of limbs, also dark taupe, mottled with small and pale blotches; dorsal tail dark taupe, alternatively ornamented with nine large pale grey and nine larger dark taupe bands, mottled at the ends; ventral skin creamy white, mosaiced with small taupe pigments.

Coloration of holotype in preservative. The coloration pattern of the specimen mostly faded. Dorsal surfaces of head, neck, and body black taupe, but compared to the living status, much wider body area irregularly creamy white, and still alternatively ornamented with eight large creamy white and seven black taupe wide bands from neck to the sacrum. A creamy white vertebral line extends from the nape to the tail terminal; dorsal surfaces of limbs creamy white, mottled with small taupe blotches; dorsal tail dark taupe, alternatively decorated with nine large creamy white and nine larger taupe bands, and mottled towards the end. Ventral skin creamy white, mosaicked with small taupe pigments, though some areas turned creamy yellow due to prolonged alcohol storage.

Variation. All paratypes are very similar to the holotype. Variation of the mensural characters and meristic features among individuals of the type series are presented in Table 4.

Figure 7. Habitats of *Gekko alpinus* sp. nov. **A** macrohabitat: Jinsha River dry-hot valley in Zhubalong Village at the border between Batang County, Sichuan Province and Mangkang County, Xizang Autonomous Region **B** microhabitat: house walls **C** one individual found on the dry rocky cliffs **D** one individual found in the rock crevices on cliff **E** one individual found on a house wall. Photos by S-C Shi.

Distribution and habits. *Gekko alpinus* sp. nov. is currently known only from the Jinsha River Basin between the border of Mangkang County, Xizang Autonomous Region and Batang County, Sichuan Province, China, at elevations ranging from 2400 to 2542 meters above sea level. This new species is nocturnal and inhabits shrubs or dry rocky cliffs in the arid Jinsha River valley, as well as on building walls (Fig. 7). Ants, discovered in the gut of one specimen, are among the recorded food choices of this species.

Etymology. The specific name *alpinus* is derived from Latin, alpinus, -a, -um, meaning from *Alpēs* ("the Alps") + *-īnus*, of or pertaining to the Alps, alpine. This refers to the "great high mountains", referring to not only its distribution range in the great high Hengduan Mountains, but also the highest distribution elevation for all currently known *Japonigekko* species. The suggested common English name is "Alpine Gecko" and the Chinese name is "高山壁虎" (Gāo Shān Bì Hǔ).

Discussion

The discovery of *Gekko alpinus* sp. nov. raises the total species number of the genus *Gekko* to 89, in the subgenus *Japonigekko* to 34, and within this subgenus in China to 21, including six species distributed in Sichuan Province (*Gekko alpinus* sp. nov., *G. chinensis*, *G. cib*, *G. japonicus*, *G. jinjiangensis*, and *G. scabridus*). Additionally, this is the only *Gekko* species recorded in Xizang Autonomous Region, marking a new provincial record of this genus in Xizang (Li et al. 2010; Cai et al. 2018; Che et al. 2020; Hou et al. 2021; Lyu et al. 2021).

Hou et al. (2021) reported that the elevation range of *G. jinjiangensis* as 2000 m to 2476 m a.s.l. However, the type series of *G. jinjiangensis* was only found from 2045 m to 2114 m a.s.l. The 2476 m of *G. jinjiangensis* record originally

pertains to a *Gekko* population in Batang County, which is actually *Gekko alpinus* sp. nov., as described in this study. Consequently, we revise the elevation range of *G. jinjiangensis* to 2045–2114 m a.s.l., while *Gekko alpinus* sp. nov. is distributed between 2400 m to 2542 m a.s.l., making it the highest-altitude *Japonigekko* species currently recognized. Future surveys are recommended to assess the population status of this new species.

The dry-hot valley of Jinsha River in the Hengduan Mountain features habitat heterogeneity and diverse topographic complexity, which supports a variety of reptile species and promotes rapid species evolutionary changes. This is particularly evident in species of *Diploderma* Hallowell, 1861 (Squamata, Agamidae) (Wang et al. 2020; Cai et al. 2022). The discovery of *Gekko alpinus* sp. nov. also highlights the previously underestimated reptile diversity of this area. The *Gekko alpinus* sp. nov. populations found on each side of the Jinsha River do not exhibit significant genetic differentiation (uncorrected *p*-distance among No 1, 2, 6, 7 of *16S*/*ND2*: 0–0.2%/0–0.2%) (Tables 2, 3), similar to *Diploderma batangense* (Li, Deng, Wu & Wang, 2001) (uncorrected *p*-distance of *ND2*: 0–0.4%), implying that the Jinsha River of Hengduan Mountain in Batang and Mangkang do not pose a significant geographical isolation barrier for local reptiles (Wang et al. 2020). To gain a deeper understanding of the reptile diversity patterns and evolutionary histories of Jinsha River Basin in Hengduan Mountain, future field surveys and comprehensive multidimensional analyses are essential.

Acknowledgements

We send sincere thanks herein to Xian-Guang Guo and Qun-De Zhang (Chengdu Institute of Biology, Chinese Academy of Sciences) for their help in the field survey. We greatly thank Jun-Da Zhao from Seattle University for carefully polishing the manuscript.

Additional information

Conflict of interest

The authors have declared that no competing interests exist.

Ethical statement

No ethical statement was reported.

Funding

This work was supported by the Second Tibetan Plateau Scientific Expedition and Research Program (STEP: 2019QZKK05010503) and China Biodiversity Observation Networks (Sino BON – Amphibian & Reptile).

Author contributions

Conceptualization: SM, SCS, JPJ. Data curation: SCS, SM. Formal analysis: SM. Funding acquisition: JPJ. Investigation: SM, JPJ, SCS, CS, LMC. Methodology: JPJ, SM. Project administration: JPJ. Resources: LMC, CS, JPJ. Software: SM. Supervision: JPJ. Validation: JPJ, SCS. Visualization: SM. Writing - original draft: SM. Writing - review and editing: SM, SCS, JPJ, LMC, CS.

Author ORCIDs

Shun Ma https://orcid.org/0009-0003-8611-4550
Sheng-Chao Shi https://orcid.org/0000-0003-2337-6572
Li-Ming Chang https://orcid.org/0000-0002-2411-6978
Jian-Ping Jiang https://orcid.org/0000-0002-1051-7797

Data availability

All of the data that support the findings of this study are available in the main text.

References

Cai B, Lyu K, Chen YY, Li JT, Wang YZ, Gu HJ, Gu XD (2018) The distributional list of amphibians and reptiles in Sichuan Province, China. Science Data Bank 3(1). [in Chinese with English abstract] https://doi.org/10.11922/sciencedb.524

Cai B, Zhang MH, Li J, Du SM, Xie F, Hou M, Zhou HM, Jiang JP (2022) Three New Species of *Diploderma* Hallowell, 1861 (Reptilia: Squamata: Agamidae) from the Shaluli Mountains in Western Sichuan, China. Asian Herpetological Research 13(4): 205–223. https://doi.org/10.16373/j.cnki.ahr.220040

Chan KO, Grismer LL (2021) A standardized and statistically defensible framework for quantitative morphological analyses in taxonomic studies. Zootaxa 5023(2): 293–300. https://doi.org/10.11646/zootaxa.5023.2.9

Che J, Jiang K, Yan F, Zhang YP (2020) Amphibians and Reptiles in Tibet—Diversity and Evolution. Science Press, Beijing, 691 pp. [in Chinese]

Edgar RC (2004) MUSCLE: multiple sequence alignment with high accuracy and high throughput. Nucleic Acids Research 32(5): 1792–1797. https://doi.org/10.1093/nar/gkh340

Goris RC, Maeda N (2004) Guide to the Amphibians and Reptiles of Japan. Florida, Malabar: Krieger Publishing Company, 176–178.

Hoang DT, Chernomor O, Haeseler AV, Minh BQ, Vinh LS (2018) UFBoot2: improving the ultrafast bootstrap approximation. Molecular Biology and Evolution 35(2): 518–522. https://doi.org/10.1093/molbev/msx281

Hou YM, Shi SC, Wang G, Shu GC, Zheng PY, Qi Y, Liu GH, Jiang JP, Xie F (2021) A new species of the *Gekko japonicus* group (Squamata: Gekkonidae) from southwest China. Asian Herpetological Research 12(1): 36–48. https://doi.org/10.16373/j.cnki.ahr.200064

Jonniaux P, Kumazawa Y (2008) Molecular phylogenetic and dating analyses using mitochondrial DNA sequences of eyelid geckos (Squamata: Eublepharidae). Gene 407: 105–115. https://doi.org/10.1016/j.gene.2007.09.023

Kalyaanamoorthy S, Minh BQ, Wong TKF, Haeseler AV, Jermiin LS (2017) ModelFinder: fast model selection for accurate phylogenetic estimates. Nature Methods 14(6): 587–589. https://doi.org/10.1038/nmeth.4285

Li PP, Zhao EM, Dong BJ (2010) Amphibians and Reptiles of Tibet. Beijing: Science Press.

Lleonart J, Salat J, Torres GJ (2000) Removing allometric effects of body size in morphological analysis. Journal of Theoretical Biology 205(1): 85–93. https://doi.org/10.1006/jtbi.2000.2043

Luu VQ, Calame T, Nguyen TQ, Le MD, Bonkowski M, Ziegler T (2014) A new species of the *Gekko japonicus* group (Squamata: Gekkonidae) from central Laos. Zootaxa 3895: 73–88. https://doi.org/10.11646/zootaxa.3895.1.4

Luu VQ, Calame T, Nguyen TQ, Le MD, Ziegler T (2015) Morphological and molecular review of the *Gekko* diversity of Laos with descriptions of three new species. Zootaxa 3986: 279–306. https://doi.org/10.11646/zootaxa.3986.3.2

Luu VQ, Nguyen TQ, Le MD, Bonkowski M, Ziegler T (2017) A new karst dwelling species of the *Gekko japonicus* group (Squamata: Gekkonidae) from central Laos. Zootaxa 4263: 179–193. https://doi.org/10.11646/zootaxa.4263.1.10

Lyu ZT, Lin CY, Ren JL, Jiang K, Zhang YP, Qi S, Wang J (2021) Review of the *Gekko* (*Japonigekko*) *subpalmatus* complex (Squamata, Sauria, Gekkonidae), with description of a new species from China. Zootaxa 4951: 236–258. https://doi.org/10.11646/zootaxa.4951.2.2

Ngo VT, Thai PH, Phimvohan A, David P, Teynié A (2015) *Gekko aaronbaueri*, a new gecko (Squamata: Gekkonidae) from central Laos. Zootaxa 3914: 144–156. https://doi.org/10.11646/zootaxa.3914.2.4

Nguyen TQ, Wang YY, Yang JH, Lehmann T, Le MD, Ziegler T, Bonkowski M (2013) A new species of the *Gekko japonicus* group (Squamata: Sauria: Gekkonidae) from the border region between China and Vietnam. Zootaxa 3652: 501–518. https://doi.org/10.11646/zootaxa.3652.5.1

Nguyen LT, Schmidt HA, Haeseler AV, Minh BQ (2015) IQ-TREE: a fast and effective stochastic algorithm for estimating maximum likelihood phylogenies. Molecular Biology and Evolution 32(1): 268–274. https://doi.org/10.1093/molbev/msu300

Phung TM, Ziegler T (2011) Another new *Gekko* species (Squamata: Gekkonidae) from southern Vietnam. Zootaxa 3129: 51–61. https://doi.org/10.11646/zootaxa.3129.1.4

Pyron RA, Burbrink FT, Wiens JJ (2013) A phylogeny and revised classification of Squamata, including 4161 species of lizards and snakes. BMC Evolutionary Biology 13: 93. https://doi.org/10.1186/1471-2148-13-93

Reist JD (1985) An empirical evaluation of several univariate methods that adjust for size variation in morphometric data. Canadian Journal of Zoology 64(6): 1429–1439. https://doi.org/10.1139/z85-213

Ronquist F, Teslenko M, Van DMP, Ayres DL, Darling A, Hohna S (2012) MrBayes 3.2: efficient Bayesian phylogenetic inference and model choice across a large model space. Systematic Biology 61(3): 539–542. https://doi.org/10.1093/sysbio/sys029

Rösler H, Ziegler T, Vu NT, Herrmann HW, Böhme W. (2005 "2004") A new lizard of the genus *Gekko* Laurenti, 1768 (Squamata: Sauria: Gekkonidae) from the Phong Nha-Ke Bang National Park, Quang Binh Province, Vietnam. Bonner zoologische Beiträge 53: 135–148.

Rösler H, Bauer AM, Heinicke MP, Greenbaum E, Jackman T, Nguyen TQ, Ziegler T (2011) Phylogeny, taxonomy, and zoogeography of the genus *Gekko* Laurenti, 1768 with the revalidation of *G. reevesii* Gray, 1831 (Sauria: Gekkonidae). Zootaxa 2989: 1–50. https://doi.org/10.11646/zootaxa.2989.1.1

Simon C, Frati F, Beckenbach A, Crespi B, Liu H, Flook P (1994) Evolution, weighting and phylogenetic utility of mitochondrial gene sequences and a compilation of conserved polymerase chain reaction primers. Annals of the Entomological Society of America 87(6): 651–701. https://doi.org/10.1093/aesa/87.6.651

Sitthivong S, Lo OV, Nguyen TQ, Ngo HT, Khotpathoom T, Le MD, Ziegler T, Luu VQ (2021) A new species of the *Gekko japonicus* group (Squamata: Gekkonidae) from Khammouane Province, central Laos. Zootaxa 5082: 553–571. https://doi.org/10.11646/zootaxa.5082.6.3

Song MT (1985) A new species of *Gekko* from Shaanxi. Acta Herpetologica Sinica 4: 329–330. [in Chinese with English abstract]

Stejneger L (1907) Herpetology of Japan and adjacent territory. Bulletin of the United States National Museum 58: 165–169. https://doi.org/10.5479/si.03629236.58.i

Stephane G, Jean-franc OD, Vincent L, Maria A, Wim H, And OG (2010) New algorithms and methods to estimate Maximum-likelihood phylogenies: Assessing the performance of PhyML 3.0. Systematic Biology 59(3): 307–321. https://doi.org/10.1093/sysbio/syq010

Tamura K, Stecher G, Kumar S (2021) MEGA11: molecular evolutionary genetics analysis version 11. Molecular Biology and Evolution 38(7): 3022–3027. https://doi.org/10.1093/molbev/msab120

Thorpe RS (1975) Quantitative handling of characters useful in snake systematics with particular reference to intraspecific variation in the Ringed Snake *Natrix natrix* (L.). Biological Journal of the Linnaean Society 7(1): 27–43. https://doi.org/10.1111/j.1095-8312.1975.tb00732.x

Thorpe RS (1976) Biometric analysis of geographic variation and racial affinities. Biological reviews of the Cambridge Philosophical Society 51(4): 407–452. https://doi.org/10.1111/j.1469-185X.1976.tb01063.x

Thorpe RS (1983) A Review of the Numerical Methods for Recognising and Analysing Racial Differentiation. In: Felsenstein J (Ed.) Numerical Taxonomy. Springer Verlag, Berlin, 404–423. https://doi.org/10.1007/978-3-642-69024-2_43

Toda M, Sengoku S, Hikida T, Ota H (2008) Description of two new species of the genus *Gekko* (Squamata: Gekkonidae) from the Tokara and Amami Island Groups in the Ryukyu Archipelago, Japan. Copeia 2008: 452–466. https://doi.org/10.1643/CH-06-281

Uetz P, Freed P, Aguilar R, Reyes F, Kudera F, Hošek J (2024) The Reptile Database. http://www.reptile-database.org [accessed 9 February 2024]

Wang K, Ren JL, Wu JW, Jiang K, Jin JQ, Hou SB, Zheng PY, Xie F, Siler CD, Che J (2020) Systematic revision of mountain dragons (Reptilia: Agamidae: *Diploderma*) in China, with descriptions of six new species and discussion on their conservation. Journal of Zoological Systematics and Evolutionary Research 67: 222–263. https://doi.org/10.1111/jzs.12414

Wang HT, Qi S, Zhou DY, Wang YY (2024) Description of a new karst-adapted species of the subgenus *Japonigekko* (Squamata: Gekkonidae: *Gekko*) from Guangxi, southern China. Vertebrate Zoology 74: 121–132. https://doi.org/10.3897/vz.74.e113899

Wood PL, Guo XG, Travers SL, Su YC, Olson KV, Bauer AM, Grismer LL, Siler CD, Moyle RG, Andersen MJ, Brown RM (2020) Parachute geckos free fall into synonymy: *Gekko* phylogeny, and a new subgeneric classification, inferred from thousands of ultraconserved elements. Molecular Phylogenetics and Evolution 146: 106731. https://doi.org/10.1016/j.ympev.2020.106731

Yang JH (2015) A new species of the genus *Gekko* Laurenti (Squamata: Sauria: Gekkonidae) from Guangxi, China. Zootaxa 3936: 287–295. https://doi.org/10.11646/zootaxa.3936.2.9

Zhang D, Gao FL, Jakovlić I, Zou H, Zhang J, Li WX, Wang GT (2020) PhyloSuite: an integrated and scalable desktop platform for streamlined molecular sequence data management and evolutionary phylogenetics studies. Molecular Ecology Resources 20(1): 348–355. https://doi.org/10.1111/1755-0998.13096

Zhang CW, Wu AF, Cai B, Wang LR, Pang DP, Ma HH, Yu L, Li XY, Huang H, Zeng L, Li L, Yan J, Li P, Zhang BW (2023) A new species of the genus *Gekko* (Squamata: Sauria: Gekkonidae) from the Dabie Mountains, China. Animals 13: 3796. https://doi.org/10.3390/ani13243796

Zhao E, Zhao K, Zhou K (1999) Fauna Sinica Reptilia, Vol. 2: Squamata, Lacertilia. Science Press, Beijing, xi + 394 pp. [in Chinese]

Zhou K, Wang Q (2008) New species of *Gekko* (Squamata: Sauria: Gekkonidae) from China: morphological and molecular evidence. Zootaxa 1778: 59–68. https://doi.org/10.11646/zootaxa.1778.1.5

Zhou KY, Liu YZ, Li DJ (1982). Three new species of *Gekko* and remarks on *Gekko hokouensis* (Lacertiformes, Gekkonidae). Acta Zootaxonomica Sinica 7: 438–446. [in Chinese with English abstract]

ZooKeys 1215: 311–334 (2024)
DOI: 10.3897/zookeys.1215.129410

Research Article

Type designation and redescription of *Scolopendra spinosissima* Kraepelin, 1903 (Scolopendromorpha, Scolopendridae), with remarks on related taxa

Carles Doménech[1]

1 *Departament de Ciències Ambientals i Recursos Naturals, Universitat d'Alacant, Carretera de Sant Vicent del Raspeig s/n C.P. 03690, San Vicent del Raspeig, Alacant, Spain*

Corresponding author: Carles Doménech (carles.domenech.perez@gmail.com)

Abstract

The recent description of the scolopendromorph centipede *Scolopendra paradoxa* Doménech, 2018 raised questions concerning the morphological limits of its closest relative *S. spinosissima* Kraepelin, 1903. Following the works of this author and other evidence, the specimens making up the type series of *S. spinosissima* and a lectotype are fixed, redescribed, and illustrated; these are then compared with this species' unique available voucher and with *S. paradoxa* type material. Specimens making up the *S. spinosissima* type series are fixed including only four of the five individuals stored in the collection of Zoological Museum of Hamburg and, the voucher is identified as *S. spinosissima*. Its sister species, *S. paradoxa*, is confirmed as a morphologically and molecularly distinguishable taxon. Additionally, new data on the *S. spinosissima* type series are provideda and observations involving the excluded original type, reidentified as *Ethmostigmus rubripes rubripes* (Brandt, 1840), are given. Finally, the presence of *S. multidens* Newport, 1844 in the Philippines is proposed as dubious and a revised key for the *Scolopendra* of this archipelago is presented.

Key words: *Ethmostigmus*, *multidens*, *paradoxa*, Philippines, *rubripes*, *Scolopendra*, *spinosissima*

Academic editor: Alessandro Minelli
Received: 11 June 2024
Accepted: 17 July 2024
Published: 17 October 2024

ZooBank: https://zoobank.org/7473119D-1697-4767-AE4D-691F5778C6EE

Citation: Doménech C (2024) Type designation and redescription of *Scolopendra spinosissima* Kraepelin, 1903 (Scolopendromorpha, Scolopendridae), with remarks on related taxa. ZooKeys 1215: 311–334. https://doi.org/10.3897/zookeys.1215.129410

Introduction

Centipedes, class Chilopoda, are one of the basal extant groups of terrestrial arthropods (Thomas et al. 2020). They are distributed across the world's tropical, temperate, and subarctic areas, with their predatory activities occurring mostly at night. With a total of 3300 extinct and extant recognised taxa, centipedes are placed in five different orders (Edgecombe and Giribet 2007; Schileyko et al. 2020). One of the best-known of these is Scolopendromorpha, which accommodates the emblematic and quite diverse – with ~ 100 described species within (Bonato et al. 2016) – genus *Scolopendra* Linnaeus, 1758.

In the Philippines, the genus *Scolopendra* currently comprises six valid taxa, three of them endemic (Doménech et al. 2018). One of these, the reddish-brown *S. spinosissima* Kraepelin, 1903 (Fig. 1A, B), was initially described

as a variety of *S. subspinipes* Leach, 1815. For the original description of this species, Kraepelin (1903) based the type series on an unspecified number of specimens stored at the Zoological Museum of Hamburg (ZMH collection, Germany), which were, in turn, on loan from the Natural History National Museum Paris (MNHN collection, France). Kraepelin (1903) did not indicate the exact type locality for the species, instead only assigning it to their origin country, Philippines. In 1904, a year after the description of this variety, this same taxonomist confirmed the presence of other *S. spinosissima* specimens in the MNHN collection (Kraepelin 1904b). In this catalogue, he also documented the sampling dates and localities, as well as names of collectors and previous examiners, but again he did not specify if these other specimens made up part of the type series.

In line with the remarks provided in Kraepelin's original work (1903), Attems (1930) raised *S. subspinipes* var. *spinosissima* to its current specific status. In that scrutiny, which was an almost literal transcription of Kraepelin's (1903) text, a schematic illustration of an unidentified specimen of *S. spinosissima* was also added, detailing the ventral view of its ultimate leg-bearing segment and ultimate legs' prefemora (Attems 1930: fig. 44; Doménech et al. 2018: fig. 14E).

Since Attems (1930), few reports on this species have been published. These citations were restricted to old distribution data (Wang 1951, 1962) (Fig. 1C), museum catalogues (Weidner 1960; Wang 1962; Rack 1974; Thofern et al. 2021), a dichotomous key (Lewis 2010), illustrations of its defensive behaviour (Kronmüller and Lewis 2015: fig. 2A), and recently, ethological notes (Acuña et al. 2021).

Notwithstanding, it was not until the integrated description of *S. paradoxa* Doménech, 2018 that the morphological limits of *S. spinosissima* were questioned. The doubts regarding the morphology of the last-mentioned species derived from the ancient works of Kraepelin (1903) and Attems (1930), where some omitted, controversial, or unrestrictive data complicated these species differentiations. Inconsistent with the differences found at the genetic level (Doménech et al. 2018), it was noted that when the *S. paradoxa* type series was compared with the description of *S. spinosissima*, a few taxonomic traits of each species occasionally overlapped. This revealed that the existing morphological standard of *S. spinosissima* was inadequately defined, and as a result, the need for this species redescription emerged (Doménech et al. 2018).

To emend this situation, related literature, additional external sources (including museum catalogues and labels), and all probable specimens making up the *S. spinosissima* type series (Kraepelin 1903, 1904b; Thofern et al. 2021) were examined in detail. As a result, the specimens making up the type series of *S. spinosissima* were fixed and a lectotype was designated (Fig. 2A–C). The taxon was redescribed and illustrated before comparing it with the unique available voucher of this same species and with the *S. paradoxa* type material (ICZN 1999: Preamble, Art. 13, Recommendation 13A; Doménech et al. 2018; Buckner et al. 2021). Based on unexpected findings, some considerations regarding the distribution and taxonomy of two other Asian species of Scolopendridae are also briefly discussed, and a revised key for *Scolopendra* species from the Philippines is provided.

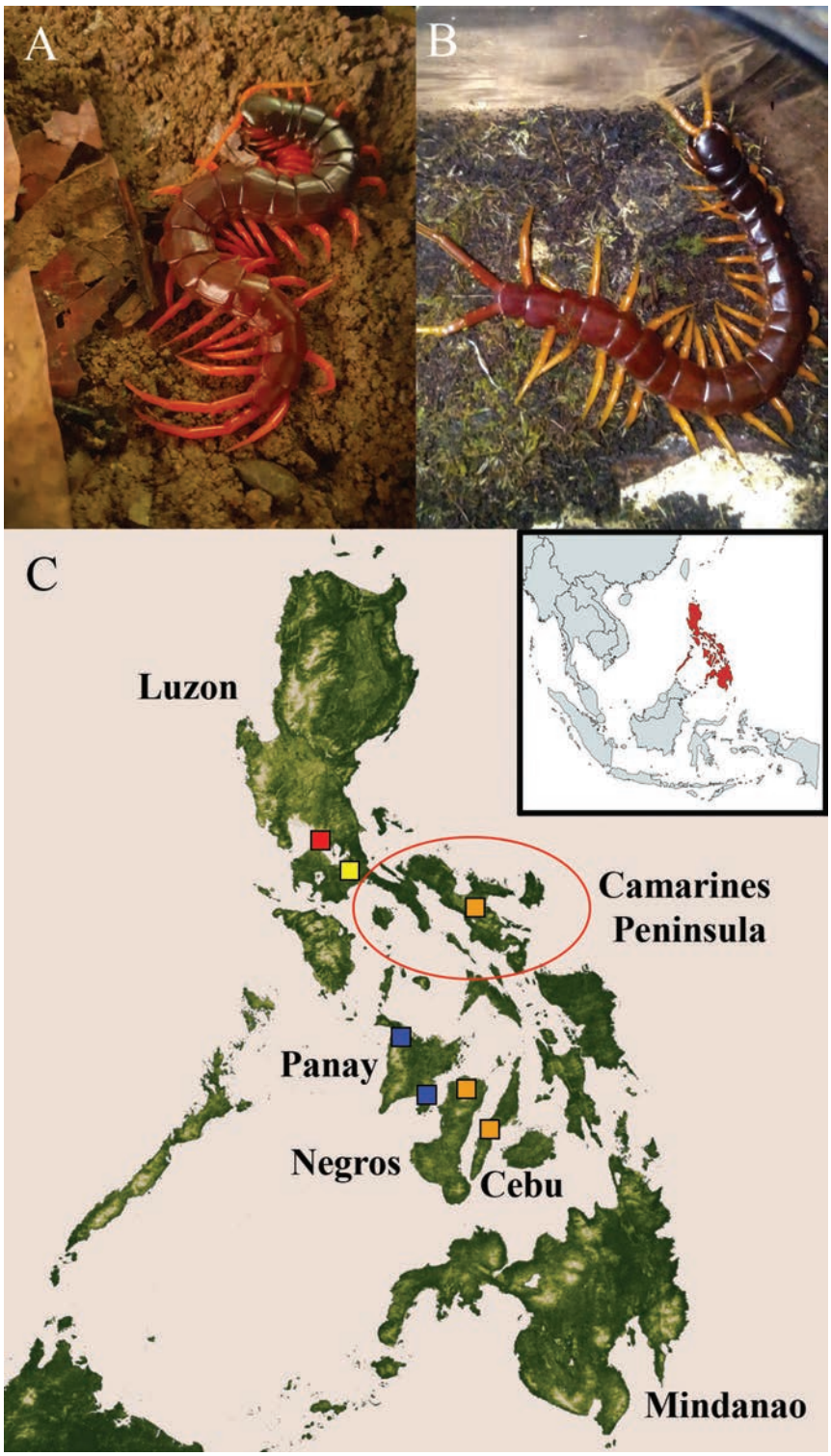

Figure 1. *Scolopendra spinosissima* Kraepelin, 1903 **A**, **B** habitus in vivo showing the only two known variations of colouration; specimens from Panay Is. (**A**) and Guimaras Is. (**B**) (photographs courtesy of E. Währen; individuals uncollected) **C** distribution, 20th century records: red square = lectotype, Manila, Luzon Is.; red circle = paralectotypes 1–3, Camarines Peninsula, Luzon Is.; yellow square = non-types, Dolores, Quezon province (previously Tayabas), Luzon Is. (in the literature erroneously placed in Dolores, Camarines Peninsula, indicated by a red circle). 21st century data: orange squares = (top) Mt. Isarog, Camarines Sur province, Luzon Is.; (middle) Cadiz, Negros Occidental province, Negros Is.; (bottom) Barili, Cebu Prov., Cebu Is. New data: blue squares: (top) Idiacacan, Pandan (Antique), Panay Is. (~ 11.683537**;** 122.114986); (bottom) Jordan, Guimaras Is. (~ 10.652871; 122.602054) (credits: E. Währen). Mindanao Is. indicates the origin of the specimen "Mus. Paris. I.XI.03" misidentified by Kraepelin as "*S. spinosissima*" (specimen currently excluded from the type series).

Materials and methods

Morphological and taxonomic analysis

The specimens from the collection of Zoological Museum of Hamburg (**ZMH**) and Colección Entomológica de la Universidad de Alicante (**CEUA**) were checked at the Universidad de Alicante (**UA**) under a Leica M205C stereo microscope, connected with a montage imaging system Leica DFC450 operated under the Cell'D program. Measurements were made with a Monzana® Digital Vernier Caliper. The specimens from Natural History National Museum in Paris (**MNHN**) collection were examined using a Wild Heerbrugg M3C stereomicroscope and photographed with a Nikon Coolpix P5100 digital camera.

Species identification and the proposed key were based on Newport (1844), Pocock (1898), Kraepelin (1903), Attems (1930), Schileyko and Stagl (2004), Lewis (2010), Kronmüller and Lewis (2015), Schileyko and Stoev (2016), Siriwut et al. (2016), Doménech et al. (2018), and Joshi and Edgecombe (2018). Sex determination and genitalia descriptions were based on the previous works of Demange and Richard (1969), Iorio (2003), Siriwut et al. (2016), and Doménech et al. (2018). Standardised terminology for centipede morphology follows Bonato et al. (2010). Labels and handwritten lists' authorships were verified by comparing their typology and calligraphy with each other and those presented in Harms and Dupérré (2018), Monod et al. (2019), and Thofern et al. (2021). Labels were actualised following Wheeler et al. (2001). Throughout the text, the citation of the type series of the nominal taxon of *S. subspinipes* var. *spinosissima* is replaced by the shorter and currently valid nomenclature *S. spinosissima*. Distribution maps have been created according to data from Kraepelin (1903, 1904b; also labels and notes), Attems (1930), Wang (1962), Lewis (2010), Doménech et al. (2018), Acuña et al. (2021), and iNaturalist (2022) database (https://www.inaturalist.org/observations/106848806 and https://www.inaturalist.org/observations/104968341; E. Währen pers. comm. April–May 2022). Fig. 1C was generated on the base maps obtained from the National Oceanic and Atmospheric Administration, National Weather Service (NOAA/NWS) website (www.noaa.gov; accessed Nov. 2022; reproduced and modified according to their licenses and personal instructions; 7 Dec. 2022) and Mapchart free software (https://www.mapchart.net). Finally, image modifications – background removal, contrast, brightness, notes, and references in the illustrations – were made using Adobe Photoshop CS6 software.

Institutional abbreviations

BMB-DENR Biodiversity Management Bureau – Department of Environment and Natural Resources, Philippines
CEUA Colección Entomológica de la Universidad de Alicante (UA), San Vicent del Raspeig, Alacant, Spain
MNHN Natural History National Museum, Paris, France
PAE Philippines Association of Entomologists, Inc., Philippines
PNM Philippine National Museum, Philippines
PNU Philippine Normal University, Philippines
WRD-DENR Wildlife Resources Division - Department of Environment and Natural Resources, Philippines
ZMH Zoological Museum of Hamburg, Germany

Morphological abbreviations

General morphology:

AP	apical spine	**T**, **TT**	tergite/s
DM	dorso-median process	**UL**	ultimate legs
LS	lateral spine	**ULBS**	ultimate leg-bearing segment
M	median process	**V**	ventral process
S, **SS**	sternite/s	**VL**	ventro-lateral process
SAP	subapical spine	**VM**	ventro-median process
SP	spine on prefemoral corner process		

Genital region:

AV	anal valve	**SGS I**	sternite of genital segment 1
LA	lamina adanalis	**SGS II**	sternite of genital segment 2
LS	lamina subanalis		

Comparative, supporting, and other related materials

ZMH – **Philippines** • 1 unsexed *Ethmostigmus rubripes rubripes* (Brandt, 1840) [determined by Kraepelin as *S. spinosissima*]; Mindanao; 1902; H. W. Brölemann leg.; "*Scolopendra subspinipes* Leach. var. *spinosissima* Krpln. Mus. Paris. I.XI.03- Mindanao Philippinen", ZMH-A00016061 (see listed material of this institution below).

ZMH other material: Kraepelin's handwritten ZMH catalogue (p.102) and draft (p. 92; pointing to the definitive condition of the catalogue); containing determination dates, localities, previous storage emplacements, type status for each specimen, and page numbers referencing the samples ascribed to Kraepelin's (1903) original publication (Fig. 2C). Widner's card files referencing the ZMH *S. spinosissima* specimens type status, Kraepelin's handwritten catalogue and the number of the pages in which the species was described as well as its historical nomenclatural considerations, according to Kraepelin (1903) and Attems (1930).

MNHN – **Philippines** • 1 unsexed adult *S. paradoxa* [determined by Kraepelin as *S. spinosissima*]; Luzon Island, Manila. "Manille"; 1902; H. W. Brölemann leg.; "Léveillé an *multidens* Nwpt. [unreadable] DCCXXIX", "*Scolopendra subspinipes* Leach var. *spinosissima* Krpl.", "Muséum Paris. Manille. Coll H. Brölleman, 1902. *Scolopendra subspinipes* Leach var. *spinosissima* Krpl. Auct. dét. 1903. (N° 729) (Léveillé) [Mus. staff summit label]"; MNHN N° 387; • 7 adults, 3 subadults, unsexed *S. spinosissima*; Luzon Island, Tayabas [Currently Quezon Province], Dolores; same collection data as above; "Dolores Tayabas. I. Philippines. Pen. Camarines [sic.]; • ? *multidens* C[?]XXXIX. Eug. Simon", "*Scolopendra subspinipes* Leach var. *spinosissima* Krpl.", "Muséum Paris. I. Philippines. Pen. Camarines [sic.]. Dolores Tayabas. Coll H. Brölleman, 1902. *Scolopendra subspinipes* Leach var. *spinosissima* Krpl. Auct. dét. 1903. (N° 149) (Eug. Simon) [Mus. staff summit label]"; MNHN N° 388.

CEUA – **Philippines** • 1 unsexed *S. spinosissima*; DNA voucher specimen, non-type; GenBank: KY888682.1; remaining data ibid. Doménech et al. (2018) CEUA016-Mr0009; • 1 adult male, 1 adult female, and 10 subadult unsexed *S. paradoxa* (type series and DNA vouchers); remaining data ibid. Doménech et al. (2018); CEUA016-Mr0000 to Mr0008 and CEUA017-Mr0000 to Mr0002. These materials were originally described in Doménech et al. (2018) and deposited at CEUA. They will be transferred to a permanent repository in a yet undetermined Philippine public institution based on an agreement with BMD-DENR [Biodiversity Management Bureau; Office BMB202305107 – Department of Environment and Natural Resources (DENR)]; document signed on 18 October 2023 (https://bmb.gov.ph). The use of these specimens has been approved for research purposes, including molecular studies, with prior notification to DENR. The author of this article would like to expressly indicate that access to biological resources in the Philippines always requires appropriate research permits from the DENR.

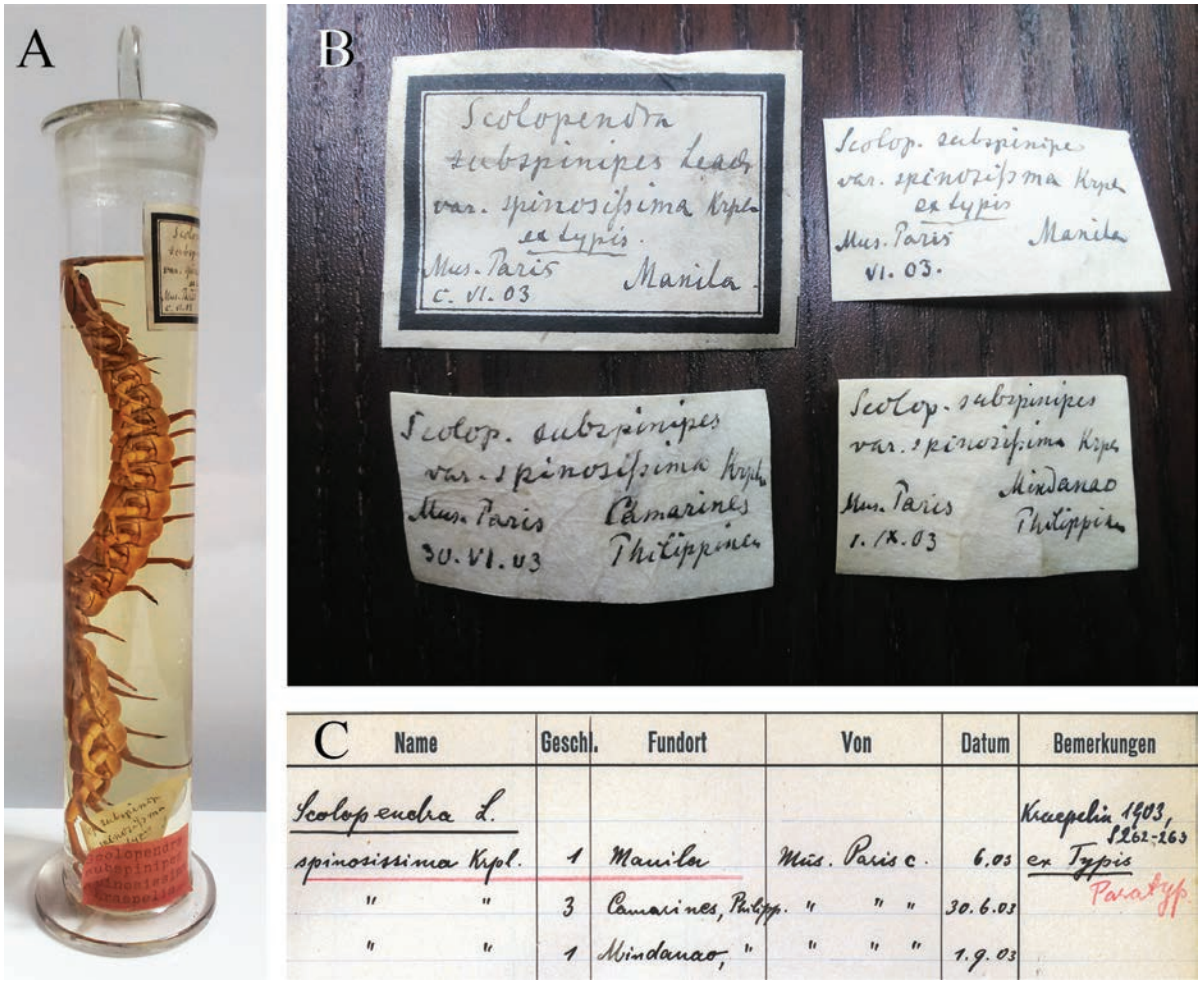

Figure 2. A *Scolopendra spinosissima* Kraepelin, 1903; lectotype in original container (ZMH-A0000633). Notice the two labels inside and the red label fixed outside the jar, indicating type status **B** labels of the original type series proposed by Kraepelin in 1903: lectotype from Manila (two labels on top), paralectotypes from Camarines (bottom left), and specimen "Mus. Paris. I.XI.03" from Mindanao (bottom right, specimen excluded from the type series) **C** the manuscript list in which Kraepelin pointed out the type status of these specimens, localities, and identification dates. Notice that these five specimens, making up the type series, are ascribed to the data "S. 262–263": S. is an abbrev. of "Seiten", meaning pages in German, which is a reference to the page numbers of the 1903 publication containing the original description. Photograph courtesy of N. Dupérré.

Results

Systematics

Order Scolopendromorpha Pocock, 1895
Family Scolopendridae Leach, 1814
Subfamily Scolopendrinae Leach, 1814
Tribe Scolopendrini Leach, 1814
Genus *Scolopendra* Linnaeus, 1758

***Scolopendra spinosissima* Kraepelin, 1903**
Figs 1–4, 5A, C, E, 6, 8E, Table 1

Scolopendra subspinipes var. *spinosissima* Kraepelin, 1903: 262–263.
Scolopendra spinosissima: Attems 1930: 31–32, fig. 44 (transcription, illustration; specimen unidentified); Lewis 2010: 92, 110, fig. 18 (in keys); Kronmüller and Lewis 2015: 269–278, fig. 2A (not type); Doménech et al. 2018: 401–427, table 4, figs 3A, B (not types), 4 (current paralectotype 3), and 15 (voucher, not type); Acuña et al. 2021: 417–419, figs 1, 2 (not type).

Diagnosis. Colouration dark red to brownish. Antennae reaching posterior border of T3, rarely T4; with 19 antennal articles, basal four glabrous. Paramedian sutures on tergites highly variable in TT1–7, in TT8–20 complete. Paramedian sutures on sternite incomplete in SS 2–20. Free coxopleuron edge not extending beyond the T21 posterior edge. Coxopleural process moderately long and not inflected with coxopleuron, forming together an angle of ~ 120°. Coxopleural process with one AP and one smaller dorsal SAP, rarely with an extra ventral SAP. UL prefemur with single spine tipping long spinous processes disposed in VL: 1, V: 2, VM: 2, M: 1, DM: 2 and SP: 1. Penis, gonopods, and secondary sexual characters in males absent.

Lectotype (new designation). Philippines • 1 unsexed adult; Luzon Island, Manila; 1902; H. W. Brölemann leg.; "*Scolopendra subspinipes* Leach. var. *spinosissima* Krpln. ex Typis. Mus. Paris. [unreadable].VI.03. Manila", "*Scolop. subspinipes* Leach. var. *spinosissima* Krpln. ex Typis. Mus. Paris. VI.03. Manila", "*Scolopendra subspinipes spinosissima* Kraepelin [red label fixed in jar]"; ZMH-A0000633. ***Paralectotypes*.** Philippines • 1 ♂, 1 ♀, 1 unsexed; Luzon Island, Quezón Province, Dolores; same collection data as for the lectotype; "*Scolop. subspinipes* Leach. var. *spinosissima* Krpln. Mus. Paris. 30.VI.03. Camarines. Philippinen"; ZMH-A00016058 to A00016060.

Type locality. Since a lectotype is now designated, Manila, Luzon Island, Philippines (and not just Philippines) is the current type locality (Figs 1C, 2B, C) (ICZN 1999: Art. 73.2.3, 76.2; Kraepelin 1903).

Type depository (new data). All type material is deposited in the collection of ZMH, Hamburg (Germany).

Legitum (new data). H. W. Brölemann, 1902.

Distribution. Philippines, endemic. Known from the islands of Luzon, Cebu, Negros, Guimaras, and Panay (Fig. 1C).

Current rank and status. Accepted species.

Lectotype redescription (variation of paralectotypes given in parentheses). Body length reaching 147 mm.

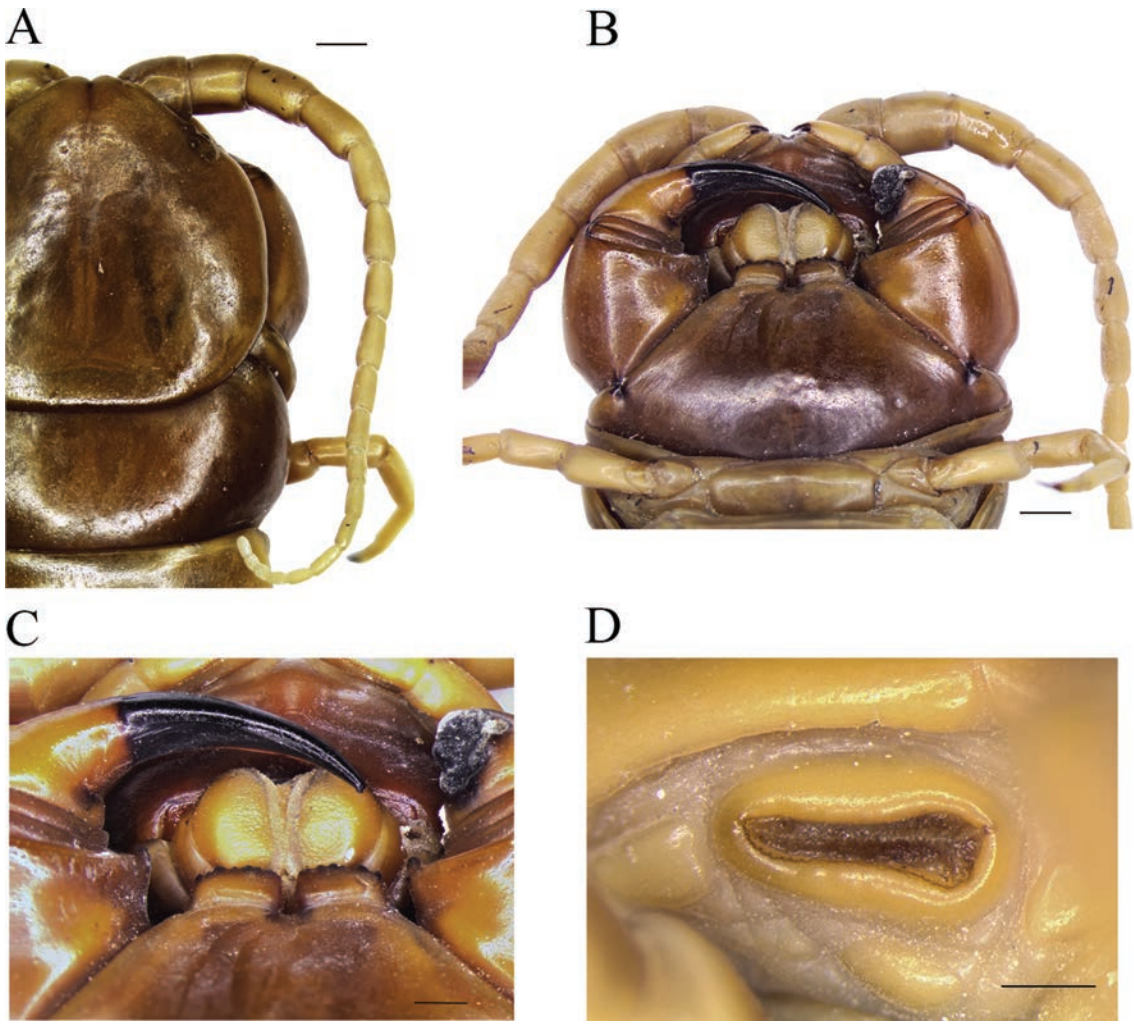

Figure 3. *Scolopendra spinosissima* Kraepelin, 1903; lectotype (ZMH-A0000633) **A** cephalic plate and right antenna, dorsal view **B** forcipular segment, ventral view **C** tooth-plates, ventral view **D** left spiracle on segment 8. Scale bars: 0.5 mm (**C, D**); 2 mm (**A, B**).

Live specimens dark red to brownish with cephalic plate and TT8–11 usually darker. Antennae and coxopleuron orange. Legs reddish to yellowish orange. Coxosternal surface and SS pale yellow (Fig. 1A, B).

Antennae reaching posterior border on T3 (T4 in paralectotype 1), with 19 articles (17–20 in paralectotypes 1 and 2), the basal four glabrous dorsally and ventrally (Fig. 3A). Cephalic plate with four ocelli in each side. Surface covered by dispersed small puncta allocating a short sensillum each; median sulcus absent. Posterior part of cephalic plate without paramedian sulci, overlapping the anterior margin of T1 (Fig. 3A). Coxosternite surface essentially smooth, counting with few isolated and less deep puncta; median suture absent (Fig. 3B, C). Article 2 of second maxillary telopodite with spur (Fig. 3C). Forcipula surface covered by dispersed small puncta. Left tarsungulum lost. Forcipular trochanteroprefemoral process with denticles in two groups, apically with two teeth on the right and three on the left, and proximally, one tooth on the right and two teeth on the left (a total of 2–5 in paralectotypes). Tooth-plates longer than wide, with small dispersed puncta and 7+8 teeth divided in two groups (5+5 in paralectotype 1). Tooth-plate with straight, transverse basal suture (Fig. 3C; Table 1).

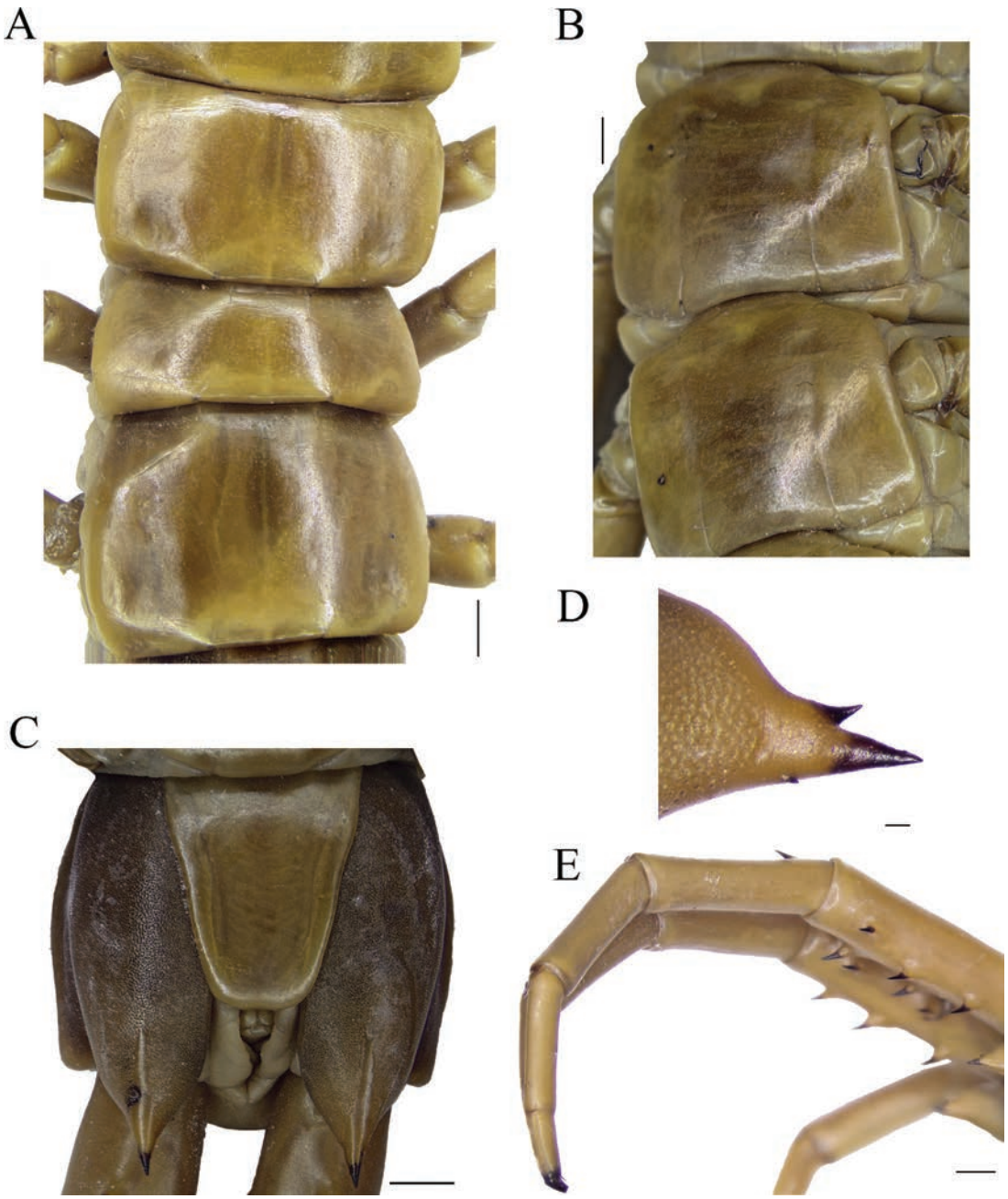

Figure 4. *Scolopendra spinosissima* Kraepelin, 1903; lectotype (ZMH-A0000633) **A** tergites 3–5 **B** sternites 10 and 11 **C** ultimate leg-bearing segment, ventral view **D** left coxopleural process, lateral view **E** ultimate leg, right lateral view. Scale bars: 1 mm (**A, B, D**); 2 mm (**C, E**).

Spiracles positioned in segments 3, 5, 8, 10, 12, 14, 16, 18 and 20, triangular in form and tri-valved (Fig. 3D). Tergite surface with shallow, small, and more dispersed puncta compared to the cephalic plate (Fig. 4A). Paramedian sutures of tergites faint and variable; in paralectotype sutures on T1 and T21 absent, T2 incomplete posteriorly, T3, T5, and T7 incomplete posteriorly and anteriorly, T4, T6, and TT8–20 complete (see Table 1 for paralectotypes). Complete margination starting on T10 (on T12 in paralectotype 1). Tergite of ultimate leg-bearing segment with disperse and non-deep puncta, without depression or sutures; posterior margin rounded. Ratio of width:length of tergite of ultimate leg-bearing segment 1.14:1.Sternite surfaces essentially smooth, with

dispersed, small, shallow puncta. Paramedian sutures in S1 and S21 absent; in SS2–20 incomplete and confined to proximal 10–25% and distal 5–10% of sternite length (see Table 1 for paralectotypes; Fig. 4B). Space between sutures sometimes weakly depressed. Sternite of ultimate leg-bearing segment with sides converging posteriorly (Fig. 4C); surface without depressions or sutures.

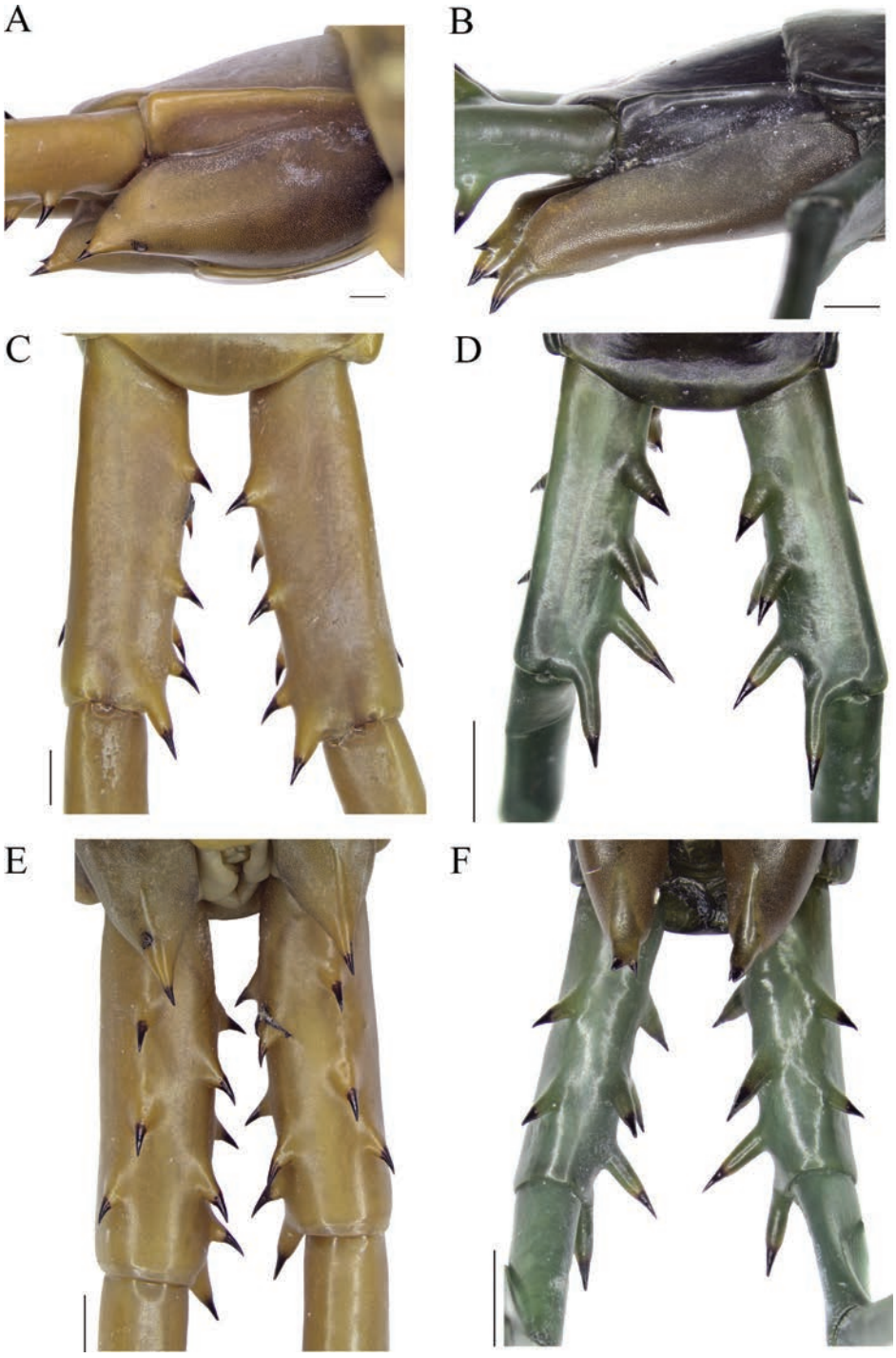

Figure 5. A, C, E *Scolopendra spinosissima* Kraepelin, 1903; lectotype (ZMH-A0000633) **B, D, F** *Scolopendra paradoxa* Doménech, 2018; holotype (CEUA017-Mr0000) **A, B** right coxopleura and coxopleural processes, lateral views **C, D** ultimate leg prefemora, dorsal views **E, F** ultimate leg prefemora, ventral views. The coxopleuron and coxopleural processes are different shapes and lengths; with the different sizes, morphologies, numbers, and positions of the prefemoral spinous processes, these are the most remarkable characters differentiating these species. Scale bars: 1 mm.

Coxopleuron with numerous coxal pores; reaching but excluding spines of the coxopleural process, not extending beyond T21 posterior margin of T21. Free edge on coxopleuron moderately long, with straight dorsal and ventral margins. Posterodorsal margin of coxopleuron not inflected into dorsal margin of coxopleural process, forming both margins at ~ 120° angle (Figs 4C, D, 5A). Coxopleural process moderately long, with isolated small pores and with two or three distal spines, two on right (one each AP and smaller dorsal SAP) and three on left (an additional minute spine in ventral SAP; Fig. 4D). Lateral or dorsal spines absent. Pore-free area extending ventrally 30% of length from proximal part of coxopleural process to margin of sternite of the ultimate leg-bearing segment (Figs 4C, 5A).

All legs without tibial spurs. Surface with shallow, dispersed, small puncta allocating a short sensillum each. One tarsal spur on legs 1–19 or 20, right and left legs, respectively (all paralectotypes with spur on legs 1–20). UL long, slender, with length ratios prefemur and femur = 1.2:1, femur and tibia = 1.07:1, tibia and tarsus 2 = 2:1; tarsus 1 and tarsus 2 = 1.45:1 (Fig. 4E). Prefemora flattened dorsally, with long wider base processes located backwards at 45° angle with respect to the prefemur. Spines of the spinous processes slightly curved backwards. Prefemoral spinous processes formula: VL: 1, V: 2, VM: 2, M: 1, DM: 2 (Figs 4E, 5C, E), (in paralectotype 3, proximal spine in VM position in right prefemur is absent (preserving the prefemoral process); Doménech et al. 2018: fig. 4). Prefemoral corner process slightly longer and with a narrow base in respect to other prefemoral processes, ending with a single non-curved spine (Figs 4E, 5C, E). Tarsus 1 partially lost in left UL (Fig. 4E).

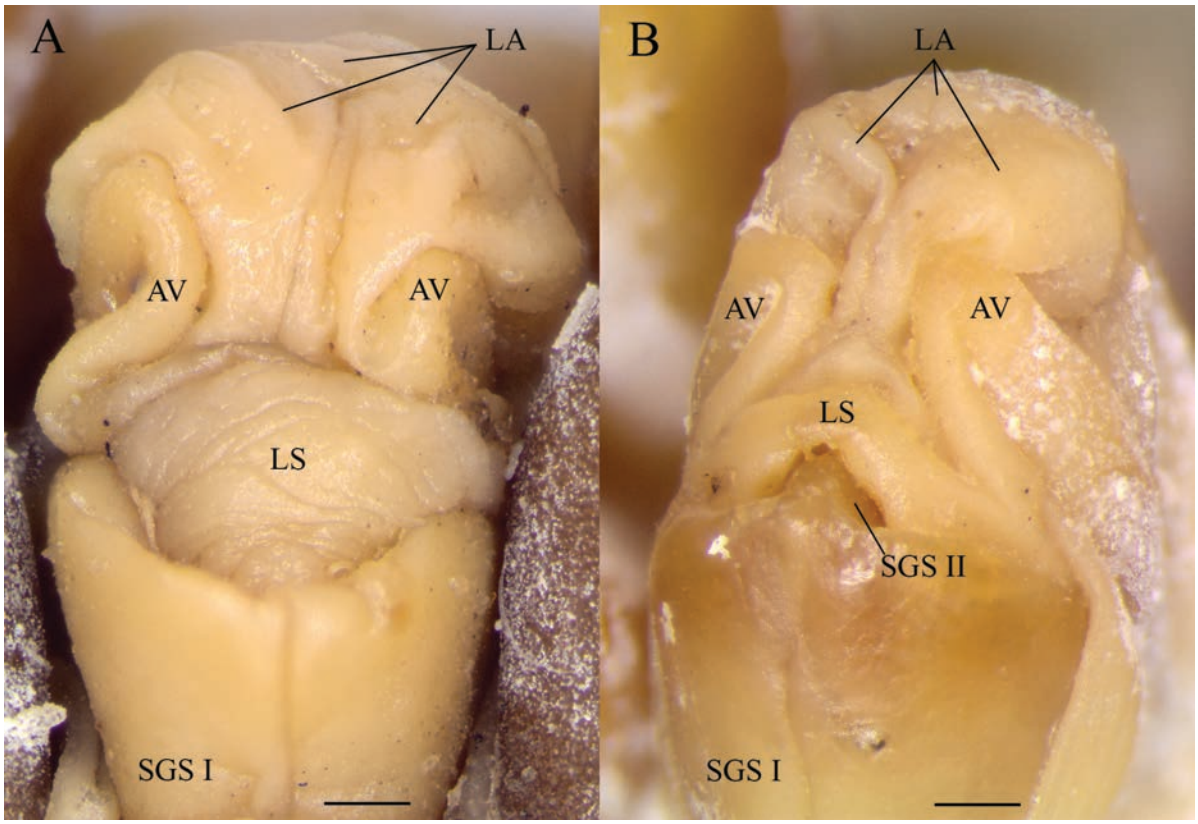

Figure 6. *Scolopendra spinosissima* Kraepelin, 1903; genital apparatus **A** paralectotype 2, female (ZMH-A00016059) **B** paralectotype 3, male (ZMH-A00016060). Abbreviations: AV = anal valve; LA = lamina adanalis; LS = lamina subanalis; SGS I = sternite of genital segment I; SGS II = sternite of genital segment II. Scale bars: 0.5 mm.

Genitalia in the lectotype and paralectotype 1 retracted. In paralectotypes 2 and 3 well-developed (Fig. 6A, B, respectively), partially retracted, reaching further than the distance between posterior margin of ULBS sternite and distal part of the coxopleural process. The genital segment sternite 1 rounded, convex posteriorly, with a median suture. Tergite of the genital segment without small setae. In male paralectotype 3 (Fig. 6B) genital segment 2 is small, horseshoe-shaped, with small shallow puncta; penis, gonopods, and secondary sexual characters absent.

Scolopendra spinosissima differential diagnosis (*S. spinosissima* paratypes features given in parentheses)

According to Doménech et al. (2018), and re-examination of both type series, the closest relative to *S. spinosissima* is *S. paradoxa.* This species can be readily distinguished from *S. spinosissima* on the basis of the following unambiguous

Table 1. Morphological comparison between the type series of *Scolopendra spinosissima* Kraepelin, 1903, its voucher, and *S. paradoxa* Doménech, 2018 holotype. A = Absent; C = Complete; I = Incomplete; D = Distal; P = Proximal; PR = Partially retracted; R = Retracted. * = Appendix damaged. N/A = Not applicable.

	***Scolopendra paradoxa* Doménech, 2018**	***Scolopendra spinosissima* Kraepelin, 1903**				
Current type condition	Holotype – and voucher–	Lectotype	Paralectotype 1	Paralectotype 2	Paralectotype 3	Voucher (non type)
Specimen number	CEUA017-Mr0000	ZMH-A0000633	ZMH-A00016058	ZMH-A00016059	ZMH-A00016060	CEUA016-Mr0009
Reference in previous labels and catalogue	N/A	Mus. Paris c.; VI.03; "ex Typis" (holotype)	Mus. Paris c.; 30.VI.03; paratype	Mus. Paris c.; 30.VI.03; paratype	Mus. Paris c.; 30.VI.03; paratype	N/A
Body length in mm	132	147	126	120	99	87
Sex	R-Female	R	PR	Female	PR-Male	* (probably female)
Antenna reaching to tergite	T5	T3	T4	T3	T3	T4
Number of antennal articles	19/19	19/19	17/20	18/19	19/19	19/19
Number of proximal glabrous articles	4/4 dorsally 5½/5½ ventrally	4/4 dorsally and ventrally	4/4 dorsally and ventrally	4/4 dorsally and ventrally	4/4 dorsally and ventrally	4/4 dorsally and ventrally
Teeth on tooth-plate	5+5	7+8	5+5	7+7	7+7	7+7
Teeth on forcipular trochanteroprefemoral processes as total (upper group/lower group)	2 (1/1) – 1(1/0)	3 (2/1) – 5(3/2)	5 (3/2) – 3 (2/1)	2 (1/1) – 4 (3/1)	4 (3/1) – 4 (3/1)	4 (3/1) – 5(3/2)
Tergite paramedian sutures	TT1–2 A; TT3–4 IDP; T5C; T6C (right side ID); T7IDP; TT9–20C; T21 A	TT1–2 A; T3 IP; T4 C; T5 IP; T6 C; T7IDP; TT9–20C; T21 A	TT1A; TT2 ID; TT3–5 IDP; T6 C; TT7–8 IDP; TT9–20 C; T21 A	T1 A; T2 ID; T3 IDP; T4 C; T5 IDP; TT6–20C; T21 A	T1 A; T2 ID; T3 IDP; T4 C; T5 IDP; T6 C; TT7–20C; T21 A	TT1–2 A; T3 IP; T4–20 C; T21 A
First tergite with complete margination	10	10	12	10	10	12
Paramedian sutures on sternites	SS 1–2 A; SS3–18 C; SS19–21 A	S1 A; SS2–20 IDP; S21 A	S1 A; SS2–20 IDP; S21 A	S1 A; SS2–4 IP; SS5–19 IPD; SS20–21 A	S1 A; SS2–5 C; SS6–19 IPD; SS20–21 A	S1 A; SS2–12C; SS13–19 IP; S20–21 A
Spines in coxopleural process	AP: 1; SAP: 1	AP: 1; SAP: 1; (left with 1 extra ventral SAP spinula)	AP: 1; SAP: 1	AP: 1; SAP: 1	AP: 1; SAP: 1	AP: 1; SAP: 1
Coxopleural process extending beyond T21	Yes	No	No	No	No	No
Spinous process formula on prefemora of ultimate legs	VL: 2/2; V: 0/0; VM: 1/1; M: 1/1; DM: 2/2; SP: 1/1	VL: 1/1; V: 2/2; VM: 2/2; M: 1/1; DM: 2/2; SP: 1/1	VL: 1/1; V: 2/2; VM: 2/2; M: 1/1; DM: 2/2; SP: 1/1; (left M and VM proximal spinous processes with spines*)	VL: 1/1; V: 2/2; VM: 2/2; M: 1/1; DM: 2/2; SP: 1/1	VL: 1/1; V: 2/2; VM: 2/2; M: 1/1; DM: 2/2; SP: 1/1; (right VM proximal spinous process hardly noticeable, without spine); (Doménech et al. 2018: fig. 4A–C)	VL: 1/1; V: 2/2; VM: 2/2; M: 1/1; DM: 2/2; SP: 1/1; (left VL with a small medial extra aberrant process)
Legs with one tarsal spur	1–18 (left leg 18*)	1–20 (right leg 19)	1–20	1–20 (several mid body legs *)	1–20	1–20 (right leg 19)

characters: 1) antennae usually reaching T5 (vs T3, rarely T4); 2) first four basal antennal articles glabrous dorsally and first 5–5½ glabrous ventrally (vs four basal glabrous over all their surfaces); 3) cephalic plate surface covered only anteriorly by disperse small puncta (vs whole cephalic plate covered by small sparse puncta); 4) coxopleuron free edge very long, clearly extending beyond the posterior edge of T21 (vs coxopleuron reaching but not extending beyond T21) (Fig. 5A, B); 5) posterodorsal margin of coxopleuron forming an angle of ~ 180° angle with dorsal margin of coxopleural process (vs ~ 120° in *S. spinosissima*) (Fig. 5A, B); 6) coxopleural process elongate and large, with two spines (vs short and smaller, with two or rarely three spines) (Fig. 5A, B); 7) UL prefemoral spinous with seven, extremely long, narrow base processes; spines almost straight, consistently two in VL position, zero in V position, and just one in VM position (vs nine distinctly shorter spinous processes with a wide base, and with spines slightly curved backwards, constantly with a single distal process in VL and with two each in V and VM positions) (Fig. 5C–F); 8) legs with one tarsal spur in 1–18, rarely 1–19 (vs generally 1–20); 9) evident aposematic colouration, with orange antennae, dichromatic tergites orange, yellowish, or dark green anteriorly, and dark blue or brown posteriorly, cyan legs (vs not so pronounced aposematic colouration, with monochromatic brownish or dark red tergites, and with orange antennae and legs); 10) size up to 176 mm (vs up to 147 mm); 11) semiaquatic behaviour (vs exclusive terrestrial lifestyle) and 12) partial cytochrome *c* oxidase (COI) sequences genetic distances between 18.2–19.6% (Doménech et al. 2018).

Moreover, *S. spinosissima* as well as *S. paradoxa*, can be differentiated from all remaining Southeast Asian congeners, but also from all species in the genus *Scolopendra* by the exclusive discontinued paramedian sutures on TT and SS (Table 1), and by the unique shape, size, and disposition of the UL spinous processes (Doménech et al. 2018).

Fixation of *Scolopendra spinosissima* specimens making up the type series

On 15 December 1903, Karl Kraepelin's paper describing *S. spinosissima* was published, lacking the type series designation or an explicit depository. These specimens were indispensable for the detailed morphological comparison with *S. paradoxa* types and to confirm the taxonomic identity of *S. spinosissima* specimen molecularly analysed by Doménech et al. (2018). When a type series is not designated, the ICZN allows the use of other information sources besides that provided in the original description paper to ensure which specimens comprise such type series (ICZN 1999: Art. 72.4.1.1).

In the original work, Kraepelin (1903) indicated that the *S. spinosissima* specimens he examined [= type series] had been previously stored at the Natural History National Museum of Paris (MNHN) with the abbreviation "Mus. Paris", without stating these samples' definitive depository. Otherwise, several authors (Weidner 1960; Rack 1974; Doménech et al. 2018; Thofern et al. 2021) showed the probable presence of these specimens at the Natural History Museum of Hamburg (ZHM), the place where Kraepelin mainly developed his career by studying his own and exchanged material (Lohmann 1915; Harms and Dupérré 2018; Monod et al. 2019; Thofern et al. 2021). At the ZHM, a total of five *S. subspinipes* var. *spinosissima* specimens were found. In their labels

and collection data, all samples were mentioned as in the original publication with the identical provenance inscription "Mus. Paris" (Fig. 2A, B). Two of these labels (top labels in Fig. 2B) indicate type material of one of the specimens by using the term "ex Typis" (meaning "coming from the type series" sensu Harms and Dupérré 2018; Monod et al. 2019; Thofern et al. 2021; N. Dupérré pers. comm. Jun. 2021). By 'adding to' the label information, the ZHM catalogue provided more collection data and clearly shows the paratype status of the four remaining specimens (Fig. 2C). At the same time, this catalogue also demonstrated the direct connection between the specimens and the 1903 publication, with reference to the pages where this species was originally described ("*S*." German abbrev. of "Seiten", pages; pp 262–263; Fig. 2A–C). Kraepelin's calligraphy on all these documents also matches with the one seen in modern literature (Harms and Dupérré 2018; Monod et al. 2019; Thofern et al. 2021). The additional information in the Weidner file cards and current ZHM catalogues are consistent with these findings (Weidner 1960; Rack 1974; Thofern et al. 2021).

Finally, once it was established that no information supported the inclusion of the other *S. spinosissima* specimens known by Kraepelin (1904b; see justification below), the entire data set provided here (ICZN 1999: Art. 72.4.7) revealed that the original description of *S. spinosissima* was based only on five specimens deposited at the ZHM collection. After morphological analysis of the five individuals originally used by the species' authority, only four of them, here fixed, make up the type series of *S. spinosissima* (ICZN 1999: Art. 72.1.1). These are the one labelled as "Mus. Paris. VI.03 ex Typis" and three labelled as "Mus. Paris. 30.VI.03" but excluding the specimen "Mus. Paris. I.IX.03" as this one does not satisfy the new proposed morphological criteria for *S. spinosissima* (see below).

Scolopendra spinosissima lectotype designation

The ICZN (1999) only allows a holotype designation in two circumstances: the express designation in the original publication or by monotypy (Art. 73.1.1, 73.1.4, 73.1.2, Recommendation 73F). Therefore, the type designation made by Kraepelin in the catalogue or labels (Fig. 2B, C) becomes nomenclaturally invalid since these do not constitute enough evidence of the fixation of a specimen as a type in the sense of 'The Code' (ICZN 1999: Art. 8, 9.8, 72.4.7, 73.1). Subsequently, all five *S. spinosissima* specimens were considered syntypes (ICZN 1999: Art. 72.1.1). However, in the interest of nomenclatural stability and with the aim of clarifying the application of the name for the taxon *S. spinosissima*, the lectotype designation (ICZN 1999: Recommendation 73F, Art. 74.7) proved justified to solve the following nomenclatural conflicts: 1) presence of two different taxa in the original *S. spinosissima* type series and 2) the need for a reference specimen for its clear morphological redefinition and, as a consequence, unambiguous differentiation in respect to its closest relative *S. paradoxa* (ICZN 1999: Preamble, Art. 13, Recommendation 73F, 74G, Art. 74, 74.7.3; Doménech et al. 2018). Kraepelin did not validly designate a holotype among the specimens making up the *S. spinosissima* type series (ICZN 1999: Art. 72.4.7, 73.1). Nonetheless, he provided sufficient evidence supporting one of these types: after reviewing the catalogue annotations where all specimens in the type series, with except of one, were [invalidly] regarded as paratypes (see in Fig. 2C the term "Paratyp" and the red line dividing the species in two groups). Therefore, the holotype being the counterpart of this term (ICZN 1999:

Art. 72.4.5) and in the absence of any additional data corroborating the existence of other types (see below), it can be inferred that Kraepelin may have selected the specimen "Mus. Paris. VI.03 ex Typis", to be deemed the benchmark of *S. spinosissima*. In line with this, based on the ZMH catalogue information (Fig. 2C), a unique red label stamped into the "Mus. Paris. VI.03 ex Typis" jar was found (Fig. 2A). Red colours on labels usually indicate the type status of a specimen (Calhoun and Hawkins 2016) but when this colour appears in a single label, it often points to the name-bearing type of a species (Ratcliffe 2013). Hence, in the absence of any other red labels, this is advocated as the author's recognition of this specimen as the reference for *S. spinosissima*. Consequently, the best developed and preserved adult syntype ("Mus. Paris. VI.03 ex Typis") is designated as lectotype, and therefore, as the name-bearing type for the species (Figs 2–4, 5A, C, E; ICZN 1999: Art. 73, 74). Any lectotype designation relegates the remainder of the type series as paralectotypes (ICZN 1999: Art. 74.1.3). Subsequently, the three specimens contained in the jar "Mus. Paris. 30.VI.03" now bear the status of paralectotypes of *S. spinosissima* (Fig. 2B, C, Table 1). The previous label of the "Mus. Paris. VI.03 ex Typis" specimen as "paratypoid" (Weidner 1960; Weidner file cards; Rack 1974) or more precisely as syntype (ICZN 1999: Art. 72.1.1, 74.1.3; Thofern et al. 2021) is now substituted by the current lectotype status (ICZN 1999: Art. 74.1.2).

With regards to the previously illustrated paralectotype 3 in Doménech et al. (2018: fig. 4) and the recommendation of clause 74B (ICZN 1999) of "Preference for illustrated specimen", it is concluded that this specimen is not eligible over the newly designated lectotype since the former specimen does not fulfil the premise of "Other things being equal", due to its subadult developmental stage, partially aberrant prefemoral processes of the UL, and Kraepelin's express designation of this specimen as a support specimen, naming it as paratype (Table 1; Fig. 2B, C; Doménech et al. 2018: fig. 4). According to this recommendation, the specimen illustrated by Attems (1930) could not be considered because it was not designated as a type nor was a determinate taxon ascribed to such an illustration (ICZN 1999: Art. 74, Recommendation 74B).

Exclusion of the Mus. Paris. I.XI.03 specimen from the type series

The "Mus. Paris. I.IX.03" specimen displays four ocelli on each side of the cephalic plate, overlapped by T1 (Fig. 7A), ten pairs of non-valved, round, or oval spiracles on segments 3, 5, 7, 8, 10, 12, 14, 16, 18, and 20, the first one being the largest (Fig. 7B), forcipular trochanteroprefemoral process absent, smooth tergites, and coxopleural process with spines in apical, dorsal, and lateral positions. All these characters place this specimen within the genus *Ethmostigmus* Pocock, 1898 (Joshi and Edgecombe 2018; Schileyko et al. 2020). In the Philippines, the genus *Ethmostigmus* is only represented by *E. rubripes platycephalus* (Newport, 1844), was only documented in the Spratly Islands (South China Sea; Schileyko and Stagl 2004; Schileyko and Stoev 2016). The current identification represents the second formal record for the genus in this archipelago, from Mindanao Island in the Philippines (Fig. 2B). The specimen "Mus. Paris. I.IX.03" shows a relatively long coxopleural process, with one apical, one subapical and two lateral spines, and a slightly arcuate edge with two or three spines (identical features to the specimen from the Moluccas Islands (Indonesia), presented in Schileyko and Stagl (2004: fig. 33–35). This specimen also has 18 antennal

articles (first basal four dorsally glabrous), tooth-plate with 3+3 teeth, complete paramedian sulci on TT3–20, weak paramedian sulci on SS3–20, and the prefemoral spinous process formula (here revised) VL: 3, V: 0, VM: 2 (3 on the left), M: 2, DM: 2 and SP: 1 (Fig. 7C, D), all of which supports its identity as *E. rubripes platycephalus* sensu Schileyko and Stagl (2004).

Ethmostigmus rubripes platycephalus mainly differs from *E. rubripes rubripes* (Brandt, 1840) in the lengths of the coxopleural processes, which in the first is more than twice as long as S21 (Attems 1930; Schileyko and Stagl 2004). As shown in Kraepelin's drawing (1903: fig. 107) and the illustration of one of the syntypes (Joshi and Edgecombe 2018: fig. 2C, E, G, H), the two reduced coxopleuron lateral spines, almost conical morphology, and the coxopleural process being greater in length in *E. rubripes platycephalus* are

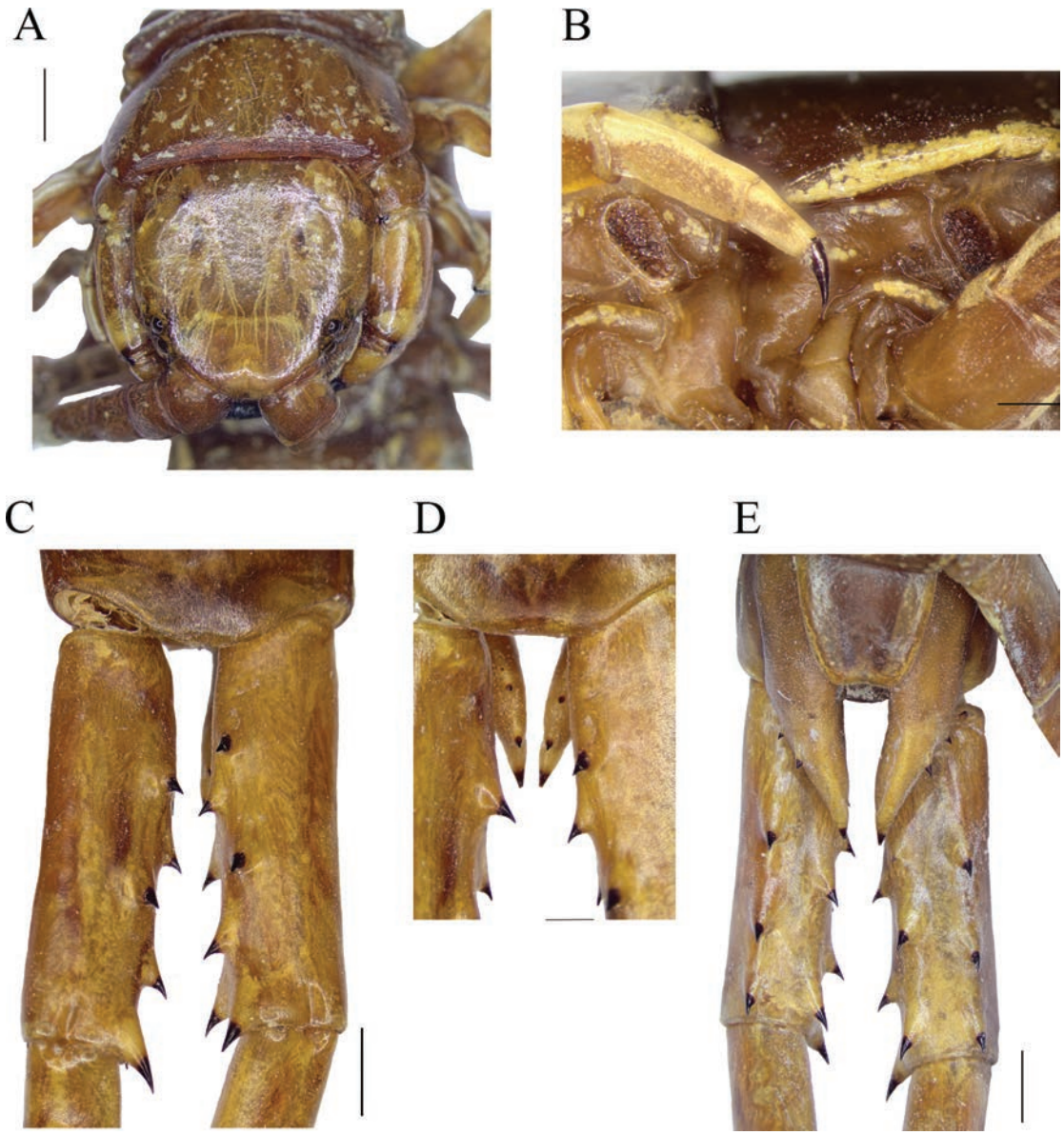

Figure 7. *Ethmostigmus rubripes rubripes* (Brandt, 1840) (ZMH-A00016061). Previously included in the type series of *S. spinosissima* under the label "Mus. Paris I.XI.03" **A** cephalic plate and tergite 1, dorsal view **B** left spiracles on segments 7 and 8 **C** UL prefemur, dorsal view **D** coxopleuron, dorsal view **E** ultimate leg-bearing segments, coxopleuron and ultimate leg prefemora, ventral view. Scale bars: 0.5 mm (**B, D**); 1 mm (**A, C, E**).

features that are obviously not present in the specimen "Mus. Paris. I.IX.03". On the basis of these morphological characters, and despite the fact that this subspecies has not been reported in the Philippines, the specimen *S. spinosissima* "Mus. Paris. I.IX.03" is here identified as *Ethmostigmus rubripes rubripes*, and therefore excluded from the type series of *S. spinosissima* (ICZN 1999: Recommendation 72B).

Non-inclusion of the MNHN *S. spinosissima* specimens as part of the type series

In addition to the material stored at the ZMH collection (Kraepelin 1903; Fig. 2A–C), Kraepelin (1904b) reported the presence of additional specimens of *S. spinosissima* at the MNHN collection. In that author's catalogue, three sets of *S. spinosissima* specimens were classified in a list according to their locality, namely: specimen/s from Luzon, det. 1875 by Laglaize [samples lost]; Jar N° 388 comprising ten specimens from Dolores, Tayabas Province (currently Quezon) [placed erroneously in the Camarines Peninsula]; and Jar N° 387, containing one specimen from Manila. The specimens in the two jars were also identified as *S. multidens* Newport, 1844 by Eugène Simon prior to Kraepelin's work (1904b) (see Materials and methods section). Morphologically, the ten specimens in jar N°388 fit with the redescription of *S. spinosissima* type series. The additional specimen in jar N°387 is confirmed as *S. paradoxa* due to the following morphological traits: antennae reaching T5, 19 antennal articles (right antenna damaged), first basal four dorsally and 5½ ventrally glabrous; punctation only in the anterior part of cephalic plate; legs 1–18 with one tarsal spur; free edge of the coxopleuron long, extending beyond the T21 with a large coxopleural process ending with two spines; and finally, the right UL (left UL regenerated) with the seven diagnostic, extremely long spinous processes, tipped with an almost straight spine, disposed in the regular prefemoral formula for this species (VL: 2, V: 0, VM: 1, M: 1, DM 2 and SP: 1; Fig. 8B–D).

Despite Kraepelin's knowledge of these eleven specimens in the MNHN collection (Kraepelin 1904b), no evidence was found to suggest that these samples were used for the original description of *S. spinosissima* (Kraepelin 1903; ICZN 1999: Art. 72.4.1.1). In his MNHN catalogue from 1904, Kraepelin (1904b) did not mention the type status of any *S. spinosissima* specimens stored there. On the contrary, the terms "Type", "Types!", and "Co-types!" were clearly ascribed to other specimens in those publications (Kraepelin 1904a, b). Some of these samples were components of a type series divided between the MNHN and ZMH collections (see Kraepelin 1904a, b; Thofern et al. 2021), but again, there was no evidence of this for *S. spinosissima*. Regarding Kraepelin's labels, he did not mention the type status of the MNHN *S. spinosissima* specimens, but again, indicated this status in the labels of other specimens belonging to species described by himself or other authors (Kraepelin 1903, 1904a, b; Doménech 2024). Therefore, this lack of explicit designation can only be understood as an intentional act by Kraepelin's of non-declaration of *S. spinosissima* specimens from the MNHN collection as part of the type series.

In addition to this absence of explicit designations, four other relevant considerations for not including of the MNHN specimens in the type series of *S. spinosissima* are as follows:

1) different publication year involving other MNHN specimens (1904, a year after the original description of *S. spinosissima* which was based exclusively on animals stored in Hamburg (Kraepelin 1903, 1904a, b; ICZN 1999: Art. 72.4.1.1);
2) Kraepelin's reference to himself in the text as *S. subspinipes* var. *spinosissma* Kraepelin [1903] in his 1904b study is impossible as there was no previous work describing the species; ICZN 1999: Chapters 3–6);
3) incompatibility between the size of the species detailed in the original description versus those of the MNHN specimens (up to 150 mm [actual 146] vs up to 176 mm) proving that Kraepelin did not use these much larger specimens in his 1903 description (see Table 1; Fig. 8A; ICZN 1999: Art. 72.4.1);
4) the presence of several Kraepelin documents confirming the exclusive type status of the ZMH specimens (Fig. 2A–C; Kraepelin 1903).

Therefore, in the absence of evidence and in the presence of other data arguing against inclusion, the consideration of the specimens from MNHN collection as part of the type series of *S. spinosissima* (Thofern et al. 2021) is finally discarded.

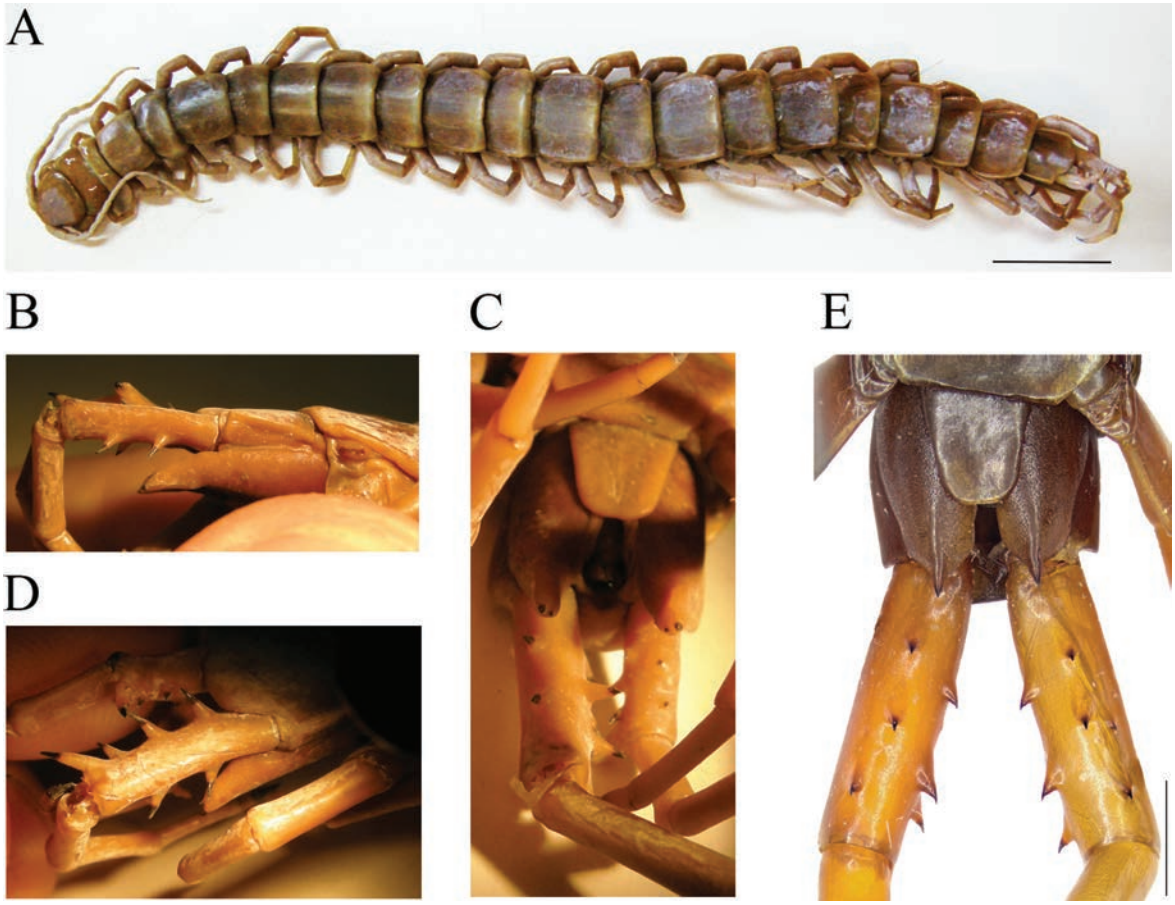

Figure 8. A–D *Scolopendra paradoxa* Doménech, 2018; non-type (MNHN N° 387), identified by Kraepelin (1904b) as *S. spinosissima* (total length 176 mm) **E** *S. spinosissima*; non-type (CEUA016-Mr0009, voucher) **A** habitus, dorsal view **B** coxopleuron and ultimate legs prefemur, right lateral view **C** ultimate leg-bearing segment and ultimate legs prefemur, ventral view **D** right ultimate leg prefemoral spinous processes (left ultimate leg regenerated), dorsolateral view **E** ultimate leg-bearing segment and ultimate legs prefemora, ventral view. Notice the smaller extra aberrant median VL spinous process in the left prefemur observed exclusively in this specimen. Scale bars: 1 mm (**E**); 20 mm (**A**).

Remarks on the *S. spinosissima* type series collector, depositories history, and type locality

In 1903, Karl Kraepelin described this taxon on the basis of specimens stored at the ZMH, which were previously loaned by the MNHN collection (Kraepelin 1903; Weidner 1960; Rack 1974; Thofern et al. 2021; see also ZMH file cards and Fig. 2B, C). However, in the MNHN, non-direct data involving the collector of *S. spinosissima* type series was located. In 1904, Kraepelin also observed, labelled, and registered the presence of other *S. spinosissima* specimens at the MNHM collection (see above; Kraepelin 1904b). Despite the fact that his catalogue was more accurate than his specimen labels, Kraepelin provided identical localities for almost all specimens deposited in Paris and in Hamburg (Fig. 2B, C; Kraepelin 1903, 1904b). Additionally, the specimens in the Paris collection date back to 1902. According to Kraepelin (1904b), the type series from Hamburg ("Mus. Paris") and date of description (1903) offered chronological compatibility, which suggests that the specimens from the ZMH and MNHN collections were collected simultaneously by the same collector. All this points to H. W. Brölemann, a taxonomist with confirmed participation in an expedition to the Philippines in 1902 (see Kraepelin 1904a, b). Therefore, it is probable that this collector deposited some *S. spinosissima* specimens in the MNHN collection and permanently loaned the remaining ones (making up the type series) to the ZMH collection (Weidner 1960; Rack 1974; Doménech et al. 2018; Thofern et al. 2021).

The previous type locality of *S. spinosissima* was simply detailed as Philippines by Kraepelin (1903). However, according to the ZMH collection data (Fig. 2A–C), the lectotype and hence the type locality are now bound to Manila, while the paralectotype locality is placed in the Camarines area. Despite lack of confirmation, this ZMH information, in combination with the previous MNHN data (Kraepelin 1903, 1904b; see also Examined material), suggests that the paralectotypes are also from Dolores, Tayabas Province (currently in Quezon), and not from somewhere in the Camarines Peninsula where no other Dolores exists, or existed (Fig. 1C).

Taxonomy of *S. spinosissima* voucher and use of its DNA barcode

In its integrative work, Doménech et al. (2018) analysed the COI partial sequence of the specimen CEUA016-Mr0009, which was identified as *S. spinosissima* (Table 1, Fig. 8E; but see also Doménech et al. 2018: fig. 15; Buckner et al. 2021). When this voucher was compared with the types of *S. paradoxa*, the morphological and molecular features showed that these specimens belong to two distinct taxa (Doménech et al. 2018). In this work, the morphology of this specimen was compared with the *S. spinosissima* lectotype, and both specimens were found to be conspecific (Table 1; Figs 5E, 8E). This confirms that the previous identification of the voucher of *S. spinosissima* was correct and is also resolved in the clear molecular and taxonomic separation of *S. spinosissima* and *S. paradoxa*.

Revised key for the species of *Scolopendra* from Philippines

Note: Due to insufficient data, *S. multidens* Newport, 1844 is excluded from the Philippines faunal catalogue until new evidence confirms its presence in the archipelago (see below).

1 4 basal antennal articles glabrous dorsally **2**
– 6 or more basal antennal articles glabrous dorsally **3**
2 Coxopleuron not clearly extending beyond the T21 posterior edge. Prefemoral formula: VL: 1, V: 2, VM: 2, M: 1, DM: 2, SP: 1.... ***S. spinosissima* Kraepelin, 1903**
– Coxopleuron clearly extending beyond the T21 posterior edge. Prefemoral formula: VL: 2, V: 0, VM: 1, M: 1, DM: 2, SP: 1..... ***S. paradoxa* Doménech, 2018**
3 T21 with median suture ..... ***S. morsitans* Linnaeus, 1758**
– T21 without median suture **4**
4 Prefemoral formula VL: 2, V: 0, VM: 0, M: 2 (1), DM: 2 (1), SP: 2. Coxopleural process with 2 AP plus 0–1 SAP spines..... ***S. subspinipes* Leach, 1816**
– Prefemoral formula VL: 3, V: 3, VM: 2, M: 2, DM: 2, SP: 4–6. Coxopleural process with 4, rarely with 3 AP spines..... ***S. subcrustalis* Kronmüller, 2009**

Discussion

The designation of the type series of *S. spinosissima* was necessary to clarify the morphological boundaries of this species, and the identities of the types and vouchers of *S. spinosissima* and *S. paradoxa*. Apart from the more precise type locality, the major improvement of this *S. spinosissima* redescription is the revised UL prefemoral processes formula. This is now more precise (i.e., V: 2), substituting the previously inaccurate range-based formula (i.e., V: 2–3). Also the position of one of the spinous processes, previously placed in the V position, was clarified as actually being on the distal VL. Other relevant morphological features added are the length, shape, and relative position of the coxopleuron in respect of the coxopleural process, the number of legs with a tarsal spur, the presence of the SS paramedian sulci, and descriptions of antennal setae distribution, tegument punctuation, and spinulation variations of the coxopleural processes.

Another important progress was the comparative morphological analysis of the voucher specimen CEUA016-Mr0009 of *S. spinosissima*, for which *S. spinosissima* sensu Doménech et al. (2018) was confirmed as *S. spinosissima* sensu Kraepelin (1903). This demonstrated that *S. paradoxa* was not described before 2018. All those facts support the previous morphological, molecular, and taxonomic outcomes (Doménech et al. 2018) for these now clearly and objectively separated species.

Repeated misidentifications of the historical specimens of *S. spinosissima* as *S. multidens* (see Examined materials), a species with only a single old citation from Mindanao (Wang 1962) (Fig. 2B), suggest that the presence of this taxon in the Philippines should be reconsidered. *Scolopendra multidens* has only been reported from southwest continental Asia, Java (Indonesia), and doubtfully from New Guinea (Bonato et al. 2016; Siriwut et al. 2015, 2016). The taxonomic re-evaluation of the specimens reported by Wang (1962) and new samples from Mindanao, New Guinea, and nearby areas could solve all these questions.

Finally, this study also revealed two distinct taxonomic criteria for the identification of the two *E. rubripes* subspecies (compare Schileyko and Stagl 2004 with Joshi and Edgecombe 2018). Following the preference for the depicted syntype (Joshi and Edgecombe 2018), the presence of *E. rubripes platycephalus* in the Philippines (Schileyko and Stagl 2004; Schileyko and Stoev 2016) needs a re-evaluation and the specimen from the Spratly Islands (Schileyko and Stagl 2004) should be assigned to *E. rubripes rubripes*. Due to the mor-

phological variability also observed between *E. rubripes* s. str. (Schileyko and Stagl 2004) and the two currently accepted subspecies, these taxa require new standardized diagnostic criteria and re-examination of taxonomic rank for the considerable distinct subspecies *E. rubripes spinosus* (Newport, 1844).

This taxonomic assessment of two species of *Scolopendra* is a primary step towards increasing biodiversity knowledge and developing conservation strategies involving these venomous arthropods with potential for agricultural and pharmaceutical applications.

Acknowledgements

The author sincerely thanks S. Rojo (UA), V. M. Barberá (UA), and E. Larriba (Universitat Miguel Hernández (UMH), Elx, Spain) for constructive advice during the preparation this manuscript. The author is also grateful to N. Dupérré and D. Harms (ZMH) and C. Rollard, E-A. Legin and J. J. Geoffroy (MNHN) for help in specimens' analysis, graphic documents, and the indispensable information provided. Also, sincere gratitude to W. Siriwut (Nakhon University, Thailand) and M. A. Alonso Zarazaga (ICZN ex-commissioner; National Museum of Natural Sciences, Madrid, Spain) for their bibliographic and nomenclatural advices, respectively; to E. Währen and J. H. Raquel for providing field pictures, location data and other relevant information involving *S. spinosissima*; to A. Aracil and M. I. Lillo (UA) for their assistance in image processing; and to the NOAA/NWS staff for their permission to use their images. Grateful acknowledgement to J. B. Warren and E. C. Jarvis for their work correcting spelling. For their invaluable support, acknowledgements are extended to S. A. Yap, G. D. Sapin, G. A. Lantican, J. J. Apolinario (PAE), P. A. C. Buenavente (PNM), V. San Juan (PNU) and, especially, to M. C. Amaro Jr. (BMB-DENR) and P. Bumanglag (WRD-DENR). Finally, the author wants to express his gratitude to the late K. M. F. M. Kraepelin, whose texts have become a source of inspiration to ongoing understanding these fascinating creatures.

Additional information

Conflict of interest

The author has declared that no competing interests exist.

Ethical statement

No ethical statement was reported.

Funding

No funding was reported.

Author contributions

The author solely contributed to this work.

Author ORCIDs

Carles Doménech https://orcid.org/0000-0003-1890-9434

Data availability

All of the data that support the findings of this study are available in the main text.

References

Acuña DC, Isagani N, Pitogo KME (2021) Predation on a McClung's Philippine False Coralsnake, *Hemibungarus mcclungi* (Weigmann 1835), by a Giant Spiny Centipede, *Scolopendra spinosissima* Kraepelin 1903, on Luzon Island, the Philippines. Reptiles & Amphibians 28 (3): 417–419. https://doi.org/10.17161/randa.v28i3.15782

Attems C (1930) Myriapoda. *2. Scolopendromorpha*. Das Tierreich 54: 308. https://doi.org/10.1515/9783112373002

Bonato L, Edgecombe GD, Lewis JGE, Minelli A, Pereira LA, Shelley RM, Zapparoli M (2010) A common terminology for the external anatomy of centipedes (Chilopoda). ZooKeys 69: 17–51. https://doi.org/10.3897/zookeys.69.737

Bonato L, Chagas-Junior A, Edgecombe GD, Lewis JGE, Minelli A, Pereira LA, Shelley RM, Stoev P, Zapparoli M (2016) ChiloBase 2.0 – A World Catalogue of Centipedes (Chilopoda). https://chilobase.biologia.unipd.it [accessed 15 July 2024]

Brandt JF (1840) Observations sur les espèces qui composent la genre *Scolopendra* suivies des caractères des espèces qui se trouvent dans le Museum zoologique de l'Académie des Sciences de St. Pétersbourg et de quelques coups d'œil sur leur distribution géographique. Bulletin Scientifique publié par l'Académie Impériale des Sciences de Saint Pétersbourg 7(11): 148–160.

Buckner JC, Sanders RC, Faircloth BC, Chakrabarty P (2021) The critical importance of vouchers in genomics. eLife 10: e68264. https://doi.org/10.7554/eLife.68264

Calhoun JV, Hawkins RL (2016) Notes about early entomological type labels in the Museum of Comparative Zoology, Harvard University. News of the Lepidopterists' Society 58: 114–118.

Demange JM, Richard J (1969) Morphologie de l'appareil génital mâle des Scolopendromorphes et son importance en systèmatique (Myriapodes Chilopodes). Bulletin du Muséum national d'Histoire naturelle, Série 2 40(5): 968–983.

Doménech C (2024) Taxonomic and nomenclatural reassessment of the Iberian Peninsula's *nomina obscura*, *Scolopendra viridipes* Dufour, 1820 and *S. chlorotes* L. Koch in Rosenhauer, 1856 (Chilopoda, Scolopendromorpha, Scolopendridae). ZooKeys 1208: 49–80. https://doi.org/10.3897/zookeys.1208.122126

Doménech C, Barbera VM, Larriba E (2018) A phylogenetic approach to the Philippines endemic centipedes of the genus *Scolopendra* Linnaeus, 1758 (Scolopendromorpha, Scolopendridae), with the description of a new species. Zootaxa 4483(3): 401–427. https://doi.org/10.11646/zootaxa.4483.3.1

Edgecombe GD, Giribet G (2007) Evolutionary biology of centipedes (Myriapoda: Chilopoda). Annual Review of Entomology 27(52): 151–170. https://doi.org/10.1146/annurev.ento.52.110405.091326

Harms D, Dupérré N (2018) An annotated type catalogue of the camel spiders (Arachnida: Solifugae) held in the Zoological Museum Hamburg. Zootaxa 4375 (1): 1–58. https://doi.org/10.11646/zootaxa.4375.1.1

ICZN (1999) International Code of Zoological Nomenclature. Fourth Edition. The International Trust for Zoological Nomenclature, London, UK, 124 pp.

iNaturalist (2022) iNaturalist. https://www.inaturalist.org [accessed 12 April 2022]

Iorio E (2003) Morphologie externe des appareils génitaux mâle et femelle de la famille Scolopendridae (Chilopoda, Scolopendromorpha). Bulletin de Phyllie 16(2): 10–16.

Joshi J, Edgecombe GD (2018) Molecular phylogeny and systematics of the centipede genus *Ethmostigmus* Pocock, 1898 (Chilopoda: Scolopendromorpha) from peninsular India. Invertebrate Systematics 32(6): 1316–1335 https://doi.org/10.1071/IS18030

Kraepelin K (1903) Revision der Scolopendriden. Mitteilungen aus dem Naturhistorischen Museum in Hamburg 20: 1–276.

Kraepelin K (1904a) Catalogue des Scolopendrides des collections du Muséum d'histroire naturelle de Paris. (Collection du Muséum déterminée par M. le professeur Karl Kraepelin, et collection H. W. Brölemann). Première partie. – Scolopendrides en dehors du genre Scolopendra. Bulletin du Muséum d'Histoire naturelle 10(5): 243–253.

Kraepelin K (1904b) Catalogue des Scolopendrides des collections du Muséum d'histroire naturelle de Paris. (Collection du Muséum déterminée par M. le professeur Karl Kraepelin, et collection H. W. Brölemann). Deuxième partie. – Genre *Scolopendra*. Bulletin du Muséum d'Histoire naturelle 10(6): 316–325.

Kronmüller C (2009) A new species of Scolopender from the Philippines (Chilopoda: Scolopendridae). Arthropoda 17(1): 48–51.

Kronmüller C, Lewis JGE (2015) On the function of the ultimate legs of some Scolopendridae (Chilopoda, Scolopendromorpha). In: Tuf IH, Tajovský K (Eds) Proceedings of the 16th International Congress of Myriapodology, Olomouc, Czech Republic. ZooKeys 510: 269–278. https://doi.org/10.3897/zookeys.510.8674

Leach WE (1814) Crustaceology. In: Brewster D (Ed.) The Edinburgh Encyclopaedia, vol. 7. Balfour, Edinburgh, 383–437.

Leach WE (1816) A tabular view of the external characters of four classes of animals, which Linné arranged under Insecta; with the distribution of the genera composing three of these classes into orders, &c. and descriptions of several new genera and species. Transactions of the Linnean Society of London 11(2): 306–400. https://doi.org/10.1111/j.1096-3642.1813.tb00065.x

Lewis JGE (2010) A key and annotated list of the *Scolopendra* species of the Old World with a reappraisal of *Arthrorhabdus* (Chilopoda: Scolopendromorpha: Scolopendridae). International Journal of Myriapodology 1(3): 83–122. https://doi.org/10.1163/187525410X12578602960380

Linnaeus C (1758) Systema naturae per regna tria naturae, secundum classes, ordines, genera, species cum characteribus, diferentiis, synonymis, locis. Tomus I. Editio Decima, Reformata. Laurentii Salvii, Holmiae. https://doi.org/10.5962/bhl.title.542

Lohmann H (1915) Karl Kraepelin als Gelehrter und Forscher. Verhandlungen des Naturwissenschafftlischen Vereins in Hamburg 7(23): 15–32.

Monod L, Dupérré N, Harms D (2019) An annotated catalogue of the scorpion types (Arachnida, Scorpiones) held in the Zoological Museum Hamburg. Part I: Parvorder Iurida Soleglad & Fet, 2003. Evolutionary Systematics 3(2): 109–200. https://doi.org/10.3897/evolsyst.3.37464

Newport G (1844) Monograph of the class myriapoda order chilopoda; with observations on the general arrangement of the articulata. Transactions of the Linnean Society of London 19(3): 265–302. https://doi.org/10.1111/j.1096-3642.1842.tb00368.x

Pocock RI (1898) List of the Arachnida and "Myriapoda" obtained in Funafuti by Prof. W.J. Sollas ad Mr. Stanley Gardiner, and in Rotuma by Mr. Stanley Gardiner. Annals and Magazine of Natural History 1(4): 321–329. https://doi.org/10.1080/00222939808677979

Rack G (1974) Die Entomologischen Sammlungen des Zoologischen Staatsinstituts und Zoologischen Museums Hamburg. III. Teil (Nachtrag) Chilopoda und Progoneata. Mitteilungen des Hamburger Zoologischen Museums Hamburg 70: 105–118.

Ratcliffe BC (2013) Best Writing and Curatorial Practices for Describing a New Species of Beetle: A Primer. The Coleopterists Bulletin 67(2): 107–113. https://doi.org/10.1649/0010-065X-67.2.107

Schileyko AA, Stagl V (2004) The collection of scolopendromorph centipedes (Chilopoda) in the Natural History Museum in Vienna: a critical re-evaluation of former taxonomic identifications. Annalen des Naturhistorischen Museum in Wien 105B: 67–137.

Schileyko AA, Stoev PE (2016) Scolopendromorpha of New Guinea and adjacent islands (Myriapoda, Chilopoda). Zootaxa 4147(3): 247–280. https://doi.org/10.11646/zootaxa.4147.3.3

Schileyko AA, Vathera V, Edgecombe GD (2020) An overview of the extant genera and subgenera of the order Scolopendromorpha (Chilopoda): a new identification key and updated diagnoses. Zootaxa 4825(1): 1–64. https://doi.org/10.11646/zootaxa.4825.1.1

Siriwut W, Edgecombe GD, Sutcharit C, Panha S (2015) The centipede genus *Scolopendra* in mainland Southeast Asia: molecular phylogenetics, geometric morphometrics and external morphology as tools for species delimitation. PLoS ONE 10(8): e0135355. https://doi.org/10.1371/journal.pone.0135355 [Erratum in PLoS ONE 10 (9): e0139182]

Siriwut W, Edgecombe GD, Sutcharit C, Tongkerd P, Panha S (2016) A taxonomic review of the centipede genus *Scolopendra* Linnaeus, 1758 (Scolopendromorpha, Scolopendridae) in mainland Southeast Asia, with description of a new species from Laos. ZooKeys 590: 1–124. https://doi.org/10.3897/zookeys.590.7950

Thofern D, Dupérré N, Harms D (2021) An annoted type catalogue of the centipedes (Myriapoda: Chilopoda) held in the Zoological Museum Hamburg. Zootaxa 4977(1): 1–103. https://doi.org/10.11646/zootaxa.4977.1.1

Thomas GWC, Dohmen E, Hughes DST, Murali SC, Poelchau M, Glastad K, Anstead CA, Ayoub NA, Batterham P, Bellair M, Binford GJ, Chao H, Chen YH, Childers C, Dinh H, Doddapaneni HV, Duan JJ, Dugan S, Esposito LA, Friedrich M, Garb J, Gasser RB, Goodisman MAD, Gundersen-Rindal DE, Han Y, Handler AM, Hatakeyama M, Hering L, Hunter WB, Ioannidis P, Jayaseelan JC, Kalra D, Khila A, Korhonen PK, Lee CE, Lee SL, Li Y, Lindsey ARI, Mayer G, McGregor AP, McKenna DD, Misof B, Munidasa M, Munoz-Torres M, Muzny DM, Niehuis O, Osuji-Lacy N, Palli SR, Panfilio KA, Pechmann M, Perry T, Peters RS, Poynton HC, Prpic NM, Qu J, Rotenberg D, Schal C, Schoville SD, Scully ED, Skinner E, Sloan DB, Stouthamer R, Strand MR, Szucsich NU, Wijeratne A, Young ND, Zattara EE, Benoit JB, Zdobnov EM, Pfrender ME, Hackett KJ, Werren JH, Worley KC, Gibbs RA, Chipman AD, Waterhouse RM, Bornberg-Bauer E, Hahn MW, Richards S (2020) Gene content evolution in the arthropods. Genome biology 21(1): 15. https://doi.org/10.1186/s13059-019-1925-7

Wang Y-HM (1951) The Myriapoda of the Philippine Islands. PhD These, University of Utah, USA.

Wang Y-HM (1962) The Chilopoda of the Philippine Islands (A revision of the Myriapoda of the Philippine Islands Part 2). Quarterly Journal of the Taiwan Museum 15(1–2): 79–106.

Weidner H (1960) Die Entomologischen Sammlungen des Zoologischen Staatsinstituts und Zoologischen Museums Hamburg. Teil III. Chilopoda und Progoneata. Mitteilungen aus dem Hamburgischen Zoologischen Museum und Institut. Jahrbuch der Hamburgischen Wissenschafftlischen. Anstalten 58: 57–104.

Wheeler TA, Huber JT, Currie DC (2001) Label Data Standards for Terrestrial Arthropods. Biological Survey of Canada (Terrestrial Arthropods) 8: 1–20.

ZooKeys 1215: 335–358 (2024)
DOI: 10.3897/zookeys.1215.128795

Research Article

Phylogeography of the Colombian water snake *Helicops danieli* Amaral, 1938 (Reptilia, Squamata, Dipsadidae) with comments on the systematics and evolution of the genus *Helicops* Wagler, 1828

Juan Pablo Hurtado-Gómez[1], Juan M. Daza[2], Mario Vargas-Ramírez[3,4], V. Deepak[1,5], Uwe Fritz[1]

1 *Museum of Zoology, Senckenberg Natural History Collections Dresden, A.B. Meyer Building, 01109 Dresden, Germany*
2 *Grupo Herpetológico de Antioquia (GHA), Instituto de Biología, Universidad de Antioquia, Medellín, Colombia*
3 *Grupo Biodiversidad y Conservación Genética, Instituto de Genética, Universidad Nacional de Colombia, Bogotá, Colombia*
4 *Estación de Biología Tropical Roberto Franco (EBTRF), Universidad Nacional de Colombia, Villavicencio, Colombia*
5 *School of Natural and Environmental Sciences, Newcastle University, Newcastle upon Tyne NE1 7RU, UK*
Corresponding author: Uwe Fritz (uwe.fritz@senckenberg.de)

Abstract

The genus *Helicops* Wagler, 1828 comprises 20 species of semiaquatic snakes. It is mostly distributed in the cis-Andean region of South America, with only two trans-Andean species (*H. danieli*, *H. scalaris*). *Helicops danieli* is endemic to Colombia and occurs through most of the trans-Andean region. Herein two mitochondrial and two nuclear genomic markers were sequenced for 16 samples of *H. danieli* across most of its distribution range to understand its phylogeography. A dated tree was also generated with additional sequences from previous studies to infer the divergence times between *H. danieli* and its cis-Andean congeners and of lineages within *H. danieli*. Using previously published data, ancestral states were estimated for putative phenotypic synapomorphies for the major clades of *Helicops*. For *H. danieli*, four clades corresponding to the main river basins within its distribution were recovered. Our dated tree suggests that the ancestor of *H. danieli* diverged from its closest congeners in the late Miocene (8.7 Mya), which can be associated with the closure of the Andalucia Pass, south of the Eastern Cordillera. Divergence within *H. danieli* commenced 1.1 Mya. Within the genus *Helicops*, two distinct hemipenial morphologies were observed, which are suggested as putative synapomorphies for the two most basal clades. Recognition of these two clades as distinct subgenera, *Helicops* sensu stricto and *Tachynectes* Fitzinger, 1843 is proposed. For the junior homonym *Tachynectes* von der Mark, 1863, rarely applied to fossil fishes, the replacement name *Ichthyotachynectes* **nom. nov.** is introduced. Furthermore, the evolution of another four phenotypic traits in *Helicops* and their phylogenetic utility are discussed.

Key words: Actinoptergyii, Andalucia Pass, *Ichthyotachynectes* nom. nov., Myctophidae, Serpentes, subgenera, *Tachynectes*

OPEN ACCESS

Academic editor: Robert Jadin
Received: 1 June 2024
Accepted: 4 September 2024
Published: 17 October 2024

ZooBank: https://zoobank.org/11120B98-7E4D-4E1B-980A-2975059B1C9C

Citation: Hurtado-Gómez JP, Daza JM, Vargas-Ramírez M, Deepak V, Fritz U (2024) Phylogeography of the Colombian water snake *Helicops danieli* Amaral, 1938 (Reptilia, Squamata, Dipsadidae) with comments on the systematics and evolution of the genus *Helicops* Wagler, 1828. ZooKeys 1215: 335–358. https://doi.org/10.3897/zookeys.1215.128795

Introduction

The genus *Helicops* Wagler, 1828 currently contains 20 species, distributed through most of the South American subcontinent (Moraes-da-Silva et al. 2022; Schöneberg and Köhler 2022). Snakes in this genus are characterized by having semiaquatic habits, eyes and nostrils dorsally located, dorsal scales keeled, a single internasal scale, and an S-shaped sulcus spermaticus in the hemipenial lobes (Zaher 1999; Schöneberg and Köhler 2022). All *Helicops* species are distributed in cis-Andean South America, except for *H. scalaris* Jan, 1865, from the Lake Maracaibo Region, and *H. danieli* Amaral, 1937, which is confined to the trans-Andean lowlands of Colombia, the inter-Andean valley of the Magdalena River, the Caribbean floodplains, and the Pacific region (Rossman 2002a; Citeli et al. 2021).

Helicops danieli was originally described by Amaral (1937) based on a single specimen from the Río Carare, Santander, Colombia, on the eastern edge of the Magdalena Valley. Later, several authors extended the knowledge about the species' morphology, describing the overall variation in scalation, measurements, and hemipenial morphology (Yuki 1994; Rossman 2002a; Citeli et al. 2021). Initially, Amaral (1937) suggested that *H. danieli* was related to *H. angulatus* and *H. scalaris*. Later, Nunes (2006) developed a morphology-based phylogenetic hypothesis and included *H. danieli* in a phylogenetic context for the first time. According to Nunes (2006), *H. danieli* is sister to a clade containing *H. angulatus*, *H. gomesi*, *H. pastazae*, *H. petersi*, *H. polylepis*, and *H. scalaris*. To date, none of the recent molecular-based phylogenies has included *H. danieli* (Costa et al. 2016; Moraes-da-Silva et al. 2019, 2021, 2022).

Helicops danieli is widely distributed across the trans-Andean lowlands of Colombia. This region comprises a variety of ecosystems and geographic units, including dry and moist forests (Etter et al. 2021), inter-Andean valleys, Pacific lowlands, the Caribbean plain, and several basins primarily associated with the Magdalena, Cauca, and Atrato rivers (Hernández-Camacho et al. 1992; Lynch et al. 1997; Mesa-S. et al. 2016). This suggests that phylogeographic variation exists in *H. danieli*.

In recent years, research on the systematics and taxonomy of the genus *Helicops* has expanded considerably, with six out of the twenty species described in the last two decades (da Frota 2005; Kawashita-Ribeiro et al. 2013; Costa et al. 2016; Moraes-da-Silva et al. 2019, 2021, 2022). Additionally, the number of taxa studied using molecular genetic approaches has increased, with up to 11 *Helicops* species analyzed to date (Moraes-da-Silva et al. 2021). Recent studies have mapped various phenotypic traits to identify synapomorphies, some of which (e.g., color pattern, subcaudal keels, reproductive mode; Moraes-da-Silva et al. 2022) have been useful for supporting minor clades within *Helicops*. However, no synapomorphies have been identified for the major clades of *Helicops*.

For the present study, we generated a dataset of four molecular markers to infer the phylogenetic position as well as the genetic and geographic structure of *H. danieli*. Additionally, we present a fossil-calibrated time tree for *Helicops* to estimate the divergence time for *H. danieli* and its cis-Andean congeners. Finally, we infer the ancestral states for five phenotypic characters of *Helicops* using our molecular phylogeny, discuss the evolution and phylogenetic value of these traits, and propose a subgeneric classification for *Helicops*.

Materials and methods

Sampling and laboratory procedures

We used 16 samples of *H. danieli* from most of its range (Fig. 1A) and one of *H. pastazae* from tissues deposited in the Banco de Tejidos de la Biodiversidad, Instituto de Genética, Universidad Nacional de Colombia, Bogotá, Colombia (**BTBC**) and the Museo de Herpetología, Universidad de Antioquia, Medellín, Colombia (**MHUA**) (Suppl. material 1: table S1). DNA was extracted using the innuPREP DNA Micro Kit (Analytik Jena GmbH, Jena, Germany) following the manufacturer's protocol. We obtained sequences from two mitochondrial (16S:

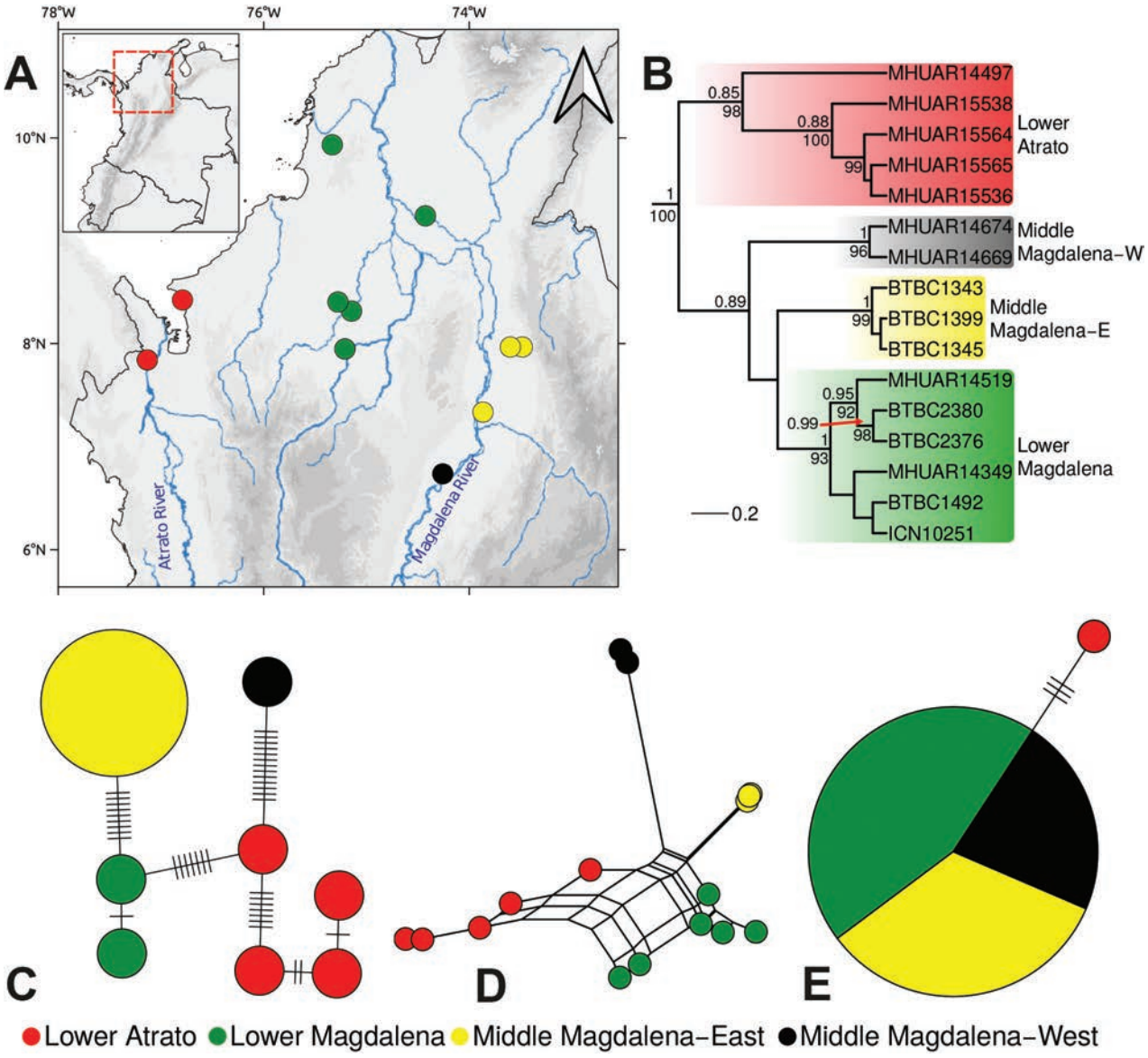

Figure 1. A Genetic sampling and clades for *Helicops danieli* **B** Bayesian tree for *H. danieli* lineages (cropped from the complete tree, see Suppl. material 2: fig. S1) based on the concatenated alignment of three mitochondrial and four nuclear molecular markers (4624 bp); values above branches indicate Bayesian posterior probabilities (> 0.85), below branches are UltraFastBootstrap values (> 90) from the ML tree (Suppl. material 2: fig. S2) **C** haplotype network for *H. danieli* based on the concatenated mtDNA alignment of 16S and cyt *b* sequences **D** Neighbor-Net for *H. danieli* samples based on the same concatenated mtDNA alignment **E** haplotype network for *H. danieli* samples based on the nuclear Rag 1 fragment.

532 bp, cyt *b*: 770 bp) and two nuclear markers (C-mos: 566 bp, Rag1: 826 bp). PCR was conducted in a reaction volume of 25 µl, containing 20–40 ng of DNA, 1 unit *Taq* polymerase (Bioron GmbH, Ludwigshafen, Germany), the buffer recommended by the supplier (complete, 10×, containing $MgCl_2$), 0.2 µM of each dNTP (Carl Roth GmbH + Co. KG, Karlsruhe, Germany), and 0.4 µM of each primer. Primers and PCR cycling conditions are described in the Suppl. material 1: table S2. Purification and sequencing followed Fritz et al. (2012). Sequences were edited with GENEIOUS 9.1.8 (Kearse et al. 2012) and aligned using MAFFT 7.39 (Katoh and Toh 2010) as implemented in GENEIOUS. To obtain a more robust hypothesis for the relationships within *Helicops*, we generated a concatenated alignment of 4624 bp length for the phylogenetic trees (see below). This alignment included three additional markers (mtDNA = 12S; nDNA = BDNF, NT3) available from previous studies (Moraes-da-Silva et al. 2019, 2021). Additional sequences for *Helicops* species and outgroups were downloaded from GenBank (Suppl. material 1: table S1). The sequences for 13 colubroid outgroup taxa originate from Zaher et al. (2019); the most distant species, the viperid *Bothrops atrox*, served for tree rooting. The individual alignments were concatenated using SEQUENCE MATRIX 1.8 (Vaidya et al. 2011). For the phylogenetic analyses, we included only one sample per species, except for *H. danieli*, for which we included all individuals, and for *H. angulatus*, which was recently retrieved as non-monophyletic (Murphy et al. 2020). For *H. angulatus*, we included one sample from Trinidad and another one from Brazil (Suppl. material 1: table S1). For the calculation of uncorrected *p* distances (see below), we included all available mitochondrial 16S and cyt *b* sequences.

Phylogenetic analyses and time-calibrated tree

The best partition scheme and substitution models for analyzing the concatenated sequences were determined using MODELFINDER (Kalyaanamoorthy et al. 2017) as implemented in IQ-TREE 2.2 (Minh et al. 2020). Model selection was performed with the parameter 'testmerge' for model selection option (-m), which implements the 'greedy' algorithm of PARTITIONFINDER 2.0 (Lanfear et al. 2016) (Suppl. material 1: table S3).

Phylogenetic trees were constructed using Maximum Likelihood (**ML**) and Bayesian Inference (**BI**). The ML tree was calculated with IQ-TREE 2.2, using partitions and substitution models obtained with MODELFINDER (Suppl. material 1: table S3). Node support for the ML tree was assessed with 5000 Ultrafast Bootstrap replicates (**UFB**), considering branches with support values of 95% and above as highly supported (Minh et al. 2013). For the BI and the relaxed molecular clock calculations (see below), we used BEAST 2.7.5 (Bouckaert et al. 2019) and two independent chains of 50 million generations, sampling every 5000th generation. For the BI analysis, we used the partitions obtained with MODELFINDER. However, substitution models were determined using BMODELTEST (Bouckaert and Drummond 2017) exploring all available models (Suppl. material 1: table S3). The Yule model was used for tree inference. For the time-calibrated tree, we applied the fast-normal relaxed clock model and three fossil calibration points from Zaher et al. (2019), as follows (fossil, minimum age, reference): (i) stem Colubroidea (Colubridae indet., 35.2 Mya; Smith 2013); (ii) stem Dipsadidae (*Paleoheterodon tiheni*, 12.5 Mya; Holman 1964, 1977);

and (iii) crown Natricidae (Natricidae incertae sedis, 13.8 Mya; Rage and Szyndlar 1986). Chain convergence and burn-in (20%) were examined using TRACER 1.7.1 (Rambaut et al. 2018). A maximum credibility tree was summarized with TREEANNOTATOR 2.7.5 implemented in BEAST 2.7.5 (Bouckaert et al. 2019). For tree annotation, plotting, and layout, we used the R program v. 4.3.1 (R Core Team 2023) in RSTUDIO (RStudio Team 2023) along with the packages 'ape' (Paradis and Schliep 2019), 'phangorn' (Schliep 2011), 'phytools' (Revell 2012), and the INKSCAPE software (https://www.inkscape.org).

Haplotype networks, Neighbor-Nets, and genetic distances

Two parsimony networks were drawn for the *H. danieli* samples using the R package PEGAS 1.2 (Paradis 2010), one for the nuclear fragment Rag1 and the other for the concatenated mitochondrial alignment (16S and cyt *b*), acknowledging that mtDNA represents a single locus. Due to the low variation in the C-mos alignment, no network was calculated for this marker.

Phylogenetic networks for the concatenated mitochondrial alignment (16S and cyt *b*) were computed using the Neighbor-Net algorithm (Bryant and Moulton 2004), implemented in the R package 'phangorn' (Schliep 2011). Given that the algorithm does not run with alignments with approximately 50% missing data (JPHG pers. obs.), specimens with only the 16S marker in the mitochondrial alignment (the shortest one) were excluded from this analysis. Due to the limited variation in the concatenated nuclear alignment, no Neighbor-Net was drawn for it.

Finally, using MEGA 11 (Tamura et al. 2021) and the pairwise deletion option, uncorrected *p* distances were computed for the 16S and cyt *b* alignments for *Helicops* species and clades retrieved for *H. danieli* in the phylogenetic trees.

Phenotypic data and ancestral state estimation

To identify putative phenotypic synapomorphies for the genus *Helicops*, we used the compiled data for all species from Murphy et al. (2020) and Moraes-da-Silva et al. (2022) on color pattern, keels on dorsal scales, subcaudal keels, and reproductive modes. Additionally, we incorporated all available information on hemipenial morphology from the literature, which included data for all *Helicops* species but *H. yacu*. The five phenotypic characters are: 1) dorsal color pattern, 2) strength of dorsal scale keels, 3) subcaudal keels, 4) reproductive mode, and 5) hemipenial lobe length.

To evaluate whether these phenotypic traits represent synapomorphies for the clades within *Helicops*, we performed an ancestral state estimation (**ASE**). First, we inferred the best fitting evolutionary model for each of the five characters, selecting among the three models equal rates (**ER**), symmetric rates (**SYM**), and all rates different (**ARD**) using the function 'fitdiscrete' in the R package 'geiger' (Harmon et al. 2007). The model with the lowest Akaike Information Criterion (AIC) value was chosen (Suppl. material 1: table S4).

For the ancestral state estimation, we used the function 'ace' in the R package 'ape'. The Bayesian phylogenetic tree cropped to the genus *Helicops* served as input, along with the chosen model for each character. Since *H. angulatus* exhibits both oviparous and viviparous reproductive modes, we coded each of the two tips for the species with a different state.

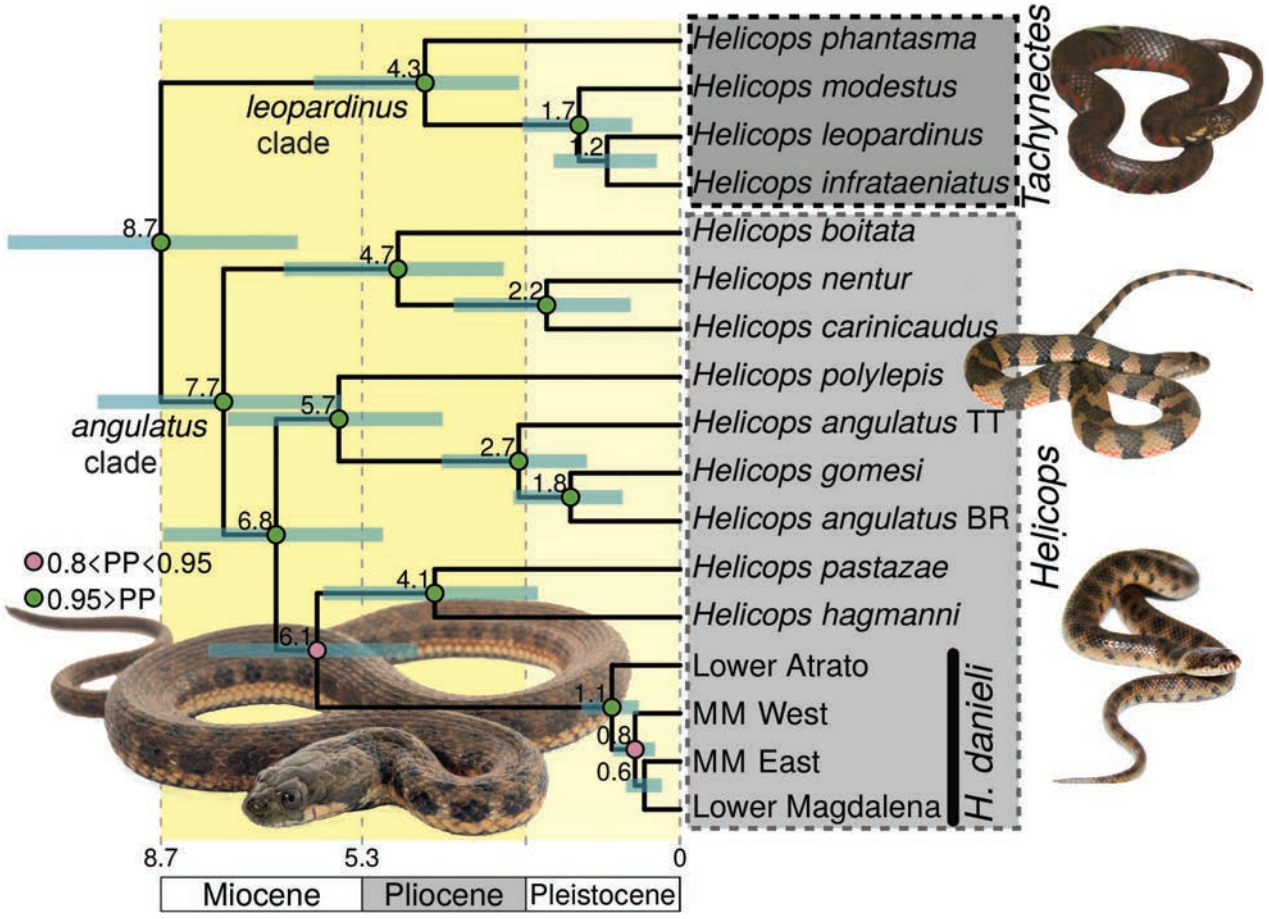

Figure 2. Bayesian time tree for the genus *Helicops* obtained with the concatenated alignment of three mtDNA and four nDNA markers, cropped from the complete tree (Suppl. material 2: fig. S1). *Helicops danieli* clades are collapsed (see Fig. 1B; Suppl. material 2: figs S1, S2). Values above branches are age estimates in million years; bluish green bars at nodes indicate 95% confidence intervals; circles at nodes represent Bayesian posterior probabilities (see legend). Boxes on branch tips and vertical names on the right indicate the subgeneric classification proposed in the present study. Abbreviations: BR, Brazil; MM, middle Magdalena; TT, Trinidad and Tobago. Photographs right: top, *H. leopardinus* (Corrientes, Argentina; A. Sabaliauskas, iNaturalist observation 94157056); center, *H. angulatus* (Guaviare, Colombia; J. P. Hurtado-Gómez); bottom, *H. pastazae* (Boyaca, Colombia; D. Gómez-Sánchez); photo left bottom, *H. danieli* (Los Katíos, Colombia; Juan M. Daza, MHUAR15536).

Results and discussion

Our phylogenetic trees returned *Helicops* as maximally supported monophylum under both the ML and BI approaches (Fig. 2; Suppl. material 2: figs S1, S2). Within *Helicops*, two main clades were consistently recovered. The first clade, termed '*leopardinus* clade', included *H. infrataeniatus*, *H. leopardinus*, *H. modestus*, and *H. phantasma* (Fig. 2). The second clade, the '*angulatus* clade', comprised the remaining species: *H. angulatus*, *H. boitata*, *H. carinicaudus*, *H. danieli*, *H. gomesi*, *H. hagmanni*, *H. nentur*, *H. pastazae*, and *H. polylepis*. Notably, *H. pastazae*, which was studied for the first time using DNA sequence data, was found to be the sister taxon of *H. hagmanni* with high support (Fig. 2; Suppl. material 2: figs S1, S2).

Helicops danieli was recovered as monophyletic with high support by both tree-building approaches (Figs 1B, 2; Suppl. material 2: figs S1, S2) and as sister to the clade containing *H. hagmanni* and *H. pastazae* in a poorly supported

Table 1. Means of interspecific uncorrected *p* distances (percentages) for 16S (below diagonal) and cyt *b* (above diagonal) sequences for *Helicops*. Sequence of taxa corresponds to Fig. 2. Cyt *b* sequences were only available for four taxa. BR, Brazil; TT, Trinidad and Tobago.

	***Helicops* species**	**1**	**2**	**3**	**4**	**5**	**6**	**7**	**8**	**9**	**10**	**11**	**12**	**13**
1	*H. danieli*		-	11.4	12.9	-	-	13.4	-	-	-	-	14.3	-
2	*H. polylepis*	5.5		-	-	-	-	-	-	-	-	-	-	-
3	*H. angulatus* TT	5.7	4.5		7.6	-	-	9.7	-	-	-	-	11.1	-
4	*H. angulatus* BR	5.6	5.6	2.6		-	-	11.2	-	-	-	-	11.8	-
5	*H. gomesi*	5.8	5.4	1.5	2.3		-	-	-	-	-	-	-	-
6	*H. hagmanni*	6.4	5.4	4.7	5.1	4.8		-	-	-	-	-	-	-
7	*H. pastazae*	4.5	4.7	4.0	4.4	4.0	3.3		-	-	-	-	14.1	-
8	*H. boitata*	6.7	6.8	7.3	7.6	7.8	7.1	7.5		-	-	-	-	-
9	*H. carinicaudus*	6.6	5.6	6.3	6.0	6.8	6.8	5.9	5.4		-	-	-	-
10	*H. nentur*	6.9	4.9	6.8	6.4	7.3	5.9	6.3	4.2	2.3		-	-	-
11	*H. phantasma*	7.3	5.2	7.3	7.1	8.0	5.9	6.4	5.4	2.8	2.8		-	-
12	*H. infrataeniatus*	6.0	5.5	6.2	6.8	6.9	6.7	5.6	6.1	4.8	4.8	4.0		-
13	*H. leopardinus*	6.3	6.1	6.7	7.1	7.2	6.9	6.3	6.1	5.5	5.5	4.2	1.0	
14	*H. modestus*	5.9	5.3	6.1	6.9	6.9	6.8	6.0	6.1	5.4	5.3	4.5	1.2	1.6

clade (Fig. 2; Suppl. material 2: figs S1, S2). Within *H. danieli*, four main clades were revealed: one from the lower Atrato River, one from the lower Magdalena River, and two from the middle Magdalena River. In the middle Magdalena Basin (as defined by Mesa-S. et al. 2016), one clade ('black') occurs east and another one ('yellow') west of the river (Figs 1A, B, 2; Suppl. material 2: figs S1, S2). These clades were corroborated by the mitochondrial haplotype networks and Neighbor-Nets (Fig. 1C, D), though not by the nuclear Rag1 haplotype network (Fig. 1E). Our mitochondrial Neighbor-Net analysis indicated that the middle Magdalena groups (east and west) are well differentiated. In contrast, those from the lower Atrato ('red') and lower Magdalena ('green') show a high degree of interconnection, despite forming separate clusters (Fig. 1D). The relationships between clades varied significantly between analyses, but with relative higher node support in the BI tree (Figs 1B, 2; Suppl. material 2: figs S1, S3).

Diversity and phylogeny of *Helicops*

The uncorrected *p* distances for the mitochondrial 16S fragment among *Helicops* species averaged 5.6%, ranging from 1.0% (between *H. leopardinus* and *H. infrataeniatus*) to 8.0% (between *H. gomesi* and *H. phantasma*; Table 1). For the cyt *b* marker, distances between *Helicops* species ranged from 9.7% (between *H. angulatus* and *H. pastazae*) to 14.3% (between *H. danieli* and *H. infrataeniatus*), averaging 11.7% (Table 1). Within *H. danieli*, uncorrected *p* distances for 16S and cyt *b* showed contrasting differentiation between the clades (Table 2). For the 16S marker, distances ranged from 0.1% (between the lower Magdalena and middle Magdalena east) to 2.0% (between the lower Atrato and middle Magdalena east). For the cyt *b* marker, distances ranged from 1.0% (between lower Atrato and lower Magdalena) to 2.0% (between lower Magdalena and middle Magdalena west).

Table 2. Means of uncorrected *p* distances (percentages) for 16S (below diagonal) and cyt *b* (above diagonal) sequences for *Helicops danieli* clades. MM, middle Magdalena.

***H. danieli* lineage**		**1**	**2**	**3**	**4**
1	Lower Atrato	-	1.7	1.1	1.0
2	MM west	1.8	-	1.9	2.0
3	MM east	2.0	0.6	-	1.1
4	Lower Magdalena	1.7	0.1	0.4	-

Our dated phylogenetic tree suggests that diversification within *Helicops* commenced in the upper Miocene, approximately 8.7 Mya (Fig. 2; Suppl. material 2: fig. S1). The '*angulatus* clade' started to diversify shortly after, around 7.7 Mya (upper Miocene). In contrast, the '*leopardinus* clade' began to radiate more recently, in the early Pliocene, approximately 4.3 Mya. Speciation events continued throughout the Pliocene and Pleistocene. *Helicops danieli* diverged from its cis-Andean congeners at least 6.1 Mya during the upper Miocene. Differentiation within *H. danieli* commenced in the early Pleistocene, approximately 1.1 Mya.

For all five phenotypic traits, the Equal Rates (ER) model was determined to be the best fit (Suppl. material 1: table S4). The ancestral state estimation (ASE) for the hemipenial lobe length indicates that each state represents a synapomorphy for the major clades within *Helicops* (Figs 3A, 4; Table 3). Short-lobed hemipenes (Fig. 4A) are prevalent among all species in the '*leopardinus* clade' (which includes *H. infrataeniatus*, *H. leopardinus*, *H. modestus*, and *H. phantasma*). Conversely, long-lobed hemipenes (Fig. 4B) are characteristic of the species in the '*angulatus* clade', including *H. angulatus*, *H. boitata*, *H. carinicaudus*, *H. danieli*, *H. gomesi*, *H. hagmanni*, *H. nentur*, *H. pastazae*, and *H. polylepis*.

We additionally observed that hemipenes with short lobes have the organ body homogeneously covered with spinules, occasionally together with few enlarged spines (e.g., *H. phantasma*; Moraes-da-Silva et al. 2021) and body pockets immediately below the lobular crotch (Fig. 4A). On the other hand, hemipenes with long lobes have spinules and/or spines throughout the body (i.e., excluding the lobes), with the spines mainly located on the sulcate surface and the lateral regions of the hemipenial body; the lobes are ornamented with papillate calyces or flounces (Fig. 4B).

ASE for the reproductive mode suggests that viviparity is the most probable ancestral state for *Helicops* (Fig. 3B; Table 3). Viviparity is common among all sampled *Helicops* species (no data available for *H. boitata* and *H. nentur*), except for four species from two different clades: (i) *H. angulatus* and *H. gomesi* as well as (ii) *H. hagmanni* and *H. pastazae*. These four species are oviparous, with *H. angulatus* having both reproductive modes. Furthermore, ASE showed that subcaudal keels are present only in the clade containing *H. angulatus* and *H. gomesi*, representing an unambiguous synapomorphy of these two species (Fig. 3C; Table 3).

Each of the three character states regarding the strength of the dorsal scale keels corresponds to a synapomorphy for three clades within *Helicops* (Fig. 3D): i) for the clade containing *H. nentur* and *H. carinicaudus*, weak dorsal scale keels represent a synapomorphy; ii) for the '*leopardinus* clade' (i.e., *H. infrataeniatus*, *H. leopardinus*, *H. modestus*, *H. phantasma*), moderately keeled dorsal scales are a synapomorphy, with a modification in *H. modestus*, which has weak keels; and iii) for the clade containing *H. angulatus*, *H. danieli*, *H. gomesi*,

Table 3. Classification of *Helicops* species as proposed in the present study and respective morphological character states.

Species	Subgenus	Dorsal pattern	Dorsal keel strength	Subcaudal keels	Reproductive mode	Hemipenial lobes	References
H. acangussu[1]	*Helicops*	Spots	Moderate	Absent	Oviparous	Long	Moraes-da-Silva et al. (2022)
H. angulatus	*Helicops*	Saddles	Strong	Present	Bimodal	Long	Cope (1895), Zaher (1999), Nunes (2006)
H. apiaka[1]	*Helicops*	Saddles	Strong	Present	Unknown	Long	Kawashita-Ribeiro et al. (2013)
H. boitata	*Helicops*	Blotches	Moderate	Absent	Unknown	Long	Moraes-da-Silva et al. (2019)
H. carinicaudus	*Helicops*	Stripes	Weak	Absent	Viviparous	Long	Zaher (1999), Nunes (2006)
H. danieli	*Helicops*	Spots	Moderate	Absent	Viviparous	Long	Zaher (1999), Nunes (2006)
H. gomesi	*Helicops*	Saddles	Strong	Present	Oviparous	Long	Nunes (2006)
H. hagmanni	*Helicops*	Spots	Strong	Absent	Oviparous	Long	Nunes (2006), Moraes-da-Silva et al. (2022)
H. nentur	*Helicops*	Uniform	Weak	Absent	Unknown	Long	Costa et al. (2016)
H. pastazae	*Helicops*	Spots	Strong	Absent	Oviparous	Long	Zaher (1999), Nunes (2006)
H. petersi[1]	*Helicops*	Spots	Strong	Absent	Unknown	Long	Rossman (1976)
H. polylepis	*Helicops*	Spots	Strong	Absent	Viviparous	Long	Zaher (1999), Nunes (2006), Moraes-da-Silva et al. (2022)
H. scalaris[1]	*Helicops*	Blotches	Strong	Present	Viviparous	Long	Nunes (2006)
H. trivittatus[1]	*Helicops*	Stripes	Moderate	Absent	Viviparous	Long	Nunes (2006)
H. yacu[1]	*Helicops*	Spots	Unknown	Unknown	Unknown	Unknown	Rossman and Dixon (1975), Rossman (1976)
H. infrataeniatus	*Tachynectes*	Stripes	Moderate	Absent	Viviparous	Short	Yuki and Lema (2005), Nunes (2006)
H. leopardinus	*Tachynectes*	Spots	Moderate	Absent	Viviparous	Short	Zaher (1999), Nunes (2006), Moraes-da-Silva et al. (2021)
H. modestus	*Tachynectes*	Stripes	Weak	Absent	Viviparous	Short	Zaher (1999), Nunes (2006)
H. phantasma	*Tachynectes*	Bands	Moderate	Absent	Viviparous	Short	Moraes-da-Silva et al. (2021)
H. tapajonicus[1]	*Tachynectes*	Uniform	Weak	Absent	Unknown	Short	da Frota et al. (2005)

[1] Species not sampled for molecular phylogenetics.

H. hagmanni, *H. pastazae*, and *H. polylepis*, strongly keeled dorsal scales are a synapomorphy, with a modification in *H. danieli* having moderately strong keels (Fig. 3D; Table 3).

ASE for the dorsal color pattern suggests that a spotted pattern is a synapomorphy for the clade comprised of *H. angulatus*, *H. danieli*, *H. gomesi*, *H. hagmanni*, *H. pastazae*, and *H. polylepis.* Within this group, a change occurs in the clade composed of *H. angulatus* and *H. gomesi*, for which a saddle pattern is an unambiguous synapomorphy (Fig. 3E; Table 3).

Phylogeography of *Helicops danieli*

Our results retrieved *Helicops danieli* as monophyletic with a distinct geographic structure (Figs 1, 2; Suppl. material 2: figs S1, S2). We distinguish the four retrieved clades based on the Colombian freshwater ecoregions (Mesa-S. et al. 2016): lower Atrato, lower Magdalena, and two in the middle Magdalena, one on the eastern side and the other on the western side of the river course (Figs 1A, 2; Suppl. material 2: figs S1, S2). A similar differentiation pattern was observed in the pitviper *Bothrops asper*, where independent lineages were identified in the middle Magdalena, lower Magdalena, and in the Pacific lowlands (Saldarriaga Córdoba et al. 2017), with the latter partially corresponding to the lower Atrato clade of *H. danieli* (Figs 1A, B, 2; Suppl. material 2: figs S1, S2).

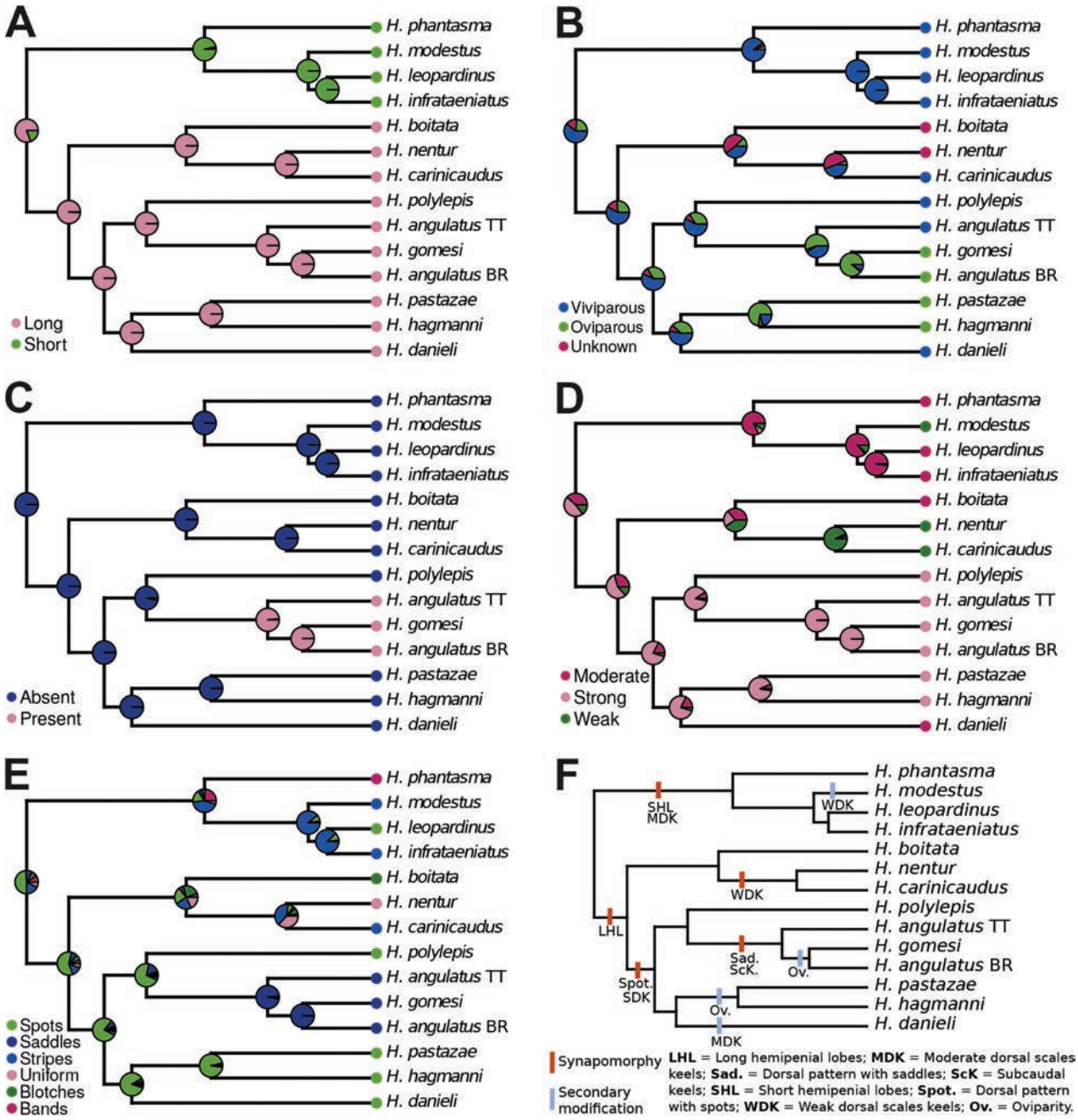

Figure 3. Ancestral state estimation using the summarized phylogeny for the genus *Helicops* for five phenotypic characters (**A** hemipenial lobe length **B** reproduction **C** subcaudal keels **D** strength of the dorsal scale keels **E** dorsal color pattern, and **F** summary of synapomorphies and secondary modifications for the nodes discussed in the text. Abbreviations (in bold) in **F** represent unambiguous synapomorphies. BR, Brazil; TT, Trinidad and Tobago.

Notably, the cladogenetic pattern found for *B. asper* by Saldarriaga Córdoba et al. (2017) resembles that of *H. danieli* in the Magdalena Basin, where the lower and middle Magdalena clades form a more inclusive clade. However, Saldarriaga Córdoba et al. (2017) did not find an east-west differentiation in *B. asper*. Given the recent diversification history of *H. danieli* (< 0.9 Mya), determining the causes of lineage differentiation is challenging due to the lack of detailed information on geological or climatic events in the distribution area during the relevant diversification period. Nonetheless, factors like isolation by distance or alterations in the river course have most likely influenced the genetic

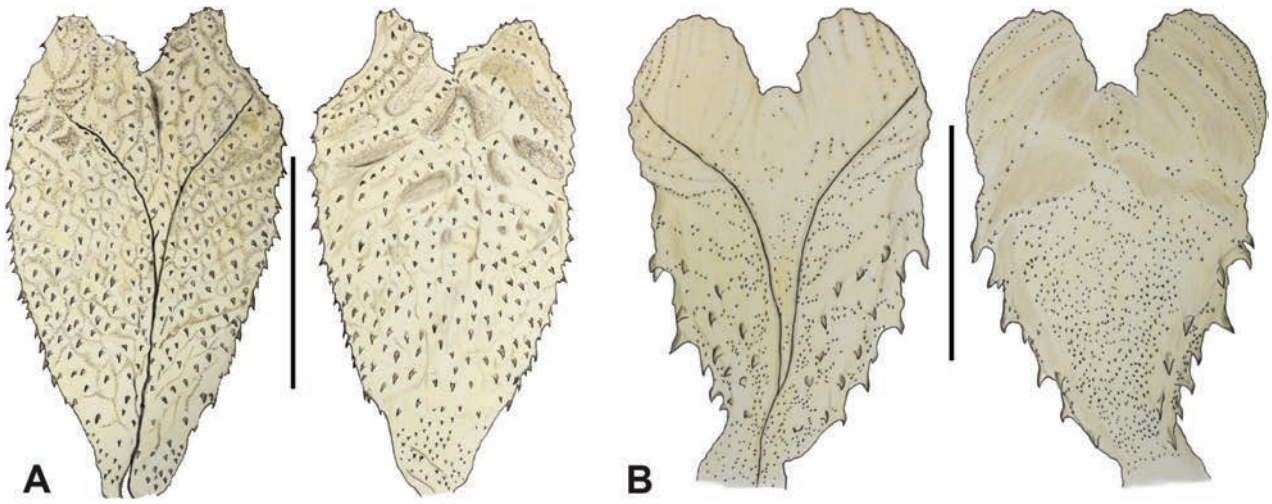

Figure 4. Hemipenes of **A** *H. leopardinus* (based on UFMTR1504 from Moraes-da-Silva et al. 2021) and **B** *H. danieli* (based on MHUAR15565) in sulcate (left) and asulcate (right) views. Scale bars: 10 mm. The hemipenis of *H. leopardinus* represents the morphology with short lobes characteristic for the subgenus *Tachynectes*; the hemipenis of *H. danieli* represents the morphology with long lobes characteristic for the subgenus *Helicops*. Note that the hemipenis is homogeneously covered with spinules in (**A**), whereas large spines are confined to the hemipenial body (i.e., excluding the lobes) on the sulcate surface and the lateral regions in (**B**). Drawings: V. Deepak.

structuring of *H. danieli*. Further downstream, there is no clear east-west pattern in the Magdalena region. Records of the 'yellow' and 'green' clades are on both sides of the river, reflecting that the lower Magdalena is slow flowing and corresponds to a swamp system in the Momposina Depression.

However, for the middle Magdalena River, the phylogeography suggests an east-west differentiation of *H. danieli*, with the respective clades ('black' and 'yellow') being non-sister (Figs 1B, 2; Suppl. material 2: figs S1–S3). This pattern suggests that the Magdalena River acts as a significant barrier to gene flow. This is at first glance counterintuitive in the face of the semiaquatic habits of *H. danieli*. However, the species is typically found in ponds and small streams in shaded areas within associated vegetation (JPH-G, MV-R pers. obs.), like other *Helicops* species (Duellman 1978; Teixeira et al. 2017) and seems to avoid fast-flowing river sections like the middle Magdalena.

An east-west differentiation as in *H. danieli* has not been reported for other lowland reptiles in the middle Magdalena region (*Mabuya* spp., Pinto-Sánchez et al. 2015; *Podocnemis lewyana*, Vargas-Ramírez et al. 2012; *Rhinoclemmys melanosterna*, Vargas-Ramírez et al. 2013; *Caiman crocodilus*, Díaz-Moreno et al. 2021; *Bothrops asper*, Saldarriaga Córdoba et al. 2017) or other vertebrates (*Ateles hybridus*, Link et al. 2015) and, to our best knowledge, such a differentiation pattern is reported here for the first time for any vertebrate.

Moraes-da-Silva et al. (2022) previously suggested that the wide and fast flowing Madeira River acts as a barrier between *H. acangussu* and its closest relative *H. hagmanni* (based on morphology), as these species occur on opposite river sides. Even though this idea was not tested with a phylogenetic hypothesis (i.e., no molecular data available for *H. acangussu*), it supports that fast-flowing rivers are a barrier to gene flow in *Helicops*. Our study, therefore, provides the first detailed phylogeographic analysis of any *Helicops* species, offering direct evidence for the role of fast-flowing rivers as barriers to gene flow.

Genetic distances of the *H. danieli* clades ranged from 0.1 to 2.0% (16S) and from 1.0 to 2.0% (cyt *b*) (Table 2). For the 16S gene, the lineage from the lower Atrato (1.7–2.0%) showed the highest divergence from the others, while for cyt *b*, it was the lineage from the middle Magdalena west (1.7–2.0%). These distances are considerably lower than the mean distances observed between *Helicops* species (5.6% for 16S; 10.0% for cyt *b*) as well as interspecific distances found in other species within the dipsadid radiation (e.g., *Hydrodynastes*, Carvalho et al. 2020; *Caaeteboia*, Montingelli et al. 2020). This suggests that the four identified lineages of *H. danieli* represent early stages of genetic divergence that do not warrant taxonomic distinction.

We dated the split between the ancestor of *H. danieli* and its cis-Andean counterparts to the late Miocene, around 6.1 Mya (Fig. 2; Suppl. material 2: fig. S1). Fossil and geological evidence suggest that the trans-Andean and Amazon aquatic fauna were connected in Colombia until at least 5 Mya (Lundberg et al. 1998; Ballen and Moreno-Bernal 2019; Montes et al. 2021; Rodriguez-Muñoz et al. 2022) through a corridor south of the Eastern Cordillera called the Andalucia Pass. Given that most *Helicops* species and the whole Hydropsini radiation (also including the genera *Hydrops* and *Pseudoeryx*) are distributed in the cis-Andean region, it is likely that the ancestor of *H. danieli* migrated during the late Miocene from this region to the trans-Andean region, through this corridor, before the connection between the Magdalena and the Amazon Basins was interrupted by the upfold of the bridge between the Eastern and Central Cordilleras due to volcanic activity and fault propagation (Montes et al. 2021).

Systematics of *Helicops*

A proposal for a subgeneric classification for *Helicops*

Our study provides the most comprehensive phylogenetic framework for the genus *Helicops* to date, covering 13 of the 20 currently recognized species (Moraes-da-Silva et al. 2022). Our phylogenetic trees (Fig. 2; Suppl. material 2: figs S1, S2) consistently recovered two more inclusive and highly supported clades within *Helicops*: the '*angulatus* clade' and the '*leopardinus* clade'. These clades have also been consistently retrieved in previous molecular phylogenetic studies, even with different taxonomic sampling (Zaher et al. 2009, 2019; Grazziotin et al. 2012; Moraes-da-Silva et al. 2019, 2021). Notably, hemipenial morphology is diagnostic for each of the clades (Figs 3A, 4; Table 3). This morphological distinctiveness, combined with the strong phylogenetic support, allows the recognition of these two clades as subgenera of *Helicops* (Figs 2, 3; Table 3).

Based on this morphological and phylogenetic evidence, we propose assigning taxa in the '*angulatus* clade' to the subgenus *Helicops* Wagler, 1828 sensu stricto (type species by monotypy: *Coluber carinicaudus* Wied-Neuwied, 1824 = *Helicops carinicaudus*). Additionally, we propose placing the taxa in the '*leopardinus* clade' in another subgenus for which the name *Tachynectes* Fitzinger, 1843 is available (type species by indication: *Homalopsis leopardina* Schlegel, 1837 = *Helicops leopardinus*); see below under 'Systematic account'.

Putative morphological synapomorphies for clades within *Helicops* and allocation of unsampled species

Beyond the hemipenial morphology that supports our proposed subgeneric classification, our ASE analysis for four additional phenotypic traits provides further phylogenetic information for various lineages within *Helicops* (Fig. 3; Table 3). These findings also allow us to tentatively assign unsampled species.

Our ASE analysis indicates that viviparity is the ancestral state for *Helicops*, with exceptions in two non-sister clades (Fig. 3B, F): one containing *H. hagmanni* and *H. pastazae*, and the other including *H. angulatus* and *H. gomesi* (with *H. angulatus* exhibiting both oviparity and viviparity; Table 3). According to our ASE analysis and phylogenetic hypothesis, oviparity has independently evolved twice within the subgenus *Helicops* (Fig. 3B; Table 3). Conversely, results of Moraes-da-Silva et al. (2022) suggest a single origin for oviparity, but this was because they inferred that all oviparous species (*H. angulatus*, *H. gomesi*, *H. hagmanni*, *H. pastazae*) are monophyletic.

The reproductive mode of six *Helicops* species remains unknown (Table 3), including two species in our phylogeny (*H. boitata* and *H. nentur*; Fig. 3B). Braz et al. (2016) proposed a geographic pattern for the bimodal reproductive mode in *H. angulatus*, but given that *H. angulatus* seems to be a species complex (cf. the deeply divergent non-sister samples of *H. angulatus* in our phylogeny; Fig. 2; Suppl. material 2: figs S1, S2), this bimodality might correspond rather to distinct taxa. Therefore, addressing these knowledge gaps requires a more comprehensive analysis for a definitive understanding of the evolution of reproductive modes in *Helicops*.

Moraes-da-Silva et al. (2022) proposed strong dorsal scale keels as a synapomorphy for the clade containing *H. angulatus*, *H. gomesi*, *H. hagmanni*, and *H. polylepis*. Our ASE results corroborate this hypothesis. Notably, *H. danieli* exhibits a modification with moderately strong dorsal keels. This putative synapomorphy is exclusive to this clade, with all other *Helicops* taxa having weak or moderate dorsal keels (Fig. 3D; Table 3).

Our ASE results also indicate that moderately keeled dorsal scales represent a synapomorphy for the subgenus *Tachynectes* (referred to as the '*leopardinus* clade' above), with a subsequent modification in *H. modestus* (with weak dorsal keels). Additionally, weak dorsal scale keels are identified as a synapomorphy for the clade containing *H. nentur* and *H. carinicaudus* (Fig. 3D, F). This is the first time that weak or moderate states of this character are identified as synapomorphies for clades within *Helicops*, highlighting the phylogenetic informativeness of dorsal scale carination.

Our results further suggest that the spotted dorsal pattern is also a synapomorphy for the clade containing *H. angulatus*, *H. danieli*, *H. gomesi*, *H. hagmanni*, *H. pastazae*, and *H. polylepis*, albeit with a secondary modification observed in the subclade *H. angulatus* + *H. gomesi*, which exhibits a dorsal pattern characterized by saddle-shaped blotches (Fig. 3E, F). The only other species in our study with a spotted pattern, *H. leopardinus* (subgenus *Tachynectes*), likely represents a case of convergence, as no other closely related species shares this pattern.

For the subclade *H. angulatus* + *H. gomesi*, Moraes-da-Silva et al. (2022) previously suggested the dorsal color pattern consisting of saddle-shaped spots and subcaudal keels as putative synapomorphies, a hypothesis supported by

our ASE results (Fig. 3E, F; Table 3). These traits are also shared by *H. apiaka* (Kawashita-Ribeiro et al. 2013), a species not included in our trees (Figs 2, 3; Suppl. material 2: figs S1, S2), which likely belongs to this clade (Table 3).

Subcaudal keels are also reported in *H. scalaris*, another unsampled species. While *H. scalaris* exhibits a polymorphic dorsal color pattern with individuals showing blotches (see photos in Rossman 2002b; Natera-Mumaw et al. 2015), some also display a saddle-like pattern (see iNaturalist observations: 129359317, 63932552, 19896494; Rossman 2002b). This suggests that *H. scalaris* might belong to the clade with saddle-shaped spots and subcaudal keels. However, *H. scalaris* is viviparous. If it truly belongs to this clade, it would support the idea of flexible reproductive modes within *Helicops* because *H. gomesi* is oviparous and *H. angulatus* exhibits both reproductive strategies. Regardless, both *H. apiaka* and *H. scalaris* possess hemipenes with long lobes, suggesting that they belong to the subgenus *Helicops* (Table 3).

Among the remaining species missing in our phylogenetic tree, *H. acangussu* Moraes-da-Silva et al. 2022, *H. petersi* Rossman, 1976, and *H. trivittatus* (Gray, 1849) possess hemipenes of the long-lobed morphotype and are therefore allocated to the subgenus *Helicops* (see Systematic account and Fig. 2; Table 3). *Helicops acangussu* and *H. petersi* both exhibit a spotted dorsal pattern and have been associated with *H. hagmanni* and *H. pastazae*, respectively, primarily based on scale counts (Rossman 1976; Moraes-da-Silva et al. 2022). Thus, *H. acangussu* and *H. petersi* most likely belong to the clade formed by *H. hagmanni* and *H. pastazae*. This is further supported by the fact that *H. petersi* has strong dorsal scale keels, a putative synapomorphy of species in this clade, and *H. acangussu* is oviparous, a reproductive mode only occurring within the subgenus *Helicops* (Fig. 3; Table 3).

Another unsampled species is *H. yacu*, a taxon with a spotted dorsal pattern (Table 3), for which information regarding the hemipenial morphology is unavailable. Nevertheless, Rossman and Dixon (1975) and Rossman (1976) associate *H. yacu* with *H. polylepis*, *H. pastazae*, and *H. petersi*, based on scalation and color pattern. Later, Rossman and Abe (1979) suggested that *H. yacu* might be conspecific with *H. pastazae* (i.e., a subspecies). Therefore, based on the reported similarities in scutellation with the aforementioned species and its spotted dorsal pattern, we tentatively assign *H. yacu* to the subgenus *Helicops*.

The last species not included in our molecular phylogeny is *H. tapajonicus* da Frota, 2005. This species has hemipenes with short lobes and is therefore allocated to the subgenus *Tachynectes* (see Fig. 2; Table 3; Systematic account).

Comments on recent taxonomic changes regarding *Helicops angulatus*

Helicops cyclops Cope, 1868 was recently resurrected from the synonymy of *H. angulatus* by Murphy et al. (2020) solely based on the morphology of the holotype (i.e., scale counts, color pattern, head shape). However, these traits show considerable overlap with *H. angulatus* (Murphy et al. 2020: table 2). Additionally, the locality of the holotype is imprecise (Bahia [State], Brazil), and Murphy et al. (2020) did not discuss the potential distribution range of *H. cyclops*. In the face of these limitations, we propose that *H. cyclops* should remain in the synonymy of *H. angulatus* pending additional evidence for its validity.

Diversification of *Helicops*

According to our results, the genus *Helicops* began to diversify in the late Miocene, around 9 Mya (Fig. 2; Suppl. material 2: fig. S1), aligning with the recent findings of Zaher et al. (2019), who suggested a similar time frame of 10.9 Mya. This period coincides with the existence of the Pebas System, a vast wetland that once covered most of the present-day Amazon Basin from approximately 20 to 5 Mya. The Pebas System was characterized by dynamic changes in landscape due to geological events and marine incursions throughout the Miocene (Hoorn et al. 2010, 2022). This dynamic wetland environment likely played a key role in the diversification of *Helicops*, and potentially the entire Hydropsini tribe (Suppl. material 2: fig. S1). This tribe includes semiaquatic snakes that diversified during the Miocene and are currently predominantly distributed in the Amazon Basin (Schöneberg and Köhler 2022).

Systematic account

Phylum: Chordata
Subphylum: Vertebrata
Superclass: Tetrapoda
Class: Reptilia
Order: Squamata
Family: Dipsadidae
Genus: *Helicops* Wagler, 1828

Subgenus: *Helicops* Wagler, 1828

Type species. *Coluber carinicaudus* Wied-Neuwied, 1824 (designated by Fitzinger 1843).

Diagnosis. Members of the subgenus *Helicops* have long hemipenial lobes decorated with papillate flounces or calyces extending to the tips, but without spinules. The hemipenial body is covered both with spines and spinules; spines are concentrated on the sulcate surface and the lateral regions of the hemipenial body (Fig. 4B).

Content. 15 species, *Helicops* (*Helicops*) *acangussu* Moraes-da-Silva et al., 2022, *H.* (*H.*) *angulatus* (Linnaeus, 1758), *H.* (*H.*) *apiaka* Kawashita-Ribeiro, Ávila & Morais, 2013, *H.* (*H.*) *boitata* Moraes-da-Silva et al., 2019, *H.* (*H.*) *carinicaudus* (Wied-Neuwied, 1824), *H.* (*H.*) *danieli* Amaral, 1938, *H.* (*H.*) *gomesi* Amaral, 1922, *H.* (*H.*) *hagmanni* Roux, 1910, *H.* (*H.*) *nentur* Costa et al., 2016, *H.* (*H.*) *pastazae* Shreve, 1934, *H.* (*H.*) *petersi* Rossman, 1976, *H.* (*H.*) *polylepis* Günther, 1861, *H.* (*H.*) *scalaris* Jan, 1865, *H.* (*H.*) *trivittatus* (Gray, 1849), *H.* (*H.*) *yacu* Rossman & Dixon, 1975.

Comments. Wagler (1828) coined the generic name *Helicops* to allocate *Coluber carinicaudus* (= *Helicops carinicaudus*) and suggested that *Coluber angulatus* Linnaeus, 1758 (= *Helicops angulatus*) and *Coluber erytrogrammus* Palisot de Beauvois in Sonnini & Latreille, 1801 (= *Farancia erytrogramma*) belonged to *Helicops* because of their similarity. Two years later, Wagler (1830) included in *Helicops* the following species: *H. carinicaudus*, *C. erytrogrammus*, *C. plicatilis*, *C. angulatus*, and *Natrix aspera* Wagler, 1824 (= *Helicops angulatus*), without designation of a type species. Fitzinger (1843) designated *H. carinicaudus* as

valid type species of *Helicops*. Since Wagler (1828) erected the name *Helicops*, the correct authorship has to be credited to Wagler (1828) and not Wagler (1830), as frequently seen (e.g., da Frota 2005; Kawashita-Ribeiro et al. 2013; Murphy et al. 2020; Schöneberg and Köhler 2022).

Subgenus: *Tachynectes* Fitzinger, 1843

Type species. *Homalopsis leopardina* Schlegel, 1837.

Diagnosis. Members of the subgenus *Tachynectes* have short hemipenial lobes decorated with spinules. The hemipenial body is homogeneously covered with spinules (Fig. 4A), occasionally a few enlarged spines may occur, e.g., in *H.* (*T.*) *phantasma*.

Content. Five species, *Helicops* (*Tachynectes*) *infrataeniatus* Jan, 1865, *H.* (*T.*) *leopardinus* (Schlegel, 1837), *H.* (*T.*) *modestus* Günther, 1861, *H.* (*T.*) *phantasma* Moraes-da-Silva et al., 2021, *H.* (*T.*) *tapajonicus* da Frota, 2005.

Comments. *Tachynectes* von der Mark, 1863, erected for a genus of fossil fishes, is a primary junior homonym of *Tachynectes* Fitzinger, 1843. As *Tachynectes* von der Mark, 1863 has only been used four times in the past 50 years according to our searches (Google Scholar, Zoological Record: Sepkoski 2002; Albert et al. 2009; Dietze 2009; Schwarzhans and Carnevale 2021), it fails to meet the criterion in Article 23.9.2 of the International Code of Zoological Nomenclature (ICZN 1999) for prevailing usage and is therefore unavailable. As a replacement name for *Tachynectes* von der Mark, 1863, we propose *Ichthyotachynectes* nom. nov. to accommodate the fossil fish species previously assigned to *Tachynectes* von der Mark, 1863.

Phylum: Chordata
Subphylum: Vertebrata
Superclass: Actinoptergyii
Class: Teleostei
Order: Myctophiformes
Family: Myctophidae

Genus: *Ichthyotachynectes* nom. nov.
https://zoobank.org/3B4D09B3-9E5A-4F4F-82FF-CBCE571D0533

Synonymy. *Tachynectes* von der Mark, 1863 (invalid junior homonym of *Tachynectes* Fitzinger, 1843)

Type species. *Tachynectes macrodactylus* von der Marck, 1863.

Diagnosis. For diagnosis and synapomorphies, see von der Marck (1863) and Dietze (2009).

Content. Three species according to Dietze (2009), *Ichthyotachynectes macrodactylus* (von der Marck, 1863), comb. nov., *I. longipes* (von der Marck, 1863), comb. nov., *I. brachypterygius* (von der Marck, 1863), comb. nov.

Etymology. The new name (male gender) means “fish that swims fast” (from the classic Greek ichthyos = fish, tachys = fast, nectes = swimming). The name intends to keep the initial meaning of *Tachynectes* (fast swimmer), but adding a prefix indicating the taxonomic group.

Comments. The homonymy of *Tachynectes* Fitzinger, 1843 and *Tachynectes* von der Mark, 1863 was already acknowledged by White and Moy-Thomas (1941), but overlooked by subsequent authors.

Conclusions

Our study reveals a pronounced phylogeographic pattern in *H. danieli*, with four distinct lineages (Figs 1, 2; Suppl. material 2: figs S1, S2). Interestingly, these lineages exhibit clear differentiation on the eastern and western sides of the middle Magdalena River, suggesting this river acts as a barrier to gene flow for this aquatic snake species. Although our sampling did not extend to the southwestern Pacific region of Colombia, it is plausible that populations there are sister to the lower Atrato lineage, mirroring patterns observed in other taxa (e.g., *Mabuya* spp., Pinto-Sánchez et al. 2015; *Bothrops asper*, Saldarriaga Córdoba et al. 2017).

Moreover, we propose a subgeneric classification for *Helicops* based on the molecular phylogeny and hemipenial morphology with two subgenera: *Helicops* and *Tachynectes*. Additionally, we offer a new interpretation of four further phenotypic and natural history traits (i.e., reproductive mode, dorsal scale keel strength, subcaudal keels, dorsal color pattern) and their value as putative synapomorphies for lineages within the subgenus *Helicops*. This reinterpretation allows us to propose the most plausible phylogenetic placement for the seven *Helicops* species not included in our molecular phylogeny.

Acknowledgements

We thank Juan Camilo Arredondo for discussions on *Helicops* hemipenial morphology and Sebastián Cuadrado for discussions on ancestral state estimation. Ralf Britz discussed the nomenclatural issues of *Tachynectes* von der Mark, 1863 with us. John Murphy and Robert Jadin made helpful comments on an earlier version of this study.

Additional information

Conflict of interest

The authors have declared that no competing interests exist.

Ethical statement

No ethical statement was reported.

Funding

JPHG was supported by a scholarship of the German Academic Exchange Service (DAAD). JMD was partially funded by the interinstitutional agreement 014-2023 between the Parques Nacionales Naturales de Colombia and the Universidad de Antioquia. MVR was supported by the Alexander von Humboldt Foundation with another research stay in Dresden, which made his contribution to the present work possible.

Author contributions

Conceptualization: JPHG, JMD, MVR, UF. Data curation: JPHG. Formal analysis: JPHG. Funding acquisition: JPHG, JMD, MVR, UF. Investigation: JPHG. Methodology: JPHG.

Project administration: JPHG, UF. Resources: JPHG, JMD, MVR, UF. Supervision: MVR, UF. Visualization: JPHG, VD. Writing – original draft: JPHG, UF. Writing – review and editing: JPHG, JMD, MVR, VD, UF.

Author ORCIDs

Juan Pablo Hurtado Gómez https://orcid.org/0000-0003-4351-2834
Mario Vargas-Ramírez https://orcid.org/0000-0001-8974-3430
V. Deepak https://orcid.org/0000-0002-8826-9367
Uwe Fritz https://orcid.org/0000-0002-6740-7214

Data availability

All of the data that support the findings of this study are available in the main text or Supplementary Information.

References

Albert JS, Johnson DM, Knouft JH (2009) Fossils provide better estimates of ancestral body size than do extant taxa in fishes. Acta Zoologica 90: 357–384. https://doi.org/10.1111/j.1463-6395.2008.00364.x

Amaral A (1937) Estudo sobre ophidios neotropicos 34. Novas notas sobre a fauna da Colombia e descrição de uma especie nova de colubrideo aglypho. Memorias do Instituto Butantan 11: 231–240.

Ballen GA, Moreno-Bernal JW (2019) New records of the enigmatic neotropical fossil fish *Acregoliath rancii* (Teleostei *incertae sedis*) from the middle Miocene Honda group of Colombia. Ameghiniana 56: 431. https://doi.org/10.5710/AMGH.17.09.2019.3266

Bouckaert R, Drummond AJ (2017) bModelTest: Bayesian phylogenetic site model averaging and model comparison. BMC Evolutionary Biology 17: 1–11. https://doi.org/10.1186/s12862-017-0890-6

Bouckaert R, Vaughan TG, Barido-Sottani J, Duchêne S, Fourment M, Gavryushkina A, Heled J, Jones G, Kühnert D, De Maio N, Matschiner M, Mendes FK, Müller NF, Ogilvie HA, du Plessis L, Popinga A, Rambaut A, Rasmussen D, Siveroni I, Suchard MA, Wu C-H, Xie D, Zhang C, Stadler T, Drummond AJ (2019) BEAST 2.5: An advanced software platform for Bayesian evolutionary analysis. PLoS Computational Biology 15: e1006650. https://doi.org/10.1371/journal.pcbi.1006650

Braz HB, Scartozzoni RR, Almeida-Santos SM (2016) Reproductive modes of the South American water snakes: A study system for the evolution of viviparity in squamate reptiles. Zoologischer Anzeiger 263: 33–44. https://doi.org/10.1016/j.jcz.2016.04.003

Bryant D, Moulton V (2004) Neighbor-Net: An agglomerative method for the construction of phylogenetic networks. Molecular Biology and Evolution 21: 255–265. https://doi.org/10.1093/molbev/msh018

Carvalho PS, Zaher H, Da Silva NJ, Santana DJ (2020) A morphological and molecular study of *Hydrodynastes gigas* (Serpentes, Dipsadidae), a widespread species from South America. PeerJ 8: 1–25. https://doi.org/10.7717/peerj.10073

Citeli NK, Klaczko J, De-Lima AKS, De-Carvalho M, Nunes PMS, Passos P, Brandão RA (2021) Taxonomy, allometry, sexual dimorphism, and conservation of the trans-Andean watersnake *Helicops danieli* Amaral 1937 (Serpentes: Dipsadidae: Hydropsini). Canadian Journal of Zoology 100: 84–196. https://doi.org/10.1139/cjz-2021-0073

Cope ED (1895) The classification of the Ophidia. Transactions of the American Philosophical Society 18: 186–219. https://doi.org/10.2307/1005387

Costa HC, Santana DJ, Leal F, Koroiva R, Garcia PCA (2016) A new species of *Helicops* (Serpentes: Dipsadidae: Hydropsini) from southeastern Brazil. Herpetologica 72: 157–166. https://doi.org/10.1655/HERPETOLOGICA-D-15-00059

da Frota JG (2005) Nova espécie de *Helicops* Wagler, 1830 (Serpentes, Colubridae) do rio Tapajós, Amazônia, Brasil. Phyllomedusa 4: 61–68. https://doi.org/10.11606/issn.2316-9079.v4i1p61-67

Díaz-Moreno DM, Hernández-Gonzalez F, Moncada-Jimenez JF, Mora C, Prada C, Jiménez-Alonso G, Balaguera-Reina SA (2021) Molecular characterization of the spectacled caiman (*Caiman crocodilus*) in the upper Magdalena River Basin, Colombia: Demographic and phylogeographic insights. Systematics and Biodiversity 19: 1040–1048. https://doi.org/10.1080/14772000.2021.1968975

Dietze K (2009) Morphology and phylogenetic relationships of certain neoteleostean fishes from the Upper Cretaceous of Sendenhorst, Germany. Cretaceous Research 30: 559–574. https://doi.org/10.1016/j.cretres.2008.11.001

Duellman WE (1978) The Biology of an Equatorial Herpetofauna in Amazonian Ecuador. Miscellaneous Publications, Museum of Natural History, University of Kansas, Lawrence, KS, 352 pp.

Etter A, Andrade Á, Zúñiga M (2021) Ecosistemas colombianos. Amenazas y riesgos. Editorial Pontificia Universidad Javeriana, Bogotá, 60 pp. https://doi.org/10.11144/Javeriana.9789587816013

Fitzinger LJ (1843) Systema reptilium. Fasciculus primus. Amblyglossae. Braumüller et Seidel, Vindobona [Vienna], 106 pp. https://doi.org/10.5962/bhl.title.4694

Fritz U, Corti C, Päckert M (2012) Mitochondrial DNA sequences suggest unexpected phylogenetic position of Corso-Sardinian grass snakes (*Natrix cetti*) and do not support their species status, with notes on phylogeography and subspecies delineation of grass snakes. Organisms Diversity & Evolution 12: 71–80. https://doi.org/10.1007/s13127-011-0069-8

Grazziotin FG, Zaher H, Murphy RW, Scrocchi GJ, Benavides MA, Zhang YP, Bonatto SL (2012) Molecular phylogeny of the New World Dipsadidae (Serpentes: Colubroidea): A reappraisal. Cladistics 28: 437–459. https://doi.org/10.1111/j.1096-0031.2012.00393.x

Harmon LJ, Weir JT, Brock CD, Glor RE, Challenger W (2007) GEIGER: Investigating evolutionary radiations. Bioinformatics 24: 129–131. https://doi.org/10.1093/bioinformatics/btm538

Hernández-Camacho JI, Hurtado A, Ortiz R, Walschburger T (1992) Unidades biogeográficas de Colombia. In: Halffter G (Ed.) La diversidad biológica de Iberoamérica I. Acta Zoologica Mexicana, Xapala, 105–151.

Holman JA (1964) Fossil snakes from the Valentine Formation of Nebraska. Copeia 1964: 631–637. https://doi.org/10.2307/1441438

Holman JA (1977) Upper Miocene snakes (Reptilia, Serpentes) from southeastern Nebraska. Journal of Herpetology 11: 323–335. https://doi.org/10.2307/1563245

Hoorn C, Wesselingh FP, Hovikoski J, Guerrero J (2010) The development of the Amazonian mega-wetland (Miocene; Brazil, Colombia, Peru, Bolivia). In: Hoorn C, Wesselingh FP (Eds) Amazonia: Landscape and Species Evolution. Wiley-Blackwell, Oxford, 123–142. https://doi.org/10.1002/9781444306408.ch8

Hoorn C, Boschman LM, Kukla T, Sciumbata M, Val P (2022) The Miocene wetland of western Amazonia and its role in neotropical biogeography. Botanical Journal of the Linnean Society 199: 25–35. https://doi.org/10.1093/botlinnean/boab098

ICZN [International Commission on Zoological Nomenclature] (1999) International Code of Zoological Nomenclature. 4th Edn. International Trust for Zoological Nomenclature, London, XXIX, 306 pp.

Kalyaanamoorthy S, Minh BQ, Wong TKF, von Haeseler A, Jermiin LS (2017) ModelFinder: Fast model selection for accurate phylogenetic estimates. Nature Methods 14: 587–589. https://doi.org/10.1038/nmeth.4285

Katoh K, Toh H (2010) Parallelization of the MAFFT multiple sequence alignment program. Bioinformatics 26: 1899–1900. https://doi.org/10.1093/bioinformatics/btq224

Kawashita-Ribeiro RA, Ávila RW, Morais DH (2013) A new snake of the genus *Helicops* Wagler, 1830 (Dipsadidae, Xenodontinae) from Brazil. Herpetologica 69: 80–90. https://doi.org/10.1655/HERPETOLOGICA-D-12-00013

Kearse M, Moir R, Wilson A, Stones-Havas S, Cheung M, Sturrock S, Buxton S, Cooper A, Markowitz S, Duran C, Thierer T, Ashton B, Meintjes P, Drummond AJ (2012) Geneious Basic: An integrated and extendable desktop software platform for the organization and analysis of sequence data. Bioinformatics 28: 1647–1649. https://doi.org/10.1093/bioinformatics/bts199

Lanfear R, Frandsen PB, Wright AM, Senfeld T, Calcott B (2016) PartitionFinder 2: New methods for selecting partitioned models of evolution for molecular and morphological phylogenetic analyses. Molecular Biology and Evolution 34: 772–773. https://doi.org/10.1093/molbev/msw260

Link A, Valencia LM, Céspedes LN, Duque LD, Cadena CD, Di Fiore A (2015) Phylogeography of the critically endangered brown spider monkey (*Ateles hybridus*): Testing the riverine barrier hypothesis. International Journal of Primatology 36: 530–547. https://doi.org/10.1007/s10764-015-9840-6

Lundberg JG, Marshall L, Guerrero J, Horton B, Malabarba MCSL, Wesselingh FP (1998) The stage for neotropical fish diversification: A history of tropical South American rivers. In: Malabarba LR, Reis RR, Vari RP, Lucena ZMS, Lucena CAS (Eds) Phylogeny and Classification of Neotropical Fishes. Edipurus, Porto Alegre, 13–48.

Lynch JD, Ruiz-Carranza PM, Ardila-Robayo M (1997) Biogeographic patterns of Colombian frogs and toads. Revista de la Academia Colombiana Ciencias Exactas Físicas y Naturales 21: 237–248. https://doi.org/10.18257/raccefyn.21(80).1997.2973

Mesa-S LM, Corzo G, Hernández-Manrique OL, Lasso CA, Galvis G (2016) Ecorregiones dulceacuícolas de Colombia: una propuesta para la planificación territorial de la región trasandina y parte de las cuencas del Orinoco y Amazonas. Biota Colombiana 17: 62–88. https://doi.org/10.21068/c2016.v17n02a06

Minh BQ, Nguyen MAT, von Haeseler A (2013) Ultrafast approximation for phylogenetic bootstrap. Molecular Biology and Evolution 30: 1188–1195. https://doi.org/10.1093/molbev/mst024

Minh BQ, Schmidt HA, Chernomor O, Schrempf D, Woodhams MD, von Haeseler A, Lanfear R (2020) IQ-TREE 2: New models and efficient methods for phylogenetic inference in the genomic era. Molecular Biology and Evolution 37: 1530–1534. https://doi.org/10.1093/molbev/msaa015

Montes C, Silva CA, Bayona GA, Villamil R, Stiles E, Rodriguez-Corcho AF, Beltran-Triviño A, Lamus F, Muñoz-Granados MD, Pérez-Angel LC, Hoyos N, Gomez S, Galeano JJ, Romero E, Baquero M, Cardenas-Rozo AL, von Quadt A (2021) A middle to late Miocene trans-Andean portal: Geologic record in the Tatacoa Desert. Frontiers in Earth Science 8: 1–19. https://doi.org/10.3389/feart.2020.587022

Montingelli GG, Barbo FE, Pereira Filho GA, Santana GG, França FGR, Grazziotin FG, Zaher H (2020) A second new species for the rare dipsadid genus *Caaeteboia* Zaher et al., 2009 (Serpentes: Dipsadidae) from the Atlantic Forest of northeastern Brazil. Cuadernos de Herpetología 34: 219–230.

Moraes-da-Silva A, Amaro RC, Nunes PMS, Strüssmann C, Teixeira MJ, Andrade AJR, Sudré V, Recoder R, Rodrigues MT, Curcio FF (2019) Chance, luck and a fortunate finding: A new species of watersnake of the genus *Helicops* Wagler, 1828 (Serpentes: Xenodontinae) from the Brazilian Pantanal wetlands. Zootaxa 4651: 445–470. https://doi.org/10.11646/zootaxa.4651.3.3

Moraes-da-Silva A, Amaro RC, Nunes PMS, Rodrigues MT, Curcio FF (2021) Long known, brand new, and possibly threatened: A new species of watersnake of the genus *Helicops* Wagler, 1828 (Serpentes; Xenodontinae) from the Tocantins-Araguaia River Basin, Brazil. Zootaxa 4903: 151–193. https://doi.org/10.11646/zootaxa.4903.2.3

Moraes-da-Silva A, Walterman S, Citeli N, Nunes PMS, Curcio FF (2022) A new oviparous species of *Helicops* Wagler, 1828 (Serpentes, Xenodontinae) from Brazilian Amazonia with reflections on the evolution of viviparity among hydropsine watersnakes. Zoologischer Anzeiger 296: 91–109. https://doi.org/10.1016/j.jcz.2021.12.001

Murphy JC, Muñoz-Mérida A, Auguste RJ, Lasso-Alcalá O, Rivas GA, Jowers MJ (2020) Evidence for cryptic diversity in the neotropical water snake, *Helicops angulatus* (Linnaeus, 1758) (Dipsadidae, Hydropsini), with comments on its ecology, facultative reproductive mode, and conservation. Amphibian and Reptile Conservation 14: 138–155.

Natera-Mumaw M, Esqueda González LF, Castelaín Fernandez M (2015) Atlas serpientes de Venezuela. Una visión actual de su diversidad. Dimacofi Negocios Avanzados SA, Santiago de Chile, 441 pp.

Nunes PMS (2006) Filogenia da tribo Hydropsini baseada em caracteres morfológicos (Serpentes: Xenodontinae). MSc Thesis, Universidade de São Paulo, São Paulo, 130 pp.

Paradis E (2010) pegas: An R package for population genetics with an integrated-modular approach. Bioinformatics 26: 419–420. https://doi.org/10.1093/bioinformatics/btp696

Paradis E, Schliep KP (2019) Ape 5.0: An environment for modern phylogenetics and evolutionary analyses in R. Bioinformatics 35: 526–528. https://doi.org/10.1093/bioinformatics/bty633

Pinto-Sánchez NR, Calderón-Espinosa ML, Miralles A, Crawford AJ, Ramírez-Pinilla MP (2015) Molecular phylogenetics and biogeography of the neotropical skink genus *Mabuya* Fitzinger (Squamata: Scincidae) with emphasis on Colombian populations. Molecular Phylogenetics and Evolution 93: 188–211. https://doi.org/10.1016/j.ympev.2015.07.016

R Core Team (2023) R: A language and environment for statistical computing. R Foundation for Statistical Computing, Vienna. https://www.R-project.org/

Rage J-C, Szyndlar Z (1986) *Natrix longivertebrata* from the European Neogene, a snake with one of the longest known stratigraphic ranges. Neues Jahrbuch für Geologie und Paläontologie 1986: 56–64. https://doi.org/10.1127/njgpm/1986/1986/56

Rambaut A, Drummond AJ, Xie D, Baele G, Suchard MA (2018) Posterior summarization in Bayesian phylogenetics using Tracer 1.7. Systematic Biology 67: 901–904. https://doi.org/10.1093/sysbio/syy032

Revell LJ (2012) phytools: An R package for phylogenetic comparative biology (and other things). Methods in Ecology and Evolution 3: 217–223. https://doi.org/10.1111/j.2041-210X.2011.00169.x

Rodriguez-Muñoz E, Montes C, Rojas-Runjaic FJM, Crawford AJ (2022) Synthesis of geological data and comparative phylogeography of lowland tetrapods suggests recent dispersal through lowland portals crossing the Eastern Andean Cordillera. PeerJ 10: e13186. https://doi.org/10.7717/peerj.13186

Rossman DA (1976) Revision of the South American colubrid snakes of the *Helicops pastazae* complex. Occasional Papers of the Museum of Zoology, Louisiana State University 50: 1–13. https://doi.org/10.31390/opmns.050

Rossman DA (2002a) Morphological variation in the endemic Colombian water snake, *Helicops danieli* Amaral, 1937 (Serpentes: Xenodontidae). Revista de la Academia Colombiana de Ciencias Exactas, Físicas y Naturales 26: 589–594. https://doi.org/10.18257/raccefyn.26(101).2002.2702

Rossman DA (2002b) Variations in the xenodontid water snake *Helicops scalaris* Jan, and the status of *H. hogei* Lancini. Occasional Papers of the Museum of Natural Science Louisiana State University 78: 1–18. https://doi.org/10.31390/opmns.078

Rossman DA, Abe AS (1979) Comments on the taxonomic status of *Helicops yacu* (Serpentes: Colubridae). Proceedings of the Louisiana Academy of Sciences 42: 7–9.

Rossman DA, Dixon JR (1975) A new colubrid snake of the genus *Helicops* from Peru. Herpetologica 31: 412–414.

RStudio Team (2023) RStudio: Integrated Development Environment for R. RStudio, PBC., Boston, MA.

Saldarriaga Córdoba MM, Parkinson CL, Daza JM, Wüster W, Sasa M (2017) Phylogeography of the Central American lancehead *Bothrops asper* (Serpentes: Viperidae). PLOS ONE 12: 1–20. https://doi.org/10.1371/journal.pone.0187969

Schliep KP (2011) phangorn: Phylogenetic analysis in R. Bioinformatics 27: 592–593. https://doi.org/10.1093/bioinformatics/btq706

Schöneberg Y, Köhler G (2022) Distribution and identification of the species in the genus *Helicops* Wagler, 1830 (Serpentes, Colubridae, Xenodontinae). Biodiversity Data Journal 10: e69234. https://doi.org/10.3897/BDJ.10.e69234

Schwarzhans W, Carnevale G (2021) The rise to dominance of lanternfishes (Teleostei: Myctophidae) in the oceanic ecosystems: A paleontological perspective. Paleobiology 47: 446–463. https://doi.org/10.1017/pab.2021.2

Sepkoski JJ (2002) A compendium of fossil marine animal genera. Bulletin of American Paleontology 363: 1–500.

Smith KT (2013) New constraints on the evolution of the snake clades Ungaliophiinae, Loxocemidae and Colubridae (Serpentes), with comments on the fossil history of erycine boids in North America. Zoologischer Anzeiger 252: 157–182. https://doi.org/10.1016/j.jcz.2012.05.006

Tamura K, Stecher G, Kumar S (2021) MEGA11: Molecular Evolutionary Genetics Analysis version 11. Molecular Biology and Evolution 38: 3022–3027. https://doi.org/10.1093/molbev/msab120

Teixeira CdC, Montag LFdA, dos Santos-Costa MC (2017) Diet composition and foraging habitat use by three species of water snakes, *Helicops* Wagler, 1830 (Serpentes:

Dipsadidae) in eastern Brazilian Amazonia. Journal of Herpetology 51: 215–222. https://doi.org/10.1670/15-161

Vaidya G, Lohman DJ, Meier R (2011) SequenceMatrix: Concatenation software for the fast assembly of multi-gene datasets with character set and codon information. Cladistics 27: 171–180. https://doi.org/10.1111/j.1096-0031.2010.00329.x

Vargas-Ramírez M, Stuckas H, Castaño-Mora OV, Fritz U (2012) Extremely low genetic diversity and weak population differentiation in the endangered Colombian river turtle *Podocnemis lewyana* (Testudines: Podocnemididae). Conservation Genetics 13: 65–77. https://doi.org/10.1007/s10592-011-0263-4

Vargas-Ramírez M, Carr JL, Fritz U (2013) Complex phylogeography in *Rhinoclemmys melanosterna*: Conflicting mitochondrial and nuclear evidence suggests past hybridization (Testudines: Geoemydidae). Zootaxa 3670: 238–254. https://doi.org/10.11646/zootaxa.3670.2.8

von der Marck W (1863) Fossile Fische, Krebse und Pflanzen aus dem Plattenkalk der jüngsten Kreide in Westphalen. Palaeontographica 11: 1–40.

Wagler J (1828) Descriptiones et Icones Amphibiorum. Fasciculus I. J.G. Cotta, Monachium (München), Stuttgartia (Stuttgart) et Tubinga (Tübingen), 28 unnumbered pages, plates I–XII. https://doi.org/10.5962/bhl.title.77350

Wagler J (1830) Natürliches System der Amphibien, mit vorangehender Classification der Säugethiere und Vögel. J.G. Cotta, München, Stuttgart, and Tübingen, VI, 354 pp., 2 plates. https://doi.org/10.5962/bhl.title.58730

White EI, Moy-Thomas JA (1941) Notes on the nomenclature of fossil fishes. Part III. Homonyms M-Z. Annals and Magazine of Natural History 7: 395–400. https://doi.org/10.1080/03745481.1941.9727941

Yuki RN (1994) Regarding *Helicops danieli* Amaral, 1937, with a description of the hemipenis (Serpentes, Colubridae, Xenodontinae). Boletim do Museu Paraense Emilio Goeldi, Série Zoologia 10: 203–209.

Yuki RN, Lema TD (2005) Análise comparativa entre as cobras d'água meridionais (*Helicops carinicaudus* (Wied, 1825) e *Helicops infrataeniatus* Jan, 1865), com a descrição do crânio e hemipênis (Serpentes: Colubridae: Xenodontinae). Comunicações do Museu de Ciências e Tecnologia da PUCRS, Série Zoologia 18: 85–128.

Zaher H (1999) Hemipenial morphology of the South American xenodontine snakes with a proposal for a monophyletic Xenodontinae and a reappraisal of colubroid hemipenes. Bulletin of the American Museum of Natural History 240: 1–168.

Zaher H, Grazziotin FG, Cadle JE, Murphy RW, Moura-Leite JC de, Bonato SL (2009) Molecular phylogeny of advanced snakes (Serpentes, Caenophidia) with an emphasis on South American xenodontines: A revised classification and descriptions of new taxa. Papéis Avulsos de Zoologia 49: 115–153. https://doi.org/10.1590/S0031-10492009001100001

Zaher H, Murphy RW, Arredondo JC, Graboski R, Machado-Filho PR, Mahlow K, Montingelli GG, Quadros AB, Orlov NL, Wilkinson M, Zhang Y-P, Grazziotin FG (2019) Large-scale molecular phylogeny, morphology, divergence-time estimation, and the fossil record of advanced caenophidian snakes (Squamata: Serpentes). PLOS ONE 14: e0216148. https://doi.org/10.1371/journal.pone.0216148

Supplementary material 1

Supplementary tables

Authors: Juan Pablo Hurtado-Gómez, Juan M. Daza, Mario Vargas-Ramírez, V. Deepak, Uwe Fritz

Data type: xlsx

Explanation note: **table S1.** Samples and their respective GenBank/ENA accession numbers and (only for the newly generated sequences) localities for the individuals used in the molecular analyses. **table S2.** Primers, sources, and PCR conditions for each of the four molecular markers. **table S3.** Partitions obtained with MODELFINDER as implemented in IQ-TREE for the concatenated analysis of six molecular markers (mtDNA = 12S, 16S, cyt *b*; nDNA = BDNF, C-mos, NT3, Rag1). **table S4.** Akaike Information Criterion values obtained for each of the five morphological characters and the three tested models.

Link: https://doi.org/10.3897/zookeys.1215.128795.suppl1

Supplementary material 2

Supplementary figures

Authors: Juan Pablo Hurtado-Gómez, Juan M. Daza, Mario Vargas-Ramírez, V. Deepak, Uwe Fritz

Data type: pdf

Explanation note: **fig. S1.** Complete Bayesian dated tree obtained with the concatenated alignment of three mtDNA and four nDNA molecular markers. BR, Brazil; TT, Trinidad and Tobago. **fig. S2.** Complete Maximum Likelihood tree obtained with the concatenated alignment of three mtDNA and four nDNA markers. Values above branches indicate UltraFast bootstrap support. BR, Brazil; TT, Trinidad and Tobago. **fig. S3.** Detailed comparison between the Bayesian (left) and Maximum Likelihood (right) topologies obtained for *Helicops danieli*, cropped from Suppl. material 2: figs S1, S2, respectively. Values above branches on the left tree indicate Bayesian posterior probabilities, and on the right tree, UltraFast bootstrap support.

Link: https://doi.org/10.3897/zookeys.1215.128795.suppl2